THESE POUR OBTENIR LE GRADE DE DOCTEUR DE L'ECOLE NATIONALE SUPERIEURE DE CHIMIE DE MONTPELLIER

En Sciences Chimiques
École doctorale Sciences Chimiques Balard
Unité de recherche UMR 5253 CNRS-UM-ENSCM

Synthesis of biobased monomers and their aqueous emulsion and photoinduced polymerizations

Présentée par **Samantha MOLINA-GUTIÉRREZ**
le 13 Novembre 2020

Sous la direction de **Patrick LACROIX-DESMAZES**
et **Roberta BONGIOVANNI**

Devant le jury composé de

Mme. Angels SERRA, Professeur, Universitat Rovira i Virgili	Rapporteuse
M. José Ramón LEIZA, Professeur, Universidad del País Vasco	Rapporteur
Mme. Maila CASTELLANO, Professeur Assistant, Università di Genova	Examinatrice
Mme. Maud SAVE, Directrice de Recherche CNRS, Université de Pau et des Pays de l'Adour	Présidente
M. Renaud PERRIN, Docteur, Synthomer UK Ltd.	Examinateur
M. Patrick LACROIX-DESMAZES, Directeur de Recherche CNRS, ENSCM	Directeur de thèse
Mme Roberta BONGIOVANNI, Professeur, Politecnico di Torino	Co-directrice de thèse
M. Sylvain CAILLOL, Directeur de Recherche CNRS, ENSCM	Invité
M. Vincent LADMIRAL, Chargé de Recherche CNRS, ENSCM	Invité

Doctoral Dissertation

Synthesis of biobased monomers and their aqueous emulsion and photoinduced polymerizations

Samantha MOLINA-GUTIÉRREZ

* * * * * *

Supervisors

Dr. Patrick LACROIX-DESMAZES, ENSCM, Supervisor
Prof. Roberta BONGIOVANNI, Politecnico di Torino, Co-Supervisor

Doctoral Examination Committee:

Prof. Angels SERRA, Universitat Rovira i Virgili	Referee
Prof. José Ramón LEIZA, Universidad del País Vasco	Referee
Dr. Maud SAVE, Université de Pau et des Pays de l'Adour	President
Assist. Prof. Maila CASTELLANO, Università di Genova	Examiner
Dr. Renaud PERRIN, Synthomer UK Ltd	Examiner
Dr. Sylvain CAILLOL, ENSCM	Invited
Dr. Vincent LADMIRAL, ENSCM	Invited

Politecnico di Torino

November 13, 2020

SAMANTHA MOLINA GUTIÉRREZ

samantha.molinag@gmail.com
samantha.molina.gutierrez
smolinagutierrez

WORK EXPERIENCE

Oct 2015 - Aug 2017 — **Research/Development Chemist**

Mexico — **Industrias Lavin de México S.A. de C.V.**

- Research project: Development of a superabsorbent polymer as raw material for the cosmetic products. Supported by the National Council of Science and Technology (CONACyT).
- Give technical advice and/or solution for any issue during the manufacturing process of cosmetic products.
- Formulation development of personal care products.

Jun 2015-Aug 2015 — **Trainee, Organic Chemistry Laboratory**

Finland — **University of Helsinki, Helsinki, Finland**

- Research project: Design of multiple hydrogen-bond arrays in order to modify and tune the interaction between supramolecular building blocks.
- Training in Organic Synthesis, NMR Spectroscopy, IR and Mass Spectrometry.

Ju 2012- Jun 2013 — **Research Assistant**

Mexico — **COMEX (PPG) GROUP**

- Development of silica containing latexes for exterior coating.
- Execution, monitoring and characterization of synthesis reactions.
- Measurement of properties as pH, density, particle size, residual initiator, percent non-volatile, mechanical stability and haze.

FORMATION

Oct 2017–Sep 2020 — **PhD in Chemical Sciences**

France / Italy — **École Nationale Supérieure de Chimie de Montpellier / Politecnico di Torino**

- Organic synthesis of biobased monomers for emulsion polymerization.
- Formulation, synthesis and characterization of latexes for coatings applications.
- Experience in NMR Spectroscopy, IR and Real Time FT-IR, Size exclusion Chromatography, Thermogravimetric analysis (TGA and DSC).

Aug 2013-May 2015 — **Master in Science**

France / Finland — **Université Lille 1 / University of Helsinki**

- Research project: Synthesis and Self Assembly of Quadruple Hydrogen-Bonded Arrays.
- Training in Organic Synthesis, NMR Spectroscopy, IR and Mass Spectrometry.

Graduated: Eximia cum laude approbatur.

July 2007-Oct 2012 — **Bachelor's degree in Chemistry**

Mexico — **National Autonomous University of Mexico (UNAM)**

- Inorganic and Organic Chemistry, Physical Chemistry and Analytical Cheimstry.

Graduated with honours.

PUBLICATIONS

- Molina-Gutiérrez, S.; Ladmiral, V.; Bongiovanni, R.; Caillol, S.; Lacroix-Desmazes, P. Radical Polymerization of Biobased Monomers in Aqueous Dispersed Media. *Green Chem*. 2019, 21 (1), 36–53. https://doi.org/10.1039/C8GC02277A
- Molina-Gutiérrez, S.; Manseri, A.; Ladmiral, V.; Bongiovanni, R.; Caillol, S.; Lacroix-Desmazes, P. Eugenol: A Promising Building Block for Synthesis of Radically Polymerizable Monomers, *Macromol. Chem. Phys.*

2019, 1900179. https://doi.org/10.1002/macp.201900179

- Molina-Gutiérrez, S.; Ladmiral, V.; Bongiovanni, R.; Caillol, S.; Lacroix-Desmazes, P., Emulsion polymerization of dihydroeugenol, eugenol and isoeugenol derived methacrylates, *Ind. Eng. Chem. Res.* 2019, 58, 21155-21164.https://doi.org/10.1021/acs.iecr.9b02338
- Molina-Gutiérrez, S.; Li, W. S. J.; Perrin, R.; Ladmiral, V.; Bongiovanni, R.; Caillol, S.; Lacroix-Desmazes, P. Radical Aqueous Emulsion Copolymerization of Eugenol-Derived Monomers for Adhesive Applications. *Biomacromolecules* 2020, https://dx.doi.org/10.1021/acs.biomac.0c00461
- Molina-Gutiérrez, S.; Dalle Vacche, S.; Vitale, A.; Ladmiral, V.; Caillol, S.; Bongiovanni, R.; Lacroix-Desmazes, P. Photoinduced Polymerization of Eugenol-Derived Methacrylates. *Molecules* 2020, 25, 3444. https://doi.org/10.3390/molecules25153444

CONGRESSES AND CONFERENCES

June 2019	▪ International Polymers and Colloids Group
Singapore	Oral communication (Graduate Research Seminar) and Poster Presentation:
June 2019	▪ European Polymer Federation
Grece	Oral communication
May 2019	▪ International Symposium on Green Chemistry
France	Oral communication
October 2018	▪ 35th Club emulsion
France	Oral communication

SKILLS

- Languages :

		Speaking	Listening	Writing	Reading
Spanish	Mother tongue				
English	Proficient User	C1	C1	C1	C1
French	Proficient User	C1	C1	B2	C1
Italian	Independent User	B1	B2	A2	B2
German	Basic User	A2	A2	A2	A2

- Digital Competences :
  - Good command of Office Suite (word processor, spread sheet, presentation software).
  - TopSpin and MestreNova (NMR spectra treatment).

- Communicationsl Skills :
  - Multilingual communication skills gained through experience in international environments.
  - Creative and logical thinking gained through academic and research experience.
  - Good explaining and technical writing ability gained through academic experience.
  - Mentoring skills gained through tutoring bachelors' and masters' thesis projects.

- Organisational Skills :
  - Good time management and planning skills gained through positions in academic and industry.

GRANTS AND SCHOLARSHIPS

- Sustainable Industrial Chemistry Program Erasmus Mundus Joint Doctorate Scholarship, École Nationale Supérieure de Montpellier/ Politecnico di Torino, October 2017-Present.
- European Master Program in Advanced Spectroscopy in Chemistry Scholarship, Universite de Lille 1, Lille, France/ University of Helsinki, Helsinki, Finland, September 2013-June 2015.
- International Exchange Program UNAM-Coca-Cola Foundation Scholarship, Université de Lille 1, Lille, France, September 2011-January 2012.
- Mexican Science Academy Excellence Grant, Mexican Science Academy, Mexico City. Mexico September 2007-September 2012.
- Dr. Bessie F. Lawrence International Summer Science Institute (ISSI) Scholarship, Weizmann Institute, Rehovot, Israel, Summer Program July 2007.

List of scientific contributions:

Published articles:

- Molina-Gutiérrez, S.; Ladmiral, V.; Bongiovanni, R.; Caillol, S.; Lacroix-Desmazes, P. Radical Polymerization of Biobased Monomers in Aqueous Dispersed Media. *Green Chem*. **2019**, 21 (1), 36–53. https://doi.org/10.1039/C8GC02277A

- Molina-Gutiérrez, S.; Manseri, A.; Ladmiral, V.; Bongiovanni, R.; Caillol, S.; Lacroix-Desmazes, P. Eugenol: A Promising Building Block for Synthesis of Radically Polymerizable Monomers, *Macromol. Chem. Phys.* **2019**, 1900179. https://doi.org/10.1002/macp.201900179

- Molina-Gutiérrez, S.; Ladmiral, V.; Bongiovanni, R.; Caillol, S.; Lacroix-Desmazes, P., Emulsion polymerization of dihydroeugenol, eugenol and isoeugenol derived methacrylates, *Ind. Eng. Chem. Res.* **2019**, 58, 21155-21164. https://doi.org/10.1021/acs.iecr.9b02338

- Molina-Gutiérrez, S.; Li, W. S. J.; Perrin, R.; Ladmiral, V.; Bongiovanni, R.; Caillol, S.; Lacroix-Desmazes, P. Radical Aqueous Emulsion Copolymerization of Eugenol-Derived Monomers for Adhesive Applications. *Biomacromolecules* **2020**, https://dx.doi.org/10.1021/acs.biomac.0c00461

- Molina-Gutiérrez, S.; Dalle Vacche, S.; Vitale, A.; Ladmiral, V.; Caillol, S.; Bongiovanni, R.; Lacroix-Desmazes, P. Photoinduced Polymerization of Eugenol-Derived Methacrylates. *Molecules* **2020**, 25, 3444. https://doi.org/10.3390/molecules25153444

Oral communications:

- Graduate Research Seminar. International Polymers and Colloids Group (IPGC 2019). June 22nd -28th 2019, Sentosa Island, Singapore.
- European Polymer Federation (EPF 2019), June 9th -14th 2019, Heraklion, Greece.
- International Symposium on Green Chemistry (ISGC 2019), May 13th - 17th, La Rochelle, France.
- 35th Club emulsion, October 9th -10th 2018, Nantes, France.

Poster presentation:

- International Polymers and Colloids Group (IPGC 2019) Poster Presentation: “Biobased polymer latexes produced by free radical emulsion polymerization of eugenol derivatives”.

This work was funded through a SINCHEM Grant.
SINCHEM is a Joint Doctorate program selected
under the Erasmus Mundus Action 1 Program
(FPA 2013-0037)

This work was supported by Synthomer UK Ltd.

ACKNOWLEDGEMENTS

This work was funded through a SINCHEM Grant. SINCHEM is a Joint Doctorate program selected under the Erasmus Mundus Action 1 Program (FPA 2013-037) and with the support of Synthomer UK Ltd.

I would like to thank the reviewers and members of the jury that evaluated my PhD thesis:

- Dr. Maud SAVE
- Prof. Angels SERRA
- Assist. Prof. Maila CASTELLANO
- Prof. José Ramón LEIZA

I would like to express my gratitude to my supervisors and industrial advisors for providing help, support, advice and encouragement during the development of this research work:

- Dr. Patrick LACROIX-DESMAZES (École Nationale Supérieure de Montpellier)
- Prof. Roberta BONGIOVANNI (Politecnico di Torino)
- Dr. Sylvain CAILLOL (École Nationale Supérieure de Montpellier)
- Dr. Vincent LADMIRAL (École Nationale Supérieure de Montpellier)
- Dr. Peter SHAW (Synthomer UK Ltd)
- Dr. Renaud PERRIN (Synthomer UK Ltd)

I also thank all the trainees, PhD students, post-doctoral students, researchers and administrative staff from the IAM who helped me throughout the three years of my PhD. Special thanks to Lisa Ebers, Jennifer Li, Céline Bonneaud, Maxinne Denis, Wassima Belhadri (best stagiaire), Amani Moussa and Nicolas Zivic, for all the help, advice, nice moments and making TP fun.

Vorrei anche ringraziare tutto il grupo di polimeri al Politecnico di Torino per accogilermi ed aiutarmi durante il mio stage. Specialmente agli “Gorditos a pranzo”: Sara Dalle Vacche, Parnian Kianfar, e Gustavo González. Mi siete mancate molto, ma non tanto comme le insalate del Mixto. Grazie a Alessandra Vitale et Giuseppe Trusiano per l’aiuto nel mio lavoro.

I would like to thank the personnel in Synthomer UK (Harlow), for their support during my PhD, especially to Theresa Scharbert, Alexander Evans, Sara Mohavedi, Anaïs Maury, Irene Basile and Brett Harding.

Thanks to all the SINCHEM family, specially to Stefania Albonetti and Francesco Di Renzo for all their support and help. Moreover, I would like to thank Ana Patricia Alves Costa Pacheco, Ferenc Martinovic, Christine Tolod, Medet Zhukush, Paola Blair Vazquez, Hua Wei, Andrés Sierra, Daniel Aguilera, Sonia Aguilera, Payal Baheti, Quang Nguyen Tran and Iqra Subair for the time shared, advice and help.

I would like to thank Dr. Aleksandar Todorov, for being the best “PhD student” and for all what he taught me during my master’s degree.

Special thanks to the people that have helped and encouraged me along the way and friends around the world, specially: Mónica P. Enríquez-Sauri, Alberto Colín-Segundo, Oscar Hernández-Fajardo, Elizabeth Yau-Flores, Oleksandr “Carlos Papalote” Zagorodko, Bertha Perez-Martínez, Zayra Mendoza-Aco and Carla Cuní-Lopez.

Quisiera agradecer a Andrea Ruiu por su amistad y ayuda durante estos años. No tengo palabras que puedan expresar mi gratitud. Grazie.

Finalmente, quisiera agradecer a mis padres y mi hermana por siempre protegerme, apoyarme y motivarme; este logro es también de ustedes.

A nosotros

ABBREVIATIONS

2-EHA	2-ethylhexyl acrylate
2-HEA	2-hydroxyethyl acrylate
2H-HBO	dihydro-5-hydroxyl furan-2-one
AC4VG	acetyl-protected 4-vinylguaiacol
ACF	autocorrelation function
ACVA	4,4′-azobis(4-cyanovaleric acid)
ADB	allylic double bond
AFAME	acrylated fatty acid methyl ester
AIBN	2,2′-Azobis(2-methylpropionitrile
AMO	acrylated methyl oleate
a_s	adsorption area per surfactant molecule
AsA	ascorbic acid
ASAP	atmospheric pressure solids analysis probe
ASTM	American Standard for Testing and Materials
BA	butyl acrylate
BDDA	1,4-butanediol diacrylate
BDT	1,4-butanedithiol
BE	butyl vinyl ether
BTMSB	1,4- bis(trimethylsilyl)benzene
$CDCl_3$	deuterated chloroform
CDMA	cyclademol acrylate
CDMMA	cyclademol methacrylate
CLA	conjugated linoleic acid
CM	cardanol methacrylate
CMC	critical micellar concentration
CNSL	cashew nut shell oil
CTA	chain transfer agent
Đ	dispersity
DBI	dibutyl itaconate
DBN	1,5-diazabicyclo[4.3.0]non-5-ene
DCM	dichloromethane
DGU	dianhydro-D-glucityl diundec-10-enoate
D_i	intensity-average particle diameter
DI water	deionized water
DLS	dynamic light scattering
DMAP	4-dimethylaminopyridine
DSC	differential scanning calorimetry
EA	ethyl acrylate

ED	ethoxy dihydroeugenol
EDA	ethoxy dihydroeugenyl acrylate
EDMA	ethoxy dihydroeugenyl methacrylate
EDTA	ethylenediaminetetraacetic acid
EE	ethoxy eugenol
EEA	ethoxy eugenyl acrylate
EEMA	ethoxy eugenyl methacrylate
EI	ethoxy isoeugenol
EIA	ethoxy isoeugenyl acrylate
EIMA	ethoxy isoeugenyl methacrylate
equiv.	molar equivalent
EtOAc	ethyl acetate
FSM	functionalized sugar-based monomer
FTIR	Fourier transform infrared spectroscopy
G’	storage modulus
G’’	loss modulus
GMA	glycidyl methacrylate
HPSBM	high oleic soybean oil-based monomer
IBOA	isorbornyl acrylate
IBOMA	isobornyl methacrylate
k_d	rate constant of decomposition
k_p	rate constant of propagation
k_t	rate constant of termination
KPS	potassium persulfate
LGO	levoglucosenone
m.p.	melting point
MAA	methacrylic acid
MBL	α-methylene-γ-butyrolactone
m-CPBA	m-chloroperbenzoic acid
MDB	methacrylic double bond
MEE	mercaptoethyl ether
MEHQ	4-methoxyphenol
MEK	methyl ethyl ketone
MeTHF	2-methyltetrahydrofuran
MFFT	minimum film forming temperature
MHU	2-(10-undecenoyloxyethyl methacrylate
MLA	methacrylated linoleic acid
MMA	methyl methacrylate
M_n	number average molecular weight
MOA	methacrylated oleic acid

NaPS	sodium persulfate
NMR	nuclear magnetic resonance
N_p	number of particles
OA	octyl acrylate
PDB	propenyl double bond
PE	polyethylene
PET	polyethylene terephthalate
PHA	polyhydroxyalkanoate
Phm	part per hundred parts of monomer
PI	photoinitiator
PIPEMA	pyperonyl methacrylate
PP	polypropylene
PSA	pressure-sensitive adhesives
PVA	poly(vinyl alcohol)
RAFT	reversible addition-fragmentation chain transfer
RNSP	regenerated starch nanoparticles
SAM	soybean acrylate macromonomer
SBR	styrene-butadiene copolymers
SDS	sodium dodecyl sulfate
SDBS	sodium dodecylbenzenesulfonate
SEC	size exclusion chromatography
SMBS	sodium metabisulfite
SNP	starch nanoparticles
STEM	scanning transmission electron microscope
STMP	sodium trimetaphosphate
TBAB	tetrabutylammonium bromide
TBHP	tert-butyl hydroperoxide
$T_{d,5\%}$	decomposition temperature at 5% weight loss
TEA	triethylamine
TEM	transmission electron microscopy
TFA	trifluoroacetic acid
T_g	glass transition temperature
TGA	thermogravimetric analysis
THF	tetrahydrofuran
THGA	tetrahydrogeraniol acrylate
THGMA	tetrahydrogeraniol methacrylate
TOF-MS	time-of-flight mass spectrometry
TSC	total solids content
UV-Vis	ultraviolet and visible spectroscopy
VOC	volatile organic compound

VOMM	vegetable oil macromonomers
wbm	weight based on monomer
wt	weight percentage
X_C	cross-link density
f	efficiency
v	kinetic chain length
μ	volumetric growth rate per particle

TABLE OF CONTENTS

Abstract - Vulgarisation

Current environmental concerns and environmental regulations have led to the necessity to synthesize monomers and polymers from renewable resources through environmentally friendly processes. Eugenol, isoeugenol and dihydroeugenol, derived from clove oil and lignin depolymerization, were used to synthesize nine monomers, reactive via radical polymerization. To provide a true green solution, environmentally friendly polymerization processes were employed. Thus, eugenol-derived methacrylates were polymerized through aqueous emulsion polymerization (water as continuous phase), and photoinduced polymerization (low energy and solvent-free) and resulted in polymers suitable for coatings and adhesives applications.

Resume - Vulgarisation

Les préoccupations et les réglementations environnementales rendent nécessaires la synthèse de monomères et de polymères à partir de ressources renouvelables en utilisant des procédés respectueux de l'environnement. L'eugénol, l'isoeugénol et le dihydroeugénol, dérivés de l'huile de clou de girofle et de la dépolymérisation de la lignine, ont été utilisés pour synthétiser neuf monomères réactifs par polymérisation radicalaire. Pour fournir une véritable solution verte, des procédés de polymérisation respectueux de l'environnement ont été utilisés. Ainsi, des méthacrylates dérivés d'eugénol ont été polymérisés par polymérisation en émulsion aqueuse (eau comme phase continue) et par polymérisation photoinduite (à faible énergie et sans solvant) qui ont abouti à des polymères appropriés pour des applications de revêtements et d'adhésifs.

Riassunto - Volgarizzazione

Le attenzioni per l’ambiente e le nuove regolamentazioni introdotte per la sua tutela, hanno portato alla necessità di sintetizzare monomeri e polimeri da fonti rinnovabili attraverso processi ecocompatibili. L’eugenolo, isoeugenolo e diidroeugenolo, derivati dall'olio di chiodi di garofano e dalla depolimerizzazione della lignina, sono stati usati per sintetizzare nove monomeri reattivi tramite polimerizzazione radicalica. Per fornire una vera soluzione verde, sono stati impiegati processi di polimerizzazione ecocompatibili. Pertanto, i metacrilati derivati dall'eugenolo sono stati polimerizzati tramite emulsione acquosa (acqua come fase continua) e polimerizzazione foto indotta (a bassa energia e senza solventi) e hanno prodotto polimeri adatti per applicazioni di rivestimenti e adesivi.

Abstract

Current environmental concerns and environmental regulations have led to the necessity to synthesize monomers and polymers from renewable resources through environmentally friendly processes. In this work, photoinduced polymerization and aqueous emulsion polymerization were selected as polymerization techniques. Natural phenols have not been widely researched and employed in the synthesis of monomers to be polymerized through the aforementioned polymerization methods. Thus, eugenol, isoeugenol and dihydroeugenol, natural phenols coming from clove oil and lignin depolymerization, were chosen as building blocks.

The synthesis of nine monomers (eight novel molecules) derived from eugenol bearing polymerizable functional groups such as (meth)acrylate, epoxy and carbonate was achieved. Successful radical polymerization in solution was achieved with the (meth)acrylated eugenol-derivatives. The polymerization rate was affected by secondary reactions involving the allylic and propenyl groups in the eugenol and isoeugenol derivatives (degradative chain transfer and cross-propagation). However, most of the allylic and propenyl groups were preserved for post-polymerization reactions.

Photoinduced polymerization was executed with the methacrylate eugenol-derived monomers. The polymerization was monitored in the absence and presence of a photoinitiator and under air or protected from air, using Real-Time Fourier Transform Infrared Spectroscopy. The polymerization rate was again affected by the presence and reactivity of the allyl and propenyl groups in the eugenol- and isoeugenol-derived methacrylates, respectively. These groups are involved in radical addition, degradative chain transfer, and termination reactions, yielding crosslinked polymers. Without photoinitiator and in the presence of air, the formation of hydroperoxides for eugenol and isoeugenol derivatives led to a second polymerization regime. The materials, in the form of films, were characterized by differential scanning calorimetry, thermogravimetric analysis, and contact angle.

Eugenol-derived methacrylates were then homopolymerized through aqueous emulsion polymerization using three different initiation systems. Latexes of poly(ethoxy dihydroeugenyl methacrylate), poly(ethoxy eugenyl methacrylate) and poly(ethoxy isoeugenyl methacrylate) with particle diameter in the 45−71 nm range were successfully obtained. Glass transition temperatures of the resulting polymers ranged between 20°C and 72°C. This study opens the way to the use of these new biobased monomers into latexes formulation for adhesives and coatings applications. Subsequently, eugenol-derived methacrylates were copolymerized by emulsion polymerization to produce latexes for adhesive applications. Latexes containing ethoxy dihydroeugenyl methacrylate and ethoxy eugenyl methacrylate with high total solids content of 50 wt% were obtained and characterized. Latexes synthesis was carried out using a semibatch process, and latexes with particle diameters in the 159−178 nm range were successfully obtained. Glass transition temperature values of the resulting polymers ranged between −32°C and −28°C. Furthermore, tack and peel measurements confirmed the possibility to use these latexes in adhesive applications.

Résumé

Les préoccupations et les réglementations environnementales rendent nécessaires la synthèse de monomères et de polymères à partir de ressources renouvelables en utilisant des procédés respectueux de l'environnement. Dans ce travail, la polymérisation photoinduite et la polymérisation en émulsion aqueuse ont été sélectionnées comme techniques de polymérisation. Les phénols naturels ont été peu étudiés dans la littérature pour la synthèse de monomères polymérisables par les procédés de polymérisation susmentionnés. Ainsi, l'eugénol, l'isoeugénol et le dihydroeugénol, des phénols naturels provenant de l'huile de girofle ou de la dépolymérisation de la lignine, ont donc été choisis comme matières premières.

La synthèse de neuf monomères (huit nouvelles molécules) dérivés d'eugénol contenant des groupes fonctionnels polymérisables tels que les groupes (méth)acrylate, époxy et carbonate, a été réalisée. Les dérivés d'eugénol (méth)acrylés ont été polymérisés avec succès par polymérisation radicalaire en solution. La vitesse de polymérisation s'est trouvée affectée par des réactions secondaires impliquant le groupe allylique de l'eugénol et propényle de l'isoeugénol (réactions de transfert de chaîne dégradatif et de propagation croisée). Cependant, la plupart des groupes allylique et propényle ont été conservés pour des réactions de post-polymérisation.

De plus, la polymérisation photoinduite a été réalisée avec les monomères méthacrylates des dérivés d'eugénol. La polymérisation a été suivie par spectroscopie infrarouge à transformée de Fourier en temps réel, en l'absence et en présence d'un photoamorceur ainsi que sous air ou à l'abri de l'air. La vitesse de polymérisation a également été affectée par la présence et la réactivité des groupes allyle et propényle dans les méthacrylates d'eugénol et d'isoeugénol, respectivement. Ces groupes sont impliqués dans des réactions d'addition de radicaux, de transfert de chaîne dégradatif, et de terminaison, donnant ainsi des polymères réticulés. Sans photoamorceur et en présence d'air, la formation de peroxydes à partir des dérivés d'eugénol et d'isoeugénol a conduit à un deuxième régime de polymérisation. Les matériaux, sous forme de films, ont été caractérisés par calorimétrie différentielle à balayage, thermogravimétrie et mesure d'angle de contact.

Les méthacrylates des dérivés d'eugénol ont ensuite été homopolymérisés par polymérisation en émulsion aqueuse en utilisant trois systèmes d'amorçage différents. Des latex de poly(méthacrylate d'éthoxy dihydroeugényle), poly(méthacrylate d'éthoxy eugényle) et poly(méthacrylate d'éthoxy isoeugényle) avec un diamètre de particules compris entre 45 et 71 nm ont été obtenus avec succès. Les températures de transition vitreuse des polymères résultants se situent entre 20°C et 72°C. Cette étude ouvre la voie à l'utilisation de ces nouveaux monomères biosourcés dans la formulation de latex pour des applications d'adhésifs et de revêtements. Par la suite, des méthacrylates des dérivés d'eugénol ont été copolymérisés par polymérisation en émulsion pour produire des latex pour des applications d'adhésifs sensibles à la pression. Des latex contenant du méthacrylate d'éthoxy dihydroeugényle (EDMA) et du méthacrylate d'éthoxy eugényle (EEMA) avec un taux de solides de 50% en poids ont été obtenus

et caractérisés. La synthèse de latex a été réalisée en utilisant un procédé semi-batch, et des latex avec des diamètres de particules dans la gamme de 159-178 nm ont été obtenus avec succès. Les valeurs de température de transition vitreuse des polymères résultants se situent entre −32°C et −28°C. De plus, les mesures de pégosité (« tack ») et de pelage (« peel ») ont confirmé la possibilité d'utiliser ces latex dans des applications d’adhésifs.

Riassunto

Le attenzioni per l'ambiente e alle nuove regolamentazioni introdotte per la sua tutela, ha portato alla necessità di sintetizzare monomeri e polimeri da fonti rinnovabili attraverso processi ecocompatibili. In questo quadro, per questo lavoro, sono state scelti come metodi di polimerizzazione la polimerizzazione foto indotta e la polimerizzazione in emulsione acquosa. L'eugenolo, l'isoeugenolo e il diidroeugenolo, fenoli naturali provenienti dal chiodo di garofano e dalla depolimerizzazione della lignina, sono stati scelti come building blocks perché, come la maggior parte dei fenoli naturali, non sono stati esaustivamente studiati nè tantomeno utilizzati per la sintesi di monomeri da usarsi con i metodi di polimerizzazione precedentemente citati.

La sintesi di nove monomeri (otto nuove molecole) derivanti dall'eugenolo è stata ottenuta tramite la funzionalizzazione con gruppi polimerizzabili come (met)acrilato, epossido e carbonato. Per i derivati (met)acrilati dell'eugenolo, la polimerizzazione radicalica in soluzione è stata condotta con successo. È stato osservato che la velocita di polimerizzazione è stata influenzata da reazioni secondarie quali il trasferimento di catena e la cross-propagation, che coinvolgono i gruppi allilici e propenilici dei derivati dell'eugenolo e dell'isoeugenolo rispettivamente. Tuttavia, la maggior parte dei gruppi allilici e propenilici è stata preservata ed è risultata presente dopo la polimerizzazione.

La polimerizzazione foto indotta è stata effettuata con i monomeri metacrilici derivati dall'eugenolo. La polimerizzazione è stata monitorata in assenza e presenza di fotoiniziatore e in assenza e presenza di aria, usando la spettroscopia infrarossa in tempo reale. Come osservato precedentemente, la velocità di polimerizzazione è influenzata dalla presenza e reattività dei gruppi allilici e propenilici dei derivati metacrilici dell'eugenolo e dell'isoeugenolo rispettivamente. Questi gruppi sono soggetti a reazioni di addizione radicalica, trasferimento degradativo di catena e reazioni di terminazione, portando a polimeri reticolati. Senza fotoiniziatore e in presenza di aria, nel caso dei derivati di eugenolo e isoeugenolo, la formazione di perossidi causa un secondo regime di polimerizzazione. I materiali, sotto forma di film, sono stati caratterizzati tramite calorimetria differenziale a scansione, analisi termogravimetrica e angolo di contatto.

I derivati metacrilici dell'eugenolo sono stati successivamente polimerizzati tramite polimerizzazione in emulsione acquosa usando tre differenti sistemi di inizializzazione. Sono stati sintetizzati lattici di poli(etossi metacrilato di diidroeugenolo), poli(etossi metacrilato di eugenolo) e poli (etossi metacrilato di isoeugenolo) con particelle di diametro medio nell'intervallo 45-71 nm. Per i polimeri ottenuti, sono state misurate temperature di transizione vetrosa tra i 20°C e 72°C. Questa ricerca apre la strada per l'utilizzo di questi monomeri ottenuti da fonti naturali per la formulazione di lattici per adesivi e rivestimenti. A questo scopo i metacrilati derivanti dall'eugenolo sono stati successivamente copolimerizzati in emulsione per farne formulazioni come adesivi. I lattici con etossi metacrilato del diidroeugenolo e dell'eugenolo sono stati ottenuti con un alto contenuto in solido pari al 50% e sono stati successivamente caratterizzati. La sintesi è stata ottenuta tramite processi semibatch, ottenendo lattici con diametro di particella compresa tra i 159-179 nm. La temperatura di transizione vetrosa per questi polimeri è risultata tra i −32°C

e −28°C. infine, misurazioni di tack e peel hanno confermato la possibilità di usare questi lattici come adesivi.

General Introduction

During the past decades environmental concerns have arisen due to the anthropogenic carbon emissions and waste production.[1] As a result, green chemistry emerged as an innovative chemistry field which follows twelve principles[2,3] that provide a framework for the design and synthesis of more sustainable monomers and polymers and to reduce the use and generation of hazardous substances. The twelve green chemistry principles are:[2]

1. Waste prevention
2. Atom economy
3. Less hazardous chemical synthesis
4. Designing safer chemicals
5. Safer solvent and auxiliaries
6. Design for energy efficiency
7. Use of renewable feedstocks
8. Reduce derivatives
9. Catalysis
10. Design for degradation
11. Real-Time analysis for pollution prevention
12. Inherently safer chemistry for accident prevention

The reduction in the use of fossil fuels to produce plastics has become a priority. Around 4% of the world oil and gas production is used as a feedstock for plastics (while 3-4% is used as energy for their manufacture).[4] Therefore, the use of renewable feedstocks, according to the seventh green chemistry principle, has become the strategy for the replacement of fossil-fuel feedstock in the production of polymers. Moreover, the use of renewable sources contributes with goal 12 (responsible consumption and production) from the 17 Sustainable Development Goals (SDGs) outlined by the United Nations.[5]

Biomass as renewable feedstock provides a wide variety of molecules to obtain the desired biobased monomers.[6] It is important to select biobased building blocks that do not affect the food supply and that derive from widely available sources. Indeed, polymers are already present in nature as natural rubber (polyisoprene),[7] polysaccharides (cellulose, hemicellulose, starch, chitin, and chitosan) and lignin.[1] Additionally, macromonomer and monomers can also be found in molecules such as: vegetable oils, terpenes, lignin derivatives, sugar derivatives and proteins.[6,8–11] Nevertheless, the physicochemical properties of the natural polymers might not be adequate for certain material applications, leading to the necessity to introduce other chemical functions to confer specific properties or enable further polymerization. Moreover, most of the available biobased building blocks are likely to be polymerized through step growth polymerization or non-radical chain polymerization as they do not possess functional groups that undergo radical polymerization. Radical polymerization is a flexible mechanism to produce copolymers as it is tolerant to protic solvents and trace impurities such as oxygen and monomer stabilizers.[12] Furthermore, polymers

with tuned properties can be synthesized by modifying the technique, initiators, chain transfer agent, or by employing reversible-deactivation radical polymerization (RDRP) techniques.[13,14] In order to execute radical polymerization, modifications to introduce the adequate functional groups such as (meth)acrylates have to be done.[11] Great advances have been achieved in the synthesis of reactive biobased-monomers for radical polymerization. However, natural phenols remain little explored and represent a considerable opportunity to generate materials that could replace oil-based aromatic monomers and bring interesting thermal and mechanical properties to polymers.[15] Lignin is the biggest source of natural phenols, although its direct utilization remains limited.[16] Despite depolymerization of lignin is not an optimized process yet, it has gained increased attention[17,18] due to its wide availability and its non-interference with the food supply. Natural phenols coming from lignin such as vanillin[10,19,20] and ferulic acid[21] and coming from lipids, as cardanol,[22–24] have been modified to introduce different functional groups and polymerized through conventional radical polymerization. Other examples of natural phenols are eugenol and eugenol-derivatives, coming from clove oil but also obtained from the depolymerization of lignin[18,25] (Figure 1). These molecules can be modified through the phenol group to introduce radically polymerizable groups. In addition, the presence of allylic and propenyl double bonds, in eugenol and isoeugenol respectively, can allow further functionalization. For the previous mentioned reasons, eugenol, isoeugenol and dihydroeugenol[26,27] were selected as the building blocks in this PhD work to synthesize a new and versatile monomer platform.

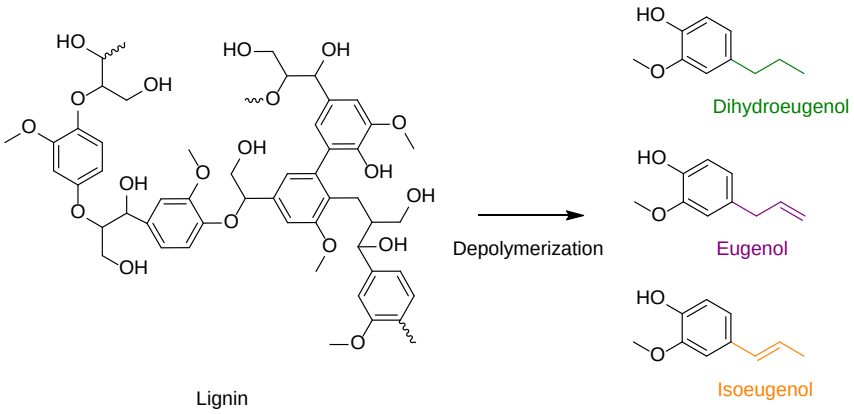

Figure 1. Lignin derivatives: eugenol, isoeugenol and dihydroeugenol.

The synthesis of biobased monomers from renewable resources is only the first step for sustainable materials. The implementation of environmentally friendly processes to polymerize them should not be neglected. Aqueous emulsion polymerization and photoinduced polymerization were chosen to perform greener polymer synthesis. In the case of aqueous emulsion polymerization, water is the continuous phase, eliminating the use of solvent and reducing the production of volatile organic compounds (VOCs).[28] In photoinduced polymerization, the process is fast, with low energy consumption and solvent-free.[29] These processes, in addition to the use of biobased monomers were implemented to follow some of the twelve green chemistry principles[30] such as:

Principle 1. Waste prevention: the use of water in emulsion polymerization reduces the production and liberation of VOCs.

Principle 3. Less hazardous chemical synthesis: as emulsion polymerization prevents hazardous residual VOCs in the formulations which could also be toxic and flammable.

Principle 5. Safer solvent and auxiliaries: use of water as the continuous phase in emulsion polymerization which is an innocuous and non-flammable solvent.

Principle 6. Design for energy efficiency: as photoinduced polymerization is a fast process that can be done at low temperature.

Principle 7. Use of renewable feedstock: by using eugenol, isoeugenol and dihydroeugenol from clove oil or lignin depolymerization.

Principle 12. Inherently safer chemistry for accident prevention: the use of water as continuous phase improves heat transfer and lower viscosity of reactions, allowing better control in case of runaway reaction rendering the synthesis safer.

By means of these techniques, the production of biobased latexes aiming at adhesive and coating applications was targeted to provide a more sustainable option for products that are used on a daily basis by consumers worldwide.[31]

Several questions emerged which defined the research strategy:

- Are eugenol and eugenol derivatives suitable building blocks to synthesize radical polymerizable monomers? Which functional groups can be introduced to create a versatile monomer platform?
- Can eugenol-derived monomers be efficiently polymerized through radical polymerization? Which are the possible secondary reactions, to which extent they happen and can they be controlled?
- Can eugenol-derived monomers be polymerized through aqueous emulsion polymerization? Would their solubility in water be a constraint and force the use of the miniemulsion polymerization process?
- Would it be possible to copolymerize eugenol-derived monomers with commercial monomers to increase biobased content in commercial formulations? Would the obtained formulations be suitable for application in coatings and adhesives?
- Would it be possible to introduce functional groups to fine tune the physicochemical properties of the polymers through post-polymerization reactions?

Derived from these questions a general objective of the project was established:

- Synthesize and characterize biobased monomers derived from eugenol and execute their polymerization via aqueous emulsion polymerization and photoinduced polymerization to produce latexes and polymers respectively, for applications in coatings and adhesives.

Moreover, the following strategy was developed and implemented to answer all the aforementioned questions and accomplish the general objective (Figure 2):

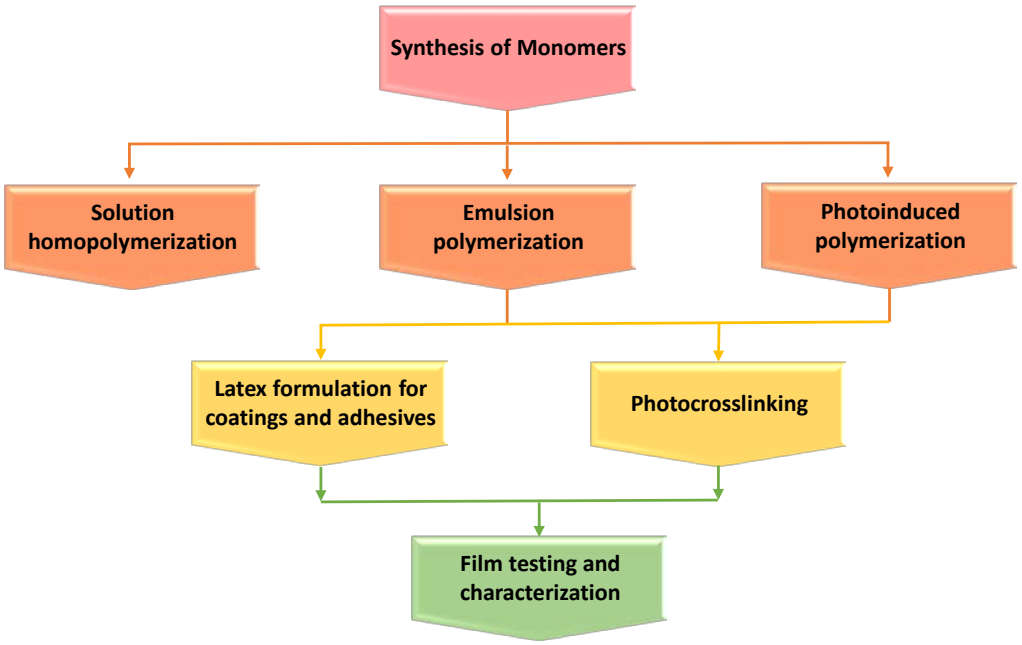

Figure 2. Research Strategy.

1. Synthesis of monomers
   - Synthesis of eugenol-derived monomers, introducing radical polymerizable functional groups
   - Characterization through NMR, TGA, DSC, FTIR, UV, Mass spectrometry.
2. Solution homopolymerization
   - Kinetics study of monomers in solution, study of secondary radical reactions.
   - Characterization of polymer though NMR, TGA, DSC, Gel content and SEC.
3. Emulsion polymerization
   - Ab initio, seeded or miniemulsion according to hydrophobicity character of monomers.
   - Characterization of latex and polymer: TGA, DSC, SEC, particle size, gel content, pH, total solids content.
   - Formulation of film forming latexes for coatings or adhesive application.
4. Photoinduced polymerization and photo-crosslinking
   - Photoinduced polymerization of monomers.
   - Synthesis of reactive polymers/latexes able to undergo photo-crosslinking.
5. Film testing and coating formulation
   - Coatings formulation and performance testing.

By executing the presented strategy, the polymerization behaviour of the eugenol-derived monomers using different techniques such as solution polymerization (to check radical

polymerizability), photoinduced polymerization, aqueous emulsion homo- and copolymerization was studied. Furthermore, the formulation of biobased latexes with adhesive properties as well as the preparation of biobased polymer for adhesive applications was also achieved.

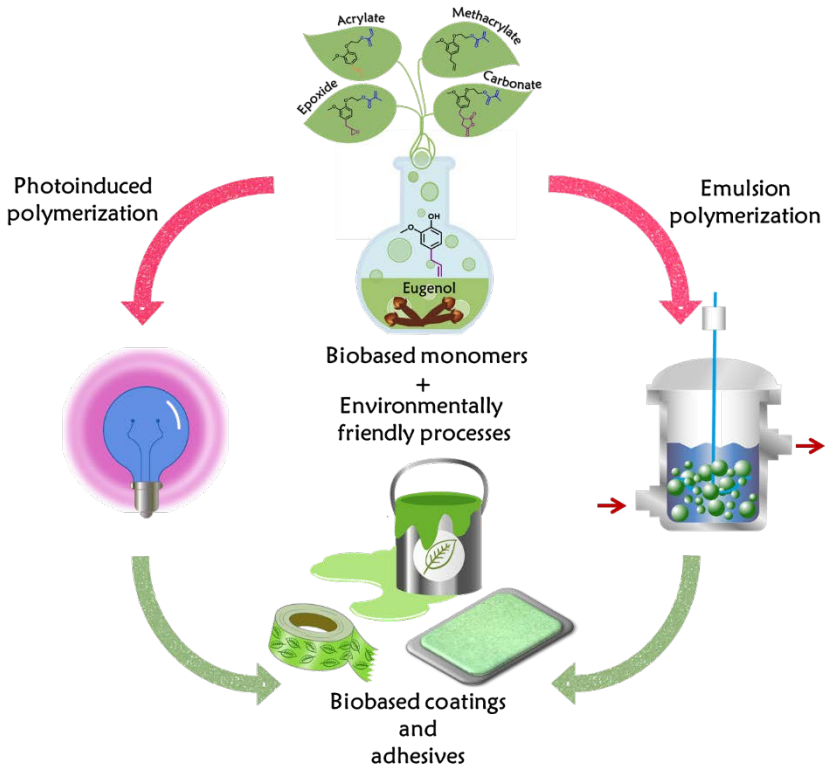

Figure 3. Research Strategy.

To discuss each part of the work, the present manuscript is divided into five chapters:

- **Chapter I: Literature overview on biobased monomers and their aqueous emulsion and photoinduced polymerizations.** Strategies for selection and synthesis of biobased monomers, selection of suitable environmentally friendly polymerization techniques, synthesis of biobased latexes and selection of the biobased building blocks for this work are described.
- **Chapter II: Biobased monomer synthesis and solution homopolymerization.** Synthesis of a platform of eugenol derived monomers bearing functional groups such as (meth)acrylates, epoxy and carbonate is introduced. The homopolymerization behaviour in solution of the synthesized monomers is then studied and discussed.
- **Chapter III: Photoinduced polymerization of eugenol-derived monomers.** The photoinduced polymerization of eugenol-derived methacrylates is studied under different conditions and using two different photoinitiators, and the behaviour of each monomer is detailed.
- **Chapter IV: Emulsion polymerization of eugenol-derived methacrylates.** The emulsion homopolymerization of the synthesized eugenol derived monomers using three different

initiation systems is presented and a discussion regarding the different polymerization behaviours of the monomers is provided.

- **Chapter V: Emulsion copolymerization of eugenol-derived methacrylates for adhesive applications.** The emulsion copolymerization of eugenol-derived methacrylates with commercial monomers to obtain adhesive formulation and the physicochemical properties of the resulting polymers are discussed and compared.

Finally, a section regarding the **General Conclusions and Perspectives** of the project is included.

This project was funded through a SINCHEM Grant. SINCHEM is a Joint Doctorate program selected under the Erasmus Mundus Action 1 Program (FPA 2013-0037): http://www.sinchem.eu/. A Category B EACEA Fellowship was granted to the PhD student for a period of 3 years. Furthermore, three institutions contributed with their expertise in the different involved fields to complete the objectives of the project, among which an industrial partner to implement the designed biobased latexes on coatings and adhesives industrial applications.

- **Home institution: École Nationale Supérieure de Chimie de Montpellier (IAM-ICGM), Montpellier France**

  Supervisor: Dr. Patrick Lacroix-Desmazes
  Co-supervisor: Dr. Sylvain Caillol
  Co-supervisor: Dr. Vincent Ladmiral

  Field of expertise: Polymer synthesis, including emulsion polymerization

- **1º Host institution: Politecnico di Torino (DISAT), Turin, Italy**

  Co-supervisor: Prof. Roberta Bongiovanni

  Field of expertise: Photoinduced polymerization

- **2º Host institution: Synthomer (UK) Ltd., Harlow, United Kingdom**

  Industrial advisor: Dr. Peter Shaw
  Industrial advisor: Dr. Renaud Perrin

  Field of expertise: Polymer synthesis, emulsion polymerization and coating formulation

References

(1) Lambert, S.; Wagner, M. Environmental Performance of Bio-Based and Biodegradable Plastics: The Road Ahead. *Chem. Soc. Rev.* **2017**, *46*, 6855.

(2) Anastas, P.; Warner, J. *Green Chemistry: Theory and Practice*; Oxford University Press: New York, 2000.

(3) Anastas, P. T.; Zimmerman, J. B. Design Through the 12 Principles of Green Engineering. *Environ. Sci. Technol.* **2003**, *37*, 94A.

(4) Hopewell, J.; Dvorak, R.; Kosior, E. Plastics Recycling: Challenges and Opportunities. *Philos. Trans. R. Soc. B Biol. Sci.* **2009**, *364*, 2115.

(5) United Nations. The 17 Sustainable Development Goals https://sdgs.un.org/goals (accessed Aug 24, 2020).

(6) Gandini, A.; Lacerda, T. M.; Carvalho, A. J. F. F.; Trovatti, E. Progress of Polymers from Renewable Resources: Furans, Vegetable Oils, and Polysaccharides. *Chem. Rev.* **2016**, *116*, 1637.

(7) Sarkar, P.; Bhowmick, A. K. Sustainable Rubbers and Rubber Additives. *J. Appl. Polym. Sci.* **2017**, *134*, 45701.

(8) Ca, V.; Lligadas, G.; Ronda, J. C.; Galia, M.; Galià, M.; Cádiz, V. Renewable Polymeric Materials from Vegetable Oils: A Perspective. *Mater. Today* **2013**, *16*, 337.

(9) Wilbon, P. A.; Chu, F.; Tang, C. Progress in Renewable Polymers from Natural Terpenes, Terpenoids, and Rosin. *Macromol. Rapid Commun.* **2013**, *34*, 8.

(10) Fache, M.; Darroman, E.; Besse, V.; Auvergne, R.; Caillol, S.; Boutevin, B. Vanillin, a Promising Biobased Building-Block for Monomer Synthesis. *Green Chem.* **2014**, *16*, 1987.

(11) Kristufek, S. L.; Wacker, K. T.; Tsao, Y.-Y. T. Y. T.; Su, L.; Wooley, K. L. Monomer Design Strategies to Create Natural Product-Based Polymer Materials. *Nat. Prod. Rep.* **2017**, *34*, 433.

(12) Nesvadba, P. Radical Polymerization in Industry. In *Encyclopedia of Radicals in Chemistry, Biology and Materials*; John Wiley & Sons, Ltd: Chichester, UK, 2012.

(13) Save, M.; Guillaneuf, Y.; Gilbert, R. G. Controlled Radical Polymerization in Aqueous Dispersed Media. *Aust. J. Chem.* **2006**, *59*, 693.

(14) Destarac, M. Controlled Radical Polymerization: Industrial Stakes, Obstacles and Achievements. *Macromol. React. Eng.* **2010**, *4*, 165.

(15) Fonseca, L. R.; Silva Sá, J. L.; Lima-Neto, B. S. Plant Oil-Based Polyester. In *Bio-Based Plant Oil Polymers and Composites*; Elsevier, 2016; pp 73–86.

(16) Strassberger, Z.; Tanase, S.; Rothenberg, G. The Pros and Cons of Lignin Valorisation in an Integrated Biorefinery. *RSC Adv.* **2014**, *4*, 25310.

(17) Azadi, P.; Inderwildi, O. R.; Farnood, R.; King, D. A. Liquid Fuels, Hydrogen and Chemicals from Lignin: A Critical Review. *Renew. Sustain. Energy Rev.* **2013**, *21*, 506.

(18) Sun, Z.; Fridrich, B.; De Santi, A.; Elangovan, S.; Barta, K. Bright Side of Lignin Depolymerization: Toward New Platform Chemicals. *Chem. Rev.* **2018**, *118*, 614.

(19) Fache, M.; Boutevin, B.; Caillol, S. Vanillin Production from Lignin and Its Use as a

Renewable Chemical. *ACS Sustain. Chem. Eng.* **2016**, *4*, 35.

(20) Zhang, H.; Deng, J.; Wu, Y. Biobased Magnetic Microspheres Containing Aldehyde Groups: Constructed by Vanillin-Derived Polymethacrylate/Fe3O4 and Recycled in Adsorbing Amine. *ACS Sustain. Chem. Eng.* **2017**, *5*, 658.

(21) Takeshima, H.; Satoh, K.; Kamigaito, M. Bio-Based Functional Styrene Monomers Derived from Naturally Occurring Ferulic Acid for Poly(Vinylcatechol) and Poly(Vinylguaiacol) via Controlled Radical Polymerization. *Macromolecules* **2017**, *50*, 4206.

(22) Voirin, C.; Caillol, S.; Sadavarte, N. V.; Tawade, B. V.; Boutevin, B.; Wadgaonkar, P. P. Functionalization of Cardanol: Towards Biobased Polymers and Additives. *Polym. Chem.* **2014**, *5*, 3142.

(23) Ladmiral, V.; Jeannin, R.; Fernandes Lizarazu, K.; Lai-Kee-Him, J.; Bron, P.; Lacroix-Desmazes, P.; Caillol, S. Aromatic Biobased Polymer Latex from Cardanol. *Eur. Polym. J.* **2017**, *93*, 785.

(24) Li, W. S. J.; Negrell, C.; Ladmiral, V.; Lai-Kee-Him, J.; Bron, P.; Lacroix-Desmazes, P.; Joly-Duhamel, C.; Caillol, S. Cardanol-Based Polymer Latex by Radical Aqueous Miniemulsion Polymerization. *Polym. Chem.* **2018**, *9*, 2468.

(25) Schutyser, W.; Renders, T.; Van den Bosch, S.; Koelewijn, S.-F.; Beckham, G. T.; Sels, B. F. Chemicals from Lignin: An Interplay of Lignocellulose Fractionation, Depolymerisation, and Upgrading. *Chem. Soc. Rev.* **2018**, *47*, 852.

(26) Kamatou, G. P.; Vermaak, I.; Viljoen, A. M. Eugenol - From the Remote Maluku Islands to the International Market Place: A Review of a Remarkable and Versatile Molecule. *Molecules*. 2012, pp 6953–6981.

(27) Khalil, A. A.; Rahman, U. ur; Khan, M. R.; Sahar, A.; Mehmood, T.; Khan, M. Essential Oil Eugenol: Sources, Extraction Techniques and Nutraceutical Perspectives. *RSC Adv.* **2017**, *7*, 32669.

(28) Asua, J. M. Emulsion Polymerization: From Fundamental Mechanisms to Process Developments. *J. Polym. Sci. Part A Polym. Chem.* **2004**, *42*, 1025.

(29) Fouassier, J. P.; Allonas, X.; Burget, D. Photopolymerization Reactions under Visible Lights: Principle, Mechanisms and Examples of Applications. *Prog. Org. Coatings* **2003**, *47*, 16.

(30) Anastas, P.; Eghbali, N. Green Chemistry: Principles and Practice. *Chem. Soc. Rev.* **2010**, *39*, 301.

(31) Antonietti, M.; Tauer, K. 90 Years of Polymer Latexes and Heterophase Polymerization: More Vital than Ever. *Macromol. Chem. Phys.* **2003**, *204*, 207.

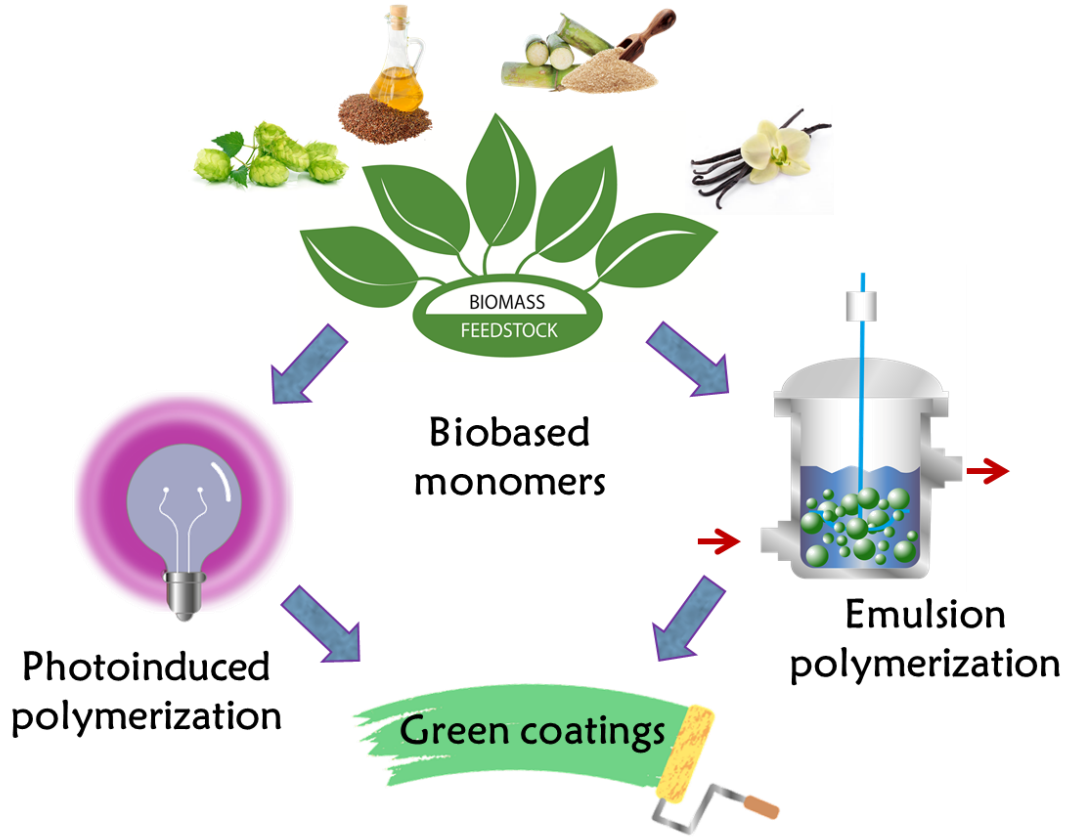

CHAPTER ONE

Literature overview on biobased monomers and their aqueous emulsion and photoinduced polymerizations

Table of contents

Chapter 1: Literature overview on biobased monomers and their aqueous emulsion and photoinduced polymerizations

Parts of this chapter have been published as a tutorial review on the subject “biobased latexes”:

- Molina-Gutiérrez, S.; Ladmiral, V.; Bongiovanni, R.; Caillol, S.; Lacroix-Desmazes, P. Radical Polymerization of Biobased Monomers in Aqueous Dispersed Media. *Green Chem.* **2019**, *21* (1), 36–53. https://doi.org/10.1039/C8GC02277.

1.1 Introduction

Current environmental concerns and more stringent environmental regulations are encouraging the design and synthesis of monomers and polymers from renewable stocks.[1,2] Several goals are pursued: the increase of biogenic carbon in polymeric material, the replacement of toxic and hazardous monomers as well as the production of materials with suitable chemical and mechanical properties which could mimic or even surpass the properties given by their petrochemical counterparts. A wide variety of renewable feedstocks are at disposal (including by-products and natural discards). However, the selection of the strategy and the consequent steps to produce monomers and polymers, should be carefully evaluated. Therefore, green chemistry principles for the synthesis of the monomers should be taken into account.[3] Moreover, in the pursuit for more sustainable materials, green engineering principles should be equally considered;[4] thus, polymerization techniques should not be neglected and processes with environmentally friendly features are to be privileged. In the following chapter, different strategies for biobased monomer production as well as greener polymerization techniques are presented. Additionally, current advances in the synthesis of monomers and polymers from biobased building blocks and their respective polymerization in aqueous dispersed media and photoinduced polymerization are reported.

1.2 Biobased monomers and polymers

The production of chemicals from renewable sources can be achieved by using different types of feedstock. In particular, gases present in the atmosphere or produced from biomass and human activity such as CH_4 and CO_2 have gained interest as C1 renewable feedstocks (Figure 1-1).[5] Methane and carbon dioxide can be processed through catalytic pathways (dry reforming and Fisher Tropsch reaction) to obtain liquid fuels.[6,7] However, atmospheric CO_2 capture costs must be reduced for this to become a viable approach.[8]

On the other hand, biomass feedstock (including vegetable oils and lipids, terpenes, lignin derivatives, carbohydrates and proteins, Figure 1-1) allows the obtention and production of biobased monomers and polymers.[9–11]

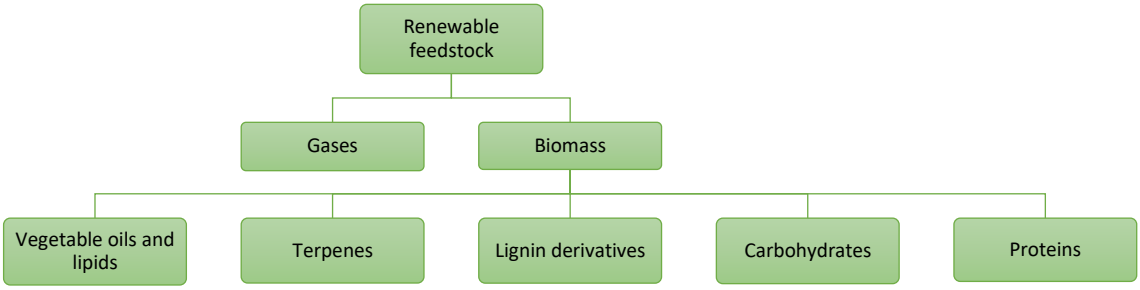

Figure 1-1. Renewable feedstock.

Biobased materials are those composed of, or derived in whole or in part from biological products issued from biomass (including plant, animal, and marine or forestry materials).[12] They are also defined by the American Standard for Testing and Materials (ASTM) as "an organic material in which carbon is derived from a renewable resource *via* biological processes. Bio-based materials include all plant and animal mass derived from CO_2 recently fixed *via* photosynthesis, per definition of a renewable resource".[13]

Biobased polymers are biobased materials that can be classified in two categories:[14]

1. Natural polymers: naturally obtained
    a. Biomass polymers: polymeric materials from biomass, directly used or modified: regenerated cellulose, starch-based materials, chitin, modified starch.
    b. Bioengineered polymers: polymers biosynthesized using microorganisms and plants (e.g. polyhydroxyalkanoates (PHA), bacterial cellulose, polyglutamic acid).
2. Synthetic polymers: synthesized from biomass-originated monomers
    a. New metabolite polymers from bio feedstocks: polylactides, polycarbonates, polyamide.
    b. Conventional petrochemical polymers from bio-derived substances: bio-polyethylene (PE), bio-polypropylene (PP).

Several recent reviews have presented the state-of-the-art in the synthesis and polymerization of biobased monomers.[13,15–18] In the last decades, most of the biobased monomers were copolymerized by step growth polymerization in bulk or solution to yield thermosetting polymers such as phenolic, polyepoxides, polyurethanes and few thermoplastic polymers such as polyesters or polyamides.[13,15,19–22] Indeed, the starting molecules obtained from biomass generally contain various functions (alcohols, phenols, carboxylic acids, amines, among others) allowing direct polycondensation, which combined with a high functionality leads easily to thermosets. In contrast, chain growth polymerization has been much less investigated. This is probably because biomass molecules rarely possess suitable reactive functions for radical polymerization. For example, the double bonds of vegetable oils are reactive by radical polymerization but the reaction is difficult to

control and can lead to thermosets,[17] while biophenols behave as radical inhibitors[23,24]. Therefore, synthesizing radically polymerizable biobased monomers is a real challenge.
From the previously mentioned reasons, the strategy followed was the selection of biobased building blocks suitable to introduce functional groups to execute radical polymerization. Biobased monomers, designed to polymerize in radical polymerization, would be then used to increase the biomass carbon content in polymer formulation.

In the pursuit of sustainable biobased polymers, green chemistry principles are observed. Not only the design of safer monomers and the use of renewable feedstock must be achieved, but less hazardous chemical synthesis involving the use of safer solvents and reactants must also be implemented.[3,25] Therefore, environmentally friendly processes such as polymerization in aqueous dispersed media and photoinduced polymerization were envisaged for the synthesis of biobased polymers.

1.3 Polymerization in aqueous dispersed media

A latex is an emulsion or a sol in which each colloidal particle contains a number of macromolecules.[26] Natural rubber latexes are usually obtained from the trunk of *Hevea brasiliensis* tree. They are composed by a polymer of *cis*-1,4-polyisoprene stabilized by various constituents such as proteins, lipids, phospholipids, fatty acids, amines and some inorganic constituents. Synthetic latexes development and production was boosted during Second World War due to the strategic importance of elastomers and the scarcity of natural rubber during that period.[27] Synthetic rubbers are produced by polymerization in aqueous dispersed media, where the continuous phase is water. The use of water as continuous phase has several advantages: it is an innocuous and non-flammable solvent, the reduction of volatile organic compounds (VOCs), reduction of the medium viscosity and improvement in heat transfer enabling easier reaction temperature control. Aqueous polymerization in dispersed media includes several related processes such as: emulsion polymerization,[28–33] miniemulsion polymerization,[34–37] microemulsion polymerization,[38] dispersion polymerization,[39] and suspension polymerization.[40,41] Emulsion and suspension polymerizations processes are used at an industrial scale. Miniemulsion polymerization offers an alternative for very hydrophobic monomers; however, this technique has several constraints which hinders its use for industrial application.[36,37]

1.3.1 Emulsion polymerization

Emulsion polymerization technique involves the emulsification of a relatively hydrophobic monomer in water by an oil-in-water emulsifier (Figure 1-2). Ionic and non-ionic surfactants are used to stabilize the oil-water interfacial area. The surfactant can be physically adsorbed (conventional surfactant) or chemically incorporated (reactive surfactants)[42,43] onto the particle surface. There are two different types of stabilization mechanisms by surfactants: electrostatic (surfactants with charge, *i.e.* anionic or cationic) or steric (surfactants without charge, *i.e.* non-ionic). Moreover, macromolecular ionic surfactants provide electrosteric stabilization.[28,32,44] The initiation of the reaction is most commonly produced by a water-soluble initiator.[30] The process is divided into three

different intervals. In the first interval, nucleation is produced by either homogeneous or micellar nucleation. Monomer droplets (micron-size), micelles (when surfactant is above its critical micellar concentration or CMC) (nanometer-size) and polymer particles (produced by nucleation) are present in water. Homogeneous nucleation occurs as polymer chains grow in the aqueous phase and become water-insoluble as a critical chain length is reached. The oligo-radical coils up and forms a particle nucleus in the aqueous phase, forming stable primary particles *via* the limited flocculation of unstable particle nuclei and adsorption of surfactant molecules on their particle surfaces.[30,45] This nucleation mechanism is promoted when the monomers have high solubility in water or when the surfactant concentration is under the CMC (no micelles present in the medium). In the micellar nucleation, the hydrophobic oligo-radical enters a micelle (surfactant concentration above the CMC) to form a polymer particle. The monomer diffuses from the monomer droplets (reservoir) to the polymer particles (locus of polymerization). More and more polymer particles are produced, where polymerization takes place, resulting in an increase of the polymerization rate (Figure 1-3, Interval I). Nucleation ceases when the capture of the new growing oligo-radicals (produced in water) by the produced latex particles is favoured compared to homogeneous or micellar nucleation; thus, the number of polymer particles remains steady. The diffusion of monomer from the monomer droplets to the polymer particles occurs producing the swelling of the polymer particles. In Interval II, the concentration of monomer in the swollen polymer particles is constant (Morton equation),[33] the number of particles is constant, resulting in a constant rate of polymerization (except when gel effect operates)[46] (Figure 1-3, Interval II). Finally, in Interval III, the monomer droplets disappear, leading to a decrease of the concentration of monomer in the swollen polymer particles, resulting in the decrease of the rate of polymerization. It is important that the monomer has a slight solubility in water to diffuse from monomer droplets to the swelling particles (Figure 1-3, Interval III). If monomers are not enough water-soluble to diffuse through the water phase, miniemulsion technique is used as an alternative, as polymerization takes place directly in the nanometer-sized monomer droplets.[28,36]

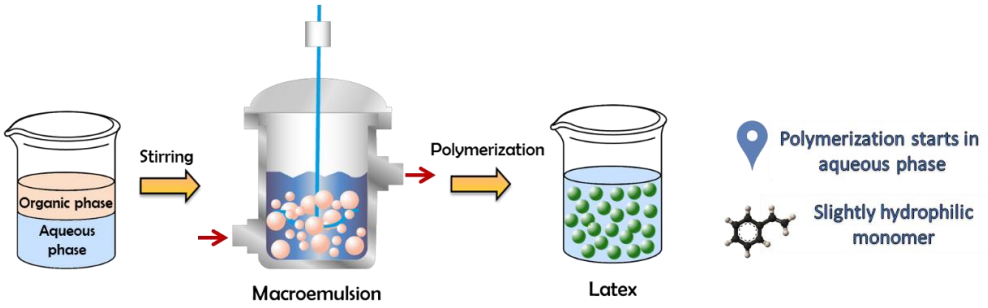

Figure 1-2. Emulsion polymerization process.

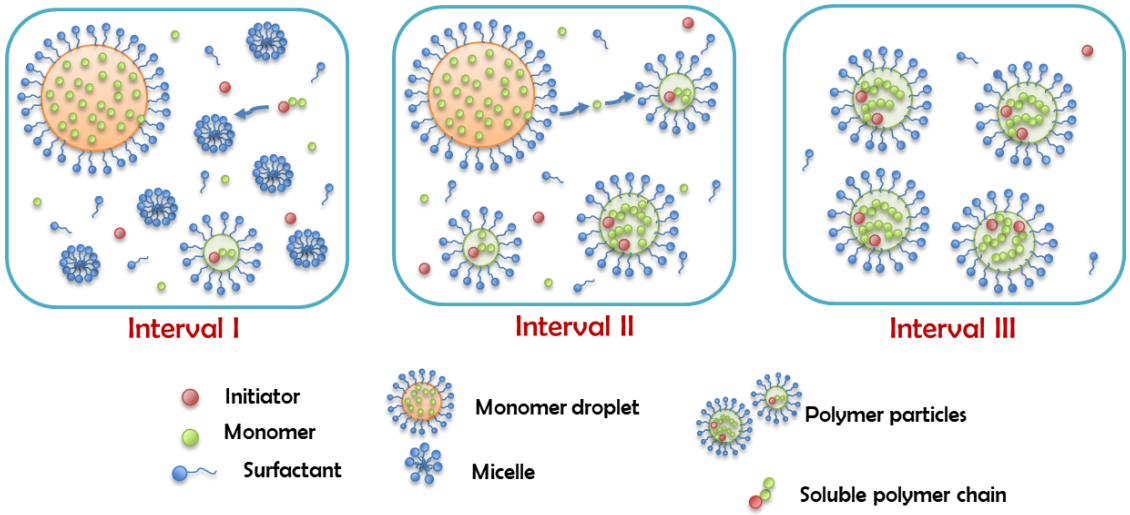

Figure 1-3. Emulsion polymerization interval.

1.3.2 Miniemulsion polymerization

Miniemulsion polymerization process is very similar to the emulsion polymerization process. However, nanometer-sized monomer droplets are produced from a micron-sized pre-emulsion by highly efficient homogenization through rotor-stator systems, sonifiers, high-pressure homogenizers, or emulsification membranes (Figure 1-4). Nanometer-sized droplets ready to be polymerized are formed in the homogenization step procedure (Figure 1-5). To avoid the transfer of monomer from small to big droplets or from droplets to particles (known as Ostwald ripening), a costabilizer is added, which is a very hydrophobic substance such as hexadecane.[36] Droplet nucleation should be fast and homogeneous nucleation minimized. Initiators can be water or oil-soluble. To prevent homogeneous nucleation, water-soluble radicals should be quickly captured by the existing droplets or particles.[47–49] As monomer diffusion through the water phase is not required in this process, it is a suitable process for highly hydrophobic monomers.

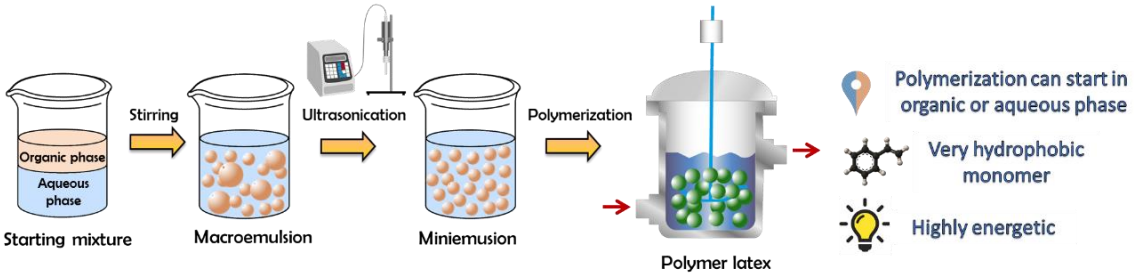

Figure 1-4. Miniemulsion polymerization processes.

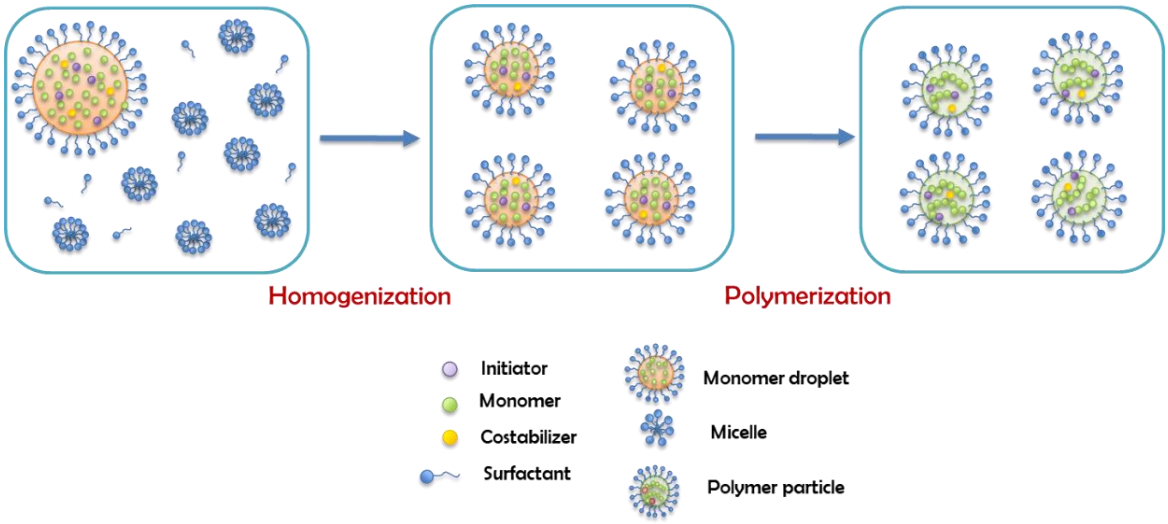

Figure 1-5. Miniemulsion polymerization stages.

Due to the variable solubility of biomass in water, from non-polar oils to polar saccharides, using these molecules as building blocks to produce suitable monomers for radical polymerizations in dispersed media is challenging.

1.3.3 Latexes applications

Synthetic latexes experienced a notable increase in production as a result from the scientific effort during the Second World War to replace natural rubber, which had suffered shortage due to the war activities in Asia. The first produced synthetic latexes were styrene-butadiene copolymers (SBR). In 1945, about 900,000 tons of synthetic rubber were produced.[50] In 2018, the production was estimated to be 15 M tons.[51] Synthetic latexes find application mainly in paper and paperboard industry, paints and coating, adhesives, sealants, and carpet backing.[24] In coatings, synthetic latexes conform the binder, which function is to form a continuous film and hold the different components of the formulation together as well as to adhere to the targeted substrate. Coating formulations may include: pigments, filters, extenders, anti-foaming agents, antimicrobial agents and rheology modifiers.[52] Different types of polymers can be identified in the coatings market such as styrene-acrylic, acrylic and vinyl acetate homo- and copolymers. As coatings for exterior applications, styrene-acrylics are preferred due to their high resistance to hydrolysis, low water absorption, good adhesion and high pigment binding capacity. Pure acrylics are better used for clear-coats, varnishes and high-gloss paints. In the adhesives market, vinyl acetate homo- and copolymers, acrylics and styrene-butadiene copolymers are the most common. Adhesives are classified in: pressure-sensitive adhesives (PSA), laminating adhesives and construction adhesives. Pressure-sensitive adhesive are materials that adhere to surfaces when pressure is applied and can be detached without leaving traces. They are mainly used in self-adhesive labels and tapes. Laminating adhesives bond polymer films to other films (as in packaging applications) or rigid materials in manufacturing processes (as in automotive and furniture industry). Construction adhesives are related to applications such as tile-adhesive and floor covering.[50] Indeed, the

extensive consumption of latexes as coatings and adhesives makes the replacement of the oil-based formulations a priority in the development of a more sustainable industry.

1.3.4 Conclusions

Aqueous emulsion polymerization represents an adequate technique to develop more sustainable products as the continuous phase is water. The reduction of VOCs is essential for environmental protection and safer products. Additionally, the improved heat transfer allows better temperature control in the process, which diminishes the possibility of thermal runaways, resulting in safer processes and working conditions. Certainly, the hydrophobicity character of the monomers defines the kind of emulsion polymerization to be used. Thus, monomers with sufficient solubility in water to diffuse are preferred, as this avoids the need of highly energetic homogenization techniques applied in miniemulsion polymerization. Additionally, the energetic cost of the homogenization in miniemulsion limits its use in some industrial processes. Nevertheless, its development should not be neglected as it can produce complex structure polymeric nanoparticles which could find use in encapsulation or biomedical applications.[53]

1.4 Photoinduced polymerization

Photoinduced polymerization is a chain process initiated by light, in which both the initiating species and the growing chains are radical or ions.[54] Photoinduced polymerization processes are also characterized by spatial and temporal control, which means that they only occur in the irradiated area and they are stop-and-go reactions, *i.e.*, they start and stop simply by switching on and off the light.[55] Therefore, they are key reactions for the emerging additive manufacturing technologies.[56–60] Most monomers do not produce initiating species with sufficiently high yields under light irradiation. Thus, photoinduced polymerization requires a photolabile molecule, called photoinitiator (PI). A photoinitiator generates either radicals or ions under illumination through different reactive pathways, such as a homolytic photoscission, an hydrogen abstraction, an heterolytic cleavage, or a redox reaction.[61] The photoinitiator can form different species that will result in cationic, anionic or radical photoinduced polymerization.

Photoinitiators for radical polymerization are classified as[57]:

- Type I, Norrish Type I (Scheme 1-1): Single molecule that undergoes bond cleavage from an excited triplet state to provide initiation radicals. The majority of these molecules are aryl ketones.

Scheme 1-1. Photoinitiator type I

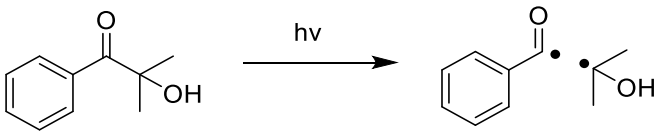

- Type II, Norrish Type II (Scheme 1-2): Two-component systems consisting in a light absorbing molecule (sensitizer) and a co-initiator (synergist). The synergist donates a hydrogen to the sensitizer and this process provides a radical.

Scheme 1-2. Photoinitiator type II

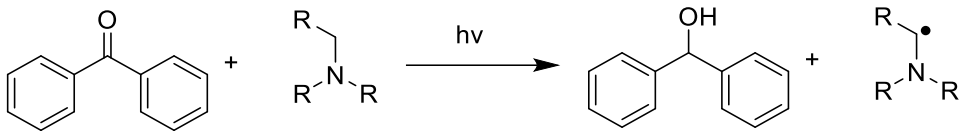

For most applications, conventional radical reactions (proceeding via propagation of macromolecular radicals after initiation triggered by irradiation) are employed, although cationic photoinitiators are also widely used.[62,63]

Cationic photopolymerization involves aryl onium salts such as diaryliodonium,[64] triarylsulfonium,[62] which bear anions of low nucleophilic character that serve as photochemical sources of strong protonic acids (Scheme 1-3and Scheme 1-4).

Scheme 1-3. Cationic photoinitiator

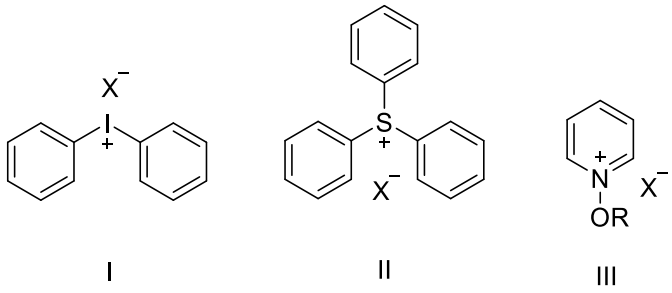

Scheme 1-4. Cationic photoinitiation mechanism

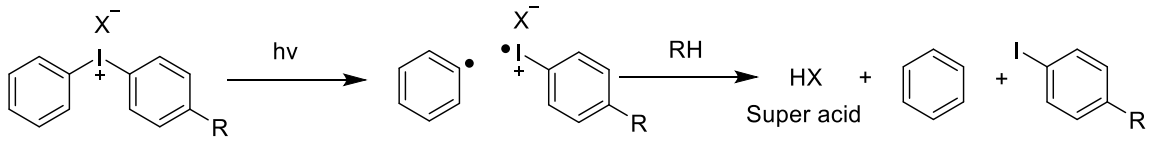

X^- = non-nucleophilic anion

On the other hand, examples of anionic photopolymerization are rare.[65] Additionally, photocross-linking, which is the formation of a covalent linkage between two macromolecules or two different parts of one macromolecule,[66] can be achieved with or without the use of a PI, according to the functional groups present in the monomer and polymer. Thiol-ene chemistry is of particular interest due to its “click” reaction characteristics, as it is highly efficient, has reduced oxygen inhibition, low shrinkage and the possibility to be executed without photoinitiator (Scheme 1-5).[67] Thiol-ene polymerizations are reactions between thiols and ene (vinyl) monomers (Scheme 1-6) that proceed *via* a step-growth radical addition mechanism (Scheme 1-7).[68,69]

Scheme 1-5. Thiol-ene reaction

Scheme 1-6. Typical enes used in Thiol-ene reactions[70]

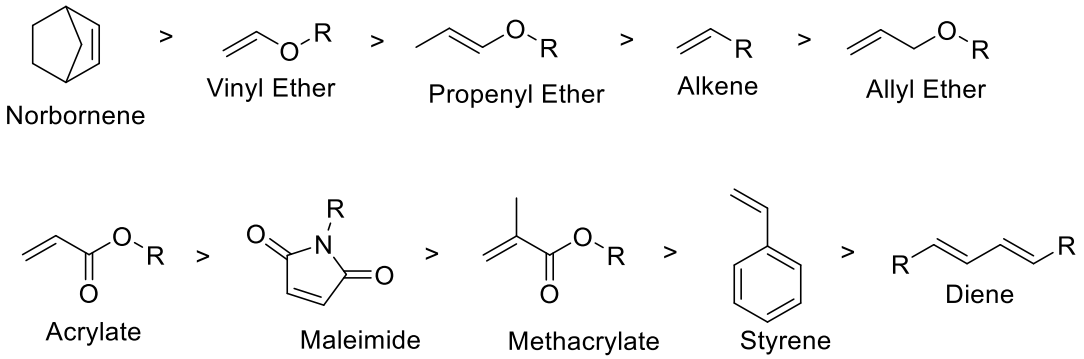

Scheme 1-7. Thiol-ene polymerization

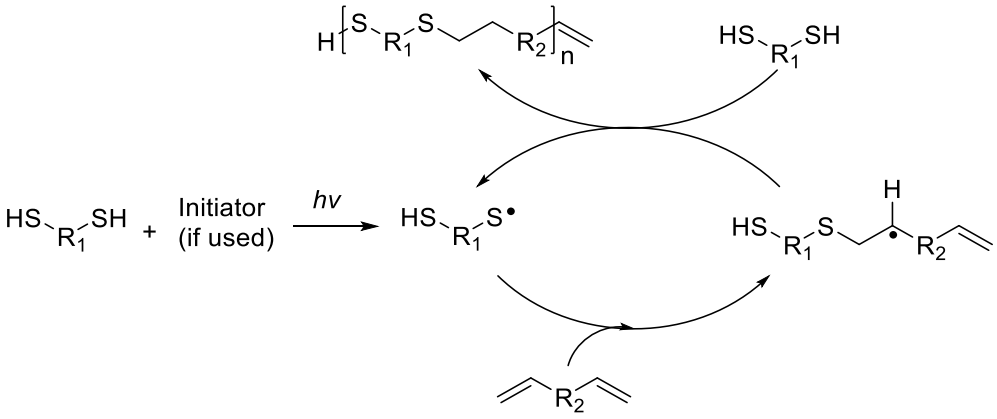

Cationic photopolymerization can also be used for photocross-linking reactions and has several advantages with respect to radical processes such as lack of oxygen inhibition, possibility of solvent-free process, post-polymerization in the dark, low shrinkage and good mechanical properties of UV-cured material and good adhesion to substrates.[71] There are several functional groups that can be cationically photopolymerized such as: vinyl, vinyl ether, oxirane, thiiranes, and oxetanes among others (Scheme 1-8).

Scheme 1-8. Cationically polymerizable monomers[71]

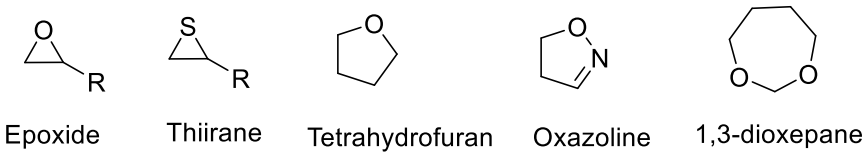

Photoinduced polymerization allows for fast processes (complete conversion within minutes) and low energy consumption (room temperature reactions). Coatings and adhesives formulations can be directly cured onto temperature sensitive substrates for used in the biomedical field.[69,72] Reactions can be solvent-free with the reduction or elimination of VOCs.[73] Additionally, it has found wide application in industrial processes. It is an established technique in the fields of coating, printing inks, adhesives and wood finishing.[74] Products from photopolymerization are present in everyday life, such as contact lenses,[75] filling for dental cavities,[76] and credit cards.[77] Recently, photopolymerization in additive manufacturing (3D printing) has gained interest due to its applications is rapid prototyping, tooling, dentistry, microfluidics, biomedical devices, tissue engineering, drug delivery, etc.[57,60,78]

The use of biobased molecules in photopolymerization is a necessary step in the quest for more sustainable materials. Some natural molecules can undergo autoxidation, isomerization, dimerization and cyclization reactions in presence of light.[79] However, most biobased building blocks require the introduction of suitable functional groups to undergo photoinduced polymerization processes either radical or ionic, such as (meth)acrylates, vinyl ethers, epoxy groups, and thiols (to be used in thiol-ene chemistry). Sugars derivatives (from galactose, glucose,[80] sucrose,[81] itaconic acid and succinic acid,[82] furanic compounds[83–85]), terpenes,[86,87] lignin derivatives (as eugenol),[88–93] vegetable oils[94–96] and lipids (cardanol)[97–99] have been modified and successfully used in radical or ionic photoinduced polymerization.

1.4.1 Oxygen inhibition in photoinduced polymerization

The majority of commercial photocurable formulations consists in (meth)acrylates. However, as these monomers undergo radical polymerization, they are vulnerable to inhibition by molecular oxygen, resulting in incomplete or failed curing and tacky surfaces. The oxygen inhibition can be produced through different mechanisms as presented in Figure 1-6. The excited state of the photoinitiator, $[PI]^T$, can be quenched by oxygen (Figure 1-6, a). Additionally, when a radical is formed it can react with oxygen to form peroxyl radicals (scavenging reaction, Figure 1-6, b). Oxygen has been reported to react very rapidly with carbon-centred radicals (k_{ox}>5×10^8 L mol^{-1}s^{-1}) forming peroxyl radicals.[100] Peroxyl radicals do not readily react with alkenic double bonds or acrylate monomer, limiting the propagation rate. On the other hand, they are prone to terminate through radical-radical recombination producing di-alkyl peroxides (Figure 1-6, d), or by hydrogen abstraction producing hydroperoxides (Figure 1-6, e). Then, peroxides and hydroperoxides can decompose under irradiation to produce initiating species (Figure 1-6, f). Other initiation mechanisms can be the formation of radicals by the hydrogen donor molecules and reducing agents (Figure 1-6, c and g respectively).

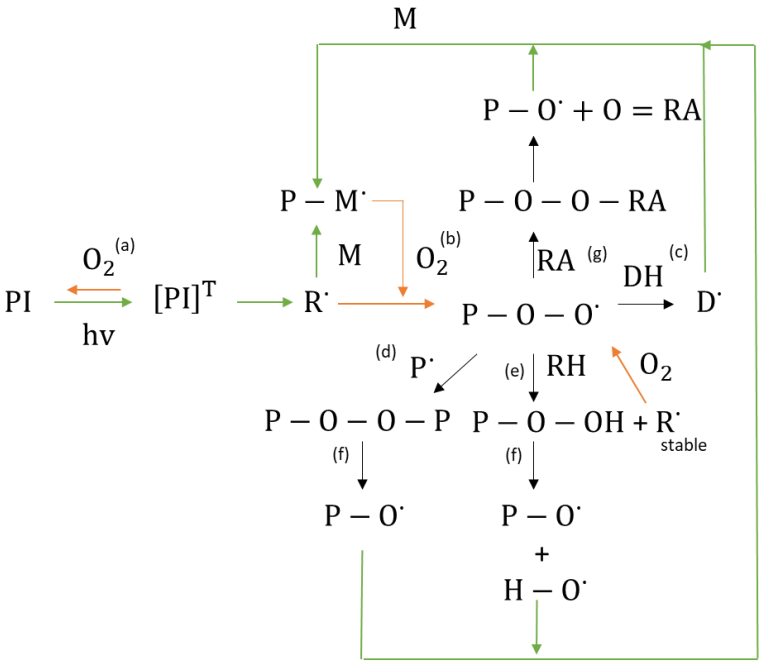

Figure 1-6. Mechanistic pathways of oxygen inhibition (initiation steps in green, oxygen in red).[100]

Several physical and chemical strategies have been developed to avoid oxygen inhibition. Among the physical strategies, the most widespread is nitrogen inerting, where oxygen is removed from the monomer and the curing surface is blanketed to avoid oxygen diffusion. This option is suitable for laboratory scale but becomes expensive at industrial scale. An alternative is to cover the resin with a solid or liquid barrier. Wax[101] or a UV-transparent film (lamination)[102] can be used to prevent oxygen ingression, although they should be removed at the end of the curing and the permeability of the material to molecular oxygen should also be considered. Increase of light intensity is another option to mitigate oxygen inhibition as it increases the availability of radicals formed by the photoinitiator.[103] The radicals will react with oxygen limiting its concentration, thus allowing the propagation reaction to compete with oxygen inhibition. Light intensity (in watts per square meter) has been found more effective in reducing oxygen inhibition than radiation dose (in joules per square meter). Nevertheless, an excessively high light intensity might cause the fast depletion of initiating species prior to chain elongation.[104]

The correct selection of type and quantity of initiator are among the chemical strategies to reduce oxygen inhibition.[105] Higher concentration of photoinitiator can reduce the oxygen inhibition (similar to increasing light intensity). Indeed, a photoinitiator should be selected to absorb in the used irradiation wavelength and have high efficiency to decompose and produce radicals. On the other hand, limitation of solubility[106] can restrain the use of high amounts of photoinitiators. Moreover, residual fragments of photoinitiators can be undesirable in certain applications such as biomedicine or food packaging.[100]

Other chemical strategies to avoid oxygen inhibition are the use of hydrogen donors (DH) and reducing agents (RA) (Figure 1-6, c and g respectively). The formed radical D· can reinitiate

polymerization, as well as the radicals produced by hydroperoxides decomposition. Other reducing agents such as organic molecules containing boron or phosphorous as well as metal-based additives[100,107] are used for the reduction of peroxyl radicals P-O-O•, leading to P-O• alkoxy radicals (Figure 1-6g).

Indeed, the combination of polymerizable biobased monomers through environmentally friendly processes, such as aqueous emulsion polymerization and photoinduced polymerization and photocross-linking, opens the possibility to further tune the thermal and the mechanical properties of the polymers and provide industry and consumers with more sustainable processes and products.

1.5 Biobased Latexes

Biobased monomers derived from the modification of natural occurring building blocks have been used in radical polymerization in aqueous dispersed media to produce partially biobased latexes aiming for different applications such as coatings and adhesives. The different types of biomass building blocks sources could be divided in: vegetable oils and lipids, terpenes, lignin derivatives, carbohydrates and proteins.[9] In the next sections, the state-of-the-art in the use of biobased monomers in aqueous emulsion polymerization is presented, ordered according to the biomass origin of the biobased molecules.

1.5.1 Vegetable oil- and lipid-based polymers

Vegetable oils and lipids are an abundant, biodegradable and low toxic renewable feedstock for polymeric materials.[108–111] The annual production of major vegetable oils was reported to be 177 million metric tons for 2015-2016 and increased to 189 million metric tons in 2016-2017.[112] The most common vegetable oils are olive oil, soybean oil, linseed oil and sunflower oil (Table 1-1).[113]

Table 1-1. Vegetable oil composition[113]

Oil type	Fatty acids				
	Saturated (wt%)		Unsaturated (wt%)		
	Stearic $C_{18}H_{36}O_2$	Palmitic $C_{16}H_{32}O_2$	Oleic $C_{18}H_{34}O_2$	Linoleic $C_{18}H_{32}O_2$	Linolenic $C_{18}H_{30}O_2$
Olive	7.5-20	0.5-5	65-85	3.5-20	0-1.5
Sunflower	3-6	1-3	14-35	44-75	1-2
Soybean	7-11	2-6	22-34	43-56	7-10
Linseed	4-7	2.5	12-34	17-24	35-60

Vegetable oils are composed of triglycerides (esters of glycerol and fatty acids). Fatty acids are carboxylic acids with long aliphatic chains which may be saturated, monounsaturated or polyunsaturated. To increase their reactivity towards radical polymerization processes, these molecules can be modified through their carboxylic acid function, alkene groups or allylic protons.[114] However, most of the chemical modifications are performed on the carboxylic group.[115] Fatty acids

are indeed one of the main components of alkyd resins as binders.[111] By virtue of their aliphatic chain, fatty acid monomers can be excellent plasticizers and facilitate coalescence during film formation. They are thus key biomass feedstocks to generate monomers for coatings and adhesives applications.[116] Polymerization has been achieved *via* different functionalization reactions as exemplified in several reviews.[13,17,115,117,118] Initially, they were incorporated to emulsion polymerization processes to produce alkyd-acrylic hybrids systems where the faster physical drying of acrylics could be combined with the oxidative curing of the alkyd leading to better chemical and water resistance properties.[119–121] Decrease in the polymerization rate was observed, although minimum film forming temperature (MFFT) improved in comparison with cosolvent-free acrylic formulations. Long aliphatic chains from fatty acids are likely to have difficulties to diffuse through the aqueous continuous phase, from the monomer droplets to the nucleated polymer particles. Fatty acids low water solubility can lead to long induction periods in emulsion polymerization,[122] although surfactants may play an important role to solve this issue.[123] Indeed, miniemulsion polymerization may be a more suitable option for the polymerization in dispersed aqueous media of such highly hydrophobic monomers.[124,125] Similar studies done in miniemulsion polymerization, showed that 20-30% of the double bonds in the aliphatic chain reacted.[126,127] In addition, vegetable oils could be also used as co-stabilizers in miniemulsion polymerization for nanocapsules production for medical applications.[128] Several examples of biobased latexes synthesized at solids content typically ranging from 20 to 40% are presented in the next section.

1.5.1.1 Fatty acid emulsion polymerization

The unsaturation on fatty acids has traditionally been used for oxidative coupling reactions in alkyd resins for paint and varnish binders. However, Bunker and Wool[129–131] functionalized methyl oleate through its chain double bonds by means of an epoxidation to obtain acrylated methyl oleate (AMO) (Scheme 1-9); and performed emulsion homopolymerization to prepare biobased pressure-sensitive adhesives (PSA). Very low conversion and low molar mass polymers were obtained due to the low AMO solubility in water (estimated to be 10^{-7} M). Therefore, AMO was copolymerized with hydrophilic acrylic acid to enhance nucleation. Likewise, Jensen *et al.*[132] reported the emulsion copolymerization of AMO and styrene. They showed that the conversion and the average molar mass decreased as the concentration of AMO increased. Polymerizations conducted with more than 15 wt% of AMO resulted in an increase in the induction time and in the decrease of particle nucleation and conversion. At 30 wt% of AMO, very low polymer concentrations were obtained, and large quantities of initiator were necessary to increase the monomer conversion. Similar results were obtained by the same group in the emulsion copolymerization of acrylated soybean oil and methyl methacrylate (MMA).[133] These results illustrate the difficulties encountered in the nucleation phase of emulsion polymerization of such hydrophobic monomers.

Scheme 1-9. Synthesis of acrylated fatty acid methyl ester (AFAME) and acrylated methyl oleate (AMO)

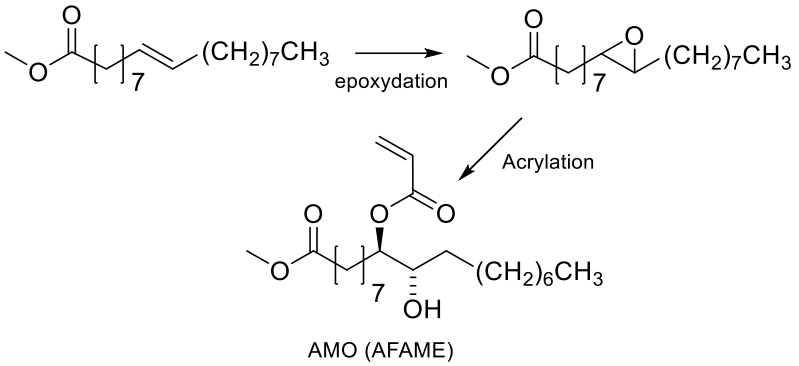

Vegetable oil derivatives with pendant acrylate functions easily undergo degradative chain transfer with the remaining allylic double bonds of the fatty acid, resulting in low conversion, high gel contents and branching.[134] Indeed, Thames *et al.*[135], reported the emulsion copolymerization of functionalized vegetable oil macromonomers (VOMM's) featuring at least one cross-linkable double bond in the aliphatic chain. The seeded emulsion copolymerization of MMA with soyamide monomers acrylated at their chain-end (after amidation of soybean oil with N-methyl ethanolamine)[136,137] was also reported (Scheme 1-10). In this case, the allylic functionalities were preserved to further undergo auto-oxidation during the drying of the latex for ambient self-crosslinking. Emulsion copolymerizations of acrylamides (Scheme 1-10)[138,139] derived from olive, soybean, sunflower and linseed oil with styrene[140] and vinyl acetate[113] were also studied. The copolymerization with styrene (up to 20 wt% of oil-based monomer) followed the Smith-Ewart theory, predicting the formation of latex particles *via* micellar nucleation and proportionally to the surfactant and initiator concentrations. Moreover, the reaction order of these copolymerizations was not affected by the degree of unsaturation of the monomers. However, an increase in the degree of unsaturation and in the proportion of biobased monomers in the reaction mixture led to copolymers of lower molar masses due to degradative chain transfer and allylic termination.

Scheme 1-10. Synthesis of soyamide monomers and vegetable oils acrylamide monomers

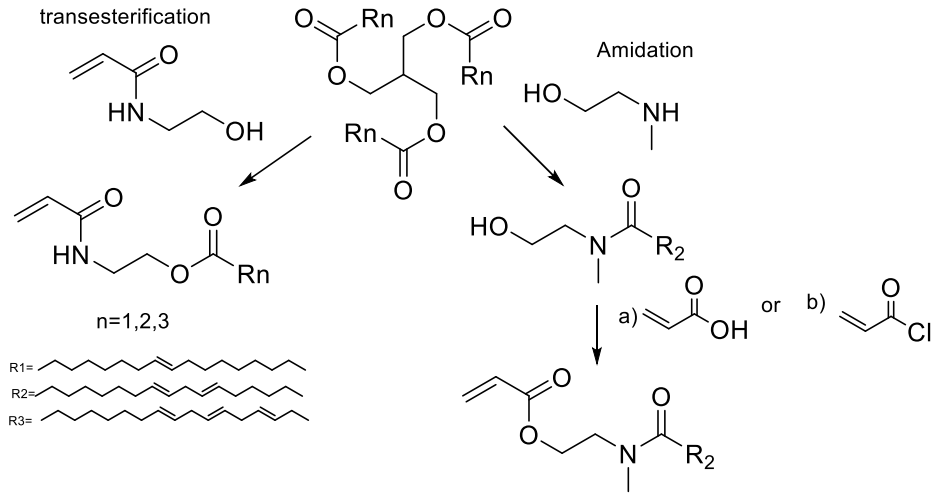

Roberge and Dubé,[141] used cost-effective conjugated linoleic acid (CLA) with impurities (74 wt% CLA, 13 wt% oleic acid and 13 wt% saturated fatty acid) to partially replace butyl acrylate (BA) in PSA formulations with styrene and BA, acrylic acid, *n*-dodecyl mercaptan as chain transfer agent (CTA), and divinyl benzene as cross-linker. CLA was integrated in the polymer formulation at 16, 23 and 30 wt% of the total monomer. Two different factorial designs were conducted to study the performance of the obtained PSA. This work revealed that oleic acid, present as an impurity, helped the introduction of CLA into the terpolymer. Moreover, as mentioned before, the increase in CLA (possessing allylic double bonds) reduced the polymerization rate and decreased the polymer molar mass.

Recently, in an attempt to synthesize a PSA with a higher biobased content, Badía *et al.*,[142] prepared waterborne pressure adhesives with biobased contents up to 72% using partially commercial 2-octyl acrylate (OA, bio-content of 73%, T_g of - 44°C, derived from castor oil) and isobornyl methacrylate (IBOMA, bio-content of 71%, T_g of 150°C, derived from pine resin) (Scheme 1-11). PSA formulations are composed mainly of a low T_g monomer, which provides tackiness, and a small quantity of hard monomer, which provides cohesion to the system, combined with an unsaturated carboxylic acid for wettability and good peel and shear strength properties. The copolymerization (IBOMA, OA and MAA) was done through a seeded process under starved monomer feed. The seed was composed of isobornyl acrylate (IBOA), 2-octyl acrylate and AA. The peel, loop tack, work of adhesion, gel content, molar mass, shear and shear adhesion failure temperature, storage modulus and tan delta were assessed. The formulation of the PSA had to be adjusted and a chain transfer agent had to be added to achieve a microstructure that yielded adhesive performance as good as the oil-based formulation. Later, piperonyl methacrylate (PIPEMA, coming from black pepper, Scheme 1-11) was also included in a formulation with 2-octyl acrylate and MMA to produce latexes for PSA applications.[143] The performance of the polymers containing PIPEMA was compared to polymers containing IBOMA at the same % wbm. Higher tack and peel values were obtained in the formulation with 15% wbm of PIPEMA than with 15% wbm of IBOMA. Moreover, PIPEMA was then used to execute photocross-linking as benzodioxole derivatives undergo hydrogen donation, producing radicals that rearrange by β-scission and then terminate (Scheme 1-12). The polymers were irradiated at 254 nm for up to 2 hours. Cross-linking increased with irradiation time, while peel and tack decreased.

Scheme 1-11. Biobased monomer OA, IBOA, IBOMA and PIPEMA

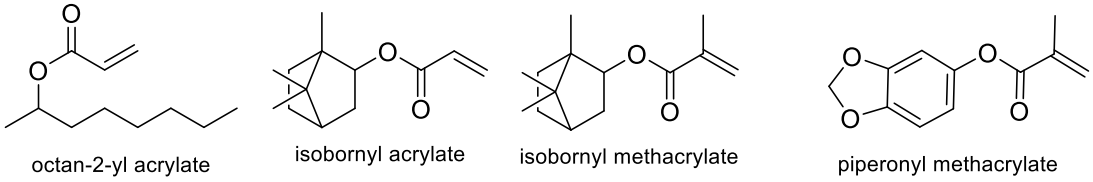

Scheme 1-12. Photo-crosslinking of pyperonyl units

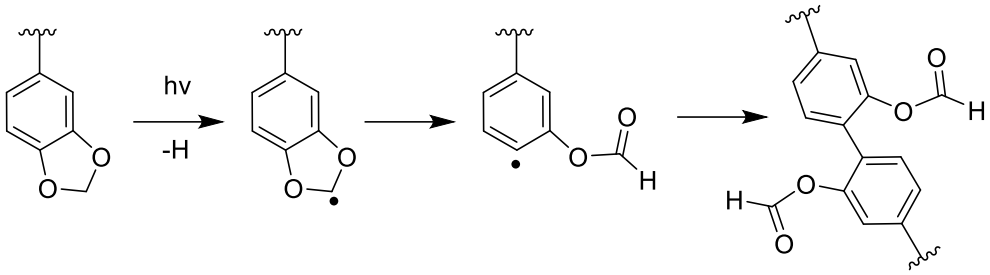

1.5.1.2 Fatty acid miniemulsion polymerization

To improve the results obtained by emulsion polymerization of AMO, Bunker *et al.*[144] conducted a comparative study of the copolymerization of AMO (Scheme 1-9) with MMA, 1,4-butanediol diacrylate (BDDA) and 2-ethylhexyl acrylate (2-EHA) under emulsion and miniemulsion polymerization conditions. It was observed that the reaction time decreased from 18 h to 1 h and that the surfactant concentration could be reduced from 15 wt% to 2 wt% when using miniemulsion polymerization. Furthermore, copolymers with suitable properties for application as pressure sensitive adhesives (PSA) were obtained.

Similarly, Quintero *et al.*[125] used soybean acrylate macromonomer (SAM) [145] (Scheme 1-13) as a copolymerizable hydrophobe in miniemulsion polymerization The stability of the miniemulsion droplets was confirmed with dynamic light scattering measurements. SAM was copolymerized with MMA and BA. Gel content measurements showed that the unsaturation was preserved and could undergo oxidative curing during the drying process.

Scheme 1-13. Soybean acrylated macromonomer (SAM) structure

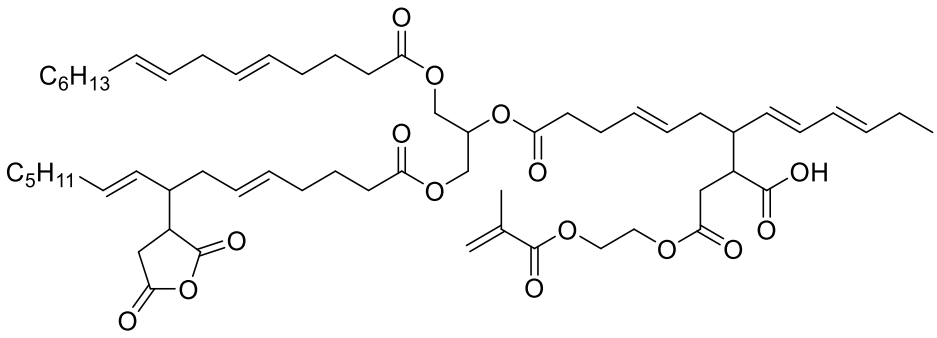

Guo and Schork[124] studied the miniemulsion copolymerization of MMA and BA with sunflower seed oil and linoleic acid (66% and 97%) (Table 1-1) without any further functionalization. As the content of linoleic acid (two unsaturations in the aliphatic chain) increased, the polymerization rate and the monomer conversion decreased. Moreover, molar mass distributions were broad due to chain transfer reactions leading to radical species with different reactivities in propagation and termination.

Copolymerization of styrene with transesterified soybean oil, acrylated through the double bond of the aliphatic chains, was also performed *via* miniemulsion polymerization.[146] In this system, increasing the concentration of acrylated fatty acid methyl ester (AFAME) from soybean oil (Scheme 1-9), resulted in an increase of the latex particle size and a decrease of the total monomer

conversion. This was explained by an increase of viscosity at an AFAME/styrene molar ratio higher than 5/95. Moreover, both the glass transition temperature and the thermal stability decreased, whereas the gel fraction increased when the proportion of AFAME increased. Likewise, ricinoleic acid (castor oil) was also acrylated through the internal double bonds (Scheme 1-14), then copolymerized with MMA *via* miniemulsion to prepare a variety of polymers with T_g ranging from 50°C to 124°C.[147] Similar drawbacks (bigger particle size, lower polymerization rates and lower molar masses) were encountered as the acrylated ricinoleic acid concentration increased.

Scheme 1-14. Synthesis of acrylated ricinoleic acid

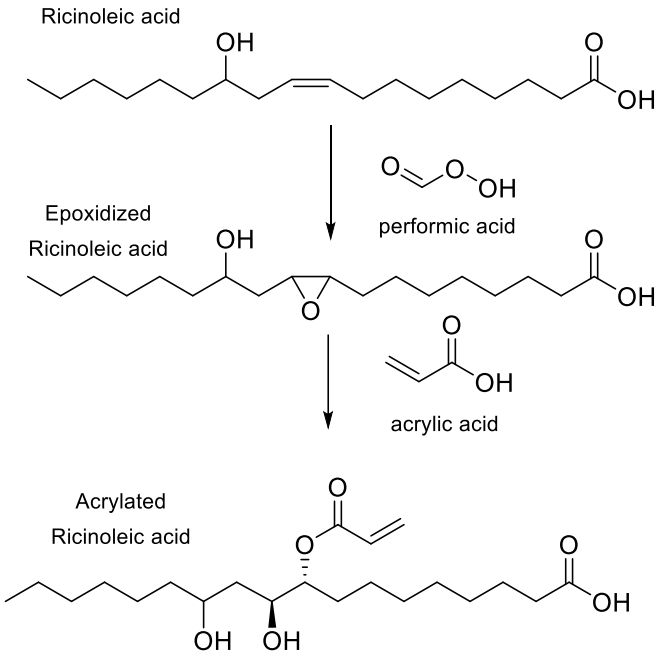

To avoid the use of chromium catalyst to synthesize acrylate derivatives from epoxidized vegetable oils,[129] Maassen *et al.*[148,149] described different synthesis pathways to suitable monomers for pressure-sensitive adhesives based on acrylated methyl oleate (AMO) and acrylated methyl erucate (Scheme 1-15). These monomers were copolymerized using solution and miniemulsion polymerizations. Shorter reactions times were possible using miniemulsion polymerization whereas the resulting modulus, tack, and peel values were better for the solution polymerization materials. The authors proposed that appropriate comonomers should be included to produce shorter segments between entanglements and thus improve cohesive properties at high temperatures.

Scheme 1-15. Synthesis of oleate and erucate derivatives

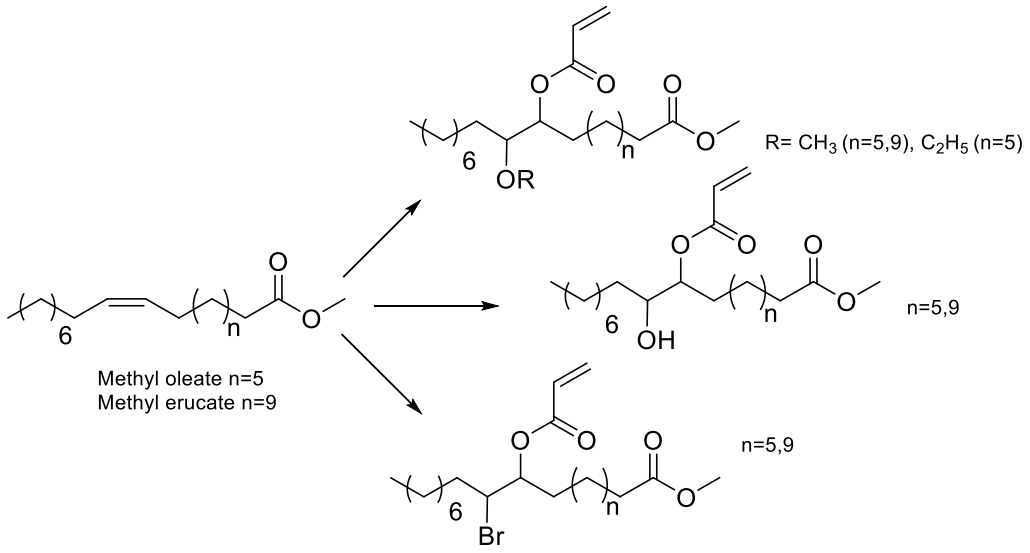

Biobased acrylamido monomers, obtained by condensation of N-(hydroxylethyl)acrylamide (Scheme 1-10) with fatty acids (soybean, sunflower, linseed and olive oils), were copolymerized with styrene in solution.[113] The Q-e parameters of the biobased monomers were determined by using the Alfrey-Price equations. These Q-e values were then applied to determine the reactivity ratios with MMA and vinyl acetate. Subsequently, copolymers of olive, soybean and linseed oils with MMA and vinyl acetate were obtained by miniemulsion polymerization.[113] The molar mass decreased with the increasing degree of unsaturation of the vegetable oil monomers due to degradative chain transfer. A type of seeded miniemulsion polymerization (a miniemulsion of biobased monomer fed into another miniemulsion of MMA containing the initiator) was used to limit the extent of degradative chain transfer. In addition, copolymers of olive, soybean, linseed and hydrogenated soybean oil and styrene were prepared by miniemulsion polymerization.[150] The cross-linking density increased proportionally with the unsaturation amount of the monomer feed and the latex properties could be adjusted by combining different oil-based monomers in the formulation. Furthermore, the plasticization effect of soybean oil and olive oil was studied through miniemulsion copolymerization with styrene and MMA.[151] It was demonstrated that the increase of OVM or SBM biobased monomer in formulations led to lower T_g and that the increase in unsaturations led to an increase in cross-link density. The unsaturation amount was used as a parameter to compare the physico-chemical and thermo-mechanical properties of the latexes. The highest values for the cross-hatch adhesion and König pendulum hardness tests were obtained when formulations had 60% wt of OVM or SBM, containing the highest unsaturation amount.

Moreno *et al.*[152,153] synthesized methacrylate monomers from oleic and linoleic acid by methacrylation of the carboxylic acid with glycidyl methacrylate thus preserving the double bonds on the long alkyl chain for further curing (Scheme 1-16).[154] After methacrylation of the fatty acids, approximately 12-14 wt% of oleic acid and 13 wt% of linoleic acid remained unreacted. This unreacted carboxylic acid functional group was later reacted with potassium hydroxide solution to produce surfactants *in situ,* able to form stable miniemulsions.[155] Miniemulsion polymerizations were performed using thermal (potassium persulfate, KPS) and redox initiators (*tert*-butyl

hydroperoxide and ascorbic acid, TBHP/AsA). The polymerization kinetics were slower for KPS as termination in the aqueous phase was overtaking propagation. Moreover, it was found that 30% of the double bonds on the aliphatic chain of the methacrylated oleic acid reacted during the miniemulsion polymerization.[152]

Scheme 1-16. Synthesis of oleic and linoleic methacrylates

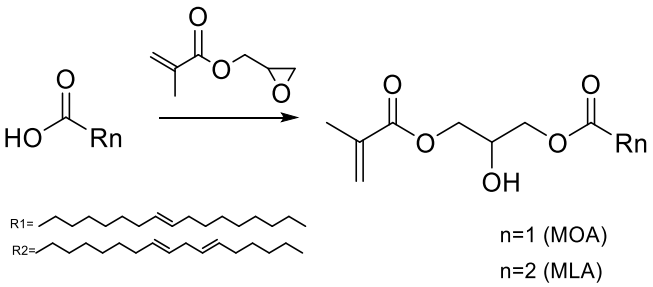

Furthermore, in the case of MLA only the TBHP/AsA initiation system promoted gel formation.[153] This was ascribed to the lability of the two hydrogen atoms of the methylene group next to the double bonds (allylic protons). Indeed, the radical thus generated is stabilized by conjugation, less prone to propagation but still able to undergo termination. This effect was enhanced because under redox initiation, hydrophobic *tert*-butoxy radicals can improve droplet nucleation compared to the water soluble $SO_4^{-\bullet}$ radicals produced by KPS, leading to an increase of the radical availability, increasing both droplet nucleation and rate of polymerization.[156]

To develop polymers for coating applications, Moreno *et al.*[157] synthesized latexes by miniemulsion polymerization from methacrylated oleic acid and α-methylene-γ-butyrolactone (Tulipalin-A). The homopolymer of α-methylene-γ-butyrolactone, a cyclic analogue to methyl methacrylate, has a T_g of 195°C.[158,159] Several concentrations of α-methylene-γ-butyrolactone (MBL) were copolymerized with methacrylated oleic acid (MOA) *via* miniemulsion copolymerization. MBL reacted slower than the methacrylated oleic acid leading to lower yields as its concentration in the feed increased. Moreover, higher gel contents were obtained as the amount of MOA increased due to the free reactive double bonds of this monomer. Finally, copolymers of MOA, methacrylated linoleic acid (MLA), MBL and MMA were reported and used in paint formulations.[160] Properties such as hardness, gloss, rheological behaviour and open time were measured and compared with commercial samples.

Machado *et al.*[161] reported the thiol-ene miniemulsion polymerization of dianhydro-D-glucityl diundec-10-enoate (DGU), synthesized from 10-undecenoic acid (derived from castor oil) and isosorbide, with 1,4-butanedithiol to produce a polymer with encapsulation properties for potential use in uterine and colon cancer treatments (Scheme 1-17). Different conditions were tested by varying reaction time, temperature, emulsifier and amount of initiator. Miniemulsion polymerization resulted in higher molar masses than bulk polymerization, due to radical compartmentalization where bimolecular termination was reduced (*i.e.* radicals remained active for a longer time). High viscosity at low reaction temperatures (60°C, *i.e.* at lower temperature than the melting temperature of the polymer, which is about 68°C) produced low molar masses due to restricted molecular mobility. A reaction temperature of 80°C provided the highest molar masses. Finally, organo-soluble

azobisisobutyronitrile (AIBN) was preferred as initiator over water-soluble KPS which may favour thiyl-thiyl termination in the water phase before thiyl radicals could enter the monomer droplets.

Scheme 1-17. Synthesis of Poly(Dianhydro-D-glucityl diundec-10-enoate-*co*-Butanedithiol)

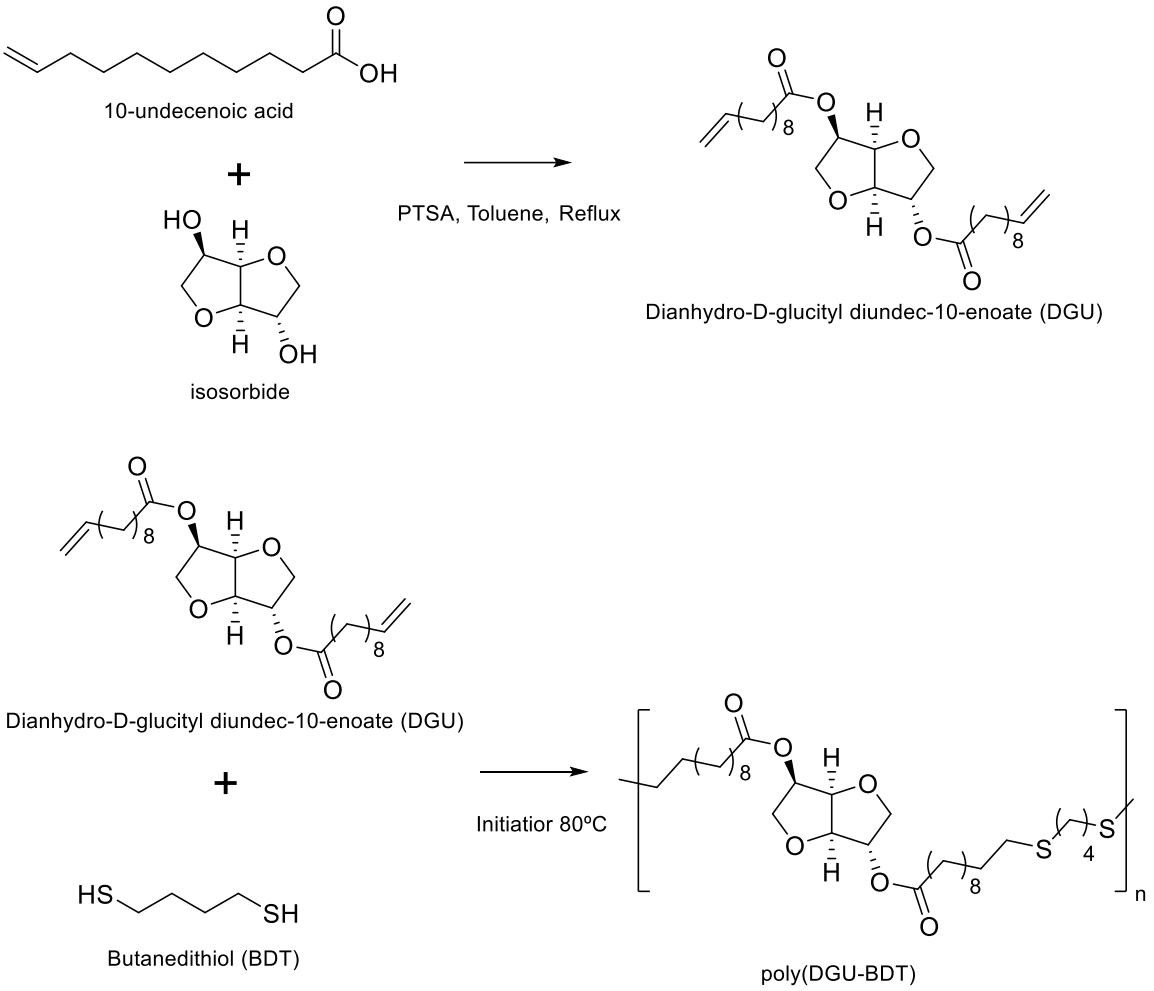

Likewise, 10-undecanoic acid was reacted with 1,3 propanediol to prepare a difunctionalized monomer which was later reacted with dithiol, mercaptoethyl ether (MEE) or 1,4-butanedithiol (BDT), *via* a thiol-ene miniemulsion polymerization (Scheme 1-18).[162] Increasing the quantity of initiator led to an increase of the molar mass due to the step-growth nature of the system. Lower molar masses were obtained when 2-mercaptoethyl was used. This could be due to the fact that MEE is more hydrophilic which induced a stoichiometric misbalance at the polymerization locus. Cytotoxic studies were also performed as the target applications for these polymers were temporary implants, tissue engineering or drug delivery systems.

Scheme 1-18. Thiol-ene miniemulsion polymerization from 10-undecanoic acid derivatives and dithiols

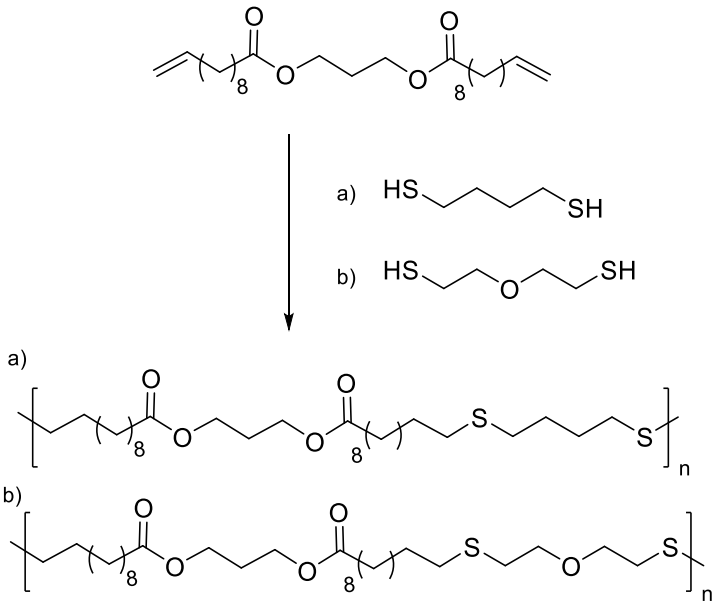

Similarly, Oliveira *et al.*,[163] executed the enzymatic esterification of 10-undecenoic acid (derived from castor oil) and 2-hydroxyethyl methacrylate to obtain 2-(10-undecenoyloxyethyl methacrylate (MHU)(Scheme 1-19). This monomer possessed an allylic and a methacrylate group. Then, it was polymerized by miniemulsion thiol-ene polymerization with 1,4-butanedithiol for 4 hours at 80°C using different types and amounts of surfactants (SDS and Lutensol AT50). Higher stability was produced by SDS (electrostatic stabilization) at 9 µmol cm^{-3} while Lutensol AT50 had to be used at a concentration of 13.5 µmol cm^{-3} to produce colloidal stability by steric hindrance. No need of costabilizer was found as the miniemulsions were stable due to the hydrophobicity of MHU. Molecular weights for stoichiometric thiol-ene molar ratios were similar both in bulk and miniemulsion polymerization. If the ratio MHU/1,4-BDT increased the importance of free radial mechanism increased, making the compartmentalization effect more pronounced, yielding higher molecular weights in miniemulsion than in bulk.

Scheme 1-19. Thiol-ene miniemulsion polymerization from MHU and 1,4-butanedithiol

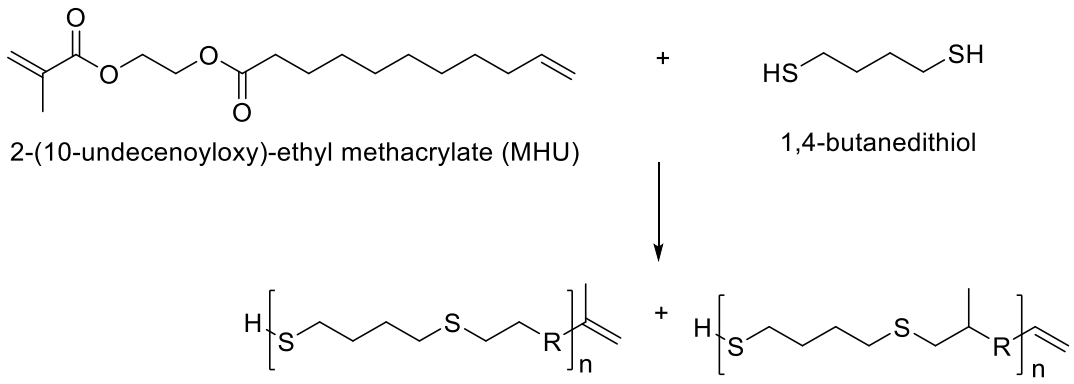

Recently, nitroxide-mediated copolymerization in miniemulsion of a mixture of methacrylic esters

with an average of 13 units (C13MA, obtained from plant oils) and IBOMA was executed.[164] Molecular weight dispersities between 1.62 and 1.73 were obtained, with conversions above 83% and the total solids content was 24%. Glass transition temperatures could be tuned between -52°C and 123°C.

As mentioned before, due to their long aliphatic chain, vegetables oils do not diffuse easily through the aqueous phase. Indeed, only monomers possessing water solubility greater than 10^{-7} wt% are capable of diffusing through the aqueous phase on a reasonable timescale.[145] Thus, for vegetable oil derivatives, miniemulsion polymerization is preferred to emulsion polymerization. However, miniemulsion is not currently well suited to industrial processes, hence the use of vegetable oils in polymerization in large scale remains a challenge. Moreover, double bonds within the aliphatic chains easily undergo degradative chain transfer due to the easy abstraction of allylic hydrogen atoms.[165] These allylic transfer reactions are detrimental to the polymerization, and lead to low monomer conversion and high gel content. Efforts have been made to understand these reactions and develop kinetic models for the preservation and exploitation of allylic double bonds.[166–168] The modification of biobased precursors to introduce functional groups suitable for free radical polymerization is often conducted using harmful chemicals and producing a considerable amount of waste (reducing the atom economy of the process). It is important to mention, that although a percentage of vegetable oils is dedicated to industrial applications instead of food supply, preference should be given to non-edible vegetable oils for the production of biobased materials.[169,170] In addition, chemical and mechanical properties of the vegetable oil based monomers often do not match the performance of their oil-based counterparts. As a consequence, the use of monomer mixtures (oil-based and biobased monomers) is still necessary nowadays in new formulations to meet the requirements of commercial products.

1.5.1.3 Lipid emulsion polymerization

Recently, Ladmiral *et al.*[171] reported for the first time the synthesis of a biobased latex from a cardanol derivative. Cardanol is a naturally occurring phenol extracted from Cashew Nut Shell Liquid (CNSL),[20] which can be regarded as a valuable renewable material for the substitution of aromatic monomers such as styrene. Cardanol methacrylate (Scheme 1-20) was copolymerized with MMA by emulsion copolymerization and the resulting latex was cast into films which were photocross-linked *via* thiol-ene chemistry. Gel formation during the copolymerizations of cardanol methacrylate and MMA was ascribed to hydrogen abstraction of the isopropyl alcohol proton group in the monomer or polymer (transfer reaction) by the highly electrophilic oxygen-centered sulfate radicals used as initiator. Therefore, another synthetic approach was proposed to obtain a new cardanol-based methacrylate: hydroxyethylation of cardanol and further methacrylation (Scheme 1-21).[172] In this synthesis, the use of epichlorohydrin was avoided. Due to the high hydrophobicity of the monomer, miniemulsion homo- and copolymerization were performed. The miniemulsion polymerization proceeded faster than the solution polymerization. Likewise, the miniemulsion copolymerization of cardanol methacrylate with MMA proceeded faster than homopolymerization, although higher dispersity in particle sizes was obtained when increasing MMA content, due to

possible secondary nucleation. On the other hand, gel content increased with decreasing content of MMA and reached 83 wt% for the biobased homopolymer.

Scheme 1-20. Synthesis of cardanol methacrylate

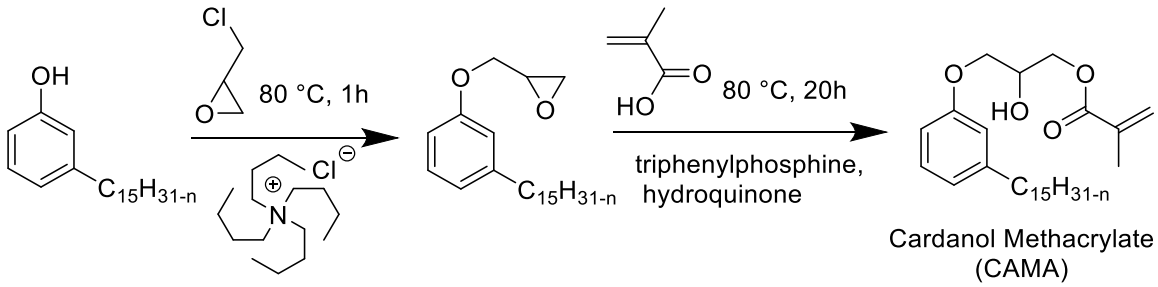

Scheme 1-21. Alternative synthesis of cardanol methacrylate

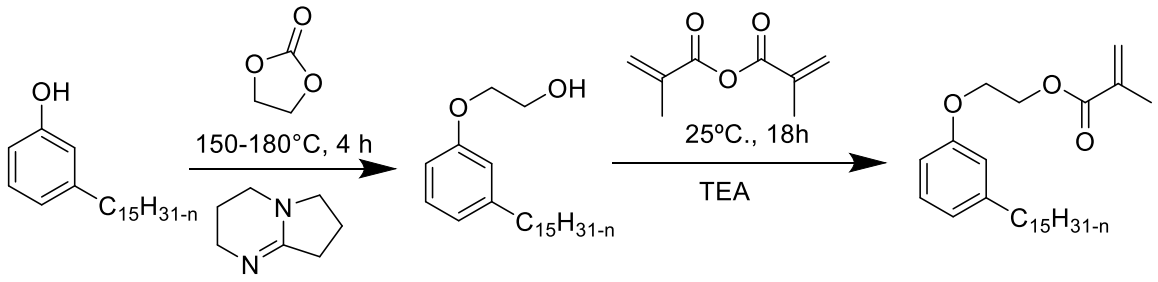

More recently, cardanol methacrylate (CM) was copolymerized *via* miniemulsion polymerization with high oleic soybean oil-based monomer (HOSBM).[173] Latexes containing different quantities of cardanol methacrylate (from 10 to 75% wbm) and HOSBM (from 25 to 90% wbm) with 29 to 31% total solids content were synthesized. The unsaturation amount in each monomer was measured and resulted higher for CM. Lower number average molecular weight was obtained as the amount of CM increased in the formulation allylic hydrogen abstraction (chain transfer reaction). The presence of allylic double bonds was exploited to cure the films by autoxidation without catalyst at 135°C for 4-5 h. The cross-link density, T_g, pencil hardness, cross-cut adhesion, water and solvent resistance increased with the CM content in the formulation.

Similar to vegetable oil derived monomers, lipid derived monomers show diffusion limitations in aqueous phase. The miniemulsion technique is thus more suitable than emulsion polymerization. It is important to mention, that cardanol is an abundant non-edible by-product of the cashew nut industry.[174] The use of nonedible raw materials is preferred in the synthesis of new biobased monomers. Equally important, the new synthetic pathway (Scheme 1-21) prevented the use of toxic reactants such as epichlorohydrin, thus making the biobased monomer synthesis more environmentally friendly. Still, some efforts towards solvent-free and low energy consuming reactions (which can be performed at ambient temperature for example) should be pursued for the synthesis of novel biobased monomers.

1.5.2 Terpene-based polymers

Terpenes, terpenoids and rosin are hydrocarbon-based molecules with one or more isoprene (2-methyl-1,3-butadiene) units that comprise the largest single group of natural products.[175–177] Terpenes have been particularly important for fine chemistry and fragrance industry. Due to their low cost and ease of separation, α-pinene, β-pinene, limonene and myrcene have been studied relatively extensively as starting materials for the synthesis of polymers.[178,179] Pinene has been used in cationic polymerization for adhesives, coatings and inks.[180,181] Limonene has been reacted to prepare polyesters, polyamides and polyurethanes through thiol-ene functionalization.[182] Several other examples of solution and condensation polymerization with terpene derivatives have been discussed in recent articles and reviews.[178,183,184] However, only a few examples of emulsion polymerization to produce latexes with 30% solids content exist, and they mostly concern acyclic terpenes such as myrcene and alloocimene. Myrcene is an acyclic monoterpene similar to some oil-based unsaturated hydrocarbons such as 1,3-butadiene and isoprene. Myrcene can be obtained in small percentages from hop, celery, ginger root, rosemary, nutmeg and sage. However, it can be produced on a large scale by pyrolysis of β-pinene. Ocimene and alloocimene are isomers of myrcene and very sensitive to oxidation. Ocimene is prepared by thermal cracking of α-pinene, but it isomerizes to alloocimene at high temperatures.[185]

1.5.2.1 Terpene emulsion polymerization

Sarkar and Bhowmick[186] reported the synthesis of a β-myrcene homopolymer *via* free radical emulsion polymerization using either thermal or redox initiation. According to ^{1}H NMR measurements, the thermal polymerization promoted the formation of 1,4-*cis* and 1,4-*trans* mixture and 1,2 *vinyl* and 3,4 structure as side reactions (Scheme 1-22a), whereas in the redox initiated polymyrcene neither 3,4 *structure* nor 1,2 *vinyl* structure were formed and the microstructure predominantly contained 1,4 addition products.

At room temperature, side reactions and chain transfer effects were suppressed. The T_g value was found to be -73°C for the thermal polymerization and -60°C for the redox process. Similarly, free radical emulsion copolymerization of methacrylate molecules (stearyl, lauryl and butyl) and β-myrcene was reported (Scheme 1-22 b).[187] The rate of copolymerization and the molar mass decreased with the increase of the alkyl chain length of the methacrylic pendant group due to diffusion constraints. Moreover, only the myrcene-butyl methacrylate copolymer was devoid of 1,2 *vinyl* and 3,4 addition myrcene microstructures. This was related to the higher rate of copolymerization of butyl methacrylate which prevented side reactions. Furthermore, for the emulsion copolymerization of β-myrcene and styrene (Scheme 1-22c),[188] higher gel content and lower rate of copolymerization were observed as the mass fraction of styrene decreased. Only 1,4-*cis* and 1,4-*trans* microstructures were found for those copolymers prepared with a 40 wt% or higher styrene contents.

Scheme 1-22. Polymerization of myrcene

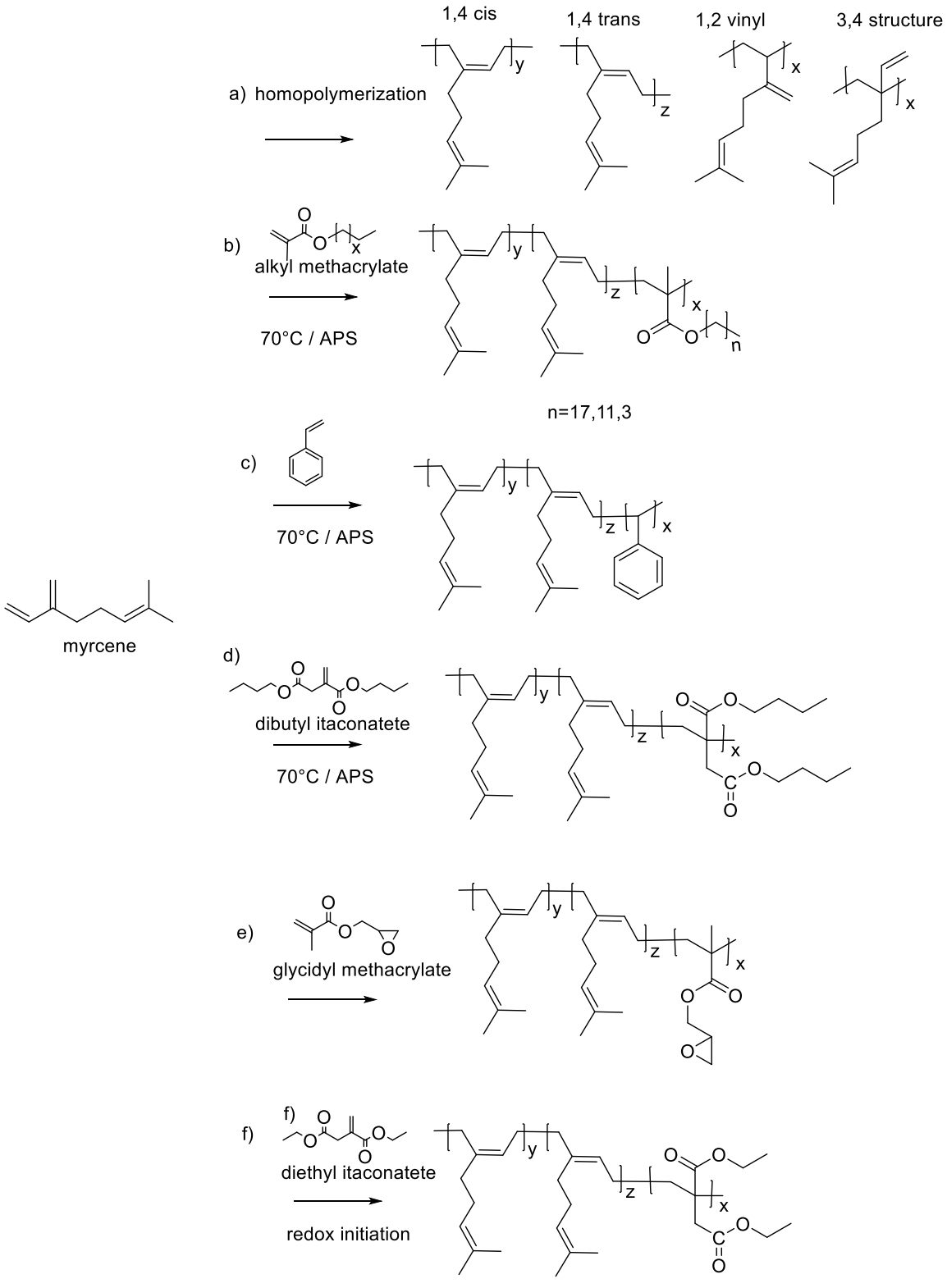

The synthesis of poly(myrcene-*co*-dibutyl itaconate) by emulsion copolymerization (Scheme 1-22 d)[189] showed a delayed nucleation process due to the polar character of dibutyl itaconate (DBI). As DBI feed content increased, oligomers formed in the aqueous phase did not diffuse promptly into the micelles. In addition, DBI radicals are more stable than myrcene radicals, thus less prone to chain propagation. Consequently, as DBI was introduced (10 wt% of the total monomer), the copolymer yield and its molar mass increased until 50 wt% of myrcene and 50 wt% DBI in the copolymer mixture was reached, then reductions in the yield and molar mass were observed. Moreover, the gel content increased with the content of myrcene. In addition, elastomers such as polymyrcene and its copolymers with styrene, dibutyl itaconate and butyl methacrylate at a 30 wt% of the comonomer were compounded and vulcanized. Carbon black was used as a filler to improve mechanical properties. Myrcene constituted 70 wt% of the total monomer feed mass in the formulation to maintain low T_gs. Properties such as tensile strength, elongation at break, cross-link density, hardness and thickness were measured. The presence of aromatic rings in the copolymer of styrene and myrcene increased the stiffness of the polymer backbone resulting in a higher T_g in spite of having lower cross-link density than polymyrcene homopolymer.[190] However, no comparison with commercial products was given. Furthermore, the copolymerization of glycidyl methacrylate (GMA) (Scheme 1-22 e) and myrcene was carried out to prepare a functional polymer capable of covalent interaction with silica for tyre reinforcement.[191]The reaction temperature was maintained at 20°C to avoid cross-linking reactions that occurred as the mass fraction of GMA increased in the comonomer mixture. The copolymerization between myrcene and GMA corresponded to an azeotropic copolymerization.

Lei *et al.*,[192] performed the synthesis of a nanocomposite of myrcene and diethyl itaconate *via* redox emulsion polymerization employing sodium hydroxymethane sulfonate/Fe-EDTA/*tert*-butyl hydroperoxide as initiating system at room temperature (Scheme 1-22 f). Diethyl itaconate was used to improve the polarity of the resulting macromolecules. Only 1,4-*cis* and 1,4-*trans* microstructures of myrcene were found in the copolymers according ^{1}H NMR spectra. Nano silica, which is non-petroleum based, was used as a filler instead of carbon black. Physical and mechanical properties of the vulcanized silica/poly (myrcene-*co*-diethyl itaconate) elastomers were studied, achieving a tensile strength of 9.2 MPa and 443% of elongation at break for the 60 wt% myrcene formulation. Similar tendencies in the polymerization yield as the ones observed for dibutyl-itaconate[189] were found. The highest yield was reached at a 70/30 weight ratio of myrcene/diethyl itaconate comonomer mixture.

Sahu *et al.*[193] reported the emulsion homopolymerization of alloocimene (Scheme 1-23) using two redox emulsion polymerization reaction systems: $FeSO_4 \cdot 7H_2O$/TBHP and $FeSO_4 \cdot 7H_2O/Na_2S_2O_5$ at different temperatures (15°C, 25°C and 35°C). A rubbery-type polymer was obtained in 20-25% yield. The authors claimed that, at 35°C, the thermal decomposition of the polymer chains

increased, leading to the reduction of the molar masses. The polymerization was thus preferably performed at room temperature to control side reactions and prevent cross-linking reactions.

Later, Sahu and Bhowmick, used a redox initiated emulsion polymerization for the polymerization of β-myrcene, β-farnesene and β-ocimene.[194] In this work, different surfactants (anionic, nonionic and cationic), initiators and reducing agents were studied. Reactions were followed up to 24 h and done at 20-25°C to produce less branched and less cross-linked polymers. The reaction using potassium oleate as surfactant and *tert*-butyl hydroperoxide (TBHP) as initiator produced the maximum yield and higher molecular mass polymers. Moreover, 1,4 *cis* and 1,4- *trans* microstructures were mainly observed according to NMR characterization. Yields from 38 to 65% were obtained and gel content was in the range of 0 to 8% in the different β-myrcene formulations.

Scheme 1-23. Alloocimene polymerization

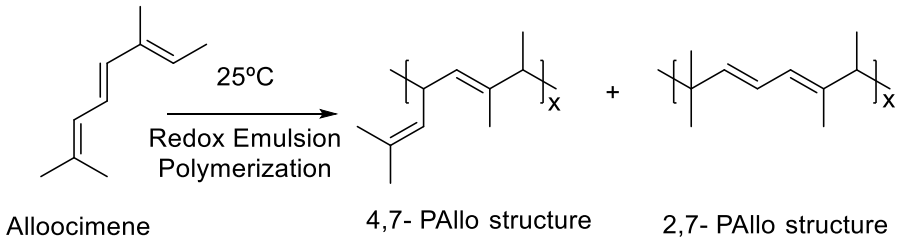

Isobornyl methacrylate (IBOMA), derived from camphene in pine resin, was copolymerized with 2-hydroxyethyl acrylate (2-HEA), acrylic acid and butyl acrylate through emulsion polymerization.[195] Adhesive properties such as tack and peel were measured. IBOMA containing formulations exhibited peel and tack forces similar to the reference formulations containing only oil-based monomers. Similar studies were done using 2-octyl acrylate and 2-EHA instead of 2-HEA or butyl acrylate as mentioned in the vegetable oil section.[142]

1.5.2.1 Terpene miniemulsion polymerization

Noppalit et al,[196] synthetized tetrahydrogeraniol acrylate (THGA) and cyclademol acrylate (CDMA), both molecules derived from terpenes. RAFT (Reversible addition-fragmentation chain transfer) polymerization was executed through miniemulsion polymerization, using AIBN at 70°C, aiming for the synthesis of PSAs. It was possible to obtain a polymer with adequate peel resistance for PSA applications (6.0 N/25mm) and a dispersity of 1.6. Later, tetrahydrogeraniol methacrylate (THGMA) and cyclademol methacrylate (CDMMA) were used in the synthesis of a diblock copolymers, also aiming for PSAs applications.[197] A seed containing THGMA and stearyl methacrylate (co-stabilized) was synthesized *via* nitroxide-mediated miniemulsion polymerization and then CDMMA dissolved in acetone was added to the seed. The reaction was done at 97°C for 8 hours. Dispolred 007 (3-(((2-cyanopropan-2-yl)oxy)(cyclohexyl)amino)-2,2-dimethyl-3-phenylpropanenitrile) was used as a regulator. Experimental number average molecular weights were close to the theoretical ones for both the seed and diblock latexes synthesis with dispersity from 1.24 to 1.68 for all experiments.

The obtained polymers showed comparable performance to partially oil-based formulations for PSAs applications.

Linear terpenes remain highly valuable monomers for their resemblance to isoprene. The physico-chemical properties of the resulting polymers are greatly influenced by the reaction conditions; thus, side reactions and chain transfer should be avoided to control the microstructure of the polymers. Stereoselective solution polymerization of myrcene at 70°C has been done succesfully.[198] Likewise, this has been achieved in emulsion polymerization using low temperature redox initiation. Reactivity ratios of the biobased monomers should be studied and adequate copolymer mixtures should be formulated to reach high polymerization yields and suitable molar mass for the targeted applications. Miniemulsion polymerization remains a suitable option for monomers suffering from diffusion constraints although it will restrict their use in industrial processes. Seeded emulsion (co)polymerization with more hydrophilic monomers also offers a solution to overcome difficulties encountered in the nucleation step in *ab initio* emulsion polymerization Furthermore, more exploration should be done regarding the cyclic terpene-derived monomer, as several cyclic terpene-derived methacrylates[199] have been developed but only a few molecules, such IBOMA and THGA have made their way to emulsion and miniemulsion polymerization.

1.5.3 Lignin derivatives-based polymers

Lignin is the main renewable source of phenolic compounds; which provides a platform of aromatic chemicals that can be used for the production of polymers with different thermomechanical properties.[200,201] Lignocellulosic biomass is mostly cell wall material and is composed of three main kind of molecules: cellulose (40-50 wt%), hemicellulose (20-30 wt%), and lignin (15-35 wt%). Hemicellulose and cellulose, are polymers and copolymers of C5 and C6 sugars.[202] Lignin constitutes 15–35% of dry lignocellulose and is the largest renewable source of aromatics on Earth. Lignin is a cross-linked amorphous copolymer produced from the radical polymerization of substituted phenyl propylene units: coumaryl, coniferyl, and sinapyl alcohols containing zero, one, and two methoxy groups, respectively.[203,204] The depolymerization process of lignin has been widely studied.[176,200,202,205] Interestingly, lignocellulose is the non-edible part of the plant; therefore its use to produce polymer materials does not compete with food supply. Different small molecules such as vanillin, ferulic acid, eugenol, creosol and sinapyl alcohol derivatives can be isolated from lignin and can be used for the synthesis of biobased polymer. Several polymers have been prepared from these building blocks.[15,22,206,207]

Although the reactivity and functionalization of lignin derivatives have already been widely studied,[22,203,207] emulsion polymerization reactions of lignin derivatives has been little studied so far. Exploring this kind of polymerization processes taking advantage of the functionalization pathways already developed and building on the existing solution polymerization studies of molecules such as eugenol or vanillin is a valuable opportunity.[21,208,209]

1.5.3.1 Lignin derivative emulsion polymerization

Ferulic acid, a natural occurring phenol found in plant cell walls, was used as building block to produce a monomer with a vinyl group AC4VG (acetyl-protected 4-vinylguaiacol).[210,211] This monomer was polymerized using a semi-batch seeded emulsion polymerization to produce core-shell particles. The seed was composed of poly(BA). Particles with a poly(BA) core, partially encapsulated by a poly(AC4VG) shell (Janus like) were observed by TEM. Glass transition measurement confirmed the presence of a phase separation as three different temperatures were observed, −48°C for poly(BA), 52°C for the interphase and 112°C for poly(AC4VG).

1.5.3.2 Lignin derivative suspension polymerization

The aqueous suspension polymerization of methacrylated eugenol (Scheme 1-24) in the presence of poly(vinyl alcohol) (PVA) as a steric stabilizer produced cross-linked microspheres with diameters ranging from 500 to 800 µm.[212] These particles exhibited large oil absorbency and were targeted for applications in wastewater treatment. Concentrations of AIBN (initiator) and of PVA (stabilizer) were found to be key factors of the reaction. The allylic double bond was also involved in the radical polymerization, thus avoiding the need of a cross-linking agent.

Scheme 1-24. Eugenol methacrylation

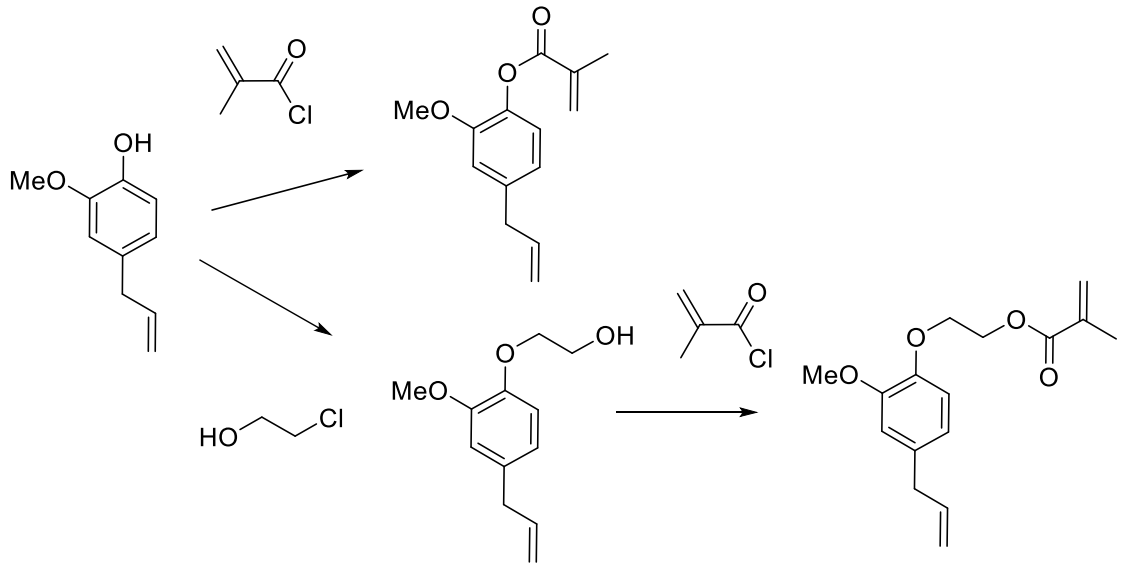

Scheme 1-25. Vanillin methacrylate suspension polymerization

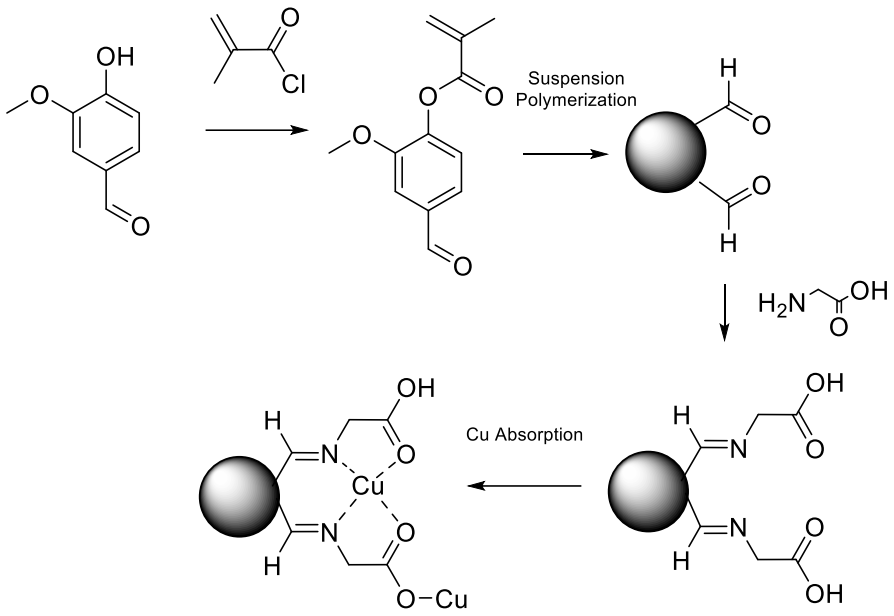

Similarly, Zhang *et al.*[213] reported the suspension polymerization of vanillin methacrylate to obtain porous microspheres also for wastewater treatment applications (Scheme **1-25**). In this case, chloroform and toluene were used as cosolvents since vanillin methacrylate is solid at the reaction temperature. The vanillin aldehyde group present on the resulting microspheres was reacted with glycine, to form Schiff–bases with remarkable Cu^{2+} complexation capability. On the other hand, magnetic microspheres were prepared *via* suspension polymerization using vanillin methacrylate as monomer and methacrylated-Fe_3O_4 magnetic nanoparticles as magnetic substrates.[214] The aldehyde-containing magnetic microspheres were reacted with *para*-anisidine (used as a model amine) to determine their absorption capacity. The absorption of amines, by the formation of a Schiff base, was studied and a facile recovery of the microspheres was achieved thanks to their magnetic properties.

Currently, degradation of lignin into smaller molecules of interest has to be optimized.[215] Molecules such as eugenol and vanillin are still prepared from selected natural sources. Nevertheless, continuous research in the exploitation of natural feedstocks such as lignin could provide efficient and cost-effective synthetic routes to produce biobased building blocks in large quantities. The development of lignin-derived monomers and their polymerization processes is thus very timely.

1.5.4 Carbohydrate-based polymers

Carbohydrates represent roughly 75% of the annually renewable biomass (200 billion tons),[216] thus they represent an important feedstock for the production of polymeric materials as presented in recent reviews.[15,16,217,218] The synthesis of carbohydrate macromers for emulsion polymerization can be performed *via* the hydroxyl, carboxylic acid and amine groups. Vinyl groups have been introduced by esterification of carbohydrates using (meth)acryloyl chlorides or (meth)acrylic anhydrides (Scheme 1-26 a).[219] Brune *et al.*[220] prepared a starch based macromer by a

condensation reaction between the hydroxyl groups from starch and bifunctional monomers such as *N*-methylolmethacrylamide, *N*-methylolacrylamide, hydroxyethyl methacrylate, or hydroxypropylmethacrylate in the presence of a catalyst. The resulting macromonomers were subsequently copolymerized with vinyl monomers such as styrene in emulsion polymerization to form starch-grafted latex particles. Another approach has been the free-radical polymerization through the "grafting from" technique using persulfate initiators (hydrogen abstraction from a C-H bond in the carbohydrate backbone) (Scheme 1-26 b).[221] This technique is employed to minimize the quantity of carbohydrate in the continuous phase of the latex as it can induce flocculation or coagulation.[222,223] Biopolymers containing amine functions, such as chitosan, have been copolymerized with acrylates using surfactant-free emulsion polymerization.[224,225]

Scheme 1-26. Grafting techniques on carbohydrates

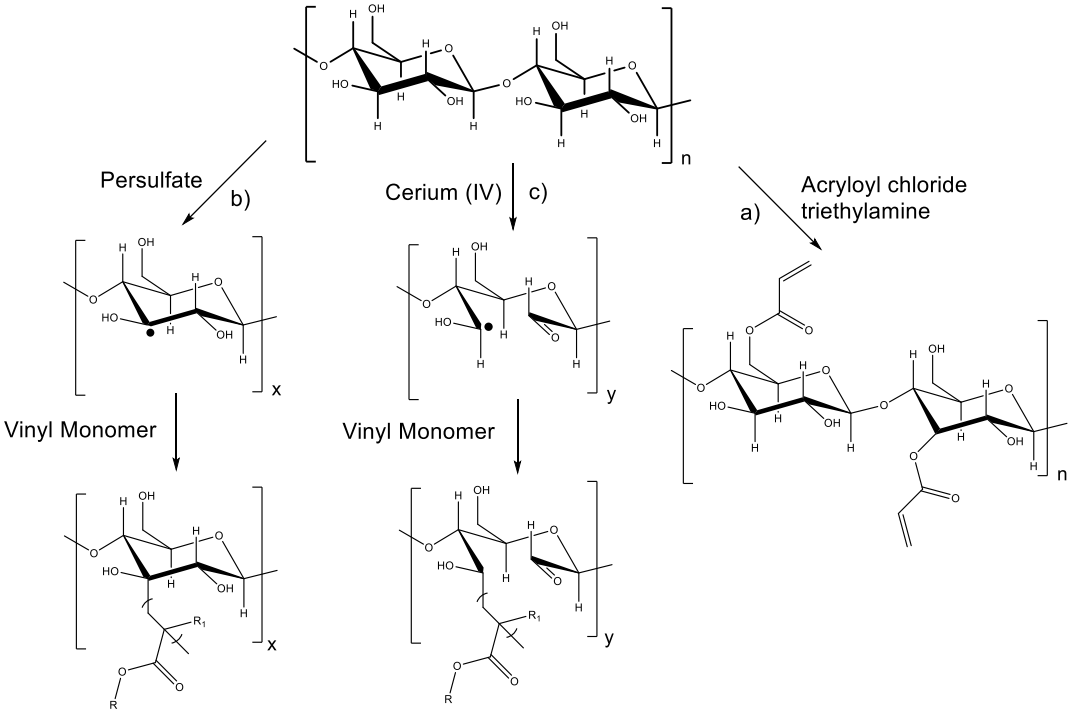

Although more selective grafting techniques which involve the use of oxidant cations such as cerium (Ce^{4+}), iron (Fe^{3+}), manganese (Mn^{4+}) or copper (Cu^{2+}) ions able to react with the hydroxyl groups of carbohydrates (Scheme 1-26 c)[226] can be used (redox chemistry), they induce colouring in the final latexes. Consequently, the use of persulfate is often preferred.

Möller and Glittenberg reported the emulsion copolymerization of styrene-butadiene in the presence of corn starches. The final hybrid latexes contained 50 phm (parts per hundred monomer) of starch exhibiting improved performances for paper coating applications.[227] A similar example was presented by Wang *et al.*[228] where potato starch was degraded *in-situ* using potassium persulfate to prepare latexes containing butyl acrylate and methyl methacrylate. Then, diacetone acrylamide was copolymerized as a functional monomer to produce a latex that could be further cross-linked by reaction with adipic acid dihydrazide (ADH). These latexes exhibited humidity control properties,

and could be used as indoor coatings. Similarly, Gaborieau *et al.*[226] used Ce^{4+} redox initiator to produce core-shell particles from hydrophobic core-forming vinyl monomers and cationic carbohydrate shell. However, as Ce^{4+} ions can lead to coloration of the latexes, hydrogen abstraction by alkyl hydroperoxides on amino groups of certain biopolymers was reported by Li *et al.*[224] As low molar mass polyamines can form redox pairs with alkyl hydroperoxide, a radical is generated on the nitrogen atoms in the amino group which subsequently initiated graft polymerization.[229] Graft polymerization resulted in amphiphilic polymers that could self-assemble into micelle-like domains, leading to core-shell particles structures. Following a different approach, Smeets *et al.*[230] reported the sonochemical homolytic chain scission of hydroxyethyl cellulose in presence of hydrophobic monomers (such as butyl acrylate) to form functional hairy latex particles. Cummins *et al.*[231] used dent corn sourced regenerated starch nanoparticles (RNSP's) modified with vinyl groups in a semi-batch, monomer-starved seeded emulsion copolymerization of butyl acrylate, methyl methacrylate and acrylic acid. Stable latexes were produced at 40 wt% solids and 25 wt% of RNSP loading (40 wt% incorporation into the latex).

Later, starch nanoparticles (SNPs) were introduced in a latex formulation aiming at adhesive applications.[232] Due to the hydrophilic nature of SNPs, several strategies were implemented to incorporate them in the latex particles. First, cross-linking followed by the attachment of vinyl groups to the SNP surfaces with the subsequence polymerization of "tie-layer" monomer with a moderate hydrophilic character. Sodium trimetaphosphate (STMP) was used as the cross-linker, a functionalized sugar-based monomer (FSM) was used as source of the vinyl groups chemically bounded to the surface of the SNP and finally, butyl vinyl ether (BE) was used as the "tie-layer" monomer. The latexes were synthesized through a semi batch process where the initial charge contained the cross-linked functionalized SNPs. The obtained copolymers containing SNPs at 15% wbm (with BVE, BA, MMA and AA, to a total solids content of 40%) presented higher tack and peel properties but lower shear strength than the completely oil-based reference recipe (containing BA, MMA and AA) or blends of oil-based latex and SNPs. Moreover, by using STEM and TEM, it was observed that SNPs were encapsulated in an acrylic core. Later, the SNP content in the latexes was successfully increased from 15 to 45% wbm in formulation with 55% total solids content.[233] Core-shell morphology was preserved (SNPs core/acrylic polymer shell). Nevertheless, a reduction of tack and peel properties was observed as the SNP was increased in the formulations. Comprehensive reviews on the use of starch in emulsion polymerization,[234] as well as the use of carbohydrates as surfactants/stabilizers, macromonomers and transfer agents to prepare hybrid latex particles have been published.[235]

Abeylath *et al.*[236] examined the emulsion copolymerization of ethyl acrylate and several monosaccharide acrylates and acrylamide. These sugar acrylates were derived from glucose, ribose, mannose, galactose and glucosamine and their hydroxyl groups were protected and unprotected to study the particle formation efficiency and size (Scheme 1-27). Hydroxyl groups were protected by acetonides in the case of glucofuranose, mannofuranose, galactofuranose and ribofuranose and acetylated in the case of glucosamine. Morover, ribofuranose hydroxyl groups were also protected with benzyl groups and glucosamine hydroxy goups with benzoyl groups. The

copolymerizations were successful when the acetonide-protected derivatives were used and resulted in particles with an average diameter of 42 nm. However, the *O*-benzyl- and *O*-benzoyl-protected monosaccharide acrylates polymerized only to low conversions. This was explained by the effect of the bulky groups that may affect their reactivity. Emulsion polymerization of protected carbohydrate monomers resulted in a latex characterized by particles with an average diameter of 40 nm; however, unprotected monomers produce particles of approximately 80 nm. The particles size increased with the proportion of unprotected carbohydrate monomer in the copolymer (ethyl acrylate as comonomer).

Scheme 1-27. Carbohydrate monomers (a) 3-*O*-acryloyl-1,2:5,6-di-*O*-isopropylidene-α-D-glucofuranose, b) 1-*O*-acryloyl-2,3:5,6-di-*O*-isopropylidene- α -D-mannofuranose, c) 5-*O*-acryloyl-1-methoxy- 2,3-isopropylidene-β-D-ribofuranose, d) 6-*O*- acryloyl-1,2:3,4-di-*O*-isopropylidene-α-D-galactopyranose, e) N-acryloyl-1,3,4,6-tetra-*O*-acetyl-β-D-glucosamine

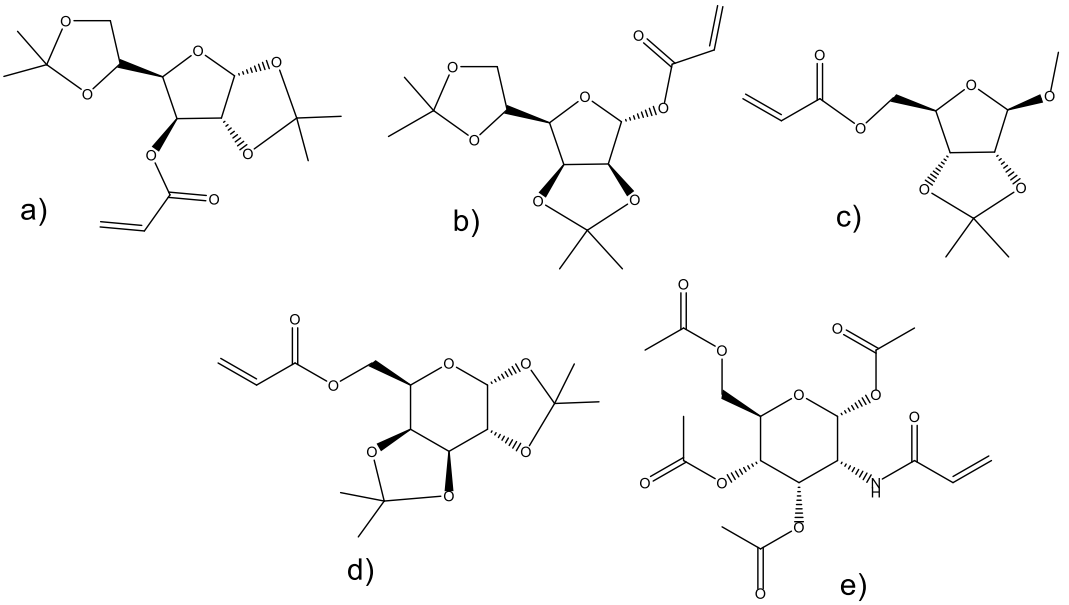

Cellulose and hemicellulose can be degraded to obtain C5 and C6 sugar derivatives which can be used to synthesise several biobased building blocks.[2] For example, levoglucosenone (LGO), can be produced by pyrolysis of cellulose[237]. Dihydro-5-hydroxyl furan-2-one (2H-HBO) is a LGO-derived compound produced by Baeyer-Villiger oxidation. It was methacrylated and used in emulsion homo- and copolymerization and reversible addition-fragmentation chain transfer (RAFT) emulsion polymerization to prepare latexes at 30% solids content.[238] The yield of emulsion homopolymerization was 82% and the T_g of the resulting polymer was approximately 108°C. Copolymerizations with commercially available monomers in water were also attempted. These experiments showed that the methacrylated 2H-HBO copolymerized well with polar monomers such as MMA and HEMA. However low incorporation of the biobased monomer was obtained in copolymerization with styrene, producing copolymers with low molar mass and rich in styrene.

Villanova *et al.* [239] functionalized pectin with GMA (Scheme 1-28) to introduce methacrylic moieties and copolymerized the resulting monomer with MMA, BMA and ethyl acrylate (EA) *via* redox

($FeSO_4$/APS/Sodium dithionite) emulsion polymerization. The desired latexes were thought to have good mucoadhesive properties for use as pharmaceutical excipients, as coating agents or matrix agent. The functionalized pectin monomer was introduced in 2, 3.5, 5 and 6 wt% in the total monomer feed. The increase in viscosity after the addition of mucin proved the formation of intermolecular interactions which confirmed the potential use of these materials as bioadhesives.

Scheme 1-28. Functionalization of pectin

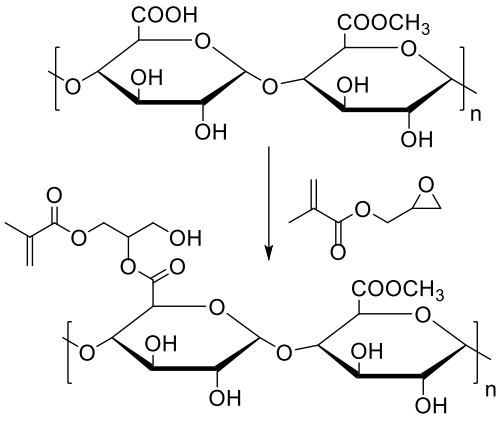

Another approach in exploiting carbohydrates as biobased monomers was the synthesis of methacrylated monomers using galactose and fructose-derived molecules (Scheme 1-29).[240–242] A commercially available fructose-based monosaccharide bearing acetonide protecting groups was used in the synthesis of a methacrylated monomer, taking advantage of the peculiar reactivity of primary alcohol in the anomeric position. The resulting methacrylate was used in emulsion homopolymerization and copolymerization with butyl acrylate, reaching up to 45% solids. The homopolymer glass transition temperature was reported to be approximately 115°C. Under copolymerization conditions, polymerization rates increased with increasing amount of fructose-methacrylate. Moreover, the gel content increased with increasing butyl acrylate content. Surprisingly, the gel content decreased with decreasing the amount of potassium persulfate as initiator. However, as the gel content measurements were not performed systematically, this difference could be caused by the evolution of the latexes during storage.

Scheme 1-29. Methacrylation of protected fructose

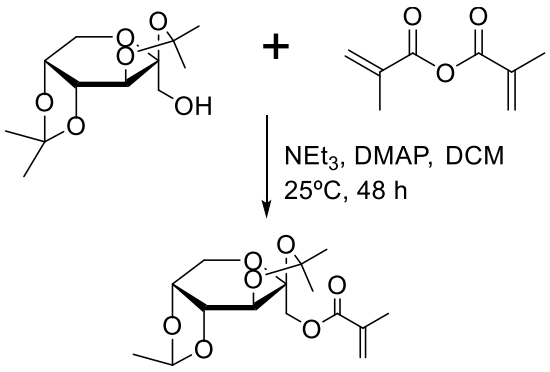

Neqal *et al.* [243] prepared acrylate and methacrylate from protected galactopyranose (1,2:3,4-di-*O*-isopropylidene-D-galactopyranose) (Scheme 1-30) and polymerized these monomers under emulsion polymerization conditions. The melting point of these glycomonomers was approximately 60°C. Coagulation was observed when emulsion polymerization was carried out without any cosolvent. For the emulsion polymerization to proceed properly, the monomers had to be dissolved in toluene prior to the emulsification. However, coagulation was still not efficiently prevented; thus, ethyl acetate was used instead of toluene. In addition, the initiator amount was increased and the solids content was decreased from 10 to 5 wt%. Moreover, due to the high tendency of acrylate glycomonomer to autopolymerize, the study was carried out only on the methacrylate glycomonomer as it could be safely stored. The polymerizations proceeded to full conversions. The polymers were deprotected using trifluoroacetic acid (TFA) and finally an *N*-alkylation reaction using dodecylamine was carried out. *N*-dodecylgalactosylamine has been proven to possess antifungal properties.[244] Nevertheless, in case of the functionalized polymer particles, the antifungal activity was not as pronounced in the case of N-dodecylgalactosylamine.

Scheme 1-30. Synthesis of poly(6-*O*-methacryloyl-*N*-alkyl-β-D-galactosylamine)

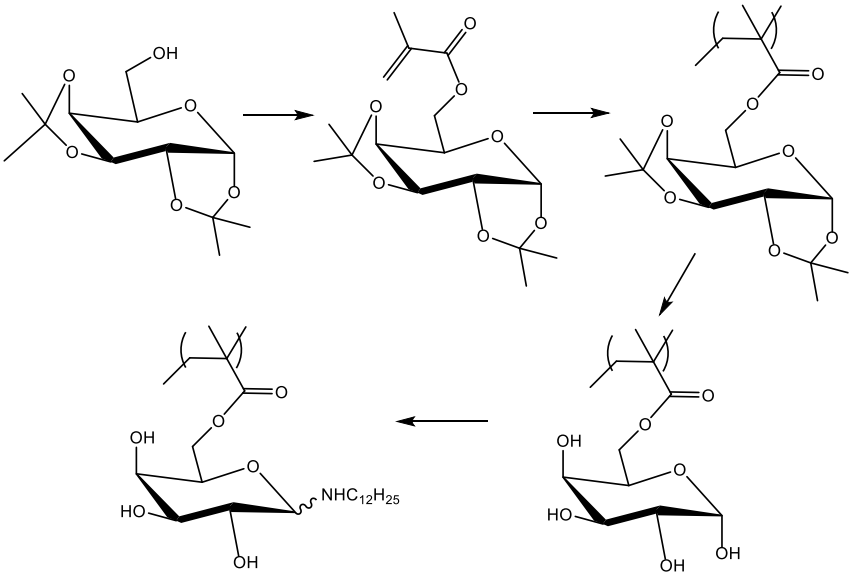

Recently, Badía et al.[245] included isosorbide methacrylates in PSA formulation containing IBOA, IBOMA, octyl acrylate and MAA. It was shown that low percentages (1%) of ISOMA (isosorbide methacrylate) and a mixture of isosorbide mono and di- methacrylates provided the polymers with enhanced flexibility and cohesiveness improving the adhesion performance. Moreover, the presence of hydroxyl groups promoted the complete removability of the PSA tapes in water, which is interesting in applications where labels need to be removed easily, preferably without the use of organic solvents.

Due to the water solubility of saccharides and their lack of polymerizable functional groups able to undergo direct free radical polymerization, several structure modifications are often required to obtain suitable monomers. These modifications sometimes involve the use of protecting groups which are highly undesirable according to green chemistry principles.[246] In consequence,

alternatives have been examined. For example, the use of grafting techniques is an option, although the control of these reactions is not straightforward. However, this water-solubility which is a source of problems when saccharides are used as monomers, can be turned into an advantage if these saccharides are derivatized into surfactants or surfmers.[247] Biobased surfactants and surfmers will not be presented here since they are beyond the scope of the present review.

1.5.5 Protein-based polymers

Milk proteins, casein and whey proteins, are important for human nutrition. Moreover, they have found application in wood and paper adhesives.[248] Casein, a protein derived from bovine milk, has good biocompatibility and biodegradability, high purity and low cost and exhibits a high T_g (~180°C).[249] Therefore, it can form a hard phase in biphasic acrylic copolymers. By addition of casein, binders employed in waterborne coatings can show a reasonable minimum film forming temperature (MFFT) and have an acceptable blocking resistance. Thus, casein in combination with soft acrylic monomers was employed. Emulsion polymerization of butyl acrylate *via* grafting to caprolactam-casein particles using persulfate initiators and in the absence of emulsifier has been reported.[250] Improvements in grafting efficiency resulted in higher elongation at break and tensile strength. To improve the mechanical properties, nano-silica was introduced into the copolymer[251], and core-shell particles were obtained. However, casein is easily oxidized and the resulting polymer acquired a yellow colour when persulfate initiators were used. As in the case of carbohydrates, the grafting of polymers on casein could be achieved using redox initiation based on amino functional groups (Scheme 1-31 a). This approach was applied to casein, bovine serum albumin and gelatin.[222] Thus, in the pursuit of a hybrid acrylic-casein latex with potential applications in coatings, Picchio *et al.*[249,252] investigated the emulsion polymerization of butyl acrylate and methyl methacrylate in the presence of casein at different concentrations, using a redox initiation system based on TBHP as oxidant and the amine of casein as reductant. As previously mentioned, TBHP radicals react with the amino groups of the protein leading to a grafting reaction with the methacrylates.[222] The polymerization rate of the reaction increased as the content of casein increased due to the enhanced generation of amino radicals.[252] However, the acrylic grafting efficiency decreased with the increasing casein concentration. Due to the presence of ungrafted protein, particle size distributions of the resulting polymers showed two populations of particles (bimodal distribution) and the resulting films showed weak water resistance.

A different approach was presented for the copolymerization of casein and methacrylic monomers.[253] Casein was functionalized with glycidyl methacrylate (Scheme 1-31 b) to prepare methacrylated casein which was later copolymerized with methyl methacrylate and butyl acrylate in a surfactant-free emulsion copolymerization using TBHP as the initiator. The degree of grafting was determined using *o*-phthalaldehyde as colouring agent in combination with UV spectroscopy. The maximum functionality reached was thirty-two vinyl double bonds per molecule of casein. In this case, the increase in methacrylic groups decreased the polymerization rate and the polymerization yield, because the initiation reaction is triggered by the reaction between the TBHP (oxidant) and the remaining amino groups in the casein.[254]

Scheme 1-31. Casein functionalization

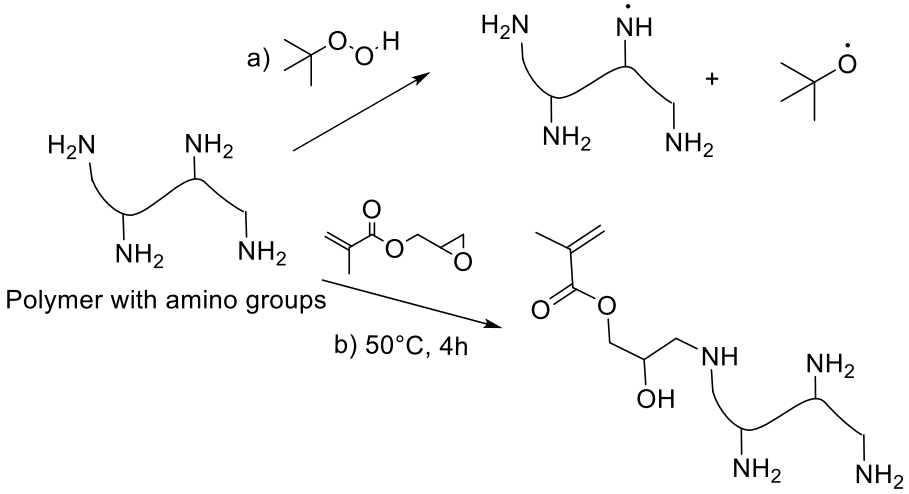

However, an increase in the degree of methacrylation allowed the adequate control of casein grafting efficiency,[252] which varied from 20% to 76%. The transmission electron microscopy (TEM) micrographs showed dark regions corresponding to ungrafted casein in the polymers prepared with native casein, whereas polymers prepared with highly methacrylated casein exhibited a reduction in free casein content, as larger fraction of casein were grafted to the (meth)acrylic polymer. Moreover, copolymers prepared from methacrylated casein had better water and solvent (methyl ethyl ketone, MEK) resistance compared to copolymers prepared from native casein. Finally, a statistical study to optimize the formulation of casein-based clear coatings (*i.e.* without pigments) was carried out. The study revealed that the casein latexes prepared at 35% solids content exhibited good minimum film forming temperature (MFFT), blocking resistance, opacity and mechanical properties. However, low hardness and poor chemical resistance was observed in comparison to commercial binders.

Similar to carbohydrates, the use of proteins as building blocks for monomers in free radical polymerization may require significant modification of their chemical structure. Nevertheless, they might also be thought of as potential surfmers due to their hydrophilic character. At present, it is still necessary to use them in a mixture with oil-based monomer, but the biogenic carbon content could be increased in the polymeric materials, which is the starting point for the replacement of fossil-based polymers.

1.5.6 Conclusion

Polymerization in aqueous dispersed media such as emulsion and miniemulsion polymerizations of biobased monomers is a promising strategy to produce green latexes for coating and adhesive applications. Molecules from different types of biomass have been already included in such formulations. Nevertheless, several constraints remain to be overcome such as the design and synthesis of monomers with adequate solubility in water to allow nucleation in *ab initio* emulsion polymerization. The control of chain transfer reactions, gel formation (cross-linking) and grafting efficiency should also be carefully examined. Although it has been less explored so far, suspension

polymerization of biobased monomers should not be disregarded as it represents a valuable alternative to produce polymers in aqueous dispersed media. In addition, polymers produced *via* suspension polymerization are easily recovered by filtration. In the quest for greener latexes, other components in formulations such as initiators,[255] surfactants,[256,257] costabilizers, pigments, etc., should not be neglected. In addition, the new biobased monomers, which will arise from the growing field of research on biobased latexes, will possibly bring unexpected new properties (thanks to the combination of many new functional groups and structures, *e.g.* aromatics from lignocellulosic derivatives), which can in turn open the road to new applications.

1.6 General conclusions

The literature review reported in this chapter demonstrates that the variety of available biomass provides a wide choice of molecules for the synthesis of novel biobased monomers. Biobased building blocks used in the synthesis of biobased monomers should not interfere with the food supply and be produced *via* a cost- and atom-efficient facile synthesis with a straightforward purification pathway to comply with green chemistry principles.[258] Most biobased building blocks require structure modification to introduce functional groups if they are desired to react by radical mechanisms. The introduction of acrylate and methacrylate groups in biobased building blocks is currently done using non-biobased sources. Nevertheless, acrylic acid[259,260] and more recently, methacrylic acid[261,262] can be obtained from renewable resources, making this pathway sustainable. Indeed, the synthesis optimization will be a crucial step for these biobased monomers to have any significant industrial use and impact, provided that their adequate performance is demonstrated.

Additionally, to provide a true green solution, environmentally friendly polymerization processes should also be employed. Photoinduced polymerization can be solvent-free, low energy consuming, and with spatial and temporal control. Aqueous emulsion polymerization allows the reduction of VOCs (as water is the continuous phase), better temperature control of reactions and lower viscosities than bulk reactions. In aqueous emulsion polymerization, monomers should possess the adequate hydrophobic character to diffuse through the aqueous. On the contrary, miniemulsion polymerization is a suitable option for very hydrophobic biobased monomers, although it has a higher energetic cost. Recent advances demonstrate that biobased latexes are a promising option in the replacement of oil-based latexes in applications such as coatings and adhesives. Even though the main objective is the production of polymers with similar or better properties than the ones obtained with oil-based monomers, the synthesis of novel biobased materials such as stimuli responsive,[263] nanostructured and/or self-healing materials,[264] taking advantage of the functional groups present in the biomass, should also be encouraged.

From the literature review, it was possible to conclude that natural phenols had not been widely researched in aqueous emulsion polymerization. The presence of the aromatic ring can give interesting properties to the polymers in terms of high thermal stability and mechanical strength derived from the interactions between aromatic side chains.[265] Eugenol, a natural phenol extracted from clove oil but also derived from lignin, represents an interesting biobased building block as it is

possible to functionalize it to obtain monomers that react through radical mechanisms. Additionally, it possesses an allylic pendant bond that can be used for further functionalization or cross-linking reactions. Therefore, it was selected in our work as the biobased molecule to create a monomer platform. In the following chapters, we will present the synthesis of eugenol-based monomers and their polymerization in various conditions, such as aqueous emulsion polymerization and photoinduced polymerization. The aim is to target products for daily use applications, such as coatings and adhesives, in the pursuit of a circular economy.

1.7 References

(1) Williams, C.; Hillmyer, M. Polymers from Renewable Resources: A Perspective for a Special Issue of Polymer Reviews. *Polym. Rev.* **2008**, *48*, 1.

(2) Gallezot, P. Conversion of Biomass to Selected Chemical Products. *Chem. Soc. Rev.* **2012**, *41*, 1538.

(3) Anastas, P.; Warner, J. *Green Chemistry: Theory and Practice*; Oxford University Press: New York, 2000.

(4) Anastas, P. T.; Zimmerman, J. B. Peer Reviewed: Design Through the 12 Principles of Green Engineering. *Environ. Sci. Technol.* **2003**, *37*, 94A.

(5) Schubert, T. Production Routes of Advanced Renewable C1 to C4 Alcohols as Biofuel Components – a Review. *Biofuels, Bioprod. Biorefining* **2020**, *14*, 845.

(6) Cai, X.; Hu, Y. H. Advances in Catalytic Conversion of Methane and Carbon Dioxide to Highly Valuable Products. *Energy Sci. Eng.* **2019**, *7*, 4.

(7) Panzone, C.; Philippe, R.; Chappaz, A.; Fongarland, P.; Bengaouer, A. Power-to-Liquid Catalytic CO2 Valorization into Fuels and Chemicals: Focus on the Fischer-Tropsch Route. *J. CO2 Util.* **2020**, *38*, 314.

(8) Figueroa, J. D.; Fout, T.; Plasynski, S.; McIlvried, H.; Srivastava, R. D. Advances in CO2 Capture Technology—The U.S. Department of Energy's Carbon Sequestration Program. *Int. J. Greenh. Gas Control* **2008**, *2*, 9.

(9) Sheldon, R. A. Green and Sustainable Manufacture of Chemicals from Biomass: State of the Art. *Green Chem.* **2014**, *16*, 950.

(10) Gandini, A. The Irruption of Polymers from Renewable Resources on the Scene of Macromolecular Science and Technology. *Green Chem.* **2011**, *13*, 1061.

(11) Gandini, A. Polymers from Renewable Resources: A Challenge for the Future of Macromolecular Materials. *Macromolecules* **2008**, *41*, 9491.

(12) Vert, M.; Doi, Y.; Hellwich, K.-H.; Hess, M.; Hodge, P.; Kubisa, P.; Rinaudo, M.; Schué, F. Terminology for Biorelated Polymers and Applications (IUPAC Recommendations 2012). *Pure Appl. Chem.* **2012**, *84*, 377.

(13) Kristufek, S. L.; Wacker, K. T.; Tsao, Y.-Y. T. Y. T.; Su, L.; Wooley, K. L. Monomer Design Strategies to Create Natural Product-Based Polymer Materials. *Nat. Prod. Rep.* **2017**, *34*, 433.

(14) Masutani, K.; Kimura, Y. *Encyclopedia of Polymeric Nanomaterials*; Kobayashi, S., Müllen, K., Eds.; Springer Berlin Heidelberg: Berlin, Heidelberg, 2021.

(15) Gandini, A.; Lacerda, T. M. From Monomers to Polymers from Renewable Resources: Recent Advances. *Prog. Polym. Sci.* **2015**, *48*, 1.

(16) Gandini, A.; Lacerda, T. M.; Carvalho, A. J. F. F.; Trovatti, E. Progress of Polymers from Renewable Resources: Furans, Vegetable Oils, and Polysaccharides. *Chem. Rev.* **2016**, *116*, 1637.

(17) Ca, V.; Lligadas, G.; Ronda, J. C.; Galia, M.; Galià, M.; Cádiz, V. Renewable Polymeric Materials from Vegetable Oils: A Perspective. *Mater. Today* **2013**, *16*, 337.

(18) Harmsen, P. F. H.; Hackmann, M. M.; Bos, H. L. Green Building Blocks for Bio-Based Plastics. *Biofuels, Bioprod. Biorefining* **2014**, *8*, 306.

(19) Sharma, V.; Kundu, P. P. P. Condensation Polymers from Natural Oils. *Prog. Polym. Sci.* **2008**, *33*, 1199.

(20) Voirin, C.; Caillol, S.; Sadavarte, N. V.; Tawade, B. V.; Boutevin, B.; Wadgaonkar, P. P. Functionalization of Cardanol: Towards Biobased Polymers and Additives. *Polym. Chem.* **2014**, *5*, 3142.

(21) Fache, M.; Darroman, E.; Besse, V.; Auvergne, R.; Caillol, S.; Boutevin, B. Vanillin, a Promising Biobased Building-Block for Monomer Synthesis. *Green Chem.* **2014**, *16*, 1987.

(22) Fache, M.; Boutevin, B.; Caillol, S. Vanillin Production from Lignin and Its Use as a Renewable Chemical. *ACS Sustain. Chem. Eng.* **2016**, *4*, 35.

(23) Fujisawa, S.; Kadoma, Y. Action of Eugenol as a Retarder against Polymerization of Methyl Methacrylate by Benzoyl Peroxide. *Biomaterials* **1997**, *18*, 701.

(24) Rigoussen, A.; Verge, P.; Raquez, J.-M.; Dubois, P. *Chemistry and Technology of Emulsion Polymerisation*; van Herk, A. M., Ed.; John Wiley & Sons Ltd: Oxford, UK, 2013; Vol. 6.

(25) Anastas, P. T.; Zimmerman, J. B. Design Through the 12 Principles of Green Engineering. *Environ. Sci. Technol.* **2003**, *37*, 94A.

(26) Latex. In *IUPAC Compendium of Chemical Terminology*; IUPAC: Research Triagle Park, NC, 2008; Vol. 577, p 3484.

(27) Sarkar, P.; Bhowmick, A. K. Sustainable Rubbers and Rubber Additives. *J. Appl. Polym. Sci.* **2017**, *134*, 45701.

(28) *Emulsion Polymerization and Emulsion Polymers*; Lovell, P. A., El-Aasser, M. S., Eds.; John Wiley & Sons Ltd: Sussex, 1997.

(29) Asua, J. M. Emulsion Polymerization: From Fundamental Mechanisms to Process Developments. *J. Polym. Sci. Part A Polym. Chem.* **2004**, *42*, 1025.

(30) Chern, C. S. Emulsion Polymerization Mechanisms and Kinetics. *Prog. Polym. Sci.* **2006**, *31*, 443.

(31) Save, M.; Guillaneuf, Y.; Gilbert, R. G. Controlled Radical Polymerization in Aqueous Dispersed Media. *Aust. J. Chem.* **2006**, *59*, 693.

(32) Daniel, J.-C.; Pichot, C. *Les Latex Synthétiques: Élaboration et Applications*; Tec&Doc-Lavoisier, 2006.

(33) Thickett, S. C.; Gilbert, R. G. Emulsion Polymerization: State of the Art in Kinetics and Mechanisms. *Polymer (Guildf).* **2007**, *48*, 6965.

(34) Ugelstad, J.; El-Aasser, M. S.; Vanderhoff, J. W. Emulsion Polymerization: Initiation of Polymerization in Monomer Droplets. *J. Polym. Sci. Polym. Lett. Ed.* **1973**, *11*, 503.

(35) Antonietti, M.; Landfester, K. Polyreactions in Miniemulsions. *Prog. Polym. Sci.* **2002**, *27*, 689.

(36) Asua, J. M. Miniemulsion Polymerization. *Prog. Polym. Sci.* **2002**, *27*, 1283.

(37) Asua, J. M. Challenges for Industrialization of Miniemulsion Polymerization. *Prog. Polym. Sci.* **2014**, *39*, 1797.

(38) Demirci, S.; Sahiner, N. Microemulsion Polymerization. In *Encyclopedia of Polymer Science and Technology*; Wiley, 2019; pp 1–24.

(39) Sáenz, J. M.; Asua, J. M. Dispersion Polymerization in Polar Solvents. *J. Polym. Sci. Part A Polym. Chem.* **1995**, *33*, 1511.

(40) Brooks, B. Suspension Polymerization Processes. *Chem. Eng. Technol.* **2010**, *33*, 1737.

(41) Pinto, M. C. C.; Santos, J. G. F.; Machado, F.; Pinto, J. C. Suspension Polymerization Processes. In *Encyclopedia of Polymer Science and Technology*; John Wiley & Sons, Inc.: Hoboken, NJ, USA, 2013.

(42) Guyot, A.; Tauer, K.; Asua, J. M.; Van Es, S.; Gauthier, C.; Hellgren, A. C.; Sherrington, D. C.; Montoya-Goni, A.; Sjoberg, M.; Sindt, O.; Vidal, F.;Unzue, M.;Schoonbrood, H.;Shipper, E.; Lacroix-Desmazes, P. Reactive Surfactants in Heterophase Polymerization. *Acta Polym.* **1999**, *50*, 57

(43) Guyot, A. Advances in Reactive Surfactants. *Adv. Colloid Interface Sci.* **2004**, *108–109*, 3.

(44) Napper, D. H. *Polymeric Stabilization of Colloidal Dispersions, Ed. R. H. Ottewill and R. L. Rowell, Academic Press, 1983*; Ottewillt, R. H., Rowell, R. L., Eds.; Academic Press: London, 1983.

(45) Gilbert, R. G. *Emulsion Polymerization, a Mechanistic Approach*, Academic P.; London, 1995.

(46) Russell, G. T.; Gilbert, R. G.; Napper, D. H. Chain-Length-Dependent Termination Rate Processes in Free-Radical Polymerizations. 1. Theory. *Macromolecules* **1992**, *25*, 2459.

(47) Schork, F. J.; Luo, Y.; Smulders, W.; Russum, J. P.; Butté, A.; Fontenot, K. Miniemulsion Polymerization. In *Advances in Polymer Science*; 2005; Vol. 175, pp 129–255.

(48) Asua, J. M. Miniemulsion Polymerization. In *Encyclopedia of Polymeric Nanomaterials*; Springer Berlin Heidelberg: Berlin, Heidelberg, 2015; pp 1267–1275.

(49) Masa, J. A.; De Arbina, L. L.; Asua, J. M. A Comparison between Miniemulsion and Conventional Emulsion Terpolymerization of Styrene, 2-Ethylhexyl Acrylate and Methacrylic Acid. *J. Appl. Polym. Sci.* **1993**, *48*, 205.

(50) Van Herk, A. M. *Chemistry and Technology of Emulsion Polymerisation*; van Herk, A. M., Ed.; John Wiley & Sons Ltd: Oxford, UK, 2013.

(51) Malaysian Rubber Board. Natural Rubber Statistic 2018 http://www.lgm.gov.my/nrstat/Statistics Website 2018 (Jan-Dec).pdf (accessed May 3, 2020).

(52) Bieleman, J. Additives for Coatings. *Pigment Resin Technol.* **2007**, *36*, prt. 2007.12936bac.005.

(53) Landfester, K. Miniemulsion Polymerization and the Structure of Polymer and Hybrid Nanoparticles. *Angew. Chemie Int. Ed.* **2009**, *48*, 4488.

(54) Yagci, Y.; Jockusch, S.; Turro, N. J. Photoinitiated Polymerization: Advances, Challenges, and Opportunities. *Macromolecules* **2010**, *43*, 6245.

(55) Corrigan, N.; Yeow, J.; Judzewitsch, P.; Xu, J.; Boyer, C. Seeing the Light: Advancing Materials Chemistry through Photopolymerization. *Angew. Chemie Int. Ed.* **2019**, *58*, 5170.

(56) Vitale, A.; Hennessy, M. G.; Matar, O. K.; Cabral, J. T. A Unified Approach for Patterning via Frontal Photopolymerization. *Adv. Mater.* **2015**, *27*, 6118.

(57) Ligon, S. C.; Liska, R.; Stampfl, J.; Gurr, M.; Mülhaupt, R. Polymers for 3D Printing and Customized Additive Manufacturing. *Chem. Rev.* **2017**, *117*, 10212.

(58) Zhang, J.; Xiao, P. 3D Printing of Photopolymers. *Polym. Chem.* **2018**, *9*, 1530.

(59) Leibfarth, F. A.; Mattson, K. M.; Fors, B. P.; Collins, H. A.; Hawker, C. J. External Regulation of Controlled Polymerizations. *Angew. Chemie Int. Ed.* **2013**, *52*, 199.

(60) Bagheri, A.; Jin, J. Photopolymerization in 3D Printing. *ACS Appl. Polym. Mater.* **2019**, *1*, 593.

(61) Vitale, A.; Bongiovanni, R.; Ameduri, B. Fluorinated Oligomers and Polymers in Photopolymerization. *Chem. Rev.* **2015**, *115*, 8835.

(62) Crivello, J. V.; Lam, J. H. W. Triarylsulfonium Salts as Photoinitiators of Free Radical and Cationic Polymerization. *J. Polym. Sci. Polym. Lett. Ed.* **2003**, *17*, 759.

(63) Atif, M.; Bongiovanni, R.; Yang, J. Cationically UV-Cured Epoxy Composites. *Polym. Rev.* **2015**, *55*, 90.

(64) Crivello, J. V.; Lam, J. H. W. Diaryliodonium Salts. A New Class of Photoinitiators for Cationic Polymerization. *Macromolecules* **1977**, *10*, 1307.

(65) Jarikov, V. V.; Neckers, D. C. Anionic Photopolymerization of Methyl 2-Cyanoacrylate and Simultaneous Color Formation. *Macromolecules* **2000**, *33*, 7761.

(66) Photocrosslinking. In *IUPAC Compendium of Chemical Terminology*; IUPAC: Research Triagle Park, NC, 2008; Vol. 2223, p 4592.

(67) Cramer, N. B.; Reddy, S. K.; Cole, M.; Hoyle, C.; Bowman, C. N. Initiation and Kinetics of Thiol-Ene Photopolymerizations without Photoinitiators. *J. Polym. Sci. Part A Polym. Chem.* **2004**, *42*, 5817.

(68) Hoyle, C. E.; Bowman, C. N. Thiol-Ene Click Chemistry. *Angew. Chemie - Int. Ed.* **2010**, *49*, 1540.

(69) Machado, T. O.; Sayer, C.; Araujo, P. H. H. Thiol-Ene Polymerisation: A Promising Technique to Obtain Novel Biomaterials. *Eur. Polym. J.* **2017**, *86*, 200.

(70) Hoyle, C. E.; Lee, T. Y.; Roper, T. Thiol-Enes: Chemistry of the Past with Promise for the Future. *J. Polym. Sci. Part A Polym. Chem.* **2004**, *42*, 5301.

(71) Lazauskaitė, R.; Gražulevičius, J. V. Synthesis and Cationic Photopolymerization of Electroactive Monomers Containing Functional Groups. *Polym. Adv. Technol.* **2005**, *16*, 571.

(72) Melchels, F. P. W.; Feijen, J.; Grijpma, D. W. A Review on Stereolithography and Its Applications in Biomedical Engineering. *Biomaterials* **2010**, *31*, 6121.

(73) Fouassier, J. P.; Allonas, X.; Burget, D. Photopolymerization Reactions under Visible Lights: Principle, Mechanisms and Examples of Applications. *Prog. Org. Coatings* **2003**, *47*, 16.

(74) Crivello, J. V.; Reichmanis, E. Photopolymer Materials and Processes for Advanced Technologies. *Chem. Mater.* **2014**, *26*, 533.

(75) Childs, A.; Li, H.; Lewittes, D. M.; Dong, B.; Liu, W.; Shu, X.; Sun, C.; Zhang, H. F.

Fabricating Customized Hydrogel Contact Lens. *Sci. Rep.* **2016**, *6*, 34905.

(76) Stansbuty, J. W. Curing Dental Resins and Composites by Photopolymerization. *J. Esthet. Restor. Dent.* **2000**, *12*, 300.

(77) Lloret, T.; Navarro-Fuster, V.; Ramírez, M.; Ortuño, M.; Neipp, C.; Beléndez, A.; Pascual, I. Holographic Lenses in an Environment-Friendly Photopolymer. *Polymers (Basel).* **2018**, *10*, 302.

(78) Zhang, J.; Xiao, P. 3D Printing of Photopolymers. *Polym. Chem.* **2018**, *9*, 1530.

(79) Fertier, L.; Koleilat, H.; Stemmelen, M.; Giani, O.; Joly-Duhamel, C.; Lapinte, V.; Robin, J.-J. The Use of Renewable Feedstock in UV-Curable Materials – A New Age for Polymers and Green Chemistry. *Prog. Polym. Sci.* **2013**, *38*, 932.

(80) Baek, S.-S. S.; Hwang, S.-H. H. Eco-Friendly UV-Curable Pressure Sensitive Adhesives Containing Acryloyl Derivatives of Monosaccharides and Their Adhesive Performances. *Int. J. Adhes. Adhes.* **2016**, *70*, 110.

(81) Yu, A. Z.; Sahouani, J. M.; Webster, D. C. Highly Functional Methacrylated Bio-Based Resins for UV-Curable Coatings. *Prog. Org. Coatings* **2018**, *122*, 219.

(82) Brännström, S.; Malmström, E.; Johansson, M. Biobased UV-Curable Coatings Based on Itaconic Acid. *J. Coatings Technol. Res.* **2017**, *14*, 851.

(83) Jeong, J.; Kim, B.; Shin, S.; Kim, B.; Lee, J. S.; Lee, S. H.; Cho, J. K. Synthesis and Photo-Polymerization of Bio-Based Furanic Compounds Functionalized by 2-Hydroxypropyl Methacrylate Group(S). *J. Appl. Polym. Sci.* **2013**, *127*, 2483.

(84) Jang, N. R.; Kim, H. R.; Hou, C. T.; Kim, B. S. Novel Biobased Photo-Crosslinked Polymer Networks Prepared from Vegetable Oil and 2,5-Furan Diacrylate. *Polym. Adv. Technol.* **2013**, *24*, 814.

(85) Larsen, D. B.; Sønderbæk-Jørgensen, R.; Duus, J.; Daugaard, A. E. Investigation of Curing Rates of Bio-Based Thiol-Ene Films from Diallyl 2,5-Furandicaboxylate. *Eur. Polym. J.* **2018**, *102*, 1.

(86) Prandato, E.; Livi, S.; Melas, M.; Auclair, J.; Verney, V.; Fleury, E.; Méchin, F. Effect of Bio-Based Monomers on the Scratch Resistance of Acrylate Photopolymerizable Coatings. *J. Polym. Sci. Part B Polym. Phys.* **2015**, *53*, 379.

(87) Voet, V. S. D.; Strating, T.; Schnelting, G. H. M.; Dijkstra, P.; Tietema, M.; Xu, J.; Woortman, A. J. J.; Loos, K.; Jager, J.; Folkersma, R. Biobased Acrylate Photocurable Resin Formulation for Stereolithography 3D Printing. *ACS Omega* **2018**, *3*, 1403.

(88) Yoshimura, T.; Shimasaki, T.; Teramoto, N.; Shibata, M. Bio-Based Polymer Networks by Thiol-Ene Photopolymerizations of Allyl-Etherified Eugenol Derivatives. *Eur. Polym. J.* **2015**, *67*, 397.

(89) Dai, J.; Jiang, Y.; Liu, X.; Wang, J.; Zhu, J. Synthesis of Eugenol-Based Multifunctional Monomers via a Thiol-Ene Reaction and Preparation of UV Curable Resins Together with Soybean Oil Derivatives. *RSC Adv.* **2016**, *6*, 17857.

(90) Modjinou, T.; Versace, D. L.; Abbad-Andallousi, S.; Bousserrhine, N.; Dubot, P.; Langlois, V.; Renard, E. Antibacterial and Antioxidant Bio-Based Networks Derived from Eugenol

Using Photo-Activated Thiol-Ene Reaction. *React. Funct. Polym.* **2016**, *101*, 47.

(91) Guzmán, D.; Ramis, X.; Fernández-Francos, X.; De la Flor, S.; Serra, A. New Bio-Based Materials Obtained by Thiol-Ene/Thiol-Epoxy Dual Curing Click Procedures from Eugenol Derivates. *Eur. Polym. J.* **2017**, *93*, 530.

(92) Guzmán, D.; Ramis, X.; Fernández-Francos, X.; De la Flor, S.; Serra, A. Preparation of New Biobased Coatings from a Triglycidyl Eugenol Derivative through Thiol-Epoxy Click Reaction. *Prog. Org. Coatings* **2018**, *114*, 259.

(93) Modjinou, T.; Versace, D. L.; Abbad-Andaloussi, S.; Langlois, V.; Renard, E. Enhancement of Biological Properties of Photoinduced Biobased Networks by Post-Functionalization with Antibacterial Molecule. *ACS Sustain. Chem. Eng.* **2019**, *7*, 2500.

(94) Gan, Y.; Jiang, X. Photo-Cured Materials from Vegetable Oils. *RSC Green Chem.* **2015**, *2015-Janua*, 1.

(95) Bigot, S.; Daghrir, M.; Mhanna, A.; Boni, G.; Pourchet, S.; Lecamp, L.; Plasseraud, L. Undecylenic Acid: A Tunable Bio-Based Synthon for Materials Applications. *Eur. Polym. J.* **2016**, *74*, 26.

(96) Dai, J.; Liu, X.; Ma, S.; Wang, J.; Shen, X.; You, S.; Zhu, J. Soybean Oil-Based UV-Curable Coatings Strengthened by Crosslink Agent Derived from Itaconic Acid Together with 2-Hydroxyethyl Methacrylate Phosphate. *Prog. Org. Coatings* **2016**, *97*, 210.

(97) Li, S.; Yang, X.; Huang, K.; Li, M.; Xia, J. Design, Preparation and Properties of Novel Renewable UV-Curable Copolymers Based on Cardanol and Dimer Fatty Acids. *Prog. Org. Coatings* **2014**, *77*, 388.

(98) Hu, Y.; Shang, Q.; Wang, C.; Feng, G.; Liu, C.; Xu, F.; Zhou, Y. Renewable Epoxidized Cardanol-Based Acrylate as a Reactive Diluent for UV-Curable Resins. *Polym. Adv. Technol.* **2018**, *29*, 1852.

(99) Dalle Vacche, S.; Vitale, A.; Bongiovanni, R. Photocuring of Epoxidized Cardanol for Biobased Composites with Microfibrillated Cellulose. *Molecules* **2019**, *24*, 3858.

(100) Ligon, S. C.; Husár, B.; Wutzel, H.; Holman, R.; Liska, R. Strategies to Reduce Oxygen Inhibition in Photoinduced Polymerization. *Chem. Rev.* **2014**, *114*, 557.

(101) Bolon, D. A.; Webb, K. K. Barrier Coats versus Inert Atmospheres. The Elimination of Oxygen Inhibition in Free-Radical Polymerizations. *J. Appl. Polym. Sci.* **1978**, *22*, 2543.

(102) Decker, C.; Moussa, K. Real-Time Kinetic Study of Laser-Induced Polymerization. *Macromolecules* **1989**, *22*, 4455.

(103) Decker, C. The Use of UV Irradiation in Polymerization. *Polym. Int.* **1998**, *45*, 133.

(104) Lyubimova, T.; Righetti, P. G. On the Kinetics of Photopolymerization: A Theoretical Study. *Electrophoresis* **1993**, *14*, 191.

(105) Eibel, A.; Fast, D. E.; Gescheidt, G. Choosing the Ideal Photoinitiator for Free Radical Photopolymerizations: Predictions Based on Simulations Using Established Data. *Polym. Chem.* **2018**, *9*, 5107.

(106) Allen, N. S. Chapter 8. Polymer Photochemistry. In *Photochemistry*; Royal Society of Chemistry: Cambridge, 2007; Vol. 36, pp 232–297.

(107) Courtecuisse, F.; Belbakra, A.; Croutxé-Barghorn, C.; Allonas, X.; Dietlin, C. Zirconium Complexes to Overcome Oxygen Inhibition in Free-Radical Photopolymerization of Acrylates: Kinetic, Mechanism, and Depth Profiling. *J. Polym. Sci. Part A Polym. Chem.* **2011**, *49*, 5169.

(108) Xia, Y.; Larock, R. C. Vegetable Oil-Based Polymeric Materials: Synthesis, Properties, and Applications. *Green Chem.* **2010**, *12*, 1893.

(109) Zhang, C.; Garrison, T. F.; Madbouly, S. A.; Kessler, M. R. Recent Advances in Vegetable Oil-Based Polymers and Their Composites. *Prog. Polym. Sci.* **2017**, *71*, 91.

(110) Qurat-ul-Ain; Zia, K. M.; Zia, F.; Ali, M.; Rehman, S.; Zuber, M. Lipid Functionalized Biopolymers: A Review. *Int. J. Biol. Macromol.* **2016**, *93*, 1057.

(111) Meier, M. A. R. R.; Metzger, J. O.; Schubert, U. S. Plant Oil Renewable Resources as Green Alternatives in Polymer Science. *Chem. Soc. Rev.* **2007**, *36*, 1788.

(112) World, U. S. D. of A. O.; Trade, M. and. United States Department of Agriculture: Oilseeds: World Markets and Trade https://apps.fas.usda.gov/psdonline/app/index.html#/app/downloads.

(113) Demchuk, Z.; Shevchuk, O.; Tarnavchyk, I.; Kirianchuk, V.; Lorenson, M.; Kohut, A.; Voronov, S.; Voronov, A. Free-Radical Copolymerization Behavior of Plant-Oil-Based Vinyl Monomers and Their Feasibility in Latex Synthesis. *ACS Omega* **2016**, *1*, 1374.

(114) Thames, S.; Smith, O. W.; Evans, J. M.; Dutta, S.; Chen, L. Functionalized Vegetable Oil Derivaties, Latex Compositions and Coatings. 2005/0203246 A1, 2005.

(115) Sharmin, E.; Zafar, F.; Akram, D.; Alam, M.; Ahmad, S. Recent Advances in Vegetable Oils Based Environment Friendly Coatings: A Review. *Ind. Crops Prod.* **2015**, *76*, 215.

(116) Vendamme, R.; Schüwer, N.; Eevers, W. Recent Synthetic Approaches and Emerging Bio-Inspired Strategies for the Development of Sustainable Pressure-Sensitive Adhesives Derived from Renewable Building Blocks. *J. Appl. Polym. Sci.* **2014**, *131*, 40669.

(117) Mosiewicki, M. A.; Aranguren, M. I. Recent Developments in Plant Oil Based Functional Materials. *Polym. Int.* **2016**, *65*, 28.

(118) Seniha Güner, F.; Yağci, Y.; Tuncer Erciyes, A. Polymers from Triglyceride Oils. *Prog. Polym. Sci.* **2006**, *31*, 633.

(119) Nabuurs, T.; Baijards, R. A.; German, A. L. Alkyd-Acrylic Hybrid Systems for Use as Binders in Waterborne Paints. *Prog. Org. Coatings* **1996**, *27*, 163.

(120) Booth, G.; Delatte, D. E.; Thames, S. F. Incorporation of Drying Oils into Emulsion Polymers for Use in Low-VOC Architectural Coatings. *Ind. Crops Prod.* **2007**, *25*, 257.

(121) Uschanov, P.; Heiskanen, N.; Mononen, P.; Maunu, S. L.; Koskimies, S. Synthesis and Characterization of Tall Oil Fatty Acids-Based Alkyd Resins and Alkyd-Acrylate Copolymers. *Prog. Org. Coatings* **2008**, *63*, 92.

(122) Matsumoto, A.; Murakami, N.; Aota, H.; Ikeda, J.; Capek, I. Emulsion Polymerization of Lauryl Methacrylate and Its Copolymerization with Trimethylolpropane Trimethacrylate. *Polymer (Guildf).* **1999**, *40*, 5687.

(123) Boscán, F.; Paulis, M.; Barandiaran, M. J. Towards the Production of High Performance

Lauryl Methacrylate Based Polymers through Emulsion Polymerization. *Eur. Polym. J.* **2017**, *93*, 44.

(124) Guo, J.; Schork, F. J. Hybrid Miniemulsion Polymerization of Acrylate/Oil and Acrylate/Fatty Acid Systems. *Macromol. React. Eng.* **2008**, *2*, 265.

(125) Quintero, C.; Mendon, S. K.; Smith, O. W.; Thames, S. F. Miniemulsion Polymerization of Vegetable Oil Macromonomers. *Prog. Org. Coatings* **2006**, *57*, 195.

(126) Wang, S. T.; Schork, F. J.; Poehlein, G. W.; Gooch, J. W. Emulsion and Miniemulsion Copolymerization of Acrylic Monomers in the Presence of Alkyd Resin. *J. Appl. Polym. Sci.* **1996**, *60*, 2069.

(127) Wu, X. Q.; Schork, F. J.; Gooch, J. W. Hybrid Miniemulsion Polymerization of Acrylic/Alkyd Systems and Characterization of the Resulting Polymers. *J. Polym. Sci. Part A Polym. Chem.* **1999**, *37*, 4159.

(128) Bigon, J. P.; Montoro, F. E.; Lona, L. M. F. F. Vegetable Oils Acting as Encapsulated Bioactives and Costabilizers in Miniemulsion Polymerization Reactions. *Eur. J. Lipid Sci. Technol.* **2018**, *120*, 1700130.

(129) Bunker, S. P.; Wool, R. P. Synthesis and Characterization of Monomers and Polymers for Adhesives from Methyl Oleate. *J. Polym. Sci. Part A Polym. Chem.* **2002**, *40*, 451.

(130) Scala, J. La; Wool, R. P. The Effect of Fatty Acid Composition on the Acrylation Kinetics of Epoxidized Triacylglycerols. *J. Am. Oil Chem. Soc.* **2002**, *79*, 59.

(131) Wool, R. P.; Bunker, S. P. Pressure Sensitive Adhesives from Plant Oils. 6,646,033 B2, 2003.

(132) Jensen, A. T.; Sayer, C.; Araujo, P. H. H.; Machado, F. Emulsion Copolymerization of Styrene and Acrylated Methyl Oleate. *Eur. J. Lipid Sci. Technol.* **2014**, *116*, 37.

(133) Ferreira, G. R.; Braquehais, J. R.; da Silva, W. N.; Machado, F. Synthesis of Soybean Oil-Based Polymer Lattices via Emulsion Polymerization Process. *Ind. Crops Prod.* **2015**, *65*, 14.

(134) Diamond, K. L.; Pandey, R. B.; Thames, S. F. Modeling the Polymerization Behavior of Vegetable-Oil-Derived Macromonomers in Solution by Computer Simulation. *J. Polym. Sci. Part B Polym. Phys.* **2004**, *42*, 1164.

(135) Thames, S. F.; Panjani, K. G.; Fruchey, O. S. Latex Compositions Containing Ethylenically Unsaturated Esters of Long-Chan Alkenols. 6,001,913, 1999.

(136) Delatte, D.; Kaya, E.; Kolibal, L. G.; Mendon, S. K.; Rawlins, J. W.; Thames, S. F. Synthesis and Characterization of a Soybean Oil-Based Macromonomer. *J. Appl. Polym. Sci.* **2014**, *131*, 40249.

(137) Thames, S. F.; Rawlins, J. W.; Mendon, Sharathkumar K. Delatte, D. U.S. Pat. Appl. 0,143,527. **2009**, *1*.

(138) Tarnavchyk, I.; Popadyuk, A.; Popadyuk, N.; Voronov, A. Synthesis and Free Radical Copolymerization of a Vinyl Monomer from Soybean Oil. *ACS Sustain. Chem. Eng.* **2015**, *3*, 1618.

(139) Demchuk, Z.; Shevchuk, O.; Tarnavchyk, I.; Kirianchuk, V.; Kohut, A.; Voronov, S.; Voronov,

A. Free Radical Polymerization Behavior of the Vinyl Monomers from Plant Oil Triglycerides. *ACS Sustain. Chem. Eng.* **2016**, *4*, 6974.

(140) Kingsley, K.; Shevchuk, O.; Demchuk, Z.; Voronov, S.; Voronov, A. The Features of Emulsion Copolymerization for Plant Oil-Based Vinyl Monomers and Styrene. *Ind. Crops Prod.* **2017**, *109*, 274.

(141) Roberge, S.; Dubé, M. A. Emulsion-Based Pressure Sensitive Adhesives from Conjugated Linoleic Acid/Styrene/Butyl Acrylate Terpolymers. *Int. J. Adhes. Adhes.* **2016**, *70*, 17.

(142) Badía, A.; Movellan, J.; Barandiaran, M. J.; Leiza, J. R. High Biobased Content Latexes for Development of Sustainable Pressure Sensitive Adhesives. *Ind. Eng. Chem. Res.* **2018**, *57*, 14509.

(143) Badía, A.; Santos, J. I.; Agirre, A.; Barandiaran, M. J.; Leiza, J. R. UV-Tunable Biobased Pressure-Sensitive Adhesives Containing Piperonyl Methacrylate. *ACS Sustain. Chem. Eng.* **2019**, *7*, 19122.

(144) Bunker, S.; Staller, C.; Willenbacher, N.; Wool, R. Miniemulsion Polymerization of Acrylated Methyl Oleate for Pressure Sensitive Adhesives. *Int. J. Adhes. Adhes.* **2003**, *23*, 29.

(145) Thames, S. F.; Rawlins, J. W.; Mendon, S. K. Miniemulsion Polymerization of Vegetable Oil Macromonomers. In *Miniemulsion Polymerization Technology*; John Wiley & Sons, Inc.: Hoboken, NJ, USA, 2010; Vol. 57, pp 139–171.

(146) Medeiros, A. M. M. S.; Machado, F.; Rubim, J. C.; McKenna, T. F. L. Bio-Based Copolymers Obtained through Miniemulsion Copolymerization of Methyl Esters of Acrylated Fatty Acids and Styrene. *J. Polym. Sci. Part A Polym. Chem.* **2017**, *55*, 1422.

(147) Laurentino, L. S.; Medeiros, A. M. M. S.; Machado, F.; Costa, C.; Araújo, P. H. H.; Sayer, C. Synthesis of a Biobased Monomer Derived from Castor Oil and Copolymerization in Aqueous Medium. *Chem. Eng. Res. Des.* **2018**, *137*, 213.

(148) Maaßen, W.; Oelmann, S.; Peter, D.; Oswald, W.; Willenbacher, N.; Meier, M. A. R. Novel Insights into Pressure-Sensitive Adhesives Based on Plant Oils. *Macromol. Chem. Phys.* **2015**, *216*, 1609.

(149) Maaßen, W.; Meier, M. A. R.; Willenbacher, N. Unique Adhesive Properties of Pressure Sensitive Adhesives from Plant Oils. *Int. J. Adhes. Adhes.* **2016**, *64*, 65.

(150) Demchuk, Z.; Kohut, A.; Voronov, S.; Voronov, A. Versatile Platform for Controlling Properties of Plant Oil-Based Latex Polymer Networks. *ACS Sustain. Chem. Eng.* **2018**, *6*, 2780.

(151) Demchuk, Z.; Kirianchuk, V.; Kingsley, K.; Voronov, S.; Voronov, A. Plasticizing and Hydrophobizing Effect of Plant OilBased Acrylic Monomers in Latex Copolymers with Styrene and Methyl Methacrylate. *Int. J. Theor. Appl. Nanotechnol.* **2018**, *6*, 29.

(152) Moreno, M.; Goikoetxea, M.; Barandiaran, M. J. Biobased-Waterborne Homopolymers from Oleic Acid Derivatives. *J. Polym. Sci. Part A Polym. Chem.* **2012**, *50*, 4628.

(153) Moreno, M.; Miranda, J. I.; Goikoetxea, M.; Barandiaran, M. J. Sustainable Polymer Latexes Based on Linoleic Acid for Coatings Applications. *Prog. Org. Coatings* **2014**, *77*, 1709.

(154) La Scala, J. J.; Sands, J. M.; Orlicki, J. A.; Robinette, E. J.; Palmese, G. R. Fatty Acid-Based

Monomers as Styrene Replacements for Liquid Molding Resins. *Polymer (Guildf).* **2004**, *45*, 7729.

(155) Moreno, M.; Goikoetxea, M.; Barandiaran, M. J. Surfactant-Free Miniemulsion Polymerization of a Bio-Based Oleic Acid Derivative Monomer. *Macromol. React. Eng.* **2014**, *8*, 434.

(156) Ronco, L. I.; Minari, R. J.; Gugliotta, L. M. Particle Nucleation Using Different Initiators in the Miniemulsion Polymerization of Styrene. *Brazilian J. Chem. Eng.* **2015**, *32*, 191.

(157) Moreno, M. M.; Goikoetxea, M.; De La Cal, J. C.; Barandiaran, M. J. From Fatty Acid and Lactone Biobased Monomers toward Fully Renewable Polymer Latexes. *J. Polym. Sci. Part A Polym. Chem.* **2014**, *52*, 3543.

(158) Trotta, J. T.; Jin, M.; Stawiasz, K. J.; Michaudel, Q.; Chen, W.-L.; Fors, B. P. Synthesis of Methylene Butyrolactone Polymers from Itaconic Acid. *J. Polym. Sci. Part A Polym. Chem.* **2017**, *55*, 2730.

(159) Akkapeddi, M. K. Poly(α-Methylene-γ-Butyrolactone) Synthesis, Configurational Structure, and Properties. *Macromolecules* **1979**, *12*, 546.

(160) Moreno, M.; Lampard, C.; Williams, N.; Lago, E.; Emmett, S.; Goikoetxea, M.; Barandiaran, M. J. Eco-Paints from Bio-Based Fatty Acid Derivative Latexes. *Prog. Org. Coatings* **2015**, *81*, 101.

(161) Machado, T. O.; Cardoso, P. B.; Feuser, P. E.; Sayer, C.; Araújo, P. H. H. H. Thiol-Ene Miniemulsion Polymerization of a Biobased Monomer for Biomedical Applications. *Colloids Surfaces B Biointerfaces* **2017**, *159*, 509.

(162) Cardoso, P. B.; Machado, T. O.; Feuser, P. E.; Sayer, C.; Meier, M. A. R. R.; Araújo, P. H. H. H. Biocompatible Polymeric Nanoparticles From Castor Oil Derivatives via Thiol-Ene Miniemulsion Polymerization. *Eur. J. Lipid Sci. Technol.* **2018**, *120*, 1700212.

(163) Romera, C. D. O.; de Oliveira, D.; de Araújo, P. H. H.; Sayer, C. Biobased Ester 2-(10-Undecenoyloxy)Ethyl Methacrylate as an Asymmetrical Diene Monomer in Thiol–Ene Polymerization. *Ind. Eng. Chem. Res.* **2019**, *58*, 21044.

(164) Tajbakhsh, S.; Hajiali, F.; Marić, M. Nitroxide-Mediated Miniemulsion Polymerization of Bio-Based Methacrylates. *Ind. Eng. Chem. Res.* **2020**, acs. iecr.0c00840.

(165) Black, M.; Messman, J.; Rawlins, J. Chain Transfer of Vegetable Oil Macromonomers in Acrylic Solution Copolymerization. *J. Appl. Polym. Sci.* **2011**, *120*, 1390.

(166) Tsavalas, J. G.; Luo, Y.; Schork, F. J. Grafting Mechanisms in Hybrid Miniemulsion Polymerization. *J. Appl. Polym. Sci.* **2003**, *87*, 1825.

(167) Hudda, L.; Tsavalas, J. G.; Schork, F. J. Simulation Studies on the Origin of the Limiting Conversion Phenomenon in Hybrid Miniemulsion Polymerization. *Polymer (Guildf).* **2005**, *46*, 993.

(168) Costa, C.; Wagner, M.; Musyanovych, A.; Landfester, K.; Sayer, C.; Araújo, P. H. H. H. Decrease of Methyl Methacrylate Miniemulsion Polymerization Rate with Incorporation of Plant Oils. *Eur. J. Lipid Sci. Technol.* **2016**, *118*, 93.

(169) Gunstone, F. D. Supplies of Vegetable Oils for Non-Food Purposes. *Eur. J. Lipid Sci.*

Technol. **2011**, *113*, 3.

(170) Atabani, A. E. E.; Silitonga, A. S. S.; Ong, H. C. C.; Mahlia, T. M. I. M. I.; Masjuki, H. H. H.; Badruddin, I. A.; Fayaz, H. Non-Edible Vegetable Oils: A Critical Evaluation of Oil Extraction, Fatty Acid Compositions, Biodiesel Production, Characteristics, Engine Performance and Emissions Production. *Renew. Sustain. Energy Rev.* **2013**, *18*, 211.

(171) Ladmiral, V.; Jeannin, R.; Fernandes Lizarazu, K.; Lai-Kee-Him, J.; Bron, P.; Lacroix-Desmazes, P.; Caillol, S. Aromatic Biobased Polymer Latex from Cardanol. *Eur. Polym. J.* **2017**, *93*, 785.

(172) Li, W. S. J.; Negrell, C.; Ladmiral, V.; Lai-Kee-Him, J.; Bron, P.; Lacroix-Desmazes, P.; Joly-Duhamel, C.; Caillol, S. Cardanol-Based Polymer Latex by Radical Aqueous Miniemulsion Polymerization. *Polym. Chem.* **2018**, *9*, 2468.

(173) Demchuk, Z.; Li, W. S. J.; Eshete, H.; Caillol, S.; Voronov, A. Synergistic Effects of Cardanol- and High Oleic Soybean Oil Vinyl Monomers in Miniemulsion Polymers. *ACS Sustain. Chem. Eng.* **2019**, *7*, 9613.

(174) Dworakowska, S.; Cornille, A.; Bogdał, D.; Boutevin, B.; Caillol, S. Formulation of Bio-Based Epoxy Foams from Epoxidized Cardanol and Vegetable Oil Amine. *Eur. J. Lipid Sci. Technol.* **2015**, *117*, 1893.

(175) Gershenzon, J.; Dudareva, N. The Function of Terpene Natural Products in the Natural World. *Nat. Chem. Biol.* **2007**, *3*, 408.

(176) Corma, A.; Iborra, S.; Velty, A. Chemical Routes for the Transformation of Biomass into Chemicals. *Chem. Rev.* **2007**, *107*, 2411.

(177) Tracy, N. I.; Chen, D.; Crunkleton, D. W.; Price, G. L. Hydrogenated Monoterpenes as Diesel Fuel Additives. *Fuel* **2009**, *88*, 2238.

(178) Wilbon, P. A.; Chu, F.; Tang, C. Progress in Renewable Polymers from Natural Terpenes, Terpenoids, and Rosin. *Macromol. Rapid Commun.* **2013**, *34*, 8.

(179) Winnacker, M.; Rieger, B. Recent Progress in Sustainable Polymers Obtained from Cyclic Terpenes: Synthesis, Properties, and Application Potential. *ChemSusChem* **2015**, *8*, 2455.

(180) Liu, S.; Zhou, L.; Yu, S.; Xie, C.; Liu, F.; Song, Z. Polymerization of α-Pinene Using Lewis Acidic Ionic Liquid as Catalyst for Production of Terpene Resin. *Biomass and Bioenergy* **2013**, *57*, 238.

(181) Satoh, K.; Nakahara, A.; Mukunoki, K.; Sugiyama, H.; Saito, H.; Kamigaito, M. Sustainable Cycloolefin Polymer from Pine Tree Oil for Optoelectronics Material: Living Cationic Polymerization of β-Pinene and Catalytic Hydrogenation of High-Molecular-Weight Hydrogenated Poly(β-Pinene). *Polym. Chem.* **2014**, *5*, 3222.

(182) Firdaus, M.; Meier, M. A. R. R. Renewable Polyamides and Polyurethanes Derived from Limonene. *Green Chem.* **2013**, *15*, 370.

(183) Baek, S.-S. S.; Hwang, S.-H. H. Preparation and Adhesion Performance of Transparent Acrylic Pressure-Sensitive Adhesives Containing Menthyl Acrylate. *Polym. Bull.* **2016**, *73*, 687.

(184) Baek, S.-S. S.; Hwang, S.-H. H. Preparation of Biomass-Based Transparent Pressure

Sensitive Adhesives for Optically Clear Adhesive and Their Adhesion Performance. *Eur. Polym. J.* **2017**, *92*, 97.

(185) Behr, A.; Johnen, L. Myrcene as a Natural Base Chemical in Sustainable Chemistry: A Critical Review. *ChemSusChem* **2009**, *2*, 1072.

(186) Sarkar, P.; Bhowmick, A. K. Synthesis, Characterization and Properties of a Bio-Based Elastomer: Polymyrcene. *RSC Adv.* **2014**, *4*, 61343.

(187) Sarkar, P.; Bhowmick, A. K. Terpene Based Sustainable Methacrylate Copolymer Series by Emulsion Polymerization: Synthesis and Structure-Property Relationship. *J. Polym. Sci. Part A Polym. Chem.* **2017**, *55*, 2639.

(188) Sarkar, P.; Bhowmick, A. K. Terpene Based Sustainable Elastomer for Low Rolling Resistance and Improved Wet Grip Application: Synthesis, Characterization and Properties of Poly(Styrene- Co -Myrcene). *ACS Sustain. Chem. Eng.* **2016**, *4*, 5462.

(189) Sarkar, P.; Bhowmick, A. K. Green Approach toward Sustainable Polymer: Synthesis and Characterization of Poly(Myrcene- Co -Dibutyl Itaconate). *ACS Sustain. Chem. Eng.* **2016**, *4*, 2129.

(190) Sarkar, P.; Bhowmick, A. K. Terpene-Based Sustainable Elastomers: Vulcanization and Reinforcement Characteristics. *Ind. Eng. Chem. Res.* **2018**, *57*, 5197.

(191) Sahu, P.; Sarkar, P.; Bhowmick, A. K. Design of a Molecular Architecture via a Green Route for an Improved Silica Reinforced Nanocomposite Using Bioresources. *ACS Sustain. Chem. Eng.* **2018**, *6*, 6599.

(192) Lei, W.; Yang, X.; Qiao, H.; Shi, D.; Wang, R.; Zhang, L. Renewable Resource-Based Elastomer Nanocomposite Derived from Myrcene, Ethanol, Itaconic Acid and Nanosilica: Design, Preparation and Properties. *Eur. Polym. J.* **2018**, *106*, 1.

(193) Sahu, P.; Sarkar, P.; Bhowmick, A. K. Synthesis and Characterization of a Terpene-Based Sustainable Polymer: Poly-Alloocimene. *ACS Sustain. Chem. Eng.* **2017**, *5*, 7659.

(194) Sahu, P.; Bhowmick, A. K. Redox Emulsion Polymerization of Terpenes: Mapping the Effect of the System, Structure, and Reactivity. *Ind. Eng. Chem. Res.* **2019**, *58*, 20946.

(195) Zhang, L.; Cao, Y.; Wang, L.; Shao, L.; Bai, Y. Polyacrylate Emulsion Containing IBOMA for Removable Pressure Sensitive Adhesives. *J. Appl. Polym. Sci.* **2016**, *133*, 42886.

(196) Noppalit, S.; Simula, A.; Billon, L.; Asua, J. M. Paving the Way to Sustainable Waterborne Pressure-Sensitive Adhesives Using Terpene-Based Triblock Copolymers. *ACS Sustain. Chem. Eng.* **2019**, *7*, 17990.

(197) Noppalit, S.; Simula, A.; Billon, L.; Asua, J. M. On the Nitroxide Mediated Polymerization of Methacrylates Derived from Bio-Sourced Terpenes in Miniemulsion, a Step towards Sustainable Products. *Polym. Chem.* **2020**, *11*, 1151.

(198) Loughmari, S.; Hafid, A.; Bouazza, A.; El Bouadili, A.; Zinck, P.; Visseaux, M. Highly Stereoselective Coordination Polymerization of β-Myrcene from a Lanthanide-Based Catalyst: Access to Bio-Sourced Elastomers. *J. Polym. Sci. Part A Polym. Chem.* **2012**, *50*, 2898.

(199) Sainz, M. F.; Souto, J. A.; Regentova, D.; Johansson, M. K. G. G.; Timhagen, S. T.; Irvine,

D. J.; Buijsen, P.; Koning, C. E.; Stockman, R. A.; Howdle, S. M. A Facile and Green Route to Terpene Derived Acrylate and Methacrylate Monomers and Simple Free Radical Polymerisation to Yield New Renewable Polymers and Coatings. *Polym. Chem.* **2016**, *7*, 2882.

(200) Llevot, A.; Grau, E.; Carlotti, S.; Grelier, S.; Cramail, H. From Lignin-Derived Aromatic Compounds to Novel Biobased Polymers. *Macromol. Rapid Commun.* **2016**, *37*, 9.

(201) Abdelaziz, O. Y.; Hulteberg, C. P. Physicochemical Characterisation of Technical Lignins for Their Potential Valorisation. *Waste and Biomass Valorization* **2017**, *8*, 859.

(202) Li, C.; Zhao, X.; Wang, A.; Huber, G. W.; Zhang, T. Catalytic Transformation of Lignin for the Production of Chemicals and Fuels. *Chem. Rev.* **2015**, *115*, 11559.

(203) Azadi, P.; Inderwildi, O. R.; Farnood, R.; King, D. A. Liquid Fuels, Hydrogen and Chemicals from Lignin: A Critical Review. *Renew. Sustain. Energy Rev.* **2013**, *21*, 506.

(204) Ragauskas, A. J.; Beckham, G. T.; Biddy, M. J.; Chandra, R.; Chen, F.; Davis, M. F.; Davison, B. H.; Dixon, R. A.; Gilna, P.; Keller, M.; et al. Lignin Valorization: Improving Lignin Processing in the Biorefinery. *Science (80-.).* **2014**, *344*, 1246843.

(205) Sun, Z.; Fridrich, B.; De Santi, A.; Elangovan, S.; Barta, K. Bright Side of Lignin Depolymerization: Toward New Platform Chemicals. *Chem. Rev.* **2018**, *118*, 614.

(206) Ten, E.; Vermerris, W. Recent Developments in Polymers Derived from Industrial Lignin. *J. Appl. Polym. Sci.* **2015**, *132*, 42069.

(207) Holmberg, A. L.; Stanzione, J. F.; Wool, R. P.; Epps, T. H. A Facile Method for Generating Designer Block Copolymers from Functionalized Lignin Model Compounds. *ACS Sustain. Chem. Eng.* **2014**, *2*, 569.

(208) Rojo, L.; Vazquez, B.; Parra, J.; López Bravo, A.; Deb, S.; San Roman, J. From Natural Products to Polymeric Derivatives of “Eugenol”: A New Approach for Preparation of Dental Composites and Orthopedic Bone Cements. *Biomacromolecules* **2006**, *7*, 2751.

(209) Stanzione, J. F.; Sadler, J. M.; La Scala, J. J.; Wool, R. P. Lignin Model Compounds as Bio-Based Reactive Diluents for Liquid Molding Resins. *ChemSusChem* **2012**, *5*, 1291.

(210) Takeshima, H.; Satoh, K.; Kamigaito, M. Bio-Based Functional Styrene Monomers Derived from Naturally Occurring Ferulic Acid for Poly(Vinylcatechol) and Poly(Vinylguaiacol) via Controlled Radical Polymerization. *Macromolecules* **2017**, *50*, 4206.

(211) Li, W. S. J.; Ladmiral, V.; Takeshima, H.; Satoh, K.; Kamigaito, M.; Semsarilar, M.; Negrell, C.; Lacroix-Desmazes, P.; Caillol, S. Ferulic Acid-Based Reactive Core–Shell Latex by Seeded Emulsion Polymerization. *Polym. Chem.* **2019**, *10*, 3116.

(212) Deng, J.; Yang, B.; Chen, C.; Liang, J. Renewable Eugenol-Based Polymeric Oil-Absorbent Microspheres: Preparation and Oil Absorption Ability. *ACS Sustain. Chem. Eng.* **2015**, *3*, 599.

(213) Zhang, H.; Yong, X.; Zhou, J.; Deng, J.; Wu, Y. Biomass Vanillin-Derived Polymeric Microspheres Containing Functional Aldehyde Groups: Preparation, Characterization, and Application as Adsorbent. *ACS Appl. Mater. Interfaces* **2016**, *8*, 2753.

(214) Zhang, H.; Deng, J.; Wu, Y. Biobased Magnetic Microspheres Containing Aldehyde Groups:

Constructed by Vanillin-Derived Polymethacrylate/Fe3O4 and Recycled in Adsorbing Amine. *ACS Sustain. Chem. Eng.* **2017**, *5*, 658.

(215) Varanasi, P.; Singh, P.; Auer, M.; Adams, P. D.; Simmons, B. A.; Singh, S. Survey of Renewable Chemicals Produced from Lignocellulosic Biomass during Ionic Liquid Pretreatment. *Biotechnol. Biofuels* **2013**, *6*, 14.

(216) Lichtenthaler, F. W.; Peters, S. Carbohydrates as Green Raw Materials for the Chemical Industry. *Comptes Rendus Chim.* **2004**, *7*, 65.

(217) Vilela, C.; Sousa, A. F.; Fonseca, A. C.; Serra, A. C.; Coelho, J. F. J.; Freire, C. S. R.; Silvestre, A. J. D. The Quest for Sustainable Polyesters – Insights into the Future. *Polym. Chem.* **2014**, *5*, 3119.

(218) Sousa, A. F.; Vilela, C.; Fonseca, A. C.; Matos, M.; Freire, C. S. R.; Gruter, G.-J. M.; Coelho, J. F. J.; Silvestre, A. J. D. Biobased Polyesters and Other Polymers from 2,5-Furandicarboxylic Acid: A Tribute to Furan Excellency. *Polym. Chem.* **2015**, *6*, 5961.

(219) Thomas, H.; Tim, L.; Andreas, K. *Esterification of Polysaccharides*; Springer Laboratory; Springer-Verlag: Berlin/Heidelberg, 2006.

(220) Brune, D.; Eben-Worlée, R. Von. Starch-Based Graft Polymer, Process for Its Preparation, and Use Thereof in Printing Inks and Overprint Varnishes. 6,423,775 B1, 2002.

(221) George, C.; El Rassy, H.; Chovelon, J. M. Reactivity of Selected Volatile Organic Compounds (VOCs) toward the Sulfate Radical (SO4-). *Int. J. Chem. Kinet.* **2001**, *33*, 539.

(222) Li, P.; Zhu, J.; Sunintaboon, P.; Harris, F. W. New Route to Amphiphilic Core-Shell Polymer Nanospheres: Graft Copolymerization of Methyl Methacrylate from Water-Soluble Polymer Chains Containing Amino Groups. *Langmuir* **2002**, *18*, 8641.

(223) Harris, F. W.; Pei, L.; Jun Min, Z. Amphiphilic Core-Shell Latexes. 2002/0143081 A1, 2002.

(224) Ye, W.; Leung, M. F.; Xin, J.; Kwong, T. L.; Lee, D. K. L.; Li, P. Novel Core-Shell Particles with Poly(n-Butyl Acrylate) Cores and Chitosan Shells as an Antibacterial Coating for Textiles. *Polymer (Guildf).* **2005**, *46*, 10538.

(225) Xin, J. H.; Ye, W.; Pei, L. Textiles with Chitosan Core-Shell Particles. 8,349,343 B2, 2013.

(226) Gaborieau, M.; De bruyn, H.; Mange, S.; Castignolles, P.; Brockmeyer, A.; Gilbert, R. G. Synthesis and Characterization of Synthetic Polymer Colloids Colloidally Stabilized by Cationized Starch Oligomers. *J. Polym. Sci. Part A Polym. Chem.* **2009**, *47*, 1836.

(227) Möller, K., & Glittenberg, D. Novel Starch Containing Polymer Dispersions as Coating Binders. In *TAPPI PaperCon symposium*; 1990; pp 85–91.

(228) Wang, R.-M.; Wang, X.-W.; Guo, J.-F.; He, Y.-F.; Jiang, M.-L. Crosslinkable Potato Starch-Based Graft Copolymer Emulsion for Humidity Controlling Coatings. *Mater. Res.* **2013**, *16*, 1246.

(229) Ho, K. M.; Li, W. Y.; Lee, C. H.; Yam, C. H.; Gilbert, R. G.; Li, P. Mechanistic Study of the Formation of Amphiphilic Core-Shell Particles by Grafting Methyl Methacrylate from Polyethylenimine through Emulsion Polymerization. *Polymer (Guildf).* **2010**, *51*, 3512.

(230) Smeets, N. M. B.; E-Rramdani, M.; van Hal, R. C. F.; Santana, S. G.; Quéléver, K.; Meuldijk, J.; Van Herk, A. M.; Heuts, J. P. A. A Simple One-Step Sonochemical Route towards

Functional Hairy Polymer Nanoparticles. *Soft Matter* **2010**, *6*, 2392.

(231) Cummings, S.; Cunningham, M.; Dubé, M. A. The Use of Amylose-Rich Starch Nanoparticles in Emulsion Polymerization. *J. Appl. Polym. Sci.* **2018**, *135*, 46485.

(232) Zhang, Y.; Cunningham, M. F.; Smeets, N. M. B.; Dubé, M. A. Starch Nanoparticle Incorporation in Latex-Based Adhesives. *Eur. Polym. J.* **2018**, *106*, 128.

(233) Zhang, Y.; Cunningham, M. F.; Smeets, N. M. B.; Dubé, M. A. Increasing Starch Nanoparticle Content in Emulsion Polymer Latexes. *Ind. Eng. Chem. Res.* **2019**, *58*, 20987.

(234) Cummings, S.; Zhang, Y.; Smeets, N.; Cunningham, M.; Dubé, M. On the Use of Starch in Emulsion Polymerizations. *Processes* **2019**, *7*, 140.

(235) Smeets, N. M. B.; Imbrogno, S.; Bloembergen, S. Carbohydrate Functionalized Hybrid Latex Particles. *Carbohydr. Polym.* **2017**, *173*, 233.

(236) Abeylath, S. C.; Turos, E. Glycosylated Polyacrylate Nanoparticles by Emulsion Polymerization. *Carbohydr. Polym.* **2007**, *70*, 32.

(237) Sui, X.; Wang, Z.; Liao, B.; Zhang, Y.; Guo, Q. Preparation of Levoglucosenone through Sulfuric Acid Promoted Pyrolysis of Bagasse at Low Temperature. *Bioresour. Technol.* **2012**, *103*, 466.

(238) Ray, P.; Hughes, T.; Smith, C.; Simon, G. P.; Saito, K. Synthesis of Bioacrylic Polymers from Dihydro-5-Hydroxyl Furan-2-One (2H-HBO) by Free and Controlled Radical Polymerization. *ACS Omega* **2018**, *3*, 2040.

(239) Villanova, J. C. O.; Ayres, E.; Oréfice, R. L. Design, Characterization and Preliminary in Vitro Evaluation of a Mucoadhesive Polymer Based on Modified Pectin and Acrylic Monomers with Potential Use as a Pharmaceutical Excipient. *Carbohydr. Polym.* **2015**, *121*, 372.

(240) Desport, J. S.; Mantione, D.; Moreno, M.; Sardón, H.; Barandiaran, M. J.; Mecerreyes, D. Synthesis of Three Different Galactose-Based Methacrylate Monomers for the Production of Sugar-Based Polymers. *Carbohydr. Res.* **2016**, *432*, 50.

(241) Desport, J. S. Exploring the Use of Carbohydrate Resources for the Production of Waterborne Polymers, University of the Basque Country, 2017.

(242) Desport, J.; Moreno, M.; Barandiaran, M. Fructose-Based Acrylic Copolymers by Emulsion Polymerization. *Polymers (Basel).* **2018**, *10*, 488.

(243) Neqal, M.; Voisin, A.; Neto, V.; Coma, V.; Héroguez, V. New Active Supported Antifungal Systems for Potential Aeronautical Application. *Eur. Polym. J.* **2018**, *105*, 304.

(244) Neto, V.; Voisin, A.; Héroguez, V.; Grelier, S.; Coma, V. Influence of the Variation of the Alkyl Chain Length of n -Alkyl-β- d -Glycosylamine Derivatives on Antifungal Properties. *J. Agric. Food Chem.* **2012**, *60*, 10516.

(245) Badía, A.; Agirre, A.; Barandiaran, M. J.; Leiza, J. R. Removable Biobased Waterborne Pressure-Sensitive Adhesives Containing Mixtures of Isosorbide Methacrylate Monomers. *Biomacromolecules* **2020**, acs. biomac.0c00474.

(246) Anastas, P.; Eghbali, N. Green Chemistry: Principles and Practice. *Chem. Soc. Rev.* **2010**, *39*, 301.

(247) Pokeržnik, N.; Krajnc, M. Synthesis of a Glucose-Based Surfmer and Its Copolymerization

with n-Butyl Acrylate for Emulsion Pressure Sensitive Adhesives. *Eur. Polym. J.* **2015**, *68*, 558.

(248) Guo, M.; Wang, G. Milk Protein Polymer and Its Application in Environmentally Safe Adhesives. *Polymers (Basel).* **2016**, *8*, 324.

(249) Picchio, M. L.; Passeggi, M. C. G.; Barandiaran, M. J.; Gugliotta, L. M.; Minari, R. J. Waterborne Acrylic–Casein Latexes as Eco-Friendly Binders for Coatings. *Prog. Org. Coatings* **2015**, *88*, 8.

(250) Ma, J.; Xu, Q.; Zhou, J.; Gao, D.; Zhang, J.; Chen, L. Nano-Scale Core-Shell Structural Casein Based Coating Latex: Synthesis, Characterization and Its Biodegradability. *Prog. Org. Coatings* **2013**, *76*, 1346.

(251) Xu, Q.; Ma, J.; Zhou, J.; Wang, Y.; Zhang, J. Bio-Based Core-Shell Casein-Based Silica Nano-Composite Latex by Double-in Situ Polymerization: Synthesis, Characterization and Mechanism. *Chem. Eng. J.* **2013**, *228*, 281.

(252) Picchio, M. L.; Minari, R. J.; Gonzalez, V. D. G.; Passeggi, M. C. G.; Vega, J. R.; Barandiaran, M. J.; Gugliotta, L. M. Waterborne Acrylic-Casein Nanoparticles. Nucleation and Grafting. *Macromol. Symp.* **2014**, *344*, 76.

(253) Picchio, M. L.; Bohórquez, S. J.; van den Berg, P. G. C. A. C. A.; Barandiaran, M. J.; Gugliotta, L. M.; Minari, R. J. Waterborne Casein-Based Latexes with High Solids Content and Their High-Throughput Coating Optimization. *Ind. Eng. Chem. Res.* **2016**, *55*, 10271.

(254) Picchio, M. L.; Passeggi, M. C. G.; Barandiaran, M. J.; Gugliotta, L. M.; Minari, R. J. Acrylic/Casein Latexes with Controlled Degree of Grafting and Improved Coating Performance. *Prog. Org. Coatings* **2016**, *101*, 587.

(255) Van Hamersveld, E. M. S.; Van Es, J. J. G. S.; Cuperus, F. P. Oil-Acrylate Hybrid Emulsions, Mini-Emulsion Polymerization and Characterization. *Colloids Surfaces A Physicochem. Eng. Asp.* **1999**, *153*, 285.

(256) Hu, J.; Jin, Z.; Chen, T.-Y. Y.; Polley, J. D.; Cunningham, M. F.; Gross, R. A. Anionic Polymerizable Surfactants from Biobased ω-Hydroxy Fatty Acids. *Macromolecules* **2014**, *47*, 113.

(257) Hazra, C.; Arunbabu, D.; Kundu, D.; Chaudhari, A.; Jana, T. Biomimetic Fabrication of Biocompatible and Biodegradable Core-Shell Polystyrene/Biosurfactant Bionanocomposites for Protein Drug Release. *J. Chem. Technol. Biotechnol.* **2013**, *88*, 1551.

(258) Dubé, M. A.; Salehpour, S. Applying the Principles of Green Chemistry to Polymer Production Technology. *Macromolecular Reaction Engineering*. January 2014, pp 7–28.

(259) Pramod, C. V.; Fauziah, R.; Seshan, K.; Lange, J.-P. Bio-Based Acrylic Acid from Sugar via Propylene Glycol and Allyl Alcohol. *Catal. Sci. Technol.* **2018**, *8*, 289.

(260) Venkitasubramanian, P. Processes for Making Acrylic-Type Monomers and Products Made Therefrom. 9,234,064 B2, 2016.

(261) Lansing, J. C.; Murray, R. E.; Moser, B. R. Biobased Methacrylic Acid via Selective Catalytic Decarboxylation of Itaconic Acid. *ACS Sustain. Chem. Eng.* **2017**, *5*, 3132.

(262) Le Nôtre, J.; Witte-van Dijk, S. C. M.; van Haveren, J.; Scott, E. L.; Sanders, J. P. M. Synthesis of Bio-Based Methacrylic Acid by Decarboxylation of Itaconic Acid and Citric Acid Catalyzed by Solid Transition-Metal Catalysts. *ChemSusChem* **2014**, *7*, 2712.

(263) Kawamura, A.; Hata, Y.; Miyata, T.; Uragami, T. Synthesis of Glucose-Responsive Bioconjugated Gel Particles Using Surfactant-Free Emulsion Polymerization. *Colloids Surfaces B Biointerfaces* **2012**, *99*, 74.

(264) Turkenburg, D. H.; Durant, Y.; Fischer, H. R. Bio-Based Self-Healing Coatings Based on Thermo-Reversible Diels-Alder Reaction. *Prog. Org. Coatings* **2017**, *111*, 38.

(265) Imada, M.; Takenaka, Y.; Hatanaka, H.; Tsuge, T.; Abe, H. Unique Acrylic Resins with Aromatic Side Chains by Homopolymerization of Cinnamic Monomers. *Commun. Chem.* **2019**, *2*, 5.

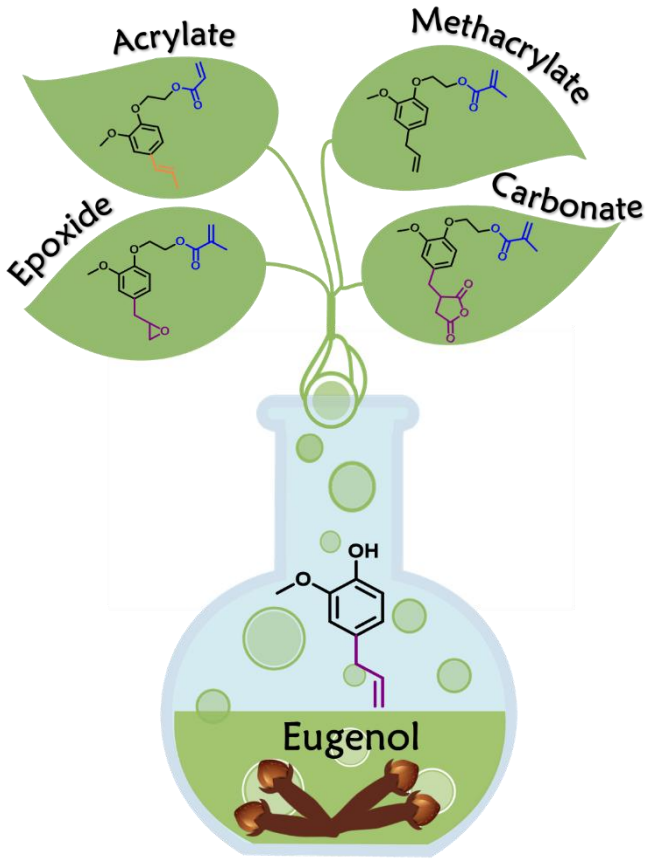

CHAPTER TWO

Monomer synthesis

and solution homopolymerization

Table of contents

Chapter 2: Biobased monomer synthesis and solution homopolymerization

Some of the results and discussion presented in this chapter have been published in the article:

- Molina-Gutiérrez, S.; Manseri, A.; Ladmiral, V.; Bongiovanni, R.; Caillol, S.; Lacroix-Desmazes, P. Eugenol: A Promising Building Block for Synthesis of Radically Polymerizable Monomers. *Macromol. Chem. Phys.* **2019**, *220* (14), 1900179. https://doi.org/10.1002/macp.201900179.

2.1 Introduction

Synthesis of biobased monomers which possess physico-chemical properties that could mimic or even surpass those of their oil-based counterparts or bring additional functionality to polymeric materials has become crucial as a consequence of the current environmental concerns and more stringent environmental regulations. Suitable molecules for this purpose can be selected from a vast biomass feedstock that includes terpenes, carbohydrates, lignin derivatives, proteins, vegetable oils and lipids.[1,2] However, biomass molecules rarely possess suitable reactive functions for radical or ionic chain growth polymerization. Therefore, the synthesis of biobased monomers containing functional groups with suitable reactivity for chain growth polymerization remains interesting for the development of novel materials and use of different polymerization processes.[3,4] Different biobased molecules have been modified to introduce into their chemical structure functional groups adapted to radical polymerization such as methacrylates or acrylates.[5,6] In particular, biobased monomers containing aromatic groups are attractive molecules as they can provide high mechanical and thermal stabilities to materials.[7] Natural phenols can be obtained from cashew nut shell liquid (CNSL), lignin, tannin, and coconut shell tar.[8] Molecules such as cardanol,[9,10] eugenol,[11] vanillin[12] and ferulic acid[13] have already been functionalized to prepare biobased radically polymerizable monomers. In these molecules, modifications have been done to obtain a methacrylate group, or in the case of the ferulic acid, a styrenic derivative, both suitable for radical polymerization.

Eugenol, extracted mainly from clove oil but also obtained from lignin depolymerization,[14] has become a very interesting building block due to its antibacterial and anti-inflammatory properties.[15–17] In this chapter, eugenol and eugenol-derived molecules were used to build a versatile monomer platform taking advantage of their chemical structure. This platform is suitable for several kinds of polymerization reactions (e.g. radical, thiol-ene, condensation, ring-opening reactions) and processes (e.g. solution, bulk, emulsion polymerization), which opens the possibility to create materials with a variety of properties and potential applications.

2.1.1 Eugenol as a building block

Eugenol is a natural phenol that can be obtained from several plants including clove buds, cinnamon bark, tulsi leaves, turmeric, pepper, ginger, oregano and thyme.[15] Moreover, eugenol can also be

obtained from depolymerization of lignin (Scheme 2-1)[18–21] Even though this process remains to be optimized, it represents a promising feedstock due to its availability.

Scheme 2-1. Eugenol isolated from lignin [19,20]

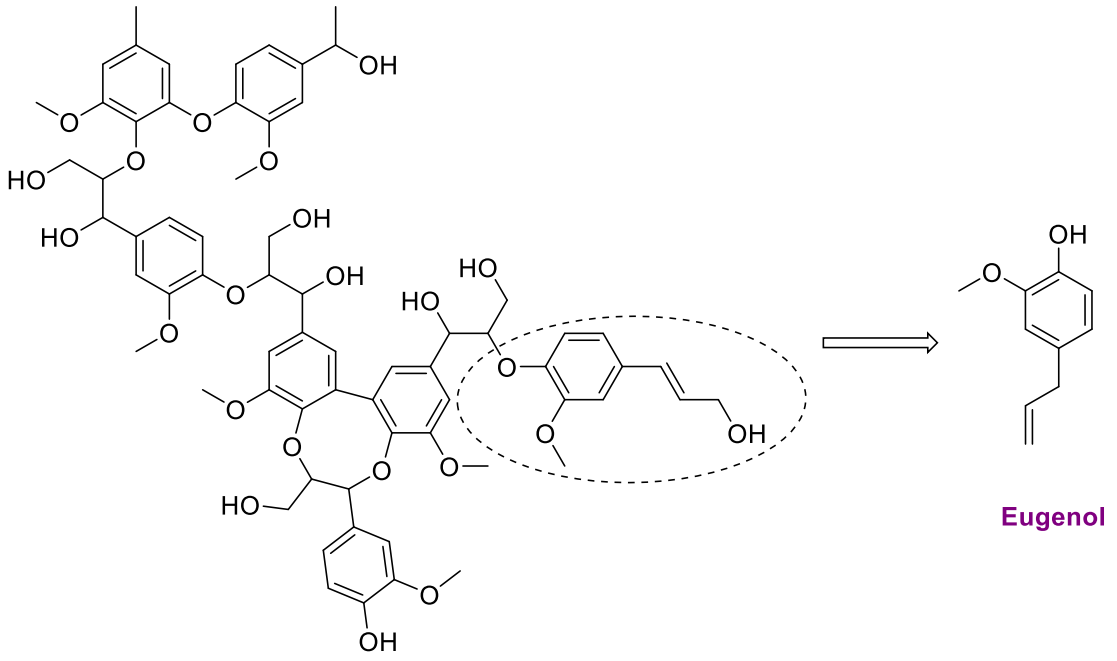

Lignin constitutes 15–35% of the dry lignocellulosic biomass and it is the largest renewable source of aromatics on earth.[14,22] As described in Chapter 1, lignin is a cross-linked amorphous copolymer produced from the radical polymerization of substituted phenyl propylene units: coumaryl, coniferyl, and sinapyl alcohols containing zero, one, and two methoxy groups, respectively (Scheme 2-2).[14] Furthermore, lignocellulose is not edible for human beings, therefore its use to produce polymeric materials does not compete with food supply.

Scheme 2-2. Lignin propylene units

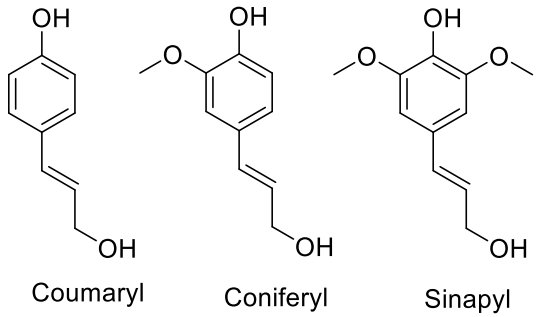

Lignin can be isolated from biomass by different methods such as: kraft process, sulfite pulping, organosolv processes, treatment with organic acids and pyrolysis of lignocellulose.[14] Lignin depolymerization is necessary to extract small molecules. This is done by several strategies: pyrolysis, homogeneous and heterogeneous catalysis (catalytic hydropyrolysis), solvolysis (base-

catalyzed depolymerization and hydrogenolysis, also using supercritical solvents and ionic liquids) and biological processes.[14,21,22] From lignin depolymerization, molecules such as sinapyl alcohol, ferulic acid, vanillin, guaiacol and eugenol can be obtained.[23,24]

In addition, eugenol possesses antioxidant, antimicrobial and anti-inflammatory properties,[25] as well as therapeutic properties against nervous disorders, digestive complications, reproductive derangements, blood cholesterol irregularity, hyper-tension, elevated blood glucose level, microbial infections, inflammatory actions and carcinogenesis.[15] As a bactericide, anti-inflammatory and analgesic, eugenol has been widely used for dental treatment materials.[26] Eugenol antibacterial activity has been assessed with positive results in polymeric material,[16,17,27–30] representing further properties to be exploited.

Isoeugenol, eugenol isomer, and dihydroeugenol, the hydrogenated form of eugenol, are also interesting building blocks for the production of new biobased monomers and polymers (Scheme 2-3). Isoeugenol can be obtained by the isomerization reaction from eugenol,[31] while dihydroeugenol by hydrogenation[19] as well as from lignin depolymerization.[21] The presence and absence of allylic and propenyl double bonds in *para* position may lead to important difference in reactivity and properties of the final materials.

Scheme 2-3. Eugenol-derived molecules

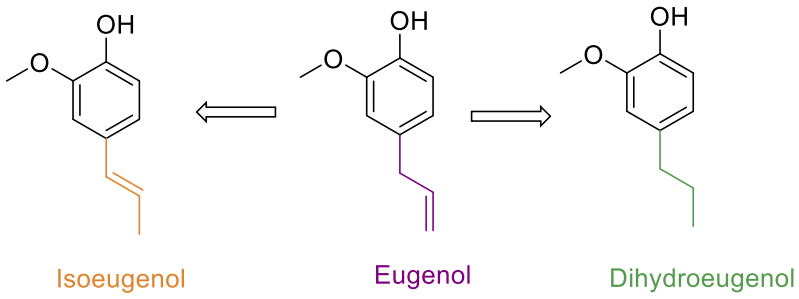

2.1.2 Eugenol-derived monomers

Eugenol has already been modified to introduce suitable functional groups for radical polymerization. Rojo *et al*.[11] functionalized eugenol to produce methacrylate derivatives for uses in orthopaedic and dental cements. The methacrylic eugenol-derived monomers were synthesized *via* incorporation of the methacrylic group directly onto the phenol group by reaction with methacryloyl chloride or after introduction of a spacer group to obtain ethoxy eugenyl methacrylate (Scheme 2-4). Both monomers were polymerized in toluene solution.

Scheme 2-4. Eugenol-derived methacrylate monomers

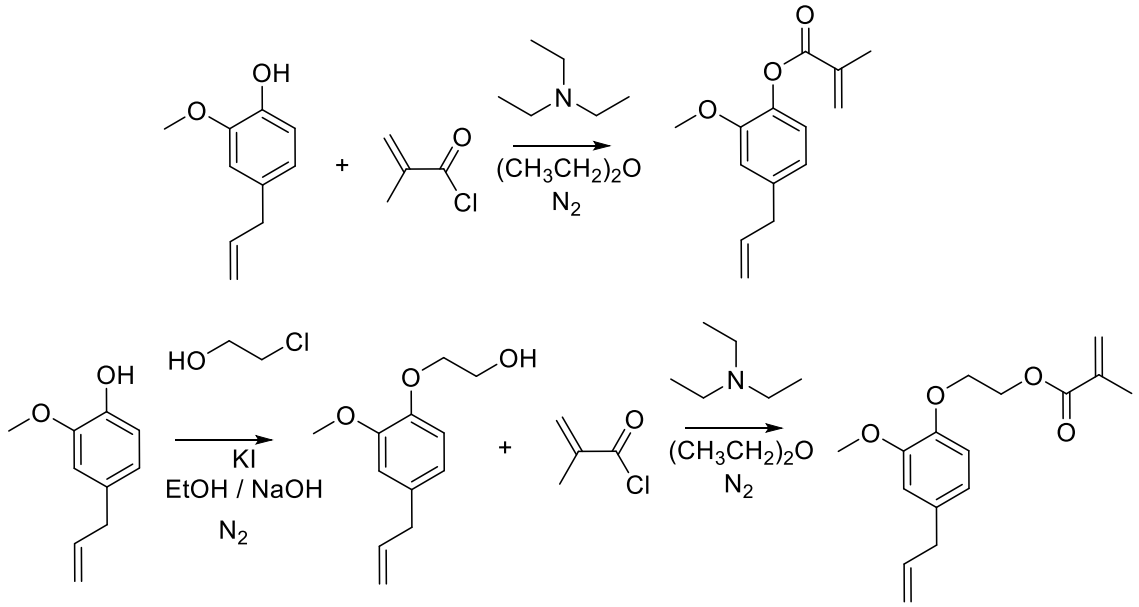

Only low conversion polymers (<10% monomer conversion) were soluble in organic solvent and characterized. It was observed that the reaction proceeded primarily through the methacrylic double bond. Moreover, eugenol methacrylate, obtained using methacrylic anhydride (Scheme 2-5), was also polymerized under suspension polymerization in aqueous dispersed media conditions using poly(vinyl alcohol) (PVA) as stabilizer.[32] In this case, eugenol methacrylate was used as the monomer and the cross-linking agent simultaneously. Microspheres with diameter ranging from 500-800 µm were obtained and their oil absorbency properties were studied.

Scheme 2-5. Synthesis of eugenol methacrylate monomers

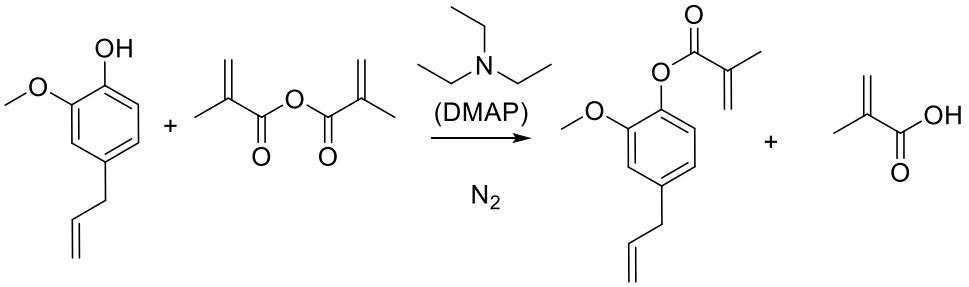

A platform of biobased monomers derived from eugenol was synthesized containing different functional groups. Eugenol, isoeugenol and dihydroeugenol have been selected as the monomers building blocks (Scheme 2-6). To reduce the risk of hydrolysis of the ester group,[33] methacrylate and acrylate moieties were not introduced directly on the aromatic phenol (Scheme 2-6). Polymerizations of these biobased monomers were carried out through conventional radical polymerization in solution and the different behaviours of these molecules were assessed with regards to the position or absence of allylic or propenyl double bonds.

Scheme 2-6. Monomer platform from eugenol derivatives

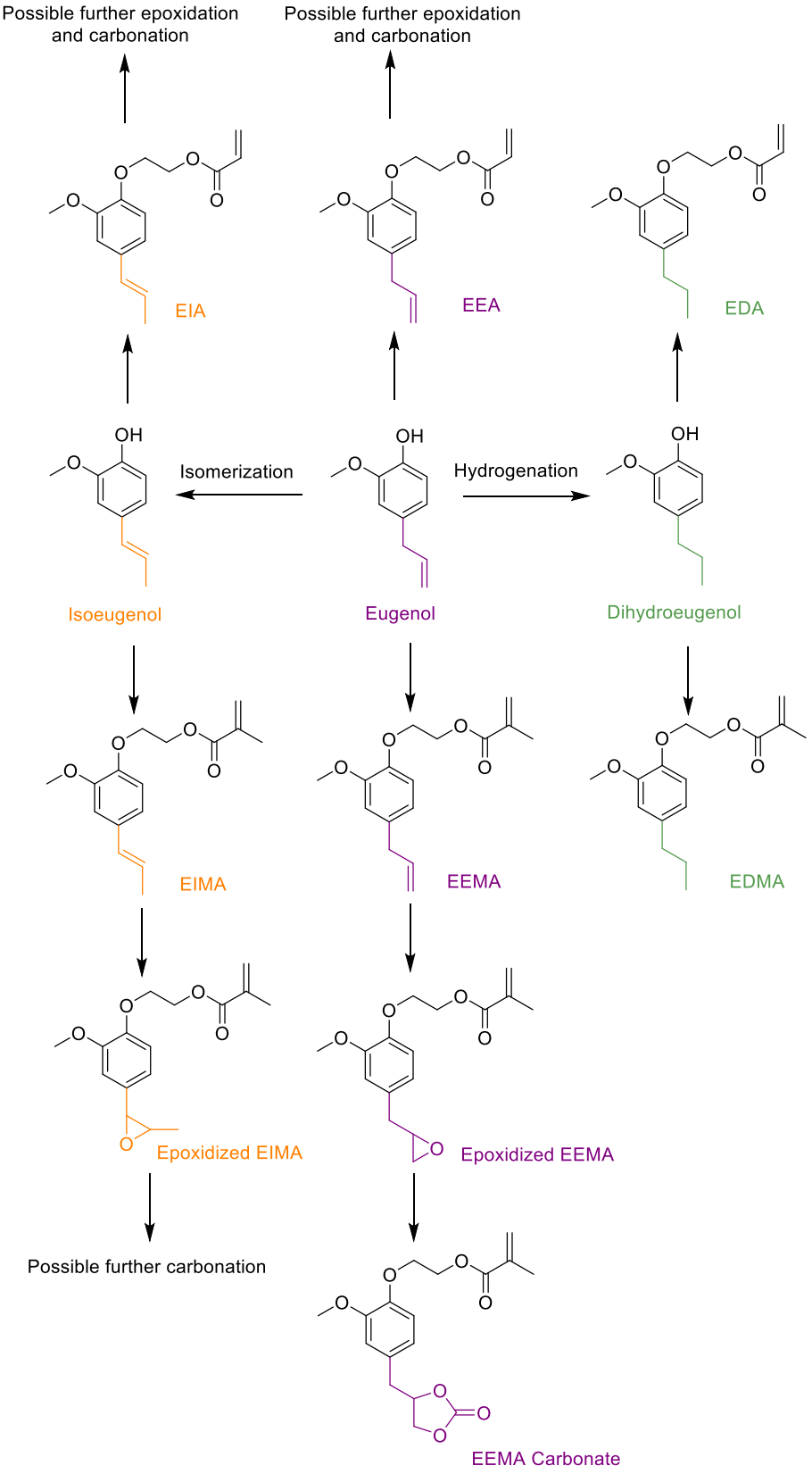

The preservation of the allyl or propenyl double bonds after the polymerization is desired as this leads to functional polymers. The properties of the resulting polymer materials could then be further tuned *via* chemical reaction on the residual allyl and propenyl groups to form networks through cross-linking for example.

Alternatively, it is possible to take advantage of the allyl and propenyl double bonds, to convert them into functional groups such as epoxy and cyclic carbonate which could be further reacted with a wide range of reactants such as amines, anhydrides, phenols, or thiols.[34,35]

2.2 Experimental

2.2.1 Materials

Eugenol (99%, Aldrich), isoeugenol (99%, Aldrich, mixture of 8% *cis* and 92% *trans*), dihydroeugenol (2-Methoxy-4-propylphenol, 98%, Aldrich), ethylene carbonate (98%, Aldrich), 1,5- diazabicyclo[4.3.0]non-5-ene (DBN, 98%, Aldrich), triethylamine (TEA, 99.5%, Aldrich), methacrylic anhydride (94%, Aldrich), acryloyl choride (>97%, Aldrich), m-CPBA (m- chloroperbenzoic acid, <77%, Aldrich), potassium peroxymonosulfate, tradename Oxone® (>99%,VWR), sodium hydrogen carbonate ($NaHCO_3$, >99% Aldrich), potassium carbonate (K_2CO_3, >99%, Aldrich), sodium sulphite (Na_2SO_3,98%, Aldrich), sodium hydroxide (NaOH, 98%, Aldrich), aluminium oxide basic (Aldrich), dichloromethane (DCM, >99%,VWR), acetone (>99%,VWR), ethyl acetate (>99%,VWR), sodium sulfate (Na_2SO_4, >99%, Aldrich), methanol (MeOH, >99%, Aldrich), 1,4- bis(trimethylsilyl)benzene (BTMSB, 96%,Aldrich), tetrabutylammonium bromide (TBAB, >99%, Acros Organics), toluene (>99%, Aldrich) were used as received. 2,2′-Azobis(2-methylpropionitrile) (AIBN, Fluka, 98%) was purified by recrystallization in methanol and dried under vacuum before use. Deionized water (DI water) (1 µS cm^{-1}) was obtained using a D8 ion exchange demineralizer from A2E Affinage de L'Eau.

2.2.2 Methods

2.2.2.1 General procedure for hydroxyethylation of eugenol and eugenol derivatives

Eugenol or eugenol derivatives (isoeugenol or dihydroeugenol) (480 mmol, 1 equiv.) and ethylene carbonate (528 mmol, 1.1 equiv.) were placed in a 2-neck round-bottom flask equipped with a reflux condenser and mixed under argon and high magnetic agitation. The flask was then immersed into an oil bath set to 150°C. Once the ethylene carbonate had completely melted and the reaction mixture was homogeneous, DBN (1.47 mmol, 0.003 equiv.) was injected into the reaction mixture *via* a syringe. The reaction proceeded at 150°C for 30 min, after which the temperature of the oil bath was increased to 180°C. The reaction was left to proceed for another 4 h. The product was dissolved in DCM and extracted twice with DI water, to remove any residues of ethylene carbonate. The organic phase was dried with Na_2SO_4 and filtered through silica gel to remove any residues of salts (Scheme 2-7).

Scheme 2-7. General synthesis of the hydroxyethylated eugenol derivatives

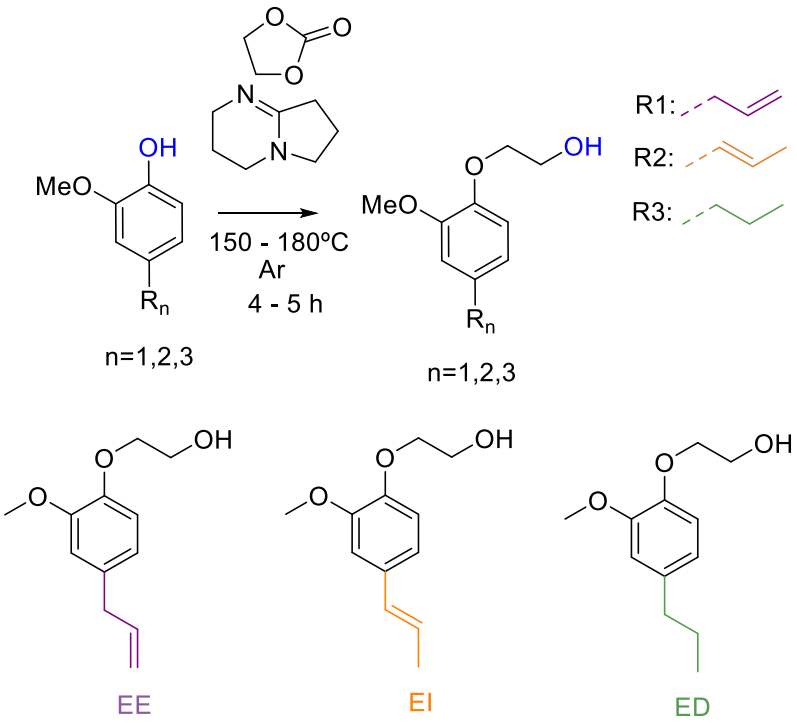

Synthesis of 2-(4-allyl-2-methoxyphenoxy)ethan-1-ol (Ethoxy eugenol) (EE). Eugenol (78.83 g, 480 mmol, 1 equiv.) and ethylene carbonate (46.49 g, 528 mmol, 1.1 equiv.), DBN (0.1829 g, 1.47 mmol, 0.003 equiv.). Yield: 95% (see Appendix Eq. A1-1). m.p.: 41°C

Synthesis of 2-(2-methoxy-4-(prop-1-en-1-yl)phenoxy)ethan-1-ol (Ethoxy isoeugenol) (EI). Isoeugenol (78.91 g, 8% *cis* and 92% *trans*, 481 mmol, 1 equiv.) and ethylene carbonate (46.61 g, 529 mmol, 1.1 equiv.), DBN (0.1414 g, 1.14 mmol, 0.002 equiv.). Yield: 95%. m.p.: 89°C.

Synthesis of 2-(2-methoxy-4-propylphenoxy)ethan-1-ol (Ethoxy dihydroeugenol) (ED). Dihydroeugenol (79.61 g, 479 mmol, 1 equiv.) and ethylene carbonate (46.39 g, 527 mmol, 1.1 equiv.), DBN (0.1629 g, 1.31 mmol, 0.003 equiv.). Yield: 97%. m.p.: 53°C.

2.2.2.2 General synthesis for eugenol and eugenol-derived methacrylates.

Hydroxyethylated eugenol derivative (449 mmol, 1 equiv.) was placed in a round-bottom flask and dissolved in DCM. TEA (1078 mmol, 2.4 equiv.) was added and the flask sealed with a septum. The mixture was purged with argon for 15 min and then immersed in an ice bath. Methacrylic anhydride (497 mmol, 1.1 equiv.) was added dropwise over 10 min to the solution. The reaction proceeded for 18 h at room temperature (*circa* 25°C). The final mixture was washed three times with 0.05 M NaOH solution and twice with DI water, then extracted with ethyl acetate. The organic phase was dried with Na_2SO_4, filtered, and the solvent was removed at 30°C under vacuum. Finally, the product was purified through flash chromatography using cyclohexane: ethyl acetate 9:1. No radical inhibitor was added (Scheme 2-8).

Scheme 2-8. Synthesis of the methacrylated eugenol derivatives

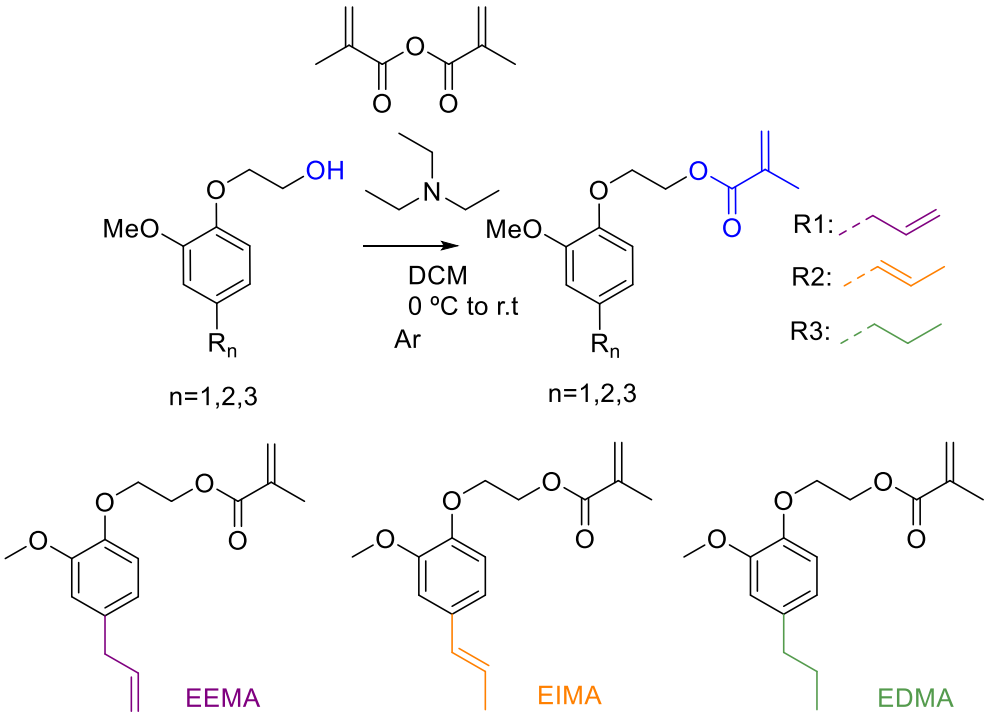

Synthesis of 2-(4-allyl-2-methoxyphenoxy)ethyl methacrylate (Ethoxy eugenyl methacrylate) (EEMA). EE (93.55 g, 449 mmol, 1 equiv.), DCM (150 mL), TEA (150 mL, 1078 mmol, 2.4 equiv.) and methacrylic anhydride (76.67 g, 497 mmol, 1.1 equiv.). Yield: 74%. m.p.:11°C. Exact Mass: 276.1361; ASAP (HRMS): $(M+H)^+$ calculated ($C_{16}H_{21}O_4$): *m/z* 277.1440, found: *m/z* 277.1427, $\Delta m/z = (m/z_{theo} - m/z_{exp})/(m/z_{theo})$ = 4.70 ppm.

Synthesis of 2-(2-methoxy-4-(prop-1-en-1-yl)phenoxy)ethyl methacrylate (Ethoxy isoeugenyl methacrylate) (EIMA). EI (75.39 g, 9% *cis* and 91% *trans*, 362 mmol, 1 equiv.), DCM (150 mL), TEA (120 mL, 869 mmol, 2.4 equiv.) and methacrylic anhydride (64.18 g, 416 mmol, 1.15 equiv.). Yield: 70%. m.p.:37°C. Exact Mass: 276,1361; ASAP (HRMS): $(M+H)^+$ calculated ($C_{16}H_{21}O_4$): *m/z* 277.1440, found: *m/z* 277.1439, $\Delta m/z$= 0.4 ppm.

Synthesis of 2-(2-methoxy-4-propylphenoxy)ethyl methacrylate (Ethoxy dihydroeugenyl methacrylate) (EDMA). ED (75.67 g, 360 mmol, 1 equiv.), DCM (150 mL), TEA (120 mL, 864 mmol, 2.4 equiv.) and methacrylic anhydride (62.13 g, 396 mmol, 1.12 equiv.). Yield: 88%. m.p.: below 0°C. Exact Mass: 278,15; ASAP (HRMS): $(M+H)^+$ calculated ($C_{16}H_{23}O_4$): *m/z* 279.1596, found: *m/z* 279.1595, $\Delta m/z$= 0.4 ppm

2.2.2.3 General synthesis for eugenol and eugenol-derived acrylates.

Hydroxyethylated eugenol derivative (48 mmol, 1 equiv.) was placed in a round-bottom flask and dissolved in dry DCM (70 mL). TEA (75 mmol, 1.56 equiv.) was added and the flask sealed with a septum. The mixture was purged with argon for 30 min and then immersed in an ice bath. Acryloyl chloride (60 mmol, 1.25 equiv.) was dissolved in 30 mL of dry DCM and added dropwise over 10 min to the reaction mixture. The reaction proceeded for 1.5 h at room temperature (*circa* 25°C).

The final mixture was filtered and then washed with 0.1 M NaOH solution twice, with 0.1 M HCl twice and with deionized DI, then the organic phase was dried with Na_2SO_4, filtered, and the solvent was removed at 30°C under vacuum. Finally, the product was purified through flash chromatography using cyclohexane:ethyl acetate 9:1. No inhibitor was added (Scheme 2-9)

Scheme 2-9. General synthesis of the eugenol-derived acrylates

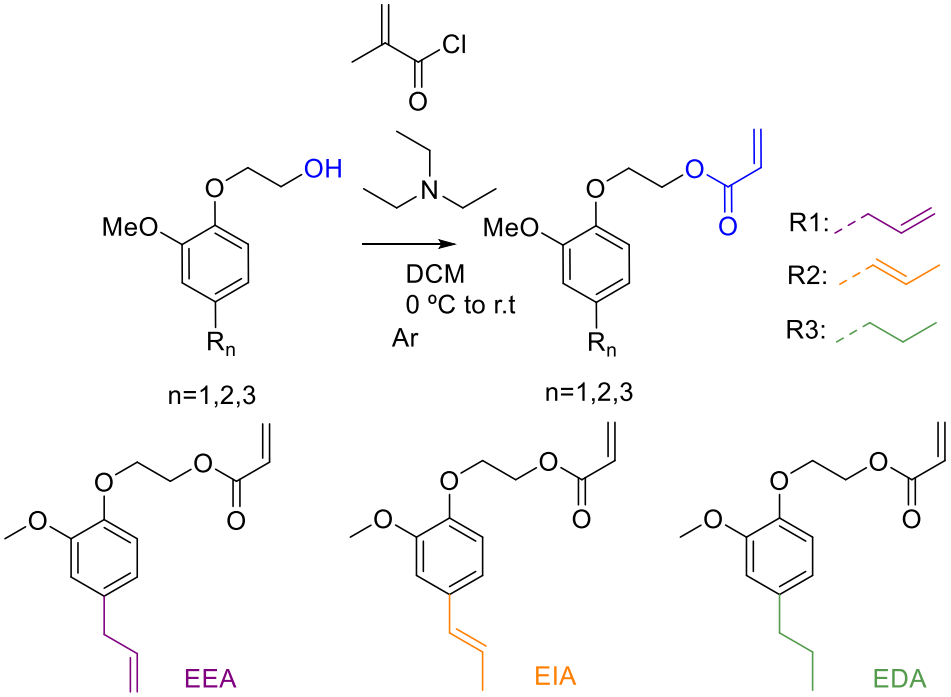

Synthesis of 2-(4-allyl-2-methoxyphenoxy)ethyl acrylate (Ethoxy eugenyl acrylate) (EEA). EE (21.98 g, 105.54 mmol, 1 equiv.), TEA (23 mL, 165 mmol, 1.56 equiv.) and acryloyl chloride (11 mL, 132 mmol, 1.25 equiv.). Yield: 68%. m.p.: below 0°C. Exact Mass: 262,1205; ASAP (HRMS): $(M+H)^+$ calculated ($C_{15}H_{19}O_4$): *m/z* 263.1283, found: *m/z* 263.1283, Δ*m/z*= 0 ppm.

Synthesis of 2-(2-methoxy-4-(prop-1-en-1-yl)phenoxy)ethyl acrylate (Ethoxy isoeugenyl acrylate) (EIA). EI (31.24 g, 9% *cis* and 91% *trans*, 150 mmol, 1 equiv.), TEA (33 mL, 234 mmol, 1.56 equiv.) and acryloyl chloride (18 mL, 188 mmol, 1.25 equiv.). Yield: 50%. m.p.: 56°C Exact Mass: 262,1205; ASAP (HRMS): $(M+H)^+$ calculated ($C_{15}H_{19}O_4$): *m/z* 263.1283, found: *m/z* 263.1282, Δ*m/z*= 0.4 ppm.

Synthesis of 2-(2-methoxy-4-propylphenoxy)ethyl acrylate (Ethoxy dihydroeugenyl acrylate) (EDA). ED (10.1 g, 48 mmol, 1 equiv.) dissolved in dry DCM (70 mL), TEA (11 mL, 75 mmol, 1.56 equiv.) and acryloyl chloride (6 mL, 60 mmol, 1.25 equiv.) dissolved in 30 mL of DCM. Yield: 81%.

2.2.2.4 Procedure for the epoxidation of eugenol-derived methacrylates

Method A with m-CPBA as oxidant. Eugenol and isoeugenol-derived methacrylates (36.19 mmol, 1 equiv.) were dissolved in 60 mL DCM and placed in a double necked flask with stirrer and purged with argon for 15 min. m-CPBA (77%) (54.28 mmol, 1.5 equiv.) was dissolved in 180 mL of DCM and added to the reaction mixture dropwise over 15 min. The reaction was left overnight under argon and stirring. Then it was washed first with 250 mL of 10 wt% of Na_2SO_3 aqueous solution, then with 250 mL of saturated aqueous solution of $NaHCO_3$ and finally with 250 mL of distilled H_2O. The aqueous phase was extracted with 250 mL of DCM. The organic phase was dried with Na_2SO_4, filtered, and the solvent was removed at 30°C under vacuum. Finally, the product was purified through flash chromatography using cyclohexane:ethyl acetate 7:3 (Scheme 2-10).

Synthesis of 2-(2-methoxy-4-(oxiran-2-ylmethyl)phenoxy)ethyl methacrylate (Epoxy Ethoxy Eugenyl Methacrylate) (Epoxy EEMA). EEMA (10.10 g, 36.19 mmol, 1 equiv.), m-CPBA (12.16 g (77%), 54.28 mmol, 1.5 equiv.) Yield: 58%. Exact Mass: 336.1209; ASAP (HRMS): $(M+H)^+$ calculated ($C_{17}H_{21}O_7$): *m/z* 337.1287, found: *m/z* 337.1284, Δ*m/z*= 0.9 ppm.

Scheme 2-10. Synthesis of the eugenol-derived epoxide

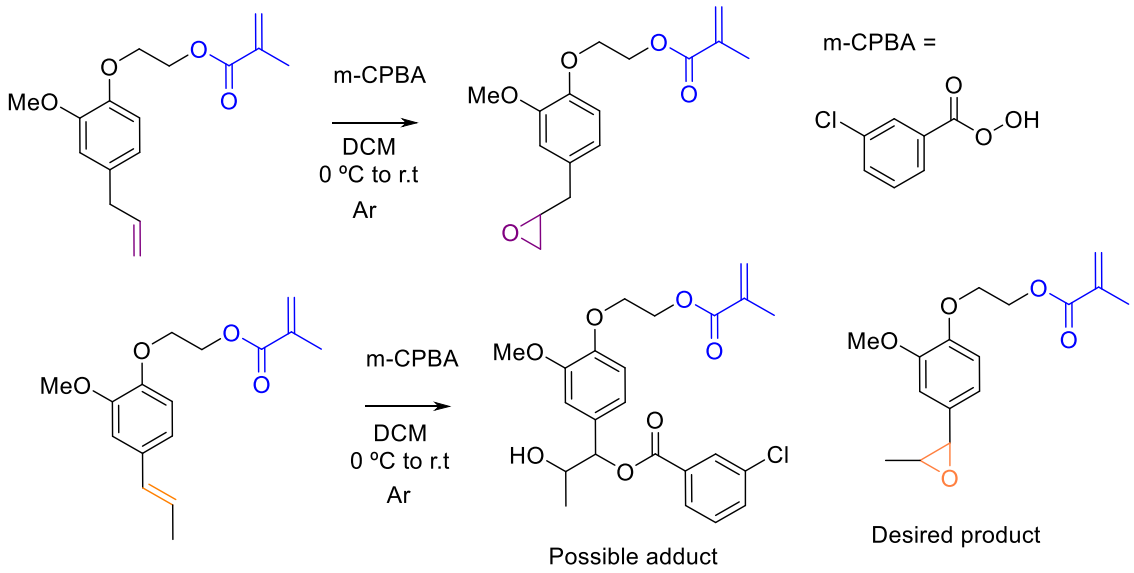

Method B with Oxone® as oxidant. Eugenol and isoeugenol-derived methacrylates (45 mmol, 1 equiv.) were dissolved in 180 mL acetone and placed in a round flask with a magnetic stirrer in an ice bath. $NaHCO_3$ (181 mmol, 4 equiv.) was added. Then, Oxone® (73.53 mmol, 1.6 equiv.) was dissolved in 110 mL of water and added dropwise. The reaction was left stirring overnight for EEMA and 4 hours for EIMA at 25°C. Then it was extracted with ethyl acetate. The organic fraction was dried with Na_2SO_4, filtered, and the solvent was removed at 30°C under vacuum. Finally, the product was purified through flash chromatography using cyclohexane:ethyl acetate 8:2 (Scheme 2-11).

Synthesis of 2-(2-methoxy-4-(oxiran-2-ylmethyl)phenoxy)ethyl methacrylate (Epoxy Ethoxy Eugenyl Methacrylate) (Epoxy EEMA). EEMA (12.44 g, 45 mmol, 1 equiv.), 180 mL acetone,

$NaHCO_3$ (15.12g, 181 mmol, 4 equiv.), Oxone® (22.60 g, 73.5 mmol, 1.6 equiv.), DI water 110 mL. Yield:34%.

Synthesis of 2-(2-methoxy-4-(3-methyloxiran-2-yl)phenoxy)ethyl methacrylate) (Epoxy EIMA). EIMA (5.53 g, 20 mmol, 1 equiv.), 80 mL acetone, $NaHCO_3$ (6.72 g, 80 mmol, 4 equiv.), Oxone® (10.05 g, 32.7 mmol, 1.6 equiv.), DI water 48 mL. Yield: 62%.

Scheme 2-11. Synthesis of the eugenol-derived epoxide with Oxone®

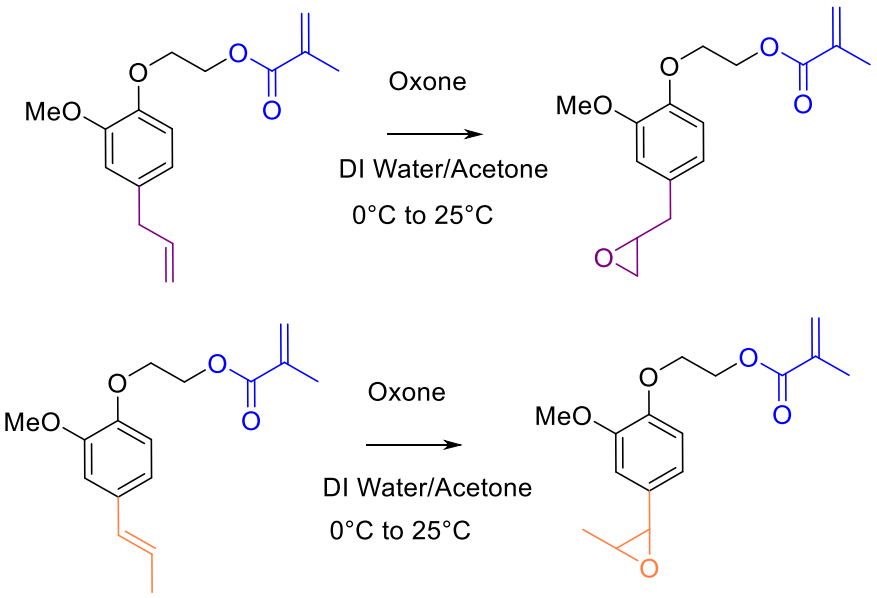

2.2.2.5 Synthesis of eugenol-derived carbonate

Synthesis of 2-(2-methoxy-4-((2-oxo-1,3-dioxolan-4-yl)methyl)phenoxy)ethyl methacrylate (Ethoxy eugenyl methacrylate carbonate) (EEMA Carbonate) (Scheme 2-12).

Epoxidized EEMA (3.00 g, 10.27 mmol) and TBAB (0.09 g, 0.03 mmol, 3 wt% of epoxide) were dissolved in 60 mL of ethyl acetate. The reaction mixture was placed in a high-pressure stainless-steel Parr Reactor equipped with a pressure gage, a turbine impeller and a split ring, which was then filled with CO_2 at a pressure of 20 bar. The reactor was heated to 80°C and left to react for 48 h under mechanical stirring. The reactor was depressurized and the reactor mixture was degassed with Ar. Then it was washed three times with 100 mL $NaHCO_3$. The organic phase was dried with Na_2SO_4 and the solvent evaporated under vacuum. Yield: 66 %.

Scheme 2-12. Synthesis of EEMA carbonate

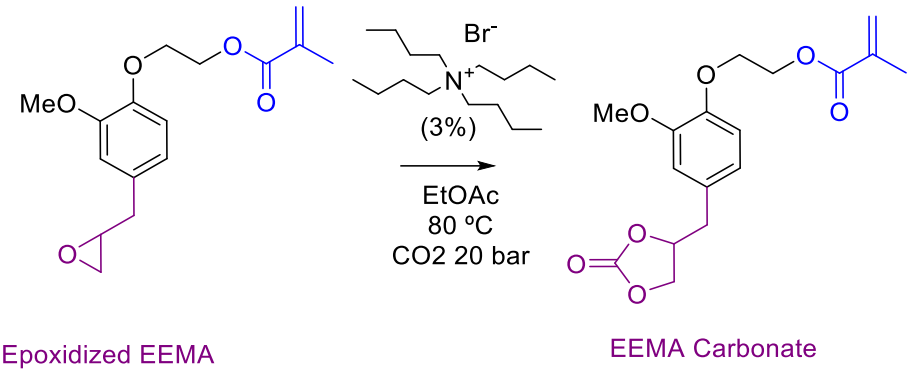

Epoxidized EEMA

EEMA Carbonate

2.2.2.6 General procedure for solution homopolymerization of eugenol, isoeugenol and dihydroeugenol-derived (meth)acrylates.

Eugenol, isoeugenol and dihydroeugenol-derived (meth)acrylates (2.763 g, 10 mmol), BTMSB (0.12 g, 0.55 mmol) and toluene (6.4 g) were placed in a double necked flask equipped with a condenser. The flask was sealed with a septum and the reaction mixture was purged with argon bubbling for 30 min. The reaction mixture was placed in an oil bath at 70°C. AIBN (0.034 g, 1.3 wt% with respect to the monomer) previously dissolved in toluene (4 g) and purged with argon for 10 min was added to the reaction mixture. The monomer conversion was followed by ^{1}H NMR.

2.2.3 Characterization

Fourier transform infrared spectroscopy (FTIR). (Appendix Figure A1-1 to Figure A1-11) FTIR spectra were acquired on a Thermo Scientific Nicolet 6700 FTIR, and were analyzed using an OMNIC Series 8.2 software from Thermo Scientific.

Thermogravimetric analysis (TGA). (Appendix Figure A1-12 to Figure A1-17) TGA analyses were carried out on 10–15 mg samples on a TGA Q50 apparatus from TA Instruments from 20°C to 590°C, in an aluminum pan, at a heating rate of 10°C min, under air. TGA under argon analyses where executed on a PERSEUS® TGA 209 F1 Libra® from Netzch using a temperature ramp of 20°C min from 20°C to 620°C under nitrogen flow of 40 mL min in an alumina crucible.

Differential Scanning Calorimetry (DSC). (Appendix Figure A1-18 to Figure A1-23) Melting points measurements were performed on 10–15 mg samples on a Netzsch DSC 200 F3 instrument using the following: first cooling ramp from room temperature (*ca.* 20°C) to −20 at 10°C min^{-1} , isotherm plateau at−20°C for 10 min, first heating ramp from −20°C to 140°C at 10°C min^{-1} cooling stage from 140°C to room temperature (*ca.* 20°C).

Heating/cooling cycle for T_g measurements (Appendix Figure A1-54 to Figure A1-68): first cooling ramp from room temperature (*ca.* 20ºC) to −40 at 20°C min^{-1}, isotherm plateau at −40°C for 10 min, first heating ramp from −40°C to 100°C at 20°C min^{-1}, cooling stage from 100°C to−40°C at

20°C min^{-1}, isotherm plateau at −40°C for 10 min, second heating ramp from −40°C to 100°C at 20°C min^{-1}, cooling ramp to −40°C at 20°C min^{-1}, isotherm plateau at −40°C for 20 min, third heating ramp from −40°C to 100°C at 20°C min^{-1}, and last cooling stage from 100°C to room temperature (*ca.* 20°C). T_g value was obtained from the third cycle. Calibration of the instrument was performed with noble metals and checked with an indium sample.

Nuclear magnetic resonance spectroscopy (NMR). (Appendix Figure A1-24 to Figure A1-47) Chemical structures were determined by ^{1}H NMR and ^{13}C NMR spectroscopies on a Bruker Avance 400 MHz spectrometer at 23°C. The spectra were recorded by dissolving 10 mg of sample in 0.5 mL of $CDCl_3$. The experimental conditions for recording ^{13}C NMR spectra were as follows: flip angle 30°, acquisition time 2 s, pulse delay 2 s and 512 scans.

Size exclusion chromatography (SEC). (Appendix Figure A1-69 to Figure A1-72) Polymer molar masses were determined from the THF-soluble fraction by SEC, using a PL-GPC 50 Plus apparatus from Polymer Laboratories (Varian Inc.) equipped with two 300 mm PL-gel 5 µm, mixed D (200–400 000 g mol^{-1}) columns thermostated at 35°C and a refractive index detector. In addition, a GPC from Agilent Technologies with its corresponding Agilent software, equipped with two PL1113-6300 ResiPore 300 x 7.5 mm columns (up to 500,000g mol^{-1}) was used. The detector suite comprised a 390-LC PL0390-0601 refractive index detector. The entire SEC-HPLC system was thermostated at 35°C. Calibration was performed with PMMA narrow standards. THF was used as the eluent at a flow rate of 1 mL $min^{-1}$and toluene as flow rate marker. Typical sample concentration was 10 mg mL^{-1}.

Atmospheric Pressure Solids Analysis Probe (ASAP) time-of-flight mass spectrometry (TOF-MS). ASAP/TOF-MS analyses were performed on a SYNAPT G2-S Mass Spectrometer (Waters) fitted with an Atmospheric Solids Analysis Probe. The samples were deposited directly onto the exterior of a glass capillary and were thermally desorbed. The mass spectra were registered in positive mode from 50 to 1500 Da. The corona discharge voltage was 15 µA and the sampling cone voltage was 30 V. The temperatures of the source and of desolvation were 140°C and 450°C respectively. The temperature of thermal desorption was ramped from 50 to 600°C.

2.3 Results and Discussion

2.3.1 Synthesis of biobased monomers-derived from eugenol.

The successful synthesis of monomers derived from eugenol containing radically polymerizable functional groups such as acrylates and methacrylates was performed. Moreover, the introduction of functional groups such as epoxy and cyclic carbonate to allow further functionalization or cross-linking was also achieved. Thus, the synthesis of six eugenol-derived (meth)acrylate monomers was executed using a two-step synthesis procedure.[10] The first step was a chain elongation whereby an ethyl spacer was introduced, to move the hydroxyl group away from the aromatic ring. This was done to increase the stability of the ester group of the methacrylate function (to avoid possible hydrolysis).[33] This reaction was performed without solvent, at high temperature (150-

180°C) for 4-5 h using DBN as catalyst. Reactions went to full conversion and yields were quantitative for all the eugenol derivatives. In the case of the eugenol, after the introduction of the spacer group, 3% mol of isoeugenol derivative was observed. This isomerisation was probably caused by the high temperature and the presence of DBN. The second step was the introduction of the methacrylate or acrylate group using methacrylic anhydride or acryloyl chloride respectively, in the presence of triethylamine. The reactions were carried out between 0°C and room temperature (*circa* 25°C). and lasted 15-20 h in the case of methacrylation and 2 h in the case of acrylation. The methacrylate monomers were produced with quantitative conversion and then purified by a flash chromatography method using cyclohexane and ethyl acetate binary mixture as eluent. Although the reactions were initially executed using DCM as a solvent, it was later proven that they can also be carried out in ethyl acetate as a less hazardous solvent (DCM is irritant and suspected to cause cancer). ^{1}H NMR spectroscopy confirmed the preparation of the desired products synthesized in ethyl acetate (Appendix Figure A1-48 to Figure A1-49).

After the successful synthesis of the (meth)acrylated monomers, the introduction of functional groups such as epoxy and cyclic carbonate was explored as this could allow the synthesis of other types of functional biobased polymers.

The epoxidation of the methacrylated monomers was carried out in DCM using m-CPBA as oxidant. This method was successful in the case of EEMA. However, in the case of EIMA, a secondary product was formed by opening of the epoxy ring by chloro-benzoic acid (Scheme 2-13).

Scheme 2-13. Reaction of epoxidation of EIMA with m-CPBA

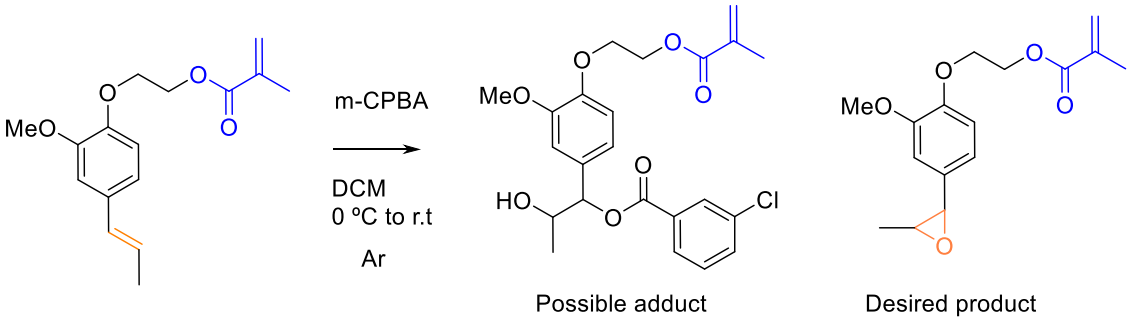

Another way reported in literature to do the epoxidation is by using Oxone® in acetone,[36] which could help not only to avoid the ring opening but it is also a greener synthetic reaction. Epoxidation of internal double bonds was done successfully with this method.[36] Thus, this reaction was executed with EEMA and EIMA. EIMA epoxy became insoluble after a month at 4°C, indicating that it is unstable and reactive.

The carbonation of the eugenol methacrylate EEMA was successfully achieved. TBAB was used to catalyse the reaction which was carried out under a CO_2 pressure of 20 bar.[37–40] This carbonate derivative could be used for further reaction, for example as a cross-linker through addition reactions with amines.[41–43] The carbonation of the EIMA-derived epoxy was not pursued, due to the complexity encountered in its synthesis and storage.

2.3.2 Solution polymerization of eugenol-derived (meth)acrylates.

After the synthesis of the novel platform of biobased monomers derived from eugenol, it was important to study the behaviour of these monomers in radical homopolymerization. The solution polymerization of the eugenol-derived monomers was performed in toluene (21% solids) at 70°C, with AIBN as initiator (1.3 wt% with respect to the monomer) and the monomer conversion was monitored by ^{1}H NMR. The monomer conversion was determined each hour for the first 7 h of reaction and then measured after 24 h reaction (Appendix A1-50 and Figure A1-51, Eq. A1-2 and Eq. A1-3), monitoring the methacrylic double bond and the *para* unsaturation when present (Figure 2-1). No additional initiator was added during the course of the reaction. The homopolymerization of EDMA (monomer without any other unsaturation than the methacrylate) reached quantitative monomer conversion (97%) after 24 h (Table 2-1).

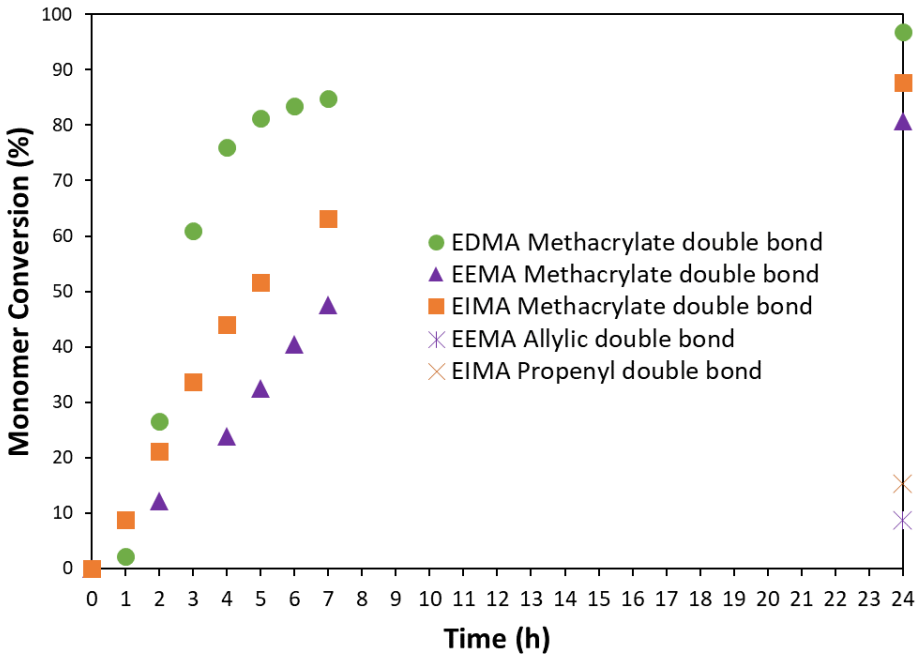

Figure 2-1. Monomer conversion of eugenol-derived methacrylates in toluene solution homopolymerization at 70°C.

Although EIMA and EEMA also reached high conversion after 24 h (80% conversion) (Table 2-1), the reaction rate R_p was noticeably slower throughout the entire reaction with respect to EDMA, *i.e.* $R_{p,EDMA} >> R_{p,EIMA} > R_{p,EEMA}$ (Appendix Figure A1-52).The presence of allylic or propenyl moieties (in the eugenol and isoeugenol-derived methacrylates, respectively) can induce secondary reactions during polymerization. Degradative chain transfer reactions such as allylic proton abstraction may occur and lead to a decrease of the polymerization rate.[44–46]

Scheme 2-14. Chain transfer and radical addition

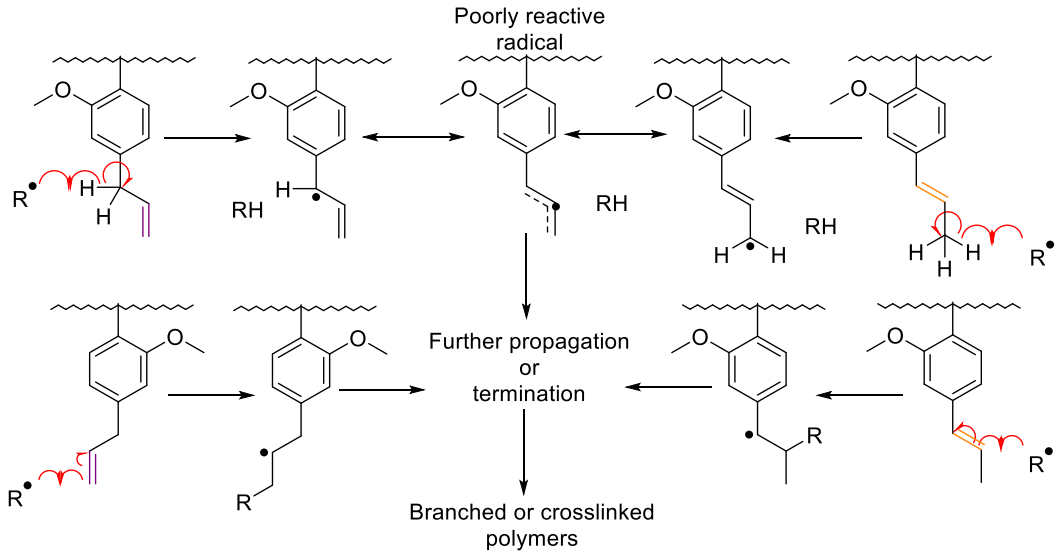

The abstraction of a hydrogen atom from both allyl and propenyl derivatives will indeed lead to virtually the same allylic radical strongly stabilized by resonance (Scheme 2-14). Moreover, radical addition can also occur directly on the double bond. Both reactions can lead to propagation (although with low probability considering the poorly reactive resonance-stabilized radical) or more probably to termination with either a radical derived from the initiator (primary termination) or with a growing polymer radical. These H-abstraction reactions, leading to resonance-stabilized radicals less prone to propagation, would ultimately result in lower polymerization rates (termination) and in branched and eventually cross-linked polymers. The consumption of the double bond was also studied by ^{1}H NMR spectroscopy (Figure 2-1). It was observed that in the case of EEMA after 24 h of reaction, 9% of the allylic double bonds and 81% of the methacrylate double bonds were consumed. In case of EIMA, 15% of the propenyl double bonds and 88% of the methacrylate double bonds were consumed after 24 h. This gives a ratio of 9:1 methacrylate double bonds/allylic double bonds consumption for EEMA and 5.8:1 methacrylate double bonds/propenyl double bonds consumption for EIMA.

Table 2-1.Characterization of homopolymers from eugenol-derived acrylates and methacrylates (Part A)

Monomer	Monomer conversion % (7h)	Monomer conversion % (24h)	T_g (°C)	Gel formation
EDMA	85	97	21	No
EIMA	63	88	40	No
EEMA	48	81	31	No
EDA	91 (6 h)	94	10	No
EIA	25	ND	ND	Yes
EEA	36	61	27	No

Thus, the propenyl double bond proved to be slightly more reactive than the allylic double bond. However, the mechanism followed by the allylic and propenyl double bonds seems to differ. Previous studies indicate that the propenyl groups are more prone to cross-propagation than to H-abstraction.[47] It was also possible to monitor the consumption of the allylic protons –Ar-C**H$_2$**-CH=CH$_2$ in the case of EEMA. It was found that 9% of the allylic protons had been consumed after 24 h. This means that there is a small abstraction of the allylic protons (10%) with the preservation of 91% of the allylic double bond occurring. Even though secondary reactions were present, the final polymers remained soluble in toluene. The monomers conversions were calculated both with the signals of the polymer (using the unreactive methoxy group as a reference) and by using the signal of an internal standard (1,4-bis(trimethylsilyl)benzene, BTMSB). The results obtained by both methods were equal, thus confirming the absence of an insoluble fraction.

SEC measurements after 7 h of reaction (Table 2-2, Appendix Figure A1-69 to Figure A1-72) show that the molar masses of poly(EEMA) and poly(EIMA) were lower than that of poly(EDMA). This is consistent with the occurrence of chain transfer during the polymerization of EEMA and EIMA. Furthermore, at longer reaction time (24 h), the average molar masses of poly(EEMA) and poly(EIMA) increased and the dispersity increased steadily for poly(EEMA) (multimodal) (Table 2-2). This suggests the formation of branched polymers. It is important to mention that the preservation of residual allylic and propenyl double bonds in the polymers was desired as it gives the opportunity to execute further cross-linking reactions or post-functionalisation of the polymers.

Table 2-2 Characterization of homopolymers from eugenol-derived acrylates and methacrylates (Part B)

Monomer	**M_n (g mol^{-1}) (7 h)**	**Đ (7 h)**	**M_n (g mol^{-1}) (24 h)**	**Đ (24 h)**
EDMA	26,900	2.3	26,700	2.5
EIMA	21,400	3.0	28,900	3.3
EEMA	19,700	2.3	28,000	Multimodal
EDA	16,300	3.0	14,000	3.5
EIA	17,500	3.8	ND	ND
EEA	9,500	3.0	15,900	Multimodal

The eugenol-derived acrylates behaved slightly differently. The solution homopolymerization of EDA was followed monitoring the disappearance of the acrylate double bond (Figure 2-2) and reached high conversion in 6 h (Table 2-1), showing as expected, the higher reactivity of the acrylate derivative compared to the analogous methacrylate in radical polymerization.[48,49] The molar mass of the poly(EDA) is lower at 24 h than at 7 h. This behaviour is consistent with the kinetics of conventional radical polymerization (quasi–steady–state approximation), where the initiation rate is approximated to be constant. Thus, as the concentration of monomer decreases

during the polymerization, the kinetic chain length diminishes with the increase of monomer conversion (Eq. 2-1)[50]

$$v = \frac{k_p[M]}{2(f k_d k_t [I])^{1/2}} \qquad \text{Eq. 2-1}$$

where k_p, k_d and k_t are the rate constants of propagation, decomposition and termination respectively, *f* is the initiator efficiency and [M] and [I] are the monomer and initiator concentration.

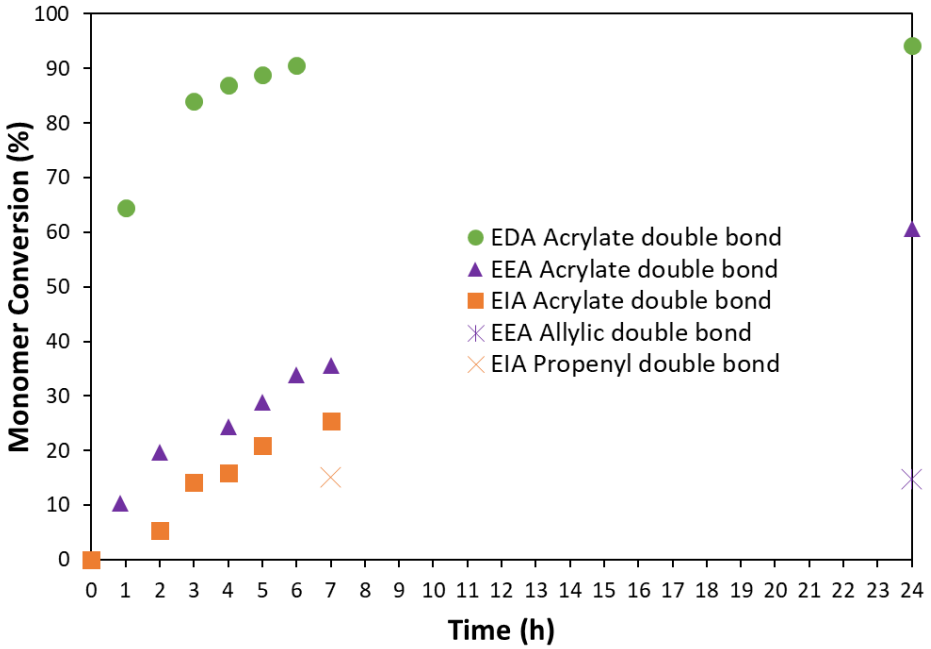

Figure 2-2. Monomer conversion of eugenol-derived acrylates in solution homopolymerization

In the case of the EEA and EIA (Figure 2-2) a lower conversion was reached in comparison with their methacrylate counterparts (Table 2-2). Furthermore, after 24 h, the polymerization of EIA led to the formation of a gel insoluble in toluene.

The monomer conversion was monitored by ^{1}H NMR through direct integration of the polymer and monomer signals (using the unreactive methoxy group as a reference) and also against the signal of the internal standard (BTMSB). In the case of the EDA and EEA polymerizations, monomer conversions were identical irrespective of the use of internal standard, implying that there was no gel formation during the polymerization. In contrast, for EIA polymerization, the two methods used to calculate conversion led to slightly different values. This suggests that gel formation occurred during the first hour of the reaction, producing a cross-linked insoluble material. The consumption of the allylic and propenyl double bonds was monitored by ^{1}H NMR (Figure 2-2).In the case of EEA, 8% of the allylic double bonds and 36% of the acrylate double bonds were consumed after 7 h of polymerization, whereas for EIA (soluble fraction), 12% of the propenyl double bonds and 25% of the acrylate double bonds were consumed during the same period of time (Figure 2-2). This gives a ratio of 4.5:1 acrylate double bonds: allylic double bonds consumption for EEA and 2.1:1 acrylate double bonds: propenyl double bonds consumption for EIA. This last value for EIA being related to

only the soluble fraction of the reaction media, the overall consumption of propenyl double bonds is underestimated and thought to be higher than 12%. Thus, in this polymerization, propenyl double bonds conversion might be due to the high reactivity of the acrylate function towards the propenyl double bond, leading to fast gelation (cross-propagation). However, it might also be due to the higher reactivity of poly(alkyl acrylate) radical towards H-abstraction, compared to poly(alkyl methacrylate) radical. The combination of a lower reactivity of the allylic double bonds compared to the propenyl double bonds (*i.e.* smaller extent of cross-propagation with acrylate) and the higher propensity to degradative chain transfer of the allylic protons (reflected by the lower molar masses, (Table 2-2 at 7 h) delays gelation in the case of EEA compared to EIA. Nevertheless, the increase of polydispersity with EEA conversion, from 3.0 at 36% conversion up to 8.7 (multimodal) at 61% conversion (Table 2-2), and the increase of molar masses clearly visible in the SEC chromatogram are signs of significant chain branching. Moreover, the consumption of the allylic protons was calculated and it was found that 15% of them had been consumed in the homopolymerization after 24 h. Similarly, in the case of EIA the monitoring of the propenyl protons showed a consumption of above 16% after 7 h (underestimated due to formation of insoluble fraction), which is slightly higher than the propenyl double bonds consumption of 12%. Nevertheless, approximately 83% of the allylic double bonds of EEA remained unreacted after 24 h of reaction, and available for cross-linking or post functionalisation of the polymers.

There was a decrease of the T_g (determined by DSC, Table 2-2, Appendix Figure A1-54 to Figure A1-58) of about 10°C between poly(methacrylates) and poly(acrylates). At first sight, this small difference is quite surprising, but small differences of T_g between poly(acrylates) and poly(methacrylates) have already been observed in polymers such as poly(isobornyl methacrylate) (T_g=110°C) and poly(isobornyl acrylate) (T_g=94°C).[51] Moreover, the secondary reactions involving the pending propenyl and allylic moieties may also contribute to this uncommon difference in T_g between these biobased poly(methacrylates) and poly(acrylates).

Samples of dried poly(EEMA) and poly(EIMA) (in form of powder) were preserved over one and half year in storage and their gel content and T_g measured again after experiencing a change of color from white to yellow. Further experiments were done preserving samples under different conditions and measuring gel content and T_g as shown in Figure 2-3 and Figure 2-4 (Appendix Figure A1-59 to Figure A1-68).

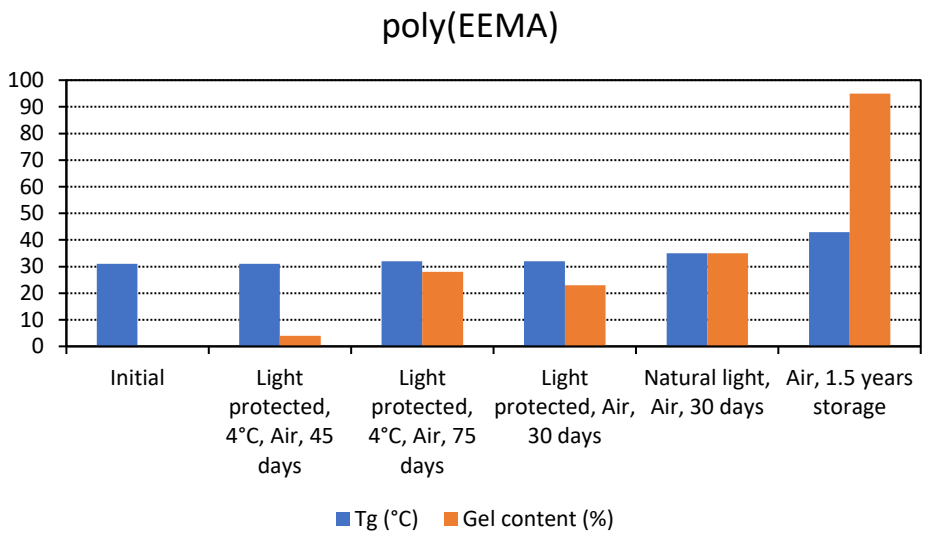

Figure 2-3. Autoxidation process of poly(EEMA) under different conditions

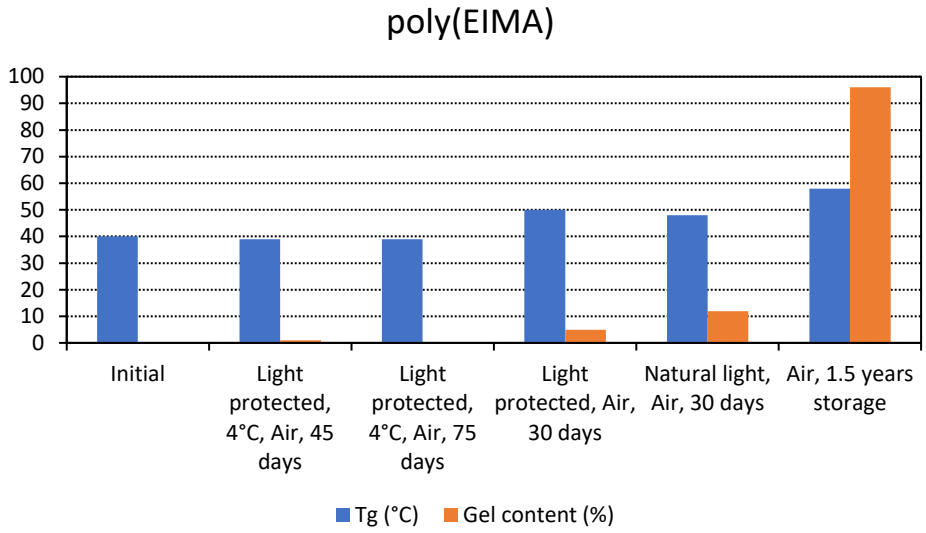

Figure 2-4. Autoxidation process of poly(EIMA) under different conditions

Oxidative curing has been observed in vegetable oils with allylic double bonds. This process, also called autoxidation, occurs quite slowly in the absence of a catalyst.[52–54] The autoxidation mechanism involves several steps such as: induction period, oxygen uptake, peroxide formation and peroxide decomposition (Scheme 2-15). When the samples were preserved under air, at 4°C and protected from light for 45 days, the T_g was not modified for both poly(EEMA) and poly(EIMA). However, after a 75 days poly(EEMA) exhibited a slight increase in T_g and 28% of gel content, while poly(EIMA) preserved the T_g and gel content value. Additionally, after an exposure of 30 days to

natural light and under air the gel content and T_g increased for both poly(EEMA) and poly(EIMA). It can be presumed that autoxidation occurs producing cross-linking even in the absence of a catalyst.

Scheme 2-15. Autoxidation process

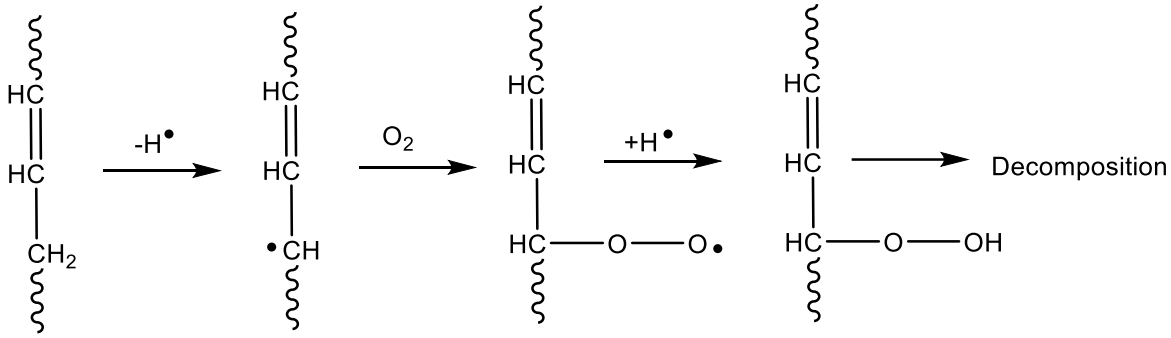

2.4 Conclusions

The syntheses of nine biobased eugenol-derived monomers (eight novel structures) are presented: ethoxy eugenyl methacrylate (EEMA), ethoxy isoeugenyl methacrylate (EIMA), ethoxy dihydroeugenyl methacrylate (EDMA), ethoxy eugenyl acrylate (EEA), ethoxy isoeugenyl acrylate (EIA), ethoxy dihydroeugenyl acrylate (EDA), epoxy EEMA and EEMA carbonate. The (meth)acrylic monomers were homopolymerized in solution (21% solids content) in toluene. The polymers exhibited T_g between 10°C and 40°C. High monomer conversions were obtained in the case of methacrylates: EDMA (98%), EIMA (89%) and EEMA (84%). The lower polymerization rates observed in the case of EIMA and EEMA compared to EDMA were probably a result of degradative chain transfer reactions (hydrogen abstraction of allylic protons) and cross-propagation (on the propenyl double bonds), both leading to resonance-stabilized poorly reactive radicals. Nevertheless, residual allylic and propenyl double bonds remained in the poly(EEMA) and poly(EIMA) polymers which are thus functional polymers. The remaining allylic and propenyl double bonds can be used to carry out further reactions such as cross-linking or post-functionalizations. For acrylates, the polymerization reached high conversion for EDA (94%), but a lower conversion was obtained for EEA (61%) and gelation was observed in the case of EIA (poly(EIA) was insoluble). Considering both the decrease of the polymerization rate and the production of branched polymers, the extent of the secondary reactions taking place on the allylic and propenyl moieties follows the decreasing order: EIA>>EEA>EEMA>EIMA. Nevertheless, in copolymerization with acrylates, EIMA is expected to show more side reactions than EEMA due to the higher reactivity of acrylates towards propenyl double bond. The resulting functional polymers possessing pending allylic or propenyl double bonds can be further functionalized to tune their properties and applications.

2.5 References

(1) Corma, A.; Iborra, S.; Velty, A. Chemical Routes for the Transformation of Biomass into Chemicals. *Chem. Rev.* **2007**, *107*, 2411.

(2) Sheldon, R. A. Green and Sustainable Manufacture of Chemicals from Biomass: State of the Art. *Green Chem.* **2014**, *16*, 950.

(3) Molina-Gutiérrez, S.; Ladmiral, V.; Bongiovanni, R.; Caillol, S.; Lacroix-Desmazes, P. Radical Polymerization of Biobased Monomers in Aqueous Dispersed Media. *Green Chem.* **2019**, *21*, 36.

(4) Li, W. S. J.; Ladmiral, V.; Takeshima, H.; Satoh, K.; Kamigaito, M.; Semsarilar, M.; Negrell, C.; Lacroix-Desmazes, P.; Caillol, S. Ferulic Acid-Based Reactive Core–Shell Latex by Seeded Emulsion Polymerization. *Polym. Chem.* **2019**, *10*, 3116.

(5) Kristufek, S. L.; Wacker, K. T.; Tsao, Y.-Y. T. Y. T.; Su, L.; Wooley, K. L. Monomer Design Strategies to Create Natural Product-Based Polymer Materials. *Nat. Prod. Rep.* **2017**, *34*, 433.

(6) Lomège, J.; Lapinte, V.; Negrell, C.; Robin, J.-J.; Caillol, S. Fatty Acid-Based Radically Polymerizable Monomers: From Novel Poly(Meth)Acrylates to Cutting-Edge Properties. *Biomacromolecules* **2019**, *20*, 4.

(7) Imada, M.; Takenaka, Y.; Hatanaka, H.; Tsuge, T.; Abe, H. Unique Acrylic Resins with Aromatic Side Chains by Homopolymerization of Cinnamic Monomers. *Commun. Chem.* **2019**, *2*, 5.

(8) Lochab, B.; Shukla, S.; Varma, I. K. Naturally Occurring Phenolic Sources: Monomers and Polymers. *RSC Adv.* **2014**, *4*, 21712.

(9) Ladmiral, V.; Jeannin, R.; Fernandes Lizarazu, K.; Lai-Kee-Him, J.; Bron, P.; Lacroix-Desmazes, P.; Caillol, S. Aromatic Biobased Polymer Latex from Cardanol. *Eur. Polym. J.* **2017**, *93*, 785.

(10) Li, W. S. J.; Negrell, C.; Ladmiral, V.; Lai-Kee-Him, J.; Bron, P.; Lacroix-Desmazes, P.; Joly-Duhamel, C.; Caillol, S. Cardanol-Based Polymer Latex by Radical Aqueous Miniemulsion Polymerization. *Polym. Chem.* **2018**, *9*, 2468.

(11) Rojo, L.; Vazquez, B.; Parra, J.; López Bravo, A.; Deb, S.; San Roman, J. From Natural Products to Polymeric Derivatives of “Eugenol”: A New Approach for Preparation of Dental Composites and Orthopedic Bone Cements. *Biomacromolecules* **2006**, *7*, 2751.

(12) Fache, M.; Darroman, E.; Besse, V.; Auvergne, R.; Caillol, S.; Boutevin, B. Vanillin, a Promising Biobased Building-Block for Monomer Synthesis. *Green Chem.* **2014**, *16*, 1987.

(13) Takeshima, H.; Satoh, K.; Kamigaito, M. Bio-Based Functional Styrene Monomers Derived from Naturally Occurring Ferulic Acid for Poly(Vinylcatechol) and Poly(Vinylguaiacol) via Controlled Radical Polymerization. *Macromolecules* **2017**, *50*, 4206.

(14) Azadi, P.; Inderwildi, O. R.; Farnood, R.; King, D. A. Liquid Fuels, Hydrogen and Chemicals from Lignin: A Critical Review. *Renew. Sustain. Energy Rev.* **2013**, *21*, 506.

(15) Khalil, A. A.; Rahman, U. ur; Khan, M. R.; Sahar, A.; Mehmood, T.; Khan, M. Essential Oil Eugenol: Sources, Extraction Techniques and Nutraceutical Perspectives. *RSC Adv.* **2017**,

7, 32669.

(16) da Silva, F. F. M.; Monte, F. J. Q.; de Lemos, T. L. G.; do Nascimento, P. G. G.; de Medeiros Costa, A. K.; de Paiva, L. M. M. Eugenol Derivatives: Synthesis, Characterization, and Evaluation of Antibacterial and Antioxidant Activities. *Chem. Cent. J.* **2018**, *12*, 34.

(17) Hu, Q.; Zhou, M.; Wei, S. Progress on the Antimicrobial Activity Research of Clove Oil and Eugenol in the Food Antisepsis Field. *J. Food Sci.* **2018**, *83*, 1476.

(18) Zakzeski, J.; Bruijnincx, P. C. A.; Jongerius, A. L.; Weckhuysen, B. M. The Catalytic Valorization of Lignin for the Production of Renewable Chemicals. *Chem. Rev.* **2010**, *110*, 3552.

(19) Nimmanwudipong, T.; Runnebaum, R. C.; Ebeler, S. E.; Block, D. E.; Gates, B. C. Upgrading of Lignin-Derived Compounds: Reactions of Eugenol Catalyzed by HY Zeolite and by Pt/γ-Al2O3. *Catal. Letters* **2012**, *142*, 151.

(20) Isikgor, F. H.; Becer, C. R. Lignocellulosic Biomass: A Sustainable Platform for the Production of Bio-Based Chemicals and Polymers. *Polym. Chem.* **2015**, *6*, 4497.

(21) Sun, Z.; Fridrich, B.; De Santi, A.; Elangovan, S.; Barta, K. Bright Side of Lignin Depolymerization: Toward New Platform Chemicals. *Chem. Rev.* **2018**, *118*, 614.

(22) Ragauskas, A. J.; Beckham, G. T.; Biddy, M. J.; Chandra, R.; Chen, F.; Davis, M. F.; Davison, B. H.; Dixon, R. A.; Gilna, P.; Keller, M.; et al. Lignin Valorization: Improving Lignin Processing in the Biorefinery. *Science (80-.).* **2014**, *344*, 1246843.

(23) Abdelaziz, O. Y.; Hulteberg, C. P. Physicochemical Characterisation of Technical Lignins for Their Potential Valorisation. *Waste and Biomass Valorization* **2017**, *8*, 859.

(24) Schutyser, W.; Renders, T.; Van den Bosch, S.; Koelewijn, S.-F.; Beckham, G. T.; Sels, B. F. Chemicals from Lignin: An Interplay of Lignocellulose Fractionation, Depolymerisation, and Upgrading. *Chem. Soc. Rev.* **2018**, *47*, 852.

(25) Kamatou, G. P.; Vermaak, I.; Viljoen, A. M. Eugenol - From the Remote Maluku Islands to the International Market Place: A Review of a Remarkable and Versatile Molecule. *Molecules*. 2012, pp 6953–6981.

(26) Markowitz, K.; Moynihan, M.; Liu, M.; Kim, S. Biologic Properties of Eugenol and Zinc Oxide-Eugenol. A Clinically Oriented Review. *Oral Surgery, Oral Med. Oral Pathol.* **1992**, *73*, 729.

(27) Chen, C.; Xiao, M.; Deng, L.; Yuan, L.; Zhang, P. An Effective Way to Biosynthesize α -Glucosyl Eugenol with a High Yield by Xanthomonas Maltophilia. *Pharm. Biol.* **2012**, *50*, 727.

(28) Chiaradia, V.; Paroul, N.; Cansian, R. L.; Júnior, C. V.; Detofol, M. R.; Lerin, L. A.; Oliveira, J. V.; Oliveira, D. Synthesis of Eugenol Esters by Lipase-Catalyzed Reaction in Solvent-Free System. *Appl. Biochem. Biotechnol.* **2012**, *168*, 742.

(29) Gazzotti, S.; Hakkarainen, M.; Adolfsson, K. H.; Ortenzi, M. A.; Farina, H.; Lesma, G.; Silvani, A. One-Pot Synthesis of Sustainable High-Performance Thermoset by Exploiting Eugenol Functionalized 1,3-Dioxolan-4-One. *ACS Sustain. Chem. Eng.* **2018**, *6*, 15201.

(30) Breloy, L.; Ouarabi, C. A.; Brosseau, A.; Dubot, P.; Brezova, V.; Abbad Andaloussi, S.; Malval, J. P.; Versace, D. L. β-Carotene/Limonene Derivatives/Eugenol: Green Synthesis of

Antibacterial Coatings under Visible-Light Exposure. *ACS Sustain. Chem. Eng.* **2019**, *7*, 19591.

(31) Kishore, D.; Kannan, S. Isomerization of Eugenol and Safrole over MgAl Hydrotalcite, a Solid Base CatalystElectronic Supplementary Information (ESI) Available: Figs. S1 and S2: PXRD Patterns. See Http://Www.Rsc.Org/Suppdata/Gc/B2/B207865a/. *Green Chem.* **2002**, *4*, 607.

(32) Deng, J.; Yang, B.; Chen, C.; Liang, J. Renewable Eugenol-Based Polymeric Oil-Absorbent Microspheres: Preparation and Oil Absorption Ability. *ACS Sustain. Chem. Eng.* **2015**, *3*, 599.

(33) Wang, F.; Finnin, J.; Tait, C.; Quirk, S.; Chekhtman, I.; Donohue, A. C.; Ng, S.; D'Souza, A.; Tait, R.; Prankerd, R. The Hydrolysis of Diclofenac Esters: Synthetic Prodrug Building Blocks for Biodegradable Drug-Polymer Conjugates. *J. Pharm. Sci.* **2016**, *105*, 773.

(34) Vidil, T.; Tournilhac, F.; Musso, S.; Robisson, A.; Leibler, L. Control of Reactions and Network Structures of Epoxy Thermosets. *Prog. Polym. Sci.* **2016**, *62*, 126.

(35) Yadav, N.; Seidi, F.; Crespy, D.; D'Elia, V. Polymers Based on Cyclic Carbonates as Trait d'Union Between Polymer Chemistry and Sustainable CO 2 Utilization. *ChemSusChem* **2019**, *12*, 724.

(36) Ferraz, H. M. C.; Muzzi, R. M.; De O. Vieira, T.; Viertler, H. A Simple and Efficient Protocol for Epoxidation of Olefins Using Dimethyldioxirane. *Tetrahedron Lett.* **2000**, *41*, 5021.

(37) Yamaguchi, K.; Ebitani, K.; Yoshida, T.; Yoshida, H.; Kaneda, K. Mg−Al Mixed Oxides as Highly Active Acid−Base Catalysts for Cycloaddition of Carbon Dioxide to Epoxides. *J. Am. Chem. Soc.* **1999**, *121*, 4526.

(38) Tamami, B.; Sohn, S.; Wilkes, G. L. Incorporation of Carbon Dioxide into Soybean Oil and Subsequent Preparation and Studies of Nonisocyanate Polyurethane Networks. *J. Appl. Polym. Sci.* **2004**, *92*, 883.

(39) Doll, K. M.; Erhan, S. Z. The Improved Synthesis of Carbonated Soybean Oil Using Supercritical Carbon Dioxide at a Reduced Reaction Time. *Green Chem.* **2005**, *7*, 849.

(40) Doll, K. M.; Erhan, S. Z. Synthesis of Carbonated Fatty Methyl Esters Using Supercritical Carbon Dioxide. *J. Agric. Food Chem.* **2005**, *53*, 9608.

(41) Webster, D. C.; Crain, A. L. Synthesis and Applications of Cyclic Carbonate Functional Polymers in Thermosetting Coatings. *Progress in Organic Coatings*. 2000, pp 275–282.

(42) Suzuki, A.; Nagai, D.; Ochiai, B.; Endo, T. Facile Synthesis and Crosslinking Reaction of Trifunctional Five-Membered Cyclic Carbonate and Dithiocarbonate. *Journal of Polymer Science, Part A: Polymer Chemistry*. 2004, pp 5983–5989.

(43) Camara, F.; Caillol, S.; Boutevin, B. Free Radical Polymerization Study of Glycerin Carbonate Methacrylate for the Synthesis of Cyclic Carbonate Functionalized Polymers. *Eur. Polym. J.* **2014**, *61*, 133.

(44) Gaylord, N. G. Allyl Polymerization. IV. Effective Chain Transfer in Polymerization of Allylic Monomers. *J. Polym. Sci.* **1956**, *22*, 71.

(45) Aota, H.; Matsumoto, A.; Kumagai, T.; Kawasaki, H.; Arakawa, R.; Aota, H.; Kawasaki, H.;

Arakawa, R. Reassessment of Free-Radical Polymerization Mechanism of Allyl Acetate Based on End-Group Determination of Resulting Oligomers by MALDI-TOF-MS Spectrometry. *Polym. J.* **2009**, *41*, 26.

(46) Zhang, Y.; Dubé, M. A.; Vivaldo-Lima, E. Modeling Degradative Chain Transfer in d -Limonene/ n -Butyl Methacrylate Free-Radical Copolymerization. *J. Renew. Mater.* **2015**, *3*, 318.

(47) Barson, C. A.; Bevingtont, J. C.; Hunt, B. J. The Effects of Some Phenyl Derivatives of Propene upon Radical Polymerizations. **1998**, *39*, 1345.

(48) Van Herk, A. M. Pulsed Initiation Polymerization as a Means of Obtaining Propagation Rate Coefficients in Free-Radical Polymerizations. II Review up to 2000. *Macromol. Theory Simulations* **2000**, *9*, 433.

(49) Beuermann, S.; Buback, M. Rate Coefficients of Free-Radical Polymerization Deduced from Pulsed Laser Experiments. *Prog. Polym. Sci.* **2002**, *27*, 191.

(50) Odian, G. *Principles of Polymerization*; John Wiley & Sons, Inc.: Hoboken, NJ, USA, 2004; Vol. 58.

(51) Sigma-Aldrich. Thermal Transitions of Homopolymers: Glass Transition & Melting Point https://www.sigmaaldrich.com/technical-documents/articles/materials-science/polymer-science/thermal-transitions-of-homopolymers.html (accessed Apr 8, 2019).

(52) Soucek, M. D.; Khattab, T.; Wu, J. Review of Autoxidation and Driers. *Prog. Org. Coatings* **2012**, *73*, 435.

(53) Ghogare, A. A.; Greer, A. Using Singlet Oxygen to Synthesize Natural Products and Drugs. *Chem. Rev.* **2016**, *116*, 9994.

(54) Jacobsen, C. Oxidative Rancidity. In *Encyclopedia of Food Chemistry*; Elsevier, 2019; pp 261–269.

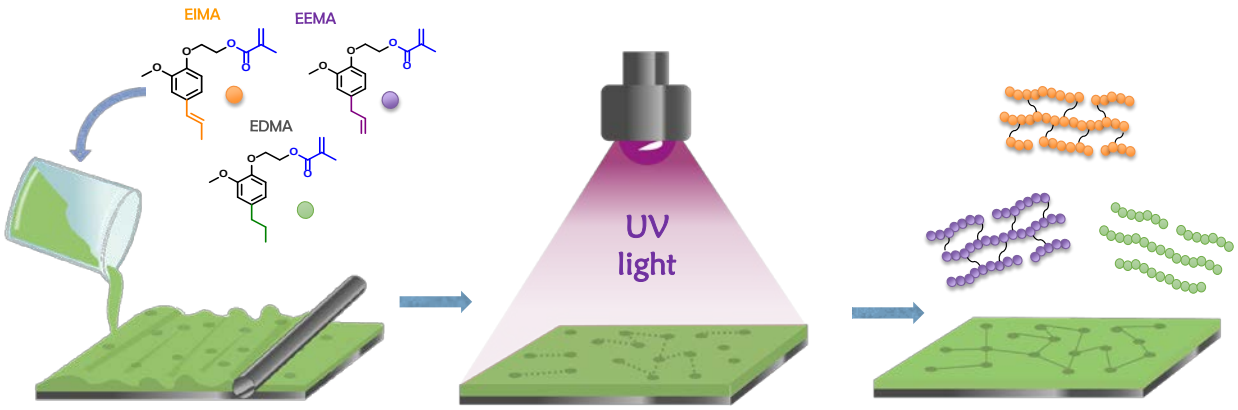

CHAPTER THREE

Photoinduced polymerization of eugenol-derived monomers

Table of Contents

Chapter 3: Photoinduced polymerization of eugenol-derived monomers

Some of the results and discussion presented in this chapter have been published in the article:

- Molina-Gutiérrez, S.; Dalle Vacche, S.; Vitale, A.; Ladmiral, V.; Caillol, S.; Bongiovanni, R.; Lacroix-Desmazes, P. Photoinduced Polymerization of Eugenol-Derived Methacrylates. *Molecules* **2020**, 25, 3444. https://doi.org/10.3390/molecules25153444.

3.1 Introduction

The need for more environmentally friendly materials and processes has led to the development of suitable biobased building blocks to produce polymers.[1] However, the use of energy-efficient polymerization techniques is also paramount. Photoinduced polymerization is a suitable option, as it allows fast processes, low energy consumption, room temperature reactions, and solvent-free conditions with the reduction or elimination of volatile organic compounds (VOCs).[2] Thanks to these advantages, it has found wide application in industrial processes. It is an established technique in the fields of coatings, inks, adhesives, and wood finishing.[3] Products from photopolymerization are present in everyday life, such as contact lenses,[4] filling for dental cavities,[5] and credit cards.[6]

3.1.1 Eugenol-derived monomers in photoinduced polymerization

In search of sustainability, it is crucial to replace oil-based monomers with bio-based ones produced from renewable sources. Among the available biobased building blocks, some natural molecules can undergo autooxidation reactions, cyclization, isomerization, dimerization, and oligomerization in the presence of light.[7,8] However, most of these require being suitably functionalized prior to photoinduced polymerization processes. The introduction of polymerizable functions on biobased building blocks is thus a crucial step.

Recently, the use of naturally occurring phenols, such as eugenol and eugenol-derivatives, has gained attention for producing biobased monomers, as they can be obtained by lignin depolymerization.[9–11] In addition, eugenol-derived monomers are attractive because they possess antioxidant, antiseptic, and antibacterial properties,[12,13] which could be exploited in photopolymers for dentistry or food packaging.[14] In particular, isoeugenol has a higher antibacterial activity than eugenol and is not genotoxic.[15] However, as many other biobased building blocks, eugenol and its derivatives do not possess functional groups that react readily through photoinduced polymerization. In addition, phenols scavenge free radicals and inhibit polymerization.[16,17] Thus, suitable functional groups must be inserted to avoid this inhibition and promote polymerization.

Besides the functionalization of eugenol with epoxy groups for cationic photopolymerization and thiol-epoxy condensation,[18–20] methacrylate functional groups have also been introduced in the molecule. Eugenol methacrylic derivatives were obtained by reacting the allylic double bond with 3-mercaptopropionic acid and thiomalic acid (*via* thiol-ene chemistry) and then reacting to the resulting carboxylic acid product and phenol group of eugenol with glycidyl methacrylate. These monomers were then used in photoinduced copolymerization with AESO (acrylated epoxidized

soybean oil) to produce biobased coatings.[21] Moreover, allyl-etherified eugenol-derivatives were copolymerized through thiol-ene reactions with pentaerythritol-based primary and secondary tetrathiol and with isocyanurate-based secondary trithiol, to prepare crosslinked polymers.[22] Similarly, allyl-etherified eugenol and linalool were copolymerized with trimethylolpropane tris(3-mercaptopropionate) to form crosslinked networks endowed with antioxidant and antibacterial properties.[14] Later, a trifunctional allyl compound, tris(4-allyl-2 methoxyphenolyl) phosphate, was synthesized and reacted with thiols with two to four functionalities *via* thiol-ene chemistry and the influence of crosslink density on the different materials was studied.[23] Thiol-ene chemistry was also employed to covalently attach eugenol through its allylic double bond to a limonene-derived polymer network and prepare antibacterial coatings.[24]

As described in Chapter 2, a monomer platform including methacrylated eugenol derivatives has been synthesized.[25] Biobased polymers obtained in the form of homogeneous and transparent films are potentially interesting for industrial development and could find application in coatings, food packaging or dentistry. Therefore, in the present chapter, we investigated the photopolymerization of films of these eugenol methacrylates under irradiation in different conditions: with or without the radical photoinitiator and in the presence or in the absence of air. Moreover, the conversion of the methacrylic double bond of the three monomers as well as the conversion of the allylic (EEMA) or propenyl (EIMA) double bonds are monitored, and the properties of the polymers were tested.

3.2 Materials and Methods

3.2.1 Materials

Ethoxy eugenyl methacrylate (EEMA), ethoxy isoeugenyl methacrylate (EIMA), ethoxy dihydroeugenyl methacrylate (EDMA) monomers were synthesized as described in Chapter 2.[25] Toluene (>98%) was purchased from Sigma-Aldrich. The radical photoinitiators 2-hydroxy-2-methylpropiophenone (tradename Darocur 1173) and phenylbis(2,4,6-trimethylbenzoyl)phosphine oxide (tradename Irgacure 819), were kindly given by BASF and used as received.

3.2.2 Photoinduced polymerization of eugenol derived methacrylates

Samples Preparation. To monitor the photopolymerization kinetics of each monomer, a mixture of monomer and PI at 2% wbm (weight based on monomer) was spread over a silicon wafer using a rod coater, forming a film with a thickness of 10 µm. Samples were irradiated up to 9 min either under air or protected from air with a 30 µm-thick polypropylene (PP) film.

Kinetics Monitoring. Photopolymerization was monitored using Real-Time Fourier Transform Infrared (FT-IR) spectroscopy on a Nicolet iS50 spectrometer. The spectra were acquired in transmission mode, in the 650–4000 cm^{-1} range, with 1 scan per spectrum and a resolution of 4 cm^{-1}.

A high-pressure mercury-xenon lamp Lightning Cure LC8 from Hamamatsu equipped with a flexible light guide was used as UV-light source (L9566-02A, 220 to 600 nm)[26] and an EIT Powerpuck® II

radiometer was used to measure the UV irradiance. The samples were irradiated with 260 mW cm^{-2} (sum of UVA, UVB, UVC, UVV). In some experiments, light was filtered using a A9616-07 filter (Hamamatsu) with a transmittance wavelength of 355–375 nm (centered at 365 nm) The filtered light had and intensity of 78 mW cm^{-2} (UVA).

Conversion Determination. (Appendix Figure A2-1 and Figure A2-2, Scheme A2-1, Table A2.1, Eq. A2-1 to Eq. A2-6) The methacrylate double bonds (MDB) conversion was monitored using the band at 1638 cm^{-1}, the allylic double bonds (ADB) conversion was monitored using the band at 995 cm^{-1}, and the propenyl double bonds (PDB) conversion was determined using the 960 cm^{-1} band.[22,27–29] Each conversion was calculated using the following Eq. 3-1:

$$Conversion\%_{t=x} = 100 \times \left(1 - \frac{\frac{A_{t=x}}{Ref.A_{t=x}}}{\frac{A_{t=0}}{Ref.A_{t=0}}}\right) \qquad \text{Eq. 3-1}$$

Where A is the absorbance of the IR band of the functional group monitored during irradiation; Ref A is the absorbance of the band of the aromatic ring (C-C stretching) taken as a reference (1540 cm^{-1} to 1490 cm^{-1}).

Absorbances were estimated as the area of the vibrational bands under examination. Data were processed using OMNIC software. All curves were smoothed using the Savitzky–Golay method with 20 points window and second polynomial order. For the determination of EEMA methacrylate double bonds conversion, an approximation was made as peaks corresponding to the allylic and methacrylate double bond superimposed at circa 1638 cm^{-1} (Appendix Eq. A2-1 to Eq. A2-6).

3.2.3 Characterization Methods

Sample preparation. Samples for thermogravimetric analysis (TGA), differential scanning calorimetry (DSC), and gel content were prepared by coating a glass slide with 200 µm films and irradiating it for 10 min using a DYMAX 5000 EC UV flood lamp in the range of 320 to 390 nm with an intensity on the sample of 156 mW cm^{-2} (UVA and UVV).

Infrared spectroscopy (IR). Spectra to determine the conversion were acquired on a Thermo Scientific Nicolet 6700 FTIR apparatus in the 650–4000 cm^{-1} range, with 32 scan per spectrum and a resolution of 4 cm^{-1} (using attenuated total reflectance technique, ATR) on both faces of the film: the one exposed to the atmosphere and the one in contact with the glass slide.

Ultraviolet and visible spectroscopy (UV-Vis). (Appendix Figure A2-3 to Figure A2-4) Spectra were recorded on a Varian Cary 50 Scan spectrophotometer from 200 to 800 nm with a scan rate of 4800 nm min^{-1}.

Thermogravimetric Analysis (TGA). Analyses were performed on 5–10 mg samples on a TGA Q50 apparatus from TA Instruments from 20°C to 580°C, in an aluminum pan, at a heating rate of 20°C min^{-1}, under nitrogen.

Differential Scanning Calorimetry (DSC). (Appendix Figure A2-5 to Figure A2-10) Measurements were performed on 10–15 mg samples, under nitrogen atmosphere, with a Netzsch DSC 200 F3 instrument using the following heating/cooling cycle: first cooling ramp from room temperature (ca. 20°C) to −40°C at 20°C min^{-1}, isothermal plateau at −40°C for 10 min, first heating ramp from −40°C to 150°C at 20°C min^{-1}, second cooling stage from 150°C to −40°C at 20 °C min^{-1}, isothermal plateau at −40°C for 10 min, second heating ramp from −40°C to 150°C at 20 °C min^{-1}, third cooling stage from 150°C to −40°C at 20°C min^{-1}, isothermal plateau at −40°C for 10 min, third heating ramp from −40°C to 150°C at 20°C min^{-1} and last cooling stage from 150°C to room temperature (ca. 20°C). T_g values are given from the evaluation of the third heating ramp. Calibration of the instrument was performed with noble metals and checked with an indium sample.

Gel content measurements. The gel content of the polymers was measured by placing approximately 30–50 mg of polymer in a Teflon pocket which was subsequently immersed in 10 mL of toluene for 24 h, then dried in a ventilated oven at 50°C for 4 h. The gel content was calculated based on the initial (W_i) and final (W_f) polymer mass according to Eq. 3-2:

$$Gel\ content(\%) = \frac{W_f \times 100}{W_i} \qquad \text{Eq. 3-2}$$

3.3 Results and Discussion

3.3.1 Kinetic monitoring of photoinduced polymerization of eugenol-derived methacrylates

The photoinduced polymerization of ethoxy eugenyl methacrylate (EEMA), ethoxy isoeugenyl methacrylate (EIMA) and ethoxy dihydroeugenyl methacrylate (EDMA) was conducted by irradiating the monomers spread on a solid substrate in the form of films. Different experimental conditions were investigated. At first, the reactions were attempted in the absence of any photoinitiator (PI). Avoiding the use of PI is a crucial step in the development of new products for many real life applications (e.g., inks for food packaging, dental materials) as photoinitiators decompose into harmful species which can uncontrollably migrate.[30] Then, reactions were done in the presence of two different Norrish Type I photoinitiators. Azo-initiators, largely used in radical polymerization, can also be used as photoinitiators. However, they have been reported to have low efficiency compared to acyl photoinitiators.[31] Thus, Darocur 1173 and Irgacure 819 were selected. As the reaction proceeds *via* a radical mechanism, the effect of oxygen was studied by irradiating the monomers either in the presence or absence of air. Experiments in the absence of air were carried out by covering the monomer films with a polypropylene (PP) film. This is a common strategy to protect polymerization samples from oxygen and reduce inhibition.[32]

3.3.1.1 Photopolymerization without photoinitiator

The kinetics of the reactions of the eugenol-derivatives EDMA, EEMA, and EIMA were monitored by Real-Time FT-IR in transmission mode while they were exposed to a UV-light source (L9566-02A, 240 nm to 400 nm, 260 mW cm^{-2})[26] in the presence or in the absence of air. The band

corresponding to the methacrylate double bond at 1638 cm^{-1} (C=C stretching vibration),[33] and the aromatic band at 1514 cm^{-1} (C-H aromatic in-plane bending)[29] as reference, were monitored over the irradiation time. The conversion of the methacrylate double bonds (MDB) for EDMA, EEMA, and EIMA are presented in Figure 3-1. Simultaneously, the conversion of the allylic double bonds (ADB) from EEMA and propenyl double bonds (PDB) from EIMA were monitored using the bands at 995 cm^{-1} and 960 cm^{-1} respectively. The results comparing allylic and propenyl double bond conversion with regards to the presence or absence of air are plotted in Figure 3-2.

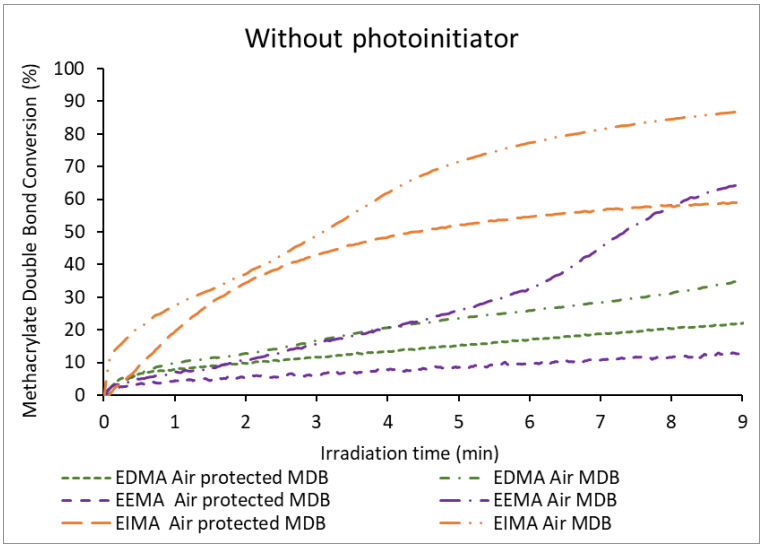

Figure 3-1. Methacrylate double bond (MDB) conversion of eugenol-derived monomers versus irradiation time in the absence of photoinitiator.

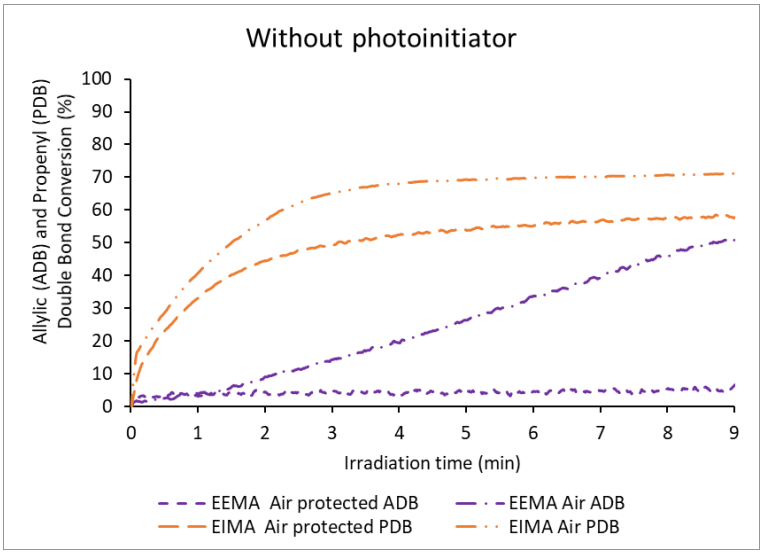

Figure 3-2. Allylic (ADB) and Propenyl double bond (PDB) conversion of eugenol-derived monomers versus irradiation time in the absence of photoinitiator.

Figure 3-1 shows that the methacrylic double bonds (MDB) of all monomers can react upon light exposure even in the absence of any photoinitiator. This was not surprising, as it has been previously reported that (meth)acrylates could undergo photopolymerization without a photoinitiator

due to self-initiation.[34–37] Interestingly, the final conversion of MDB and the conversion rate (*i.e.*, the slope of the conversion versus time curve) were different for the three monomers. The reactivity trend was as follows: EIMA >> EDMA > EEMA. EIMA was the most reactive monomer (higher slope, final conversion of 59%), while the conversion of EDMA and EEMA remained low reaching only 22% and 12% respectively at the end of the irradiation (Table 3-1). The different reactivities of the MDBs may be explained by the difference in the UV absorption spectra of the monomers (Appendix Figure A2-3). The monomers UV absorption curves overlap with the emission spectrum of the Hg lamp used as irradiation source.[26] The absorption of EIMA is significantly higher than that of EDMA and EEMA. Thus, EIMA is more likely to undergo faster self-initiation. To confirm that the monomers self-initiate due to UV absorption,[34] further polymerization experiments protected from air were performed under UV irradiation but using a filter to stop wavelengths below 365 nm. As expected, since the monomers absorb below 320 nm, no reaction was observed for any of the monomers. These experiments confirmed the hypothesis of self-initiation being responsible for the polymerization occurring in the absence of PI.

Besides the methacrylic group, the reactivity of the allyl and propenyl groups, present in EEMA and EIMA respectively, was studied during photopolymerization processes protected from air (Figure 3-2). Indeed, allylic and propenyl double bonds can experience secondary reactions such as (degradative) chain transfer reactions (allylic hydrogen abstraction produce poorly-reactive highly-stabilized radicals) and radical addition (cross-propagation) (Scheme 3-1).[25,38–40] The radicals formed from these secondary reactions can undergo further propagation or termination yielding branched and even crosslinked polymers (in the case of termination by combination). In the absence of air, the propenyl double bond (PDB) of EIMA was quite reactive and reached nearly the same conversion as the methacrylic double bonds (58%). On the other hand, the allylic double bond (ADB) of EEMA displayed a very low conversion (6%). For this monomer, a lower reaction rate and MDB conversion were obtained (Figure 3-1). EEMA allylic hydrogens can be abstracted and form highly stabilized radicals (main secondary reaction). This can affect the propagation rate as the corresponding radicals become less reactive (degradative chain transfer). This effect was not seen for EIMA, implying that PDB reacts mainly through cross-propagation reactions between propenyl and methacrylic groups, as discussed in Chapter II for the experiments of polymerization in solution.

Scheme 3-1. Scavenging and cross-propagation reactions on allylic and propenyl double bonds of eugenol-derived methacrylates

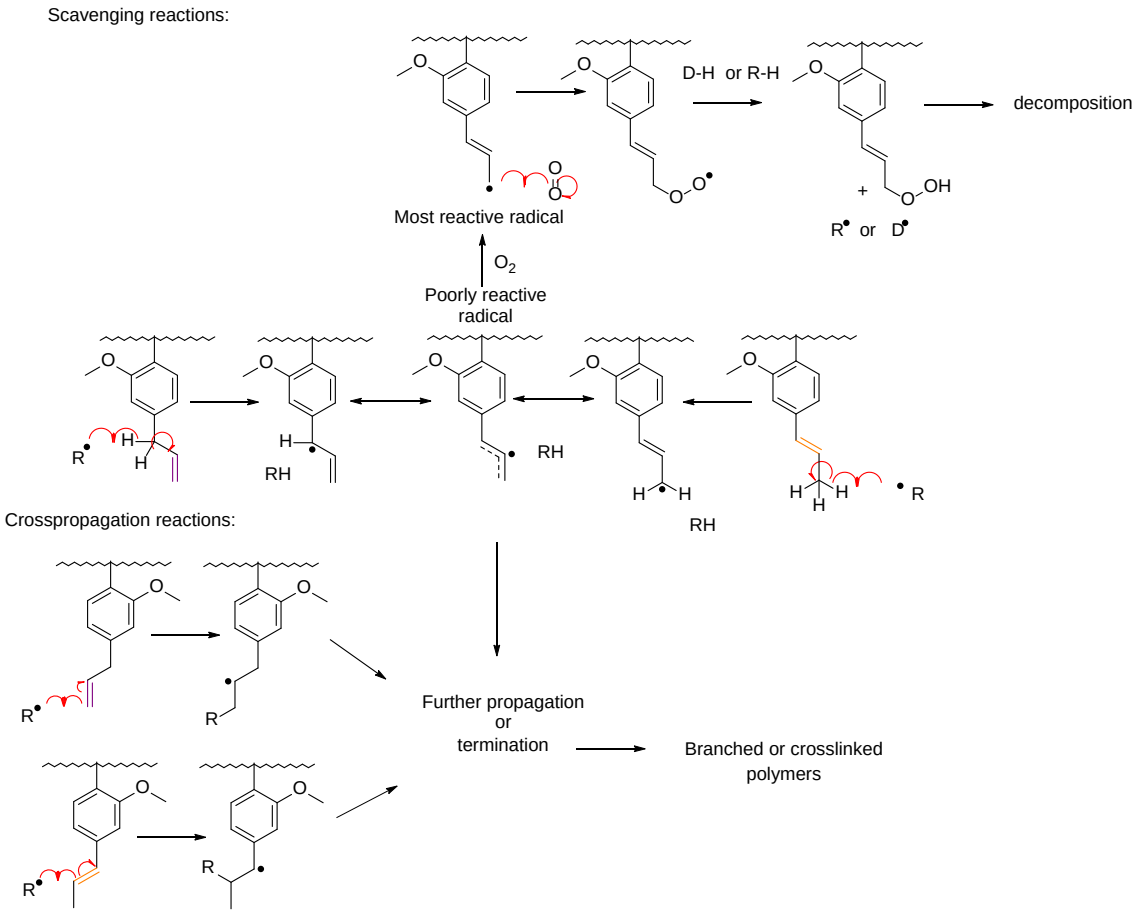

Figure 3-1 shows that the methacrylate double bond conversions under air have different profiles compared to those of the polymerization protected from air. Changes in the curve slope are visible, signaling a noticeable variation of the speed of the reaction during the irradiation. This behavior is particularly clear for EIMA and to a lower extent for EEMA (Figure 3-1), but it is negligible for EDMA. The sigmoidal profile appearing in the curves is caused by the occurrence of two polymerization regimes. These are due to the formation of hydroperoxides in the presence of oxygen, as reported in literature.[41] Indeed, radicals produced by irradiation of the monomers can react with oxygen according to Scheme 3-1 and Eq. 3-3 to Eq. 3-5:

$$R^{\cdot} + O_2 \rightarrow RO_2^{\cdot} \qquad \text{Eq. 3-3}$$

$$RO_2^{\cdot} + RH \rightarrow RO_2H + R^{\cdot} \qquad \text{Eq. 3-4}$$

$$RO_2H \xrightarrow{h\nu} RO^{\cdot} + HO^{\cdot} \qquad \text{Eq. 3-5}$$

Once peroxy radicals ($RO_2^{\cdot}$) are formed (Eq. 3-3), hydroperoxides (RO_2H) are generated by hydrogen abstraction (Eq. 3-4).[32] The three monomers possess abstractable hydrogen atoms: bis-allylic hydrogens in EEMA (Ph-C**H$_2$**-CH=CH$_2$), propenylic hydrogens in EIMA (Ph-CH=CH-C**H$_3$**), and benzylic hydrogens in EDMA (Ph-C**H$_2$**-CH$_2$-CH$_3$). Hydroperoxides react slowly, therefore

oxygen is often described as an inhibitor of radical polymerization. The phenomenon is particularly severe in photopolymerization when monomers are irradiated in films. In such a situation, a large area is exposed to oxygen, and oxygen can be continuously replaced by diffusion at the surface of the reacting formulation. However, hydroperoxides can decompose, through continued irradiation, to produce new radicals (Eq. 3-5) that are able to trigger additional initiation and a second polymerization regime.[41] Herein, IR analyses confirmed the hydroperoxides formation during the photopolymerization reactions carried out in the presence of air (Appendix Figure A2-11 to Figure A2-13).

Contrary to what was expected, all the monomers showed a higher MDB conversion in the presence of air than in the absence of air. During the first minute of irradiation, EEMA and EDMA displayed very similar MDB conversion under air or protected from air. However, conversion increased significantly at higher irradiation time in the presence of air. Specifically, for EEMA, MDB final conversion reached 66% under air (and only 12% when protected from air over the same irradiation time). For EDMA, the final conversion was 35% in the presence of air and 22% when protected from air (Table 3-1.). Finally, for EIMA, the MDB conversion and conversion rates under air were always higher than in the absence of air from the onset of irradiation. Similar to EEMA, after the first polymerization regime, the conversion rate of EIMA MDB increased (producing a second polymerization regime) and a final conversion of 86% was reached (59% in the absence of air).

Figure 3-2 shows that EEMA ADB are consumed up to 49% in the presence of air, while they are almost non-reactive in the absence of air. This can explain the high reactivity of the EEMA MDBs under air. Allylic double bonds undergo hydrogen abstraction leading to radicals that can react with oxygen to form peroxy radicals which scavenge oxygen and thus prevent the oxygen inhibition of MDB polymerization. The peroxy radicals can then form hydroperoxides that decompose to provide additional radicals for further MDB polymerization. In the case of EIMA, the conversion of PDB reached relatively higher values under air (68%) than while air-protected (58%), independently of the irradiation time (Figure 3-2 and Table 3-1). PDB can be consumed not only by the formation of peroxy and hydroperoxy radicals when oxygen is present but also by cross-propagation reactions (Scheme 3-1). Only a slightly higher consumption of PDB was observed in the polymerizations carried out under air compared to those protected from it. This suggests that although hydroperoxides are formed under air, cross-propagation is the main secondary reaction (as observed in solution homopolymerization of EIMA in Chapter 2).

In addition, higher conversion of the monomers under air can also be related to the formation of ozone induced by the UV irradiation at 242 nm and its subsequent photolysis into singlet oxygen ($^1O_2$).[42,43] Singlet oxygen can react with the ADB and PDB of both EEMA and EIMA, again forming peroxy radicals and hydroperoxides which dissociate into other radicals.[44–47]

Styrene can polymerize in the absence of a photoinitiator, due its capacity to form charge-transfer complexes with oxygen.[48,49] These complexes lead to the production of peroxides eventually leading to the production of radicals. Recently, Krueger *et al*.[50] concluded that in photoinitiator-free

styrene polymerizations, oxygen reacts photochemically with styrene at the beginning of their polymerization reactions but that peroxides are not the sole source of radical formation. The photochemical radical generation *via* photo electron transfer (PET) requires a donor-acceptor pair. In the absence of oxygen, the PET between styrene-polystyrene leads to the generation of radical ions continuing the polymerization in the absence of PI. A similar process could occur in the case of isoeugenol. Moreover, the triplet state of isoeugenol derivatives has been suspected to produce singlet oxygen able to react with the double bond to form dioxetane, which can cleave to produce aldehydes.[49,51] Nonetheless, no increment or change was noticed in the bands at 2827 cm^{-1} and 2725 cm^{-1}, corresponding to the Fermi resonance characteristic of aldehydes. Hence, the consumption of PDB does not follow this pathway here.

To avoid the absorption of light by the monomers and the possible formation of ozone, further polymerization experiments under air were performed using a 355–375 nm bandpass filter. Unsurprisingly, no reaction was observed for any of the monomers, since neither monomer homolytic cleavage nor ozone production (both leading to radicals) occur at this longer irradiation wavelength.

In conclusion, the eugenol-derived methacrylates can photopolymerize in the absence of the photoinitiator both in the presence or absence of air as long as the irradiation wavelengths are short (from 220 to 355 nm). The presence of oxygen (while irradiating at short wavelengths <365 nm) leads to higher conversion of the methacrylic, allylic, and propenyl double bonds of the eugenol-derived methacrylates as a consequence of the production of hydroperoxides and their decomposition. The presence of ADB and PDB causes secondary reactions such as allylic hydrogen abstraction and cross-propagation which could lead to branched or crosslinked structures.

Table 3-1**.**Methacrylate (MDB), allylic (ADB) and propenyl (PDB) double bond conversions under different conditions of irradiation

Monomer	**Condition**	**Conversion (%)**			
		220–600 nm		**365 nm**	
		Without PI	**Darocur 1173**	**Darocur 1173**	**Irgacure 819**
EDMA MDB	Air protected	22	100	94	96
EEMA MDB		12	66	74	76
EIMA MDB		59	100	65	78
EEMA ADB		6	7	6	3
EIMA PDB		58	56	40	12
EDMA MDB	Under air	35	61	8	8
EEMA MDB		66	81	0	7
EIMA MDB		86	92	39	40
EEMA ADB		49	64	2	9
EIMA PDB		68	76	58	30

3.3.1.2 Photopolymerization with photoinitiator

Experiments proceeded with the use of common photoinitiators. Darocur 1173 was added to the monomers at 2% wbm (weight based on monomer). It is a Norrish Type I photoinitiator that undergoes homolytic cleavage to produce two carbon-centered radicals (Scheme 3-2 and Appendix Figure A2-4).

Scheme 3-2. Homolytic cleavage under light of Darocur 1173

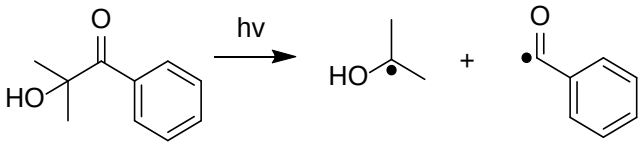

The evolutions with irradiation time of the MDB conversions of the three monomers for the photopolymerizations carried out in the presence and in the absence of air using Darocur 1173 are shown in Figure 3-3. The evolutions with time of the conversions of ADB and PDB in the same conditions are displayed in Figure 3-4. The comparison of these data with those observed for polymerizations carried out in the absence of the photoinitiator demonstrates, as expected, that the PI accelerates the polymerization.

In the absence of air, the conversion of EDMA MDB was fast and reached 100%. The polymerization rates of the difunctional methacrylates, EEMA and EIMA, were slower. EEMA MDB conversion reached 66%, whereas that of EIMA MDB reached 100% although at a lower rate than EDMA (Table 3-1.). In the case of EEMA, radicals were presumed to be consumed by the allyl groups (degradative chain transfer), even to a small extent, to form highly stabilized radicals that resulted in a lower polymerization rate and ultimately in termination reactions limiting the conversion. No increment or appearance of the band at 960 cm^{-1} corresponding to the propenyl double bonds was observed, suggesting that the isomerization of EEMA into EIMA does not occur under these experimental conditions. In addition, the conversion of allylic double bonds to propenyl double bonds would lead to the decrease of the 995 cm^{-1} peak area (corresponding to allylic double bond), which did not occur, as conversion was <10%. In the case of EIMA, the PDBs were consumed up to 56% (Table 3-1) most likely *via* cross-propagation (*vide supra*). This cross-propagation slightly slows down the polymerization but does not prevent the quantitative conversion of EIMA MDB. Moreover, as discussed above, EIMA has a higher absorption than EEMA and could form propagating species by itself, thus enhancing the conversion.

In the presence of air, the polymerization rates were lower than those observed for polymerizations carried out in the absence of air. This decrease of the polymerization rate was likely caused by oxygen inhibition. EDMA was strongly inhibited by air and presented the lowest MDB conversion (61%). EIMA and EEMA were less affected and reached high conversions: 92% and 81%, respectively (Table 3-1). As previously discussed, reactions with oxygen can lead to the formation of hydroperoxides, which decompose, causing a second polymerization regime. The corresponding sigmoidal curve is observed quite clearly for EEMA, but not for EIMA. In addition, the conversion of

PDB was higher than that of ADB (76% and 64% respectively, Figure 3-4). PDBs were also highly consumed when protected from air (56%), while ADBs were not (7%). Again, cross-propagation is the dominant reaction in the consumption of PDBs (only a fraction might be consumed by hydrogen abstraction or hydroperoxide formation). In the case of EEMA, for which bis-allylic H-abstraction and radical termination dominate, the absence of air limits the overall polymerization. However, in the presence of air, hydroperoxide dissociation provides the necessary radicals to continue EEMA MDB polymerization.

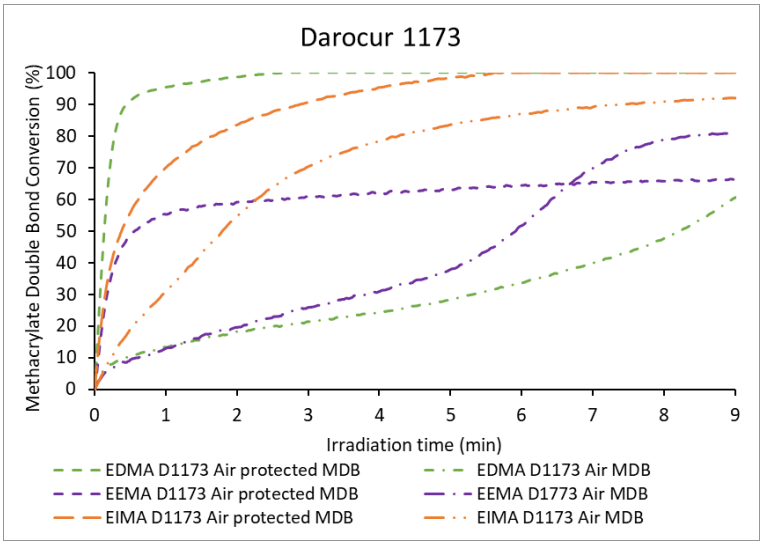

Figure 3-3. Methacrylate double bond (MDB) conversion of eugenol-derived monomers versus irradiation time in the presence of Darocur 1173.

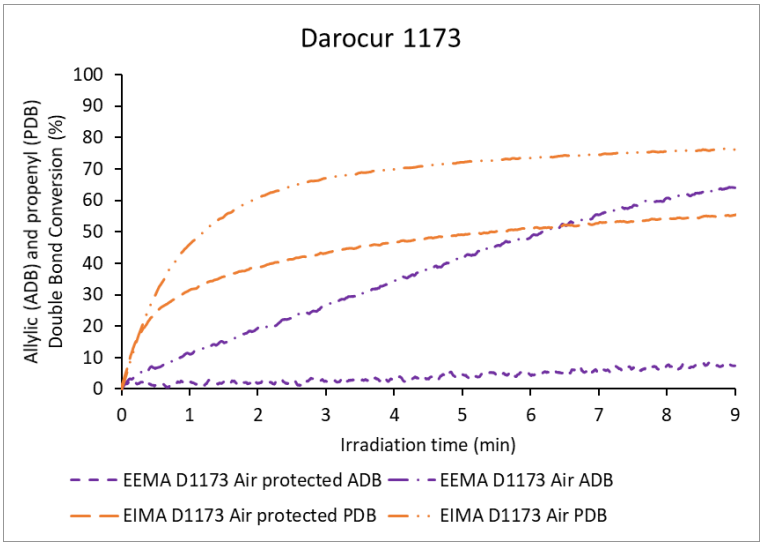

Figure 3-4. Allylic (ADB) and propenyl double bond (PDB) conversion of eugenol-derived monomers versus irradiation time in the presence of Darocur 1173.

The effect of the monomer light absorption and the possible formation of ozone on the kinetics of polymerization remained to be investigated. Thus, a bandpass filter centered at 365 nm, preventing monomer light absorption and ozone formation (<242 nm) was again used to irradiate the

formulations. Experiments with Darocur 1173 were performed and results are shown in Figure 3-5 and Figure 3-6.

In the presence of air, almost no conversion of MDB could be measured for EEMA and EDMA (conversion <10%, Figure 3-5 and Table 3-1). Similar results were observed for EEMA ADB with a conversion close to zero (2%, Figure 3-6 and Table 3-1). In the presence of the filter, the production of radicals by cleavage of the photoinitiator was strongly diminished and the scarce quantity of radicals could quickly be quenched by oxygen, while no peroxides nor hydroperoxides could be generated.[32] Nevertheless, the considerable consumption of both EIMA MDB and PDB (39% and 58% respectively, Table 3-1) was observed in spite of the presence of oxygen. This may be explained by the formation of charge-transfer complexes of EIMA with oxygen (as reported for styrene)[48,49] which leads to the production of radicals and allows propagation.

In the absence of air, both the polymerization rate and the final conversion increased significantly. MDB conversion followed the trend: EDMA (94%) > EEMA (74%) > EIMA (65%) (Table 3-1). The polymerization rate was lower than that observed for the reaction carried out using light including shorter irradiation wavelengths (*i.e.*, without filter). This may be explained by a lower radical production both from Darocur 1173 (which absorbs weakly at 365 nm) and from the monomers (which do not absorb at 365, see Appendix Figure A2-3). Moreover, the irradiance decreases because of the filter (78 mW cm^{-2} UVA). However, contrary to the experiments carried out without filter, EIMA showed lower MDB conversion than EEMA. This means that EIMA UV light absorption and cleavage (responsible for the reaction in the absence of PI) contribute to the formation of reactive species. Moreover, the consumption of the PDBs reached 40% (Table 3-1), while ADB consumption remained low (6%).

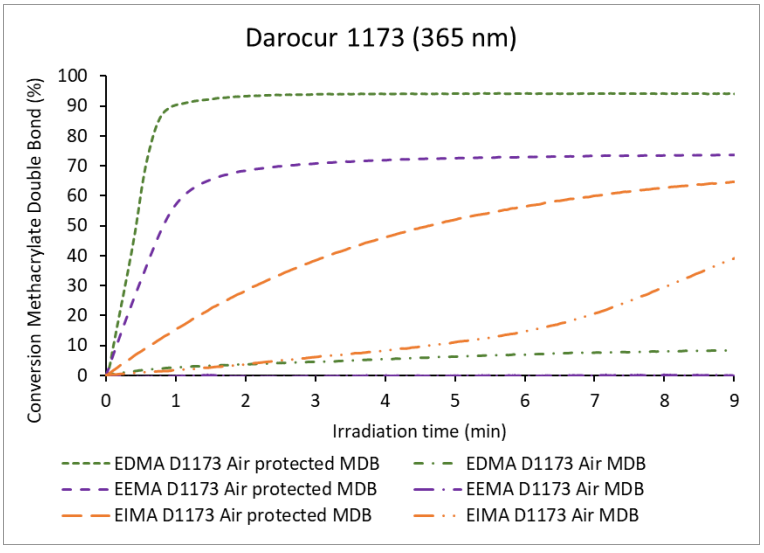

Figure 3-5. Methacrylate double bond (MDB) conversion of eugenol-derived monomers with irradiation time in the presence of Darocur 1173, irradiation under λ=365 nm.

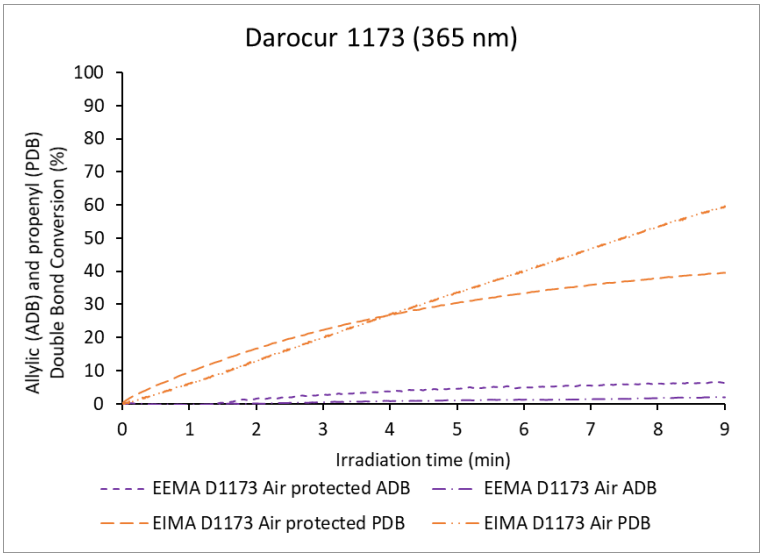

Figure 3-6. Allylic (ADB) and propenyl double bond (PDB) conversion of eugenol-derived monomers with irradiation time in the presence of Darocur 1173, irradiation under λ=365 nm.

The comparison of the results of the polymerizations irradiated with and without filter using Darocur 1173 (Norrish Type I photoinitiator) suggests that the monomer absorptions play an important role in their reactivity, especially for EIMA. Moreover, in the presence of air, reactions of peroxides and hydroperoxides, ozone formation and photolysis to singlet oxygen, contribute to the polymerization mechanism.

In a final study, a passband filter centered at 365 nm and another Norrish type I PI with high absorption at longer wavelengths (absorption in the UVA region), Irgacure 819[52] were used. The results obtained in the different conditions (with and without air) are gathered in the Appendix Scheme A2-2, Figure A2-14 and Figure A2-15). In this case, the potential cleavage of the methacrylates was prevented by the pass band filter and oxygen inhibition or the production of hydroperoxides was avoided by protecting the samples from air. In addition, the flux of radicals had been raised by using Irgacure 819, which has a higher molar extinction coefficient and quantum yield than Darocur 1173 in the UVA region.[52] A behavior similar to Darocur 1173 was observed.

The experiments executed in different conditions (with or without initiator, in the presence and absence of air, with or without filter) revealed that EDMA polymerization was always strongly inhibited in the presence of air. On the contrary, the presence of the pending allylic (EEMA) or propenyl (EIMA) double bonds could produce a second polymerization regime due to dissociation of hydroperoxides formed in-situ in the presence of air under shorter (<320 nm) wavelength irradiation). It was also shown that the dominant reaction mechanism for PDB is cross-propagation rather than hydrogen abstraction or hydroperoxide formation, as they were consumed to a high extent even in the absence of air. The polymerization of EIMA was the least affected by air.

3.3.2 Polymers Characterization

Properties of the polymers prepared by photoinduced polymerization in the presence of Darocur 1173, both in the presence and absence of air, were measured (Table 3-2). The polymerization conditions (*i.e.*, use of a UV irradiation spectrum from 320 to 390 nm and of Darocur 1173 as PI) were selected to guarantee high conversions. Polymers obtained from EDMA had a linear structure and were soluble (gel content ≈ 0%). In contrast, polymers from EEMA and EIMA were crosslinked and completely insoluble (gel content = 100%), suggesting that the unreacted functional groups potentially present (when the conversion was not quantitative, as reported in Appendix Table A2-2) were dangling from the network and that no free oligomer or monomer were present. The glass transition temperature did not vary much between the samples irradiated in the presence or in the absence of air except for poly(EDMA) prepared by irradiation under air. In this case, the presence of oligomers or unreacted monomer plasticized the resulting polymer and reduced its T_g. The obtained T_gs were higher than the ones of the polymers obtained from the solution polymerization (linear and branched polymers, see Chapter 2), and in accordance with cross-linked polymers obtained in emulsion polymerization , as it will be shown later in Chapter 4.[53]

The TGA results showed that the starting degradation temperatures of the polymers were always higher than 230°C (Figure 3-7 and Figure 3-8). Polymerization carried out in the presence of air led to crosslinked poly(EEMA) with higher decomposition temperatures, due to a higher consumption of ADBs. A slightly lower degradation temperature was registered for poly(EIMA) prepared in the presence of air but both polymers (produced under air or in the absence of air) exhibited complex profiles, indicating complex polymeric architectures. Their glass transition temperatures (ranging from 8°C and 58°C) as well as their degradation temperatures (above 230°C) make these materials suitable for application in coatings.

The water and hexadecane contact angles (Table 2) indicated that the wettability of all the polymers were independent of the structure. The polymers were almost hydrophobic and displayed moderate oleophilicity.

Table 3-2. Thermal properties, gel content, and contact angle of homopolymers produced with Darocur 1173

Monomer	Polymerization condition	Gel Content (%)	T_g (°C)	$T_{d5\%}$ (°C)	Contact angle DI water (°)	Contact angle Hexadecane (°)
EDMA	with air	2	8	236	92	24
	no air	3	23	269	84	30
EEMA	with air	100	35	298	89	33
	no air	98	34	294	85	34
EIMA	with air	100	56	246	85	24
	no air	100	58	258	82	25

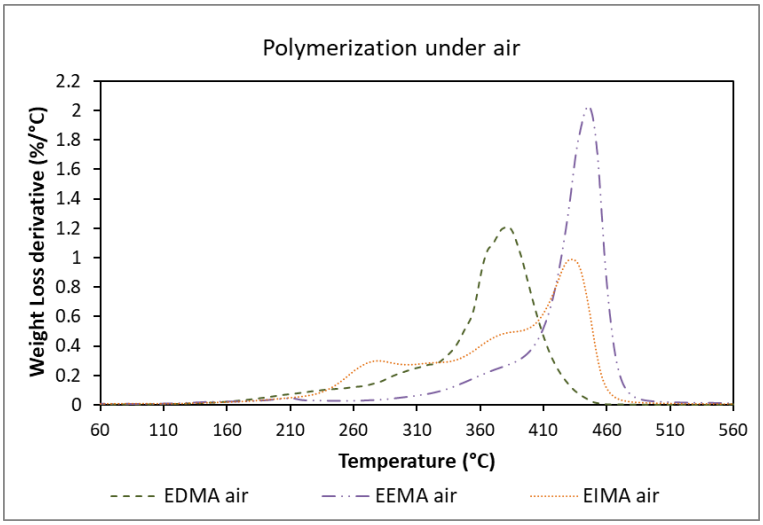

Figure 3-7. Thermogravimetric analysis of the different eugenol-derived methacrylates polymers from polymerization with Darocur 1173 under air (1º derivative).

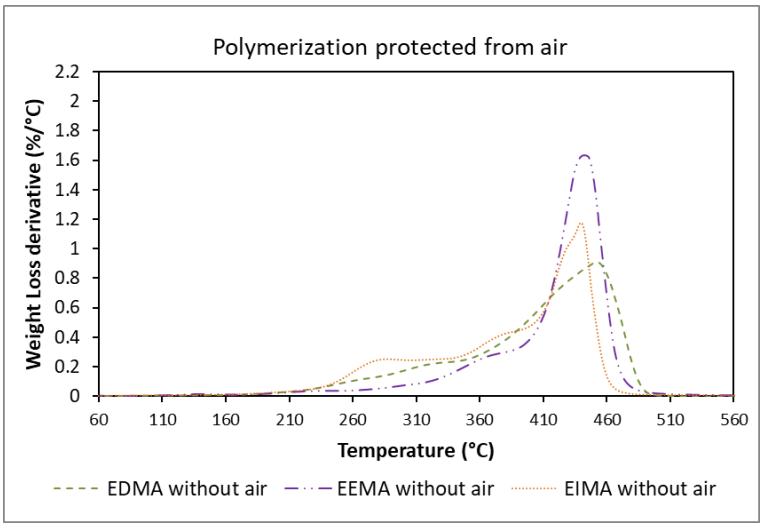

Figure 3-8. Thermogravimetric analysis of the different eugenol-derived methacrylates polymers from polymerization with Darocur 1173 protected from air (1º derivative).

3.4 Conclusions

Three eugenol-derived methacrylates (EDMA, EEMA, EIMA) were polymerized *via* photopolymerization without a photoinitiator and with two Norrish Type I photoinitiators (Darocur 1173 and Irgacure 819), under air or without air. Their polymerization behavior under the different conditions was described. The monomers were shown to polymerize in the absence of a photoinitiator, especially in the presence of oxygen, due to self-initiation and oxidation reactions. In the presence of air, EIMA showed the highest conversions in any of the conditions studied. The second polymerization regimes, due to the formation and photolysis of hydroperoxides, were observed upon irradiation at a wavelength shorter than 365 nm in air with or without PI. This effect was clearly visible for EIMA and EEMA. Moreover, both allylic and propenyl groups were reactive

in the presence of air. In addition, PDBs were shown to be predominantly polymerized *via* cross-propagation reactions while ADBs were mainly consumed under air *via* hydrogen abstraction and hydroperoxides formation. In the absence of air and using PI, EDMA reached the highest conversions. To eliminate the self-initiation of the monomers as well as the formation of hydroperoxides, a 365 nm passband filter and air-protected conditions were used. Under these conditions, the polymerization rate followed the order EDMA > EEMA > EIMA. EEMA displayed a significant reduction of the propagation rate, due to the formation of highly stabilized bis-allylic radicals. EIMA exhibited a lower MDB conversion, due to cross-propagation with the PDB. The polymers properties indicated that their use in applications in coatings and in dentistry could be envisaged.

3.5 References

(1) Gandini, A.; Lacerda, T. M.; Carvalho, A. J. F. F.; Trovatti, E. Progress of Polymers from Renewable Resources: Furans, Vegetable Oils, and Polysaccharides. *Chem. Rev.* **2016**, *116*, 1637.

(2) Fouassier, J. P.; Allonas, X.; Burget, D. Photopolymerization Reactions under Visible Lights: Principle, Mechanisms and Examples of Applications. *Prog. Org. Coatings* **2003**, *47*, 16.

(3) Crivello, J. V.; Reichmanis, E. Photopolymer Materials and Processes for Advanced Technologies. *Chem. Mater.* **2014**, *26*, 533.

(4) Childs, A.; Li, H.; Lewittes, D. M.; Dong, B.; Liu, W.; Shu, X.; Sun, C.; Zhang, H. F. Fabricating Customized Hydrogel Contact Lens. *Sci. Rep.* **2016**, *6*, 34905.

(5) Stansbuty, J. W. Curing Dental Resins and Composites by Photopolymerization. *J. Esthet. Restor. Dent.* **2000**, *12*, 300.

(6) Lloret, T.; Navarro-Fuster, V.; Ramírez, M.; Ortuño, M.; Neipp, C.; Beléndez, A.; Pascual, I. Holographic Lenses in an Environment-Friendly Photopolymer. *Polymers (Basel).* **2018**, *10*, 302.

(7) Fertier, L.; Koleilat, H.; Stemmelen, M.; Giani, O.; Joly-Duhamel, C.; Lapinte, V.; Robin, J.-J. The Use of Renewable Feedstock in UV-Curable Materials – A New Age for Polymers and Green Chemistry. *Prog. Polym. Sci.* **2013**, *38*, 932.

(8) Zielinski Goldberg, M.; Burke, L. A.; Samokhvalov, A. Selective Activation of C=C Bond in Sustainable Phenolic Compounds from Lignin via Photooxidation: Experiment and Density Functional Theory Calculations. *Photochem. Photobiol.* **2015**, *91*, 1332.

(9) Khalil, A. A.; Rahman, U. ur; Khan, M. R.; Sahar, A.; Mehmood, T.; Khan, M. Essential Oil Eugenol: Sources, Extraction Techniques and Nutraceutical Perspectives. *RSC Adv.* **2017**, *7*, 32669.

(10) Sakai, K.; Takeuti, H.; Mun, S. P.; Imamura, H. Formation of Isoeugenol and Eugenol during the Cleavage of β-Aryl Ethers in Lignin by Alcohol-Bisulfite Treatment. *J. Wood Chem. Technol.* **1988**, *8*, 29.

(11) Llevot, A.; Grau, E.; Carlotti, S.; Grelier, S.; Cramail, H. From Lignin-Derived Aromatic Compounds to Novel Biobased Polymers. *Macromol. Rapid Commun.* **2016**, *37*, 9.

(12) Kong, X.; Liu, X.; Li, J.; Yang, Y. Advances in Pharmacological Research of Eugenol. *Curr. Opin. Complement. Altern. Med.* **2014**, *1*, 8.

(13) da Silva, F. F. M.; Monte, F. J. Q.; de Lemos, T. L. G.; do Nascimento, P. G. G.; de Medeiros Costa, A. K.; de Paiva, L. M. M. Eugenol Derivatives: Synthesis, Characterization, and Evaluation of Antibacterial and Antioxidant Activities. *Chem. Cent. J.* **2018**, *12*, 34.

(14) Modjinou, T.; Versace, D. L.; Abbad-Andallousi, S.; Bousserrhine, N.; Dubot, P.; Langlois, V.; Renard, E. Antibacterial and Antioxidant Bio-Based Networks Derived from Eugenol Using Photo-Activated Thiol-Ene Reaction. *React. Funct. Polym.* **2016**, *101*, 47.

(15) Munerato, M. C.; Sinigaglia, M.; Reguly, M. L.; de Andrade, H. H. R. Genotoxic Effects of Eugenol, Isoeugenol and Safrole in the Wing Spot Test of Drosophila Melanogaster. *Mutat. Res. Toxicol. Environ. Mutagen.* **2005**, *582*, 87.

(16) Lartigue-Peyrou, F. The Use of Phenolic Compounds as Free-Radical Polymerization Inhibitors. In *Industrial Chemistry Library*; 1996; Vol. 8, pp 489–505.

(17) Fujisawa, S.; Kadoma, Y. Action of Eugenol as a Retarder against Polymerization of Methyl Methacrylate by Benzoyl Peroxide. *Biomaterials* **1997**, *18*, 701.

(18) Guzmán, D.; Ramis, X.; Fernández-Francos, X.; De la Flor, S.; Serra, A. New Bio-Based Materials Obtained by Thiol-Ene/Thiol-Epoxy Dual Curing Click Procedures from Eugenol Derivates. *Eur. Polym. J.* **2017**, *93*, 530.

(19) Guzmán, D.; Ramis, X.; Fernández-Francos, X.; De la Flor, S.; Serra, A. Preparation of New Biobased Coatings from a Triglycidyl Eugenol Derivative through Thiol-Epoxy Click Reaction. *Prog. Org. Coatings* **2018**, *114*, 259.

(20) Modjinou, T.; Versace, D. L.; Abbad-Andaloussi, S.; Langlois, V.; Renard, E. Enhancement of Biological Properties of Photoinduced Biobased Networks by Post-Functionalization with Antibacterial Molecule. *ACS Sustain. Chem. Eng.* **2019**, *7*, 2500.

(21) Dai, J.; Jiang, Y.; Liu, X.; Wang, J.; Zhu, J. Synthesis of Eugenol-Based Multifunctional Monomers via a Thiol-Ene Reaction and Preparation of UV Curable Resins Together with Soybean Oil Derivatives. *RSC Adv.* **2016**, *6*, 17857.

(22) Yoshimura, T.; Shimasaki, T.; Teramoto, N.; Shibata, M. Bio-Based Polymer Networks by Thiol-Ene Photopolymerizations of Allyl-Etherified Eugenol Derivatives. *Eur. Polym. J.* **2015**, *67*, 397.

(23) Miao, J. T.; Yuan, L.; Guan, Q.; Liang, G.; Gu, A. Water-Phase Synthesis of a Biobased Allyl Compound for Building UV-Curable Flexible Thiol-Ene Polymer Networks with High Mechanical Strength and Transparency. *ACS Sustain. Chem. Eng.* **2018**, *6*, 7902.

(24) Breloy, L.; Ouarabi, C. A.; Brosseau, A.; Dubot, P.; Brezova, V.; Abbad Andaloussi, S.; Malval, J. P.; Versace, D. L. β-Carotene/Limonene Derivatives/Eugenol: Green Synthesis of Antibacterial Coatings under Visible-Light Exposure. *ACS Sustain. Chem. Eng.* **2019**, *7*, 19591.

(25) Molina-Gutiérrez, S.; Manseri, A.; Ladmiral, V.; Bongiovanni, R.; Caillol, S.; Lacroix-Desmazes, P. Eugenol: A Promising Building Block for Synthesis of Radically Polymerizable Monomers. *Macromol. Chem. Phys.* **2019**, *220*, 1900179.

(26) Hamamatsu. Spotlight sources Lightningcure series https://www.hamamatsu.com/resources/pdf/etd/LC8_TLSZ1008E.pdf.

(27) Silverstein, R. M.; Webster, F. X.; Kiemle David J. *Spectrosmetric Identification of Organic Compounds*, 7th Editio.; Sons, J. W. &, Ed.; Hoboken, NJ, USA, 2005.

(28) Wang, L. H.; Sung, W. C. Rapid Evaluation and Quantitative Analysis of Eugenol Derivatives in Essential Oils and Cosmetic Formulations on Human Skin Using Attenuated Total Reflectance-Infrared Spectroscopy. *Spectroscopy* **2011**, *26*, 43.

(29) Chowdhry, B. Z.; Ryall, J. P.; Dines, T. J.; Mendham, A. P. Infrared and Raman

Spectroscopy of Eugenol, Isoeugenol, and Methyl Eugenol: Conformational Analysis and Vibrational Assignments from Density Functional Theory Calculations of the Anharmonic Fundamentals. *J. Phys. Chem. A* **2015**, *119*, 11280.

(30) Lalevée, J.; Fouassier, J. P.; Graff, B.; Zhang, J.; Xiao, P. Chapter 6. How to Design Novel Photoinitiators for Blue Light; Lalevée, J., Fouassier, J.-P., Eds.; Polymer Chemistry Series; Royal Society of Chemistry: Cambridge, 2018; Vol. 48, pp 179–199.

(31) Detrembleur, C.; Versace, D. L.; Piette, Y.; Hurtgen, M.; Jérôme, C.; Lalevée, J.; Debuigne, A. Synthetic and Mechanistic Inputs of Photochemistry into the Bis-Acetylacetonatocobalt-Mediated Radical Polymerization of n-Butyl Acrylate and Vinyl Acetate. *Polym. Chem.* **2012**, *3*, 1856.

(32) Ligon, S. C.; Husár, B.; Wutzel, H.; Holman, R.; Liska, R. Strategies to Reduce Oxygen Inhibition in Photoinduced Polymerization. *Chem. Rev.* **2014**, *114*, 557.

(33) Nyquist, R. A.; Fiedler, S.; Streck, R. Infrared Study of Vinyl Acetate, Methyl Acrylate and Methyl Methacrylate in Various Solvents. *Vib. Spectrosc.* **1994**, *6*, 285.

(34) Wang, H.; Brown, H. R. Self-Initiated Photopolymerization and Photografting of Acrylic Monomers. *Macromol. Rapid Commun.* **2004**, *25*, 1095.

(35) Huang, L.; Li, Y.; Yang, J.; Zeng, Z.; Chen, Y. Self-Initiated Photopolymerization of Hyperbranched Acrylates. *Polymer (Guildf).* **2009**, *50*, 4325.

(36) Hoijemberg, P. A.; Chemtob, A.; Croutxé-Barghorn, C. Two Routes Towards Photoinitiator-Free Photopolymerization in Miniemulsion: Acrylate Self-Initiation and Photoactive Surfactant. *Macromol. Chem. Phys.* **2011**, *212*, 2417.

(37) Furutani, M.; Ide, T.; Kinoshita, S.; Horiguchi, R.; Mori, I.; Sakai, K.; Arimitsu, K. Initiator-Free Photopolymerization of Common Acrylate Monomers with 254 Nm Light. *Polym. Int.* **2019**, *68*, 79.

(38) Rojo, L.; Vazquez, B.; Parra, J.; López Bravo, A.; Deb, S.; San Roman, J. From Natural Products to Polymeric Derivatives of “Eugenol”: A New Approach for Preparation of Dental Composites and Orthopedic Bone Cements. *Biomacromolecules* **2006**, *7*, 2751.

(39) Zhang, Y.; Li, Y.; Wang, L.; Gao, Z.; Kessler, M. R. Synthesis and Characterization of Methacrylated Eugenol as a Sustainable Reactive Diluent for a Maleinated Acrylated Epoxidized Soybean Oil Resin. *ACS Sustain. Chem. Eng.* **2017**, *5*, 8876.

(40) Gazzotti, S.; Hakkarainen, M.; Adolfsson, K. H.; Ortenzi, M. A.; Farina, H.; Lesma, G.; Silvani, A. One-Pot Synthesis of Sustainable High-Performance Thermoset by Exploiting Eugenol Functionalized 1,3-Dioxolan-4-One. *ACS Sustain. Chem. Eng.* **2018**, *6*, 15201.

(41) Pynaert, R.; Buguet, J.; Croutxé-Barghorn, C.; Moireau, P.; Allonas, X. Effect of Reactive Oxygen Species on the Kinetics of Free Radical Photopolymerization. *Polym. Chem.* **2013**, *4*, 2475.

(42) Schiff, H. I. Kinetics of Ozone Photochemistry. *Pure Appl. Geophys.* **1973**, *106–108*, 1464.

(43) Matsumi, Y.; Kawasaki, M. Photolysis of Atmospheric Ozone in the Ultraviolet Region. *Chem. Rev.* **2003**, *103*, 4767.

(44) Frimer, A. A. The Reaction of Singlet Oxygen with Olefins: The Question of Mechanism.

Chem. Rev. **1979**, *79*, 359.

(45) Singleton, D. A.; Hang, C.; Szymanski, M. J.; Meyer, M. P.; Leach, A. G.; Kuwata, K. T.; Chen, J. S.; Greer, A.; Foote, C. S.; Houk, K. N. Mechanism of Ene Reactions of Singlet Oxygen. A Two-Step No-Intermediate Mechanism. *J. Am. Chem. Soc.* **2003**, *125*, 1319.

(46) Ghogare, A. A.; Greer, A. Using Singlet Oxygen to Synthesize Natural Products and Drugs. *Chem. Rev.* **2016**, *116*, 9994.

(47) Parker, D. H. Laser Photochemistry of Molecular Oxygen. *Acc. Chem. Res.* **2000**, *33*, 563.

(48) Kodaira, T.; Hayashi, K.; Ohnishi, T. Photopolymerization of Styrene in the Presence of Oxygen. Role of the Charge-Transfer Complex. *Polym. J.* **1973**, *4*, 1.

(49) Kodaira, T.; Hashimoto, K.; Sakanaka, Y.; Tanihata, S.; Ikeda, K. The Role of the Charge-Transfer Complex in the Photocopolymerization of Oxygen with Styrene and α-Methylstyrene. *Bull. Chem. Soc. Jpn.* **1978**, *51*, 1487.

(50) Krüger, K.; Tauer, K.; Yagci, Y.; Moszner, N. Photoinitiated Bulk and Emulsion Polymerization of Styrene – Evidence for Photo-Controlled Radical Polymerization. *Macromolecules* **2011**, *44*, 9539.

(51) Gellerstedt, G.; Pettersson, E.-L.; Weeks, O. B. Light-Induced Oxidation of Lignin. The Behaviour of Structural Units Containing a Ring-Conjugated Double Bond. *Acta Chem. Scand.* **1975**, *29b*, 1005.

(52) Eibel, A.; Fast, D. E.; Gescheidt, G. Choosing the Ideal Photoinitiator for Free Radical Photopolymerizations: Predictions Based on Simulations Using Established Data. *Polym. Chem.* **2018**, *9*, 5107.

(53) Molina-Gutiérrez, S.; Ladmiral, V.; Bongiovanni, R.; Caillol, S.; Lacroix-Desmazes, P. Emulsion Polymerization of Dihydroeugenol-, Eugenol-, and Isoeugenol-Derived Methacrylates. *Ind. Eng. Chem. Res.* **2019**, *58*, 21155.

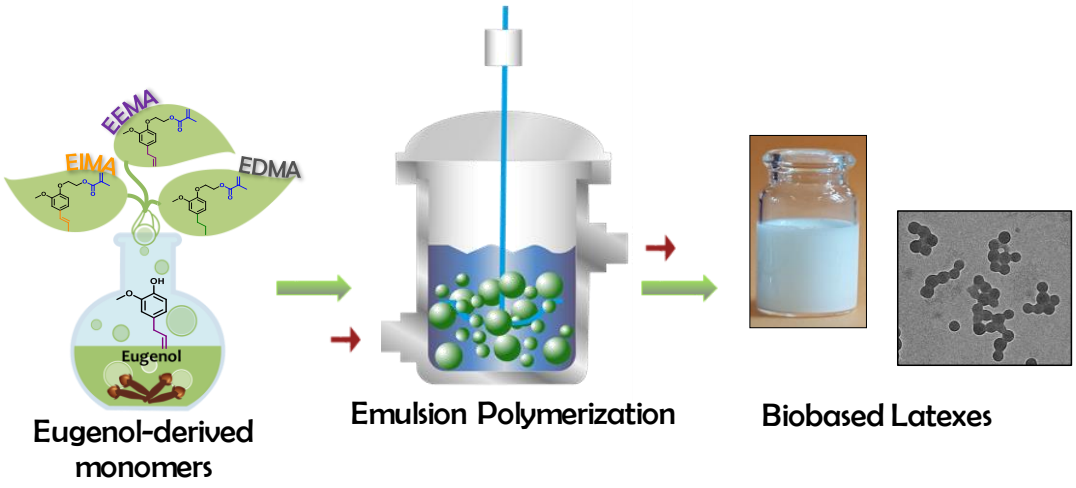

CHAPTER FOUR

Emulsion polymerization of eugenol-derived methacrylates

Table of contents

Chapter 4: Emulsion polymerization of eugenol-derived methacrylates

Some of the results and discussion presented in this chapter have been published in the article:

- Molina-Gutiérrez, S.; Ladmiral, V.; Bongiovanni, R.; Caillol, S.; Lacroix-Desmazes, P. Emulsion Polymerization of Dihydroeugenol-, Eugenol-, and Isoeugenol-Derived Methacrylates. *Ind. Eng. Chem. Res.* **2019**, *58* (46), 21155–21164. https://doi.org/10.1021/acs.iecr.9b02338.

4.1 Introduction

Green chemistry principles should be implemented in the pursuit of sustainable biobased polymers. Not only the design of monomers coming from renewable feedstock must be achieved (as presented in Chapter 2), but less hazardous chemical synthesis and processes involving the use of safer solvents and reactants must also be implemented.[1,2] The reduction of volatile organic compounds (VOCs) can be attained through environmentally friendly polymerization methods such as aqueous emulsion polymerization. The use of water as the continuous phase has several advantages: it is an innocuous and non-flammable solvent; it reduces the viscosity of the reaction medium and improves heat transfer enabling easier reaction temperature control. Polymerization in aqueous dispersed media involves several related processes such as: emulsion polymerization,[3–8] miniemulsion polymerization,[9–12] microemulsion polymerization,[13] dispersion polymerization,[14] and suspension polymerization.[15,16] Emulsion and suspension polymerizations processes are used at an industrial scale, whilst miniemulsion polymerization offers an alternative approach for very hydrophobic monomers; however, this technique has several constraints which hinders its wider industrial exploitation.[11,12] Hence, emulsion polymerization of biobased monomers is gaining increasing interest in both the academic and the industrial communities and has recently been reviewed by our team.[17]

In the present chapter, aqueous emulsion polymerization of biobased methacrylate monomers derived from eugenol, isoeugenol and dihydroeugenol (named EEMA, EIMA and EDMA, respectively; Scheme 4-1) is explored for the first time as a greener route to biobased aromatic polymer latexes.

Scheme 4-1. Eugenol-derived methacrylates

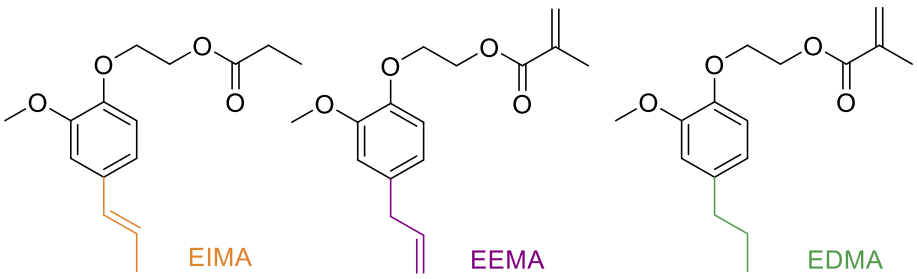

This study was conducted to assess the feasibility of this process with such biobased monomers under different experimental conditions, targeting potential applications in coatings and adhesives.

4.2 Experimental

4.2.1 Materials

Potassium persulfate (KPS, ≥99.0%, Aldrich), 4,4′-azobis(4-cyanovaleric acid) (ACVA, ≥98.0%, Fluka), sodium dodecyl sulfate (SDS, >99%, Aldrich), 1,4- bis(trimethylsilyl)benzene (BTMSB, 96%, Aldrich), sodium metabisulfite ($Na_2S_2O_5$, SMBS, 99%, Aldrich), sodium bicarbonate ($NaHCO_3$, 99.7%, Aldrich) were used as received. 2,2′-Azobis(2-methylpropionitrile) (AIBN, 98%, Fluka) was purified by recrystallization in methanol and dried under vacuum before use. Butyl acrylate (BA, ≥99.0%, Aldrich) was distilled under vacuum prior to use. Deionized water (DI water) (1 μS cm^{-1}) was obtained using a D8 ion exchange demineralizer from A2E Affinage de L'Eau. EDMA, EIMA and EEMA monomers were synthesized as described Chapter 2.[18]

4.2.2 Methods

4.2.2.1 General procedure for emulsion polymerization with thermal initiation systems

a) Potassium persulfate (KPS) at 70°C

The emulsion polymerization by thermal initiation with KPS was carried out in a 50 mL double-walled jacketed glass reactor with a U-shaped glass stirring rod. For a latex at 12.5-13.7 wt% solids content, eugenol derived methacrylate (15 mmol) was placed in a glass vial and purged with argon for 15 minutes. 31.6 g of DI water, SDS (4% wbm, weight based on monomer) and $NaHCO_3$ (2.2% wbm, 1:3.5 molar ratio KPS:$NaHCO_3$), were placed in the reactor and degassed with argon for 30 min. The reactor was heated to 70°C. The degassed monomer was added to the reactor using a syringe and a degassed solution of KPS (2% wbm) in 4 g of DI water (out of the 31.6 g of DI water previously degassed with argon) was finally added. The reaction mixture was kept under a small flux of argon and mechanical stirring at 250 rpm. Monomer conversion was followed through ^1H NMR using $CDCl_3$ as deuterated solvent. 1,4-bis(trimethylsilyl)benzene (BTMSB) was added as internal standard in the case of EEMA (Table 4-1 and Scheme 4-2).

Table 4-1. Polymerization recipe for KPS thermal initiated emulsion polymerization

Ingredient	Weight (g)	mmol	% wbm
Monomer	4.18	15.00	100.00
Surfactant (SDS)	0.17	0.58	4.00
Initiator (KPS)	0.08	0.31	2.00
Buffer ($NaHCO_3$)	0.09	1.07	2.20
Deionized water	31.64		

Emulsion polymerization of EDMA with thermal initiation using KPS. EDMA (4.183 g, 15 mmol), DI water (31.642 g), SDS (0.168 g, 4% wbm), $NaHCO_3$ (0.092 g, 2.2% wbm) and KPS (0.084 g, 2% wbm). 13.4% solids content.

Emulsion polymerization of EIMA with thermal initiation using KPS. EIMA (4.179 g, 15 mmol), DI water (31.647 g), SDS (0.167 g, 4% wbm), $NaHCO_3$ (0.093 g, 2.2% wbm of monomer) and KPS (0.084 g, 2% wbm). 13.7% solids content.

Emulsion polymerization of EEMA with thermal initiation using KPS. EEMA (4.152 g, 15 mmol), DI water (31.679 g), SDS (0.168 g, 4.0% wbm), $NaHCO_3$ (0.092 g, 2.2% wbm of monomer), BTSMB (0.181 g, 4.3% wbm) and KPS (0.084 g, 2% wbm). 12.5% solids content.

Scheme 4-2.. Emulsion homopolymerization of eugenol-derived methacrylates using KPS thermal initiation at 70°C: A) EDMA, B) EIMA, C) EEMA

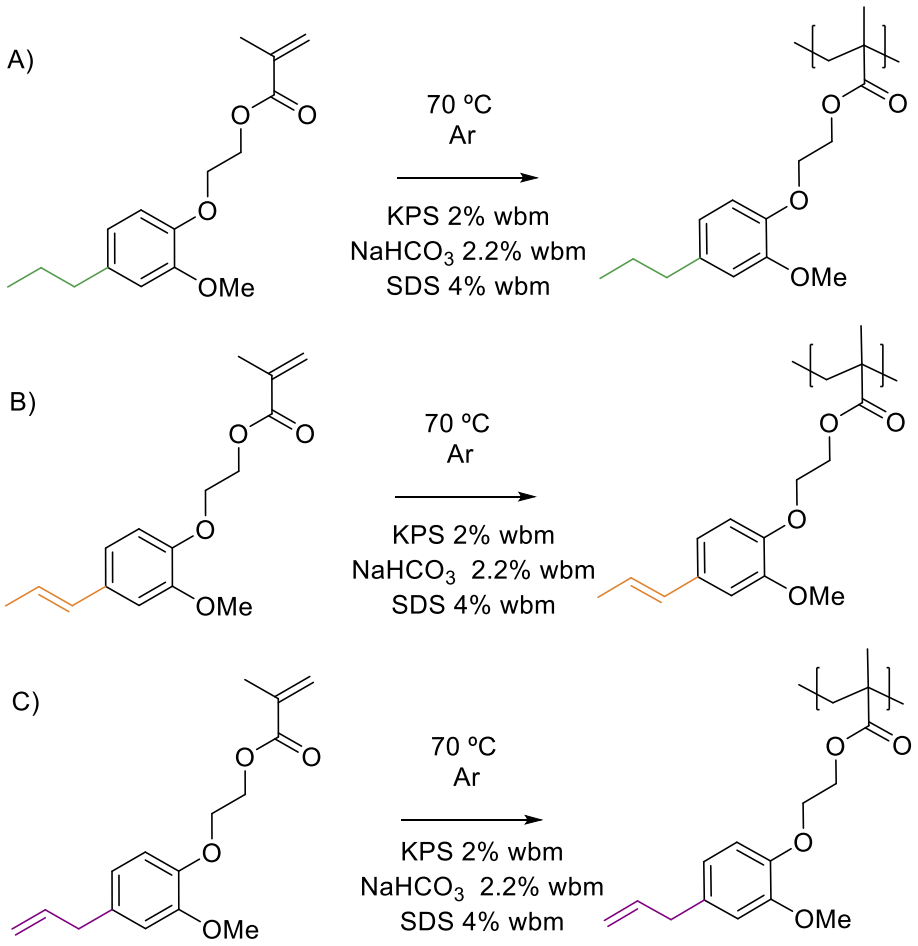

b) 4,4′-Azobis(4-cyanovaleric acid) (ACVA) at 70°C

The emulsion polymerization with 4,4′-Azobis(4-cyanovaleric acid) (ACVA) was carried out in a 50 mL double-walled jacketed glass reactor with a U-shaped glass stirring rod. For a latex at 12.5 wt% solids, the eugenol derived methacrylate (15 mmol) was placed in a glass vial and purged with argon for 15 minutes. 5 g of the total amount of DI water (31 g) were mixed with

$NaHCO_3$ (1.2% wbm, 1:2 molar ratio ACVA:$NaHCO_3$) and the mixture was used to dissolve ACVA (2% wbm). The remainder DI water was mixed with SDS (4.2% wbm), placed in the reactor and degassed with argon for 30 min. The reactor was heated to 70°C. The degassed monomer was added to the reactor through a syringe and ACVA was finally added. The reaction mixture was kept under a small flux of argon and mechanical stirring at 250 rpm. Monomer conversion was followed through ^1H NMR using $CDCl_3$ as deuterated solvent. 1,4- bis(trimethylsilyl)benzene (BTSMB) was added as internal standard in the case of EEMA (Table 4-2 and Scheme 4-3).

Table 4-2. Polymerization recipe for ACVA thermal initiated emulsion polymerization

Ingredient	Weight (g)	mmol	% wbm
Monomer	4.17	15.00	100.00
Surfactant (SDS)	0.18	0.61	4.20
Initiator (ACVA)	0.08	0.30	2.00
Buffer ($NaHCO_3$)	0.05	0.60	1.20
Deionized water	31.86		

Emulsion polymerization of EDMA with thermal initiation using ACVA. EDMA (4.171 g, 15 mmol), DI water (31.859 g), SDS (0.175 g, 4.2% wbm), $NaHCO_3$ (0.051 g, 1.2% wbm) and ACVA (0.083 g, 2.0% wbm). 12.5% solids content.

Emulsion polymerization of EIMA with thermal initiation using ACVA. EIMA (4.142 g, 15 mmol), DI water (31.104 g), SDS (0.170 g, 4.1% wbm), $NaHCO_3$ (0.050 g, 1.2% wbm) and ACVA (0.083 g, 2.0% wbm). 12.5% solids content.

Emulsion polymerization of EEMA with thermal initiation using ACVA. EEMA (4.150 g, 15 mmol), DI water (31.177 g), SDS (0.174 g, 4.2% wbm), $NaHCO_3$ (0.052 g, 1.2% wbm), BTMSB (0.034 g, 0.82% wbm) and ACVA (0.084g, 2.0% wbm). 12.5% solids content.

Scheme 4-3. Emulsion homopolymerization of eugenol-derived methacrylates using thermal ACVA initiation at 70°C: A) EDMA, B) EIMA, C) EEMA

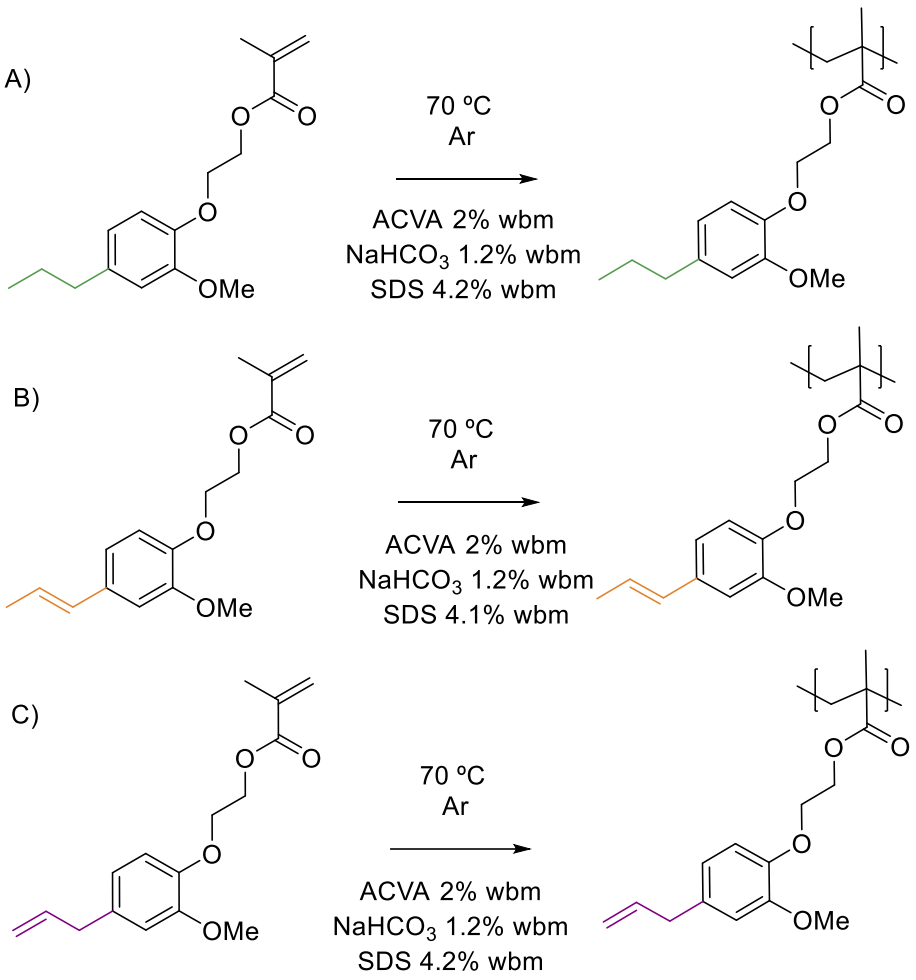

4.2.2.2 General procedure for emulsion polymerization with redox initiation system

a) Potassium persulfate (KPS) / Sodium metabisulfite (SMBS) at 40°C

The emulsion polymerization was carried out in a 50 mL double-walled jacketed glass reactor with a U-shaped glass stirring rod. Eugenol-derived methacrylate (15 mmol) was purged with argon for 15 min. KPS (2% wbm) was dissolved in 12 mL of the DI water and placed aside. SDS (4.0% wbm), $NaHCO_3$ (1.6% wbm, 1:2 molar ratio $Na_2S_2O_5$:$NaHCO_3$), $Na_2S_2O_5$ (1.8% wbm, 1.3:1 molar ratio $Na_2S_2O_5$:KPS) and the rest of the DI water were mixed, placed in the reactor, and purged with argon for 30 min. The reactor was heated to 40°C and the eugenol derived monomer was added. Finally, 4 mL of the previously prepared solution of KPS were added in one shot and this was considered as t = 0. The rest of the KPS was added over four hours at 2 mL h^{-1}. The polymerization proceeded under mechanical stirring at 250 rpm. Monomer conversion was monitored by ^1H NMR using $CDCl_3$ as deuterated solvent (50 µL of latex were mixed with 0.5 mL of $CDCl_3$ and 20 µL of solution 0.05 M of BTMSB used as external standard in deuterated chloroform) (Scheme 4-4).

Table 4-3. Polymerization recipe for $Na_2S_2O_5$: KPS redox initiated emulsion polymerization

Ingredient	Weight (g)	mmol	% wbm
Monomer	4.18	15.00	100.00
Surfactant (SDS)	0.17	0.58	4.00
Initiator oxidant (KPS)	0.08	0.31	2.00
Initiator reductant (sodium metabisulfite)	0.08	0.40	1.83
Buffer ($NaHCO_3$)	0.07	0.80	1.62
Deionized wáter	32.00		

Emulsion polymerization of EDMA with redox initiation. EDMA (4.177 g, 15 mmol), DI water (32.00 g), SDS (0.168 g, 4.0% wbm), $Na_2S_2O_5$ (0.077 g, 1.8% wbm), $NaHCO_3$ (0.068 g, 1.6% wbm) and KPS (0.084 g, 2.0% wbm). 12.5% solids content.

Emulsion polymerization of EIMA with redox initiation. EIMA (4.147 g, 15 mmol), DI water (31.761 g), SDS (0.166 g, 4.0% wbm), $Na_2S_2O_5$ (0.075 g, 1.8% wbm), $NaHCO_3$ (0.068 g, 1.6% wbm) and KPS (0.083 g, 2.0% wbm). 12.5% solids content.

Emulsion polymerization of EEMA with redox initiation. EEMA (4.159 g, 15 mmol), DI water (31.759 g), SDS (0.166 g, 4.0% wbm), $Na_2S_2O_5$ (0.076 g, 1.8% wbm), $NaHCO_3$ (0.067 g, 1.6% wbm) and KPS (0.083 g, 2.0% wbm). 12.5% solids content.

Scheme 4-4. Emulsion homopolymerization of eugenol-derived methacrylates using $Na_2S_2O_5$/KPS redox initiation at 40°C: A) EDMA, B) EIMA, C) EEMA

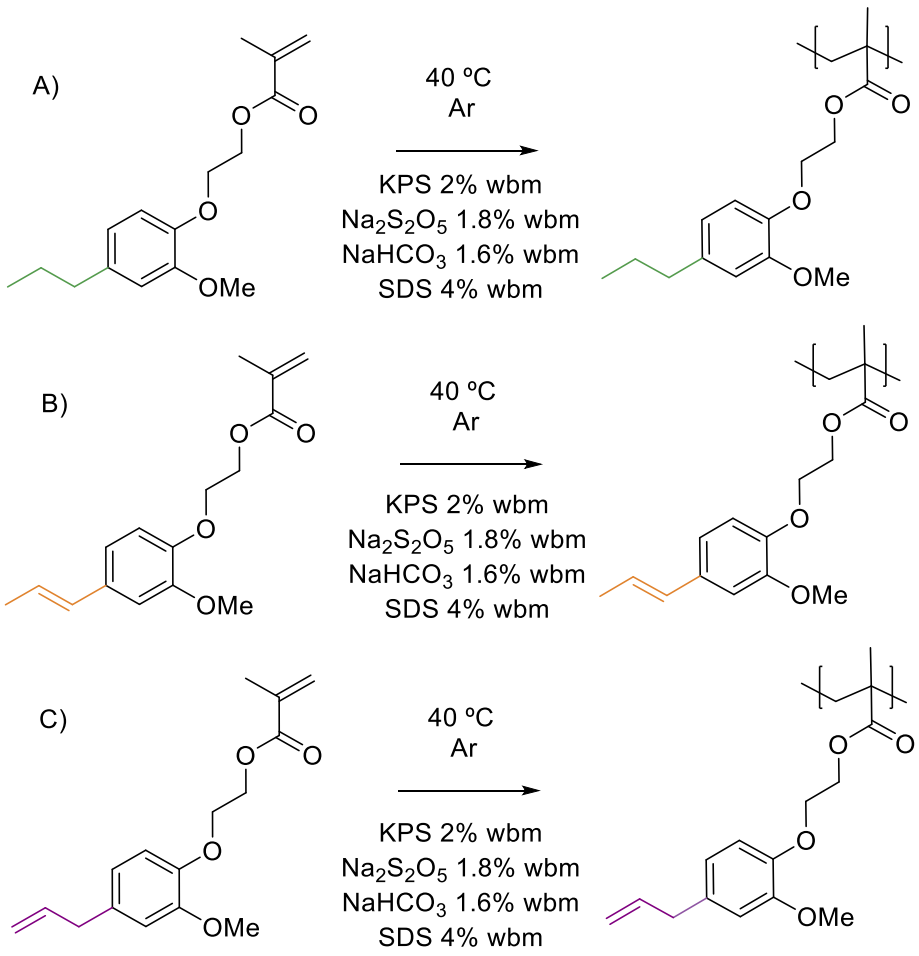

4.2.2.3 Emulsion copolymerization of ethoxy dihydroeugenyl methacrylate with butyl acrylate

The emulsion polymerization by thermal initiation was carried out in a 50 mL double-walled jacketed glass reactor with a U-shaped glass stirring rod. For a latex at 30 wt% solids, EDMA (4.175 g, 38% wbm) and butyl acrylate (6.813 g, 62% wbm) were placed in a glass vial and purged with argon for 15 minutes. DI water (26.50 g), SDS (0.143 g, 1.3% wbm) and $NaHCO_3$ (0.121 g, 1.1 % wbm, 1:3.5 molar ratio KPS:$NaHCO_3$), were placed in the reactor and degassed with argon for 30 min. The reactor was heated to 70°C. The degassed monomer was added to the reactor through a syringe and KPS (0.110 g, 1 % wbm), previously dissolved in 4 g of DI water (from the total weight) was finally added. The reaction mixture was kept under a small flux of argon and mechanical stirring at 250 rpm.

4.2.3 Characterization

Nuclear magnetic resonance spectroscopy (^{1}H NMR). Monomer conversions were determined through the monitoring of the methacrylate double bond by ^{1}H NMR spectroscopy with a Bruker Avance 400 MHz spectrometer at room temperature. The spectra were recorded

by dissolving 0.1 mL of latex in 0.5 mL of $CDCl_3$ (when not indicated otherwise). 1,4-bis(trimethylsilyl)benzene (BTMSB) was used as internal standard.

Dynamic light scattering (DLS). (Appendix Table A3-1, Figure A3-1 to Figure A3-9) Particle size measurements were performed by dynamic light scattering on a Vasco 3 nanoparticle size analyzer supplied by Cordouan Technologies at 25°C using the Cumulant model. Samples for DLS measurements were prepared by diluting one drop of latex with 5 mL of DI water. The laser power, time interval, and number of channels were adjusted for each sample to obtain a good ACF (autocorrelation function). The presented results are the average of 5-10 measurements.

Transmission Electron Microscopy (TEM). (Appendix Figure A3-10 to Figure A3-11) TEM was performed on a Jeol 1200EXII transmission electron microscope at an operating voltage of 100 kV with images captured with a Quemesa camera from Olympus Soft Imaging Solutions. One drop of latex was diluted in 5 mL of DIW and subsequently placed onto a Formvar-coated, 300-mesh copper grid, stabilized with evaporated carbon film for TEM analysis and left to dry under air prior to analysis.

Thermogravimetric Analysis (TGA). (Appendix Figure A3-12 to Figure A3-14) Thermogravimetric analysis was performed on 10 – 15 mg samples on a TGA Q50 apparatus from TA Instruments from 20°C to 590°C, in an aluminum pan, at a heating rate of 10°C min^{-1}, under nitrogen. Analyses were also performed with a PERSEUS® TGA 209 F1 Libra® from Netzch using a temperature ramp of 20°C min^{-1} from 20°C to 620°C under nitrogen flow of 40 mL min^{-1} in an alumina crucible.

Differential Scanning Calorimetry (DSC). (Appendix Figure A3-15 to Figure A3-23) Glass transition temperature measurements were performed on 10–15 mg samples, under nitrogen atmosphere, with a Netzsch DSC 200 F3 instrument using the following heating/cooling cycle: first cooling ramp from room temperature (ca. 20°C) to −40°C at 20°C min^{-1}, isotherm plateau at −40°C for 10 min, first heating ramp from −40°C to 170°C at 20°C min^{-1}, cooling stage from 170°C to −40°C at 20°C min^{-1}, isotherm plateau at −40°C for 10 min, second heating ramp from −40°C to 170°C at 20°C min^{-1}, cooling stage from 170°C to −40°C at 20°C min^{-1}, isotherm plateau at −40°C for 10 min, third heating ramp from −40°C to 170°C and last cooling stage from 170°C to room temperature (ca. 20°C). T_g values are given from the evaluation of the third heating ramp. Calibration of the instrument was performed with noble metals and checked with an indium sample.

Gel content measurements. The gel content of the polymers was measured by placing approximately 50 mg of dried polymer in a Teflon pocket which was subsequently immersed in 10 mL of THF for 24 h, then dried in a ventilated oven at 50°C for 4 hours. The gel content was calculated based on the initial (W_i) and final (W_f) polymer mass according to Eq. 4-1 below:

$$Gel\ content(\%) = \frac{W_{final\ solid} \times 100}{W_{initial\ solid}} \qquad \text{Eq. 4-1}$$

4.3 Results and Discussion

4.3.1 Emulsion homopolymerization of eugenol-derived methacrylates.

The formulations were designed to have 2% wbm of initiator (either KPS thermal peroxide initiation, ACVA thermal azo initiation, or $Na_2S_2O_5$/KPS redox initiation, 4 - 4.2 % wbm of surfactant (SDS), targeting approximately twice the value of the critical micelle concentration of SDS,[19] and $NaHCO_3$ as a buffer according to the initiator used (1.2 to 2.2% wbm). The monomer conversion was monitored only by ^{1}H NMR spectroscopy because thermogravimetric measurements were thought to be not suitable due to the high boiling point of the monomers (later it was shown that it can be performed under vacuum at 80°C as discussed in Chapter 5).

As previously discussed in Chapter 2,[18] the pendent chain comprising the allylic and propenyl groups were involved in secondary reactions during the course of radical polymerization, such as hydrogen abstraction (bis allylic protons –Ar-**CH_2**-CH=CH_2 and propenyl protons –Ar-CH=CH-**CH_3**) and cross-propagation (allylic –Ar-CH_2-**CH=CH_2** and propenyl –Ar-**CH=CH**-CH_3 double bonds). However, in solution homopolymerization in toluene, we observed that high percentages of allylic and propenyl double bonds (91% and 85% respectively) were preserved.[18] In photoinduced polymerization of the monomers, in the form of films, presented in Chapter 3, the preservation of a percentage of allylic and propenyl double bonds was also possible especially while protected from air (94% for allylic and 46% for propenyl, while using Darocur 1173 as PI). In the work presented in this chapter, keeping the highest amount of unreacted double bonds would also be beneficial to avoid extensive cross-linking during polymerization and to obtain functional latexes that could further undergo chemical reactions such as being photocured using thiol-ene chemistry for instance. This would allow tuning the properties of the coatings/adhesives after the synthesis of the latexes.

The study of the behavior of the dihydroeugenol-derived methacrylate (EDMA) monomer in emulsion polymerization was thus carried out first as this monomer does not possess any double bond, leaving only benzylic protons –Ar-**CH_2**-CH_2-CH_3 able to undergo degradative intramolecular or intermolecular chain transfer, thus limiting the risk of premature cross-linking.

The first aqueous emulsion polymerization was performed using the thermal initiation of potassium persulfate (KPS, 70°C). The decomposition mechanism of KPS is shown in Eq. 4-2 and produces oxygen-centered radicals.

$$S_2O_8^{2-} \rightarrow 2\,SO_4^{-\cdot} \qquad \text{Eq. 4-2}$$

Thermal dissociation of potassium persulfate can lead in low amount to the formation of bisulfate ions (HSO_4^-, pKa=2.0), originated from the transfer of $SO_4^{-\cdot}$ radicals to water as shown in Eq. 4-3.[20] Thus a buffer ($NaHCO_3$) was added in the formulation to control the pH and avoid possible hydrolysis of the polymer.

$$S_2O_8^{2-} + \mathrm{x}H_2O \rightarrow (2-\mathrm{x})SO_4^{-\cdot} + \mathrm{x}HSO_4^- + \mathrm{x}HO^{\cdot} \qquad \text{Eq. 4-3}$$

The reaction reached 98 % conversion after 5 h (Figure 4-1), although it showed a rather long induction period (2 h). Induction periods have already been observed with highly hydrophobic monomers. Indeed, the low concentration of monomer in the aqueous phase, due to the low monomer solubility in water, leads to radical termination rather than propagation. This in turn leads to a low concentration of oligoradicals in the aqueous phase, which decreases the probability of oligoradical entry events into the monomer-swollen micelles (micellar nucleation), therefore retarding the nucleation.[21,22] Aggregative nucleation should also be considered as a possible explanation for the observed induction period. In this case nucleation occurs when a critical supersaturation of growing dead oligomers is reached in the continuous phase, this solution becomes unstable and separates into a polymer phase.[28,29] The capture of radicals by the monomer-swollen micelles could be improved by reducing the electrostatic repulsion between the radicals (due to initiator charge, e.g. sulfate group of the KPS) and the surface of the monomer-swollen micelles (due to surfactant charge, e.g. sulfate group of SDS).[23] Thus, using weakly anionic surfactants (e.g. carboxylic acid-based surfactants) or even non-ionic surfactants (e.g. poly(ethylene oxide)-based surfactants) instead of anionic surfactants (e.g. SDS) can help to increase radical entry and shorten induction period.[24] Nevertheless, the use of weakly anionic surfactants results in latexes with lower colloidal stability (sensitivity to pH) and the use of non-ionic surfactants can lead to bigger particles and/or bimodal populations[25] due to a second nucleation period.[26] Moreover, undesired radical transfer to non-ionic surfactants has also been observed.[27] For all these reasons, the use of weakly anionic or non-ionic surfactants was not considered in this work to reduce the induction period. Efforts were instead focused on testing different initiating systems (a water soluble azo-initiator and a redox pair) as detailed below. Using KPS as initiator and SDS as surfactant, a stable latex with an average particle diameter of ca. 63 nm was obtained (Appendix Table A3-1, Figure A3-1).

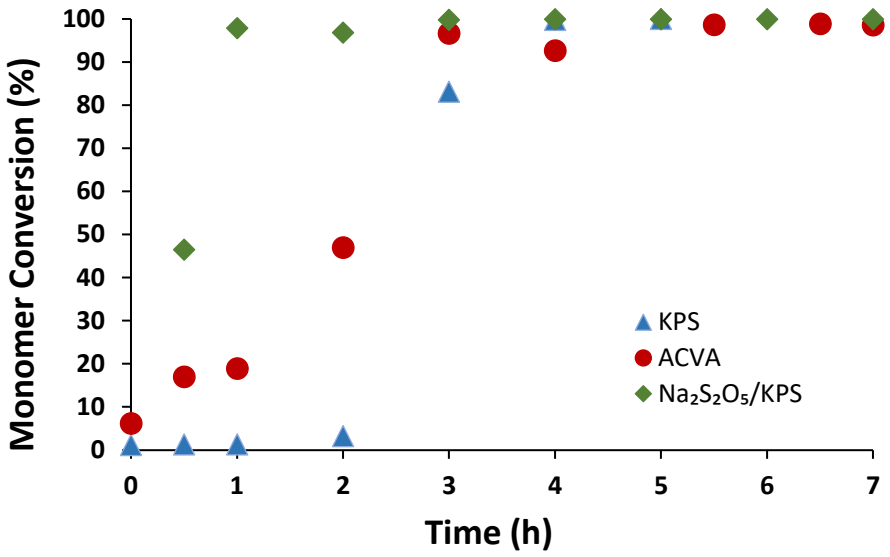

Figure 4-1. Monomer conversion versus time of emulsion homopolymerization of EDMA.

After confirming the feasibility of emulsion polymerization with the monofunctional EDMA, the difunctional EIMA and EEMA monomers were polymerized following the same procedure. The final EEMA conversion was high, as checked by ^{1}H NMR, using BTMSB as internal standard. Both poly(EIMA) and poly(EEMA) homopolymers prepared by emulsion polymerization using KPS thermal initiation were cross-linked and insoluble in organic solvents (gel content > 96 %,Table 4-4). High gel content and insoluble polymers limited the possibility to quantify propenyl and allylic double bonds consumption as the measurements were done by ^{1}H NMR. Therefore, we directed some of our efforts to prevent gel formation, aiming to minimize consumption of allylic and propenyl double bonds, as well as the formation of insoluble polymer. In addition, after two weeks, the latex derived from EIMA coagulated, whilst the one derived from EEMA sedimented. Gel content (polymer fraction insoluble in THF) should not be confused with flocculation and coagulation processes, which refer to the aggregation of the latex particles (in aqueous medium) in a reversible and irreversible manner respectively.[22] The average particle diameter of these latexes prior to coagulation and sedimentation was 70 nm and 104 nm for poly(EIMA) and poly(EEMA) respectively (Appendix Table A3-1, Figure A3-1). The increase of number of polymer particles due to increasing cross-linker content in the monomer mixture has been reported. This is due to the reduction of the monomer concentration in the growing particles, as the swelling ability is limited as the result of the cross-link density. The volume growth rate decreases leading to an increase of particle number, as shown in Eq. 4-4:[30]

$$N_p = k\left(\frac{k_d[I]}{\mu}\right)^{2/5}(a_s[S])^{3/5} \qquad \text{Eq. 4-4}$$

where N_p is number of particles, k is a numerical constant which values are in the range from 0.37 (when monomer-swollen micelles and particles compete for radical entry) to 0.53 (when all aqueous-phase radicals enter monomer-swollen micelles),[31] k_d is the initiator decomposition rate, a_s is the adsorption area per surfactant molecule, $[I]$ and $[S]$ are the concentrations of the initiator an surfactant respectively, and μ the volumetric growth rate per particle.[30] The increasing amount of particles could lead to an insufficient amount of surfactant needed to stabilize the growing particles, leading to the observed colloidal instability and later coagulation or sedimentation. The colloidal instability of these latexes was not further investigated.

To minimize the secondary reactions that led to cross-linked polymers, a water-soluble azo initiator (ACVA) was then used. Carbon-centered radicals produced by azo initiators are less likely to abstract hydrogen atoms than oxygen-centered radicals produced by thermal decomposition of KPS.[32,33]A buffer was added to solubilize the initiator. The decomposition reaction for ACVA is shown in Scheme 4-5.

Scheme 4-5. Decomposition reaction of ACVA

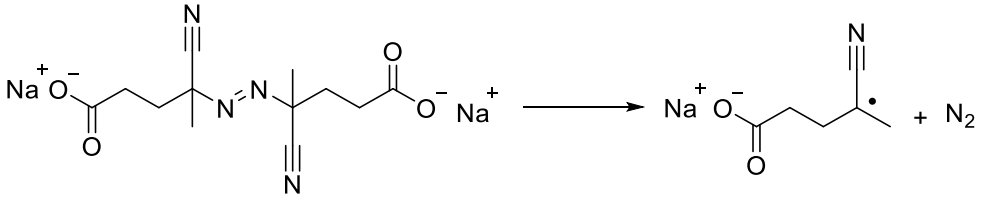

Emulsion polymerization using this initiation system was first performed with EDMA (Figure 4-1). In this case, there was no induction period. The latex particle size and thus the number of latex particles is very similar using KPS (63 nm) or ACVA (64 nm); so, the particle size is not the parameter that distinguishes these two systems. A higher radical flux would result in a higher extent of radical entry into the monomer-swollen micelles, thus leading to a shorter induction period. However, dissociation rate constants of KPS and ACVA are not significantly different in the present experimental conditions (approximately 4.3×10^{-5} s^{-1} for KPS and 3.6×10^{-5} s^{-1} for ACVA at 70°C).[32,34] Thus, in the case of ACVA, it is not a higher radical flux that eliminates the induction period. Instead, as ACVA decomposition produced a weakly charged initiator (carboxylic acid for ACVA instead of sulfate group for KPS), it leads to a higher probability of radical entry into the negatively charged monomer-swollen micelles (sulfate groups of SDS), hence promoting micellar nucleation and shortening the induction period.[23,35,36] In addition, side reactions such as hydrogen abstraction of benzylic hydrogens (degradative chain transfer to EDMA monomer or poly(EDMA) oligoradicals in the water phase) are possible in the case of the oxygen-centered radicals produced by KPS. The carbon-centered radicals produced by ACVA are less likely to abstract hydrogens.[32,33] Using ACVA as initiator and SDS as surfactant, the resulting poly(EDMA) latex was stable and the particle diameter was about 64 nm (Appendix Table A3-1, Figure A3-4). The same procedure was carried out with EIMA and EEMA. However, under these conditions, EIMA polymerization also led to polymer insoluble in organic solvents as with KPS initiation, indicating pronounced cross-linking, due to secondary reactions such as cross-propagation reaction between methacrylate and propenyl double bonds. The resulting poly(EIMA) latex was stable with a particle size of 45 nm (Appendix Table A3-1, Figure A3-4). Due to the high T_g value of this latex (63°C) and its good colloidal stability, in addition to the measurement of the particle average hydrodynamic diameter by DLS, it was also possible to perform transmission electron microscopy (TEM) analysis (Appendix Figure A3-10 and Appendix Figure A3-11) without major coalescence of the polymer particles under the electron beam. In contrast, the emulsion polymerization of EEMA with ACVA showed a soluble fraction of poly(EEMA) in $CDCl_3$ during the ^1H NMR monitoring. However, a high gel content of 98 % was obtained. The poly(EEMA) latex was stable with a particle diameter of 57 nm. (Appendix Table A3-1, Figure A3-4)

As previously mentioned in Chapter 2, it was observed that the solution homopolymerization in toluene of EIMA proceeded faster than that of EEMA, and that EIMA propenyl double bonds were also more reactive than EEMA allylic double bonds.[18] In spite of the secondary reactions, a high percentage of propenyl (85 %) and allylic (91 %) double bonds were left unreacted in solution polymerization.

The lower T_g value of poly(EEMA) (27°C) produced from the emulsion polymerization with ACVA in comparison to the T_g=48°C of the polymer obtained using KPS as initiator, suggests that the secondary reactions producing the cross-linking are not the same or do not occur in the same proportion with each initiator. This implied that the use of ACVA diminishes the secondary reactions leading to cross-linking. However, after drying, the latex displayed a gel content value

of 98 %. Thus, the polymer suffers from further cross-linking. Moreover, oxidation of the residual double bonds, could lead to higher cross-link density as it was observed in vegetable oils previously.[37,38]

Moreover, as a higher T_g was measured for EIMA emulsion polymerization using ACVA as initiator (with a T_g of more than 60°C for poly(EIMA) with either KPS or ACVA, Appendix Figure A3-16 and Figure A3-19), it could be considered that the extent of the secondary reactions led to a higher cross-link density[39] for poly(EIMA) compared to poly(EEMA). EIMA may undergo mainly cross-propagation through its propenyl double bond, leading to highly cross-linked polymers (as this cross-propagation reaction is not diminished using ACVA, resulting in a high T_g), while EEMA may undergo mainly allylic hydrogen abstraction (which is less favored with carbon-centered radical from ACVA compared to oxygen-centered radicals from KPS as initiator.

In isoprene emulsion polymerization, the reduction of temperature has been shown to decrease the relative cross-linking rate (ratio of the cross-linking rate coefficient and the propagation rate coefficient).[40] This is associated to a higher activation energy for the cross-linking reaction than for the propagation reaction.[41] Therefore, a redox initiation system was used at lower temperature, to avoid high temperatures likely promoting the secondary reactions which may lead to the cross-linking of the polymers. Thus, $Na_2S_2O_5$/KPS (molar ratio of 1.3:1 $Na_2S_2O_5$/KPS) was used as a redox initiation system.[42,43] To introduce all monomer in liquid state, the temperature reaction was fixed at 40°C (as EIMA m.p.: 36°C). The hydrolysis and redox reactions of the system are shown in Eq. 4-5 to Eq. 4-7.

$$S_2O_5{}^{2-} + H_20 \rightarrow 2HSO_3{}^{-} \quad \text{Eq. 4-5}$$

$$S_2O_8{}^{2-} + HSO_3{}^{-} \rightarrow SO_4{}^{2-} + SO_4{}^{-\cdot} + {}^{\cdot}SO_3H \quad \text{Eq. 4-6}$$

$$SO_4{}^{-\cdot} + HSO_3{}^{-} \rightarrow SO_4{}^{2-} + {}^{\cdot}SO_3H \quad \text{Eq. 4-7}$$

Two equivalents of bisulfite radicals ($^{\bullet}SO_3H$, pKa=1.9)[43] are produced per dissociation event thus a buffer was added to control the pH (however the amount of added buffer was not enough and the final pH was below 4). As for the KPS-initiated polymerizations, the first monomer to be tested was EDMA. In this case, the polymerization reached full conversion after 3 h and no induction period was observed (Figure 4-2, Appendix Figure A3-24). Slightly bigger and thus fewer latex particles are produced using $Na_2S_2O_5$/KPS redox system (71 nm) compared to KPS thermal initiation system (63 nm). Slower kinetics are expected for the redox system on the basis of the particle size, although the redox polymerization turned out to be faster. The chemical nature of the radicals produced by this $Na_2S_2O_5$/KPS redox system (sulfonate and sulfate radicals) is similar to the radicals produced by KPS thermal initiation (sulfate radicals). Therefore, contrary to the ACVA system, the nature of the produced radicals by this redox system is not responsible for the faster kinetics. The important feature of this system is that one-third of the KPS oxidant was added in one shot to start the polymerization (the remaining two-third of KPS was added semi-continuously), generating a high flux of radicals by the redox reaction between hydrogen sulfite and persulfate, thus reducing significantly any induction period.[43,44] Using $Na_2S_2O_5$/KPS redox

system as initiator and SDS as surfactant, a stable latex with particle diameter of 71 nm was obtained (Appendix Table A3-1, Figure A3-7). The same experimental conditions were then used with EIMA and EEMA. The polymerization proceeded to quantitative monomer conversion for the three monomers in 3 h, but the polymerization rate was slower for EEMA (Figure 4-2).

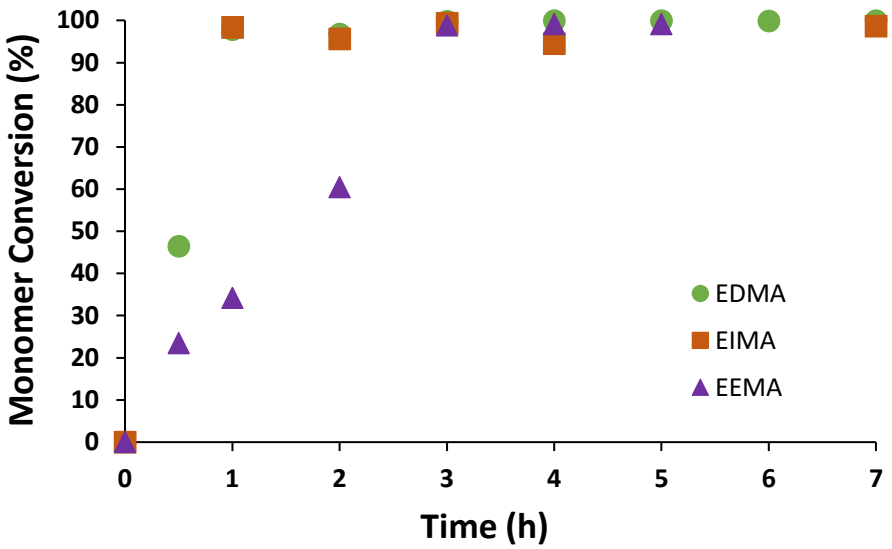

Figure 4-2. Monomer conversion versus time of eugenol-derived methacrylates in aqueous emulsion homopolymerization using redox $Na_2S_2O_5$/KPS initiation at 40°C.

These polymerization conditions with $Na_2S_2O_5$/KPS redox initiation resulted in quantitative conversions (Appendix Figure A3-25 to Figure A3-26) but high gel content (Table 4-4), with particle diameter of 163 nm for poly(EIMA) (Appendix Figure A3-7) and 53 nm for poly(EEMA) (Appendix Figure A3-7). Due to the high gel content, it was not possible to quantify the consumption of abstractable protons nor the consumption of the propenyl or allylic double bonds of EIMA and EEMA respectively. The polymerization of EIMA proceeded at a similar rate to that of EDMA while that of EEMA was much slower. This suggests that a degradative chain transfer reaction (decrease of the number of propagating radicals) occurred in the case of EEMA and that such transfer reaction did not occur (or to a much lower extent) in the case of EIMA. It is important to note that the radical formed by hydrogen abstraction of the allylic protons of EEMA is very poorly reactive as it is highly stabilized through resonance. Both poly(EEMA) obtained with ACVA and $Na_2S_2O_5$/KPS initiation system showed a low T_g=27°C and T_g=23°C respectively. Note that the high gel content (>89% for poly(EEMA)) is not synonymous to high cross-link density. Modification of the T_g value is related to the cross-link density and not solely to the presence of gel content or cross-linked polymers. The relationship between the T_g and the cross-link density is given in by the Eq. 4-8:[39]

$$\frac{T_g - T_g^0}{T_g^0} = K\frac{X_C}{1 - X_C} \qquad \text{Eq. 4-8}$$

where T_g is the glass transition temperature of the cross-linked polymer, T_g^0 is the glass transition temperature of the non-crosslinked polymer, X_C is the crosslink density in molar fraction and K a constant describing the lattice energy ratio between the non-cross-linked and cross-linked polymer.

The rather low T_g values for poly(EEMA) reflects that, although the product is insoluble (high gel content), the cross-link density in poly(EEMA) latexes is not as high as in the poly(EIMA) latexes (poly(EIMA) T_g ≈60°C).[39,45]

Furthermore, thermogravimetric analyses show that the decomposition temperatures $T_{d,5\%}$ for poly(EIMA) and poly(EEMA), according to the initiation systems, decrease in the following order: KPS > ACVA > $Na_2S_2O_5$/KPS. The thermal stability of polymers has been proved to increase as cross-link density increases,[46,47] thus higher cross-linking due to secondary reactions would be expected from emulsion polymerization using KPS at 70°C as stated above.

Table 4-4. Polymer characterization

Monomer	Initiator	Monomer conversion (%)	pH	Particle diameter D_i (nm)	Colloidal stability	Gel Content (%)	T_g (°C)	$T_{d,5\%}$ (°C)
EDMA	KPS (70°C)	100	8.9	63	Yes	1	26	247
	ACVA (70°C)	99	6.3	64	Yes	0	20	265
	$Na_2S_2O_5$/KPS (40°C)	100	2.4	71	Yes	0	28	284
EIMA	KPS (70°C)	ND	9.7	70	No	99	72	293
	ACVA (70°C)	ND	6.4	45	Yes	74	63	289
	$Na_2S_2O_5$/KPS (40°C)	99	2.4	163	No	99	61	237
EEMA	KPS (70°C)	79	8.9	104	No	96	48	297
	ACVA (70°C)	ND	8.5	57	Yes	98	27	265
	$Na_2S_2O_5$/KPS (40°C)	99	3.8	53	Yes	89	23	229

A latex with a higher solids content (30 %) was also synthesized. The comonomer used was butyl acrylate. The Fox equation (Eq. 4-9) was used to calculate the proportion of monomers to be used in the formulation to reach a T_g of −28°C, considering T_g (PBA)= −53°C[48] and T_g (PEDMA)=26°C (this work, Table 4-4).

$$\frac{1}{T_g} = \frac{w_1}{T_{g1}} + \frac{w_2}{T_{g2}} \qquad \text{Eq. 4-9}$$

From a monomer mixture of 38 wt % EDMA - 62 wt % BA, a stable latex was obtained with a particle diameter 112 nm. After 2 h of reaction, the poly(EDMA-*co*-BA) copolymer was insoluble in organic solvents, as usual for acrylate based latexes (due to intermolecular chain transfer to polymer in the case of acrylate polymerization)[49,50]. A film forming latex was obtained with a T_g=−23 °C.

4.4 Conclusion

The aqueous emulsion radical homopolymerizations of ethoxy dihydroeugenyl methacrylate (EDMA), ethoxy eugenyl methacrylate (EEMA) and ethoxy isoeugenyl methacrylate (EIMA) were successfully carried out and yielded colloidally stable biobased latexes of particle diameters of about 45-71 nm. These emulsion polymerizations did not require the use of large quantities of surfactants or of low CMC surfactants as is sometimes required for very hydrophobic monomers.[51] Emulsion polymerization with ACVA resulted in stable latexes for the three monomers. Moreover, it was possible to observe a decrease in the T_g of poly(EEMA) prepared using ACVA (T_g=23°C) in comparison to the poly(EEMA) obtained using KPS as the initiator (T_g =48°C). This indicates that ACVA as the initiator could decrease the secondary reactions leading to cross-linking. During $Na_2S_2O_5$/KPS redox emulsion polymerization at 40°C, EEMA presented the lowest rate of polymerization compared to EDMA and EIMA, possibly due to hydrogen abstraction as secondary reaction, leading to a very stable allylic radical not prone to propagate. Moreover, although quantitative conversion was reached for all monomers, the lower T_g values for poly(EEMA) compared to poly(EIMA) (23°C and 61°C respectively) suggested that the main secondary reaction in the case of EIMA is cross-propagation, leading to highly cross-linked poly(EIMA) polymers while a degradative chain transfer reaction is the main secondary reaction during EEMA redox polymerization, leading to less cross-linked poly(EEMA) polymers.

A stable poly(EDMA-*co*-BA) copolymer latex at 30 % solids content, with film-forming properties (T_g = −23°C), has also been successfully synthesized. These results opened the way to aqueous emulsion copolymerizations with commercial monomers to produce functional biobased reactive latexes for adhesives and coatings formulations as is presented in Chapter 5.

4.5 References

(1) Anastas, P.; Eghbali, N. Green Chemistry: Principles and Practice. *Chem. Soc. Rev.* **2010**, *39*, 301.

(2) Anastas, P. T.; Zimmerman, J. B. Peer Reviewed: Design Through the 12 Principles of Green Engineering. *Environ. Sci. Technol.* **2003**, *37*, 94A.

(3) *Emulsion Polymerization and Emulsion Polymers*; Lovell, P. A., El-Aasser, M. S., Eds.; John Wiley & Sons Ltd: Sussex, 1997.

(4) Asua, J. M. Emulsion Polymerization: From Fundamental Mechanisms to Process Developments. *J. Polym. Sci. Part A Polym. Chem.* **2004**, *42*, 1025.

(5) Chern, C. S. Emulsion Polymerization Mechanisms and Kinetics. *Prog. Polym. Sci.* **2006**, *31*, 443.

(6) Save, M.; Guillaneuf, Y.; Gilbert, R. G. Controlled Radical Polymerization in Aqueous Dispersed Media. *Aust. J. Chem.* **2006**, *59*, 693.

(7) Daniel, J.-C.; Pichot, C. *Les Latex Synthétiques: Élaboration et Applications*; Tec&Doc-Lavoisier, 2006.

(8) Thickett, S. C.; Gilbert, R. G. Emulsion Polymerization: State of the Art in Kinetics and Mechanisms. *Polymer (Guildf).* **2007**, *48*, 6965.

(9) Ugelstad, J.; El-Aasser, M. S.; Vanderhoff, J. W. Emulsion Polymerization: Initiation of Polymerization in Monomer Droplets. *J. Polym. Sci. Polym. Lett. Ed.* **1973**, *11*, 503.

(10) Antonietti, M.; Landfester, K. Polyreactions in Miniemulsions. *Prog. Polym. Sci.* **2002**, *27*, 689.

(11) Asua, J. M. Miniemulsion Polymerization. *Prog. Polym. Sci.* **2002**, *27*, 1283.

(12) Asua, J. M. Challenges for Industrialization of Miniemulsion Polymerization. *Prog. Polym. Sci.* **2014**, *39*, 1797.

(13) Demirci, S.; Sahiner, N. Microemulsion Polymerization. In *Encyclopedia of Polymer Science and Technology*; Wiley, 2019; pp 1–24.

(14) Sáenz, J. M.; Asua, J. M. Dispersion Polymerization in Polar Solvents. *J. Polym. Sci. Part A Polym. Chem.* **1995**, *33*, 1511.

(15) Brooks, B. Suspension Polymerization Processes. *Chem. Eng. Technol.* **2010**, *33*, 1737.

(16) Pinto, M. C. C.; Santos, J. G. F.; Machado, F.; Pinto, J. C. Suspension Polymerization Processes. In *Encyclopedia of Polymer Science and Technology*; John Wiley & Sons, Inc.: Hoboken, NJ, USA, 2013.

(17) Molina-Gutiérrez, S.; Ladmiral, V.; Bongiovanni, R.; Caillol, S.; Lacroix-Desmazes, P. Radical Polymerization of Biobased Monomers in Aqueous Dispersed Media. *Green Chem.* **2019**, *21*, 36.

(18) Molina-Gutiérrez, S.; Manseri, A.; Ladmiral, V.; Bongiovanni, R.; Caillol, S.; Lacroix-Desmazes, P. Eugenol: A Promising Building Block for Synthesis of Radically Polymerizable Monomers. *Macromol. Chem. Phys.* **2019**, *220*, 1900179.

(19) Cifuentes, A.; Bernal, J. L.; Diez-Masa, J. C. Determination of Critical Micelle Concentration Values Using Capillary Electrophoresis Instrumentation. *Anal. Chem.* **1997**,

69, 4271.

(20) Cheetham, P.; Tabner, B. A Spin-trap Study of the Peroxodisulfate-disulfite-iron Initiator System. *Die Makromol. Chemie, Rapid Commun.* **1990**, *11*, 205.

(21) Matsumoto, A.; Murakami, N.; Aota, H.; Ikeda, J.; Capek, I. Emulsion Polymerization of Lauryl Methacrylate and Its Copolymerization with Trimethylolpropane Trimethacrylate. *Polymer (Guildf).* **1999**, *40*, 5687.

(22) Van Herk, A. M. *Chemistry and Technology of Emulsion Polymerisation*; van Herk, A. M., Ed.; John Wiley & Sons Ltd: Oxford, UK, 2013.

(23) Thickett, S. C.; Gilbert, R. G. Mechanism of Radical Entry in Electrosterically Stabilized Emulsion Polymerization Systems. *Macromolecules* **2006**, *39*, 6495.

(24) Emelie, B.; Pichot, C.; Guillot, J. Batch Emulsion Copolymerization of N-Butyl Acrylate and Methyl Methacrylate in the Presence of a Nonionic Surfactant. *Die Makromol. Chemie* **1985**, *10*, 43.

(25) Piirma, I.; Chang, M. Emulsion Polymerization of Styrene: Nucleation Studies with Nonionic Emulsifier. *J. Polym. Sci. Polym. Chem. Ed.* **1982**, *20*, 489.

(26) Asua, M.; Zangi, R. Shedding Light on the Different Behavior of Ionic and Nonionic Surfactants in Emulsion Polymerization : From Atomistic Simulations to Experimental Observations †. **2017**, 31692.

(27) Wu, X. Q.; Schork, F. J. Kinetics of Miniemulsion Polymerization of Vinyl Acetate with Nonionic and Anionic Surfactants. *J. Appl. Polym. Sci.* **2001**, *81*, 1691.

(28) Tauer, K.; Ramírez, A. G.; López, R. G. Effect of the Surfactant Concentration on the Kinetics of Oil in Water Microemulsion Polymerization: A Case Study with Butyl Acrylate. *Comptes Rendus Chim.* **2003**, *6*, 1245.

(29) Tauer, K.; Nazaran, P. Mechanism and Modeling of Emulsion Polymerization: New Ideas and Concepts - 1. Particle Nucleation. *Macromol. Symp.* **2010**, *288*, 1.

(30) Suresh, K. I.; Othegraven, J.; Raju, K. V. S. N.; Bartsch, E. Mechanistic Studies on Particle Nucleation in the Batch Emulsion Polymerisation of N-Butyl Acrylate Containing Multifunctional Monomers. *Colloid Polym. Sci.* **2004**, *283*, 49.

(31) Lovell, P. A.; Schork, F. J. Fundamentals of Emulsion Polymerization. *Biomacromolecules* **2020**, acs. biomac.0c00769.

(32) Santos, A. M.; Vindevoghel, P.; Graillat, C.; Guyot, A.; Guillot, J. Study of the Thermal Decomposition of Potassium Persulfate by Potentiometry and Capillary Electrophoresis. *J. Polym. Sci. Part A Polym. Chem.* **1996**, *34*, 1271.

(33) Hioe, J.; Zipse, H. Radical Stability and Its Role in Synthesis and Catalysis. *Org. Biomol. Chem.* **2010**, *8*, 3609.

(34) Zhou, Y.; Zhang, Z.; Postma, A.; Moad, G. Kinetics and Mechanism for Thermal and Photochemical Decomposition of 4,4′-Azobis(4-Cyanopentanoic Acid) in Aqueous Media. *Polym. Chem.* **2019**, 3.

(35) Coen, E. M.; Lyons, R. A.; Gilbert, R. G. Effects of Poly(Acrylic Acid) Electrosteric Stabilizer on Entry and Exit in Emulsion Polymerization. *Macromolecules* **1996**, *29*, 5128.

(36) Cheong, I. W.; Kim, J. H. Investigation of Seeded Emulsion Polymerization Using a Calorimetric Method: Effects of the Surface Charge Density on Polymerization Rate and Average Number of Radicals per Particle. *Colloids Surfaces A Physicochem. Eng. Asp.* **1999**, *153*, 137.

(37) Mallégol, J.; Lemaire, J.; Gardette, J. Drier Influence on the Curing of Linseed Oil. *Prog. Org. Coatings* **2000**, *39*, 107.

(38) Soucek, M. D.; Khattab, T.; Wu, J. Review of Autoxidation and Driers. *Prog. Org. Coatings* **2012**, *73*, 435.

(39) Stutz, H.; Illers, K. -H; Mertes, J. A Generalized Theory for the Glass Transition Temperature of Crosslinked and Uncrosslinked Polymers. *J. Polym. Sci. Part B Polym. Phys.* **1990**, *28*, 1483.

(40) Cheong, I. W.; Fellows, C. M.; Gilbert, R. G. Synthesis and Cross-Linking of Polyisoprene Latexes. *Polymer (Guildf).* **2004**, *45*, 769.

(41) Morton, M.; Cala, J. A.; Piirma, I. Crosslinking in Isoprene Polymerization. *J. Polym. Sci.* **1955**, *15*, 167.

(42) Graillat, C.; Pichot, C.; Guyot, A. Preparation and Characterization of Low Size Polystyrene Latex Particles with Various Strong Acid Surface Charges. *Colloids and Surfaces* **1991**, *56*, 189.

(43) Garnier, J.; Dufils, P.-E.; Vinas, J.; Vanderveken, Y.; van Herk, A.; Lacroix-Desmazes, P. Synthesis of Poly(Vinylidene Chloride)-Based Composite Latexes by Emulsion Polymerization from Epoxy Functional Seeds for Improved Thermal Stability. *Polym. Degrad. Stab.* **2012**, *97*, 170.

(44) Wang, S.; Daniels, E. S.; Sudol, E. D.; Klein, A.; El-Aasser, M. S. Isothermal Emulsion Polymerization of n -Butyl Methacrylate with KPS and Redox Initiators: Kinetic Study at Different Surfactant/Initiator Concentrations and Reaction Temperature. *J. Appl. Polym. Sci.* **2016**, *133*, n/a.

(45) Bandzierz, K.; Reuvekamp, L.; Dryzek, J.; Dierkes, W.; Blume, A.; Bielinski, D. Influence of Network Structure on Glass Transition Temperature of Elastomers. *Materials (Basel).* **2016**, *9*, 607.

(46) Levchik, G. F.; Si, K.; Levchik, S. V.; Camino, G.; Wilkie, C. A. Correlation between Cross-Linking and Thermal Stability: Cross-Linked Polystyrenes and Polymethacrylates. *Polym. Degrad. Stab.* **1999**, *65*, 395.

(47) Uhl, F. M.; Levchik, G. F.; Levchik, S. V.; Dick, C.; Liggat, J. J.; Snape, C. E.; Wilkie, C. A. Thermal Stability of Cross-Linked Polymers: Methyl Methacrylate with Divinylbenzene and Styrene with Dimethacrylates. *Polym. Degrad. Stab.* **2001**, *71*, 317.

(48) Misra, S. C.; Pichot, C.; El-Aasser, M. S.; Vanderhoff, J. W. Batch and Semicontinuous Emulsion Copolymerization of Vinyl Acetate–Butyl Acrylate. II. Morphological and Mechanical Properties of Copolymer Latex Films. *J. Polym. Sci. Polym. Chem. Ed.* **2003**, *21*, 2383.

(49) Britton, D. J.; Lovell, P. A.; Heatley, F.; Venkatesh, R. Chain Transfer to Polymer in

Emulsion Copolymerizations. *Macromol. Symp.* **2001**, *175*, 95.

(50) Plessis, C.; Arzamendi, G.; Alberdi, J. M.; Agnely, M.; Leiza, J. R.; Asua, J. M. Intramolecular Chain Transfer to Polymer in the Emulsion Polymerization of 2-Ethylhexyl Acrylate. *Macromolecules* **2001**, *34*, 6138.

(51) Boscán, F.; Paulis, M.; Barandiaran, M. J. J. Towards the Production of High Performance Lauryl Methacrylate Based Polymers through Emulsion Polymerization. *Eur. Polym. J.* **2017**, *93*, 44.

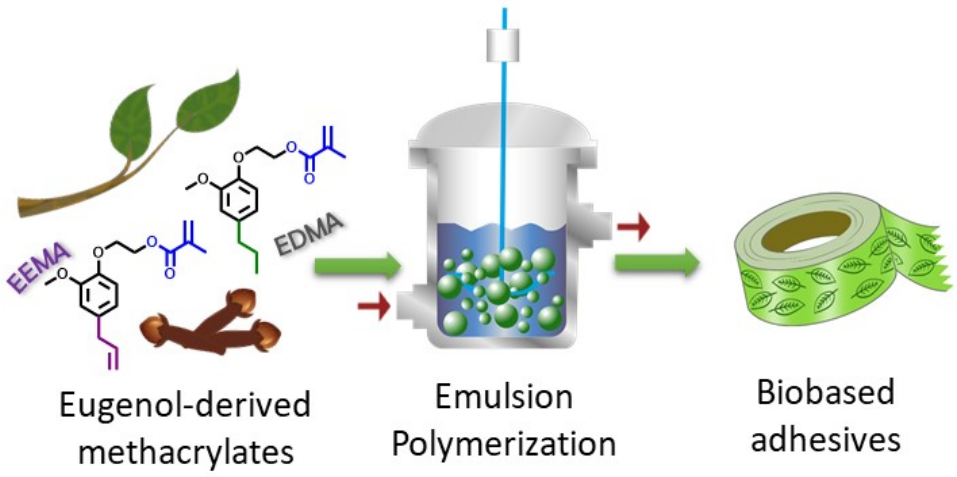

CHAPTER FIVE

Emulsion copolymerization of eugenol-derived methacrylates for adhesive applications

Table of contents

Chapter 5: Emulsion copolymerization of eugenol-derived methacrylates for adhesive applications

Some of the results and discussion presented in this chapter have been published in the article:

Molina-Gutiérrez, S.; Li, W.S.J.; Perrin, R.; Ladmiral, V.; Bongiovanni, R.; Caillol, S.; Lacroix-Desmazes, P. Radical Aqueous Emulsion Copolymerization of Eugenol-Derived Monomers for Adhesive Applications. *Biomacromolecules* **2020**, acs.biomac.0c00461. https://doi.org/10.1021/acs.biomac.0c00461.

5.1 Introduction

Pressure sensitive adhesives are defined as "*viscoelastic materials which in solvent-free form remain tacky and will adhere instantaneously to most solid surfaces with the application of very slight pressure*".[1] They are used in products such as tapes, labels and protective films. They can be produced by different polymerization techniques such as: emulsion, solution, hot-melt or photopolymerization.[2] Currently, the use of biobased monomers to produce PSAs has become a major interest as the PSAs market was valued in 7 billion dollars in 2018.[3] Emulsion polymerization, where the continuous phase is water, is an environmentally friendly process attractive for more sustainable adhesives. As discussed in Chapter 1, emulsion polymerization of biobased monomers has been widely used to produce PSAs. Monomers derived from vegetable oils,[2,4–11] terpenes[11,12] and carbohydrates[13–15] have been integrated into partially biobased PSA copolymers. The "optimal" glass transition temperature for PSAs has been reported to be –15°C to –5°C; however, commercial formulations have lower T_gs down to –60°C.[16] PSAs formulation include low T_g monomers for tack and flexibility in the adhesives, high T_g monomers for cohesion strength, and functional monomers for other properties such as adhesion strength or cross-linking.[17] The introduction of the highest amount of biobased monomer in the latex formulation is often desired. Vegetable oil- and lipid-derived monomers are of particular interest since they introduce soft segments (long aliphatic chains) in the adhesives formulation and thus contribute to yield low T_g polymers.[11] Nevertheless, most of the vegetable oil-derived monomers need to be polymerized through miniemulsion due to their low hydrophilicity. This hinders their wider use in industry.[18] Moreover, monomers derived from olive, soybean, and linseed oils possess allyl groups that can engage in secondary reactions (cross-propagation of the allylic double bond and/or allylic hydrogen abstraction) and cross-link, therefore, increasing the T_g and even producing small coagula,[19] which are undesirable in soft polymers for adhesive applications. Additionally, oxidative curing can occur as a postpolymerization process modifying the properties of the final latex film.[4,20] Thus, it is necessary to use hydrophobic biobased monomers, capable of diffusing through the aqueous phase, which can yield filmogenic polymers. Therefore, the adopted approach in this work is the gradual replacement of the monomers that increase T_g values in the latex formulations with biobased monomers. This approach has been reported using biobased monomers such as isobornyl methacrylate (IBOMA, poly(IBOMA) T_g=155°C[21]), limonene, poly(limonene) T_g=78°C), and sugar-based vinyl monomers.[21–23] Regarding

lignin-derived monomers, Wang *et al.*[24] produced a triblock copolymer from acrylates synthesized using molecules derived from lignin depolymerization. These materials possessed adequate properties for adhesive applications. Nevertheless, the polymerization was executed in solution and not in emulsion. Eugenol-derived monomers have not been used in latex formulations for adhesive purposes yet. For this reason, a general adhesive formulation including butyl acrylate (BA), methyl methacrylate (MMA) and methacrylic acid (MAA),[16] has been modified by the gradual replacement of MMA with a eugenol-derived monomer. Ethoxy dihydroeugenyl methacrylate (EDMA) was selected as the main replacement monomer as it does not possess any pending double bonds that could engage in secondary reactions. Furthermore, the use of ethoxy eugenyl methacrylate (EEMA) was tested to study its effect on the formulation while bearing an allylic double bond. The simplicity of the semibatch process used for the latex synthesis makes this study suitable for scale up.

5.1.1 PSA properties

The performance of a PSA is usually characterized by three parameters: tack, peel strength and shear strength. According to ASTM, tack is defined as *the property of an adhesive that enables it to form a bond of "measurable strength immediately after adhesive and adherend are brought into contact under low pressure"*.[1] Peel strength is defined as "*the average load per unit width of bondline required to separate progressively a flexible member from a rigid member or another flexible member"*,[1] it is related to the internal or cohesive strength of and adhesive mass. It is usually determined by measuring the force needed to remove a strip of supported adhesive from a test panel after application of a specific load (Figure 5-1,a).[25] There are several methods to measure tack such as: loop tack (Figure 5-1,b),[26] probe tack[27] and rolling ball tack.[28] Shear strength is defined as "*the maximum average stress when a force is applied parallel to an adhesive joint*" (Figure 5-1,c).[1,29] The shear test is designed to investigate the long term performance of an adhesive under a moderate load, whereas both peel and tack measurements can be used to assess the adherence of a PSA under a mostly tensile and rapid loading.[30]

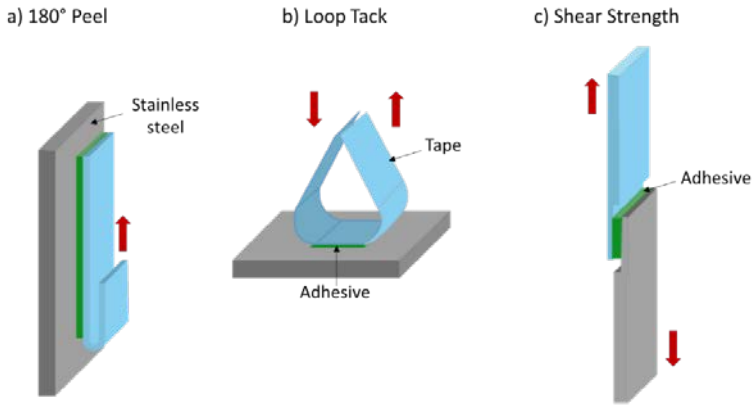

Figure 5-1. Peel, tack and shear tests.

Moreover, rheological properties can help to define the bonding/debonding behavior of the PSA. By measuring the storage (G') and loss (G'') modulus at 10^{-2} rad s^{-1} and 10^{2} rad s^{-1}, it is possible to determine the viscoelastic window of a PSA as proposed by Chang.[31] This window is correlated

to the adhesion performance of the PSA. A four-quadrant concept categorizes the different types of PSAs (Figure 5-2).

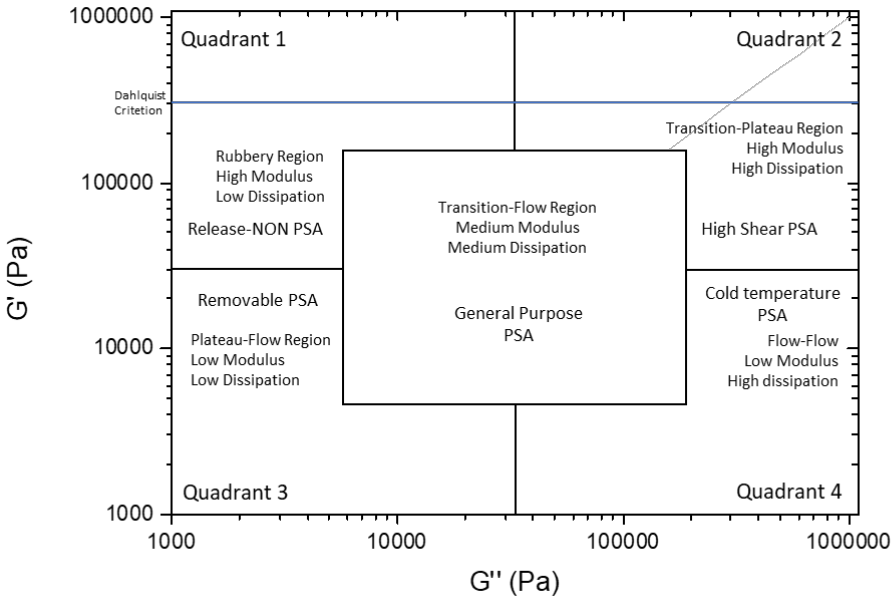

Figure 5-2. Chang's viscoelastic window of PSAs.

The Dalquist's contact criteria line indicates whether a material is contact efficient (PSA) or deficient (non-PSA). The baseline of the window should be under the Dahlquist line to possess PSA properties.

5.2 Experimental

5.2.1 Materials

Ethoxy eugenyl methacrylate (EEMA) and ethoxy dihydroeugenyl methacrylate (EDMA) monomers were synthesized as described in a previous article from our group.[32] Sodium persulfate (NaPS, ≥98.0%, Aldrich), sodium bicarbonate ($NaHCO_3$, ≥99.0%, Aldrich), sodium dodecylbenzenesulfonate (SDBS, Aldrich), 1,4-bis(trimethylsilyl)benzene (1,4-BTMSB, 96%, Aldrich), *tert*-dodecyl mercaptan (98.5%, Aldrich), tetrahydrofuran (THF, ≥99.0%, VWR), 4-methoxyphenol (MEHQ, ≥99.0%, Acros Organics), deuterated benzene (C_6D_6, 99.5%, Eurisotop), and Disponil A 3065 (65 wt% active substance, BASF) were used as received. Butyl acrylate (BA, ≥99.0%, Aldrich), methyl methacrylate (MMA, ≥99.0%, Aldrich) and methacrylic acid (MAA, ≥99.0%, Aldrich) were distilled under vacuum prior to use. 2,2′-Azobis(2-methylpropionitrile) (AIBN, Fluka, 98%) was purified by recrystallization in methanol and dried under vacuum before use. Deionized water (DI water) (1 µS cm^{-1}) was obtained using a D8 ion exchange demineralizer from A2E Affinage de L'Eau.

5.2.2 Methods

Determination of the reactivity ratios. (Appendix Table 4-1 to Table 4-3, Figure A4-1 to Figure A4-4, Eq. A4-1 to Eq. A4-12) The solution copolymerizations of EDMA and MMA were carried out at 70°C in benzene-d_6 (1 mol L^{-1} with respect to benzene-d_6) to minimize any transfer reactions to solvent. The concentration of AIBN used was 2 wt% with respect to monomers and 1,4-BTMSB was used as the internal standard (5.5 mol% with respect to benzene) to determine monomer conversions by ^{1}H NMR analysis. The feed molar fractions of EDMA ([EDMA]/([EDMA]+[MMA])) were varied from 0.1 to 0.9. The reactivity ratios were determined using three different methods: the Kelen−Tüdös method,[33] nonlinear regression based on the method of the visualization of the sum of squared residual space proposed by van den Brink,[34] and nonlinear curve fitting using the Levenberg-Marquardt algorithm.[35]

Dynamic light scattering (DLS). (Appendix Table 4-4, Figure A4-5 to Figure A4-16) Particle size measurements were performed by dynamic light scattering on a Vasco 3 nanoparticle size analyzer supplied by Cordouan Technologies at 25°C using the cumulant model. Samples for DLS measurements were prepared by diluting one drop of latex with 5 mL of DI water. The laser power, time interval, and number of channels were adjusted for each sample to obtain a good autocorrelation function (ACF). The presented results are the average of five measurements.

Total solids content measurement (TSC). 250−500 mg of latex were placed on an aluminum pan loaded with 3−5 mg of MEHQ (inhibitor) and subsequently placed in an oven at 80°C for 24 h under vacuum at 5×10^{-2} mbar. The final weight was measured and the TSC calculated according to Eq. 5-1.

$$TSC(\%) = \frac{W_{dry\ latex} \times 100}{W_{latex}} \qquad \text{Eq. 5-1}$$

where W_{latex} is the weight of the latex (without inhibitor) and $W_{dry\ latex}$ is the final weight of the dried latex (without inhibitor).

Gel content measurements. The gel content of the polymers was measured by placing 500 mg of dried polymer in a 60 mL cellulose thimble and extracting it over 24 h by Soxhlet using 180 mL of THF, at 35°C and 100 mbar. The thimble was then recovered and washed with 10 mL of THF, then dried under the fume hood overnight and in a ventilated oven at 40°C and atmospheric pressure for 2−4 hours (till the weight was constant). The gel content was calculated according to Eq. 5-2below.

$$Gel\ content(\%) = \frac{W_{final\ solid} \times 100}{W_{initial\ solid}} \qquad \text{Eq. 5-2}$$

where $W_{initial\ solid}$ is the initial polymer weight and $W_{final\ solid}$ is the weight of the polymer remaining in the thimble.

Thermogravimetric analysis (TGA). (Appendix Table 4-7, Table 4-8, Figure A4-17 to Figure A4-18) Thermogravimetric analysis was performed on 5-10 mg samples on a TGA Q50 apparatus

from TA Instruments from 20°C to 580°C, in an aluminum pan, at a heating rate of 20°C min^{-1}, under nitrogen and air.

Differential scanning calorimetry (DSC). (Appendix Figure A4-19 to Figure A4-22) DSC measurements were performed on 10–15 mg samples, under a nitrogen atmosphere, with a Netzsch DSC 200 F3 instrument using the following heating/cooling cycle: first cooling ramp from room temperature (ca. 20°C) to –100°C at 20°C min^{-1}, isotherm plateau at −100°C for 10 min, first heating ramp from −100°C to 100°C at 20°C min^{-1}, second cooling stage from 100°C to −100°C at 20°C min^{-1}, isotherm plateau at −100°C for 10 min, second heating ramp from −100°C to 100°C at 20°C min^{-1}, third cooling stage from 100°C to −100°C at 20°C min^{-1}, isotherm plateau at −100°C for 10 min, third heating ramp from −100°C to 100°C, and last cooling stage from 100°C to room temperature (ca. 20°C). T_g values are given from the evaluation of the third heating ramp. Calibration of the instrument was performed with noble metals and checked with an indium sample.

Contact angle measurements. The hydrophobicity was determined using a contact angle system OCA20 coupled with a CCD-camera from Data Physics Instrument using the software SCA20 4.1. The measurements were made on 100 µm dried polymer films prepared by casting a latex with a bar coater at 200 µm on glass plates previously cleaned with acetone. Films were dried at 25°C for 24 h under an ambient atmosphere. Static contact angle measurements were done at room temperature by the sessile drop technique with deionized water.

Size exclusion chromatography (SEC). (Appendix Table 4-9, Figure A4-23) GPC from Agilent Technologies with its corresponding Agilent software, equipped with two PL1113-6300 ResiPore 300 × 7.5 mm columns (up to 500,000 g mol^{-1}) was used. The detector suite comprised of a 390-LC PL0390–0601 refractive index detector. The entire SEC-HPLC system was thermostated at 35°C. Calibration was performed with PMMA narrow standards. THF was used as the eluent at a flow rate of 1 mL min^{-1}. Typical sample concentration was 10 mg mL^{-1}.

Tack and peel measurements. Tack and peel measurements were done using a TA.XT*plus* from Stable Micro Systems equipped with a load cell of 50 kg. Films of 100 µm were prepared using a bar coater on poly(ethyleneterephtalate) (PET) sheets. Samples were dried at 25°C for 24 h. Then 19 mm wide strips were cut.

For the peel test (Appendix Figure A4-24 to Figure A4-28), the PET-supported adhesive was applied on a glass surface and a 2 kg hand roller was rolled three times on the strip. The glass plates were clamped vertically, and the PET-supported bent adhesive strip was clamped to the moving cell at 180°. The PET support was pulled at a constant speed of 5 mm min^{-1}, and the force necessary to pull out the paper was recorded.

For the tack measurements (Appendix Figure A4-29 to Figure A4-33), the PET-supported adhesive was folded and clamped in the moving cell of the apparatus. The specimen was put in contact with a glass plate previously cleaned with ethanol and acetone and then the loop was moved upward at 5 mm min^{-1}. The force required to peel off the loop was measured.

General procedure for emulsion polymerization. The emulsion polymerization design and conditions were inspired by literature.[16,36] It was carried out in a 200 mL double-walled jacketed glass reactor with a U-shaped glass stirring rod. A solution (S1) containing NaPS (0.31 g), $NaHCO_3$ (0.34 g) and DI water (4.72 g) was prepared. Butyl acrylate (BA), methyl methacrylate (MMA), methacrylic acid (MAA), ethoxy dihydroeugenyl methacrylate (EDMA), and *tert*-butyl mercaptan (as indicated in the formulations, Table 5-1) were weighed and mixed together. In all formulations, 15% of the total monomer mixture weight was separated and purged with argon for 30 min (S2). A monomer emulsion (S3) containing SDBS (0.24 g), DI water (13.43 g) and the rest of the monomers was prepared under vigorous agitation (500 rpm). When ethoxy eugenyl methacrylate (EEMA) was present in the formulation, it was only added to the S3 mixture. The rest of the surfactants (SDBS and Disponil A 3065) were introduced as an initial load in the reactor. The water was adjusted to target a TSC of 50%. After purging the reactor with argon for 30 min, S2 was introduced in the reactor under stirring at 200 rpm followed by 12% of S1 (at 80°C under stirring at 200 rpm) and counted as time 0 min. After 10 min of reaction, the continuous feeding of S3 and 76% of S1 started and fed separately over 3 h (under 200 rpm stirring, 80°C and argon flow). The remaining S1 (12%) was introduced as a shot at the end of the polymerization. The reaction was left under stirring at 200 rpm for 50 min at 80°C as a postpolymerization step.

Table 5-1. General radical aqueous emulsion polymerization recipe

Ingredient	Mass (g)	% wbm[a]
Butyl acrylate	45.00	87.00
MMA	0-6.21	0-12
EDMA	0-6.21	0-12
EEMA	0-0.52	0-1
Methacrylic acid	0.52	1.00
***Tert*-dodecyl mercaptan**	0.03	0.06
Sodium persulfate	0.31	0.60
Sodium bicarbonate	0.34	0.66
Disponil A 3065 (65% active substance)	1.12	2.17
SDBS	0.28	0.55
Water	Adjusted for TSC of 50%	Adjusted for TSC of 50%

[a] % wbm: weight fraction based on monomers.

5.3 Results and discussion

Homopolymerization of eugenol-derived methacrylates by aqueous emulsion polymerization using different radical initiators has been reported in Chapter 4.[37] It was demonstrated that EDMA (ethoxy dihydroeugenyl methacrylate) and EEMA (ethoxy eugenyl methacrylate) were readily polymerizable under aqueous emulsion polymerization conditions using different initiation systems without using special or high quantities of surfactants. In the present chapter, the copolymerization of EDMA, the eugenol-derived monomer without pendant double bonds, with BA, MMA, and MAA,

was studied. Moreover, EEMA, which contains an allyl group, was later introduced in the formulation in a small quantity to observe the effect of a biobased functional structural unit on the properties of the resulting acrylic latex. Both EDMA and EEMA are liquid at 25°C (EDMA m.p.:<0°C; EEMA m.p.:11°C, Scheme 5-1)[32] and are miscible in the monomer mixture with up to 87% wbm of butyl acrylate. Miscibility was observed between MMA, BA, MAA, and EDMA or EEMA.

Scheme 5-1. Eugenol-derived methacrylates

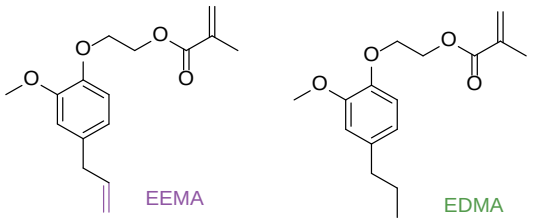

As part of this study, the reactivity ratios r_{EDMA} and r_{MMA} for the copolymerization of EDMA with MMA were determined in benzene-d_6 at 70°C. These reactivity ratios are very close to unity (Table 5-2), indicating that an almost ideal statistical copolymerization took place without a significant drift of monomer composition. Thus, EDMA behaves like MMA in radical copolymerization.

Table 5-2. Reactivity ratios of EDMA and MMA (solution copolymerization in benzene-d_6 at 70°C)

Reactivity ratios	Kelen-Tüdös	Nonlinear Least Squares[a]	Levenberg-Marquardt[b]
r_{EDMA}	1.08	0.95	1.06
r_{MMA}	0.98	1.02	1.19

[a] Refer to Annexes for joint confidence intervals.
[b] Refer to Annexes for standard errors.

To begin the investigation on the emulsion polymerization, an initial formulation containing only oil-derived monomers (BA, MMA, and MAA) was designed to obtain a theoretical T_g value of −30°C, suitable for adhesive applications. Using the Fox equation[38] and the T_g of the respective homopolymers (*i.e.,* poly(BA) T_g = –43°C,[39] poly(MMA) T_g = 105°C,[39] poly(MAA) T_g =228°C),[40] the target latex formulation shown in Table 5-1 was designed (run F1 in Table 5-33). MMA was then replaced by EDMA and EEMA (T_g of poly(EDMA) = 26°C, T_g of poly(EEMA) = 48°C)[37] and the emulsion polymerization formulation produced copolymers with T_gs close to the nonbiobased one. All formulations are described in Table 5-33.

Table 5-3. Different latex formulations composition

Run	Monomer formulation (% wbm[a])	Calculated T_g
F1	BA:MMA:MAA (87:12:1)	–30°C
F2	BA:MMA:EDMA:MAA (87:6:6:1)	–33°C
F3	BA:EDMA:MAA (87:12:1)	–35°C
F4	BA:EDMA:EEMA:MAA (87:11:1:1)	–35°C

[a]%wbm: weight fraction based on monomers.

All latexes were synthesized through a semibatch process.[16] A period of pre-polymerization of 10 min was given between the first initiator shot (addition of 12% of the total persulfate solution weight to promote nucleation) and the continuous addition of the rest of the monomers and initiator (for particle growth).[41] At the end of the pre-emulsion mixture (S3) and initiator solution addition (3 h), a final shot of 12% of the total initiator and buffer was added to the latex to promote full conversion. Particle size, pH, gel content, solids content, number average molar mass, and decomposition temperature under air and nitrogen are indicated in Table 5-4.

The first objective was to confirm that the replacing of a monomer that increases the T_g, such as MMA, with a eugenol-derived methacrylate in an emulsion polymerization formulation can be done while preserving acceptable properties for the resulting adhesives. As mentioned before, EDMA, the eugenol-derived monomer without a pendant double bond, was selected to avoid cross-linking and gel formation. EDMA has been proven to homopolymerize readily under aqueous emulsion polymerization conditions with different initiator systems and conditions such as potassium persulfate (KPS) at 70 C, 4,4-azobis(4-cyanovaleric acid) (ACVA) at 70°C and a redox system sodium metabisulfite/potassium persulfate (SMB/KPS) at 40°C (Chapter 4).[37] EDMA was introduced gradually into the formulation, starting with half of the total MMA weight fraction, reaching 6% wbm (run F2 in Table 5-33), then 100% of the MMA weight fraction, increasing to 12% wbm (run F3 in Table 5-33). In a second study, a small quantity of EEMA (possessing a pendant allyl group, Scheme 5-1) was also included in the formulation (1% wbm of EDMA was replaced with EEMA). This experiment, which corresponds to run F4 in Table 3, casts some light on the effect of this functional monomer on the polymer properties.

The instantaneous monomer conversions and the cumulative monomer conversions (by gravimetry) are reported in Figure 5-3 and Figure 5-4 (Appendix Tables A4-5 and Table A4-6, Eq. A4-13 and Eq. A4-14), respectively. All latexes exhibited instantaneous monomer conversions of above 83%, as expected for starved-feed conditions[42].

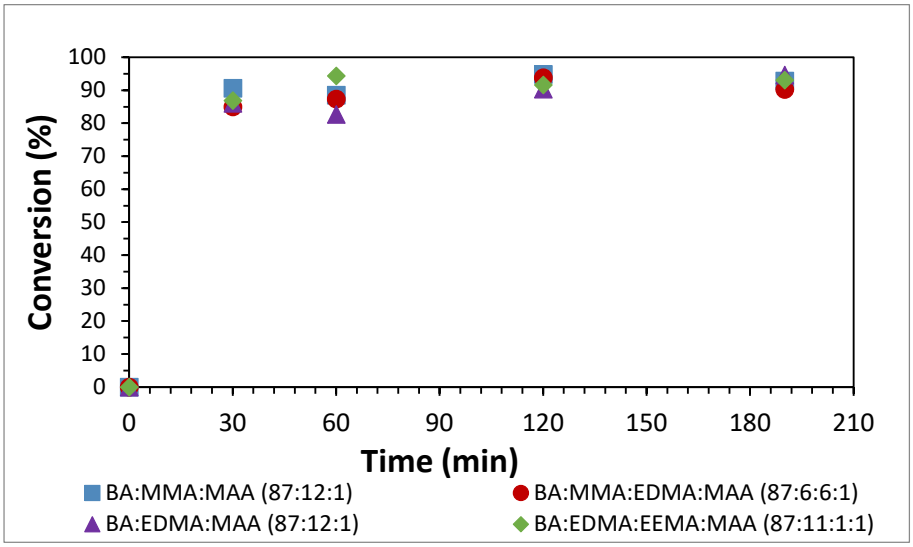

Figure 5-3. Instantaneous monomer conversions for semibatch aqueous emulsion copolymerization initiated by NaPS at 80°C of the different latex formulations.

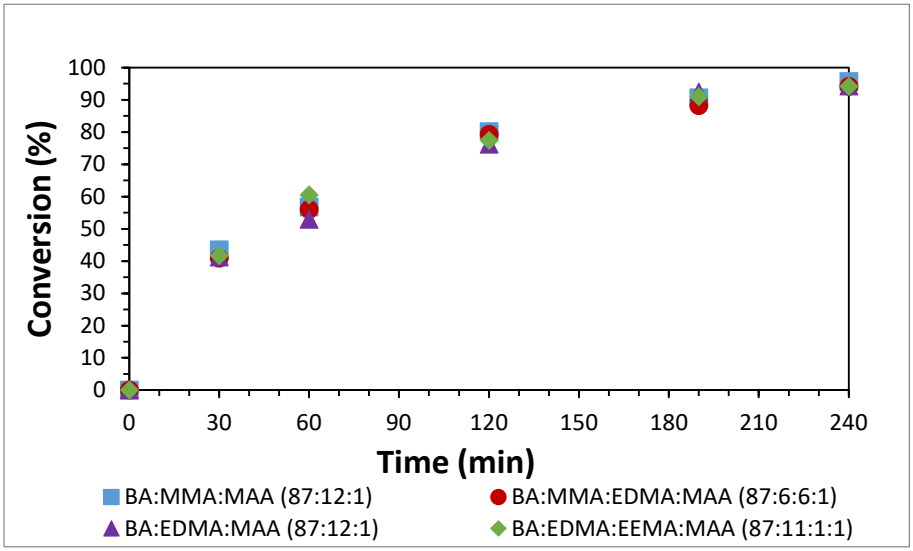

Figure 5-4. Cumulative monomer conversions for semibatch aqueous emulsion copolymerization initiated by NaPS at 80°C of the different latex formulations.

Table 5-4. Latex characterizations

Formulation	F1	F2	F3	F4
Composition in % wbm[a]	BA:MMA:MAA (87:12:1)	BA:MMA:EDMA: MAA (87:6:6:1)	BA:EDMA: MAA (87:12:1)	BA:EDMA:EEMA MAA (87:11:1:1)
pH	7.6	7.3	7.4	7.8
D_i (nm)[b]	158	159	173	178
TSC (%)[c]	50.9	49.8	50.0	49.8
Gel content (%)	64	68	69	92
$T_{d,5\%}$ Air (°C)	320	324	321	313
$T_{d,5\%}$ N_2 (°C)	335	320	340	333
M_n (g.mol^{-1})	51,700	36,100	31,200	20,300
Đ=M_w/M_n	5.58	3.27	2.78	2.55
T_g (°C)	–26	–28	–31	–32
Contact angle, DI Water (°)	98.6±1.9	103.2±2.9	107.2±1.7	100.4±0.9

[a] % wbm: weight fraction based on monomer.

[b] D_i: intensity-average particle diameter.

[c] TSC (%): total solids content by gravimetry.

The pH of the final latex did not change significantly with the addition of the biobased monomer (Table 5-4). This was expected, as a buffer was used to avoid the acidification produced by NaPS decomposition,[43] which could lead to colloidal instability or coloration of the latexes.

Total solids contents higher than 49% were reached in all cases without using seeding techniques or high amounts of surfactants (Table 5-4). The latex particle size was only slightly increased (15 nm

in F3 and 20 nm in F4) by the introduction of the biobased monomers in comparison to F1 (158 nm), but no loss of colloidal stability was observed.

Gel content was observed in all the formulations. The presence of butyl acrylate in the formulation enables intramolecular and intermolecular chain transfers to polymer. In both cases, tertiary radicals will be produced, which exhibit lower reactivity in comparison with secondary radicals. In the case of intramolecular chain transfer to polymer, usually known as backbiting, short chain branches would be obtained, whereas intermolecular chain transfer to polymer yields long chain branches. Subsequent termination by combination, after long chain branching, will produce a cross-linked network, giving rise to gel formation.[44–46] *tert*-Dodecyl mercaptan was added as a chain transfer agent to decrease the degree of cross-linking in the resulting polymers. If some gel content is desirable in adhesive formulations to increase shear strength, the content should not be so high that it affects the adhesive properties.[16] In the present experiments, gel content increased moderately with increasing EDMA biobased monomer fraction in the latex formulation (Table 5-4). However, a substantial increase in gel content was measured when EEMA was included in the formulation. The replacement of 1% wbm of EDMA in F3 by 1% wbm of EEMA to produce F4 resulted in an increase in gel content from 69% to 92%. The reactivity of a C−H bond toward hydrogen abstraction follows the order: allyl~benzyl>tertiary>secondary>primary>aryl~vinyl.[47,48] In the particular case of bis-allylic hydrogens, their dissociation energy is approximately 10 kcal mol^{-1} lower than allylic hydrogen,[49] making them more labile. EEMA abstractable hydrogens can be considered as bis-allylic due to their position with respect to the aromatic ring and the allylic double bond. Thus, more hydrogen abstraction is expected in the case of EEMA than in the case of EDMA. This has been observed in previous works related to emulsion homopolymerization reaction, as the formation of cross-linked polymers and slower kinetics of polymerization (degradative chain transfer) were observed in the case of poly(EEMA), while poly(EDMA) remained soluble (Chapter 4).[37] The F4 formulation, shows that even at very low concentrations, EEMA acts as an efficient cross-linking agent *via* side reactions involving its allyl group (cross-propagation with BA and transfer to polymer by hydrogen abstraction, followed by termination by combination).[32,37] The molar mass and dispersity of the THF-soluble fraction of the polymer decreased with increasing biobased content. This could be due to the abstraction of the benzylic hydrogens present in EDMA, by butyl acrylate propagating radicals, which are more prone to abstract hydrogens, leading to cross-linking and gelation. Thus, only the low molar mass fraction would stay soluble, artificially decreasing the molar masses.

The different contents of eugenol-derived monomers did not affect the thermal stability of the latexes as $T_{d,5\%}$ (temperature of 5% weight loss) occurred between 320°C and 340°C under nitrogen, and 313°C and 324°C under air for all the polymers synthesized and did not follow any particular tendency with the biobased monomer content (Table 5-4).

T_g values for all formulations ranged between −26°C and −32°C (Table 5-4). The expected values according to the Fox equation for the formulations were −30°C for F1, −33°C for F2, and −35°C for

F3 and F4 (Table 5-33). All the formulations showed a slightly higher T_g value, most probably due to some degree of cross-linking.[38]

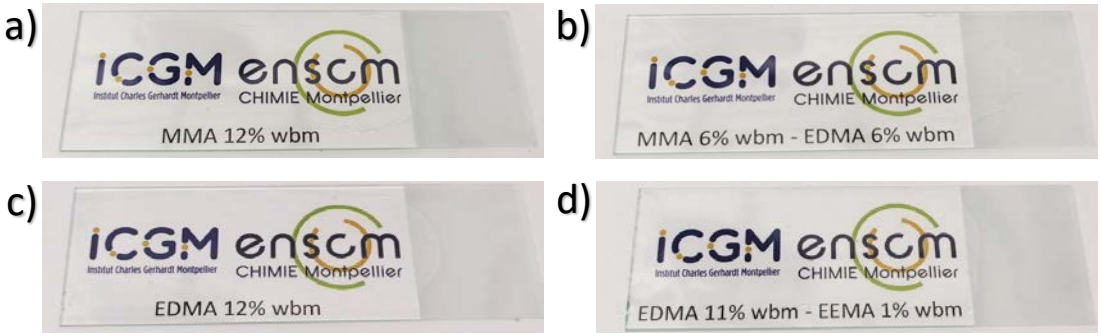

Figure 5-5. Polymer films prepared from latex formulations a) F1, b) F2, c) F3, and d) F4.

Latexes were dried at 25°C for 24 h and transparent films were obtained at the end of the drying period (Figure 5-5). Static water contact angle measurements showed an increase in hydrophobicity when MMA was replaced with eugenol-derived methacrylate, as the highest contact angle was reported for formulation F3 (107.2°) with 12% wbm of EDMA and the lowest for F1 (98.6°) with 12% wbm of MMA. The hydrophobic character of the eugenol-derived monomers is responsible for this effect. In the particular case of F4 with 11% wbm of EDMA and 1% wbm of EEMA, a reduction in the contact angle (100.4°) was observed in spite of the biobased monomer content. Possibly, the larger gel content in the case of F4 made the film formation less complete, leaving some hydrophilic channels and leading to a film with a less hydrophobic character (Table 5-4). Higher hydrophobicity is an advantageous characteristic, as it reduces the wetting ability or hydration of the surface of the adhesive films.

Peel and tack tests were executed to assess the adhesive properties of the latexes (Table 5-5). A reduction in the peel force was observed when MMA was replaced with EDMA in the latex formulations. However, the value observed for the MMA-free latex (F3), 3.18 N cm^{-1}, was higher than that of latex F2 (containing MMA and EDMA), 2.49 N cm^{-1}. The addition of EEMA (latex F4) resulted in a drastic reduction of the peel force, in which the value dropped to 0.35 N cm^{-1} (Figure 5-6). This was expected due to the high gel content in F4 which decreases the adhesive performance of the polymer.[50] Commercial product Scotch Magic Tape was also assessed for comparison. Although peel force values of F2 and F3 were lower than the peel force value of F1, they were higher than that of commercial Magic Tape (2.00 N cm^{-1}).[24] In the case of the loop tack tests, the reduction of force was also observed as the amount of biobased monomer increased (6.39 N for F2 compared to 9.35 N for F1), with again a significant drop for the formulation containing EEMA, F4 (2.75 N), due to the higher gel content. However, F2 and F3 had loop tack values of 6.39 N and 6.26 N respectively, which are higher than that measured for the commercial formulation Scotch Magic Tape (4.81 N; Figure 5-7). Thus, the overall performance of the latexes is comparable to current commercial products, opening up the possibility for these two partially biobased formulations, F2 and F3, to be used as part of commercial adhesives.

Table 5-5. Adhesive properties of the films prepared from different latex formulations

Formulation		Peel average value (N/cm)[a]		Peel maximum value (N/cm)[a]		Loop Tack (N)	
		Value	Std[b]	Value	Std[b]	Value	Std[b]
BA:MMA:MAA (87:12:1)	F1	3.76	0.14	4.34	0.19	9.35	0.44
BA:MMA:EDMA: MAA (87:6:6:1)	F2	2.49	0.10	3.08	0.12	6.39	1.34
BA:EDMA: MAA (87:12:1)	F3	3.18	0.08	3.54	0.04	6.26	0.00
BA:EDMA:EEMA MAA (87:11:1:1)	F4	0.35	ND	0.45	ND	2.75	0.17
Scotch Magic™ Tape		2.00	0.061	2.31	0.09	4.81	0.03

[a] The peel force is normalized by the tape width 1.9 cm.

[b] Std: standard deviation.

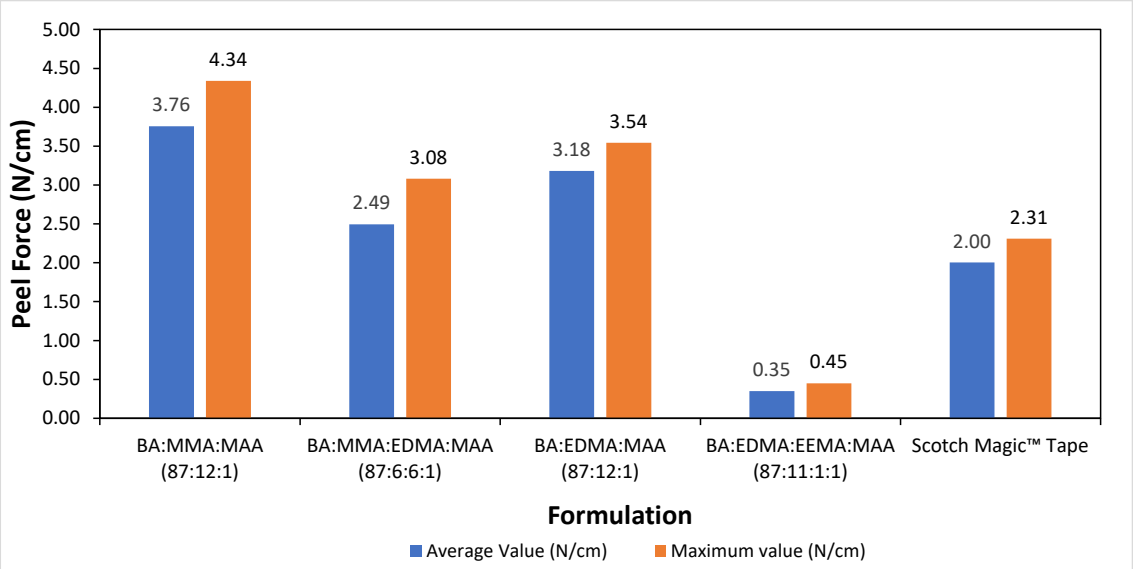

Figure 5-6. Peel averages and maximum forces of the films prepared from different latex formulations (the peel force is normalized by the tape width 1.9 cm).

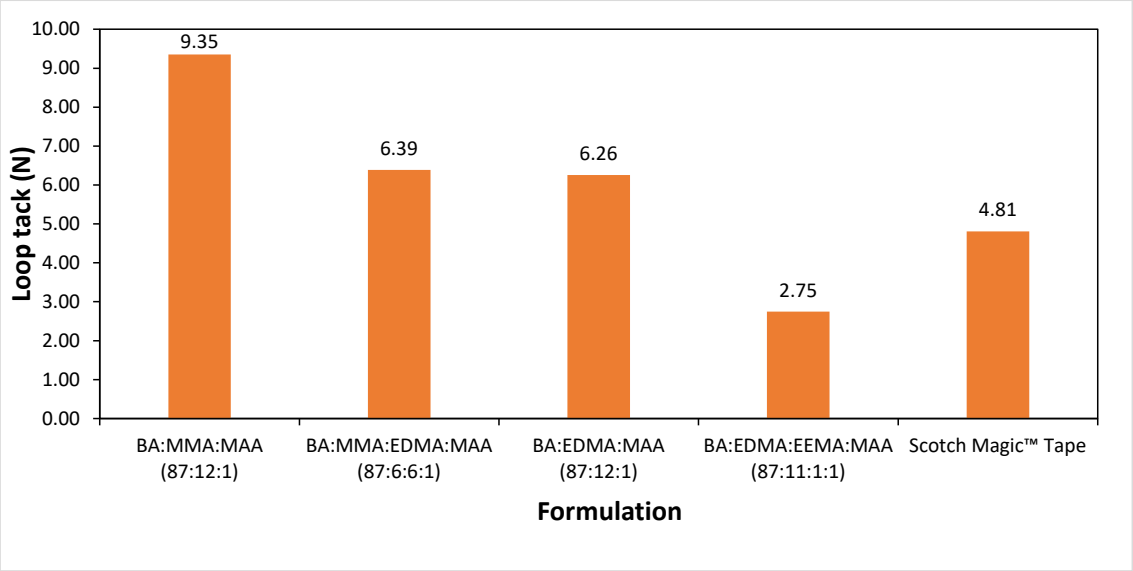

Figure 5-7. Tack forces of the films prepared from different latex formulations.

5.4 Conclusions

Latexes containing up to 12% wbm of ethoxy dihydroeugenyl methacrylate (EDMA) and 50% total solids content, suitable for application as adhesives, were successfully prepared. The latexes were synthesized using a semibatch process, which is suitable for scale-up. All formulations provided latexes with good colloidal stability and with particle sizes ranging from 159 to 178 nm in diameter. The copolymers did not show significant weight loss up to 324°C under air and their T_g ranged between −28°C and −32°C, in good agreement with the values estimated with the Fox equation. The adhesive properties of the polymers were tested and the peel and tack forces were shown to be superior to those measured for a commercial product. Thus, the formulations containing EDMA could be suitable for adhesive applications. Fine-tuning of the partial replacement of petroleum-based monomers with monomers derived from biobased building blocks is a first but essential approach in paving the way to more sustainable and greener adhesives.

5.5 References

(1) ASTM. ASTM D907-15 Standard Terminology of Adhesives. 2015, pp 1–13.

(2) Roberge, S.; Dubé, M. A. Emulsion-Based Pressure Sensitive Adhesives from Conjugated Linoleic Acid/Styrene/Butyl Acrylate Terpolymers. *Int. J. Adhes. Adhes.* **2016**, *70*, 17.

(3) Pressure Sensitive Adhesives Market Size By Technology (Water Based, Solvent Based, Hot-Melt, UV-Cured), By Product (Rubber-Based, Acrylic, Silicone), By Application (Tapes, Labels, Graphics, Films & Laminates), By Sector (Food & Beverage, Packaging, Elec https://www.gminsights.com/industry-analysis/pressure-sensitive-adhesives-market (accessed Jun 28, 2020).

(4) Moreno, M.; Goikoetxea, M.; Barandiaran, M. J. Biobased-Waterborne Homopolymers from Oleic Acid Derivatives. *J. Polym. Sci. Part A Polym. Chem.* **2012**, *50*, 4628.

(5) Maaßen, W.; Meier, M. A. R.; Willenbacher, N.; Maassen, W.; Meier, M. A. R.; Willenbacher, N. International Journal of Adhesion & Adhesives Unique Adhesive Properties of Pressure Sensitive Adhesives from Plant Oils. *Int. J. Adhes. Adhes.* **2016**, *64*, 65.

(6) Laurentino, L. S.; Medeiros, A. M. M. S.; Machado, F.; Costa, C.; Araújo, P. H. H.; Sayer, C. Synthesis of a Biobased Monomer Derived from Castor Oil and Copolymerization in Aqueous Medium. *Chem. Eng. Res. Des.* **2018**, *137*, 213.

(7) Wool, R. P.; Bunker, S. P. Pressure Sensitive Adhesives from Plant Oils. 6,646,033 B2, 2003.

(8) Bunker, S.; Staller, C.; Willenbacher, N.; Wool, R. Miniemulsion Polymerization of Acrylated Methyl Oleate for Pressure Sensitive Adhesives. *Int. J. Adhes. Adhes.* **2003**, *23*, 29.

(9) Demchuk, Z.; Kohut, A.; Voronov, S.; Voronov, A. Versatile Platform for Controlling Properties of Plant Oil-Based Latex Polymer Networks. *ACS Sustain. Chem. Eng.* **2018**, *6*, 2780.

(10) Moreno, M.; Lampard, C.; Williams, N.; Lago, E.; Emmett, S.; Goikoetxea, M.; Barandiaran, M. J. Eco-Paints from Bio-Based Fatty Acid Derivative Latexes. *Prog. Org. Coatings* **2015**, *81*, 101.

(11) Badía, A.; Movellan, J.; Barandiaran, M. J.; Leiza, J. R. High Biobased Content Latexes for Development of Sustainable Pressure Sensitive Adhesives. *Ind. Eng. Chem. Res.* **2018**, *57*, 14509.

(12) Noppalit, S.; Simula, A.; Billon, L.; Asua, J. M. Paving the Way to Sustainable Waterborne Pressure-Sensitive Adhesives Using Terpene-Based Triblock Copolymers. *ACS Sustain. Chem. Eng.* **2019**, *7*, 17990.

(13) Cummings, S.; Cunningham, M.; Dubé, M. A. The Use of Amylose-Rich Starch Nanoparticles in Emulsion Polymerization. *J. Appl. Polym. Sci.* **2018**, *135*, 46485.

(14) Zhang, Y.; Cunningham, M. F.; Smeets, N. M. B.; Dubé, M. A. Starch Nanoparticle Incorporation in Latex-Based Adhesives. *Eur. Polym. J.* **2018**, *106*, 128.

(15) Cummings, S.; Zhang, Y.; Smeets, N.; Cunningham, M.; Dubé, M. On the Use of Starch in Emulsion Polymerizations. *Processes* **2019**, *7*, 140.

(16) Jovanović, R.; Dubé, M. A. Emulsion-Base d Pressure-Sensitive Adhesives: A Review. *J.*

Macromol. Sci. Part C Polym. Rev. **2004**, *44*, 1.

(17) Baek, S.-S. S.; Hwang, S.-H. H. Preparation and Adhesion Performance of Transparent Acrylic Pressure-Sensitive Adhesives Containing Menthyl Acrylate. *Polym. Bull.* **2016**, *73*, 687.

(18) Asua, J. M. Challenges for Industrialization of Miniemulsion Polymerization. *Prog. Polym. Sci.* **2014**, *39*, 1797.

(19) Kingsley, K.; Shevchuk, O.; Demchuk, Z.; Voronov, S.; Voronov, A. The Features of Emulsion Copolymerization for Plant Oil-Based Vinyl Monomers and Styrene. *Ind. Crops Prod.* **2017**, *109*, 274.

(20) Delatte, D.; Kaya, E.; Kolibal, L. G.; Mendon, S. K.; Rawlins, J. W.; Thames, S. F. Synthesis and Characterization of a Soybean Oil-Based Macromonomer. *J. Appl. Polym. Sci.* **2014**, *131*, 40249.

(21) Zhang, L.; Cao, Y.; Wang, L.; Shao, L.; Bai, Y. Polyacrylate Emulsion Containing IBOMA for Removable Pressure Sensitive Adhesives. *J. Appl. Polym. Sci.* **2016**, *133*, 42886.

(22) Ren, S.; Trevino, E.; Dubé, M. A. Copolymerization of Limonene with n -Butyl Acrylate. *Macromol. React. Eng.* **2015**, *9*, 339.

(23) Bloembergen, S. US 6,242,593 B1, Environmentally Friendly Sugar-Based Vinyl Monomer Useful in Repulpable Adhesives and Other Applications, 2001.

(24) Wang, S.; Shuai, L.; Saha, B.; Vlachos, D. G.; Epps, T. H. From Tree to Tape: Direct Synthesis of Pressure Sensitive Adhesives from Depolymerized Raw Lignocellulosic Biomass. *ACS Cent. Sci.* **2018**, *4*, 701.

(25) ASTM. Standard Test Method for Peel Adhesion of Pressure-Sensitive Tape. **2003**.

(26) ASTM. Standard Test Methods for Loop Tack. **2003**, *15*, 1.

(27) ASTM. Standard Test Method for Pressure-Sensitive Tack of Adhesives Using an Inverted Probe Machine. **2001**, *03*, 3.

(28) ASTM. Standard Test Method for Tack of Pressure-Sensitive Adhesives by Rolling Ball. **1999**, *94*, 3121.

(29) ASTM. Standard Test Methods for Shear Adhesion of Pressure-Sensitive Tapes. *Am. Sociaty Test. Mater.* **2002**, *01*, 3.

(30) Pandey, V.; Fleury, A.; Villey, R.; Creton, C.; Ciccotti, M. Linking Peel and Tack Performances of Pressure Sensitive Adhesives. *Soft Matter* **2020**, *16*, 3267.

(31) Chang, E. P. Viscoelastic Windows of Pressure-Sensitive Adhesives. *J. Adhes.* **1991**, *34*, 189.

(32) Molina-Gutiérrez, S.; Manseri, A.; Ladmiral, V.; Bongiovanni, R.; Caillol, S.; Lacroix-Desmazes, P. Eugenol: A Promising Building Block for Synthesis of Radically Polymerizable Monomers. *Macromol. Chem. Phys.* **2019**, *220*, 1900179.

(33) Kelen, T.; Tüdös, F. Analysis of the Linear Methods for Determining Copolymerization Reactivity Ratios. I. A New Improved Linear Graphic Method. *J. Macromol. Sci. Part A - Chem.* **1975**, *9*, 1.

(34) Van Den Brink, M.; Van Herk, A. M.; German, A. L. Nonlinear Regression by Visualization

of the Sum of Residual Space Applied to the Integrated Copolymerization Equation with Errors in All Variables. I. Introduction of the Model, Simulations and Design of Experiments. *J. Polym. Sci. Part A Polym. Chem.* **1999**, *37*, 3793.

(35) Moré, J. J. The Levenberg-Marquardt Algorithm: Implementation and Theory; 1978; pp 105–116.

(36) Mishra, S.; Singh, J.; Choudhary, V. Synthesis and Characterization of Butyl Acrylate/Methyl Methacrylate/Glycidyl Methacrylate Latexes. *J. Appl. Polym. Sci.* **2010**, *115*, 549.

(37) Molina-Gutiérrez, S.; Ladmiral, V.; Bongiovanni, R.; Caillol, S.; Lacroix-Desmazes, P. Emulsion Polymerization of Dihydroeugenol-, Eugenol-, and Isoeugenol-Derived Methacrylates. *Ind. Eng. Chem. Res.* **2019**, *58*, 21155.

(38) Fox, T. G.; Loshaek, S. Influence of Molecular Weight and Degree of Crosslinking on the Specific Volume and Glass Temperature of Polymers. *J. Polym. Sci.* **1955**, *15*, 371.

(39) Penzel, E.; Rieger, J.; Schneider, H. A. The Glass Transition Temperature of Random Copolymers: 1. Experimental Data and the Gordon-Taylor Equation. *Polymer (Guildf).* **1997**, *38*, 325.

(40) Jones, J. A.; Novo, N.; Flagler, K.; Pagnucco, C. D.; Carew, S.; Cheong, C.; Kong, X. Z.; Burke, N. A. D.; Stöver, H. D. H. Thermoresponsive Copolymers of Methacrylic Acid and Poly(Ethylene Glycol) Methyl Ether Methacrylate. *J. Polym. Sci. Part A Polym. Chem.* **2005**, *43*, 6095.

(41) Li, B.; Brooks, B. W. Semi-Batch Processes for Emulsion Polymerisation. *Polym. Int.* **1992**, *29*, 41.

(42) Van Herk, A. M. *Chemistry and Technology of Emulsion Polymerisation*; van Herk, A. M., Ed.; John Wiley & Sons Ltd: Oxford, UK, 2013.

(43) Santos, A. M.; Vindevoghel, P.; Graillat, C.; Guyot, A.; Guillot, J. Study of the Thermal Decomposition of Potassium Persulfate by Potentiometry and Capillary Electrophoresis. *J. Polym. Sci. Part A Polym. Chem.* **1996**, *34*, 1271.

(44) Britton, D. J.; Lovell, P. A.; Heatley, F.; Venkatesh, R. Chain Transfer to Polymer in Emulsion Copolymerizations. *Macromol. Symp.* **2001**, *175*, 95.

(45) Chauvet, J.; Asua, J. M.; Leiza, J. R. Independent Control of Sol Molar Mass and Gel Content in Acrylate Polymer/Latexes. *Polymer (Guildf).* **2005**, *46*, 9555.

(46) González, I.; Leiza, J. R.; Asua, J. M. Exploring the Limits of Branching and Gel Content in the Emulsion Polymerization of n -BA. *Macromolecules* **2006**, *39*, 5015.

(47) Carey, F. A.; Sundberg, R. J. *Advanced Organic Chemistry Part A: Structure and Mechanisms*, 5º Ed.; Springer, Ed.; New York, 2008.

(48) Zhou, C.-W.; Simmie, J. M.; Somers, K. P.; Goldsmith, C. F.; Curran, H. J. Chemical Kinetics of Hydrogen Atom Abstraction from Allylic Sites by 3 O 2 ; Implications for Combustion Modeling and Simulation. *J. Phys. Chem. A* **2017**, *121*, 1890.

(49) Porter, N. A.; Caldwell, S. E.; Mills, K. A. Mechanisms of Free Radical Oxidation of Unsaturated Lipids. *Lipids* **1995**, *30*, 277.

(50) Lee, J.-H.; Lee, T.-H.; Shim, K.-S.; Park, J.-W.; Kim, H.-J.; Kim, Y.; Jung, S. Effect of

Crosslinking Density on Adhesion Performance and Flexibility Properties of Acrylic Pressure Sensitive Adhesives for Flexible Display Applications. *Int. J. Adhes. Adhes.* **2017**, *74*, 137.

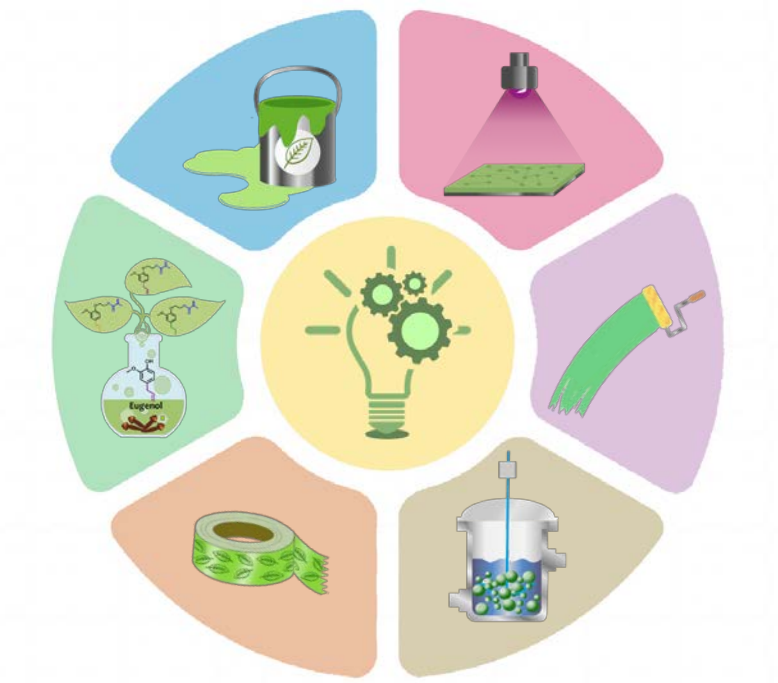

CHAPTER SIX

Conclusions and Perspectives

Table of contents

Chapter 6: Conclusions and Perspectives

6.1 Conclusions

Environmental concerns and stringent regulations have resulted in the development of a new field of chemistry, “Green Chemistry”, aiming for sustainable chemical syntheses and processes. The twelve principles of Green Chemistry[1] and the twelve principles of Green Engineering[2] have given guidelines and strategies to achieve such sustainability.[3] In 2018, the world plastic production reached 359 million tonnes. Around 4% of the world oil and gas production is used as a feedstock for plastics (while 3-4% is used as energy for their manufacture).[4] Thus, the use of renewable sources to replace fossil sources has become a priority. These renewable feedstocks should be widely available and should not interfere with food supply. Certainly, one of the immediate goals is the production of monomers and polymers that can mimic the properties of their petroleum counterparts. Thus, one of the strategies to pursue this goal is to synthesize already existing monomers (normally obtained from oil, such as ethylene[5]) from renewable sources. However, the design and synthesis of novel monomers should be explored as materials with new properties and applications can come to light from this research. Moreover, to provide a true green solution, environmentally friendly polymerization processes should also be employed.

For the previously mentioned reasons, the objective of this research work was to synthesize and characterize biobased monomers from renewable resources and then polymerize them through environmentally friendly processes such as aqueous emulsion, and photoinduced polymerization to produce polymers suitable for coatings and adhesives applications. Indeed, some coatings and adhesives are not destined for easy degradation and recycling,[6,7] thus the use of biobased monomers to produce them can render these materials more sustainable.

Radical polymerization was selected as the main polymerization mechanism to be used in the present work. Most biobased building blocks require the introduction of functional groups readily reactive under radical polymerization conditions. These modifications need to be done in a cost- and atom-efficient way and using facile synthesis with a straightforward purification to comply with green chemistry principles. The bibliographic research presented in Chapter 1 revealed that natural phenols had not been widely investigated in radical polymerization.[8] The presence of the aromatic ring can give interesting properties to the polymers in terms of high thermal stability and mechanical strength. Thus, eugenol, isoeugenol and dihydroeugenol, natural phenols extracted from clove oil but which can also be derived from lignin, were selected as biobased building blocks and functionalized to obtain monomers that react through radical mechanisms. These new monomers can then be copolymerized bringing interesting properties to the polymers by means of their aromatic ring. Moreover, these molecules were selected to compare the reactivity of their pendant double bonds (or lack of it) during radical polymerization in different processes (solution, bulk, emulsion polymerization). Additionally, the presence of pendant double bonds after polymerization allows the synthesis of reactive polymers (further reactions through the pendant double bonds).

The syntheses of nine biobased eugenol-derived monomers (**eight novel molecules**) were successfully established:[9]

- Ethoxy eugenyl methacrylate (EEMA)
- **Ethoxy isoeugenyl methacrylate (EIMA)**
- **Ethoxy dihydroeugenyl methacrylate (EDMA)**
- **Ethoxy eugenyl acrylate (EEA)**
- **Ethoxy isoeugenyl acrylate (EIA)**
- **Ethoxy dihydroeugenyl acrylate (EDA)**
- **Epoxy EEMA**
- **Epoxy EIMA**
- **EEMA carbonate**

The functionalization of the biobased building blocks was performed using non-biobased sources. Nevertheless, acrylic acid[10,11] and more recently, methacrylic acid[12,13] can be obtained from renewable sources. The valorisation of monomers through different applications (such as coatings and adhesives) will encourage their synthesis optimization.

The solution homopolymerization (21% w/w of monomer content in toluene) of the methacrylates and acrylates eugenol-derived monomers was done as well as the characterization of the obtained polymers.

All polymerizations reached conversions above 84% in the case of methacrylates; and no gel formation was found. In the case of acrylates, low conversion was obtained for EEA, whereas EIA polymerization resulted in gel formation. The polymers exhibited T_g between 10°C and 40°C. EEMA and EIMA exhibited lower rates of polymerization in comparison to EDMA, as well as EEA and EIA in comparison to EDA. These lower polymerization rates were probably a result of degradative chain transfer reactions (hydrogen abstraction of allylic protons, leading to poorly reactive highly stabilized radical) and cross-propagation (on the propenyl double bonds). Considering both the decrease of the polymerization rate and the production of branched polymers, the extent of the secondary reactions taking place on the allylic and propenyl moieties follows the decreasing order: EIA>>EEA>EEMA>EIMA. Nevertheless, residual allylic and propenyl double bonds remained in the poly(EEMA) and poly(EIMA) polymers which are thus functional polymers. Autoxidation was observed in dried polymers which could hinder their further functionalization or controlled crosslinking. Further studies on the autoxidation of the polymers should be envisaged.

Afterwards, photoinduced polymerization of eugenol-derived methacrylates was studied to assess the possibility to produce films in solvent-free conditions. The photoinduced polymerization of EDMA, EEMA and EIMA was carried out under different conditions:[14]

- In the absence of photoinitiator and with two different Norrish Type I photoinitiators (Darocur 1173 and Irgacure 819)
- Under air or without air (laminated).

- Irradiated from 240 to 600 nm and only at 365 nm (using a filter).

All three monomers showed self-initiation without photoinitiator when irradiated at wavelengths from 240 to 600 nm in the presence or absence of air. In the presence of oxygen with or without PI, peroxides formation and their photolysis resulted in second polymerization regimes, only when irradiated at wavelengths from 240 to 400 nm.[15] Secondary reactions involving allylic and propenyl groups were observed under all conditions, although higher reactivity was shown in the presence of air. Propenyl double bonds (PDBs) were shown to be predominantly polymerized via cross-propagation reactions while allyl double bonds (ADBs) were mainly consumed under air via hydrogen abstraction and hydroperoxides formation.

EDMA reached the highest conversions only in the absence of air and with the use of PI, revealing that peroxide formation is an important pathway to reinitiate the polymerization in the cases of EEMA and EIMA.

When self-initiation and peroxides formation was prevented (use of PI, air protection and 365 nm pass-band filter), the polymerization rate followed the order EDMA > EEMA > EIMA. Secondary reactions of EEMA and EIMA were responsible for the reduction in polymerization rate.

The successful photoinduced polymerization of the eugenol-derived methacrylates makes these monomers good candidates for applications in coatings and in dentistry for example. Moreover, this technique allows solvent free conditions and fast polymerization reactions.

After studying the behaviour of eugenol-derived methacrylates in radical solution thermal polymerization (Chapter 2) and bulk photopolymerization (Chapter 3), aqueous emulsion polymerization was attempted. Three different initiation systems (potassium persulfate (KPS) at 70°C, 4,4-azobis(4-cyanovaleric acid) (ACVA) at 70°C and $Na_2S_2O_5$/KPS at 40°C) were tested in aqueous emulsion homopolymerization.[16] Eugenol-derived monomers were sufficiently soluble in water to execute *ab-initio* emulsion polymerization. Stable latexes of particle diameters of about 45-71 nm were obtained without the use of large quantities of surfactants or of low CMC surfactants as is sometimes required for very hydrophobic monomers.[17]

Emulsion polymerization with KPS at 70°C yielded a colloidally stable latex only with EDMA, while ACVA, also at 70°C, resulted in stable latexes for the three monomers. Moreover, a decrease in the T_g of poly(EEMA) while using ACVA (T_g= 23°C) and $Na_2S_2O_5$/KPS (T_g= 27°C) in comparison to poly(EEMA) obtained using KPS as the initiator (T_g = 48°C) was observed. This indicates that the initiator affects the extent of secondary reactions leading to crosslinking (higher crosslinking density by using KPS). During redox emulsion polymerization the rate of polymerization followed the order EDMA>EIMA>EEMA, possibly due to hydrogen abstraction as secondary reaction, leading to a very stable allylic radical not prone to propagate (degradative chain transfer). The lower T_g values measured for poly(EEMA) compared to poly(EIMA) suggested that the main secondary reaction was cross-propagation in the case of EIMA (leading to highly cross-linked polymers), and degradative chain transfer reaction for EEMA (leading to less crosslinked polymers), as observed in Chapter 2.

In a preliminary trial, a stable poly(EDMA-*co*-BA) copolymer latex at 30 % solids content (with T_g of -23°C), was successfully synthesized. These results encouraged us to investigate the synthesis of copolymers of a eugenol-derived monomer with monomers commonly used in commercial formulation of adhesives to increase the biobased content of such formulations (Chapter 5).

Latexes containing up to 12% wbm of ethoxy dihydroeugenyl methacrylate (EDMA) and 50% total solids content, suitable for application as adhesives, were successfully prepared.[18] The latexes were synthesized using a semibatch process, and all formulations provided latexes with good colloidal stability and with particle diameters ranging from 159 to 178 nm. The copolymers remained stable up to 324°C under air and their T_g ranged between −28°C and −32°C. The adhesive properties of the polymers were tested and the peel and tack forces were shown to be superior to those measured for a commercial product. Thus, the formulations containing EDMA could be suitable for adhesive applications.

In conclusion, the synthesis of a platform of eugenol-derived monomers and their polymerization through environmentally friendly processes for coatings and adhesives applications were successfully achieved.

Green Chemistry principles were applied throughout the work. Renewable feedstock (principle 7) was used for the synthesis of the monomer platform. Photoinduced polymerization of the eugenol-derived monomers to produce coatings is an energy efficient (principle 6) and solvent-free technique (principle 5). Aqueous emulsion polymerization uses safer solvents (principle 5), reduces waste (reduction of VOCs) (principle 1), and results in a less hazardous chemical synthesis which helps for accident prevention (principle 3 and 12). This work provides bases to develop a broader lignin-derived monomer platform as well as polymers for coatings applications. The synthesis and use of biobased monomers to replace oil-derived monomers and the use of efficient polymerization techniques are necessary steps towards sustainability and circular economy.

6.2 Specific perspectives

6.2.1 Perspectives on eugenol-derived monomer synthesis

A eugenol-derived monomer platform was successfully synthesised giving the opportunity to use these biobased monomers in different types of reactions. Indeed, synthetic reactions should follow the Green Chemistry principles.[1] Valorisation of the eugenol-derived monomer platform was the main focus of the current PhD project. Nonetheless, several aspects remain to be improved in the synthesis of these monomers.

The first step in the synthesis of all these monomers is a solvent-free ethoxylation reaction with ethylene carbonate at high temperature. Improvements in the ethoxylation step have been reported, thus rendering this reaction promising by means of other bases such as TBAF (Tetrabutylamonium fluoride).[19] Methacrylation reaction was done in ethyl acetate instead of DCM as initially done. However, further efforts should be devoted to use greener solvents. MeTHF could be used as a suitable option to replace EtOAc, but effective removal of residual amine and salts may become an issue.[20,21]

New technologies are arising to improve the efficiency and sustainability of methacrylation reaction between methacrylic acid and alcohols through catalysis.[22] Certainly, as biobased-monomers produced from lignin depolymerization molecules continue to be valorised in different applications, more research and new green synthetic methods will be developed.

It should be of interest to carry out complementary studies using some of the substances most commonly obtained by lignin reductive depolymerization[23] (Scheme 6-1) similar to dihydroeugenol (no pendant double bond) such as:

Scheme 6-1. Biobased building blocks from reductive lignin depolymerization

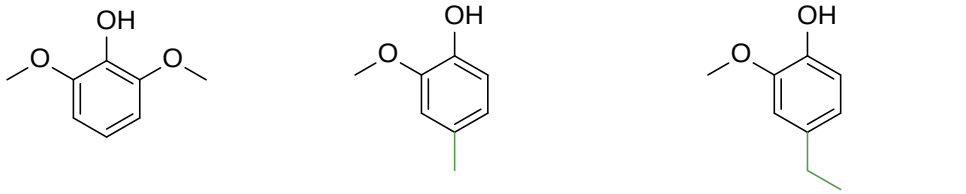

2,6-dimethoxyphenol
Syringol

2-methoxy-4-methylphenol
4-methyl guaiacol

4-ethyl-2-methoxyphenol
4-ethyl guaiacol

These building blocks could be used after purification or as crude mixtures.[24] No secondary reactions during polymerization are expected from these building blocks, once functionalized (with radically polymerizable functional group) they could be easily integrated into formulations as aromatic monomers.

The most common products of the lignin oxidative depolymerization[23] are vanillin and syringaldehyde (Scheme 6-2); thus, these molecules should not be neglected. Ethoxylation and methacrylation of these molecules can be achieved using the synthetic pathway used for eugenol-

derived monomers. The reactivity of aldehydes with diols and amines could be explored in post-polymerization reactions.

Scheme 6-2. Biobased building blocks from oxidative lignin depolymerization

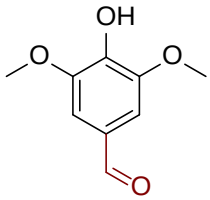

4-hydroxy-3,5-dimethoxybenzaldehyde

Syringaldehyde

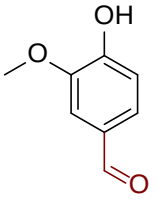

4-hydroxy-3-methoxybenzaldehyde

Vanillin

Functionalization of eugenol-derived molecules through their reaction with itaconic and maleic anhydride should be contemplated as well.

On the other hand, autoxidation studies of the homopolymers of eugenol-derived acrylates and methacrylates should be performed to determine their stability in solution and dry polymer. Moreover, a careful temporal monitoring should be done to determine the exact conditions (temperature, light, exposure to oxygen and time) where the autoxidation takes places.

6.2.2 Perspectives on photoinduced polymerization of eugenol-derived monomers

Additive manufacturing, also known as three-dimensional printing, is a technique that produces parts layer by layer directly from computer-aided design files.[25,26] Numerous applications have been developed such as in consumer products,[27] dentistry,[28] biomaterials and tissue engineering,[26,29–31] among others. By 2022, the global 3D bioprinting market is expected to reach $1.82 billion and to include products and materials for dental, medical, analytical, and food applications.[32] Biobased polymers such as cellulose-derived polymers, PLA, PHAs, and soybean protein, alginate, gelatin, collagen, chitosan, fibrin, and hyaluronic acid have made their way into 3D printing.[33] Three-dimensional printing by means of photoinduced polymerization (photocuring or photocross-linking) of liquid resins through light irradiation has also become attractive. Biobased monomers are currently used in 3D photopolymer printing. Among these monomers, there are acrylates and methacrylates such as isobornyl acrylate,[34] acrylated epoxidized soybean oil,[35] eugenol derived acrylate (3,6-dioxa-1,8-octanedithiol eugenol acrylate), guaiacol methacrylate, vanillyl alcohol dimethacrylate[36] or limonene dimethacrylate.[37] Fast polymerization and high crosslinking is desired although the resulting materials should not be brittle. Eugenol-derived acrylates could be interesting biobased monomers for 3D printing, as they have higher polymerization rates than their methacrylates counterparts. EDMA and EDA could be of particular interest as they have the highest polymerization rate and no secondary reactions (degradative chain transfer), while formulations including different amounts of EIMA and EIA could be used to fine tune the cross-linking density and T_g of the materials.

Furthermore, biobased monomers for dentistry is another application that can be envisaged.[38,39] Eugenol and eugenol-derivatives have antibacterial and anti-inflammatory properties which are desirable in dental treatment.[40–42] Further polymerization trials with eugenol-derived acrylates and methacrylates could be done with photoinitiators usually employed in dentistry such as camphorquinone[43] and ethyl 4-diethylaminobenzoate which absorb at wavelengths of 468 nm (blue light).

6.2.3 Perspectives on emulsion polymerization of eugenol-derived methacrylates

Colloidal stability issues were encountered for EEMA and EIMA while using potassium persulfate as radical initiator at 70°C. Although stable latexes where obtained while using ACVA, it is still interesting to produce stable latexes using persulfate initiators as they are preferred in industrial processes. Several strategies can be followed to reach this objective:

a) Continuous addition of surfactant: total amount of surfactant to be divided into an initial charge, always above the CMC of the respective surfactant to allow micellar nucleation but to limit the number of particles created, followed by the addition of more surfactant to sufficiently stabilize the growing polymer particles. However, excessive use of surfactant should be avoided as it can be detrimental for film formation and the overall properties of the dry polymer.
b) Use of other surfactants with lower CMC and non-ionic surfactant to introduce steric stabilization.
c) A combination of the aforementioned strategies.

In the case of redox initiation at 40°C, poly(EIMA) latex was unstable while poly(EEMA) latex was colloidally stable and with a lower T_g. Similar strategy regarding the surfactants can be followed in this case.

6.2.4 Perspectives on emulsion polymerization of eugenol-derived methacrylates for adhesive applications

Redox initiated emulsion homopolymerization of EEMA at low solids content (12.5% wt) yielded high gel content but low T_g. Thus, cross-linking density was reduced in comparison to the KPS initiation methods. Following this premise, the use of redox initiation with the same adhesive copolymer (BA/MMA/EEMA/MAA) could be employed for EEMA in percentages at high as 12% wbm to prepare a reactive latex. If colloidally stable latexes with high conversion were obtained, residual allylic double bonds could be quantified by IR and depending on the results, further tuning of the polymer properties (adhesive performances) could be achieved by post-crosslinking of the residual double bond.

Moreover, although the main objective of this chapter was the preparation of eugenol-derived copolymers for adhesive applications and, thus, low T_g values were required (T_g ranging from −28 down to −32°C were obtained), higher T_g polymers are also interesting. Copolymerizations aiming

for coatings such as paintings (with T_g of around 0ºC) should be attempted. The desired T_g value would allow a greater amount of eugenol-derived monomer to be introduced, increasing the total biobased content of the formulation. A colloidally stable poly(EDMA-*co*-BA) copolymer (30 % TSC, 38 % wbm EDMA-62 % wbm BA), was already synthesised.[16] It can be expected that a copolymer latex with BA, MMA, eugenol-derived monomer and MAA could be synthesised with up to *circa* 30 % wbm of lignin-derived monomer with colloidal stability. As the use of EEMA in the adhesive formulations resulted in increased cross-linking and a formulation containing 6 % wbm of EEMA resulted in large amounts of coagulum, synthesis should be attempted first with EDMA monomers or similar molecules (as syringol, 4-methyl guaiacol and 4-ethyl guaiacol). Alternatively, EEMA could be tried instead of EDMA with the redox initiating system (instead of KPS) to produce a reactive copolymer latex (BA/MMA/EEMA/MAA) bearing free allylic pendant groups that could be investigated for post-reactive coatings. EIMA is expected to produce high cross-linking and brittle films, irrespective of the initiating system (due to cross-propagation), not ideal for paintings. Properties such as gloss, hardness, cross-cutting test should be measured in this type of application.

6.3 General perspectives

6.3.1 Reactive polymers

Emulsion polymerization of epoxy EEMA and carbonate EEMA is another research line currently under development. The objective is to obtain reactive polymers which properties can be tuned by executing post-polymerization crosslinking reactions (through condensation or cationic photopolymerization) harnessing the reactivity of pendant epoxy or carbonate groups. Two different strategies have been imagined:

1) Emulsion copolymerization of n-hexylmethacrylate with epoxy EEMA.
2) Emulsion copolymerization of BA, MMA and epoxy EEMA.

The characteristics of the latexes are expected to be:

- Total solids contents of 50% (adequate viscosity to form films)
- T_g close to 0°C
- pH close to 7 (to avoid the opening of epoxy groups)

n-Hexylmethacrylate was chosen for the first strategy to avoid the cross-linking common to acrylates. It leads to a polymer with low T_g (−5°C) allowing film forming; and it has adequate hydrophobicity to polymerize *via* emulsion polymerization. Moreover, the homopolymer is soluble in organic solvents. It is expected that the copolymerization with epoxy EEMA will also produce soluble polymers which will allow characterization by liquid ^{1}H NMR. Quantification of epoxy group in the polymers is important and could be achieved using techniques such as liquid ^{1}H NMR (if the polymer is soluble in deuterated solvents) and/or titration.[44,45]

The second strategy implies the use of acrylate monomers. In this case, high gel content is expected due to the presence of BA (intermolecular termination).[46] Therefore, post-polymerization

crosslinking reactions would only be assessed by mechanical and chemical properties such as T_g, gel content, hardness and cross-cut adhesion test.

In order to preserve the epoxy group, a redox initiation system is used to execute the reaction at low temperature (40°C). The polymerization can be executed in semi-batch with the addition of preemulsion and oxidant (redox pair).

Successful formulation of latexes at high total solids using a redox pair as initiator has been achieved. Cross-linking tests are currently underway.

6.3.2 Vitrimers

Vitrimers have gained interest in the last decade. They are covalent adaptable networks that can undergo a reversible exchange (not reversible debonding).[47] Several examples have been reported involving transesterification, transamination of vinylogous urethanes or trans-N-alkylation of 1,2,3-triazolium salts for example.[48,49] Carbonates can undergo transcarbonation exchange with free hydroxyl groups, a reaction analogous to transesterification. Recently, it was demonstrated that hydroxy-functionalized polycarbonate networks could be reprocessed while preserving their mechanical and chemical properties.[50] Monomers derived from eugenol could be used to synthesize similar networks. Copolymers containing a certain percentage of carbonated EEMA or EEMA / EIMA diol could be synthesized via solution or emulsion polymerization (Scheme 6-3) and further reacted in transcarbonation (Scheme 6-4).

Scheme 6-3. Eugenol derived monomers for vitrimers

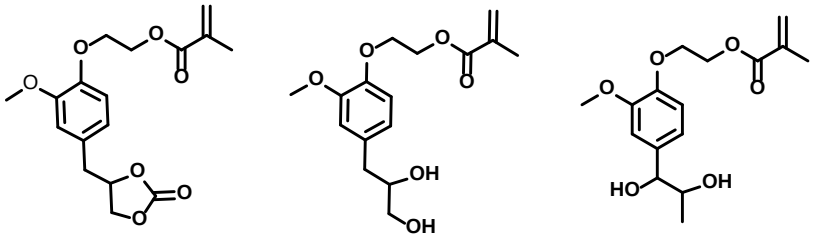

Scheme 6-4. Transcarbonation reaction

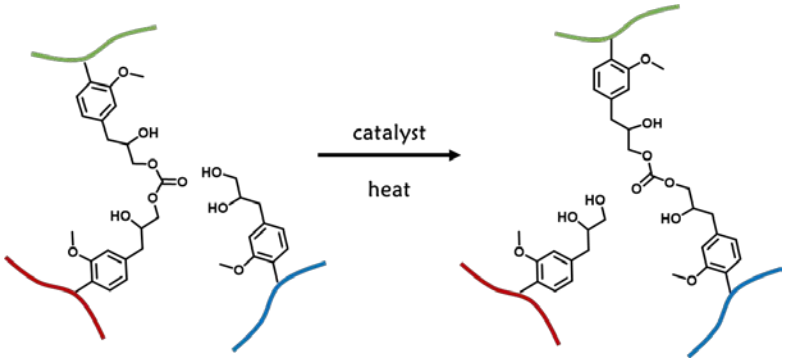

6.3.3 Electrospinning

Polymers synthesized in the present work could be also use in electrospinning for the production of ultrathin fibers. Electrospinning involves an electrohydrodynamic process in which a liquid droplet is electrified to generate a jet, followed by stretching and elongation to generate fibers.[51] Many natural and synthetic polymers have been used to produce fibers through electrospinning. The main requirement is that polymers should be soluble in appropriate solvents (solution electrospinning) or melt without degradation (melt electrospinning). Moreover, polymers should have sufficiently high molar mass. Common solvents are alcohol, dichloromethane, chloroform, dimethylformamide, tetrahydrofuran, acetone or dimethyl sulfoxide among others. Water is not favourable due to its dielectric constant which attenuates the electrostatic repulsion.[51] However, some experiments in electrospinning aqueous dispersions of poly(styrene) latex with poly(vinyl alcohol) and other latexes have been reported.[52,53]

In the case of solution electrospinning using organic solvents, poly(EDMA) and poly(EDMA-*co*-epoxy EEMA) could be interesting polymers. Poly(EDMA) is soluble in solvents such as acetone, chloroform and ethyl acetate. After the production of fibers with poly(EDMA-*co*-epoxy EEMA), the epoxy groups could be photocross-linked using cationic photoinitiators, allowing the tuning of mechanical and chemical properties of these fibers. Additionally, latexes from all eugenol-derived methacrylates could also be used in electrospinning processes.

Potential applications of these fibers in the form of mats and membranes could be patches for drug delivery,[54,55] water treatment,[56,57] and food packaging.[58]

6.4 References

(1) Anastas, P.; Warner, J. *Green Chemistry: Theory and Practice*; Oxford University Press: New York, 2000.

(2) Anastas, P. T.; Zimmerman, J. B. Design Through the 12 Principles of Green Engineering. *Environ. Sci. Technol.* **2003**, *37*, 94A.

(3) Anastas, P.; Eghbali, N. Green Chemistry: Principles and Practice. *Chem. Soc. Rev.* **2010**, *39*, 301.

(4) Hopewell, J.; Dvorak, R.; Kosior, E. Plastics Recycling: Challenges and Opportunities. *Philos. Trans. R. Soc. B Biol. Sci.* **2009**, *364*, 2115.

(5) Mohsenzadeh, A.; Zamani, A.; Taherzadeh, M. J. Bioethylene Production from Ethanol: A Review and Techno-Economical Evaluation. *ChemBioEng Rev.* **2017**, *4*, 75.

(6) Onusseit, H. The Influence of Adhesives on Recycling. *Resour. Conserv. Recycl.* **2006**, *46*, 168.

(7) Post, W.; Susa, A.; Blaauw, R.; Molenveld, K.; Knoop, R. J. I. A Review on the Potential and Limitations of Recyclable Thermosets for Structural Applications. *Polym. Rev.* **2020**, *60*, 359.

(8) Molina-Gutiérrez, S.; Ladmiral, V.; Bongiovanni, R.; Caillol, S.; Lacroix-Desmazes, P. Radical Polymerization of Biobased Monomers in Aqueous Dispersed Media. *Green Chem.* **2019**, *21*, 36.

(9) Molina-Gutiérrez, S.; Manseri, A.; Ladmiral, V.; Bongiovanni, R.; Caillol, S.; Lacroix-Desmazes, P. Eugenol: A Promising Building Block for Synthesis of Radically Polymerizable Monomers. *Macromol. Chem. Phys.* **2019**, *220*, 1900179.

(10) Pramod, C. V.; Fauziah, R.; Seshan, K.; Lange, J.-P. Bio-Based Acrylic Acid from Sugar via Propylene Glycol and Allyl Alcohol. *Catal. Sci. Technol.* **2018**, *8*, 289.

(11) Venkitasubramanian, P. Processes for Making Acrylic-Type Monomers and Products Made Therefrom. 9,234,064 B2, 2016.

(12) Lansing, J. C.; Murray, R. E.; Moser, B. R. Biobased Methacrylic Acid via Selective Catalytic Decarboxylation of Itaconic Acid. *ACS Sustain. Chem. Eng.* **2017**, *5*, 3132.

(13) Le Nôtre, J.; Witte-van Dijk, S. C. M.; van Haveren, J.; Scott, E. L.; Sanders, J. P. M. Synthesis of Bio-Based Methacrylic Acid by Decarboxylation of Itaconic Acid and Citric Acid Catalyzed by Solid Transition-Metal Catalysts. *ChemSusChem* **2014**, *7*, 2712.

(14) Molina-Gutiérrez, S.; Dalle Vacche, S.; Vitale, A.; Ladmiral, V.; Caillol, S.; Bongiovanni, R.; Lacroix-Desmazes, P. Photoinduced Polymerization of Eugenol-Derived Methacrylates. *Molecules* **2020**, *25*, 3444.

(15) Pynaert, R.; Buguet, J.; Croutxé-Barghorn, C.; Moireau, P.; Allonas, X. Effect of Reactive Oxygen Species on the Kinetics of Free Radical Photopolymerization. *Polym. Chem.* **2013**, *4*, 2475.

(16) Molina-Gutiérrez, S.; Ladmiral, V.; Bongiovanni, R.; Caillol, S.; Lacroix-Desmazes, P. Emulsion Polymerization of Dihydroeugenol-, Eugenol-, and Isoeugenol-Derived Methacrylates. *Ind. Eng. Chem. Res.* **2019**, *58*, 21155.

(17) Boscán, F.; Paulis, M.; Barandiaran, M. J. J. Towards the Production of High Performance Lauryl Methacrylate Based Polymers through Emulsion Polymerization. *Eur. Polym. J.* **2017**, *93*, 44.

(18) Molina-Gutiérrez, S.; Li, W. S. J.; Perrin, R.; Ladmiral, V.; Bongiovanni, R.; Caillol, S.; Lacroix-Desmazes, P. Radical Aqueous Emulsion Copolymerization of Eugenol-Derived Monomers for Adhesive Applications. *Biomacromolecules* **2020**.

(19) Kao, S.; Lin, Y.; Ryu, I.; Wu, Y. Revisiting Hydroxyalkylation of Phenols with Cyclic Carbonates. *Adv. Synth. Catal.* **2019**, *361*, 3639.

(20) Jessop, P. G. Searching for Green Solvents. *Green Chem.* **2011**, *13*, 1391.

(21) Clarke, C. J.; Tu, W.-C.; Levers, O.; Bröhl, A.; Hallett, J. P. Green and Sustainable Solvents in Chemical Processes. *Chem. Rev.* **2018**, *118*, 747.

(22) Hu, H.; Ota, H.; Baek, H.; Shinohara, K.; Mase, T.; Uozumi, Y.; Yamada, Y. M. A. Second-Generation Meta-Phenolsulfonic Acid-Formaldehyde Resin as a Catalyst for Continuous-Flow Esterification. *Org. Lett.* **2020**, *22*, 160.

(23) Sun, Z.; Fridrich, B.; De Santi, A.; Elangovan, S.; Barta, K. Bright Side of Lignin Depolymerization: Toward New Platform Chemicals. *Chem. Rev.* **2018**, *118*, 614.

(24) Wang, S.; Shuai, L.; Saha, B.; Vlachos, D. G.; Epps, T. H. From Tree to Tape: Direct Synthesis of Pressure Sensitive Adhesives from Depolymerized Raw Lignocellulosic Biomass. *ACS Cent. Sci.* **2018**, *4*, 701.

(25) Wendel, B.; Rietzel, D.; Kühnlein, F.; Feulner, R.; Hülder, G.; Schmachtenberg, E. Additive Processing of Polymers. *Macromol. Mater. Eng.* **2008**, *293*, 799.

(26) Jungst, T.; Smolan, W.; Schacht, K.; Scheibel, T.; Groll, J. Strategies and Molecular Design Criteria for 3D Printable Hydrogels. *Chem. Rev.* **2016**, *116*, 1496.

(27) Ligon, S. C.; Liska, R.; Stampfl, J.; Gurr, M.; Mülhaupt, R. Polymers for 3D Printing and Customized Additive Manufacturing. *Chem. Rev.* **2017**, *117*, 10212.

(28) Dawood, A.; Marti, B. M.; Sauret-Jackson, V.; Darwood, A. 3D Printing in Dentistry. *Br. Dent. J.* **2015**, *219*, 521.

(29) Xing, J. F.; Zheng, M. L.; Duan, X. M. Two-Photon Polymerization Microfabrication of Hydrogels: An Advanced 3D Printing Technology for Tissue Engineering and Drug Delivery. *Chem. Soc. Rev.* **2015**, *44*, 5031.

(30) Cui, H.; Nowicki, M.; Fisher, J. P.; Zhang, L. G. 3D Bioprinting for Organ Regeneration. *Adv. Healthc. Mater.* **2017**, *6*.

(31) Zhang, J.; Xiao, P. 3D Printing of Photopolymers. *Polym. Chem.* **2018**, *9*, 1530.

(32) Jose, R. R.; Rodriguez, M. J.; Dixon, T. A.; Omenetto, F.; Kaplan, D. L. Evolution of Bioinks and Additive Manufacturing Technologies for 3D Bioprinting. *ACS Biomater. Sci. Eng.* **2016**, *2*, 1662.

(33) Yang, E.; Miao, S.; Zhong, J.; Zhang, Z.; Mills, D. K.; Zhang, L. G. Bio-Based Polymers for 3D Printing of Bioscaffolds. *Polym. Rev.* **2018**, *58*, 668.

(34) Voet, V. S. D.; Strating, T.; Schnelting, G. H. M.; Dijkstra, P.; Tietema, M.; Xu, J.; Woortman, A. J. J.; Loos, K.; Jager, J.; Folkersma, R. Biobased Acrylate Photocurable

Resin Formulation for Stereolithography 3D Printing. *ACS Omega* **2018**, *3*, 1403.

(35) Skliutas, E.; Lebedevaite, M.; Kasetaite, S.; Rekštytė, S.; Lileikis, S.; Ostrauskaite, J.; Malinauskas, M. A Bio-Based Resin for a Multi-Scale Optical 3D Printing. *Sci. Rep.* **2020**, *10*, 9758.

(36) Ding, R.; Du, Y.; Goncalves, R. B.; Francis, L. F.; Reineke, T. M. Sustainable near UV-Curable Acrylates Based on Natural Phenolics for Stereolithography 3D Printing. *Polym. Chem.* **2019**, *10*, 1067.

(37) Schimpf, V.; Asmacher, A.; Fuchs, A.; Stoll, K.; Bruchmann, B.; Mülhaupt, R. Low-Viscosity Limonene Dimethacrylate as a Bio-Based Alternative to Bisphenol A-Based Acrylic Monomers for Photocurable Thermosets and 3D Printing. *Macromol. Mater. Eng.* **2020**, *305*, 2000210.

(38) Berlanga Duarte, M. L.; Reyna Medina, L. A.; Reyes, P. T.; González Pérez, S. E.; Herrera González, A. M. Biobased Isosorbide Methacrylate Monomer as an Alternative to Bisphenol A Glycerolate Dimethacrylate for Dental Restorative Applications. *J. Appl. Polym. Sci.* **2017**, *134*, 1.

(39) Herrera-González, A. M.; Pérez-Mondragón, A. A.; Cuevas-Suárez, C. E. Evaluation of Bio-Based Monomers from Isosorbide Used in the Formulation of Dental Composite Resins. *J. Mech. Behav. Biomed. Mater.* **2019**, *100*, 103371.

(40) Rojo, L.; Vazquez, B.; Parra, J.; López Bravo, A.; Deb, S.; San Roman, J. From Natural Products to Polymeric Derivatives of “Eugenol”: A New Approach for Preparation of Dental Composites and Orthopedic Bone Cements. *Biomacromolecules* **2006**, *7*, 2751.

(41) Modjinou, T.; Versace, D. L.; Abbad-Andallousi, S.; Bousserrhine, N.; Dubot, P.; Langlois, V.; Renard, E. Antibacterial and Antioxidant Bio-Based Networks Derived from Eugenol Using Photo-Activated Thiol-Ene Reaction. *React. Funct. Polym.* **2016**, *101*, 47.

(42) Khalil, A. A.; Rahman, U. ur; Khan, M. R.; Sahar, A.; Mehmood, T.; Khan, M. Essential Oil Eugenol: Sources, Extraction Techniques and Nutraceutical Perspectives. *RSC Adv.* **2017**, *7*, 32669.

(43) Bagheri, A.; Jin, J. Photopolymerization in 3D Printing. *ACS Appl. Polym. Mater.* **2019**, *1*, 593.

(44) Garnier, J.; Dufils, P.-E.; Vinas, J.; Vanderveken, Y.; van Herk, A.; Lacroix-Desmazes, P. Synthesis of Poly(Vinylidene Chloride)-Based Composite Latexes by Emulsion Polymerization from Epoxy Functional Seeds for Improved Thermal Stability. *Polym. Degrad. Stab.* **2012**, *97*, 170.

(45) Garnier, J.; Van Herk, A.; Lacroix-Desmazes, P. *Elaboration of Poly(Vinylidene Chloride)-Based Nanostructured Latexes by Emulsion Polymerization*; 2012.

(46) González, I.; Leiza, J. R.; Asua, J. M. Exploring the Limits of Branching and Gel Content in the Emulsion Polymerization of n -BA. *Macromolecules* **2006**, *39*, 5015.

(47) Montarnal, D.; Capelot, M.; Tournilhac, F.; Leibler, L. Silica-like Malleable Materials from Permanent Organic Networks. *Science (80-.).* **2011**, *334*, 965.

(48) Denissen, W.; Winne, J. M.; Du Prez, F. E. Vitrimers: Permanent Organic Networks with

Glass-like Fluidity. *Chem. Sci.* **2016**, *7*, 30.

(49) Guerre, M.; Taplan, C.; Winne, J. M.; Du Prez, F. E. Vitrimers: Directing Chemical Reactivity to Control Material Properties. *Chem. Sci.* **2020**, *11*, 4855.

(50) Snyder, R. L.; Fortman, D. J.; De Hoe, G. X.; Hillmyer, M. A.; Dichtel, W. R. Reprocessable Acid-Degradable Polycarbonate Vitrimers. *Macromolecules* **2018**, *51*, 389.

(51) Xue, J.; Wu, T.; Dai, Y.; Xia, Y. Electrospinning and Electrospun Nanofibers: Methods, Materials, and Applications. *Chem. Rev.* **2019**, *119*, 5298.

(52) Stoiljkovic, A.; Ishaque, M.; Justus, U.; Hamel, L.; Klimov, E.; Heckmann, W.; Eckhardt, B.; Wendorff, J. H.; Greiner, A. Preparation of Water-Stable Submicron Fibers from Aqueous Latex Dispersion of Water-Insoluble Polymers by Electrospinning. *Polymer (Guildf).* **2007**, *48*, 3974.

(53) Venkatesh, R.; Klimov, E. US2011/0104761 A1, 2011.

(54) Sa'adon, S.; Abd Razak, S. I.; Ismail, A. E.; Fakhruddin, K. Drug-Loaded Poly-Vinyl Alcohol Electrospun Nanofibers for Transdermal Drug Delivery: Review on Factors Affecting the Drug Release. *Procedia Comput. Sci.* **2019**, *158*, 436.

(55) Dodero, A.; Alloisio, M.; Castellano, M.; Vicini, S. Multilayer Alginate–Polycaprolactone Electrospun Membranes as Skin Wound Patches with Drug Delivery Abilities. *ACS Appl. Mater. Interfaces* **2020**, *12*, 31162.

(56) Ray, S. S.; Chen, S. S.; Li, C. W.; Nguyen, N. C.; Nguyen, H. T. A Comprehensive Review: Electrospinning Technique for Fabrication and Surface Modification of Membranes for Water Treatment Application. *RSC Adv.* **2016**, *6*, 85495.

(57) Jiang, S.; Schmalz, H.; Agarwal, S.; Greiner, A. Electrospinning of ABS Nanofibers and Their High Filtration Performance. *Adv. Fiber Mater.* **2020**, *2*, 34.

(58) Zhang, C.; Li, Y.; Wang, P.; Zhang, H. Electrospinning of Nanofibers: Potentials and Perspectives for Active Food Packaging. *Compr. Rev. Food Sci. Food Saf.* **2020**, *19*, 479.

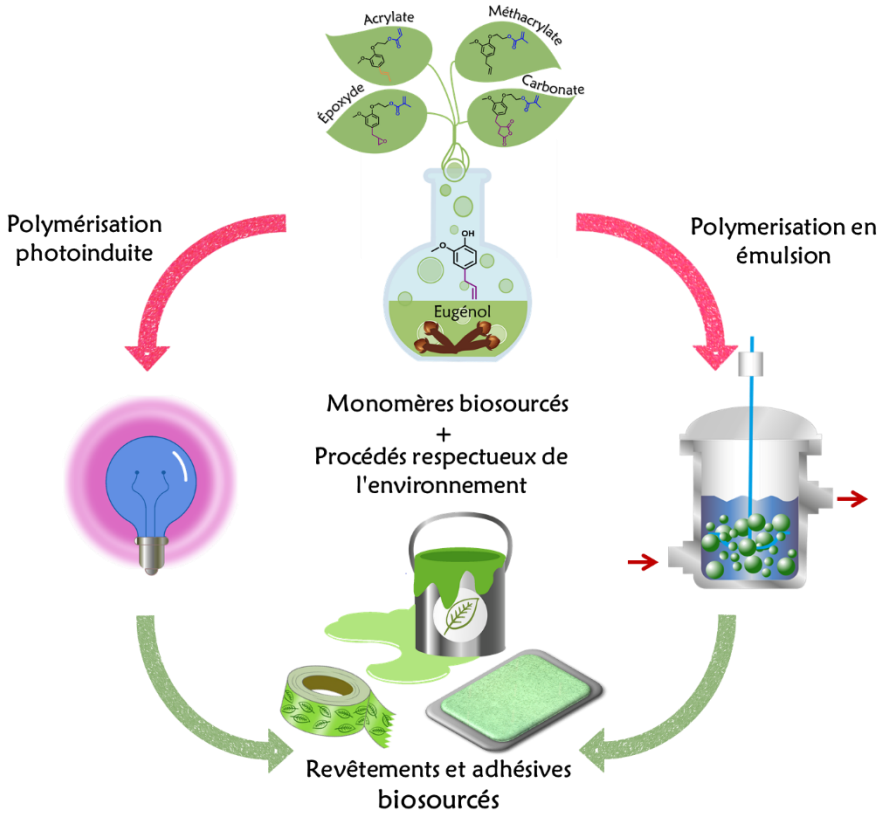

RÉSUMÉ ÉTENDU

Synthèse de monomères biosourcés et leurs polymérisations en émulsion aqueuse et photoinduite

Table des matières

Résumé étendu

7.1 Introduction

Les préoccupations environnementales croissantes liées aux émissions de carbone anthropiques et à la production de déchets ont contribué à l'essor de la « chimie verte ».[1,2] La chimie verte est basée sur douze principes :

1. Prévention des déchets
2. Économie d'atomes
3. Conception de méthodes de synthèse moins dangereuses
4. Conception de produits chimiques plus surs
5. Solvant et auxiliaires moins polluants
6. Recherche du rendement énergétique
7. Utilisation de ressources renouvelables
8. Réduction du nombre de dérivés
9. Catalyse
10. Conception de produits en vue de leur dégradation
11. Observation en temps réel en vue de prévenir la pollution
12. Une chimie fondamentalement plus fiable

Environ 4% de la production mondiale de pétrole et de gaz est utilisée comme matière première pour les plastiques (tandis que 3-4% est utilisé comme énergie pour leur fabrication).[3] La réduction de l'utilisation de combustibles fossiles pour produire des plastiques est devenue une priorité. L'utilisation de matières premières renouvelables, selon le septième principe de la chimie verte, est devenu la principale stratégie pour remplacer les matières premières dérivées des combustibles fossiles dans la production de polymères. De plus, l'utilisation de ressources renouvelables contribue à l'objectif 12 (consommation et production responsables) des 17 objectifs de développement durable définis par les Nations Unies.[4]

La biomasse, en tant que matière première renouvelable, fournit une grande variété de molécules qui peuvent être utilisées pour la synthèse des monomères biosourcés.[5] Les molécules (et ressources) sélectionnées ne doivent pas interférer avec l'approvisionnement alimentaire et elles doivent être largement disponibles. En fait, les polymères sont déjà présents dans la nature comme le caoutchouc naturel (polyisoprène),[6] les polysaccharides (cellulose, hémicellulose, amidon, chitine et chitosane) et la lignine.[7] De plus, les huiles végétales, les terpènes, les dérivés de la lignine, les dérivés de sucre et les protéines peuvent être utilisés comme des monomères et macromonomères.[5,8–11] Néanmoins, les propriétés physico-chimiques des polymères naturels peuvent ne pas être appropriées pour certaines applications, ce qui conduit à la nécessité d'introduire des groupes fonctionnels réactifs pour conférer des propriétés spécifiques au matériau résultant. Par ailleurs, la plupart des molécules biosourcés disponibles sont susceptibles d'être

polymérisées, mais essentiellement par polymérisation par étapes ou par polymérisation en chaîne non radicalaire car ils ne possèdent pas de groupes fonctionnels réactifs en polymérisation radicalaire. La polymérisation radicalaire est une technique de polymérisation robuste et flexible pour produire des copolymères car elle est tolérante aux solvants protiques et aux traces d'impuretés telles que l'oxygène.[12] De plus, des polymères avec des propriétés ajustées peuvent être synthétisés en modifiant le procédé, les amorceurs, l'agent de transfert de chaîne ou en employant des techniques de polymérisation radicalaire par désactivation réversible.[13,14] Afin d'exécuter la polymérisation radicalaire, des groupes fonctionnels comme les (méth)acrylates doivent être introduits dans les molécules.[11] Plusieurs études ont été réalisées concernant la synthèse de monomères biosourcés réactifs par voie radicalaire. Cependant, les phénols naturels restent peu explorés et représentent une opportunité considérable pour remplacer les monomères aromatiques pétrosourcés et apporter des propriétés thermiques et mécaniques intéressantes aux matériaux polymères.[15]

La lignine est la plus grande source de phénols naturels, bien que son utilisation directe reste limitée.[16] Même si la dépolymérisation de la lignine n'est pas encore un procédé optimisé, il y a beaucoup de recherche en cours en raison de la large disponibilité de la lignine et sa non-interférence avec l'approvisionnement alimentaire.[17,18] Des phénols naturels provenant de la lignine comme la vanilline[10,19,20] et l'acide férulique,[21] et aussi provenant des lipides comme le cardanol,[22–24] ont été modifiés et polymérisés par voie radicalaire. L'eugénol et les dérivés de l'eugénol, provenant de l'huile de girofle mais également obtenus à partir de la dépolymérisation de la lignine (Schéma 1), sont d'autres exemples de phénols naturels.[18,25]

Schéma 1. Dérivés de lignine: eugénol, isoeugénol et dihydroeugénol

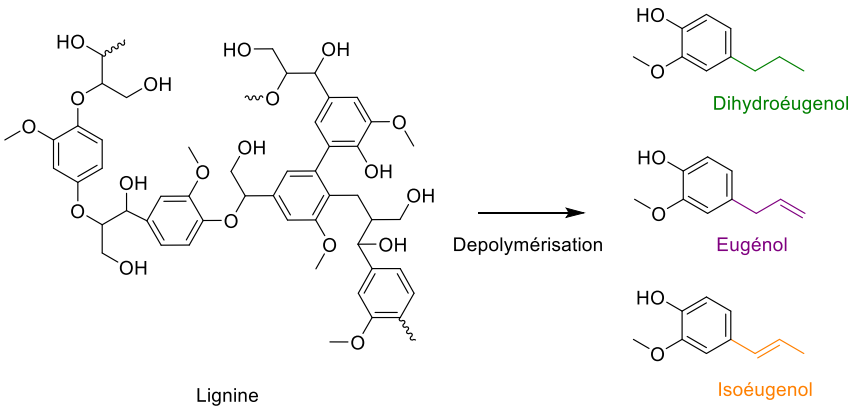

L'un des objectifs immédiats en chimie verte appliquée aux matériaux polymères est la production de monomères et de polymères biosourcés qui peuvent imiter les propriétés de leurs homologues pétrosourcés. Ainsi, l'une des stratégies pour poursuivre cet objectif est de synthétiser des monomères déjà existants (comme l'éthylène[26]) à partir de ressources renouvelables. Une autre stratégie consiste à explorer la synthèse de nouveaux monomères, car des matériaux avec de nouvelles propriétés et applications peuvent être mis au jour à partir de cette recherche.

De plus, la synthèse de monomères biosourcés à partir de ressources renouvelables n'est qu'une première étape vers des matériaux durables. La mise en œuvre de procédés de polymérisation respectueux de l'environnement constitue une deuxième étape. La polymérisation en émulsion aqueuse et la polymérisation photoinduite sont des procédés qui permettent une synthèse plus verte des polymères. Dans le cas de la polymérisation en émulsion aqueuse, l'eau est la phase continue, réduisant l'utilisation de solvant et la production de composés organiques volatils.[27] En polymérisation photoinduite, le processus est rapide, avec une faible consommation d'énergie et sans solvant.[28]

Pour les raisons mentionnées précédemment, l'objectif de ce travail de recherche était de synthétiser et de caractériser des monomères biosourcés à partir de ressources renouvelables, puis de les polymériser par polymérisation radicalaire en utilisant des procédés respectueux de l'environnement tels que la polymérisation en émulsion aqueuse et la polymérisation photoinduite pour produire des polymères adaptés aux applications de revêtements et d'adhésifs.

Ce projet a été financé par SINCHEM. SINCHEM est un programme doctoral qui s'inscrit dans le cadre du programme Action 1 Erasmus Mundus (FPA 2013-0037): http://www.sinchem.eu/. Une bourse de catégorie B EACEA a été accordée à la doctorante pour une période de 3 ans. Par ailleurs, trois partenaires ont contribué à la réalisation des objectifs du projet, parmi lesquels un partenaire industriel pour mettre en œuvre les latex biosourcés conçus pour des applications industrielles de revêtements et adhésifs.

- **Établissement d'origine (coordinateur) : École Nationale Supérieure de Chimie de Montpellier (IAM-ICGM), Montpellier France**

  Superviseur: Dr Patrick Lacroix-Desmazes

  Co-encadrant: Dr Sylvain Caillol

  Co-encadrant: Dr Vincent Ladmiral

Domaine d'expertise: synthèse de polymères, y compris la polymérisation en émulsion

- **1º Institution hôte: Politecnico di Torino (DISAT), Turin, Italie**

  Co-encadrant: Prof. Roberta Bongiovanni

Domaine d'expertise: Polymérisation photoinduite

- **2º Institution hôte: Synthomer (UK) Ltd., Harlow, Royaume-Uni**

  Conseiller industriel: Dr Peter Shaw

  Conseiller industriel: Dr Renaud Perrin

Domaine d'expertise: synthèse de polymères, polymérisation en émulsion et formulation de revêtements

7.2 Synthèse de monomères dérivés de l'eugénol

La polymérisation radicalaire a été choisie comme principal mécanisme de polymérisation dans ce travail. Comme indiqué précédemment, la plupart des molécules biosourcés nécessitent l'introduction de groupes fonctionnels réactifs par voie radicalaire. Ces modifications doivent être effectuées de manière efficace en termes d'économie d'atomes et avec une synthèse et purification simple pour être conforme aux principes de la chimie verte. La recherche bibliographique (présentée au chapitre 1)[29] a montré que les phénols naturels n'ont pas été largement étudiés en polymérisation radicalaire. Ainsi, l'eugénol, l'isoeugénol et le dihydroeugénol, phénols naturels extraits de l'huile de girofle et aussi dérivés de la lignine, ont été sélectionnés comme matières premières biosourcées et fonctionnalisés pour obtenir des monomères qui réagissent par des mécanismes radicalaires.

Les synthèses de neuf monomères biosourcés dérivés d'eugénol (**huit nouvelles molécules**) a été faite avec succès (Schéma 2) :[30]

- Méthacrylate d'éthoxy eugényle (EEMA)
- **Méthacrylate d'éthoxy isoeugényle (EIMA)**
- **Méthacrylate d'éthoxy dihydroeugényle (EDMA)**
- **Acrylate d'éthoxy eugényle (EEA)**
- **Acrylate d'éthoxy isoeugényle (EIA)**
- **Acrylate d'éthoxy dihydroeugényle (EDA)**
- **EEMA époxydé**
- **EIMA époxidé**
- **EEMA carbonaté**

La fonctionnalisation de l'eugénol, isoeugénol et dihydroeugénol a été réalisée à l'aide de molécules non biosourcées. Néanmoins, l'acide acrylique[31,32] et plus récemment l'acide méthacrylique[33,34] peuvent être obtenus à partir de ressources renouvelables. La valorisation de ces monomères à travers différentes applications (comme les revêtements et les adhésifs) favorisera l'optimisation de leur synthèse.

Schéma 2. Plateforme de monomères dérivés de l'eugénol

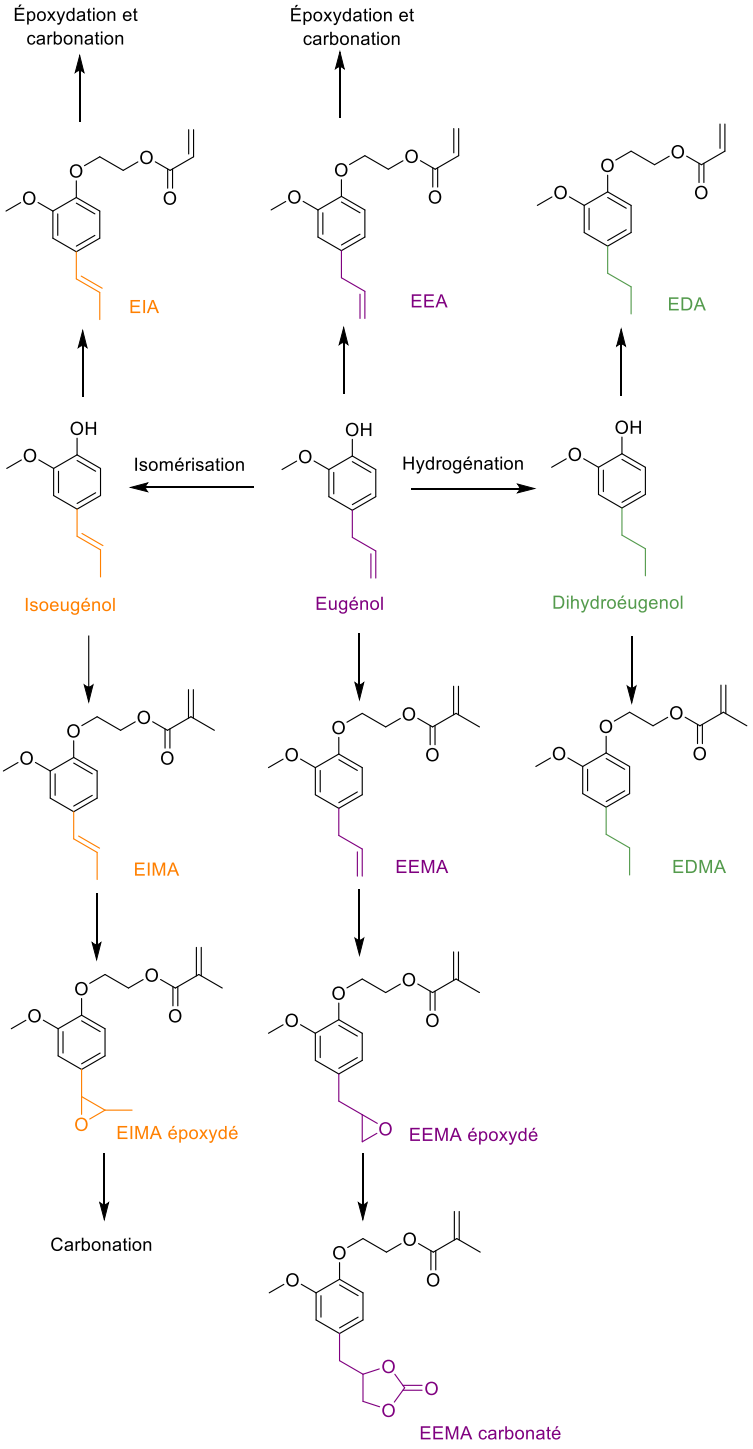

L'homopolymérisation en solution par voie radicalaire (21% massique de monomères par rapport au toluène) des méthacrylates et acrylates dérivés de l'eugénol, isoeugénol et dihydroeugénol a été réalisée ainsi que la caractérisation des polymères obtenus.

Toutes les polymérisations ont atteint des conversions supérieures à 84% dans le cas des méthacrylates. La formation de gel (fraction insoluble de polymère) n'a pas été observée. Dans le cas des acrylates, une faible conversion a été obtenue pour l'EEA, tandis que la polymérisation de l'EIA a entraîné la formation de gel. Les polymères obtenus ont une valeur de T_g entre 10°C et 40°C. L'EEMA et l'EIMA ont présenté des vitesses de polymérisation inférieures par rapport à l'EDMA, et ceci est aussi vrai pour l'EEA et l'EIA par rapport à l'EDA. Ces vitesses de polymérisation plus faibles sont probablement le résultat de réactions de transfert de chaîne dégradatif (abstraction d'hydrogènes allyliques, conduisant à un radical fortement stabilisé peu réactif) et d'une propagation croisée (sur la double liaison propényle) (Schéma 3). En considérant la diminution de la vitesse de polymérisation et la production de polymères ramifiés, le degré de réactions secondaires sur les groupes allylique et propényle suit l'ordre décroissant suivant : EIA >> EEA > EEMA > EIMA. Néanmoins, il reste des doubles liaisons allyliques et propényles résiduelles dans les chaînes polymères poly(EEMA) et poly(EIMA) qui sont donc des polymères fonctionnels. L'auto-oxydation a été observée dans les polymères séchés, ce qui pourrait limiter leur fonctionnalisation ultérieure ou leur réticulation contrôlée. D'autres études sur l'autoxydation des polymères doivent être envisagées.

Schéma 3. Réactions secondaires des groups allylique et propényle

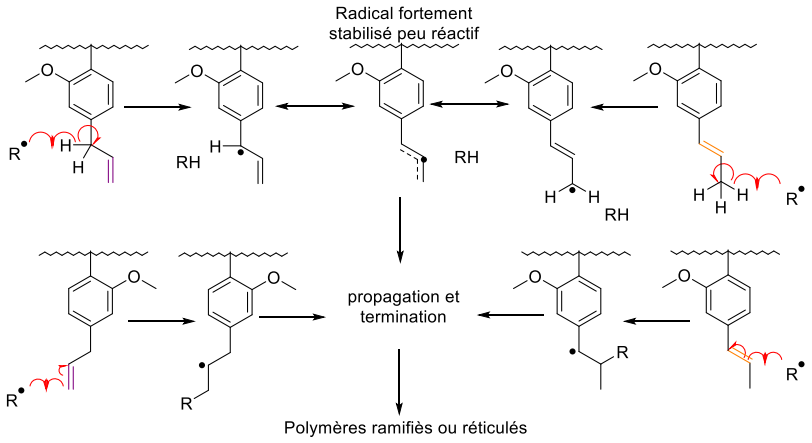

7.2.1 Perspectives sur la synthèse des monomères dérivés de l'eugénol

Une plateforme de monomères dérivés de l'eugénol a été synthétisée avec succès, ce qui a permis d'utiliser ces monomères biosourcés dans différents types de réactions. Néanmoins, plusieurs aspects restent à améliorer dans la synthèse de ces monomères qu'il convient de traiter.

La première étape de la synthèse des monomères présentés dans la plateforme est une réaction d'éthoxylation sans solvant avec du carbonate d'éthylène à haute température. Des améliorations dans l'étape d'éthoxylation ont été rapportées dans la littérature, rendant ainsi cette réaction prometteuse.[35] Par ailleurs, la réaction de méthacrylation a été effectuée dans de l'acétate d'éthyle pour éviter l'utilisation du dichlorométhane. Cependant, des efforts supplémentaires devraient être faits pour utiliser des solvants plus écologiques (par exemple le MeTHF)[36,37] et concevoir une méthode de purification efficace pour l'élimination des amines et oxydes d'amine résiduels. D'autre

part, de nouvelles technologies sont capables d'augmenter l'efficacité pour la réaction de méthacrylation entre l'acide méthacrylique et les alcools par catalyse.[38]

D'un autre côté, des études complémentaires avec d'autres molécules facilement obtenues par dépolymérisation réductive de la lignine[18] (Schéma 4), similaires au dihydroeugénol (sans double liaison pendante), pourraient être effectuées.

Ces molécules peuvent être fonctionnalisées de la même manière que l'dihydroeugénol et utilisées après purification ou sous forme de mélanges bruts dans des formulations en tant que monomères aromatiques.[39] En raison de l'absence de double liaison pendante, aucune réaction secondaire n'est attendue au cours de la polymérisation de ces molécules.

Schéma 4. Produits de la dépolymérisation réductive de la lignine

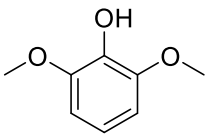

2,6-diméthoxyphénol

Syringol

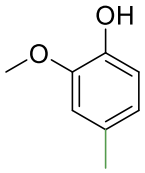

2-méthoxy-4-méthylphénol

4-méthyl gaïacol

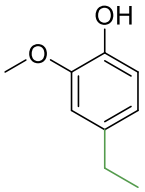

4-éthyl-2-méthoxyphénol

4-éthyl gaïacol

De plus, les produits les plus courants de la dépolymérisation oxydative de la lignine, la vanilline et le syringaldéhyde (Schéma 5), pourraient aussi être méthacrylés. La réaction de l'aldéhyde avec des diols et des amines donnerait accès à de la post-réticulation.

Schéma 5. Produits de la dépolymérisation oxydative de la lignine

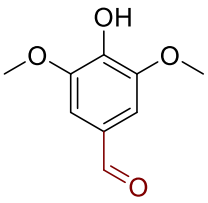

4-hydroxy-3,5-diméthoxybenzaldéhyde

Syringaldéhyde

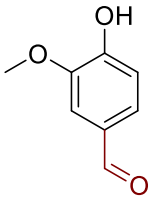

4-hydroxy-3-méthoxybenzaldéhyde

Vanilline

Des études d'autoxydation des homopolymères d'acrylates et de méthacrylates dérivés d'eugénol devraient être effectuées pour déterminer leur stabilité en solution et en polymère sec. De plus, un suivi devrait être effectué pour déterminer les conditions exactes (température, lumière, exposition à l'oxygène et durée) dans lesquelles l'autoxydation a lieu.

7.3 Polymérisation photoinduite de monomères dérivés de l'eugénol

La polymérisation photoinduite de méthacrylates dérivés d'eugénol a été étudiée pour évaluer la possibilité de produire des films dans des conditions sans solvant (polymérisation en masse). La

polymérisation photoinduite de l'EDMA, de l'EEMA et de l'EIMA a été réalisée dans différentes conditions:[40]

- En l'absence de photoamorceur ou avec deux photoamorceur Norrish Type I différents (Darocur 1173 et Irgacure 819)
- Sous air ou sans air (film protecteur)
- Irradié de 240 à 600 nm ou uniquement à 365 nm (à l'aide d'un filtre).

Les trois monomères ont montré un autoamorçage sans photoamorceur lorsqu'ils sont été irradiés à des longueurs d'onde de 240 à 600 nm (en présence ou en l'absence d'air). En présence d'oxygène, avec ou sans photoamorceur, la formation de peroxydes et leur photolyse a conduit à un deuxième régime de polymérisation, uniquement lorsque la formulation est irradiée à des longueurs d'onde de 240 à 400 nm.[40] Les réactions secondaires impliquant les groupes allylique ou propényle ont été observées dans toutes les conditions, bien qu'une contribution plus élevée ait été observée en présence d'air. Il a été démontré que les doubles liaisons propényles (PDB) ont été principalement consommées par des réactions de propagation croisée, tandis que les doubles liaisons allyliques (ADB) ont été principalement consommées sous air via l'abstraction d'hydrogène et la formation d'hydroperoxydes.

L'EDMA atteint les conversions les plus élevées à l'abri de l'air et avec l'utilisation de photoamorceur, montrant que la formation de peroxyde est une voie importante pour ré-amorcer la polymérisation dans les cas de l'EEMA et de l'EIMA.

Lorsque les contributions de l'autoamorçage et de la formation de peroxydes ont été minimisées (par utilisation d'un photoamorceur, d'un film protecteur contre l'air et d'un filtre passe-bande à 365 nm), la vitesse de polymérisation a suivi l'ordre suivant : EDMA > EEMA > EIMA. Les réactions secondaires de l'EEMA et de l'EIMA sont responsables de la réduction de la vitesse de polymérisation.

La polymérisation photoinduite des méthacrylates dérivés d'eugénol a été conduite avec succès. Ces polymères ont des propriétés qui en font de bons candidats pour des applications dans les revêtements et en dentisterie.

7.3.1 Perspectives sur la polymérisation photoinduite de monomères dérivés d'eugénol

La fabrication additive, également appelée impression tridimensionnelle (impression 3D), est une technique qui produit des pièces couche par couche.[41,42] De nombreuses applications ont été développées telles que les produits de consommation,[43] la dentisterie,[44] les biomatériaux et ingénierie tissulaire,[42,45–47] entre autres. D'ici 2022, le marché mondial de la bio-impression 3D atteindra 1,82 milliard de dollars. Les polymères biosourcés tels que les polymères dérivés de la cellulose, l'acide polylactique, les polyhydroxyalcanoates et les protéines de soja, l'alginate, la gélatine, le collagène, le chitosane, la fibrine et l'acide hyaluronique ont fait leur chemin dans l'impression 3D.[48] Également, les monomères biosourcés sont actuellement utilisés dans l'impression de photopolymères 3D. Parmi ces monomères, il y a les acrylates et méthacrylates

tels que : l'acrylate d'isobornyle,[49] l'huile de soja époxydée acrylée,[50] l'acrylate dérivé d'eugénol (acrylate de 3,6-dioxa-1,8-octanedithiol eugénol), le méthacrylate de guaïacol, le diméthacrylate d'alcool de vanille,[51] ou diméthacrylate de limonène.[52] Une polymérisation rapide et des matériaux mécaniquement résistants sont souhaités. Les acrylates dérivés de l'eugénol pourraient être des monomères biosourcés intéressants pour l'impression 3D, car ils ont des vitesses de polymérisation plus élevées que leurs homologues méthacrylates. L'EDMA et l'EDA pourraient être intéressants en raison de leur vitesse de polymérisation élevée et de l'absence de réactions secondaires (pas de transfert de chaîne dégradatif). En outre, des formulations comprenant différentes quantités d'EIMA et d'EIA pourraient être utilisées pour affiner la densité de réticulation et la T_g des matériaux.

7.4 Polymérisation en émulsion de méthacrylates dérivés d'eugénol

Après avoir étudié le comportement des méthacrylates dérivés de l'eugénol dans la polymérisation thermique en solution radicalaire (Chapitre 2) et la photopolymérisation en masse (chapitre 3), nous avons étudié leur polymérisation en émulsion aqueuse. Trois systèmes d'amorçage (persulfate de potassium (KPS) à 70°C, 4,4-azobis (acide 4-cyanovalérique) (ACVA) à 70°C et KPS/$Na_2S_2O_5$ à 40°C) ont été testés dans l'homopolymérisation en émulsion aqueuse.[53] Les monomères dérivés de l'eugénol se sont révélés suffisamment solubles dans l'eau pour exécuter la polymérisation en émulsion *ab-initio* (plutôt que la polymérisation en mini-émulsion). Des latex stables de diamètres de particules d'environ 45 à 71 nm ont été obtenus sans l'utilisation de grandes quantités de tensioactifs ou de tensioactifs à faible CMC comme cela est parfois nécessaire pour les monomères très hydrophobes.

La polymérisation en émulsion avec le KPS à 70°C a produit un latex stable (stabilité colloïdale) uniquement avec l'EDMA, tandis que l'ACVA, également à 70°C, a produit des latex stables pour les trois monomères. De plus, nous avons observé une diminution de la valeur de la T_g du poly(EEMA) en utilisant l'ACVA (T_g = 23°C) et le KPS/$Na_2S_2O_5$ (T_g = 27°C), par rapport au poly(EEMA) obtenu en utilisant le KPS comme amorceur (T_g = 48°C). Ceci indique que l'amorceur affecte le degré des réactions secondaires conduisant à la réticulation (densité de réticulation plus élevée en utilisant le KPS). Au cours de la polymérisation en émulsion amorcée par le système redox, la vitesse de polymérisation a suivi l'ordre suivant : EDMA > EIMA > EEMA, peut-être en raison de l'abstraction d'hydrogène comme réaction secondaire, qui produit un radical allylique très stable, peu susceptible à propager (transfert de chaîne dégradatif). Les valeurs de T_g plus faibles mesurées pour le poly(EEMA) par rapport au poly(EIMA) suggèrent que la principale réaction secondaire était la propagation croisée dans le cas de l'EIMA (conduisant à des polymères hautement réticulés) et la réaction de transfert de chaîne dégradatif pour l'EEMA (conduisant à des polymères moins réticulés), comme observé au chapitre 2.

Dans un essai préliminaire, un latex copolymère poly(EDMA-*co*-BA) stable à 30% de taux de solides (avec une T_g de −23°C) a été synthétisé avec succès. Ces résultats nous ont encouragé à étudier la synthèse de copolymères d'un monomère dérivé de l'eugénol avec des monomères

commerciaux utilisés dans la formulation d'adhésifs pour augmenter le contenu biosourcé de ces formulations (chapitre 5).

7.4.1 Perspectives sur la polymérisation en émulsion de méthacrylates dérivés d'eugénol

Des problèmes de stabilité colloïdale ont été rencontrés pour l'EEMA et l'EIMA lors de l'utilisation du KPS comme amorceur radicalaire à 70°C, alors que des latex stables ont été obtenus en utilisant l'ACVA. Il serait intéressant d'obtenir des latex stables en utilisant des amorceurs persulfates parce qu'ils sont préférés dans les procédés industriels. Plusieurs stratégies peuvent être suivies pour atteindre cet objectif :

a) Ajout de tensioactif en continu : quantité totale de tensioactif divisée en une charge initiale moindre pour limiter le nombre de particules créées (concentration au-dessus de la CMC pour permettre la nucléation micellaire), suivie de l'ajout du reste de tensioactif pour stabiliser suffisamment les particules de polymère en croissance. Cependant, une utilisation excessive d'agent tensioactif doit être évitée car elle peut affecter la bonne filmification et les propriétés globales du film polymère.

b) Utilisation d'autres tensioactifs avec une CMC inférieure et des tensioactifs non ioniques pour introduire une stabilisation stérique.

c) Une combinaison des stratégies susmentionnées.

7.5 Polymérisation en émulsion de méthacrylates dérivés d'eugénol pour applications adhésives

Des latex contenant jusqu'à 12% en poids de méthacrylate d'éthoxy dihydroeugényle (EDMA) et un taux de solides de 50%, pour des applications comme adhésifs, ont été préparés avec succès.[54] Les latex ont été synthétisés en utilisant un procédé semibatch, et toutes les formulations ont fourni des latex avec une bonne stabilité colloïdale et avec des diamètres de particules allant de 159 à 178 nm. Les copolymères sont restés stables jusqu'à 324°C sous air et leurs valeurs de T_g étaient comprises entre −28°C et −32°C. Les propriétés adhésives des films polymères ont été testées et les valeurs de force de pelage « peel » et de pégosité « tack » ont été trouvées supérieures à celles mesurées pour un produit commercial. Ainsi, les formulations contenant de l'EDMA pourraient convenir aux applications adhésives.

7.5.1 Perspectives sur la polymérisation en émulsion de méthacrylates dérivés d'eugénol pour applications adhésives

L'homopolymérisation de l'EEMA en émulsion amorcée par un système redox à faible taux de solides (12,5%) a donné une quantité élevée de gel mais une valeur de T_g faible (Chapitre 4). Ainsi, la densité de réticulation est réduite par rapport aux méthodes d'amorçage avec le KPS et on peut donc s'attendre à une proportion plus élevée de doubles liaisons allyliques résiduelles sur la chaîne polymère. En conséquence, l'utilisation du système d'amorçage redox avec le même copolymère adhésif (BA/MMA/EEMA/MAA) pourrait être employée pour l'EEMA (avec le monomère biosourcé

à 12% en poids de la masse totale en monomères) afin de préparer un latex réactif. Si des latex stables sont obtenus avec une conversion élevée, les doubles liaisons allyliques résiduelles pourraient être quantifiées par infrarouge. En fonction des résultats, des propriétés du film polymère (performances adhésives) pourrait être modifiées par post-réticulation des doubles liaisons allyliques résiduelles.

De plus, bien que l'objectif principal du chapitre 5 ait été la préparation de latex copolymères dérivés d'eugénol avec des faibles valeurs de T_g pour les applications adhésives, des polymères de T_g plus élevées sont aussi intéressants pour d'autres applications. Par exemple, des latex copolymères visant des applications pour des revêtements tels que des peintures (avec une T_g d'environ 0°C) peuvent être envisagés. La valeur de T_g plus élevée permettra l'introduction d'une plus grande quantité de monomère dérivé d'eugénol dans la formulation (autour de 30% massique, pour obtenir des T_g d'environ 0°C au lieu de 12% massique pour les applications adhésives). Les propriétés telles que la brillance, la dureté, l'essai d'adhérence peuvent être mesurées pour ce type d'application.

En conclusion, la synthèse d'une plateforme de monomères dérivés de l'eugénol et leur polymérisation par des procédés respectueux de l'environnement pour les applications de revêtements et d'adhésifs ont été réalisées avec succès.

Les principes de la chimie verte ont été appliqués tout au long du travail. Des matières premières renouvelables (principe 7) ont été utilisées pour la synthèse de la plateforme de monomères. La polymérisation photoinduite des monomères dérivés de l'eugénol pour produire des revêtements est une technique que peut consommer peu énergie (principe 6) et sans solvant (principe 5). La polymérisation en émulsion aqueuse utilise des solvants plus sûrs (principe 5), réduit les déchets (réduction des composés organiques volatils) (principe 1) et aboutit à une synthèse chimique moins dangereuse qui contribue à la prévention des accidents (principes 3 et 12). Ces travaux fournissent des bases pour développer une plateforme plus large de monomères dérivés de la lignine ainsi que des polymères pour les applications de revêtements. La synthèse de monomères biosourcés pour remplacer les monomères dérivés du pétrole et leur polymérisation par des techniques de polymérisation respectueuses de l'environnement sont des étapes nécessaires vers la durabilité et l'économie circulaire.

7.6 Références

(1) Anastas, P.; Warner, J. *Green Chemistry: Theory and Practice*; Oxford University Press: New York, 2000.

(2) Anastas, P. T.; Zimmerman, J. B. Design Through the 12 Principles of Green Engineering. *Environ. Sci. Technol.* **2003**, *37*, 94A.

(3) Hopewell, J.; Dvorak, R.; Kosior, E. Plastics Recycling: Challenges and Opportunities. *Philos. Trans. R. Soc. B Biol. Sci.* **2009**, *364*, 2115.

(4) United Nations. The 17 Sustainable Development Goals https://sdgs.un.org/goals (accessed Aug 24, 2020).

(5) Gandini, A.; Lacerda, T. M.; Carvalho, A. J. F. F.; Trovatti, E. Progress of Polymers from Renewable Resources: Furans, Vegetable Oils, and Polysaccharides. *Chem. Rev.* **2016**, *116*, 1637.

(6) Sarkar, P.; Bhowmick, A. K. Sustainable Rubbers and Rubber Additives. *J. Appl. Polym. Sci.* **2017**, *134*, 45701.

(7) Lambert, S.; Wagner, M. Environmental Performance of Bio-Based and Biodegradable Plastics: The Road Ahead. *Chem. Soc. Rev.* **2017**, *46*, 6855.

(8) Ca, V.; Lligadas, G.; Ronda, J. C.; Galia, M.; Galià, M.; Cádiz, V. Renewable Polymeric Materials from Vegetable Oils: A Perspective. *Mater. Today* **2013**, *16*, 337.

(9) Wilbon, P. A.; Chu, F.; Tang, C. Progress in Renewable Polymers from Natural Terpenes, Terpenoids, and Rosin. *Macromol. Rapid Commun.* **2013**, *34*, 8.

(10) Fache, M.; Darroman, E.; Besse, V.; Auvergne, R.; Caillol, S.; Boutevin, B. Vanillin, a Promising Biobased Building-Block for Monomer Synthesis. *Green Chem.* **2014**, *16*, 1987.

(11) Kristufek, S. L.; Wacker, K. T.; Tsao, Y.-Y. T. Y. T.; Su, L.; Wooley, K. L. Monomer Design Strategies to Create Natural Product-Based Polymer Materials. *Nat. Prod. Rep.* **2017**, *34*, 433.

(12) Nesvadba, P. Radical Polymerization in Industry. In *Encyclopedia of Radicals in Chemistry, Biology and Materials*; John Wiley & Sons, Ltd: Chichester, UK, 2012.

(13) Save, M.; Guillaneuf, Y.; Gilbert, R. G. Controlled Radical Polymerization in Aqueous Dispersed Media. *Aust. J. Chem.* **2006**, *59*, 693.

(14) Destarac, M. Controlled Radical Polymerization: Industrial Stakes, Obstacles and Achievements. *Macromol. React. Eng.* **2010**, *4*, 165.

(15) Fonseca, L. R.; Silva Sá, J. L.; Lima-Neto, B. S. Plant Oil-Based Polyester. In *Bio-Based Plant Oil Polymers and Composites*; Elsevier, 2016; pp 73–86.

(16) Strassberger, Z.; Tanase, S.; Rothenberg, G. The Pros and Cons of Lignin Valorisation in an Integrated Biorefinery. *RSC Adv.* **2014**, *4*, 25310.

(17) Azadi, P.; Inderwildi, O. R.; Farnood, R.; King, D. A. Liquid Fuels, Hydrogen and Chemicals from Lignin: A Critical Review. *Renew. Sustain. Energy Rev.* **2013**, *21*, 506.

(18) Sun, Z.; Fridrich, B.; De Santi, A.; Elangovan, S.; Barta, K. Bright Side of Lignin Depolymerization: Toward New Platform Chemicals. *Chem. Rev.* **2018**, *118*, 614.

(19) Fache, M.; Boutevin, B.; Caillol, S. Vanillin Production from Lignin and Its Use as a

Renewable Chemical. *ACS Sustain. Chem. Eng.* **2016**, *4*, 35.

(20) Zhang, H.; Deng, J.; Wu, Y. Biobased Magnetic Microspheres Containing Aldehyde Groups: Constructed by Vanillin-Derived Polymethacrylate/Fe3O4 and Recycled in Adsorbing Amine. *ACS Sustain. Chem. Eng.* **2017**, *5*, 658.

(21) Takeshima, H.; Satoh, K.; Kamigaito, M. Bio-Based Functional Styrene Monomers Derived from Naturally Occurring Ferulic Acid for Poly(Vinylcatechol) and Poly(Vinylguaiacol) via Controlled Radical Polymerization. *Macromolecules* **2017**, *50*, 4206.

(22) Voirin, C.; Caillol, S.; Sadavarte, N. V.; Tawade, B. V.; Boutevin, B.; Wadgaonkar, P. P. Functionalization of Cardanol: Towards Biobased Polymers and Additives. *Polym. Chem.* **2014**, *5*, 3142.

(23) Ladmiral, V.; Jeannin, R.; Fernandes Lizarazu, K.; Lai-Kee-Him, J.; Bron, P.; Lacroix-Desmazes, P.; Caillol, S. Aromatic Biobased Polymer Latex from Cardanol. *Eur. Polym. J.* **2017**, *93*, 785.

(24) Li, W. S. J.; Negrell, C.; Ladmiral, V.; Lai-Kee-Him, J.; Bron, P.; Lacroix-Desmazes, P.; Joly-Duhamel, C.; Caillol, S. Cardanol-Based Polymer Latex by Radical Aqueous Miniemulsion Polymerization. *Polym. Chem.* **2018**, *9*, 2468.

(25) Schutyser, W.; Renders, T.; Van den Bosch, S.; Koelewijn, S.-F.; Beckham, G. T.; Sels, B. F. Chemicals from Lignin: An Interplay of Lignocellulose Fractionation, Depolymerisation, and Upgrading. *Chem. Soc. Rev.* **2018**, *47*, 852.

(26) Mohsenzadeh, A.; Zamani, A.; Taherzadeh, M. J. Bioethylene Production from Ethanol: A Review and Techno-Economical Evaluation. *ChemBioEng Rev.* **2017**, *4*, 75.

(27) Asua, J. M. Emulsion Polymerization: From Fundamental Mechanisms to Process Developments. *J. Polym. Sci. Part A Polym. Chem.* **2004**, *42*, 1025.

(28) Fouassier, J. P.; Allonas, X.; Burget, D. Photopolymerization Reactions under Visible Lights: Principle, Mechanisms and Examples of Applications. *Prog. Org. Coatings* **2003**, *47*, 16.

(29) Molina-Gutiérrez, S.; Ladmiral, V.; Bongiovanni, R.; Caillol, S.; Lacroix-Desmazes, P. Radical Polymerization of Biobased Monomers in Aqueous Dispersed Media. *Green Chem.* **2019**, *21*, 36.

(30) Molina-Gutiérrez, S.; Manseri, A.; Ladmiral, V.; Bongiovanni, R.; Caillol, S.; Lacroix-Desmazes, P. Eugenol: A Promising Building Block for Synthesis of Radically Polymerizable Monomers. *Macromol. Chem. Phys.* **2019**, *220*, 1900179.

(31) Pramod, C. V.; Fauziah, R.; Seshan, K.; Lange, J.-P. Bio-Based Acrylic Acid from Sugar via Propylene Glycol and Allyl Alcohol. *Catal. Sci. Technol.* **2018**, *8*, 289.

(32) Venkitasubramanian, P. Processes for Making Acrylic-Type Monomers and Products Made Therefrom. 9,234,064 B2, 2016.

(33) Lansing, J. C.; Murray, R. E.; Moser, B. R. Biobased Methacrylic Acid via Selective Catalytic Decarboxylation of Itaconic Acid. *ACS Sustain. Chem. Eng.* **2017**, *5*, 3132.

(34) Le Nôtre, J.; Witte-van Dijk, S. C. M.; van Haveren, J.; Scott, E. L.; Sanders, J. P. M. Synthesis of Bio-Based Methacrylic Acid by Decarboxylation of Itaconic Acid and Citric Acid Catalyzed by Solid Transition-Metal Catalysts. *ChemSusChem* **2014**, *7*, 2712.

(35) Kao, S.; Lin, Y.; Ryu, I.; Wu, Y. Revisiting Hydroxyalkylation of Phenols with Cyclic Carbonates. *Adv. Synth. Catal.* **2019**, *361*, 3639.

(36) Jessop, P. G. Searching for Green Solvents. *Green Chem.* **2011**, *13*, 1391.

(37) Clarke, C. J.; Tu, W.-C.; Levers, O.; Bröhl, A.; Hallett, J. P. Green and Sustainable Solvents in Chemical Processes. *Chem. Rev.* **2018**, *118*, 747.

(38) Hu, H.; Ota, H.; Baek, H.; Shinohara, K.; Mase, T.; Uozumi, Y.; Yamada, Y. M. A. Second-Generation Meta-Phenolsulfonic Acid-Formaldehyde Resin as a Catalyst for Continuous-Flow Esterification. *Org. Lett.* **2020**, *22*, 160.

(39) Wang, S.; Shuai, L.; Saha, B.; Vlachos, D. G.; Epps, T. H. From Tree to Tape: Direct Synthesis of Pressure Sensitive Adhesives from Depolymerized Raw Lignocellulosic Biomass. *ACS Cent. Sci.* **2018**, *4*, 701.

(40) Molina-Gutiérrez, S.; Dalle Vacche, S.; Vitale, A.; Ladmiral, V.; Caillol, S.; Bongiovanni, R.; Lacroix-Desmazes, P. Photoinduced Polymerization of Eugenol-Derived Methacrylates. *Molecules* **2020**, *25*, 3444.

(41) Wendel, B.; Rietzel, D.; Kühnlein, F.; Feulner, R.; Hülder, G.; Schmachtenberg, E. Additive Processing of Polymers. *Macromol. Mater. Eng.* **2008**, *293*, 799.

(42) Jungst, T.; Smolan, W.; Schacht, K.; Scheibel, T.; Groll, J. Strategies and Molecular Design Criteria for 3D Printable Hydrogels. *Chem. Rev.* **2016**, *116*, 1496.

(43) Ligon, S. C.; Liska, R.; Stampfl, J.; Gurr, M.; Mülhaupt, R. Polymers for 3D Printing and Customized Additive Manufacturing. *Chem. Rev.* **2017**, *117*, 10212.

(44) Dawood, A.; Marti, B. M.; Sauret-Jackson, V.; Darwood, A. 3D Printing in Dentistry. *Br. Dent. J.* **2015**, *219*, 521.

(45) Xing, J. F.; Zheng, M. L.; Duan, X. M. Two-Photon Polymerization Microfabrication of Hydrogels: An Advanced 3D Printing Technology for Tissue Engineering and Drug Delivery. *Chem. Soc. Rev.* **2015**, *44*, 5031.

(46) Cui, H.; Nowicki, M.; Fisher, J. P.; Zhang, L. G. 3D Bioprinting for Organ Regeneration. *Adv. Healthc. Mater.* **2017**, *6*.

(47) Zhang, J.; Xiao, P. 3D Printing of Photopolymers. *Polym. Chem.* **2018**, *9*, 1530.

(48) Yang, E.; Miao, S.; Zhong, J.; Zhang, Z.; Mills, D. K.; Zhang, L. G. Bio-Based Polymers for 3D Printing of Bioscaffolds. *Polym. Rev.* **2018**, *58*, 668.

(49) Voet, V. S. D.; Strating, T.; Schnelting, G. H. M.; Dijkstra, P.; Tietema, M.; Xu, J.; Woortman, A. J. J.; Loos, K.; Jager, J.; Folkersma, R. Biobased Acrylate Photocurable Resin Formulation for Stereolithography 3D Printing. *ACS Omega* **2018**, *3*, 1403.

(50) Skliutas, E.; Lebedevaite, M.; Kasetaite, S.; Rekštytė, S.; Lileikis, S.; Ostrauskaite, J.; Malinauskas, M. A Bio-Based Resin for a Multi-Scale Optical 3D Printing. *Sci. Rep.* **2020**, *10*, 9758.

(51) Ding, R.; Du, Y.; Goncalves, R. B.; Francis, L. F.; Reineke, T. M. Sustainable near UV-Curable Acrylates Based on Natural Phenolics for Stereolithography 3D Printing. *Polym. Chem.* **2019**, *10*, 1067.

(52) Schimpf, V.; Asmacher, A.; Fuchs, A.; Stoll, K.; Bruchmann, B.; Mülhaupt, R. Low- Viscosity

Limonene Dimethacrylate as a Bio- Based Alternative to Bisphenol A- Based Acrylic Monomers for Photocurable Thermosets and 3D Printing. *Macromol. Mater. Eng.* **2020**, *305*, 2000210.

(53) Molina-Gutiérrez, S.; Ladmiral, V.; Bongiovanni, R.; Caillol, S.; Lacroix-Desmazes, P. Emulsion Polymerization of Dihydroeugenol-, Eugenol-, and Isoeugenol-Derived Methacrylates. *Ind. Eng. Chem. Res.* **2019**, *58*, 21155.

(54) Molina-Gutiérrez, S.; Li, W. S. J.; Perrin, R.; Ladmiral, V.; Bongiovanni, R.; Caillol, S.; Lacroix-Desmazes, P. Radical Aqueous Emulsion Copolymerization of Eugenol-Derived Monomers for Adhesive Applications. *Biomacromolecules* **2020**, acs. biomac.0c00461.

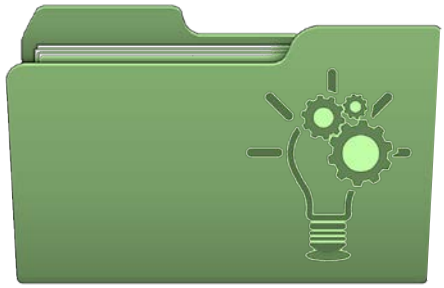

APPENDIX

Table of contents

APPENDIX:

A1 CHAPTER 2

A1.1 Infrared Spectroscopy

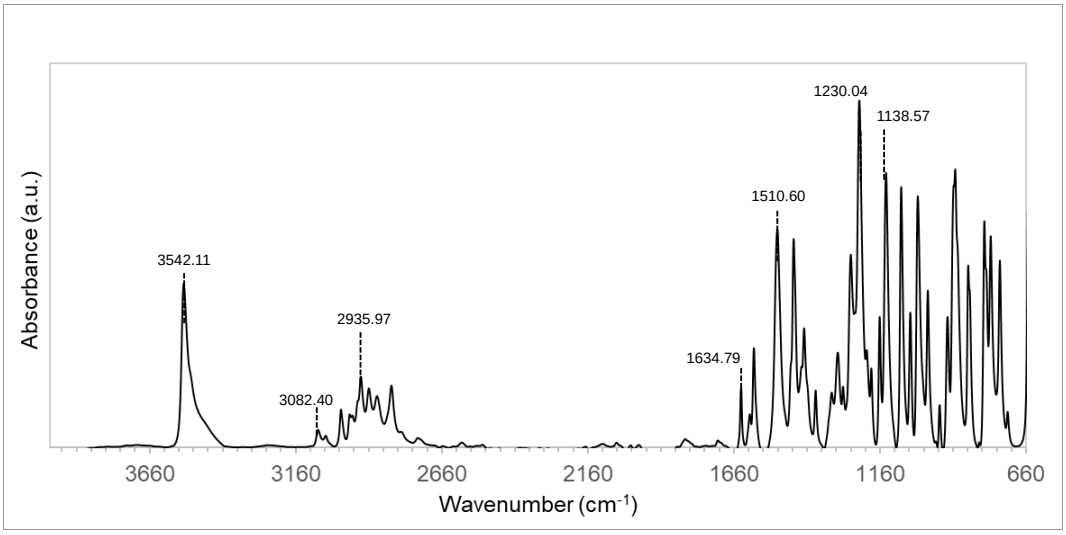

Figure A1-1. Ethoxy Eugenol (EE) ATR FTIR Spectrum.

ATR-FTIR (cm^{-1}): 3542.11 (s, sh, OH stretch), 3082.40 (w, C=C alkene stretch), 2830-3000 (s, CH_3, CH_2 stretch), 1634.79 (S, C=C alkene stretch), 1510.60 (s, C=C aromatic ring stretch), 1230.04 (s, C-O stretch), 1138.57 (s, C-O stretch).

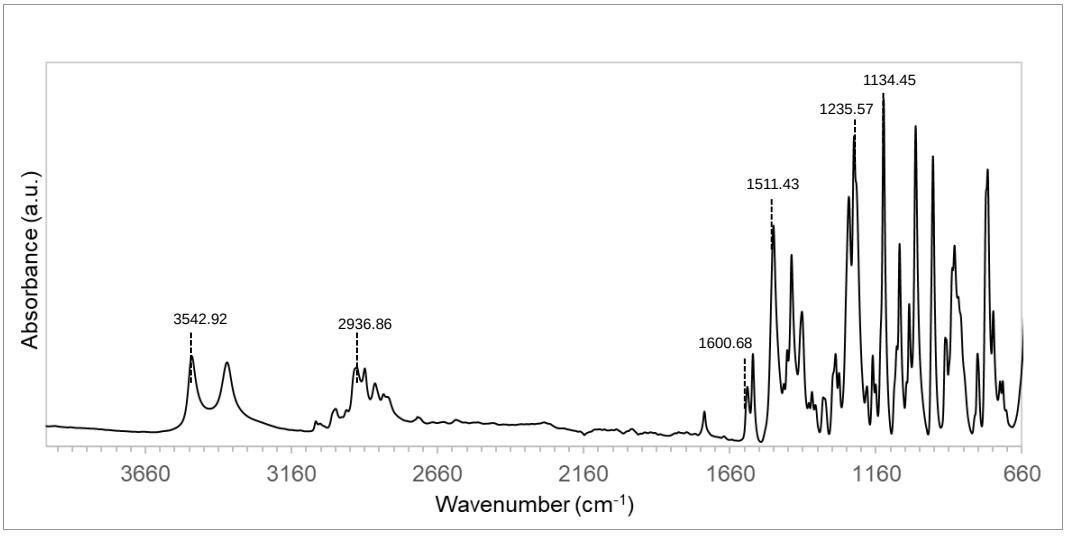

Figure A1-2. Ethoxy Isoeugenol (EI) ATR FTIR Spectrum.

ATR-FTIR (cm^{-1}): 3501.58 (s, sh, OH stretch), 3076.88 (w, C=C alkene stretch), 2830-3000 (s, CH_3, CH_2 stretch), 1600.68 (s, C=C aromatic ring stretch), 1511.43 (s, C=C aromatic ring stretch), 1235.57(s, C-O stretch), 1134.45 (s, C-O stretch).

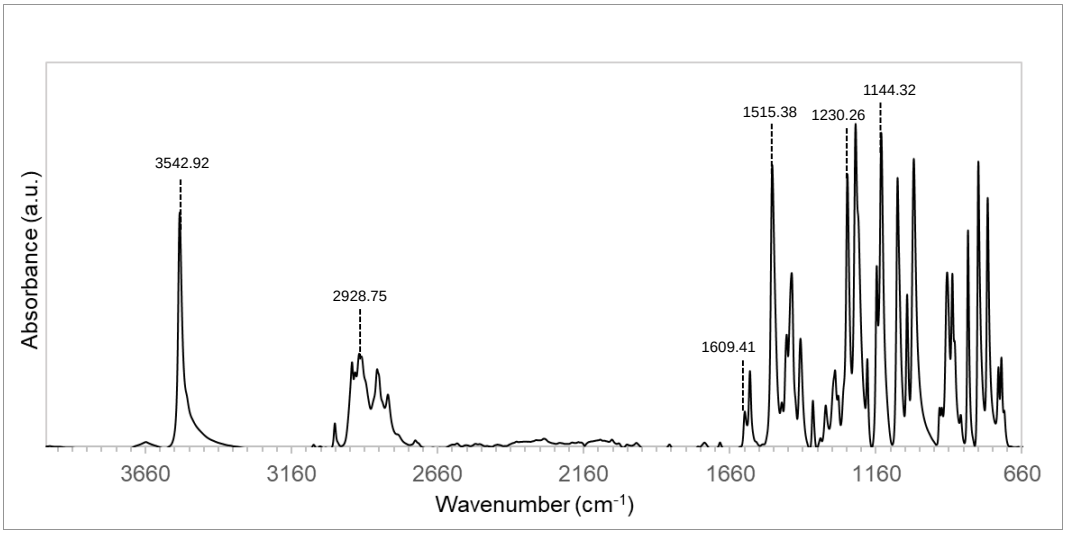

Figure A1-3. Ethoxy Dihydroeugenol (ED) ATR FT-IR Spectrum

ATR-FTIR (cm^{-1}): 3542.92 (s, sh, OH stretch), 2830-3000 (s, CH_3, CH_2 stretch), 1609.41 (m, C=C aromatic ring stretch), 1515.38 (s, C=C aromatic ring stretch), 1230.26 (s, C-O stretch), 1144.32 (s, C-O stretch).

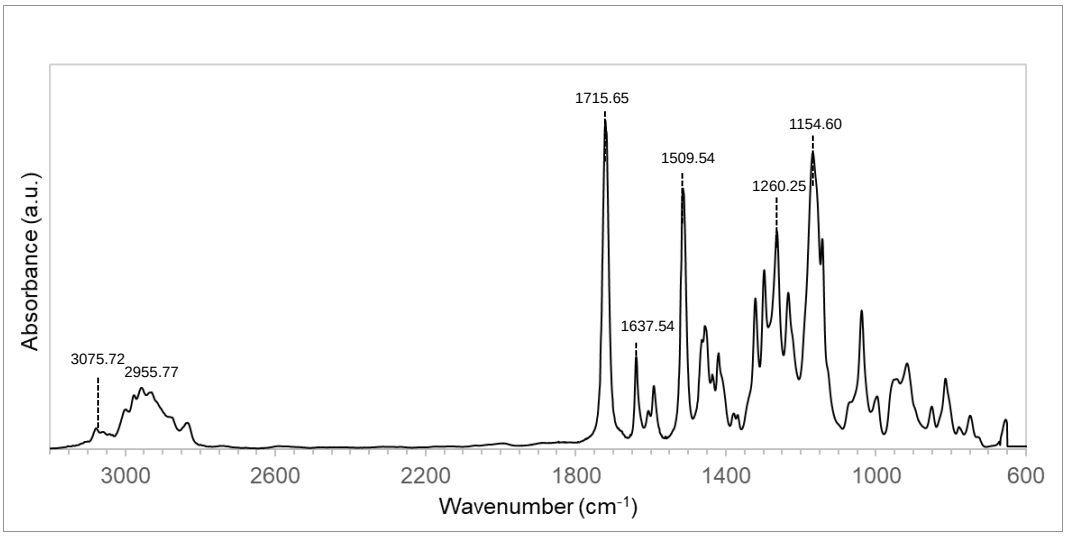

Figure A1-4. Ethoxy Eugenyl Methacrylate (EEMA) ATR FTIR Spectrum

ATR-FTIR (cm^{-1}): 3075.72 (w, C=C alkene stretch), 2830-3000 (s, CH_3, CH_2 stretch), 1715.65 (s, C=O stretch), 1637.54 (w, C=C alkene stretch), 1509.54 (s, C=C aromatic ring stretch), 1260.25 (s, C-O stretch), 1154. 60 (s, C-O stretch).

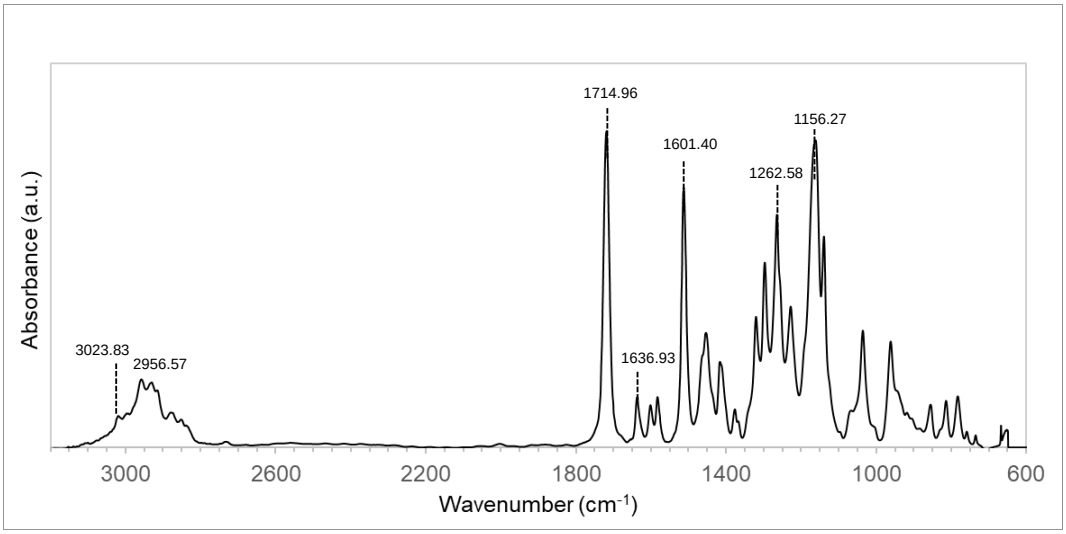

Figure A1-5. Ethoxy Isoeugenyl Methacrylate (EIMA) ATR FTIR Spectrum.

ATR-FTIR (cm^{-1}): 3023.83 (w, C=C alkene stretch), 2830-3000 (s, CH_3, CH_2 stretch), 1714.96 (s, C=O stretch), 1636.93 (w, C=C alkene stretch), 1601.40 (C=C aromatic ring stretch), 1262.58 (s, C-O stretch), 1156.27 (s, C-O stretch).

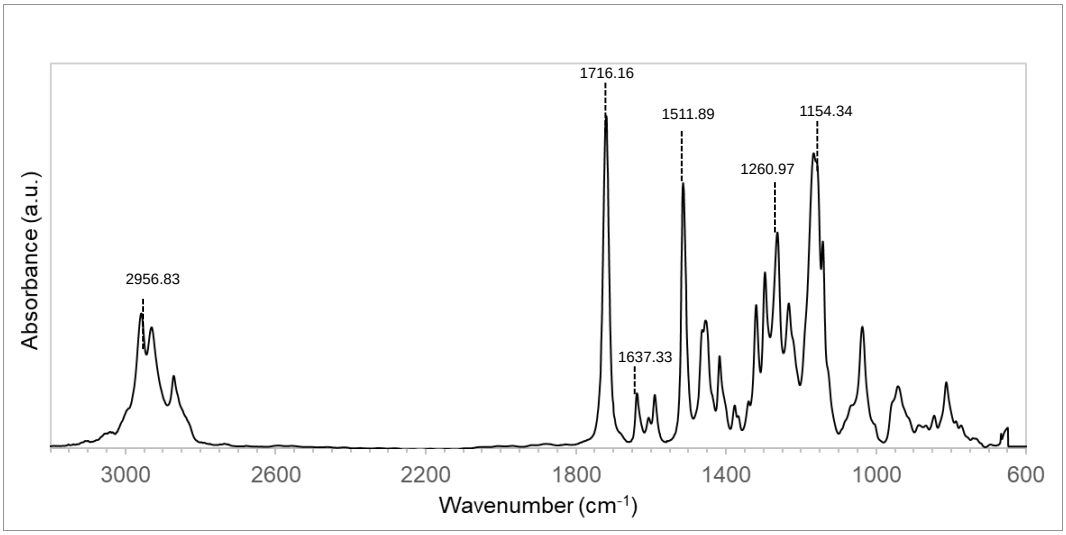

Figure A1-6. Ethoxy Dihydroeugenyl Methacrylate (EDMA) ATR FTIR Spectrum

ATR-FTIR (cm^{-1}): 2830-3000 (s, CH_3, CH_2 stretch), 1716.16 (s, C=O stretch), 1637.33 (w, C=C alkene stretch), 1511.89 (s, C=C aromatic ring stretch), 1260.97 (s, C-O stretch), 1154.34 (s, C- O stretch).

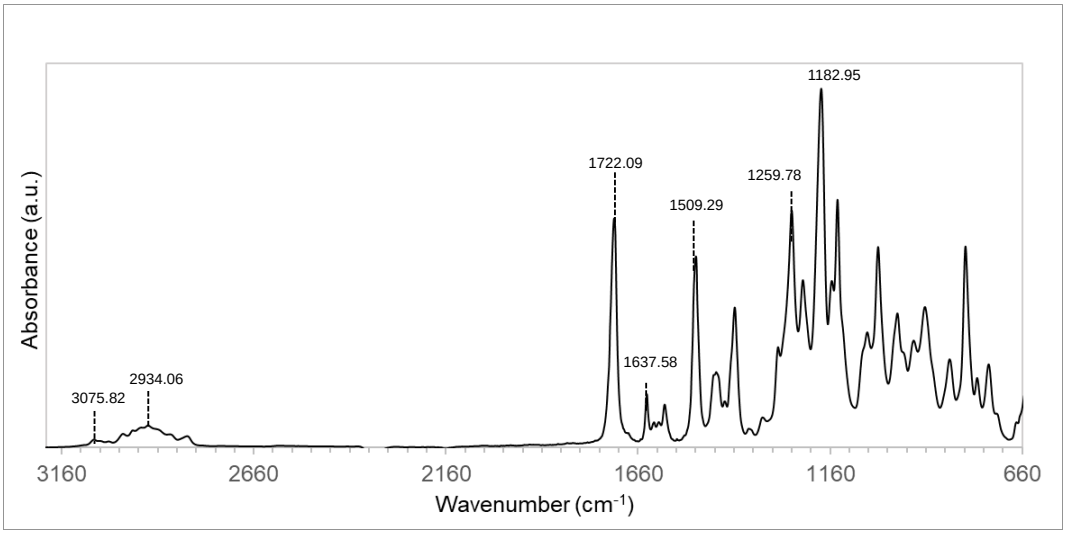

Figure A1-7. Ethoxy Eugenyl Acrylate (EEA) ATR FTIR Spectrum.

ATR-FTIR (cm^{-1}): 3075.82 (w, C=C alkene stretch), 2830-3000 (s, CH_3, CH_2 stretch), 1722.09 (s, C=O stretch), 1637.58 (w, C=C alkene stretch), 1509.29 (C=C aromatic ring stretch), 1259.78 (s, C-O stretch), 1182.95 (s, C-O stretch).

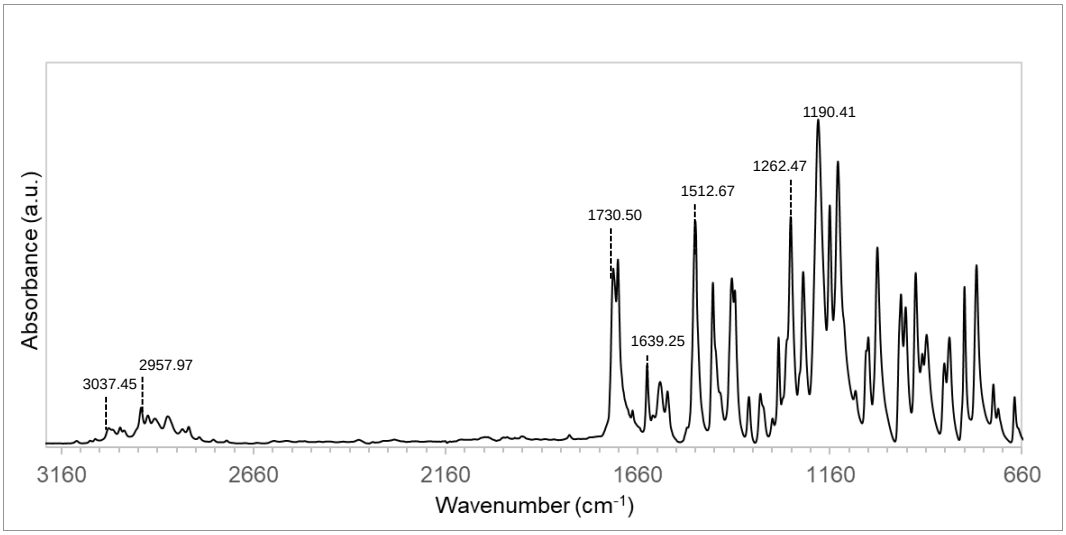

Figure A1-8. Ethoxy Isoeugenyl Acrylate (EIA) ATR FTIR Spectrum.

ATR-FTIR (cm^{-1}): 3037.45 (w, C=C alkene stretch), 2830-3000 (s, CH_3, CH_2 stretch), 1730.50 (s, C=O stretch), 1639.25 (w, C=C alkene stretch), 1512.67 (C=C aromatic ring stretch), 1262.47(s, C-O stretch), 1190.41 (s, C-O stretch).

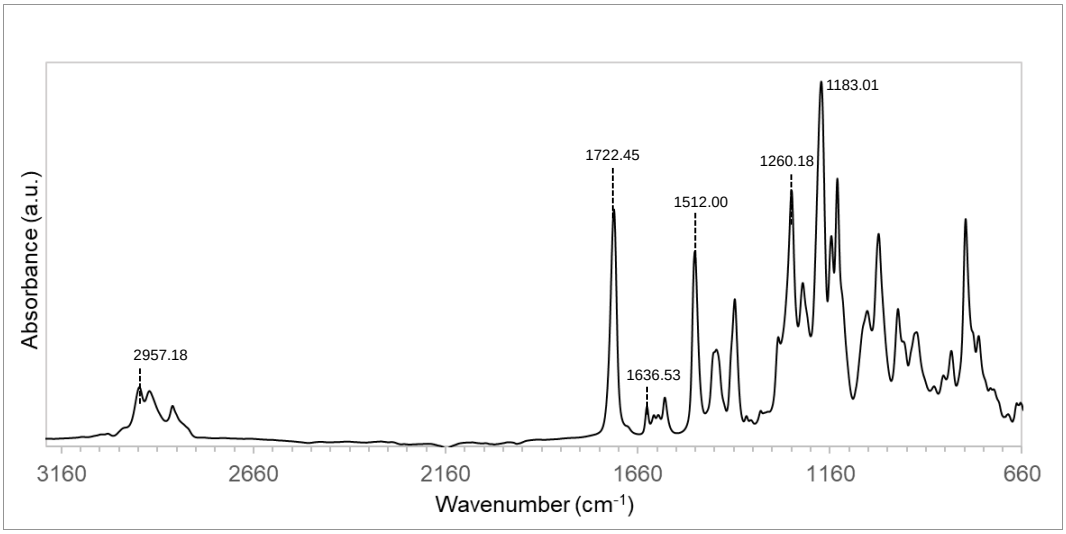

Figure A1-9. Ethoxy Dihydroeugenyl Acrylate (EDA) ATR FTIR Spectrum.

ATR-FTIR (cm^{-1}): 2870-3000 (s, CH_3, CH_2 stretch), 1722.45 (s, C=O stretch), 1636.53 (w, C=C alkene stretch), 1512.00 (s, C=C aromatic ring stretch), 1260.18 (s, C-O stretch), 1183.01 (s, C- O stretch).

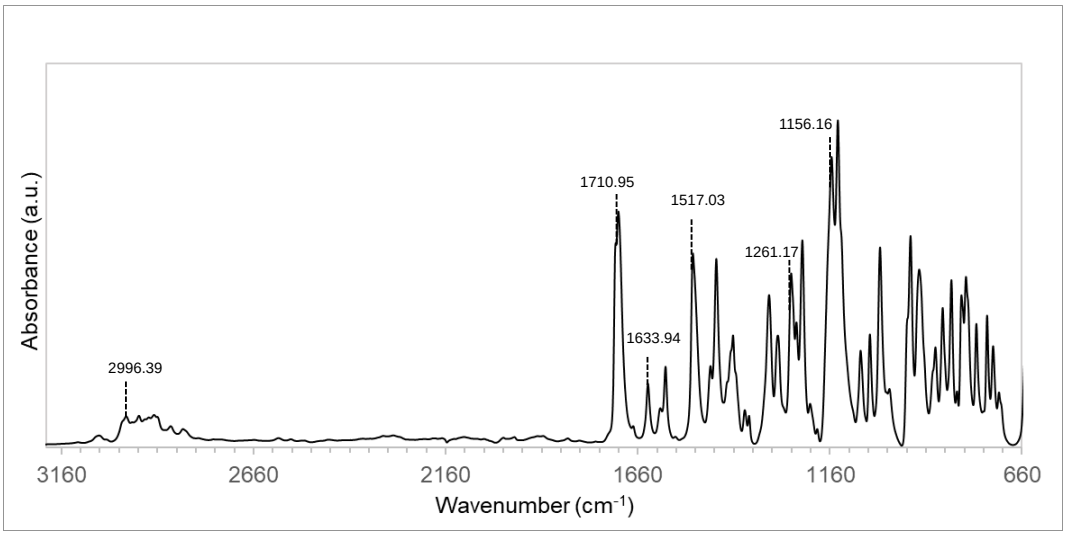

Figure A1-10. Epoxy EEMA ATR FTIR Spectrum.

ATR-FTIR (cm^{-1}): 2830-3000 (s, CH_3, CH_2 stretch), 1710.95 (s, C=O stretch), 1633.94 (w, C=C alkene stretch), 1517.03 (C=C aromatic ring stretch), 1261.17 (s, C-O stretch), 1156.16 (s, C-O stretch).

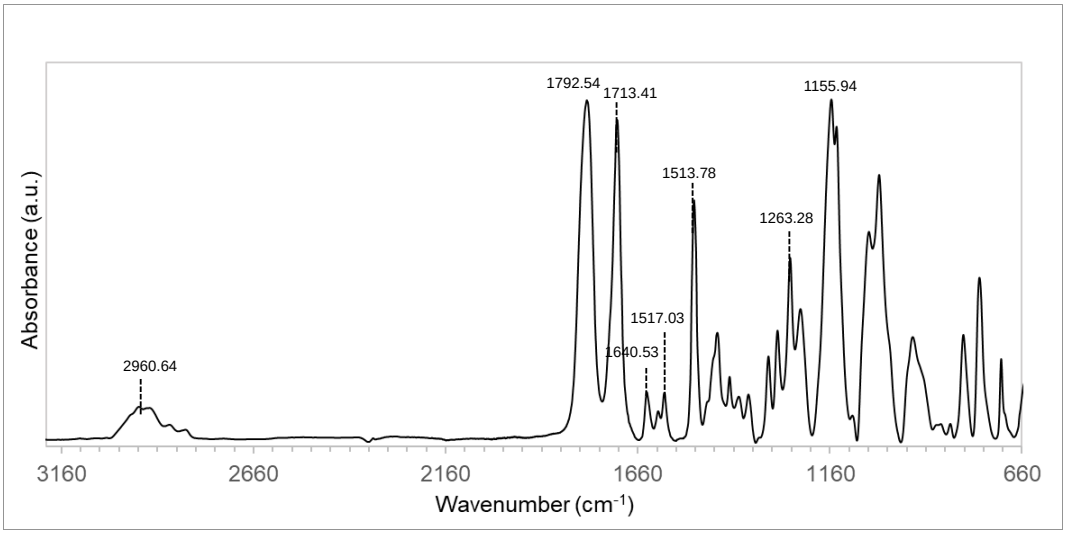

Figure A1-11. EEMA Carbonate ATR FTIR Spectrum.

ATR-FTIR (cm^{-1}): 2870-3000 (s, CH_3, CH_2 stretch), 1792.54 (s, C=O, stretch, carbonate), 1713.41 (s, C=O stretch), 1640.53 (w, C=C alkene stretch), 1587.37 (s, C=C aromatic ring stretch), 1263.28 (s, C-O stretch), 1155.94 (s, C- O stretch).

A1.2 Thermogravimetric analysis under air

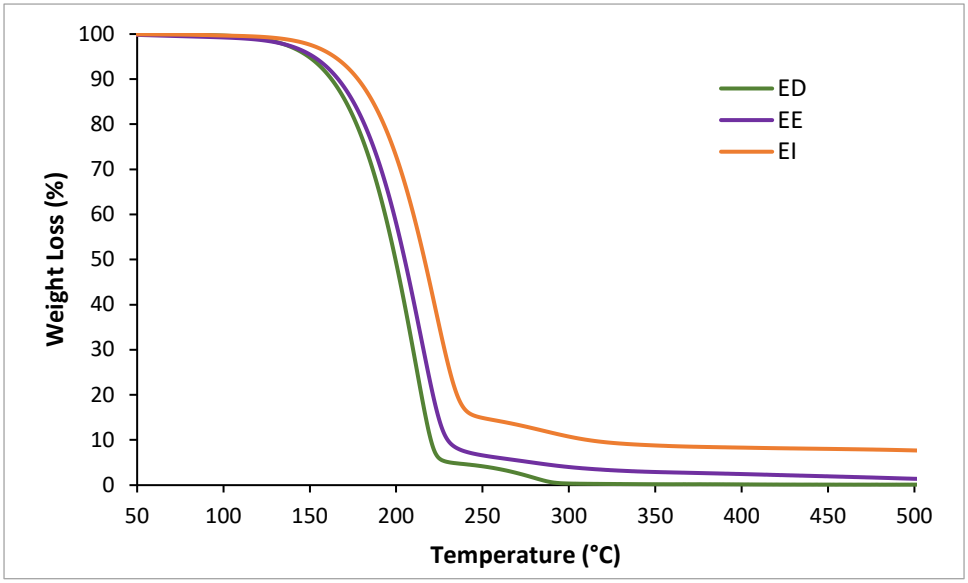

Figure A1-12. TGA (under air) of ethoxylated eugenol-derivatives.

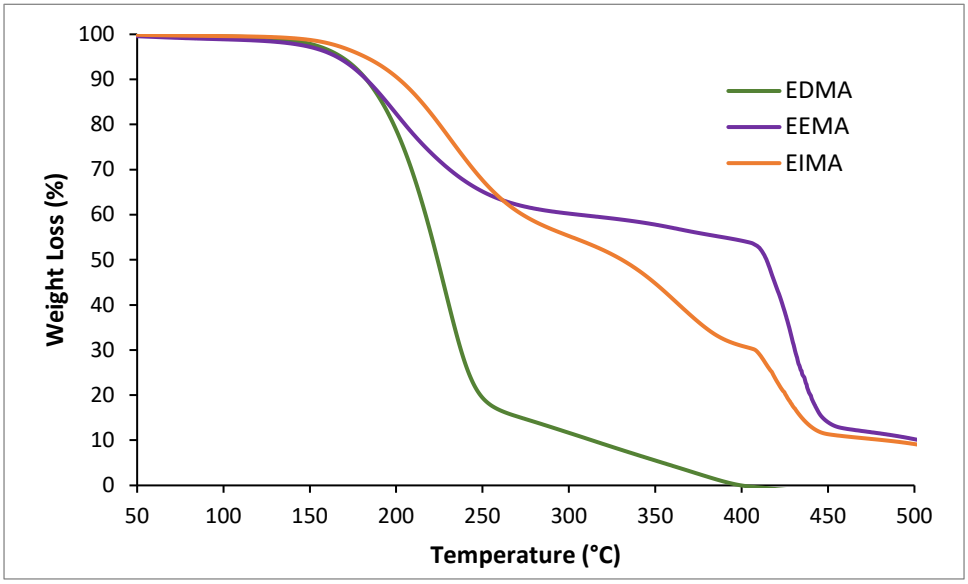

Figure A1-13. TGA (under air) of ethoxylated eugenol-derived methacrylates.

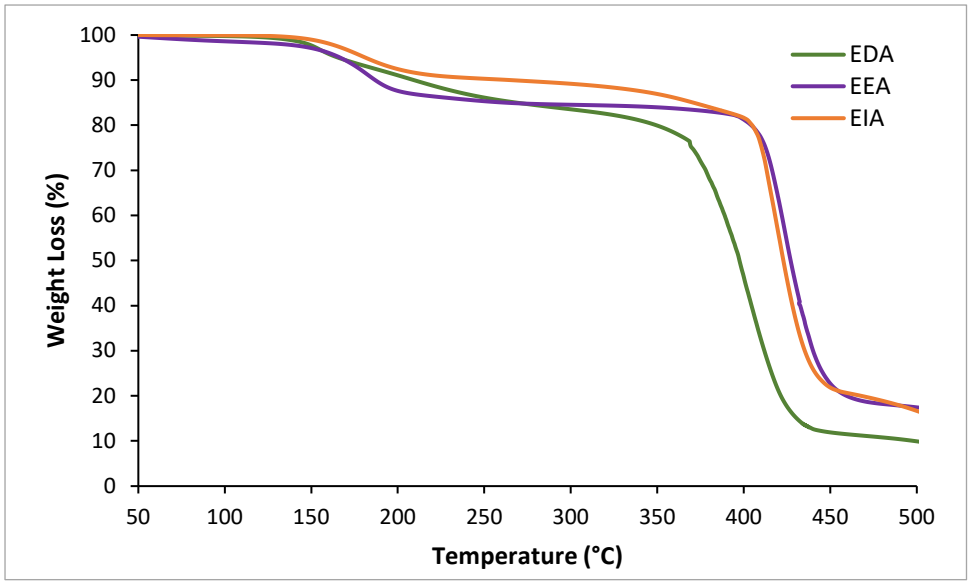

Figure A1-14. TGA (under air) of ethoxylated eugenol-derived acrylates

A1.3 Thermogravimetric analysis under N_2.

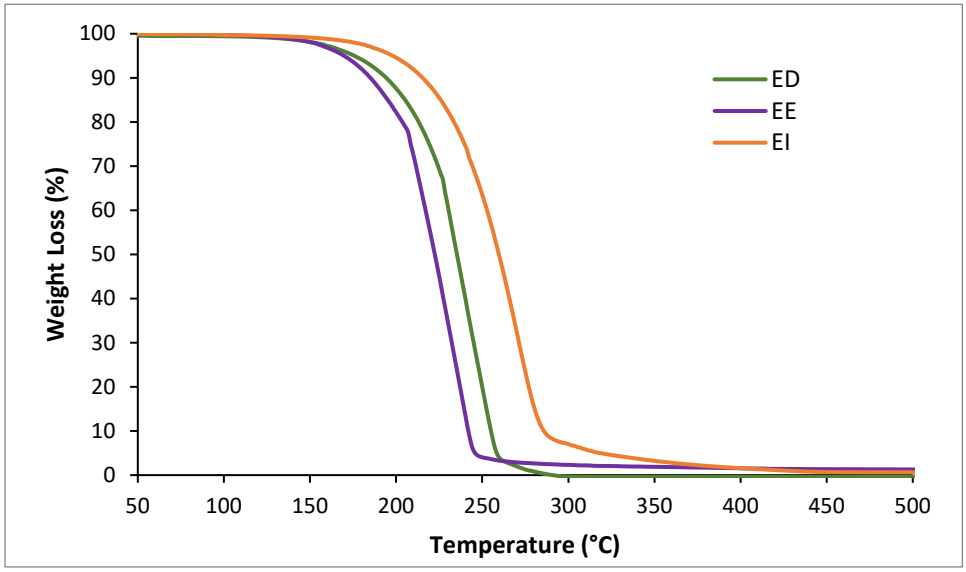

Figure A1-15. TGA (under N_2) of ethoxylated eugenol-derivatives.

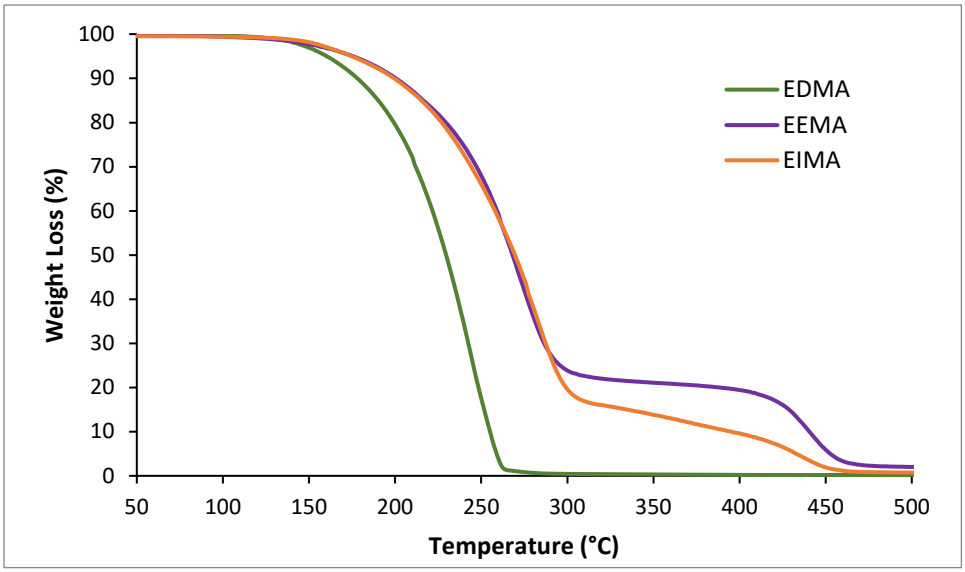

Figure A1-16. TGA (under N_2) of ethoxylated eugenol-derived methacrylates.

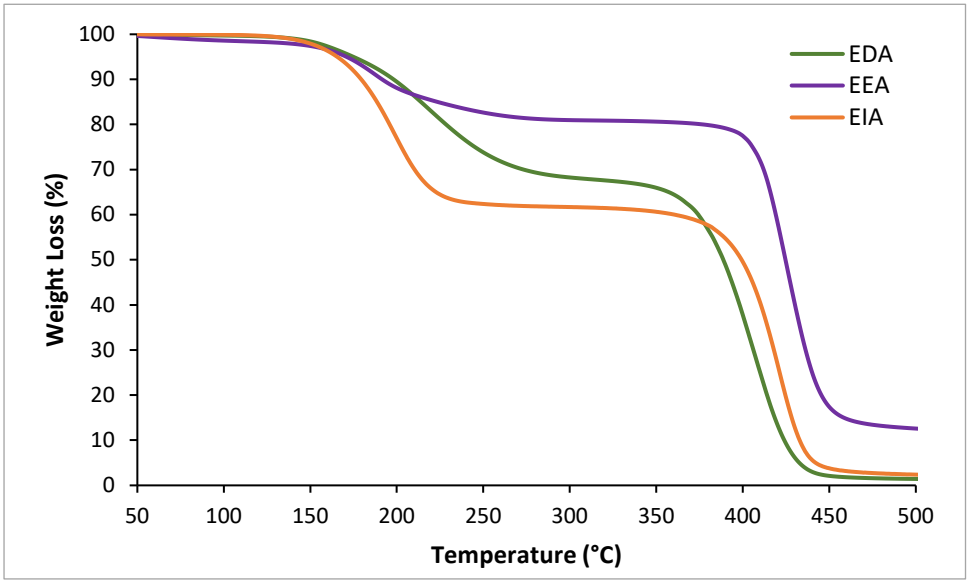

Figure A1-17. TGA (under N_2) of ethoxylated eugenol-derived acrylates.

A1.4 Melting point

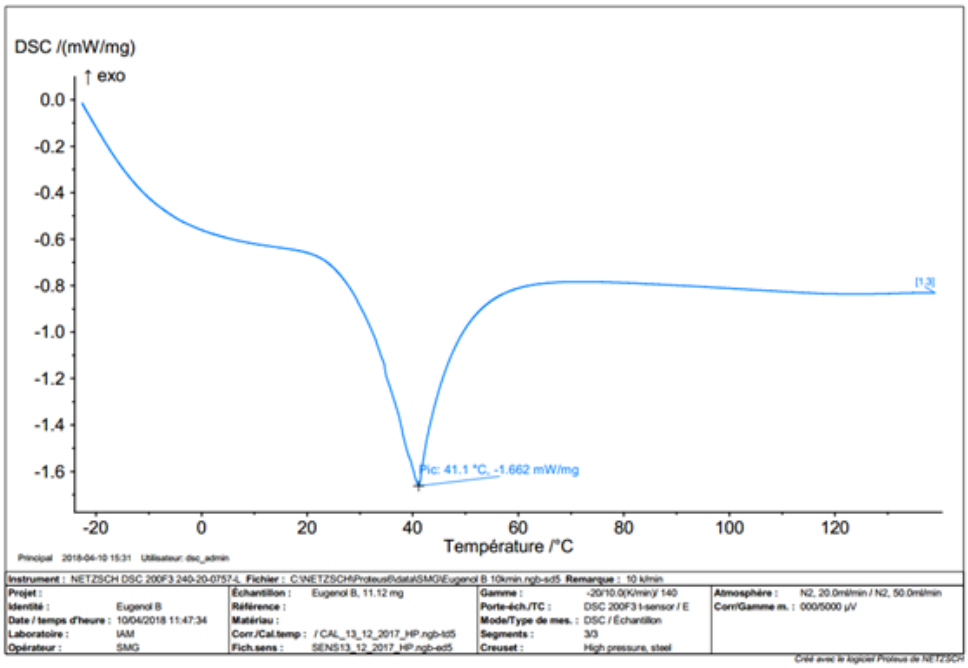

Figure A1-18. DSC of Ethoxy Eugenol (EE).

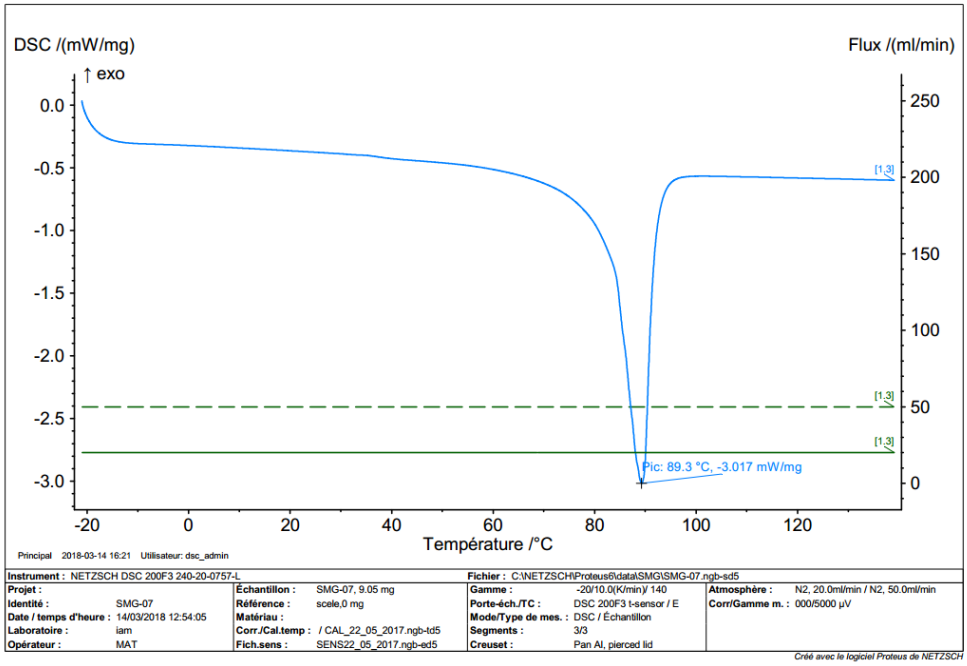

Figure A1-19. DSC of Ethoxy Isoeugenol (EI).

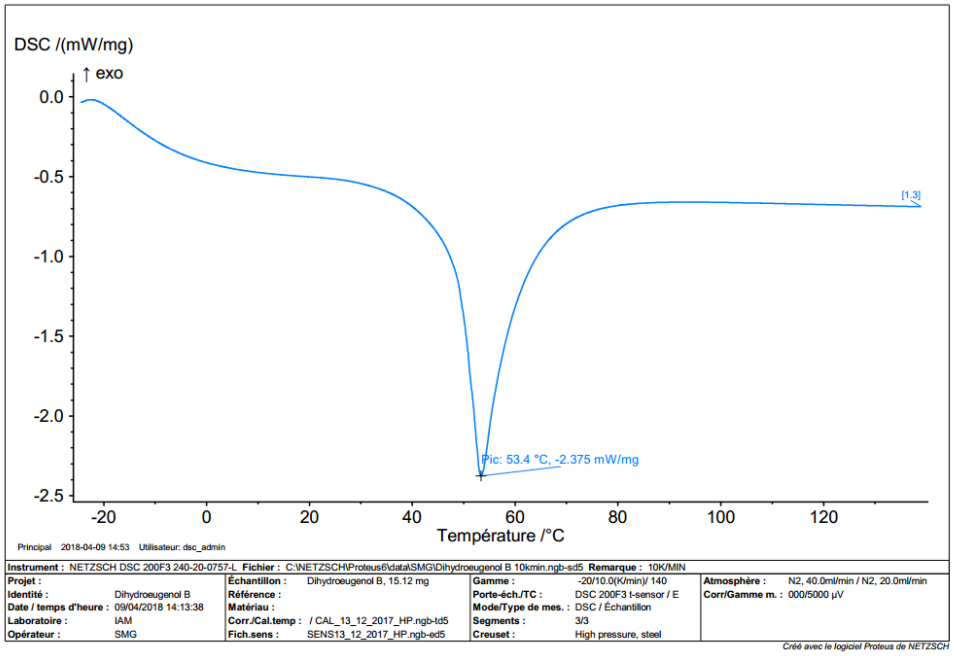

Figure A1-20. DSC of Ethoxy Dihydroeugenol (ED).

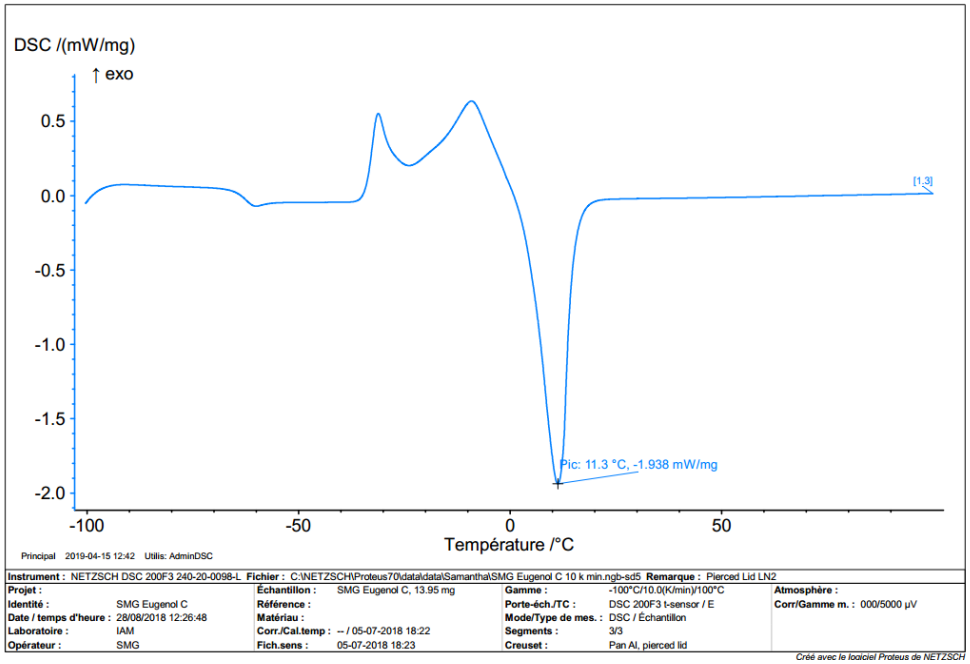

Figure A1-21. DSC of Ethoxy Eugenyl Methacrylate (EEMA).

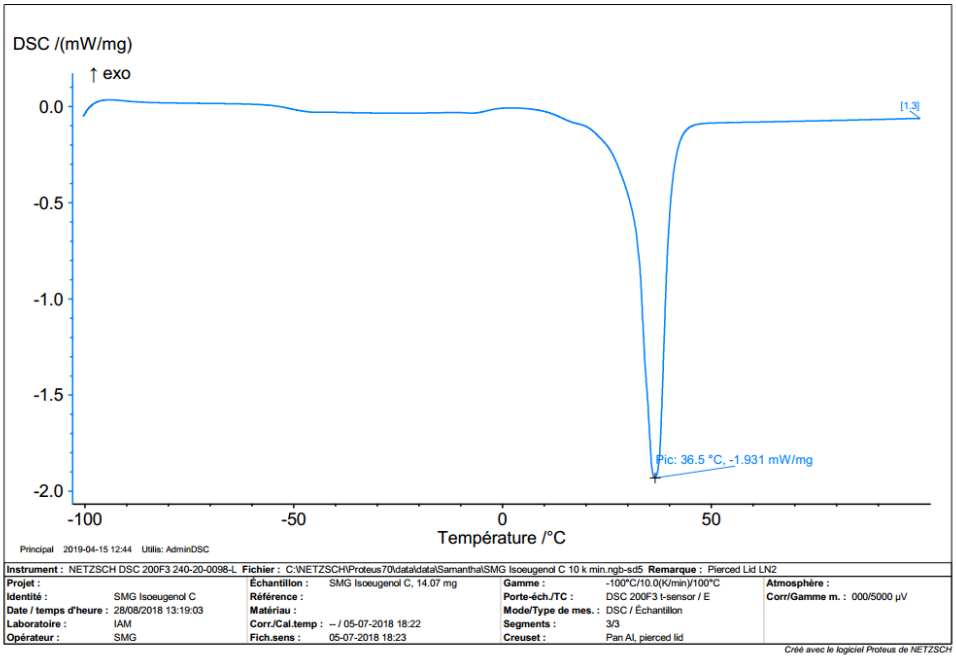

Figure A1-22. DSC of Ethoxy Isoeugenyl Methacrylate (EIMA).

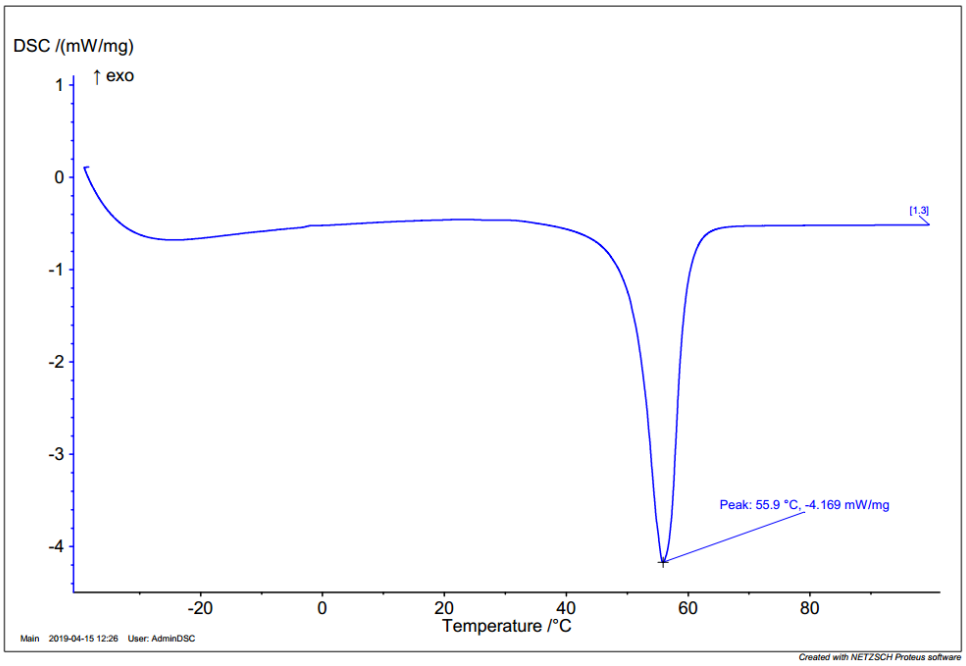

Figure A1-23. DSC of Ethoxy Isoeugenyl Acrylate (EIA).

A1.5 ^{1}H NMR

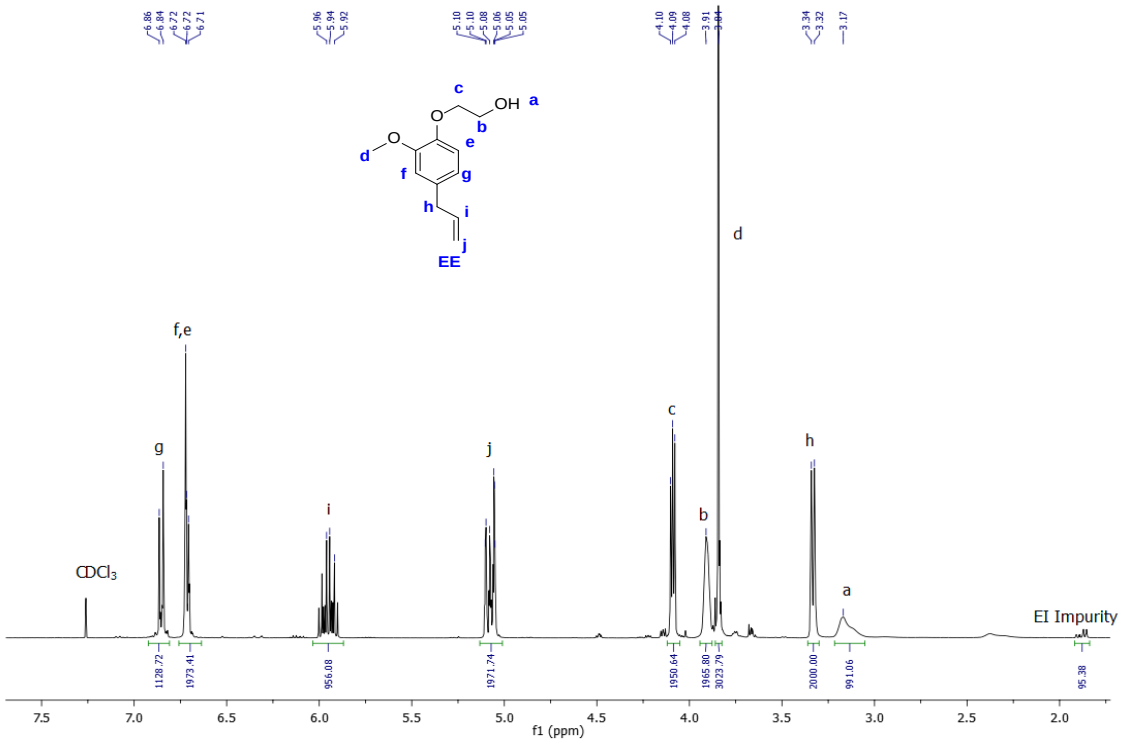

Figure A1-24. ^{1}H NMR Spectrum of Ethoxy Eugenol (EE) in $CDCl_3$.

^{1}H NMR spectrum (400 MHz, $CDCl_3$, δ, ppm): δH 7.26 ($CHCl_3$), 6.85 (d, 1H, H_5-Ar), 6.72 (m, 2H, $H_{3,6}$-Ar), 5.94 (ddt, 1H, $PhCH_2C\mathbf{H}=CH_2$), 5.08 (m, 2H, $PhCH_2CH=C\mathbf{H_2}$), 4.09 (t, 2H, $HOCH_2C\mathbf{H_2}OPh$), 3.91 (t, 2H, $HOC\mathbf{H_2}CH_2OPh$), 3.84 (s, 3H, $C\mathbf{H_3}OPh$), 3.33 (d, 2H, $PhC\mathbf{H_2}CH=CH_2$), 3.17 (s, 1H, $\mathbf{H}OCH_2CH_2OPh$)

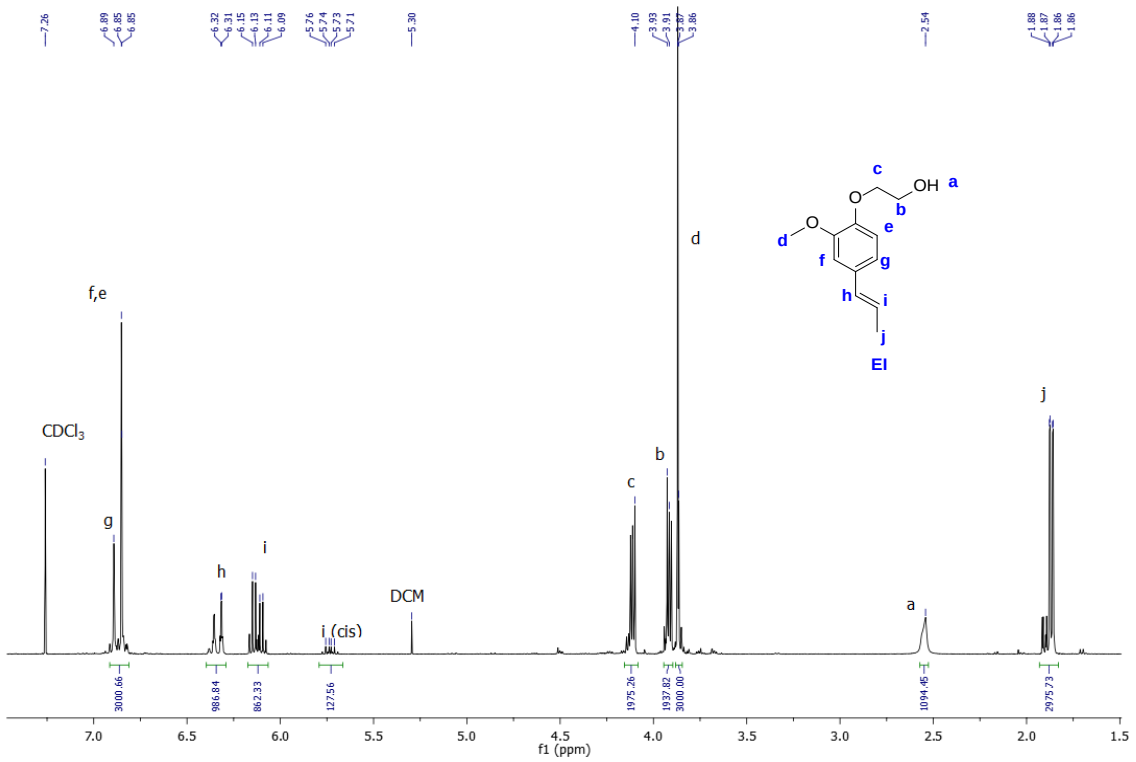

Figure A1-25. ^{1}H NMR Spectrum of Ethoxy Isoeugenol (EI) in $CDCl_3$.

^{1}H NMR spectrum (400 MHz, $CDCl_3$, δ, ppm): δH 7.26 ($CHCl_3$), 6.89 (d, 1H, , H_5-Ar), 6.85 (2H, $H_{3,6}$-Ar), 6.32 (d, 1H, PhC**H**=CHCH$_3$), 6.12 (dq, 1H, PhCH=**CH**CH$_3$, trans, *J*= 15.6, 6.4 Hz), 5.74 (dq, 1H, PhCH=C**H**CH$_3$, cis, *J*= 11.6, 6.8 Hz), 4.10 (t, 2H, HOCH$_2$C**H$_2$**OPh), 3.91 (t, 2H, HOC**H$_2$**CH$_2$OPh), 3.86 (s, 3H, C**H$_3$**OPh), 2.54 (s, **H**OCH$_2$CH$_2$OPh) 1.86 (d, 3H, PhCH=CHC**H$_3$**, cis-trans).

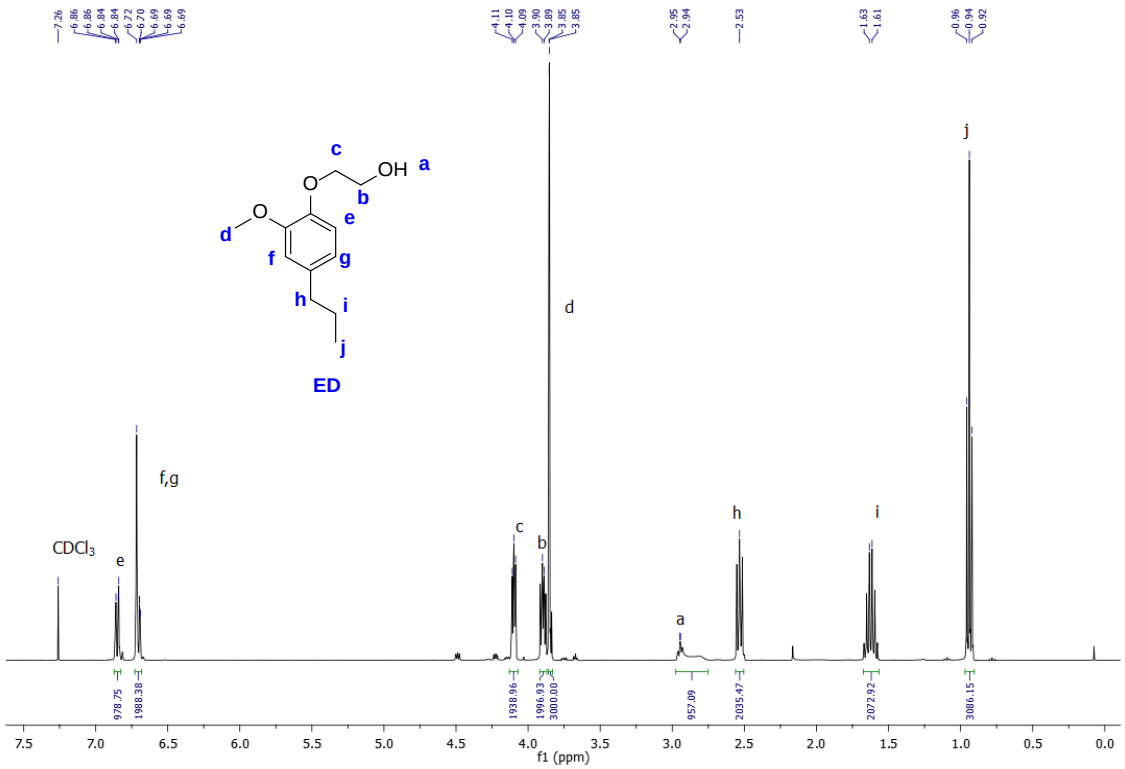

Figure A1-26. ^{1}H NMR Spectrum of Ethoxy Dihydroeugenol (ED) in $CDCl_3$.

^{1}H NMR spectrum (400 MHz, $CDCl_3$, δ, ppm): δH 7.26 ($CHCl_3$), 6.86 (d, 1H, H_6-Ar), 6.69 (m, 2H, $H_{3,5}$-Ar), 4.10 (t, 2H, $HOCH_2C\mathbf{H_2}OPh$), 3.90 (t, 2H, $HOC\mathbf{H_2}CH_2OPh$), 3.85 (s, 3H, $C\mathbf{H_3}OPh$), 2.94 (s, $\mathbf{H}OCH_2CH_2OPh$) , 2.53 (t, 2H, $CH_3CH_2C\mathbf{H_2}Ph$), 1.62 (sex, 2H, $CH_3C\mathbf{H_2}CH_2Ph$), 0.94 (t, 3H, $C\mathbf{H_3}CH_2CH_2Ph$).

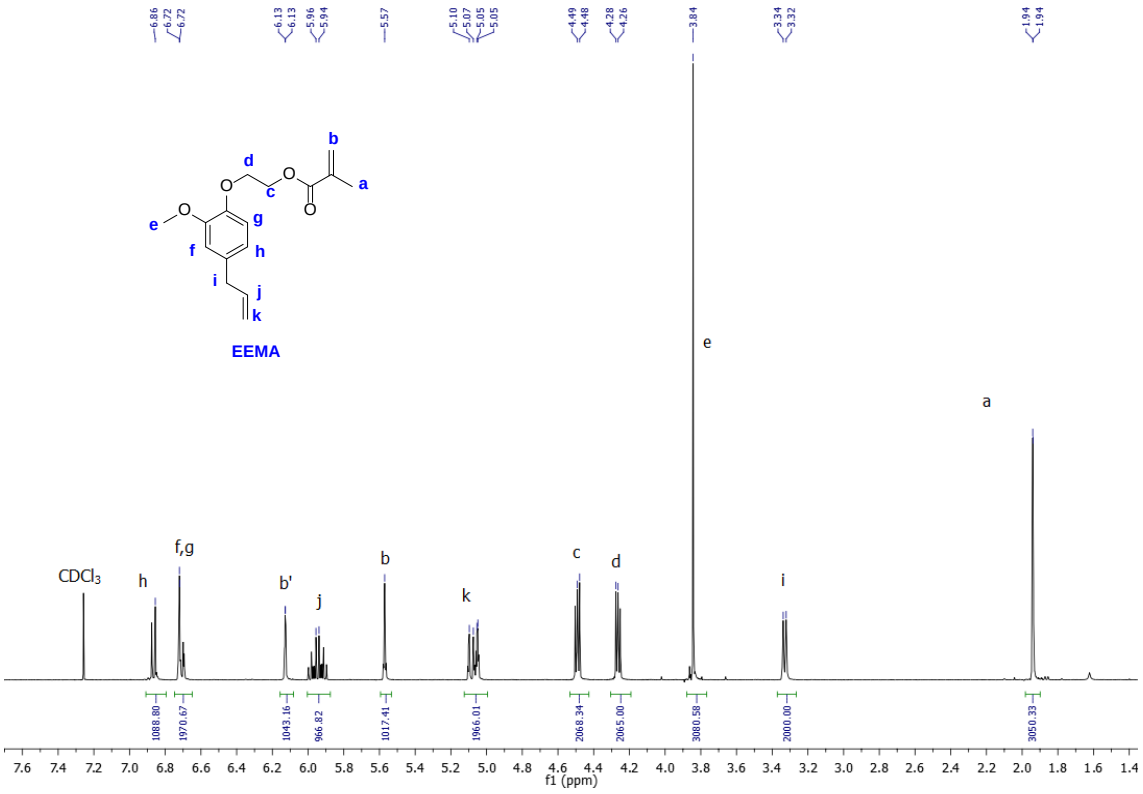

Figure A1-27. ^{1}H NMR Spectrum of Ethoxy Eugenyl Methacrylate (EEMA) in $CDCl_3$.

^{1}H NMR spectrum (400 MHz, $CDCl_3$, δ, ppm): δH 7.26 ($CHCl_3$), 6.86 (d, 1H, H_5-Ar), 6.72 (m, 2H, $H_{3,6}$-Ar), 6.13 (s, 1H, OC=OC(CH_3)=C**H**$_{2\alpha,\beta}$), 5.95 (ddt, 1H, PhCH_2C**H**=CH_2), 5.57 (s, 1H, OC=OC(CH_3)=C**H**$_{2\alpha,\beta}$), 5.07 (m, 2H, PhCH_2CH=C**H$_2$**), 4.48 (t, 2H, OC**H$_2$**CH_2OPh), 4.27 (t, 2H, OCH_2C**H$_2$**OPh), 3.84 (s, 3H, C**H$_3$**OPh), 3.33 (d, 2H, PhC**H$_2$**CH=CH_2), 1.94 (s, 3H, OC=OC(C**H$_3$**)=C$H_{2\alpha,\beta}$)

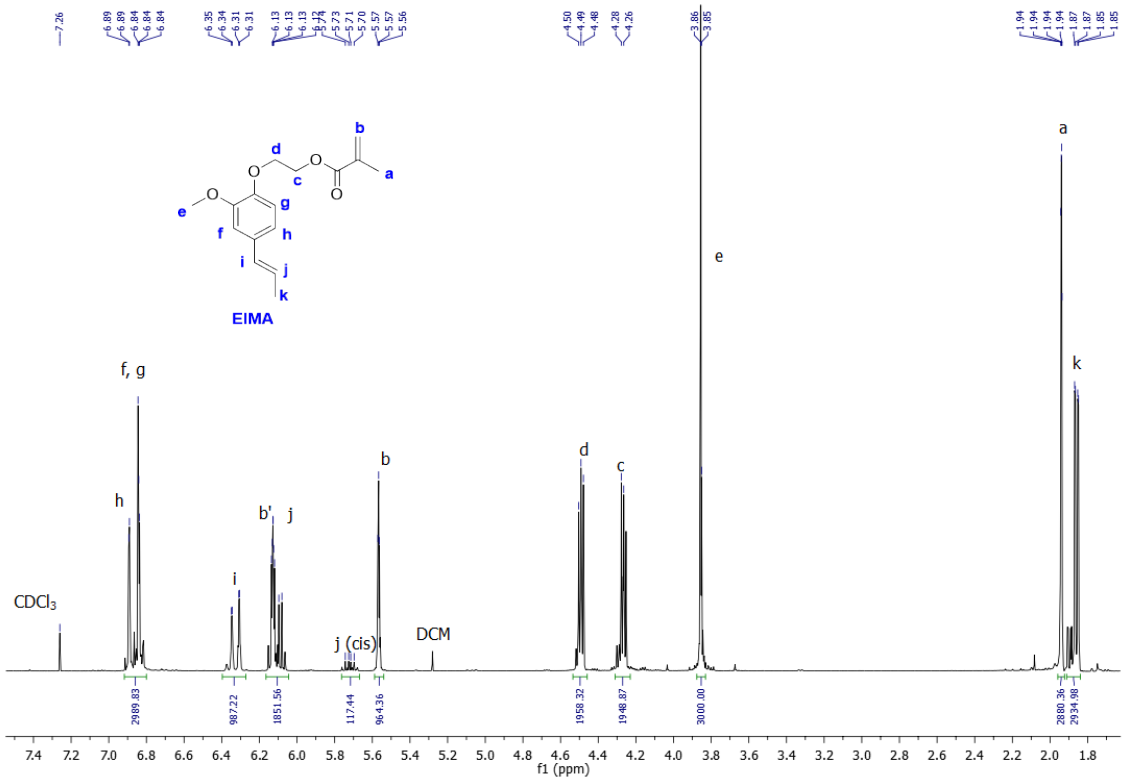

Figure A1-28. ^{1}H NMR Spectrum of Ethoxy Isoeugenyl Methacrylate (EIMA) in $CDCl_3$.

^{1}H NMR spectrum (400 MHz, $CHCl_3$, δ, ppm): δH 7.26 ($CHCl_3$), 6.87 (m, 3H, $H_{5,3,6}$-Ar), 6.33 (d, 1H, PhC**H**=CHCH$_3$), 6.13 (s, 1H, OC=OC(CH$_3$)=C**H**$_{2\alpha,\beta}$), 6.12 (dq, 1H, PhCH=C**H**CH$_3$, trans, *J*= 15.6, 6.4 Hz), 5.71 (dq, 1H, PhCH=C**H**CH$_3$, cis, *J*= 11.6, 6.8 Hz), 5.57 (s, 1H, OC=OC(CH$_3$)=C**H**$_{2\alpha,\beta}$), 4.49 (t, 2H, OC**H$_2$**CH$_2$OPh), 4.27 (t, 2H, OCH$_2$C**H$_2$**OPh), 3.86 (s, 3H, C**H$_3$**OPh), 1.94 (s, 3H, OC=OC(C**H$_3$**)=CH$_{2\alpha,\beta}$), 1.86 (d, 3H, PhCH=CHC**H$_3$**, cis-trans).

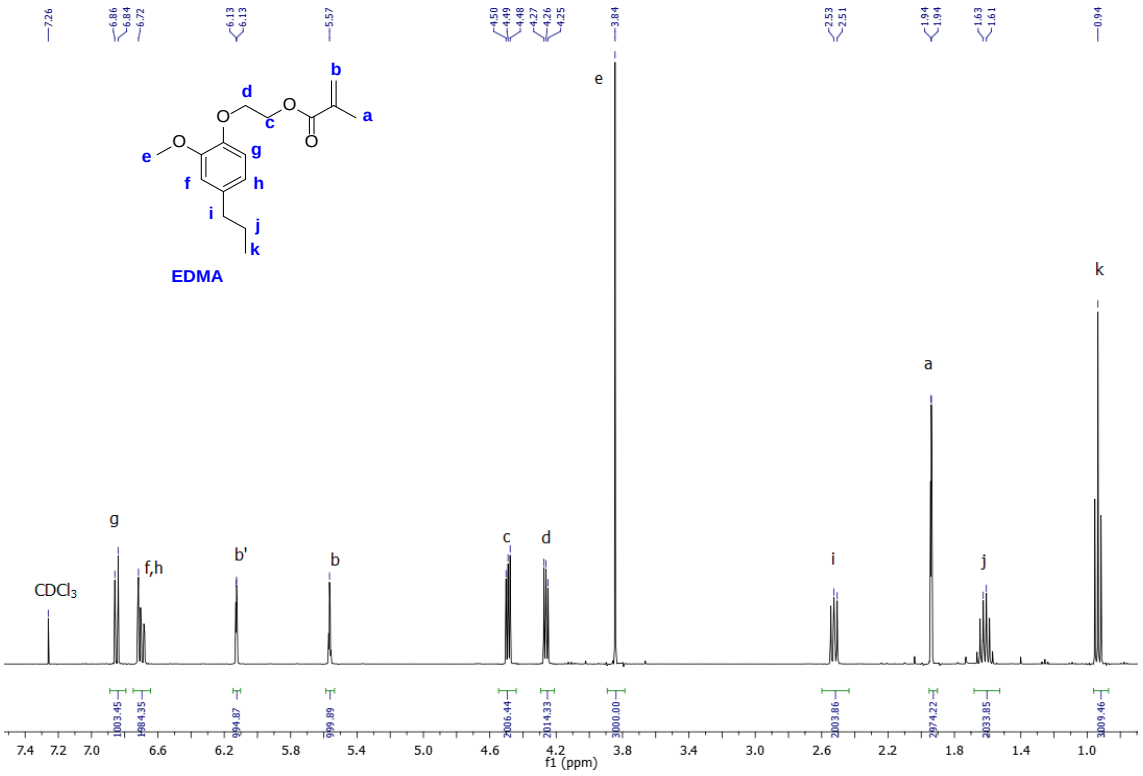

Figure A1-29. ^{1}H NMR Spectrum of Ethoxy dihydroeugenyl methacrylate (EDMA) in $CDCl_3$.

^{1}H NMR spectrum (400 MHz, $CHCl_3$, δ, ppm): δH 7.26 ($CHCl_3$), 6.85 (d, 1H, H_5-Ar), 6.72 (m, 2H, $H_{3,6}$-Ar), 6.13 (s, 1H, OC=OC(CH_3)=C**H**$_{2\alpha,\beta}$), 5.57 (s, 1H, OC=OC(CH_3)=C**H**$_{2\alpha,\beta}$), 4.49 (t, 2H, OC**H**$_2$$CH_2$OPh), 4.26 (t, 2H, O$CH_2$C**H**$_2$OPh), 3.84 (s, 3H, C**H**$_3$Oph), 2.53 (t, 2H, CH_3CH_2C**H**$_2$Ph), 1.94 (s, 1H, OC=OC(C**H**$_3$)=$CH_{2\alpha,\beta}$), 1.62 (sex, 2H, CH_3CH_2**CH**$_2$Ph), 0.94 (t, 3H, C**H**$_3$$CH_2CH_2$Ph).

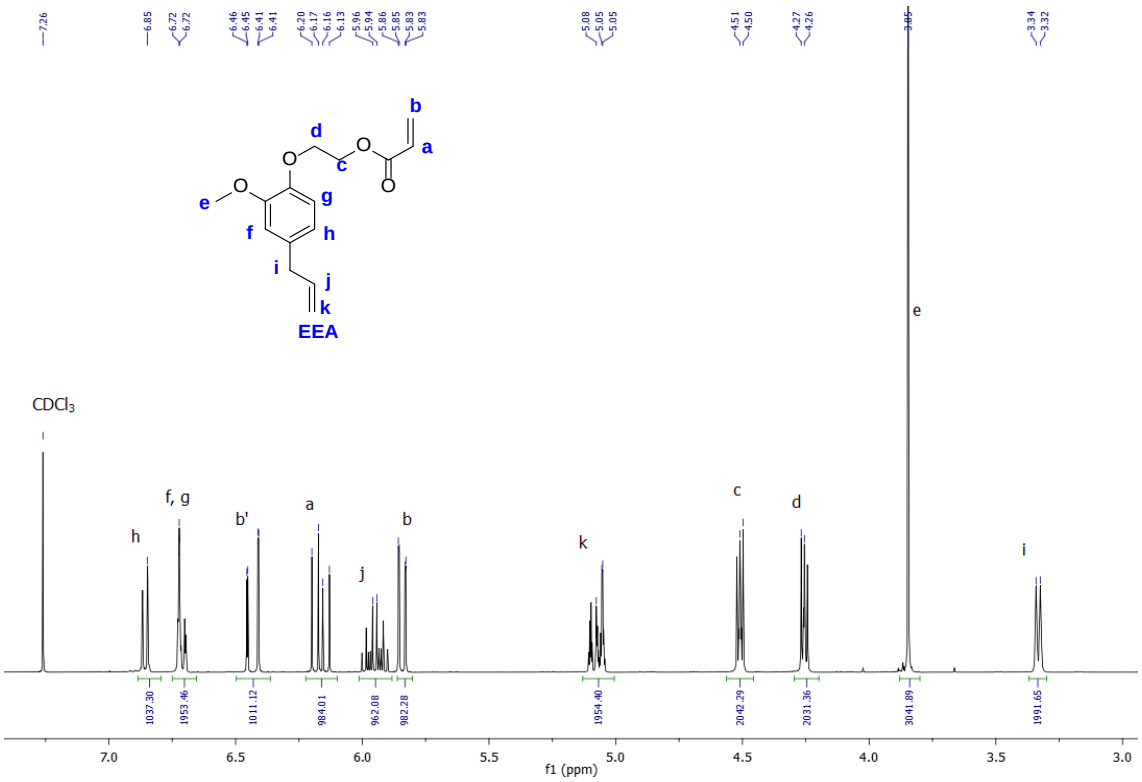

Figure A1-30. ^{1}H NMR Spectrum of Ethoxy Eugenyl Acrylate (EEA) in $CDCl_3$.

^{1}H NMR spectrum (400 MHz, $CDCl_3$, δ, ppm): δH 7.26 ($CHCl_3$), 6.85 (d, 1H, H_5-Ar), 6.72 (m, 2H, $H_{3,6}$-Ar), 6.43 (dd, 1H, OC=OCH=C**H**$_{2\alpha,\beta}$), 6.16 (dd, 1H, OC=OCH=C**H**$_{2\alpha,\beta}$), 5.95 (ddt, 1H, $PhCH_2C$**H**$=CH_2$), 5.84 (dd, 1H, OC=OC**H**$=CH_{2\alpha,\beta}$), 5.07 (m, 2H, $PhCH_2CH=C$**H**$_2$), 4.50 (t, 2H, O**C**H_2CH_2OPh), 4.26 (t, 2H, OCH_2C**H**$_2OPh$), 3.85 (s, 3H, C**H**$_3OPh$), 3.33 (d, 2H, $PhCH_2CH=C$**H**$_2$)

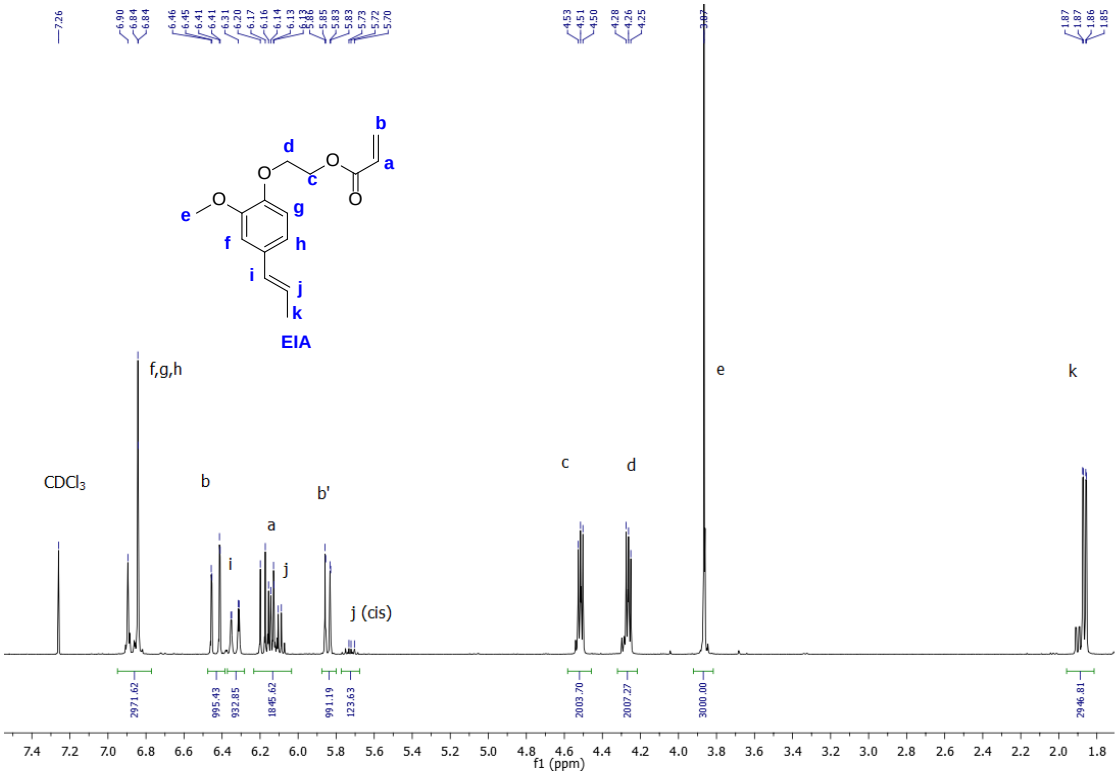

Figure A1-31. ^{1}H NMR Spectrum of Ethoxy Isoeugenyl Acrylate (EIA) in $CDCl_3$.

^{1}H NMR spectrum (400 MHz, $CHCl_3$, δ, ppm): δH 7.26 ($CHCl_3$), 6.87 (m, 3H, $H_{5,3,6}$-Ar), 6.44 (dd, 1H, OC=OCH=C**H**$_{2\alpha,\beta}$), 6.31 (dq, 1H, PhC**H**=CHCH$_3$), 6.16 (dd, 1, OC=OCH=C**H**$_{2\alpha,\beta}$), 6.10 (dq, 1H, PhCH=C**H**CH$_3$, trans, *J*=15.6, 6.4 Hz), 5.85 (dd, 1H, OC=OCH=C**H**$_{2\alpha,\beta}$), 5.72 (dq, 1H, PhCH=C**H**CH$_3$, cis, *J*=11.6, 6.8 Hz), 4.52 (t, 2H, OC**H$_2$**CH$_2$OPh), 4.27 (t, 2H, OCH$_2$C**H$_2$**OPh), 3.87 (s, 3H, C**H$_3$**OPh), 1.87 (d, 3H, PhCH=CHC**H$_3$**).

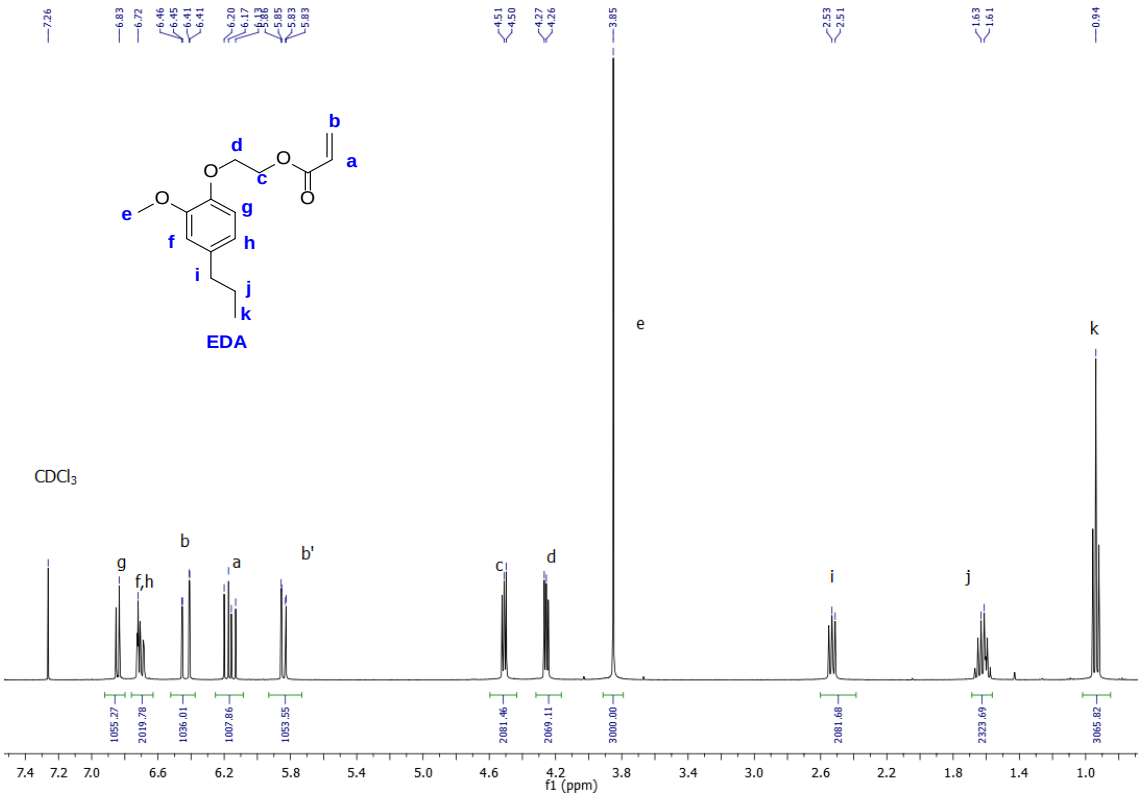

Figure A1-32. ^{1}H NMR Spectrum of Ethoxy Dihydroeugenyl Acrylate (EDA) in $CDCl_3$.

^{1}H NMR spectrum (400 MHz, $CDCl_3$, δ, ppm): δH 7.26 ($CHCl_3$), 6.83 (d, 1H, H_5-Ar), 6.72 (m, 2H, $H_{3,6}$-Ar), 6.44 (dd, 1H, OC=OCH=C**H**$_{2\alpha,\beta}$), 6.17 (dd, 1H, OC=OC**H**=$CH_{2\alpha,\beta}$), 5.83 (dd, 1H, OC=OC(CH_3)=C**H**$_{2\alpha,\beta}$), 4.50 (t, 2H, OC**H**$_2$$CH_2$OPh), 4.25 (t, 2H, OCH_2C**H**$_2$OPh), 3.85 (s, 3H, C**H**$_3$OPh), 2.53 (t, 2H, CH_3CH_2C**H**$_2$Ph, 1.62 (sex, 2H, CH_3C**H**$_2$$CH_2$Ph), 0.94 (t, 3H, C**H**$_3$$CH_2CH_2$Ph).

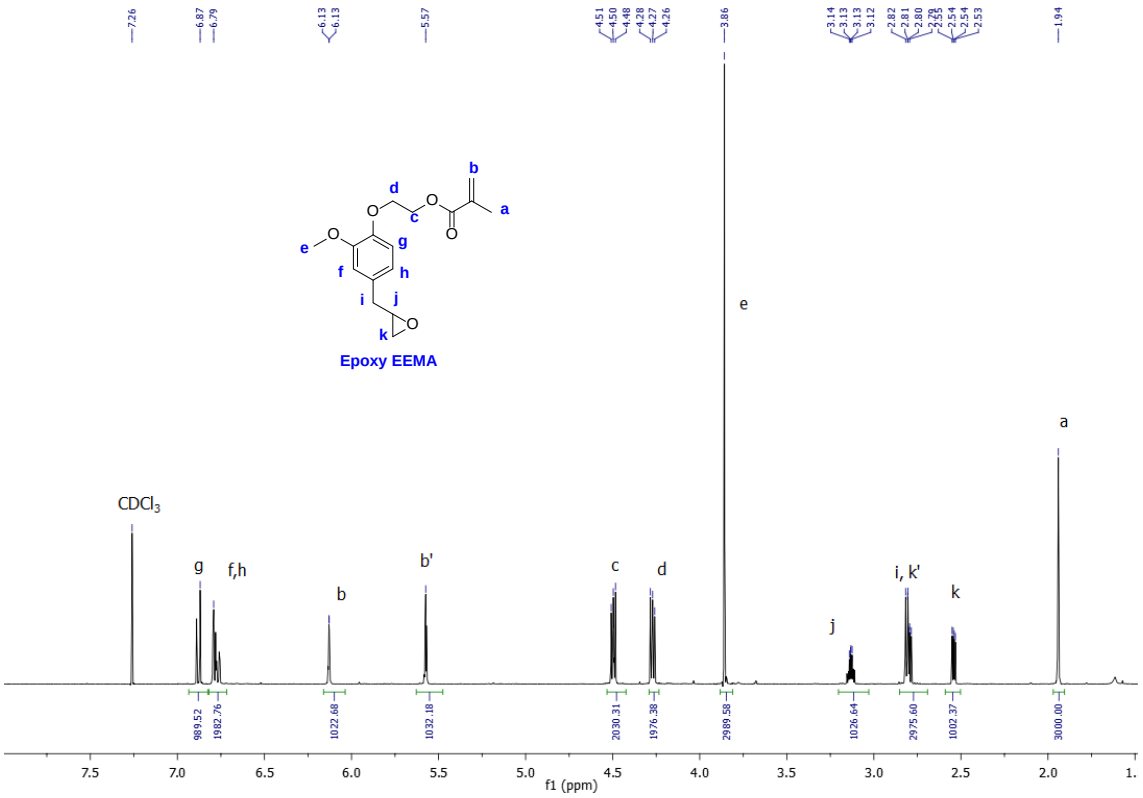

Figure A1-33. ^{1}H NMR Spectrum of Epoxy EEMA in $CDCl_3$.

^{1}H NMR spectrum (400 MHz, $CDCl_3$, δ, ppm): δH 7.26 ($CHCl_3$), 6.87 (d, 1H, H_6-Ar), 6.79 (m, 2H, $H_{3,5}$-Ar), 6.13 (dt, 1H, OC=OC(CH_3)=C**H**$_{2\alpha,\beta}$), 5.57 (dt, 1H, OC=OC(CH_3)=C**H**$_{2\alpha,\beta}$), 4.50 (t, 2H, OC**H**$_2$$CH_2$OPh), 4.27 (t,2H, OCH_2C**H**$_2$OPh), 3.86 (s, 3H, C**H**$_3$OPh), 3.13 (ddt, 1H, $PhCH_2$C**H**O(CH_2)), 2.81 (m, 2H, PhC**H**$_2$CHO(CH_2)), 2.82-2.54 (m, 2H, $PhCH_2$CHO(C**H**$_2$)), 1.94 (s, 3H, OC=OC(C**H**$_3$)=$CH_{2\alpha,\beta}$).

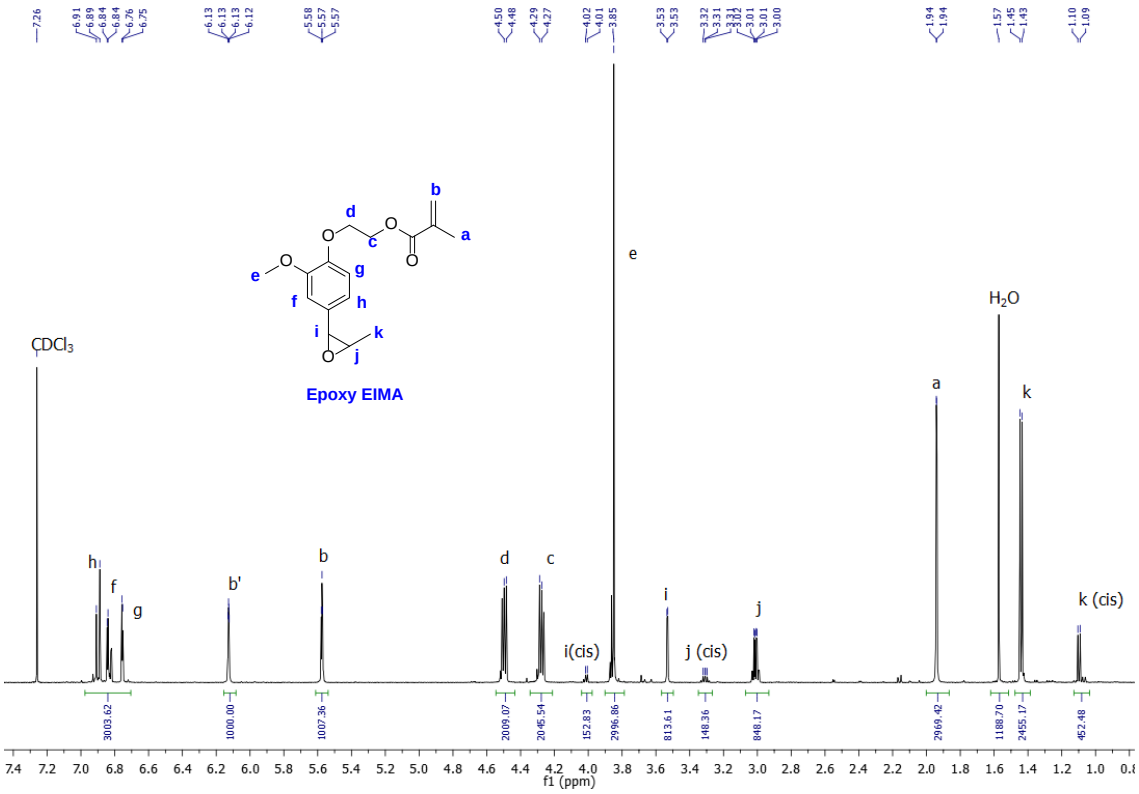

Figure A1-34. ^{1}H NMR Spectrum of Epoxy EIMA in $CDCl_3$.

^{1}H NMR spectrum (400 MHz, $CDCl_3$, δ, ppm): δH 7.26 ($CHCl_3$), 6.90 (d, 1H, H_6-Ar), 6.84 (d, 1H, H_5-Ar), 6.76 (d, 1H, H_5-Ar), 6.13 (dt, 1H, OC=OC(CH_3)=C**H**$_{2\alpha,\beta}$), 5.57 (dt, 1H, OC=OC(CH_3)=C**H**$_{2\alpha,\beta}$), 4.50 (t, 2H, OC**H**$_2$$CH_2$OPh), 4.27 (t,2H, OC$H_2$C**H**$_2$OPh), 4.02 (d, 1H, Ph**C**H(O1)CH(O1)CH_2, *cis*), 3.85 (s, 3H, C**H**$_3$OPh), 3.53 (d, 1H, Ph**C**H(O1)CH(O1)CH_2), 3.31 (qd, 1H, PhCH(O1)**C**H(O1)CH_2, *cis*), 3.01 (qd, 1H, PhCH(O1)**C**H(O1)CH_2), 1.94 (s, 3H, OC=OC(C**H**$_3$)=$CH_{2\alpha,\beta}$), 1.57 (H_2O), 1.43 (d, 2H, PhCH(O1)CH(O1)C**H**$_2$), 1.10 (d, 2H, PhCH(O1)CH(O1)C**H**$_2$,*cis*)

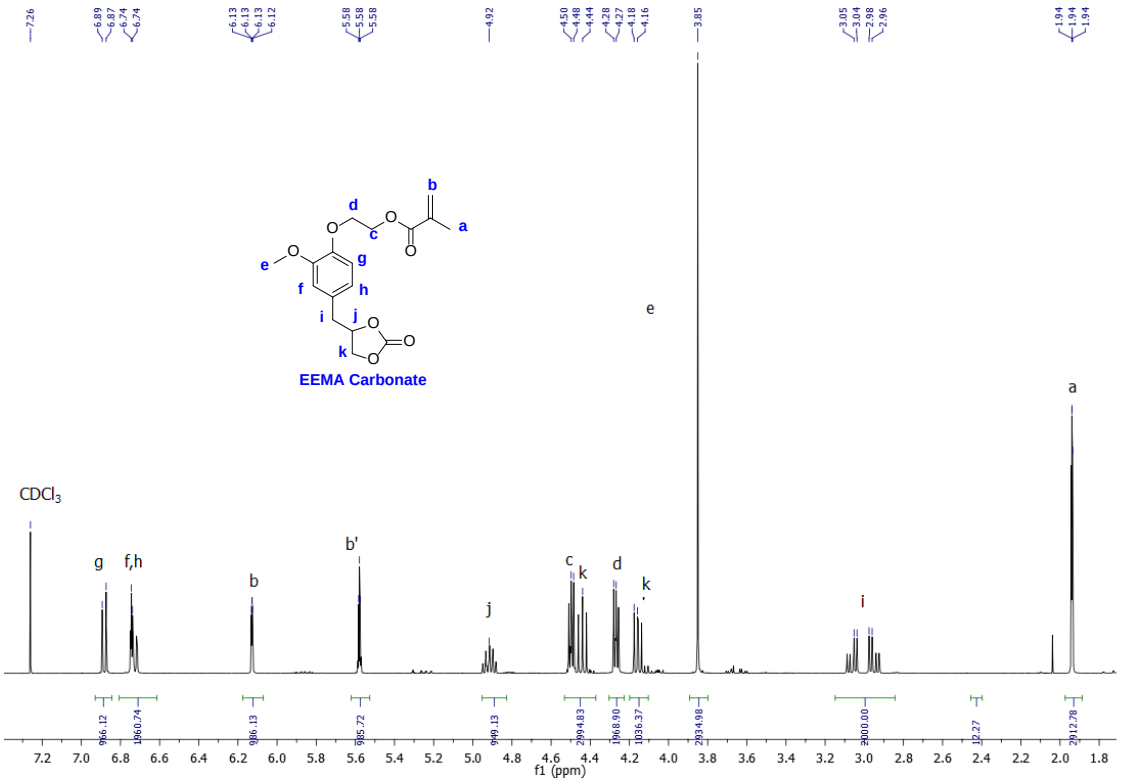

Figure A1-35. ^{1}H NMR Spectrum of EEMA Carbonate in $CDCl_3$.

^{1}H NMR spectrum (400 MHz, $CDCl_3$, δ, ppm): δH 7.26 ($CHCl_3$), 6.88 (d, 1H, H_6-Ar), 6.74 (m, 2H, $H_{3,5}$-Ar), 6.13 (dt, 1H, OC=OC(CH_3)=C**H**$_{2\alpha,\beta}$), 5.58 (dt, 1H, OC=OC(CH_3)=C**H**$_{2\alpha,\beta}$), 4.92 (dt, 1H, PhCH_2C**H**(O)CH_2(O)), 4.50 (t, 2H, OC**H$_2$**CH_2OPh), 4.44 (dd, 1H, PhC$H_{2\alpha,\beta}$CH(O)C**H$_{2\alpha,\beta}$**(O)), 4.27 (t, 'H, OCH_2C**H$_2$**OPh), 4.16 (dd, 1H, PhCH_2CH(O)C**H$_{2\ \alpha,\beta}$**(O)), 3.85 (s, 3H, C**H$_3$**OPh), 3.03 (dd, 1H, PhC**H$_{2\alpha,\beta}$**CH(O)C$H_{2\alpha,\beta}$(O)), 2.95 (dd, 1H, PhC**H$_{2\alpha,\beta}$**CH(O)C$H_{2\alpha,\beta}$(O)), 1.94 (s, 3H, OC=OC(C**H$_3$**)=C$H_{2\alpha,\beta}$).

A1.6 ^{13}C NMR

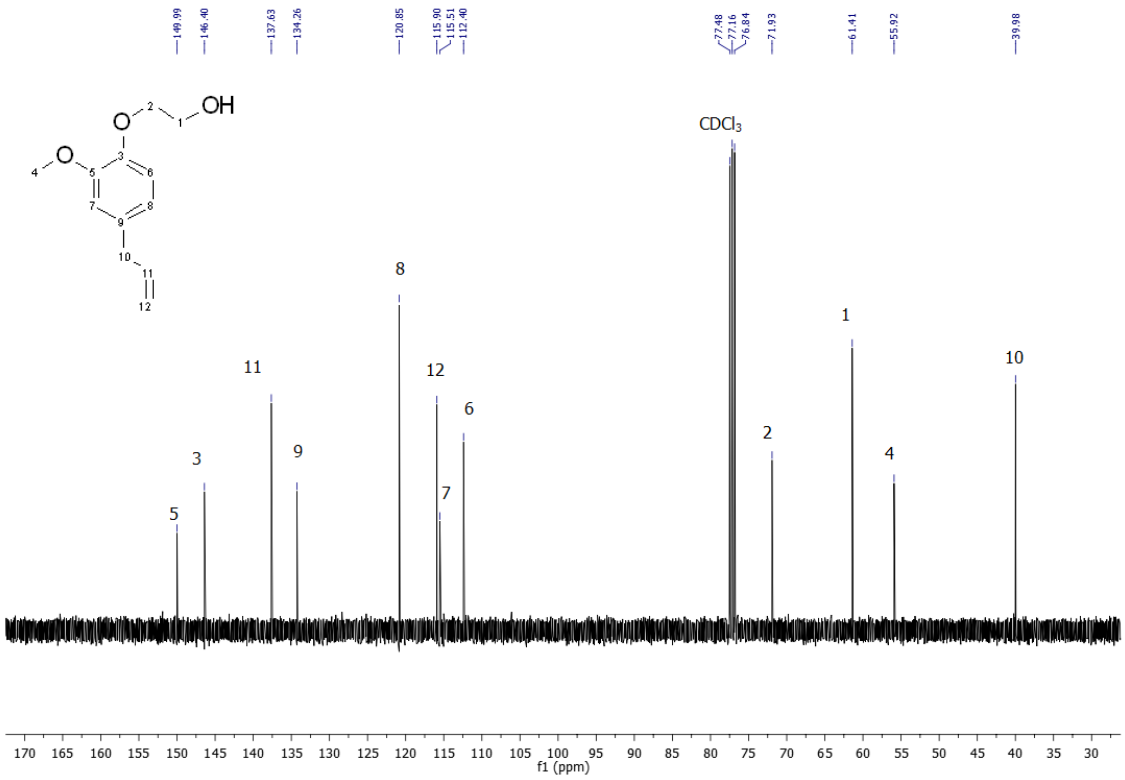

Figure A1-36. ^{13}C NMR Spectrum of Ethoxy Eugenol (EE) in $CDCl_3$.

^{13}C NMR spectrum (CDCl3): δC 149.99 (**C_2**-Ar), 146.40 (**C_1**-Ar), 137.63 ($PhCH_2$**C**$H=CH_2$), 134.26 (**C_4**-Ar), 120.85 (**C_5**-Ar), 115.90 ($PhCH_2CH=$**C**H_2), 115.51 (**C_6**-Ar), 112.40 (**C_3**-Ar), 77.16 ($CDCl_3$), 71.93 ($HOCH_2$**C**H_2OPh), 61.41 (HO**C**H_2CH_2OPh), 55.92 (**C**H_3O Ph), 39.98 (Ph**C**$H_2CH=CH_2$).

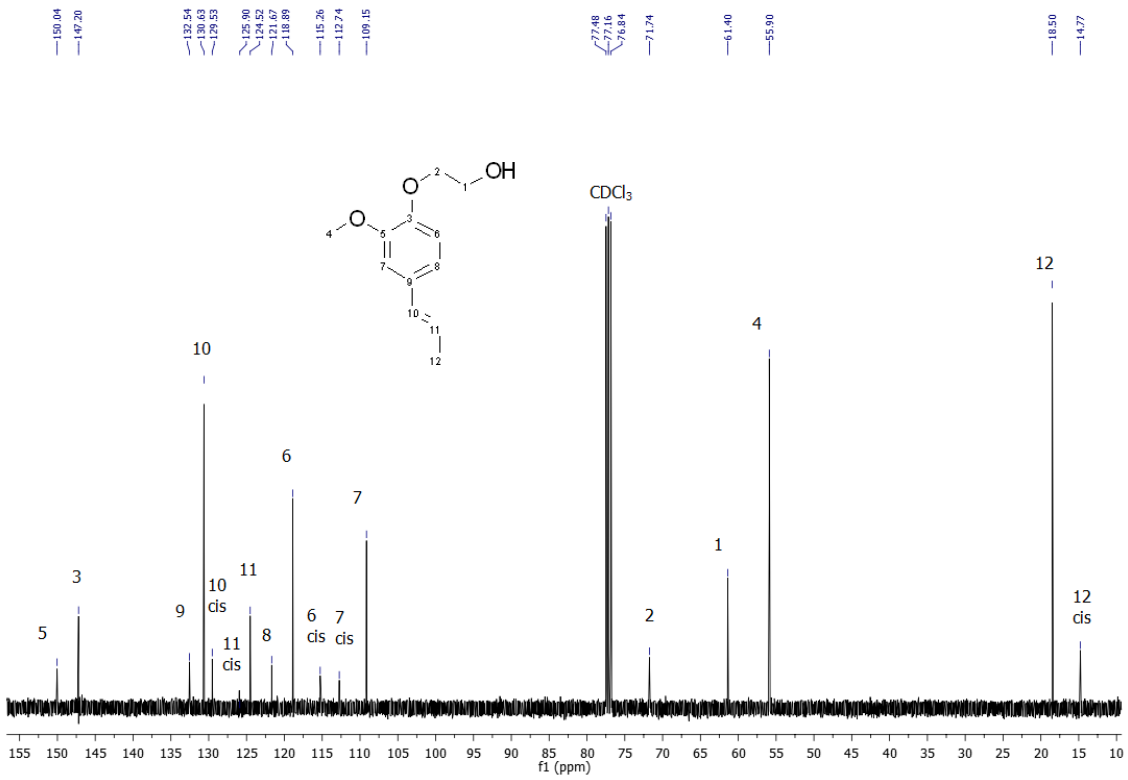

Figure A1-37. ^{13}C NMR Spectrum of Ethoxy Isoeugenol (EI) in $CDCl_3$.

^{13}C NMR spectrum ($CDCl_3$): δC 150.04 (**C_2**-Ar), 147.20 (**C_1**-Ar), 132.54 (**C_4**-Ar), 130.63 (Ph**C**H=CHCH$_3$), 129.53 (Ph**C**H=CHCH$_3$, cis), 125.90 (PhCH=**C**HCH$_3$, cis), 124.52 (PhCH=**C**HCH$_3$, trans), 121.67 (**C_5**-Ar), 118.89 (**C_6**-Ar, trans), 115.26 (**C_6**-Ar, cis), 112.74 (**C_3**-Ar, cis), 109.15 (**C_3**-Ar, trans), 77.16($CDCl_3$), 71.74 (HOCH$_2$**C**H$_2$OPh), 61.40 (HO**C**H$_2$CH$_2$OPh), 55.90 (**C**H$_3$OPh), 18.50 (PhCH=CH**C**H$_3$), 14.77 (PhCH=CH**C**H$_3$, cis).

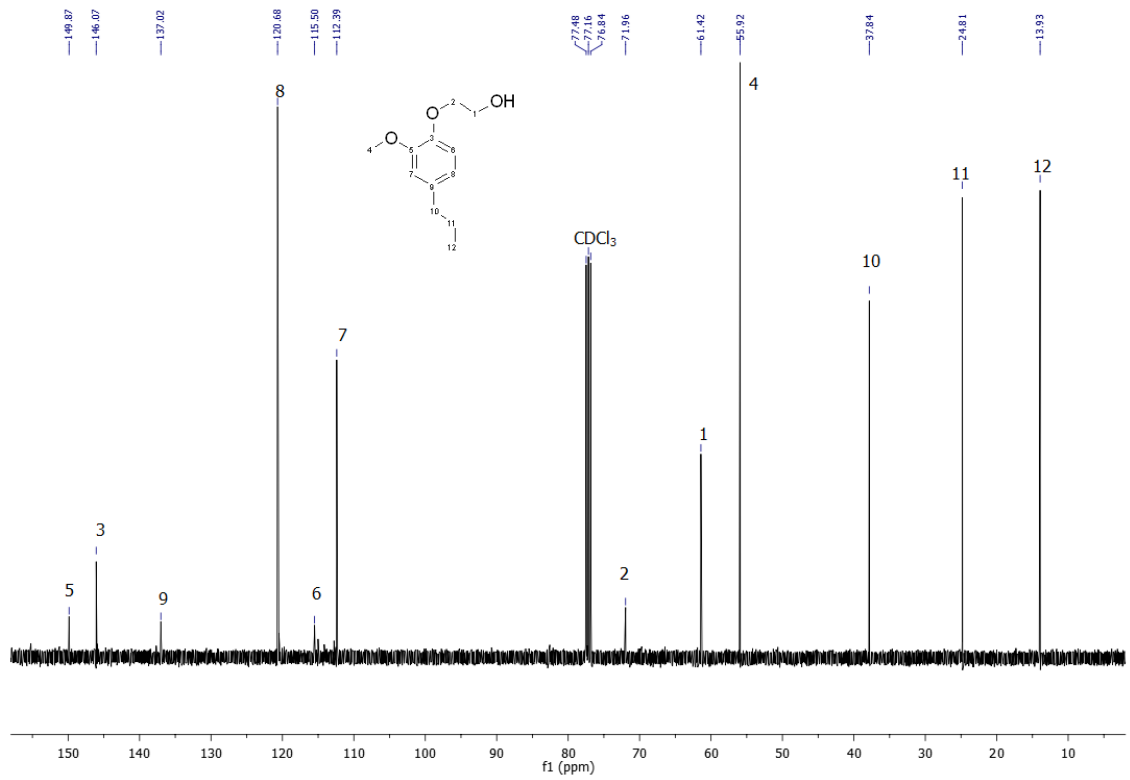

Figure A1-38. ^{13}C NMR Spectrum of Ethoxy Dihydroeugenol (ED) in $CDCl_3$.

^{13}C NMR spectrum ($CDCl_3$): δC 149.87 (**C_2**-Ar), 146.07 (**C_1**-Ar), 137.02 (**C_4**-Ar), 120.68 (**C_5**-Ar), 115.50 (**C_6**-Ar), 112.39 (**C_3**-Ar), 77.16 ($CDCl_3$), 71.96 ($HOCH_2$**C**H_2OPh), 61.42 (HO**C**H_2CH_2OPh), 55.92 (**C**H_3OPh), 37.84 (CH_3CH_2**C**H_2Ph), 24.81 (CH_3**C**H_2CH_2Ph), 13.93(**C**$H_3CH_2CH_2Ph$).

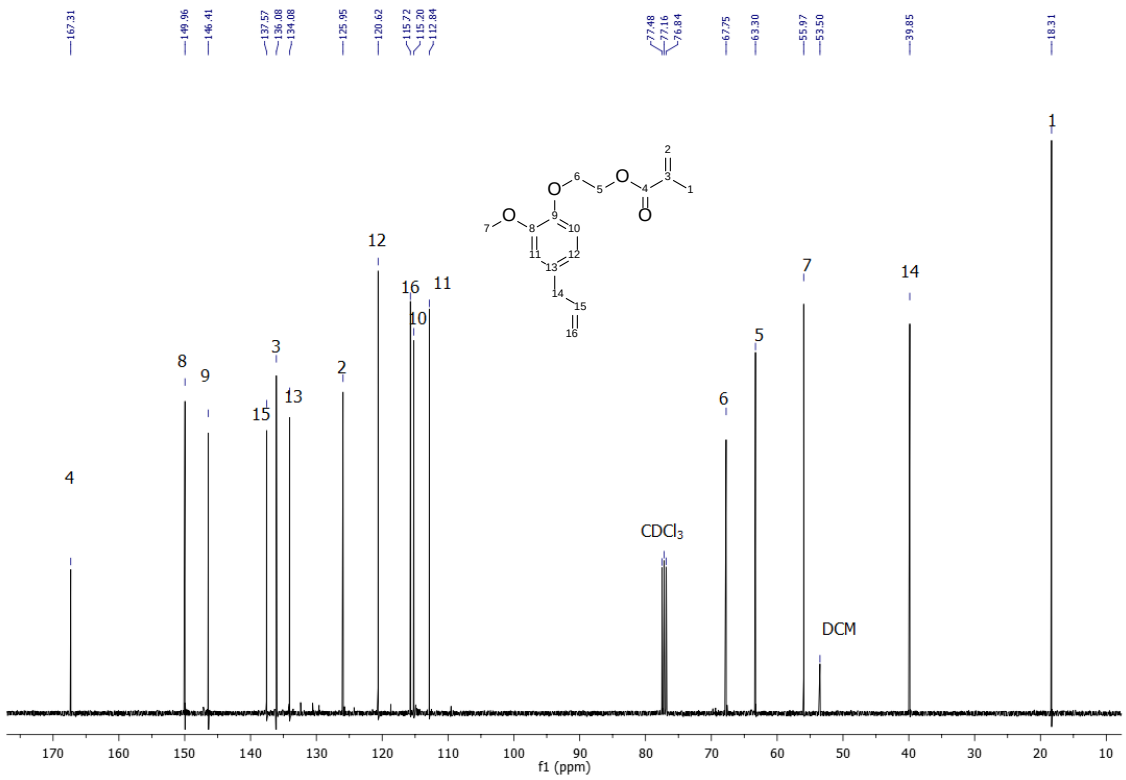

Figure A1-39. ^{13}C NMR Spectrum of Ethoxy Eugenyl Methacrylate (EEMA) in $CDCl_3$.

^{13}C NMR spectrum ($CDCl_3$): δC 167.21 (O**C**=OC(CH_3)=CH_2), 149.96 (**C_2**-Ar), 146.41 (**C_1**-Ar), 137.57 (PhC**H_2**CH=CH_2), 136.08 (OC=O**C**(CH_3)=CH_2), 134.08 (**C_4**-Ar), 125.95 (OC=OC(CH_3)=**C**H_2), 120.62 (**C_5**-Ar), 115.72 (PhCH_2CH=**C**H_2), 115.20 (**C_6**-Ar), 112.84 (**C_3**-Ar), 77.16 ($CDCl_3$), 67.75 (OCH_2**C**H_2OPh), 63.30 (O**C**H_2CH_2OPh), 55.97 (**C**H_3OPh), 39.85 (Ph**C**H_2CH=CH_2) 18.31 (OC=OC(**C**H_3)=CH_2).

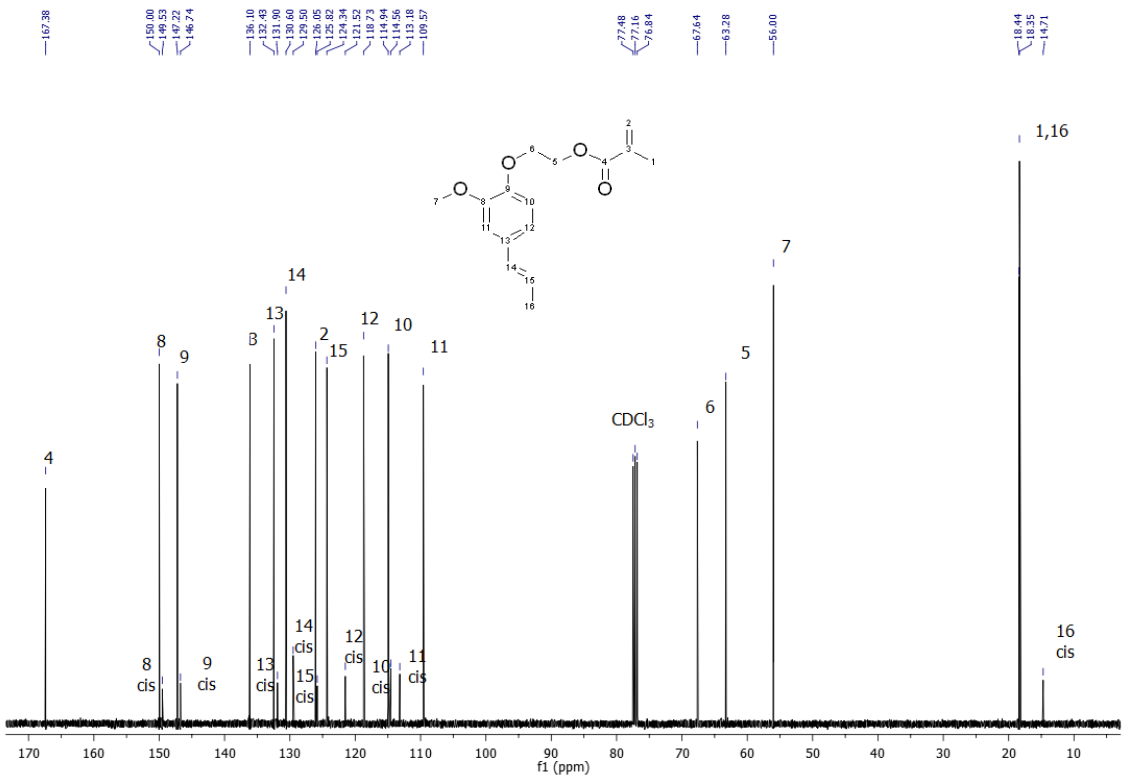

Figure A1-40. ^{13}C NMR Spectrum of Ethoxy Isoeugenyl Methacrylate (EIMA) in $CDCl_3$.

^{13}C NMR spectrum ($CDCl_3$): δC 167.38 (O**C**=OC(CH_3)=CH_2), 150.00 (**C_2**-Ar, trans), 149.53 (**C_2**-Ar, cis), 147.22 (**C_1**-Ar, trans), 146.74 (**C_1**-Ar, cis), 136.10 (OC=O**C**(CH_3)=CH_2), 132.43 (**C_4**-Ar, trans), 131.90 (**C_4**-Ar, cis) 130.60 (Ph**C**H=CHCH_3, trans), 129.50 (Ph**C**H=CHCH_3, cis), 126.05 (OC=OC(CH_3)=**C**H_2), 125.82 (PhCH=**C**HCH_3, cis), 124.34 (PhCH=**C**HCH_3, trans), 121.52 (**C_5**-Ar, cis), 118.73(**C_5**-Ar, trans), 114.94 (Ph**C**H=CHCH_3, trans), 114.56 (Ph**C**H=CHCH_3, cis) 113.18 (**C_3**-Ar, cis), 109.57 (**C_3**-Ar, trans), 77.16 ($CDCl_3$), 67.64 (OCH_2**C**H_2OPh), 63.28 (O**C**$H_2$$CH_2$OPh), 56.00 (**C**$H_3$OPh), 18.44 (PhCH=CH**C**H_3, trans), 18.35 (PhCH=CHC**H_3**, cis-trans), 14.71 (PhCH=CH**C**H_3, cis).

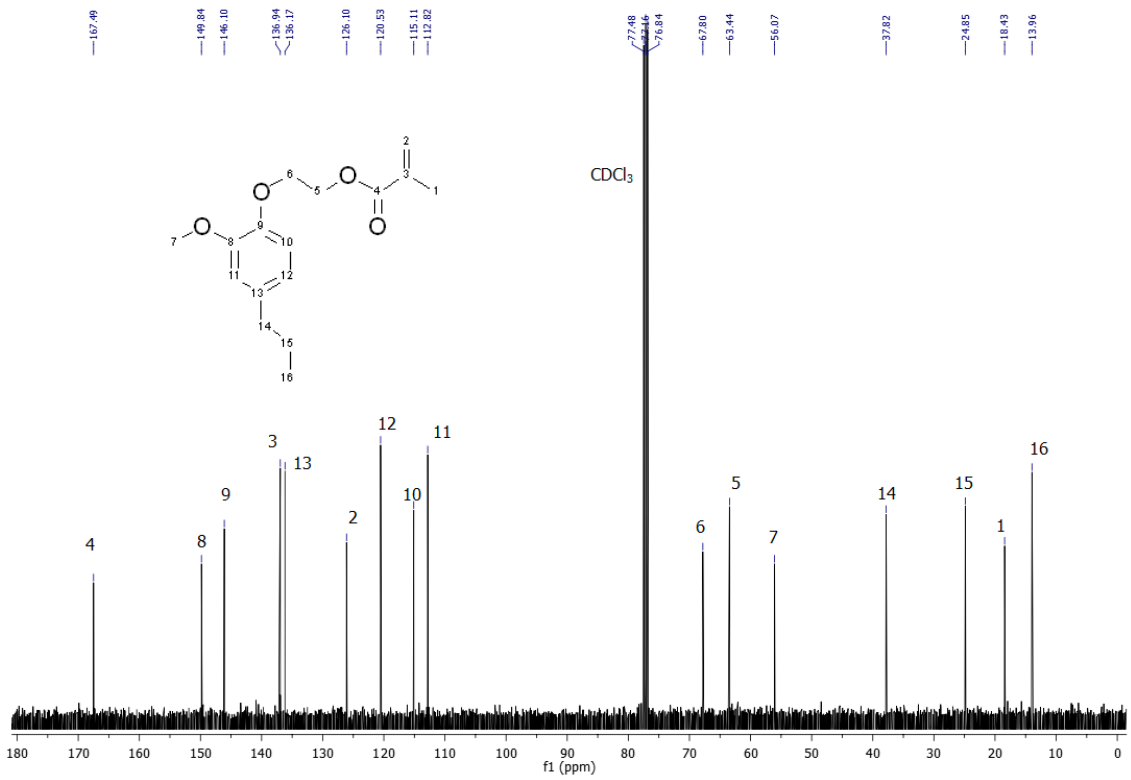

Figure A1-41. ^{13}C NMR Spectrum of Ethoxy dihydroeugenyl Methacrylate (EDMA) in $CDCl_3$.

^{13}C NMR spectrum ($CDCl_3$): δC 167.49 (O**C**=O), 149.84 (**C_2**-Ar), 146.10 (**C_1**-Ar), 136.94 (OC=O**C**(CH_3)=CH_2), 136.17 (**C_4**-Ar), 126.10 (OC=OC(CH_3)=**C**H_2), 120.53 (**C_5**-Ar), 115.11 (**C_6**-Ar), 112.82 (**C_3**-Ar), 77.16 ($CDCl_3$), 67.80 (OCH_2**C**H_2OPh), 63.44(O**C**$H_2$$CH_2$OPh), 56.07 (**C**$H_3$OPh), 37.82 ($CH_3CH_2$**C**$H_2$Ph), 24.85 ($CH_3$**C**$H_2CH_2$Ph), 18.43 (OC=OC(**C**$H_3$)=$CH_2$), 13.96 (**C**$H_3CH_2CH_2$Ph).

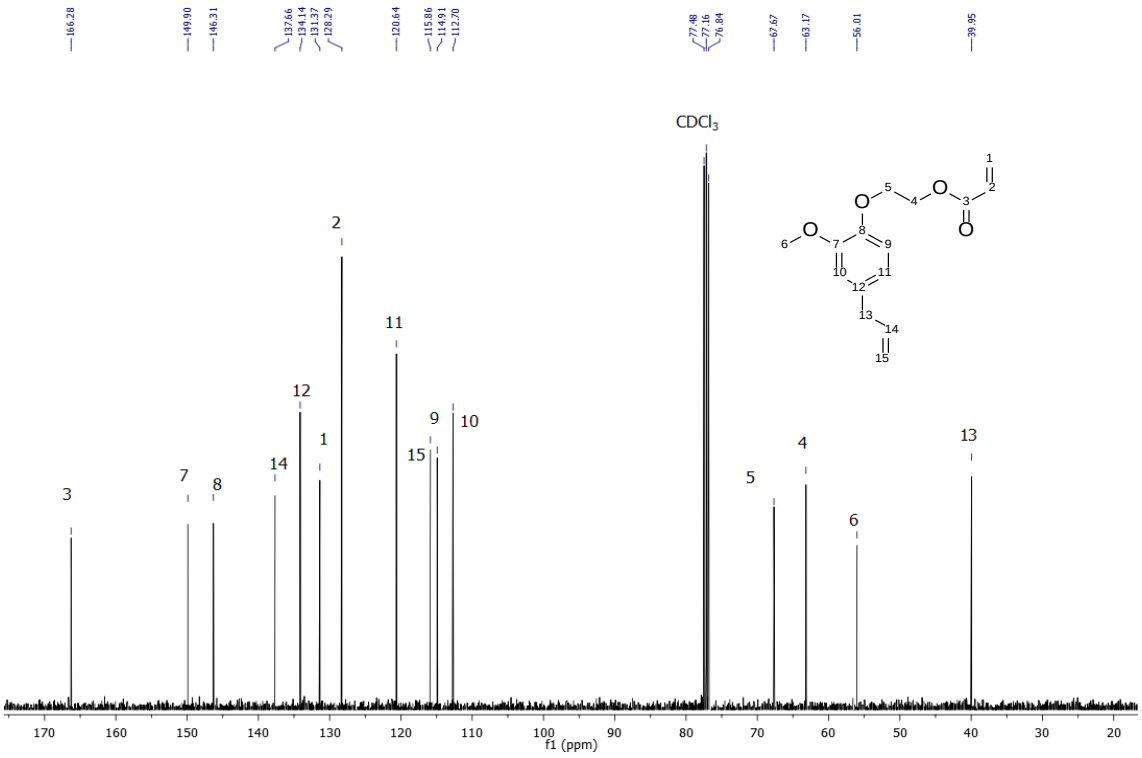

Figure A1-42. ^{13}C NMR Spectrum of Ethoxy Eugenyl Acrylate (EEA) in $CDCl_3$.

^{13}C NMR spectrum ($CDCl_3$): δC 166.28 (O**C**=OC(CH_3)=CH_2), 149.90 (**C_2**-Ar), 146.31 (**C_1**-Ar), 137.66 (PhC**H_2C**H=CH_2), 134.14 (**C_4**-Ar), 131.37 (OC=OCH=**C**H_2), 128.29 (OC=O**C**H=CH_2), 120.64 (**C_5**-Ar), 115.86 (PhCH_2CH=**C**H_2), 114.91 (**C_6**-Ar), 112.70 (**C_3**-Ar), 77.16 ($CDCl_3$), 67.67 (OCH_2**C**H_2OPh), 63.17 (O**C**H_2CH_2OPh), 56.01 (**C**H_3OPh), 39.95 (Ph**C**H_2CH=CH_2).

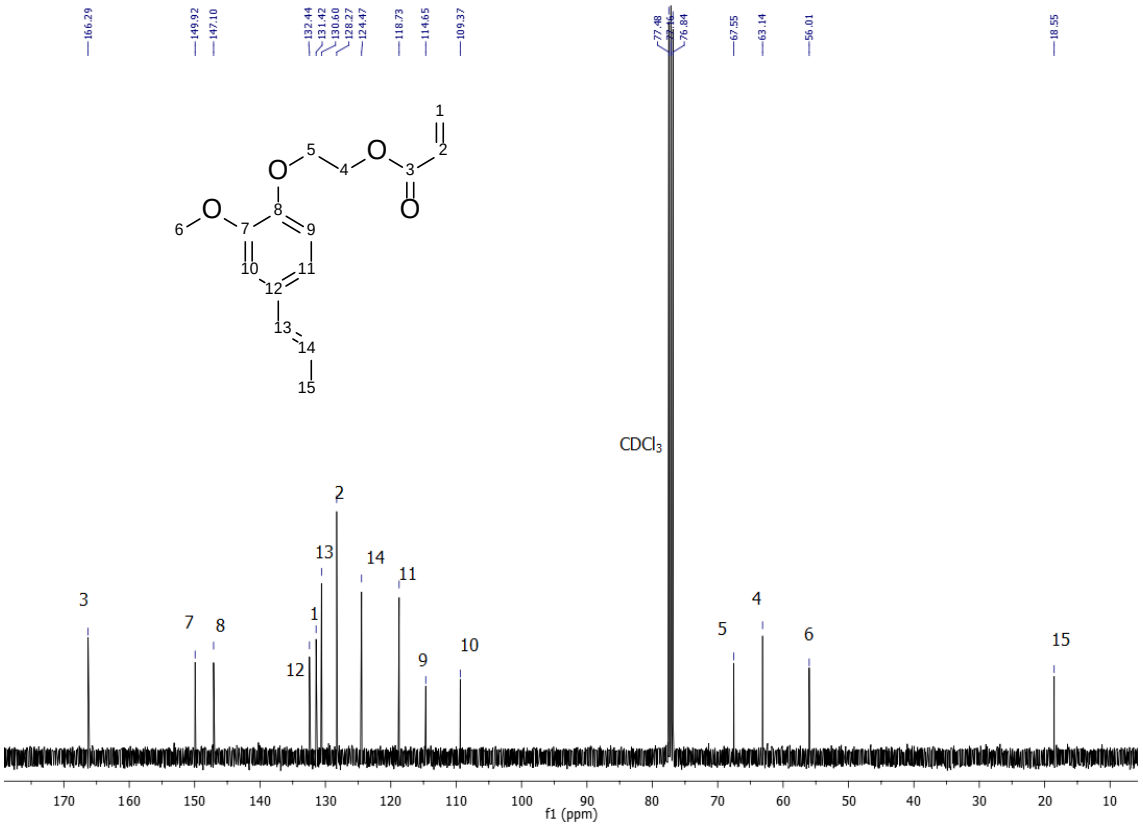

Figure A1-43. ^{13}C NMR Spectrum of Ethoxy Isoeugenyl Acrylate (EIA) in $CDCl_3$.

^{13}C NMR spectrum ($CDCl_3$): δC 166.29 (O**C**=OCH=CH_2), 149.92 (**C$_2$**-Ar), 147.10 (**C$_4$**-Ar), 132.44 (OC=OCH=**C**H_2), 131.42 (**C$_1$**-Ar), 130.60 (Ph**C**H=$CHCH_3$), 128.27(OC=O**C**H=CH_2), 124.47 (PhCH=**C**HCH_3), 118.73 (**C$_5$**-Ar), 114.65 (**C$_6$**-Ar), 109.37 (**C$_3$**-Ar), 77.16 ($CDCl_3$), 67.55 (OCH_2**C**H_2OPh), 63.14 (O**C**H_2CH_2OPh), 56.01 (**C**H_3OPh), 18.55 (PhCH=CH**C**H_3).

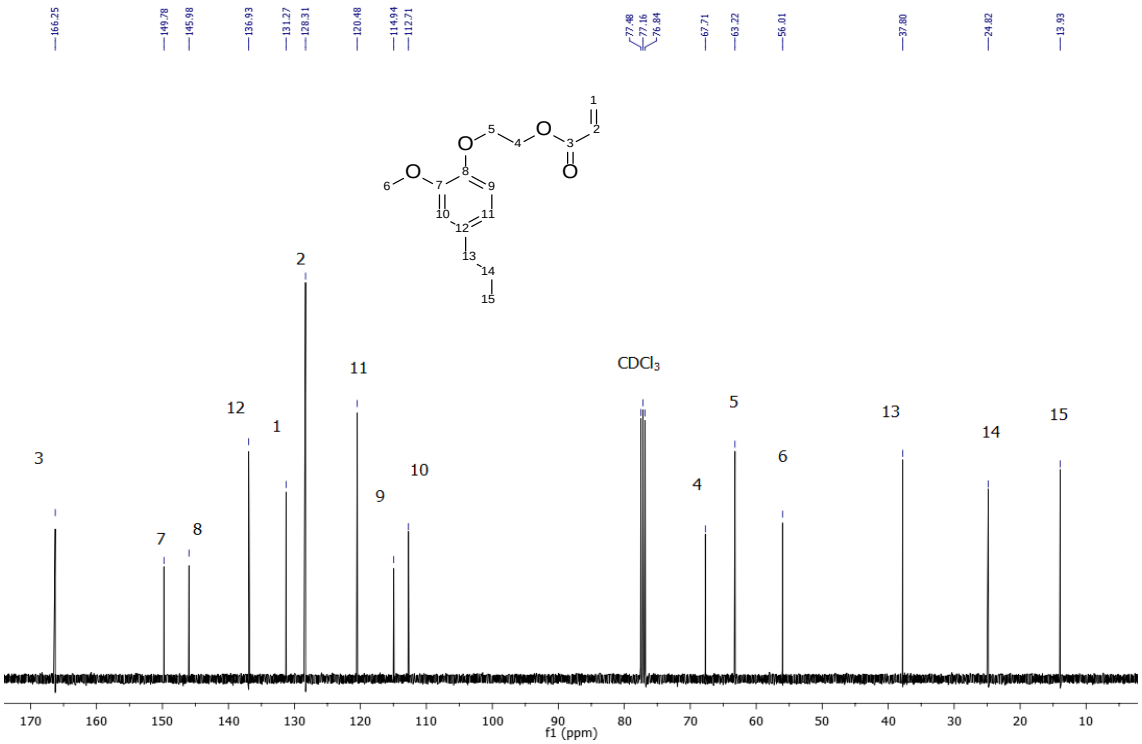

Figure A1-44. ^{13}C NMR Spectrum of Ethoxy Dihydroeugenyl Acrylate (EDA) in $CDCl_3$.

^{13}C NMR spectrum ($CDCl_3$): δC 166.25 (O**C**=O), 149.78 (**C_2**-Ar), 145.98 (**C_4**-Ar), 136.93 (**C_1**-Ar), 131.27 (OC=OCH=**C**H_2), 128.31 (OC=O**C**H=CH_2), 120.48 (**C_5**-Ar), 114.94 (**C_6**-Ar), 112.71 (**C_3**-Ar), 77.16 ($CDCl_3$), 67.71 (OCH_2**C**H_2OPh), 63.22(O**C**$H_2$$CH_2$OPh), 56.01 (**C**$H_3$OPh), 37.80 ($CH_3CH_2$**C**$H_2$Ph), 24.82 ($CH_3$**C**$H_2CH_2$Ph), 13.93 (**C**$H_3CH_2CH_2$Ph).

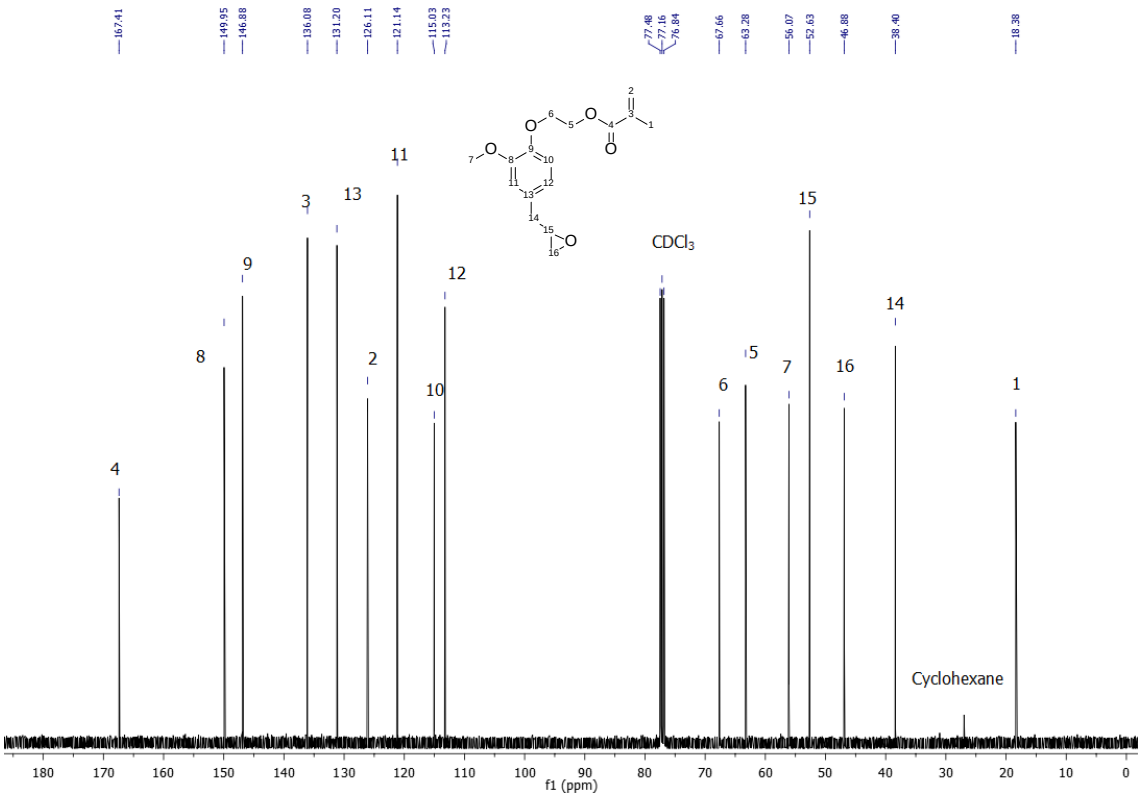

Figure A1-45. ^{13}C NMR Spectrum of Epoxy EEMA in $CDCl_3$.

^{13}C NMR spectrum ($CDCl_3$): δC 167.41 (O**C**=OC(CH_3)=CH_2), 149.95 (**C_2**-Ar), 146.88 (**C_1**-Ar), 136.08 (OC=O**C**(CH_3)=CH_2), 131.20 (**C_4**-Ar), 126.11 (OC=OC(CH_3)=**C**H_2), 121.14 (**C_3**-Ar), 115.03 (**C_6**-Ar), 113.23 (**C_5**-Ar), 77.16 ($CDCl_3$), 67.66(OCH_2**C**H_2OPh), 63.28 (O**C**H_2CH_2OPh), 56.07 (**C**H_3OPh), 52.63 (PhCH_2**C**HO(CH_2)), 46.88 (PhCH_2CHO(**C**H_2)), 38.40 (Ph**C**H_2CHO(CH_2)), 18.38 (OC=OC(**C**H_3)=CH_2).

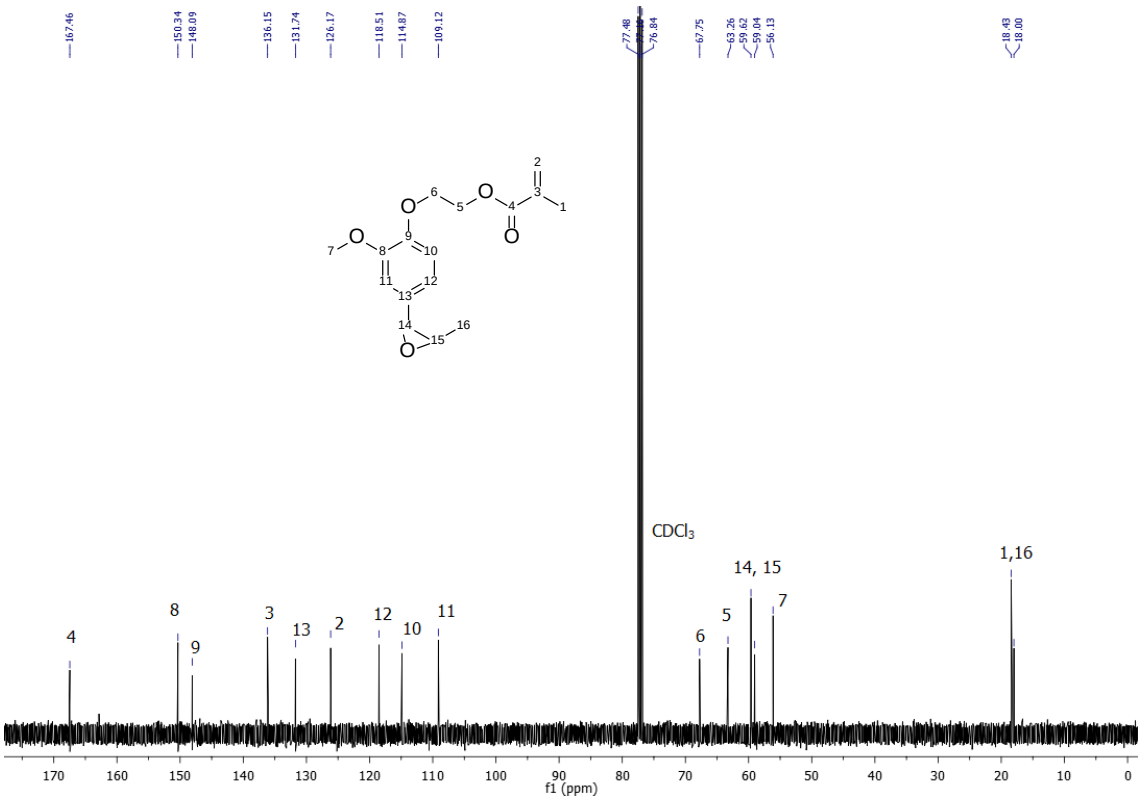

Figure A1-46. ^{13}C NMR Spectrum of Epoxy EIMA in $CDCl_3$.

^{13}C NMR spectrum ($CDCl_3$): δC 167.46 (O**C**=OC(CH_3)=CH_2), 150.34 (**C_2**-Ar), 1480.0 (**C_1**-Ar), 136.15 (OC=O**C**(CH_3)=CH_2), 131.74 (**C_4**-Ar), 126.17 (OC=OC(CH_3)=**C**H_2), 118.51 (**C_3**-Ar), 114.87 (**C_6**-Ar), 109.12 (**C_5**-Ar), 77.16 ($CDCl_3$), 67.75 (OCH_2**C**H_2OPh), 63.26 (O**C**$H_2$$CH_2$OPh), 59.62 (**C**$H_3$OPh), 59.04 (Ph**C**H(O1)CH(O1)CH_2), 56.13 (PhCH(O1)**C**H(O1)CH_2), 18.43 (PhCH(O1)CH(O1)**C**H_2), 18.00 (OC=OC(**C**H_3)=CH_2).

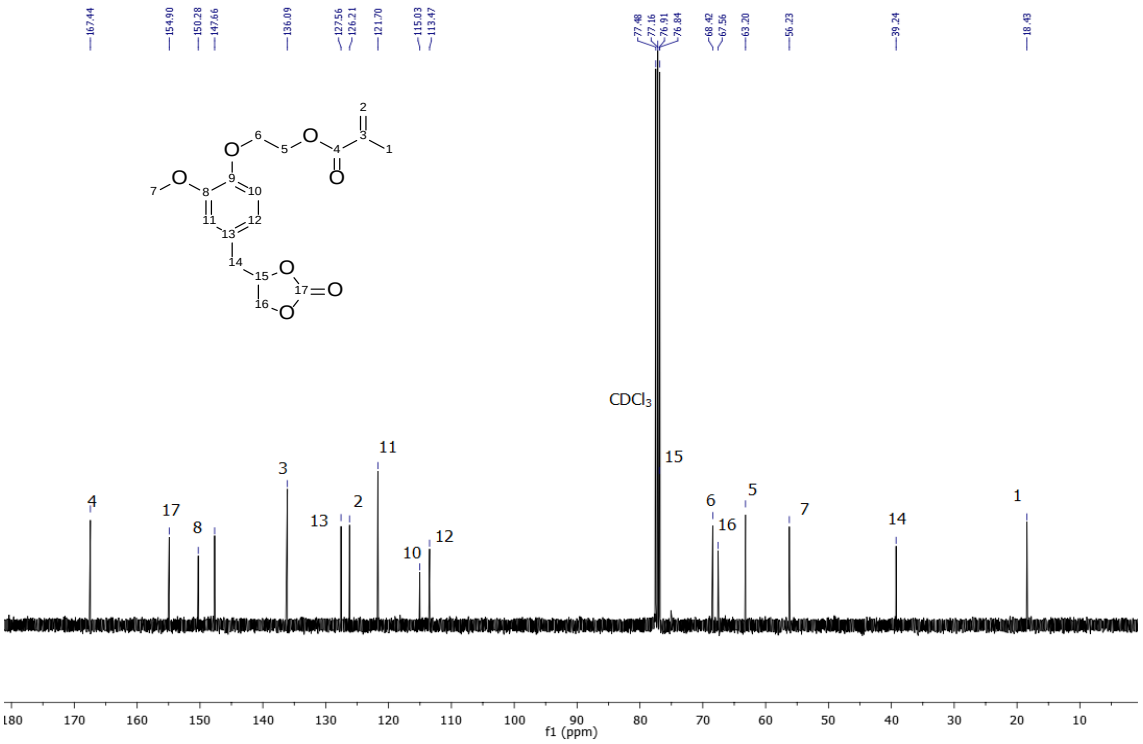

Figure A1-47. ^{13}C NMR Spectrum of EEMA Carbonate in $CDCl_3$.

^{13}C NMR spectrum ($CDCl_3$): δC 167.44 (O**C**=OC(CH_3)=CH_2), 154.90 (PhCH_2CH(O1)CH_2(O2)**C**=O(O1)), 150.28 (**C_2**-Ar), 147.66 (**C_1**-Ar), 136.09 (OC=O**C**(CH_3)=CH_2), 127.56 (**C_4**-Ar), 126.21 (OC=OC(CH_3)=**C**H_2), 121.70 (**C_3**-Ar), 115.03 (**C_6**-Ar), 113.47 (**C_5**-Ar), 77.16 ($CDCl_3$), 76.91 (PhCH_2**C**H(O1)CH_2(O2)C=O(O1)), 68.42 (O**C**H_2CH_2OPh), 67.56 (PhCH_2CH(O1)**C**H_2(O2)C=O(O1)),63.18 (OCH_2**C**H_2OPh), 56.23 (**C**H_3OPh), 39.24 (Ph**C**H_2CH(O1)CH_2(O2)C=O(O1)), 18.43 (OC=OC(**C**H_3)=CH_2).

A1.7 Yield calculation

Yields of synthesis products were obtained gravimetrically using the following equation:

$$Yield(\%) = 100 \times \frac{Obtained\ mass\ (after\ purification) in\ g}{Total\ expected\ mass\ in\ g} \qquad \text{Eq. A1-1}$$

The expected mass derives from the initial mol amount taking into account a 100% conversion.

A1.8 Optimization of reactions:

- Greener solvent for methacrylation:

Use of DCM was substituted by ethyl acetate in the pursuit of a cleaner reaction.

EI (2 g, 9% cis and 91% trans, 9.6 mmol, 1 equiv.), ethyl acetate (20 mL), triethylamine (6.0 g, 60 mmol, 2.4 equiv.) and methacrylic anhydride (1.76 g, 11.5mmol, 1.2 equiv.).

Conversion reached 88% after 35 h of reaction.

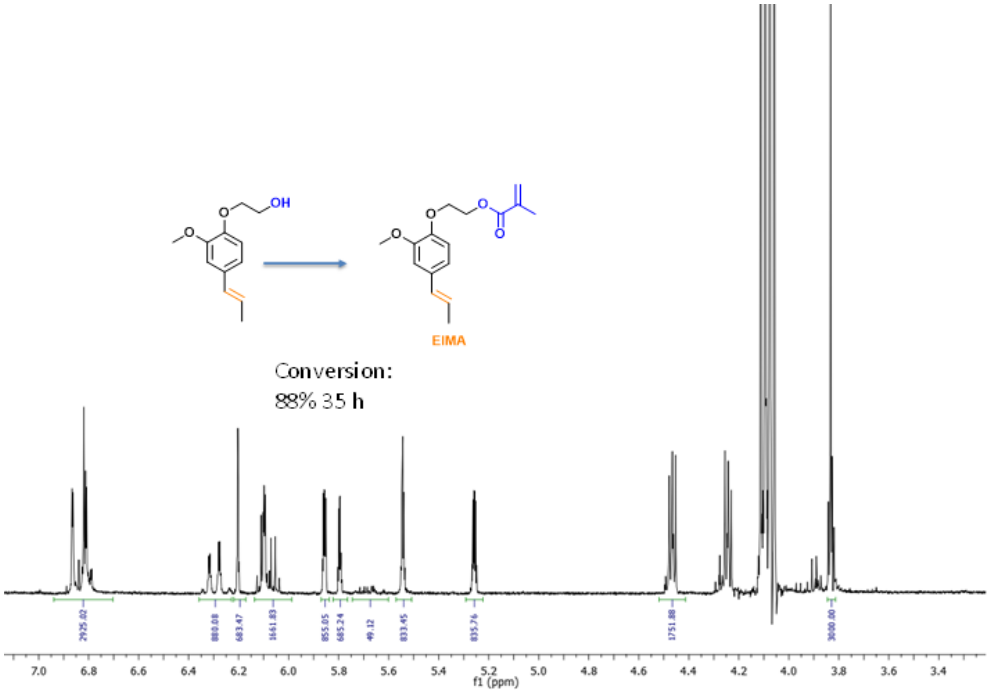

Figure A1-48. ^{1}H NMR of methacrylation of EI in ethyl acetate after 35h of reaction.

Greener solvent for acrylation:

Use of DCM was substituted by ethyl acetate in the pursuit of a cleaner reaction.

EI (2 g, 9% cis and 91% trans, 9.6 mmol, 1 equiv.), triethylamine (1.5 g, 15 mmol, 1.56 equiv.) and acryloyl chloride (1.1 g, 12 mmol, 1.25 equiv.), ethyl acetate (27 mL).

Conversion reached 42% after 2h of reaction.

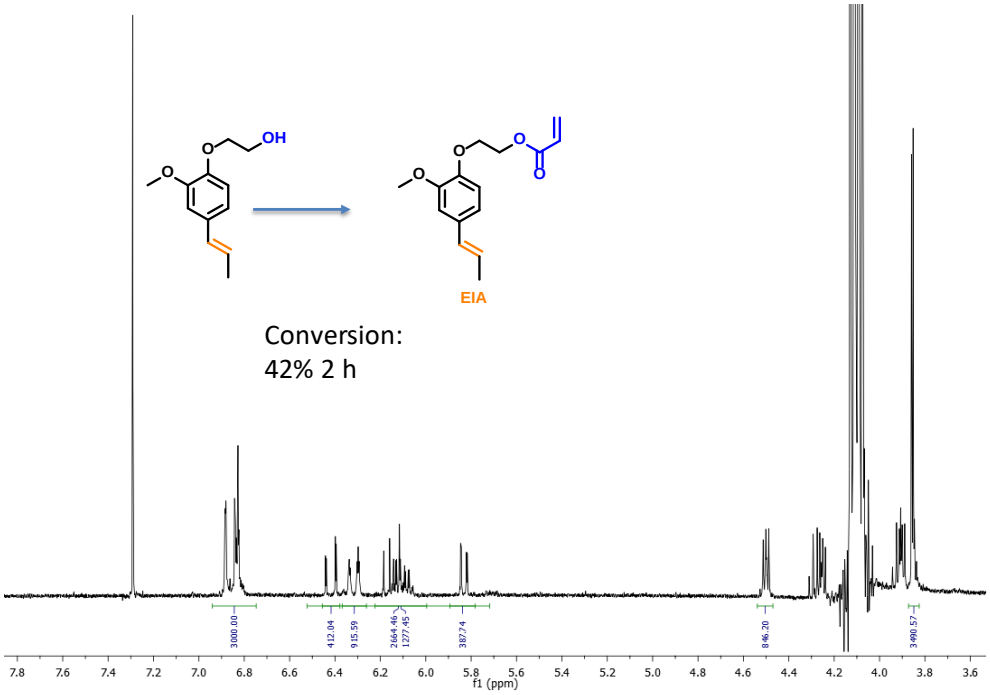

Figure A1-49. ^{1}H NMR of acrylation of EI in ethyl acetate after 2h of reaction.

A1.9 Kinetics of polymerization:

Calculation example:

Monomer conversion for solution polymerization of EEMA at t=7 hours

Calculation with Internal Standard (1-4-bis(trimethylsilylbenzene), BTMSB) :

Eq. A1-2

$$Monomer\ conversion = 100 \times \left(1 - \left(\frac{\frac{Signal\ integration_{t=x}}{IS\ integration_{t=x}}}{\frac{Signal\ integration_{t=0}}{IS\ integration_{t=0}}}\right)\right)$$

$$nomer\ conversion = 100 \times \left(1 - \left(\frac{\frac{540.16 + 534.04}{993.77}}{\frac{958.75 + 980.53}{940.30}}\right)\right) = 47.6\%$$

Calculation of Monomer conversion directly with signal of a reference peak (methoxy group of EEMA monomer) :

Eq. A1-3

$$Monomer\ conversion = 100 \times \left(1 - \left(\frac{\frac{Signal\ integration\ of\ double\ bond_{t=x}}{Number\ of\ protons\ from\ double\ bond\ signal\ _{t=x}}}{\frac{Signal\ integration\ of\ a\ reference\ signal\ (methoxy)_{t=x}}{Number\ of\ protons\ from\ reference\ signal\ (3)\ _{t=x}}}\right)\right)$$

$$Monomer\ conversion = 100 \times \left(1 - \left(\frac{\frac{540.16 + 534.04}{2}}{\left(\frac{3000}{3}\right)}\right)\right) = 46.3\%$$

The reported monomer conversion of EEMA solution homopolymerization at t=7 hours in (Figure A1-51) is 47.6%.

In the case of the allylic double bond consumption (**CH_2=CH**-CH_2-), using the internal standard, it gave:

$$Allylic\ double\ bond\ consumption = 100 \times \left(1 - \left(\frac{\frac{913.86 + 1877.48}{993.77}}{\frac{923.37 + 1880.51}{940.30}}\right)\right) = 5.8\%$$

For the consumption of the allylic protons (CH_2=CH-**CH_2**-), the calculation followed the same procedure using the internal standard:

$$Allylic\ protons\ consumption = 100 \times \left(1 - \left(\frac{\frac{1890.95}{993.77}}{\frac{1922.68}{940.30}}\right)\right) = 6.9\%$$

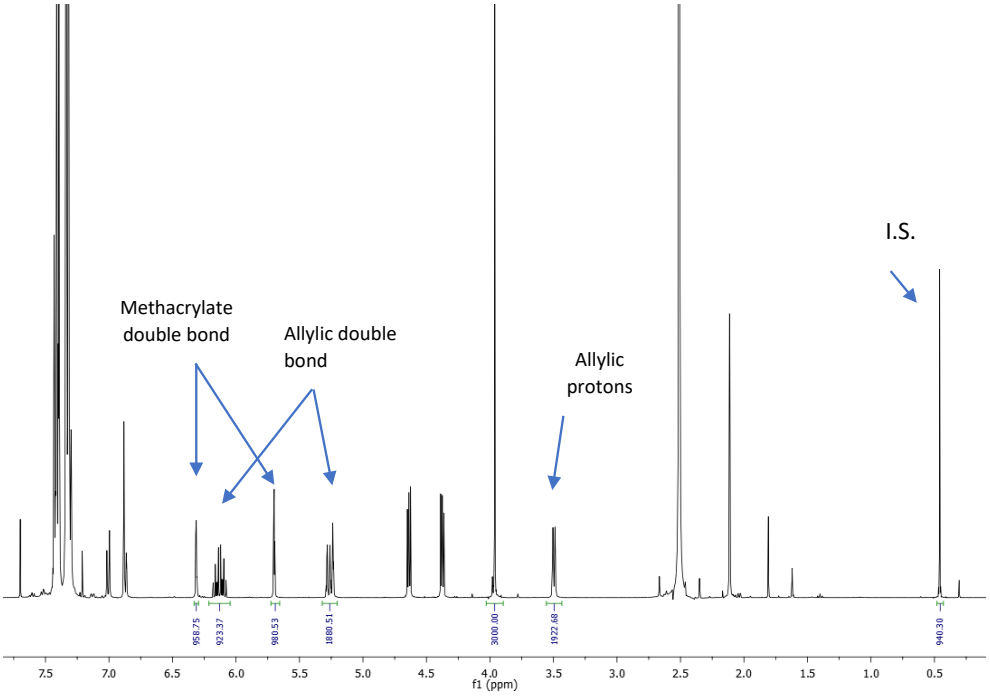

Figure A1-50. ^{1}H NMR EEMA solution polymerization t=0.

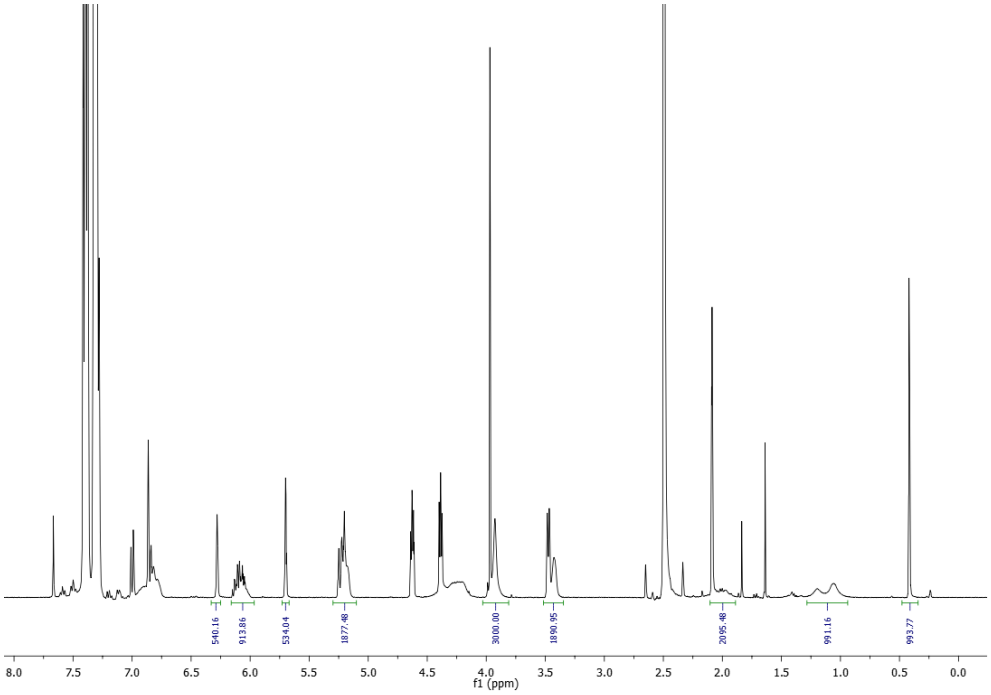

Figure A1-51. ^{1}H NMR EEMA solution polymerization t= 7 hours.

A1.10 Kinetic plots:

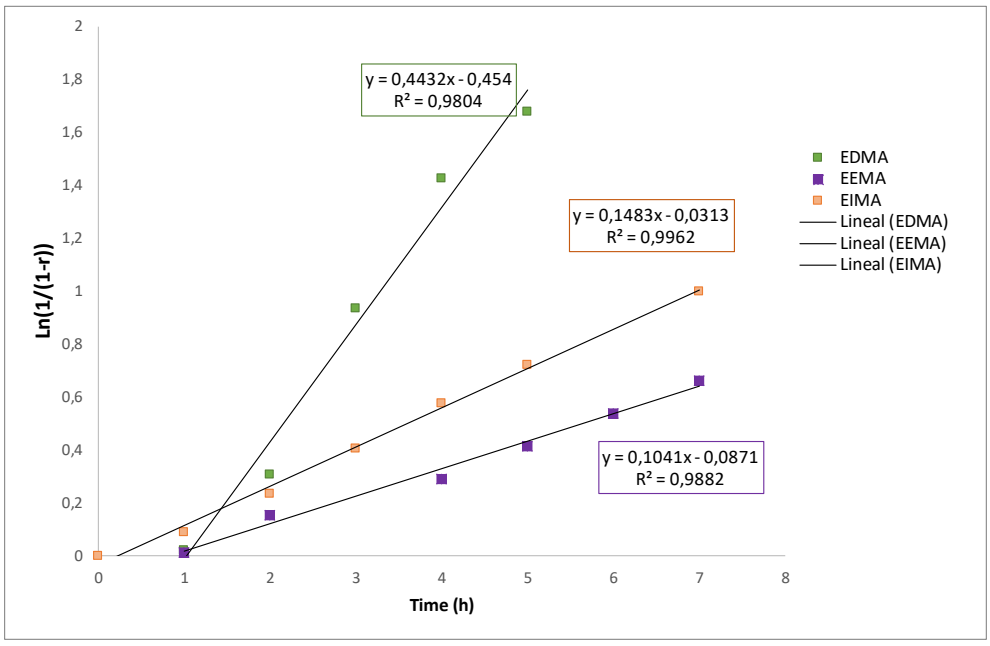

Figure A1-52. Evolution of Ln($[M]_0$/[M]) versus time for the solution homopolymerization of eugenol derived methacrylates EEMA, EIMA and EDMA.

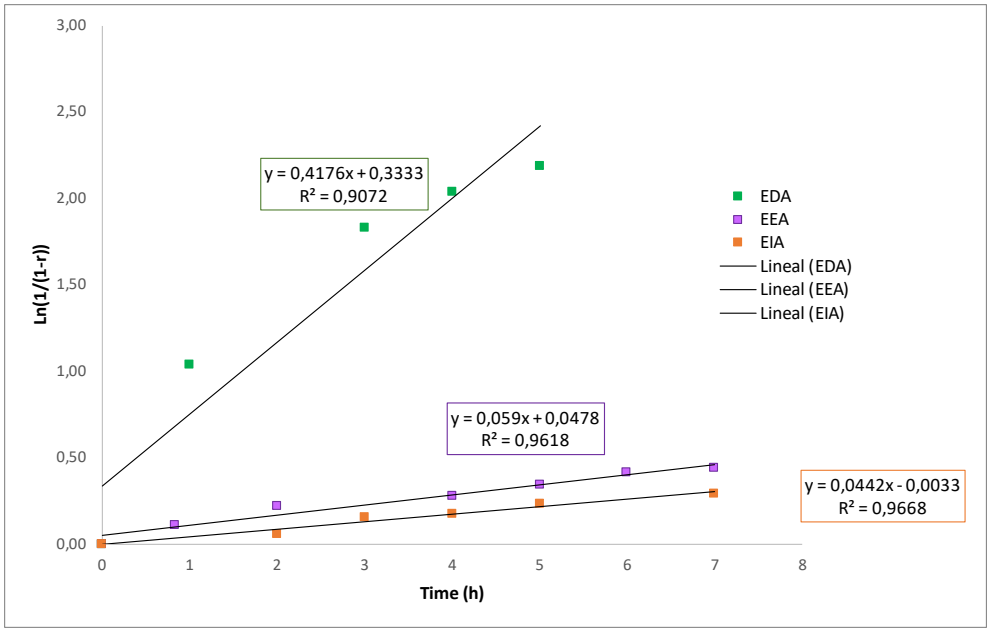

Figure A1-53. Evolution of Ln($[M]_0/[M]$) versus time for the solution homopolymerization of different eugenol derived acrylates EEA, EIA and EDA.

A1.11 DSC measurements (Tg)

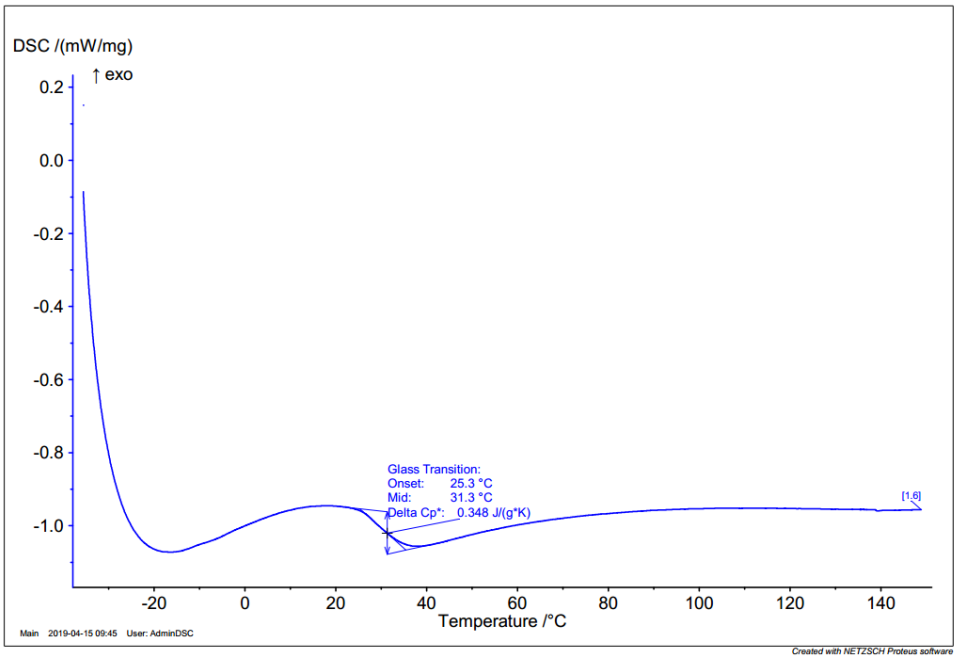

Figure A1-54. DSC of poly(EEMA).

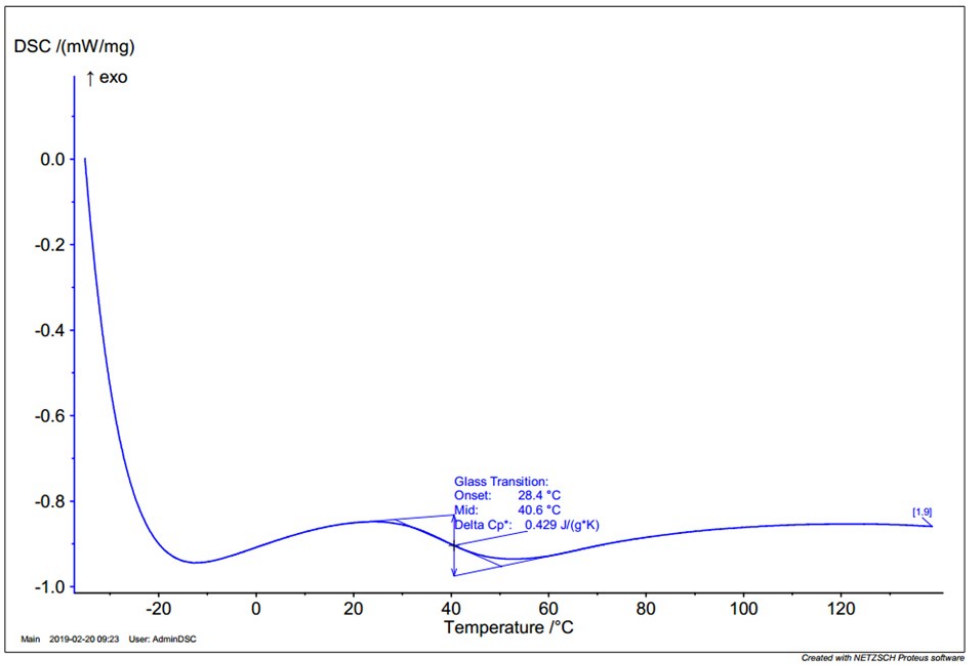

Figure A1-55. DSC of poly(EIMA).

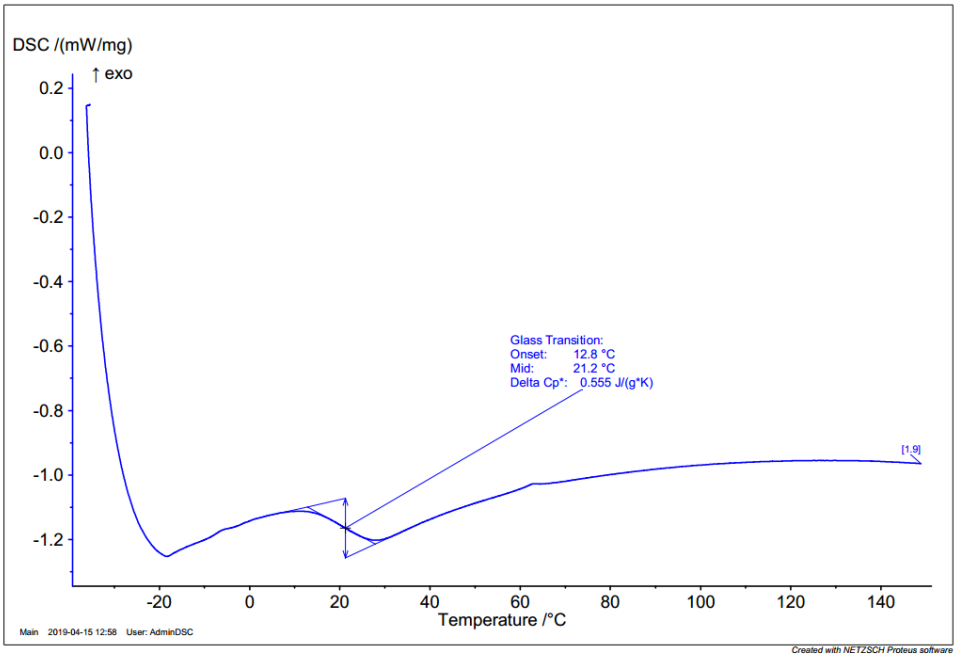

Figure A1-56. DSC of poly(EDMA).

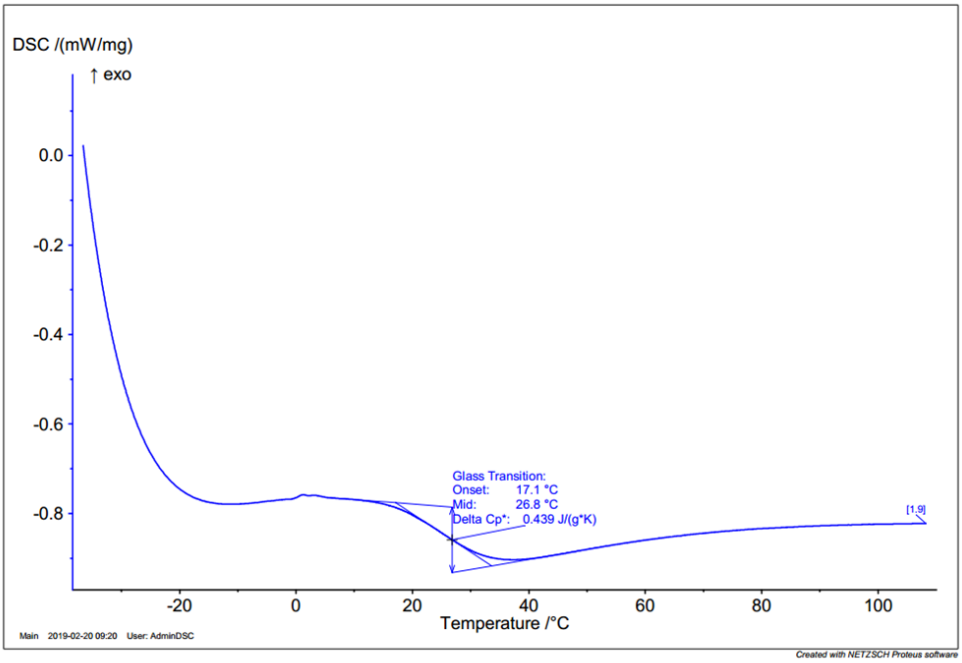

Figure A1-57. DSC of poly(EEA).

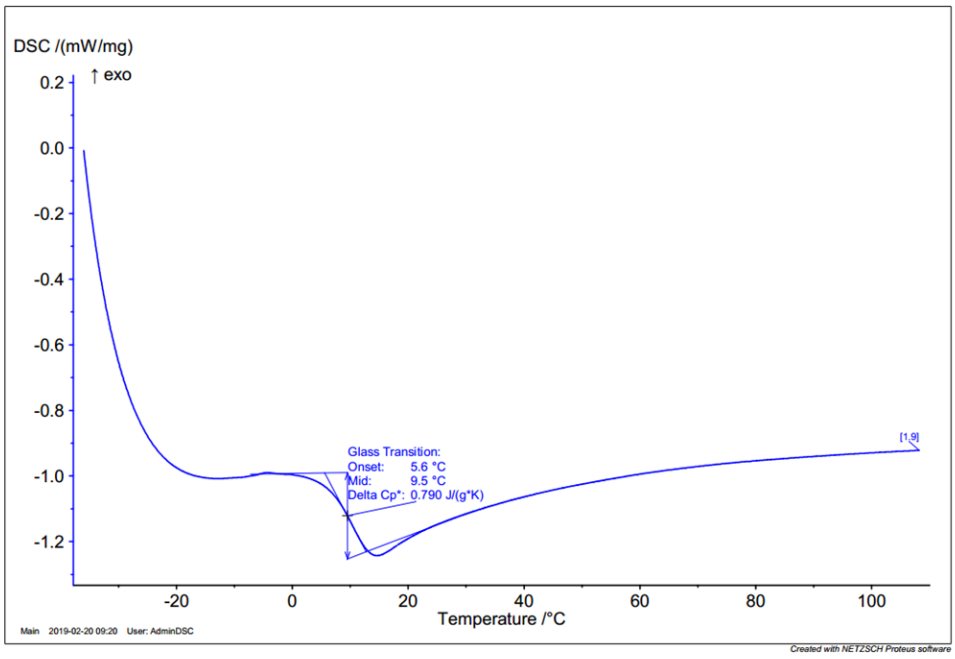

Figure A1-58. DSC of poly(EDA).

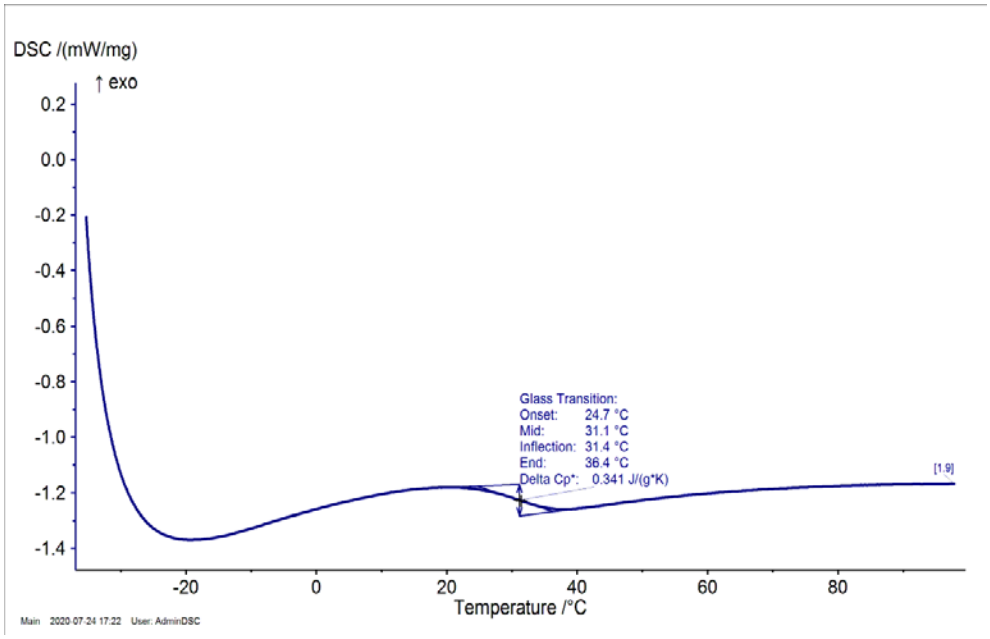

Figure A1-59. DSC of poly(EEMA) under air at 4ºC, light protected for 45 days.

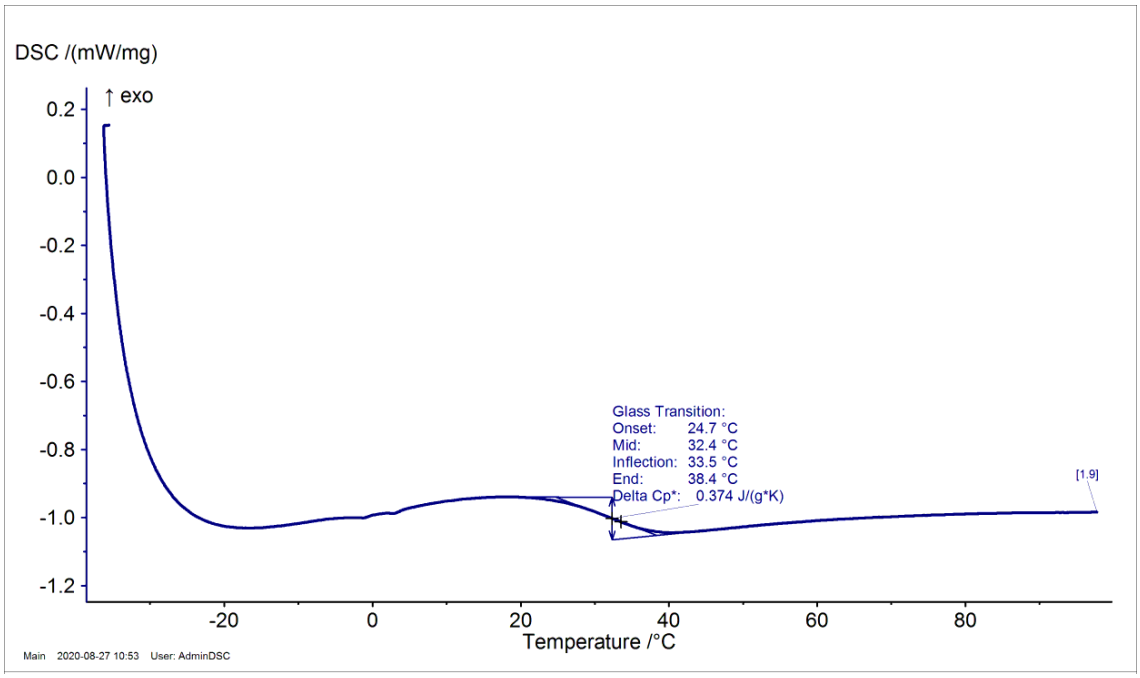

Figure A1-60. DSC of poly(EEMA) under air at 4ºC, light protected for 75 days.

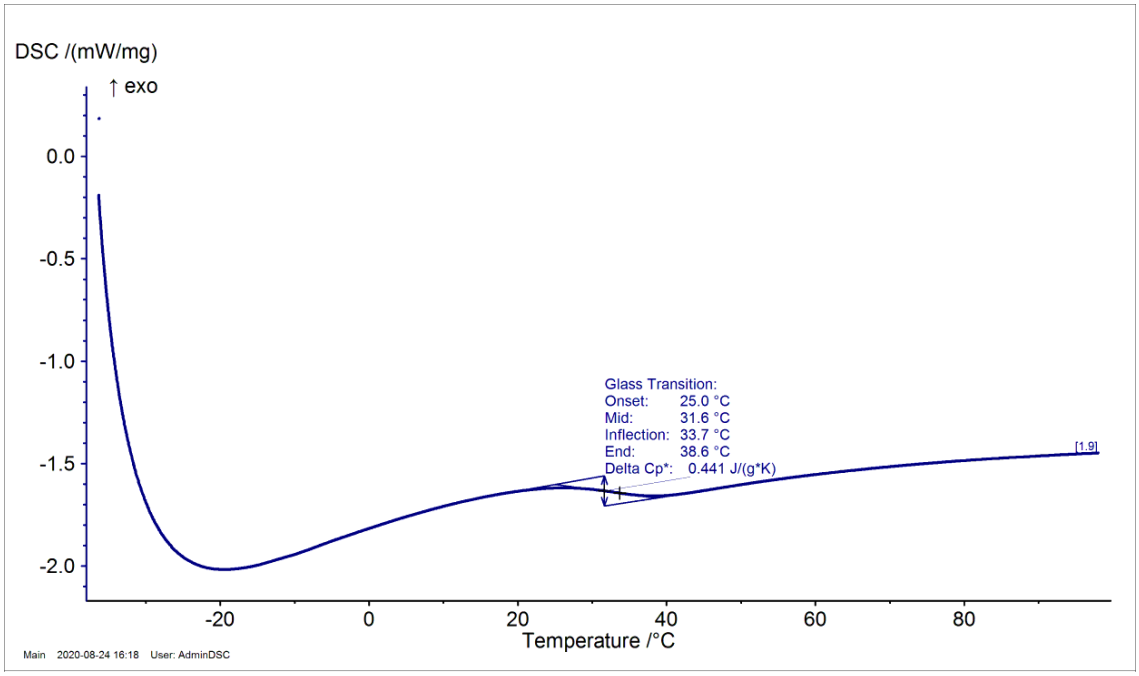

Figure A1-61. DSC of poly(EEMA) under air and light protected for 30 days.

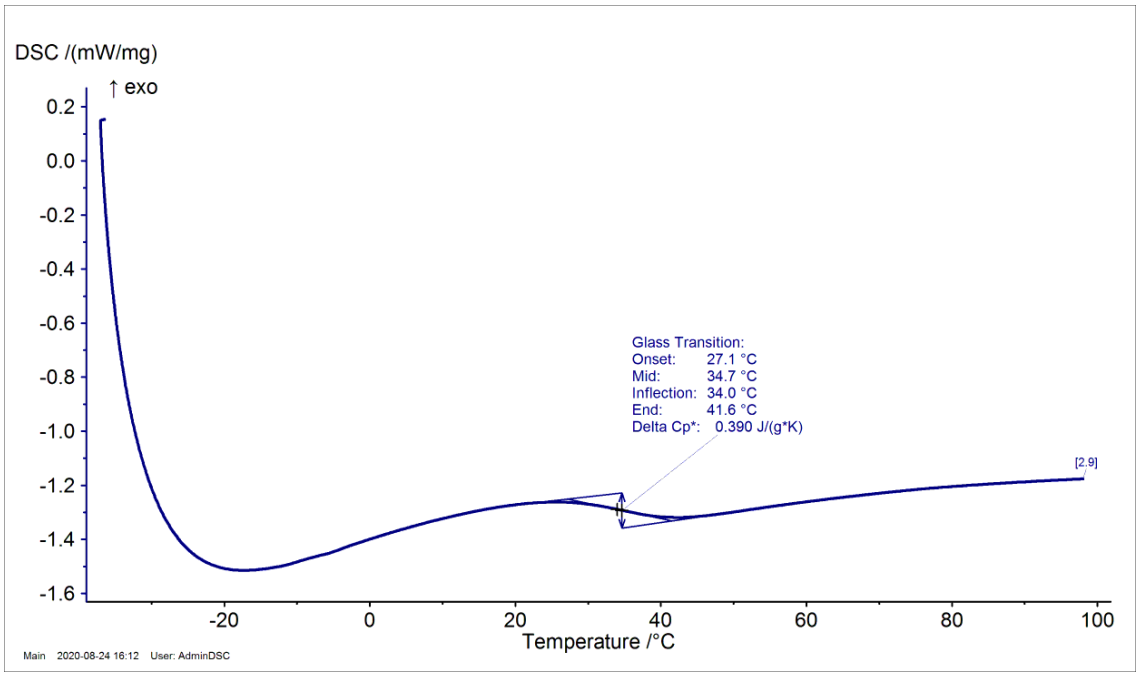

Figure A1-62. DSC of poly(EEMA) under air under natural light for 30 days.

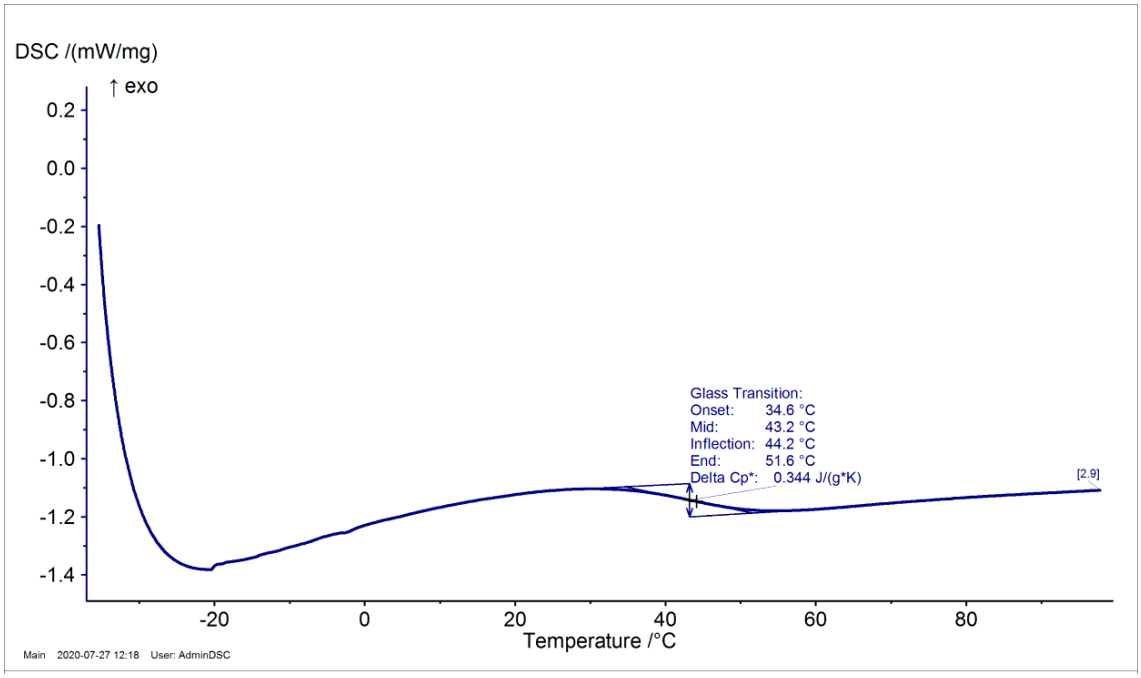

Figure A1-63. DSC of poly(EEMA) under air and 1.5 years of storage.

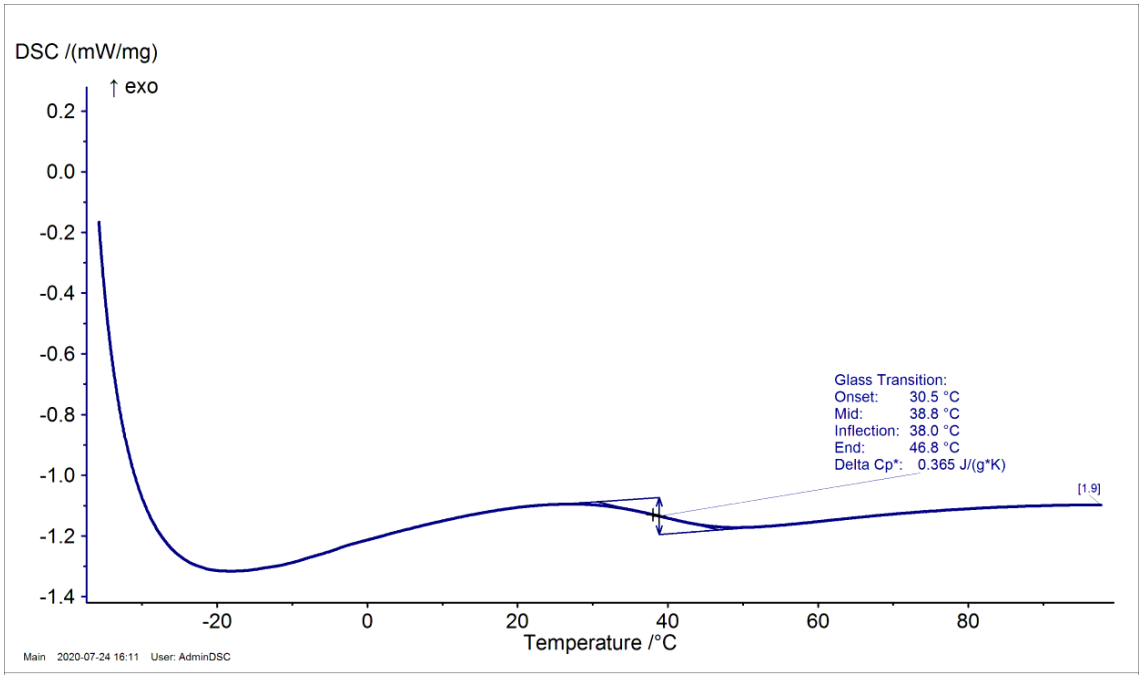

Figure A1-64. DSC of poly(EIMA) under air at 4ºC, light protected for 45 days.

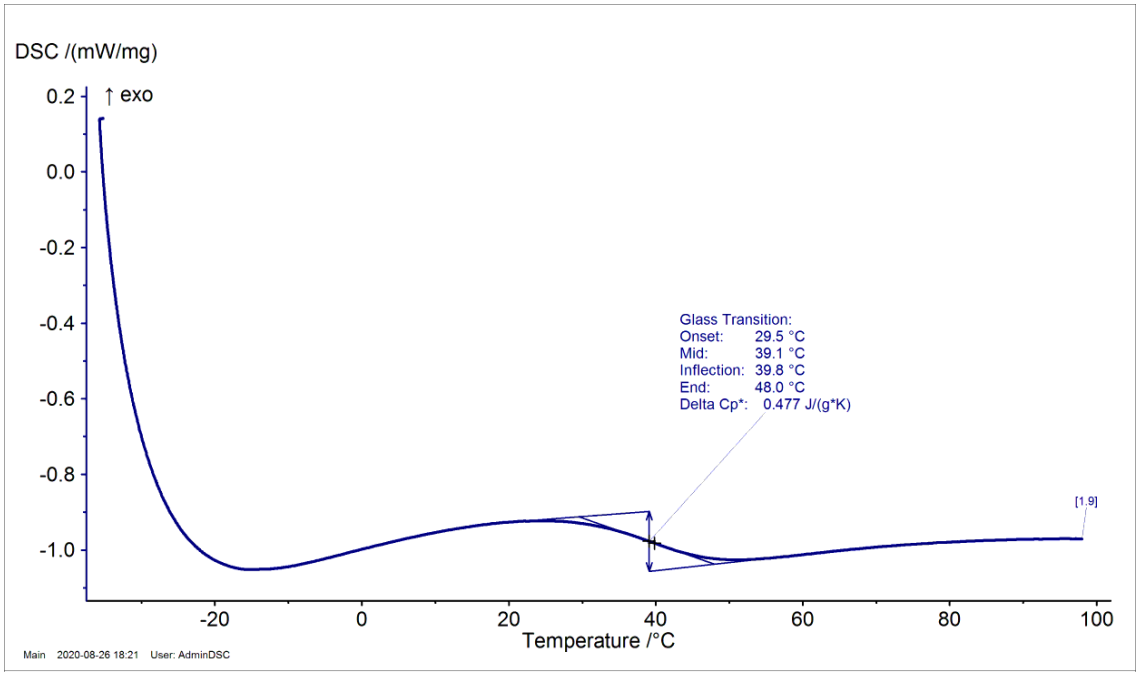

Figure A1-65. DSC of poly(EIMA) under air at 4ºC, light protected for 75 days.

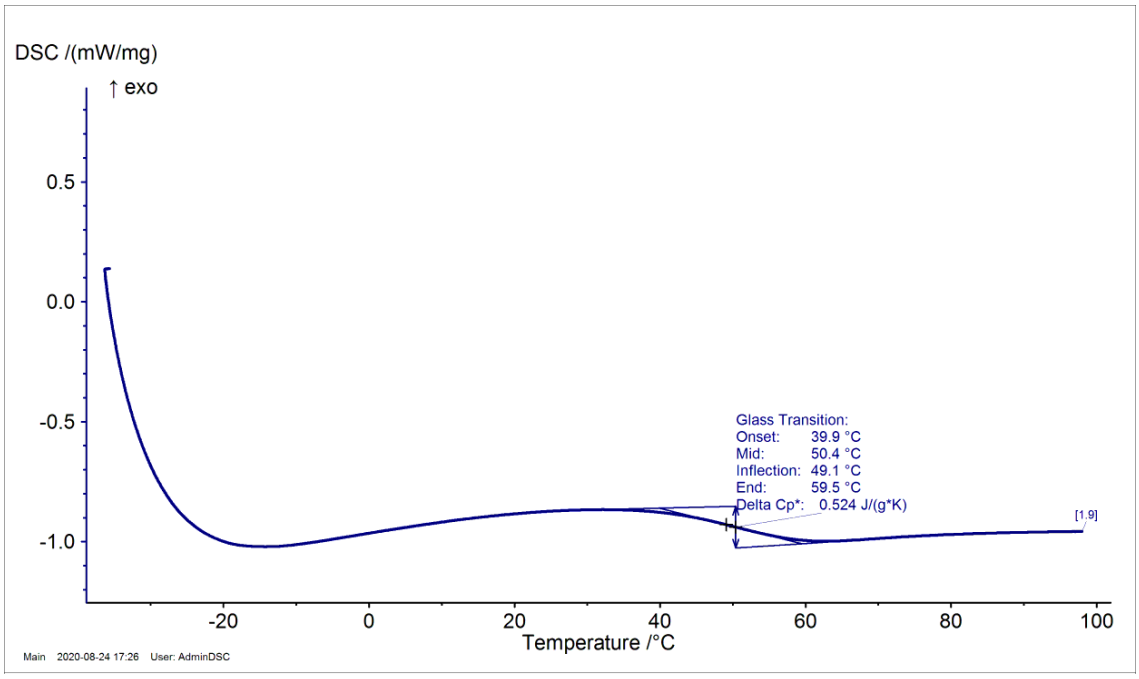

Figure A1-66. DSC of poly(EIMA) under air and light protected for 30 days.

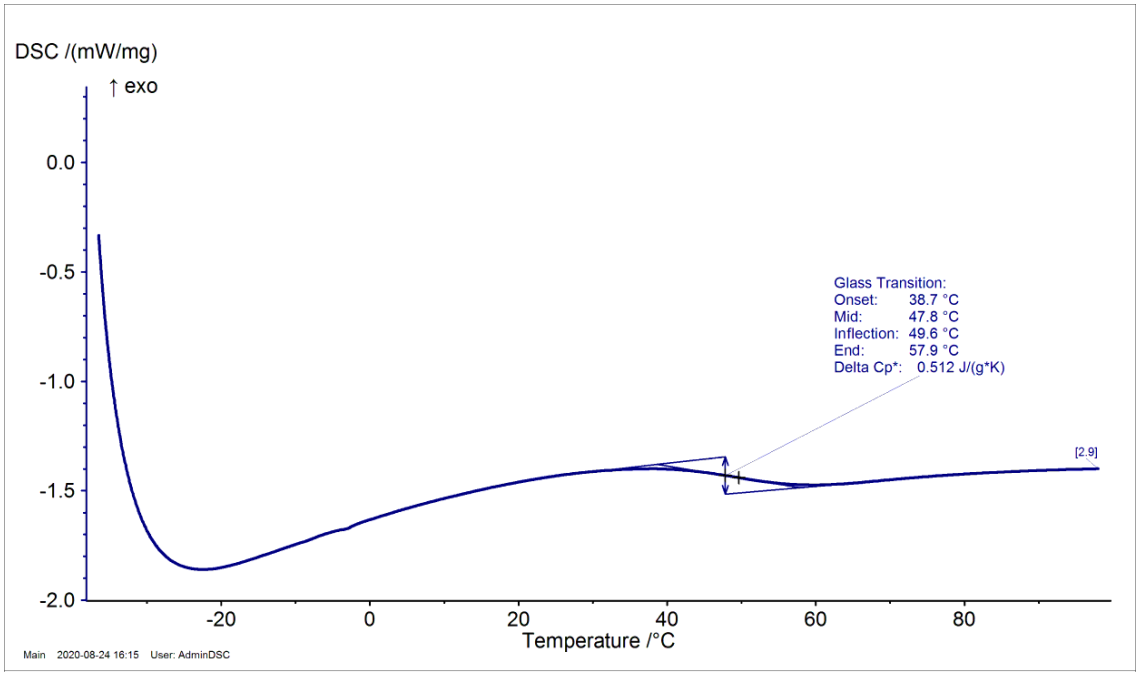

Figure A1-67. DSC of poly(EIMA) under air and under natural light for 30 days.

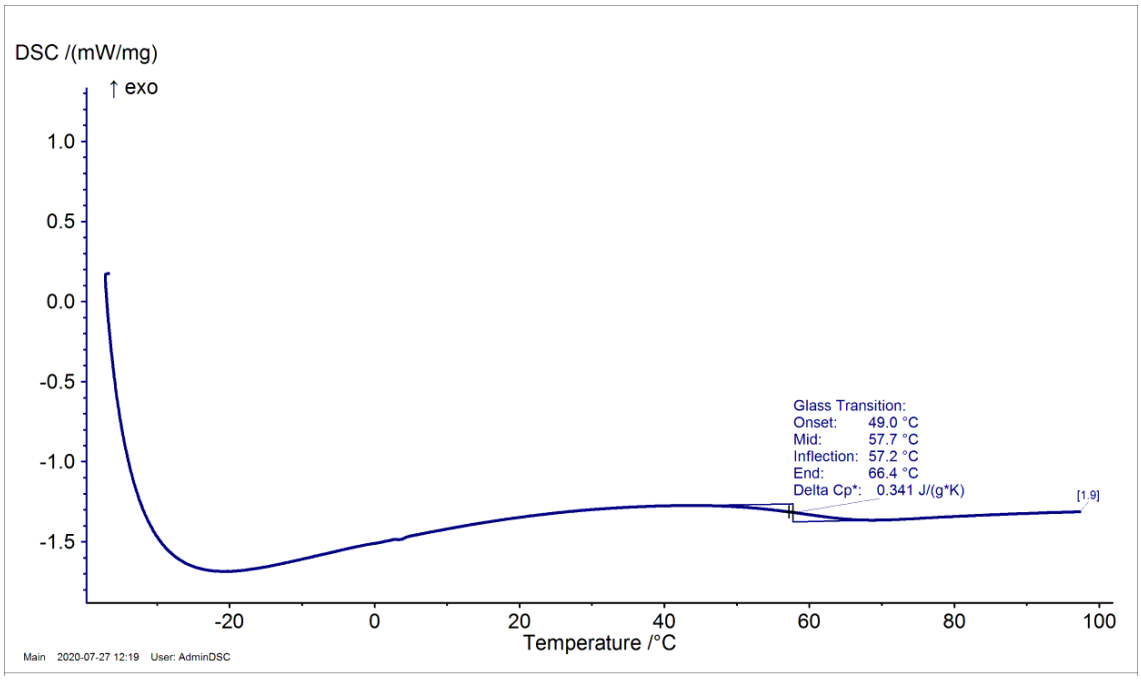

Figure A1-68. DSC of (EIMA) under air and after 1.5 years of storage.

A1.12 SEC Measurements

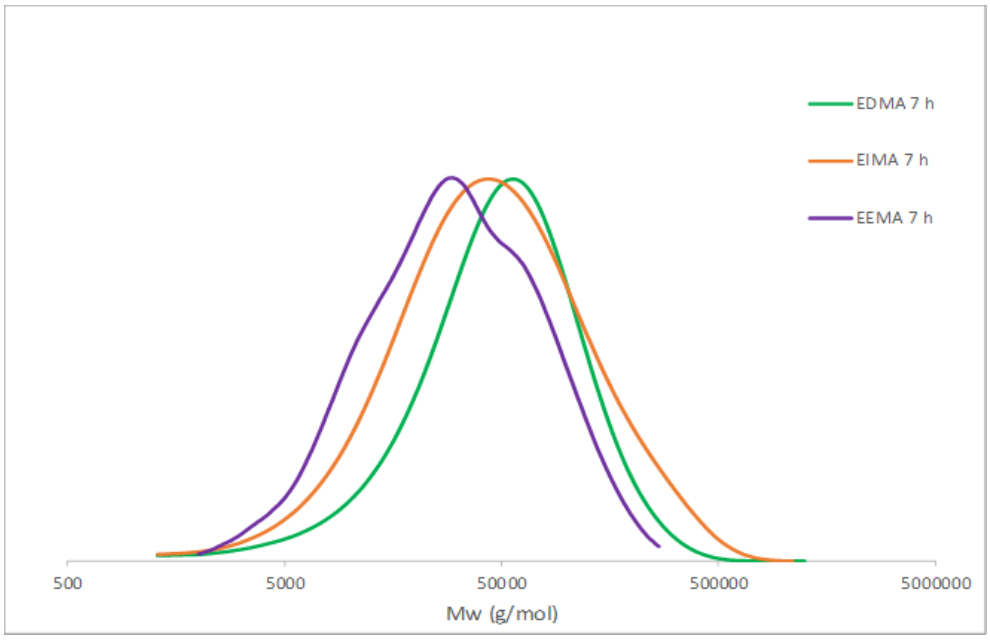

Figure A1-69. SEC measurements of solution homopolymerization of eugenol derived methacrylates at 7 hours.

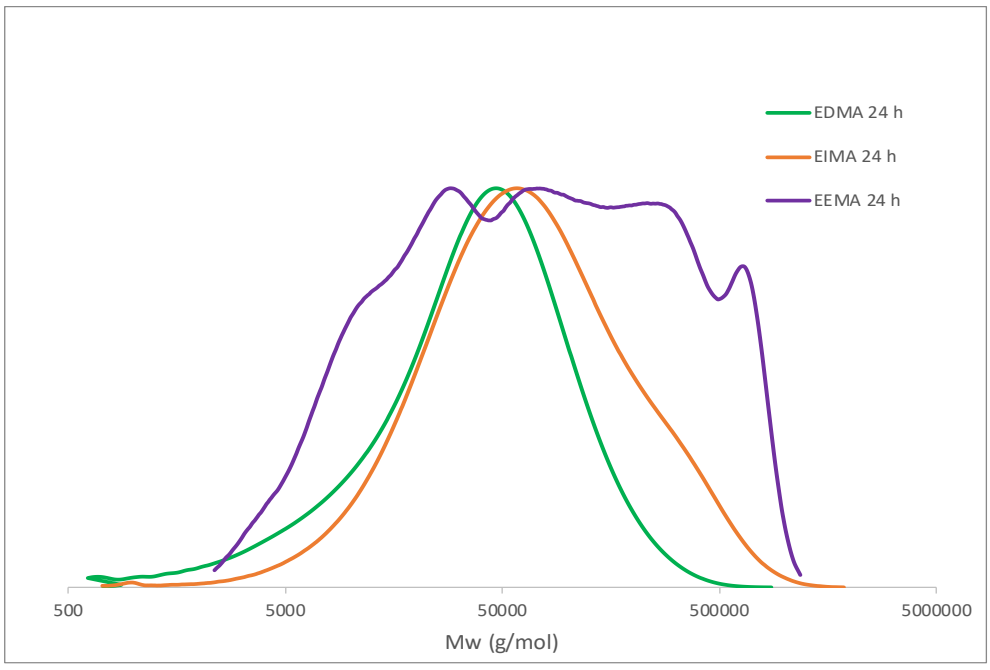

Figure A1-70. SEC measurements of solution homopolymerization of eugenol derived methacrylates at 24 hours.

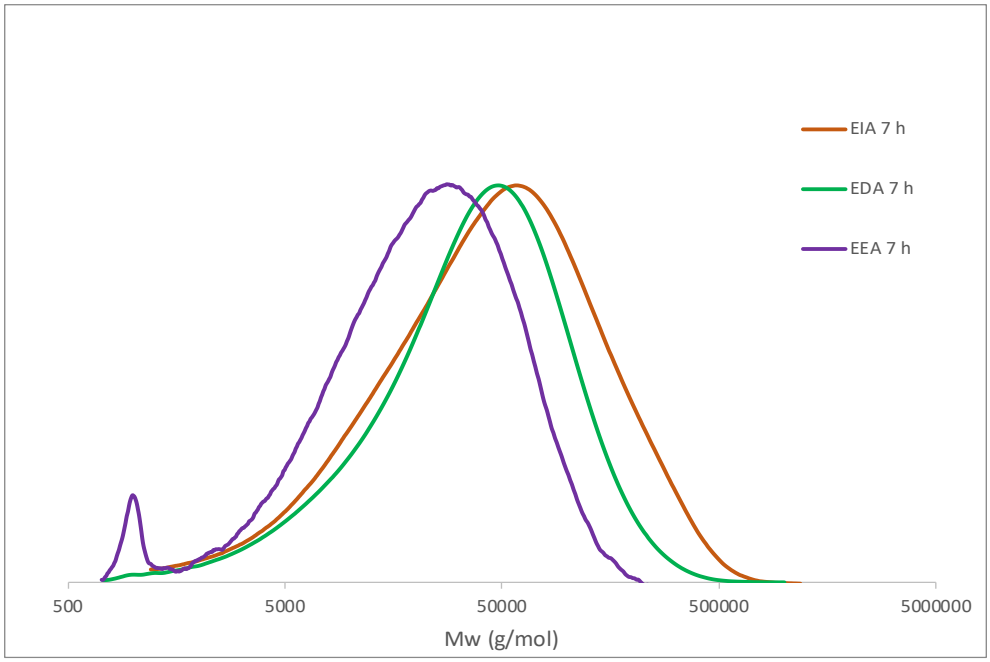

Figure A1-71. SEC measurements of solution homopolymerization of eugenol derived acrylates at 7 hours.

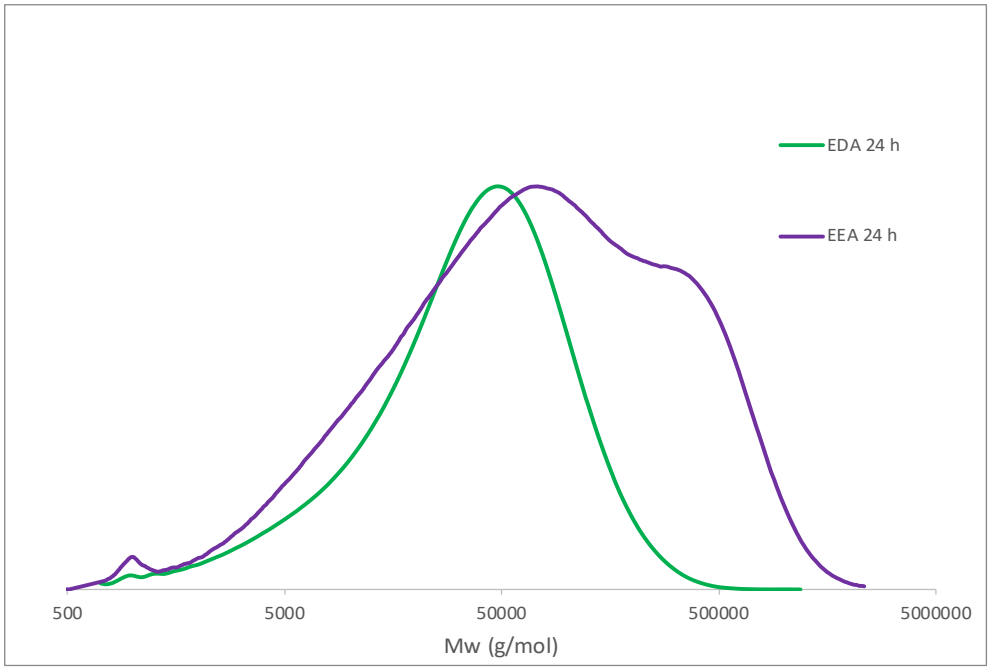

Figure A1-72. SEC measurements of solution homopolymerization of eugenol derived acrylates at 24 hours.

A2 CHAPTER 3

A2.1 IR spectra of eugenol-derived methacrylates

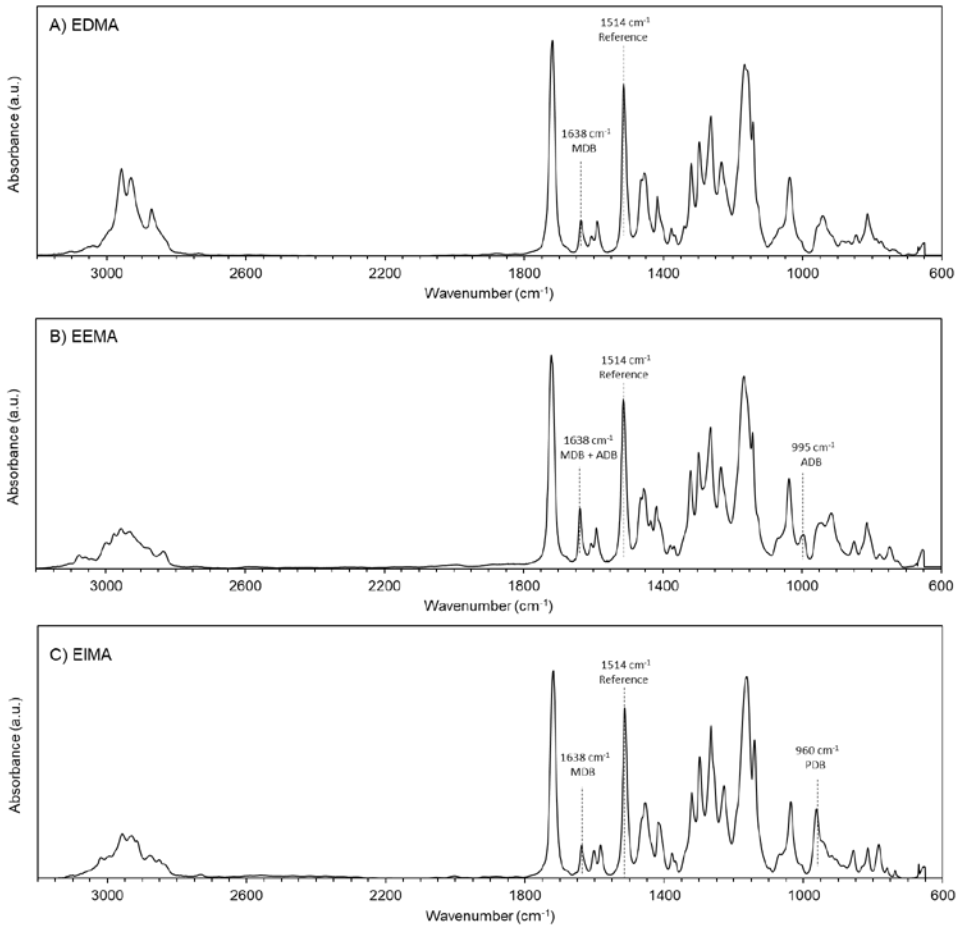

Figure A2-1. IR spectra in transmission of the different eugenol derived methacrylates: A) EDMA, B) EEMA and C) EIMA.

A2.2 Calculation of the conversion of the eugenol-derived monomers during photoinduced polymerization

As reported in the experimental part, IR spectra of the monomers were collected in real time during irradiation and the conversion of the double bonds was estimated according to Eq. A2-1:

$$Conversion\%_{t=x} = 100 \times (1 - \frac{\frac{A_{t=x}}{Ref.A_{t=x}}}{\frac{A_{t=0}}{Ref.A_{t=0}}}) \qquad \text{Eq. A2-1}$$

where A is the absorbance of the IR band of the functional group monitored during irradiation; Ref A is the absorbance of the band of the aromatic ring (C-C stretching) taken as a reference (1540 cm^{-1} to 1490 cm^{-1}).

For EDMA, the functional group monitored was the methacrylic double bond (MDB) band at 1638 cm^{-1}. For EIMA, both the methacrylic double bond (MDB) band at 1638 cm^{-1} and the propenyl double bond (PDB) band at 960 cm^{-1} were monitored.

In the case of EEMA, the band at *circa* 1638 cm^{-1} is not only due to the methacrylic double bond (MDB), but also to the allyl double bond (ADB). In fact, this ADB band is already present in the IR spectra of both eugenol and ethoxy eugenol (EE) (Scheme A2-1 and Figure A2-2), precursors of the methacrylated EEMA molecule.

Scheme A2-1. Eugenol, ethoxy eugenol and ethoxy eugenyl methacrylate

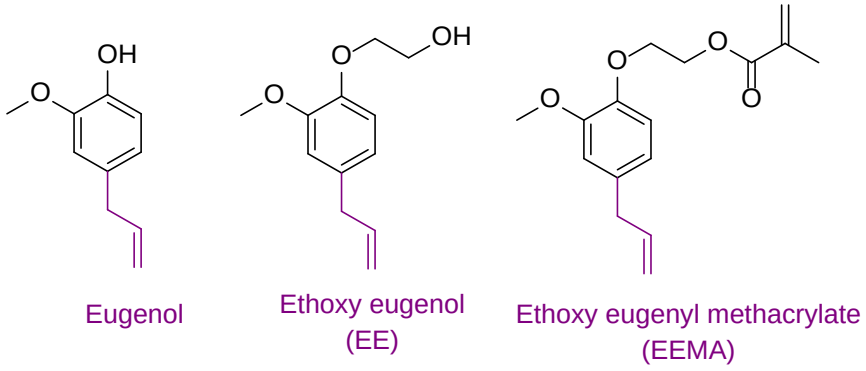

Transmission spectra of the precursos and monomers were done on a Thermo Scientific Nicolet 6700 FTIR apparatus in the 525–4000 cm^{-1} range, with 32 scan and a resolution of 2 cm^{-1}

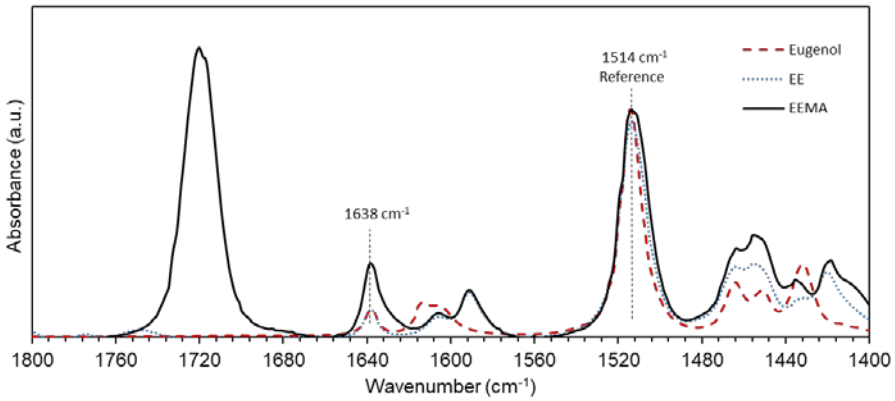

Figure A2-2. Transmission spectra of eugenol, ethoxyeugenol and ethoxy eugenyl methacrylate.

The overlap of the signals coming from methacrylic (MDB) and allylic (ADB) groups of EEMA clearly hinders the direct monitoring of the methacrylic double bond conversion through the area of the peak at 1638 cm^{-1} as conducted for EDMA and EIMA.

As the peaks from methacrylic and allylic groups are centered at the same wavenumber, thus superimposed, the deconvolution process of the band was not able to accurately separate the two contributions of MDB and ADB for EEMA at 1638 cm^{-1}. Therefore, another strategy was chosen. Spectra from EEMA precursors, i.e. eugenol and ethoxy eugenol EE (Figure A2-2) were recorded

and processed as follows. The areas of the allyl group in eugenol and ethoxy eugenol were measured and normalized (using the reference peak at 1514 cm^{-1}) (Table A2-1). The normalized values 0.057 and 0.065 were averaged. The average value 0.061, was considered as representing the allylic contribution (ADB) to the band at 1638 cm^{-1} in the EEMA spectrum with respect to the area of the reference band (Eq. A2-2).

$$A_{ADB\,(1638cm^{-1})_{t=0}} = A_{Ref\,(1514cm^{-1})_{t=0}} \times 0.061 \qquad \text{Eq. A2-2}$$

And

$$A_{MDB\,(1638cm^{-1})_{t=0}} = A_{peak\,(1638cm^{-1})_{t=0}} - A_{ADB\,(1638cm^{-1})_{t=0}} \qquad \text{Eq. A2b}$$

$$= A_{peak\,(1638cm^{-1})_{t=0}} - A_{Ref\,(1514cm^{-1})_{t=0}} \times 0.061$$

Table A2-1. Normalization of the allylic band area for Eugenol and EE

Band	Eugenol	EE
Area (a.u.): Peak 1638 cm^{-1}	1.042 (allylic)	0.558 (allylic)
Area (a.u.): Reference 1514 cm^{-1}	18.373 (aromatic)	8.540 (aromatic)
Normalized Area (a.u.) ($A_{ADB\,(1638cm^{-1})}$ / $A_{Ref\,(1514cm^{-1})}$)	0.057	0.065

The conversion of the methacrylic double bond (MDB) of EEMA was calculated as follows:

The allylic group contribution (ADB) at any time in the composed peak at 1638 cm^{-1} is calculated using Eq. A2-3, used in the form of Eq. A2-4.

The area corresponding to the allylic group contribution at the 1638 cm^{-1} peak at any given time, calculated by Eq. S4, is subtracted from the total area of the 1638 cm^{-1} peak to give the area corresponding to the MDB as shown in Eq. A2-5.

Conversion of MDB at 1638 cm^{-1} is then calculated using reference peak as shown in Eq. A2-6.

$$R = \frac{A_{ADB\,(1638cm^{-1})_{t=0}}}{A_{ADB\,(995cm^{-1})_{t=0}}} = \frac{A_{Ref\,(1514cm^{-1})_{t=0}} \times 0.061}{A_{ADB\,(995cm^{-1})_{t=0}}} = \frac{A_{ADB\,(1638cm^{-1})_{t=x}}}{A_{ADB\,(995cm^{-1})_{t=x}}} \qquad \text{Eq. A2-3}$$

$$A_{ADB\,(1638cm^{-1})_{t=x}} = \frac{A_{Ref\,(1514cm^{-1})_{t=0}} \times 0.061}{A_{ADB\,(995cm^{-1})_{t=0}}} \times A_{ADB\,(995cm^{-1})_{t=x}} \qquad \text{Eq. A2-4}$$

$$A_{MDB\,(1638cm^{-1})_{t=x}} = A_{peak\,(1638cm^{-1})_{t=x}} - A_{ADB\,(1638cm^{-1})_{t=x}}$$

$$= A_{peak\,(1638cm^{-1})_{t=x}} - \frac{A_{Ref\,(1514cm^{-1})_{t=0}} \times 0.061}{A_{ADB\,(995cm^{-1})_{t=0}}} \times A_{ADB\,(995cm^{-1})_{t=x}} \quad \text{Eq. A2-5}$$

$$EEMA\ MDB\ Conversion\ \%_{t=x} = 100 \times \left(1 - \frac{\frac{A_{MDB\,(1638cm^{-1})_{t=x}}}{A_{Ref\,(1514cm^{-1})_{t=x}}}}{\frac{A_{MDB\,(1638cm^{-1})_{t=0}}}{A_{Ref\,(1514cm^{-1})_{t=0}}}}\right) \quad \text{Eq. A2-6}$$

$$= 100 \times \left(1 - \frac{\frac{A_{peak\,(1638cm^{-1})_{t=x}} - A_{ADB\,(1638cm^{-1})_{t=x}}}{A_{Ref\,(1514cm^{-1})_{t=x}}}}{\frac{A_{MDB\,(1638cm^{-1})_{t=0}}}{A_{Ref\,(1514cm^{-1})_{t=0}}}}\right)$$

$$= 100 \times \left(1 - \frac{\frac{A_{peak\,(1638cm^{-1})_{t=x}} - \frac{A_{Ref\,(1514cm^{-1})_{t=0}} \times 0.061}{A_{ADB\,(995cm^{-1})_{t=0}}} \times A_{ADB\,(995cm^{-1})_{t=x}}}{A_{Ref\,(1514cm^{-1})_{t=x}}}}{\frac{A_{MDB\,(1638cm^{-1})_{t=0}}}{A_{Ref\,(1514cm^{-1})_{t=0}}}}\right)$$

$$= 100 \times \left(1 - \frac{\frac{A_{peak\,(1638cm^{-1})_{t=x}} - \frac{A_{Ref\,(1514cm^{-1})_{t=0}} \times 0.061}{A_{ADB\,(995cm^{-1})_{t=0}}} \times A_{ADB\,(995cm^{-1})_{t=x}}}{A_{Ref\,(1514cm^{-1})_{t=x}}}}{\frac{A_{peak\,(1638cm^{-1})_{t=0}} - A_{Ref\,(1514cm^{-1})_{t=0}} \times 0.061}{A_{Ref\,(1514cm^{-1})_{t=0}}}}\right)$$

A2.3 UV Spectra

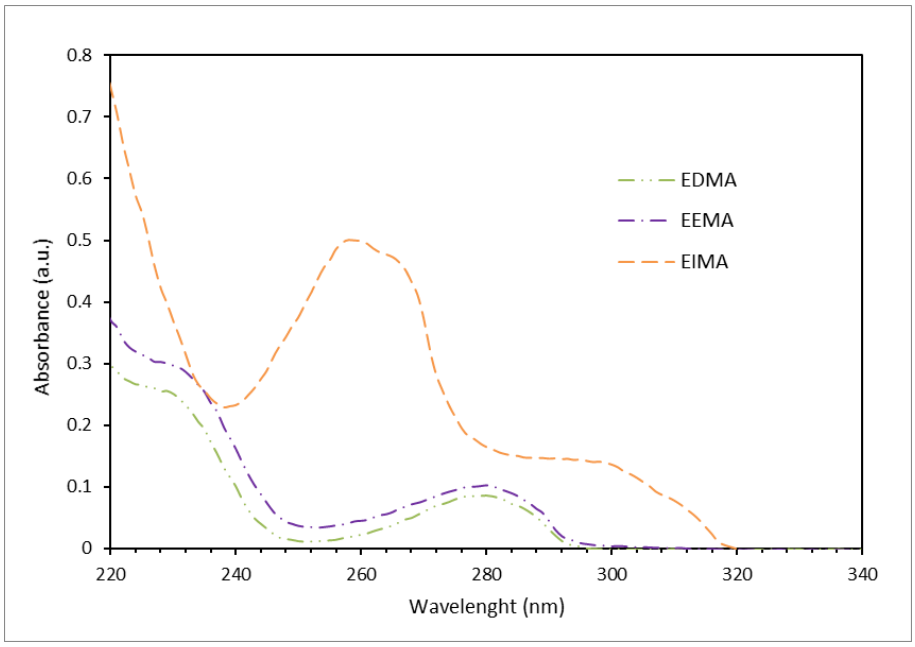

Figure A2-3. UV absorption spectra of the eugenol-derived methacrylates, in acetonitrile 0.002 wt%.

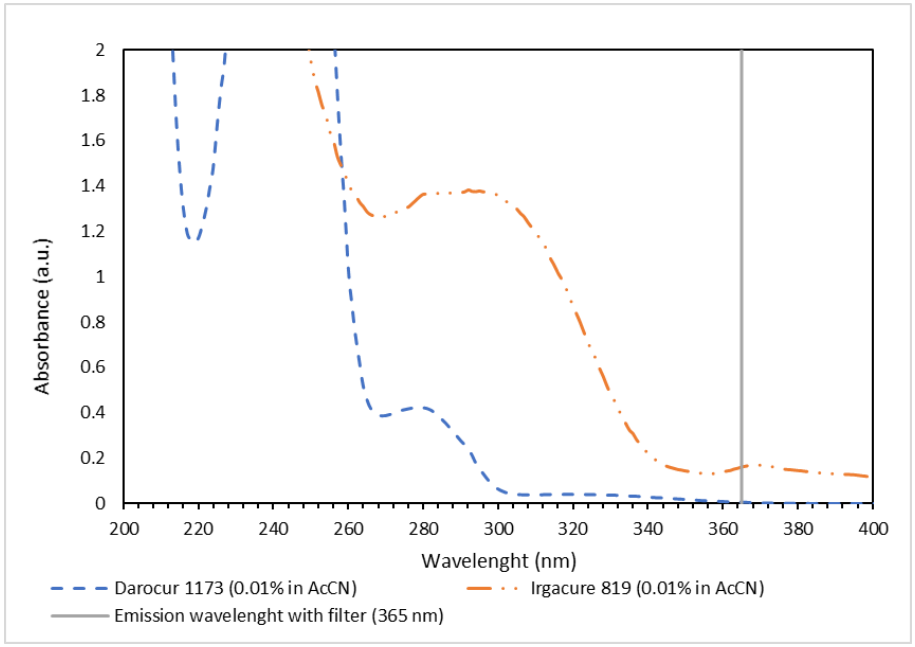

Figure A2-4. UV Absorption of photoinitiators.

A2.4 DSC Measurements

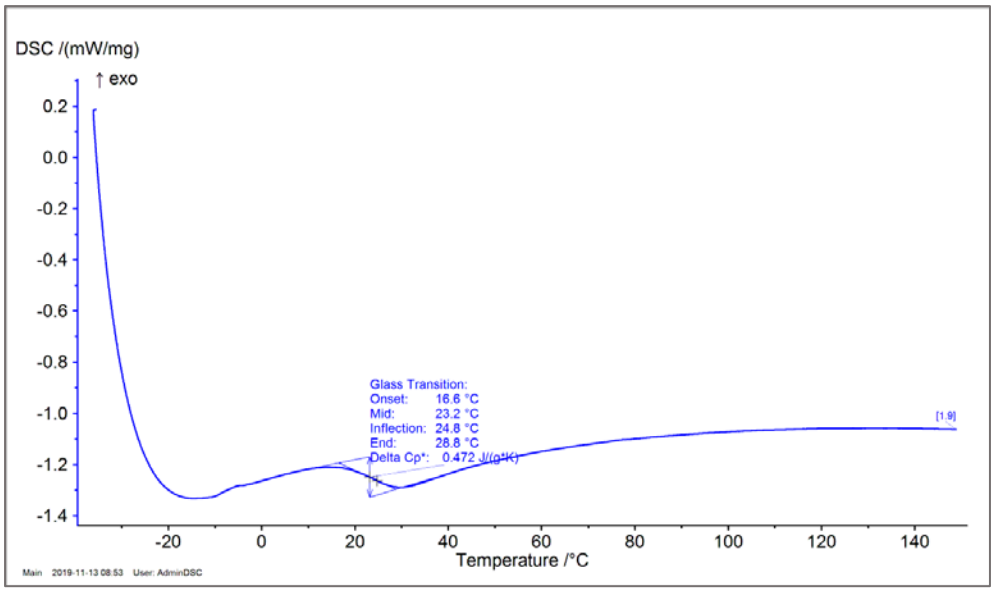

Figure A2-5. DSC measurement of poly(EDMA) obtained from photoinduced polymerization with Darocur 1173 (2% wbm) under nitrogen.

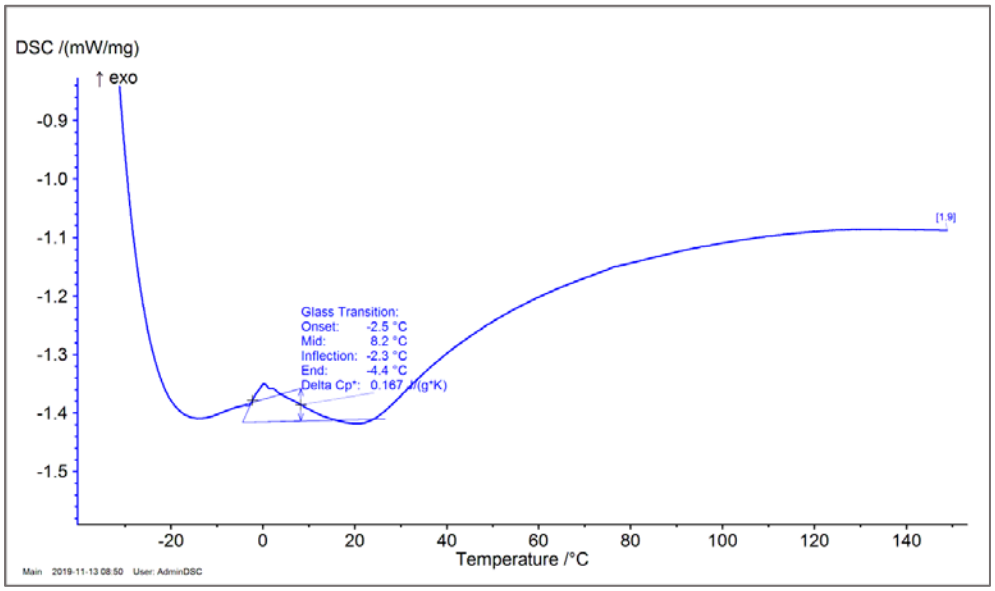

Figure A2-6. DSC measurement of poly(EDMA) obtained from photoinduced polymerization with Darocur 1173 (2% wbm) under air.

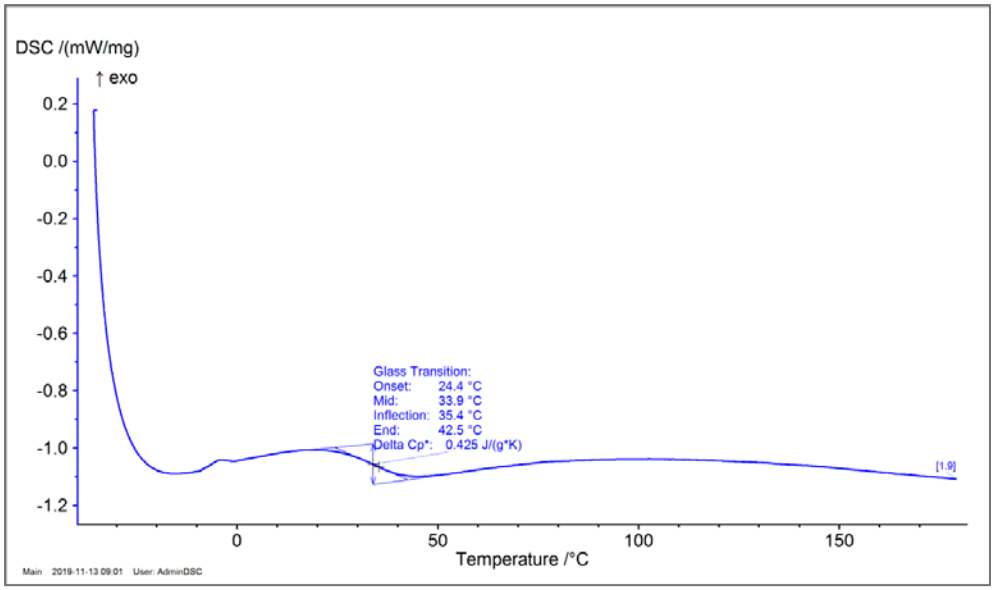

Figure A2-7. DSC measurement of poly(EEMA) obtained from photoinduced polymerization with Darocur 1173 (2% wbm) under nitrogen.

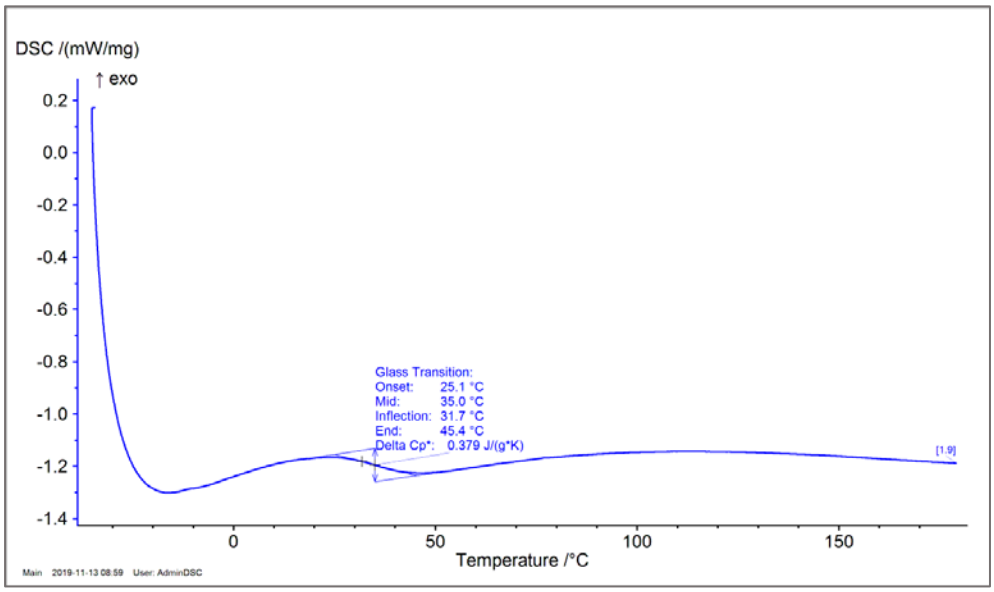

Figure A2-8. DSC measurement of poly(EEMA) obtained from photoinduced polymerization with Darocur 1173 (2% wbm) under air.

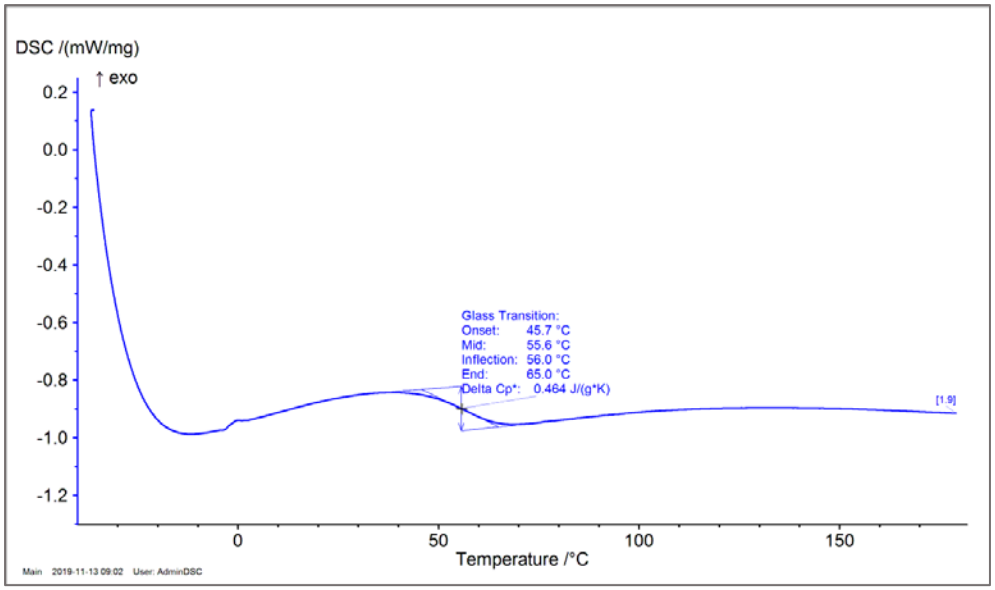

Figure A2-9. DSC measurement of poly(EIMA) obtained from photoinduced polymerization with Darocur 1173 (2% wbm) under nitrogen.

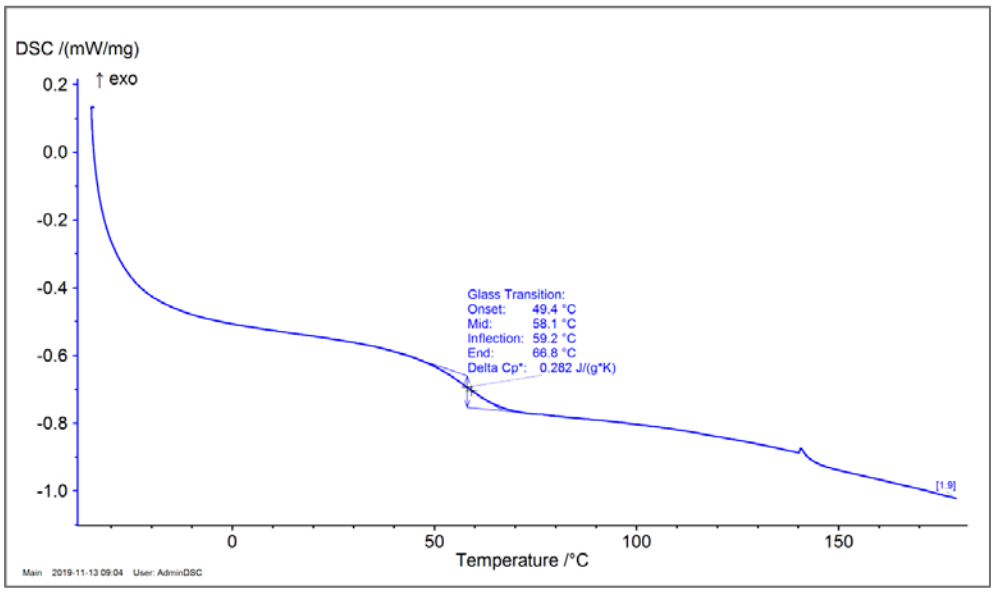

Figure A2-10. DSC measurement of poly(EIMA) obtained from photoinduced polymerization with Darocur 1173 (2% wbm) under air.

A2.5 Hydroperoxide formation

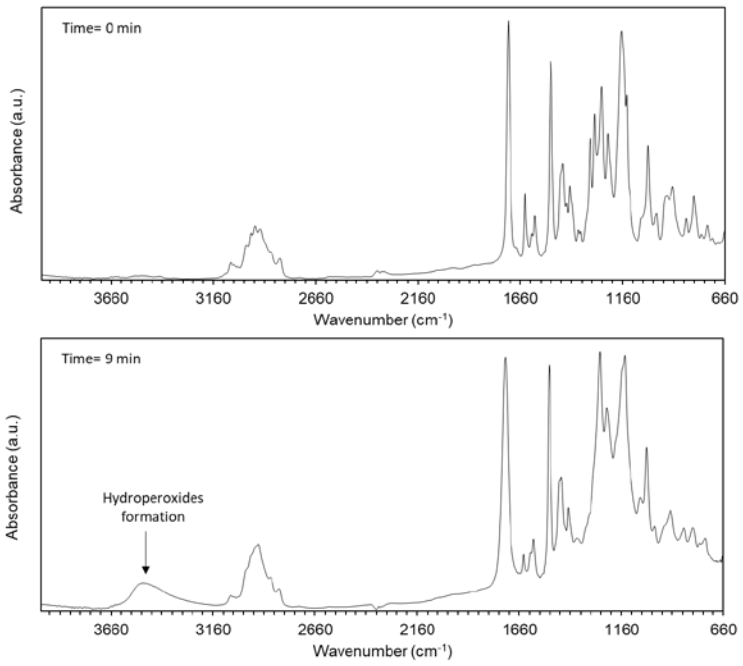

Figure A2-11. FT-IR spectra at time=0 and time=9 minutes denoting the formation of hydroperoxides during photopolymerization of EEMA in the absence of PI under air.

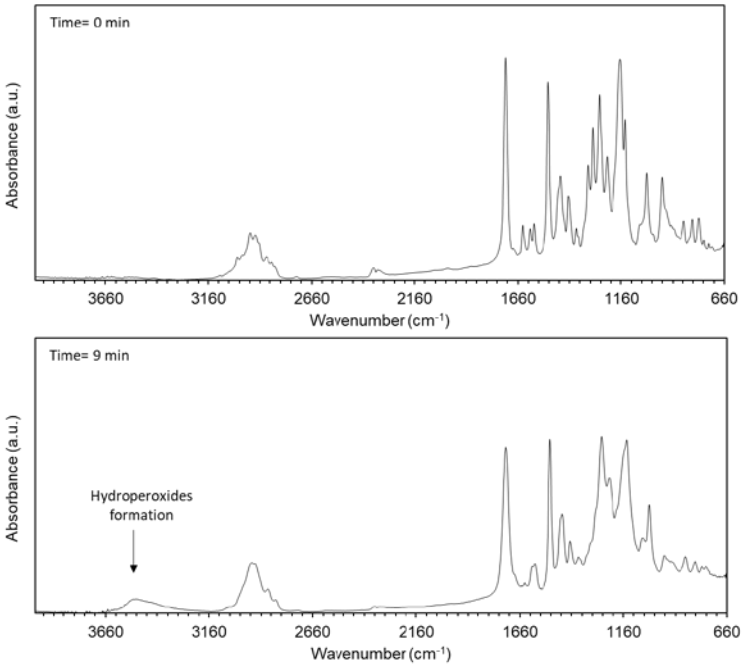

Figure A2-12. FT-IR spectra at time=0 and time=9 minutes denoting the formation of hydroperoxides during photopolymerization of EIMA in the absence of PI under air.

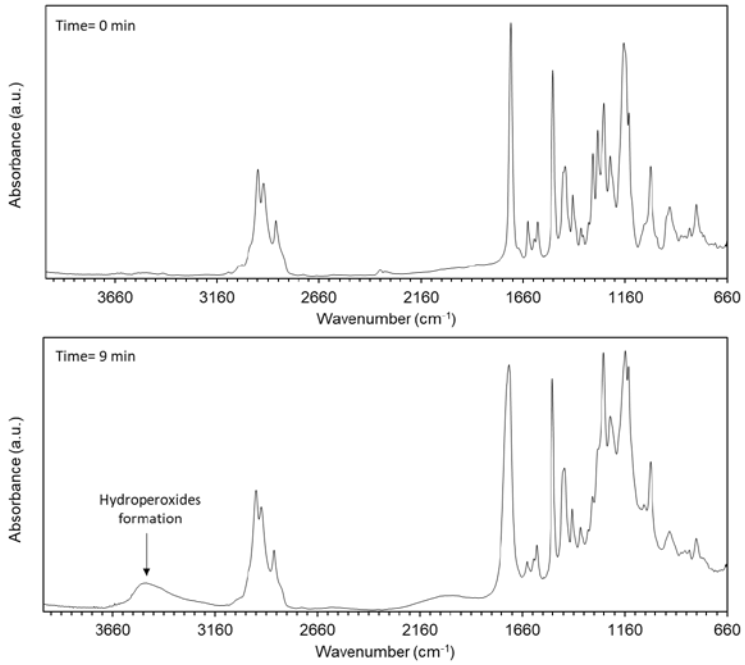

Figure A2-13. FT-IR spectra at time=0 and time=9 minutes denoting the formation of hydroperoxides during photopolymerization of EDMA in the absence of PI under air.

A2.6 Photoinduced polymerization of eugenol-derived methacrylates with Irgacure 819.

Photoinduced polymerization of eugenol-derived monomers was done with Irgacure 819®. The homolytic cleavage of Irgacure 819® is shown in (Scheme A2-2) and its UV spectrum in Figure A2-4.

Scheme A2-2.Irgacure 819, its homolytic cleavage under light

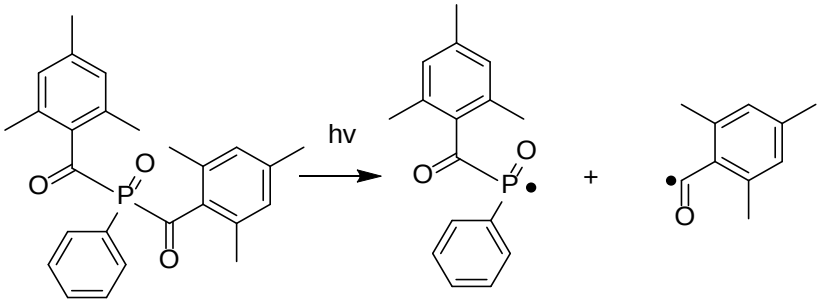

A behavior similar to that of Darocur 1173 was observed. Conversion of MDB, ADB and PDB for the respective monomers are presented in and Figure A2-14 and Figure A2-15. In the presence of oxygen, no significant reaction took place for EDMA and EEMA MDB (8% and 7% conversion respectively) while EIMA MDB reached a conversion of 40%. EIMA may be able to produce charge-transfer complexes leading to the formation of peroxides and radicals, allowing polymerization to proceed to a limited extent. In the absence of air, the conversion order was as follows: EDMA (96%) > EIMA (78%) >EEMA (76%). EDMA was the most reactive monomer (through the methacrylate

double bond) as no secondary reactions are present. EEMA followed with only a slight reduction of polymerization rate due to the formation of highly stable bis-allylic radicals. Finally, EIMA came last due to cross-propagation between propenyl and methacrylate double bonds. This secondary reaction only marginally affected the methacrylate double bond conversion, which reached values very close to those of EEMA.

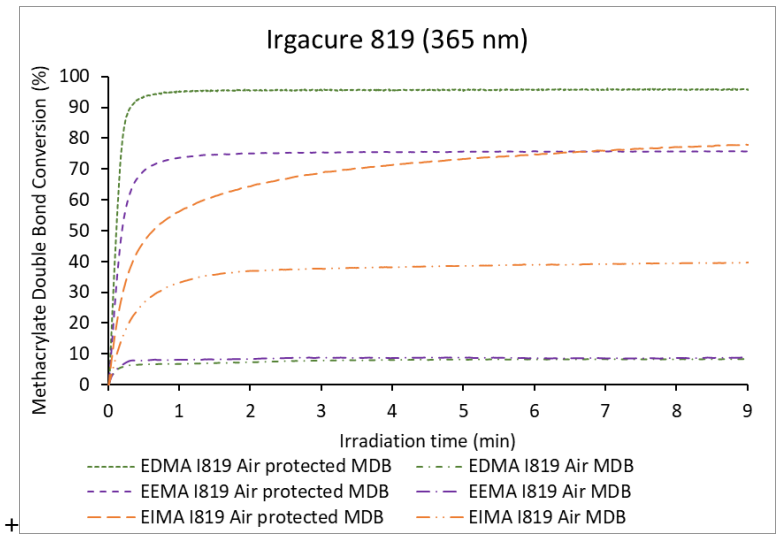

Figure A2-14. Methacrylate double bond conversion for eugenol-derived monomer versus irradiation time with Irgacure 819 and filter.

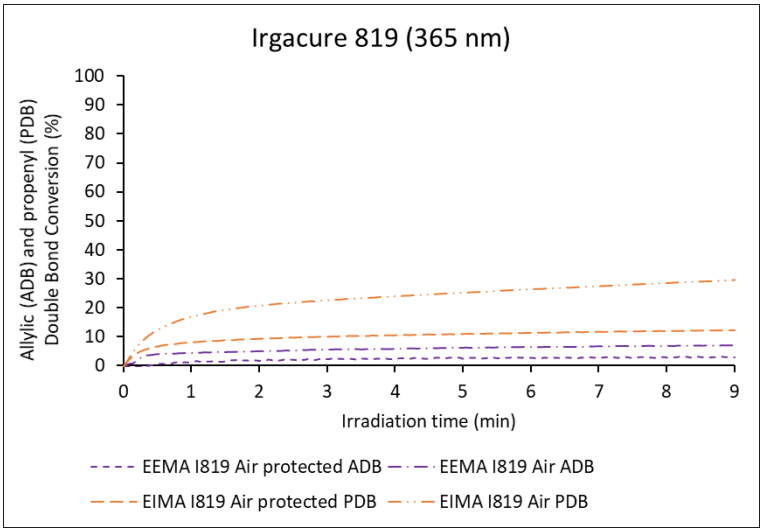

Figure A2-15. Allylic and Propenyl double bond conversion for eugenol-derived monomers versus irradiation time with Irgacure 819 and filter.

A2.7 Monomer conversion

Table A2-2. Monomer conversion of films used for polymer characterization (by ATR-FTIR)

Monomer	Condition	Darocur 1173	
		Upper side (contact with atmosphere) (%)	**Lower side (contact with glass substrate) (%)**
EDMA MDB	Air protected	100	100
EEMA MDB		85	85
EIMA MDB		99	98
EEMA ADB		27	0
EIMA PDB		96	99
EDMA MDB	Air	91	92
EEMA MDB		81	57
EIMA MDB		99	99
EEMA ADB		74	7
EIMA PDB		94º	65

A3 CHAPTER 4

A3.1 DLS measurements

Table A3-1. Intensity, number and volume-average particle diameter sizes of poly(EDMA), poly(EIMA) and poly(EEMA) latexes using KPS, ACVA and $Na_2S_2O_5$/KPS initiation systems

Monomer	Initiator	D_i (nm)	D_n (nm)	D_v (nm)	D_z (nm)	PDI
EDMA	KPS (70°C)	63	30	43	49	0.135
	ACVA (70°C)	64	49	56	58	0.044
	$Na_2S_2O_5$/KPS (40°C)	71	28	44	52	0.167
EEMA	KPS (70°C)	104	81	92	96	0.041
	ACVA (70°C)	57	29	41	45	0.119
	$Na_2S_2O_5$/KPS (40°C)	53	39	45	48	0.054
EIMA	KPS (70°C)	70	33	48	54	0.135
	ACVA (70°C)	45	30	37	39	0.073
	$Na_2S_2O_5$/KPS (40°C)	163	110	135	143	0.067

A3.2 Emulsion polymerization using KPS as the initiator:

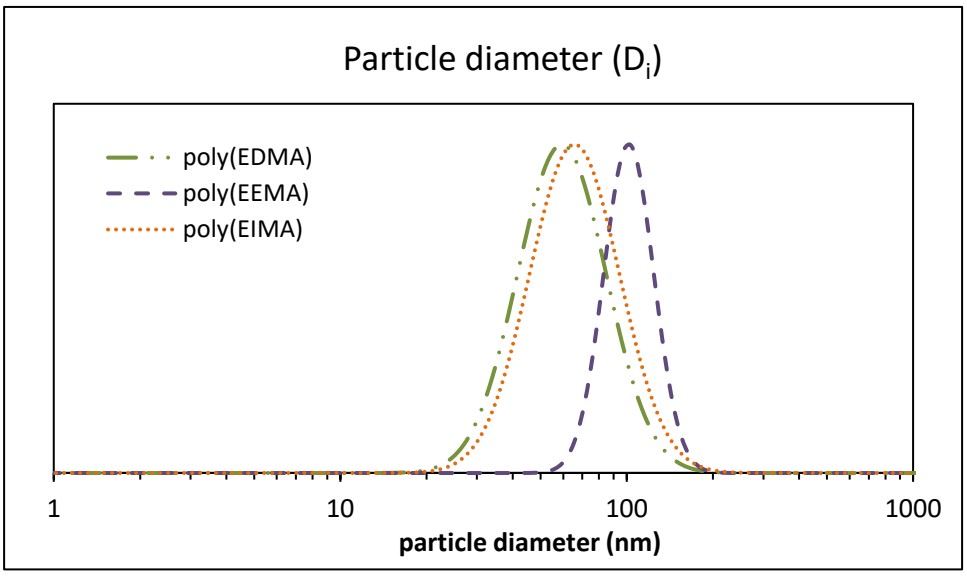

Figure A3-1. Intensity-average particle size distributions (Cumulants model) for poly(EDMA), poly(EIMA) and poly(EEMA) obtained from emulsion polymerization using KPS thermal initiation.

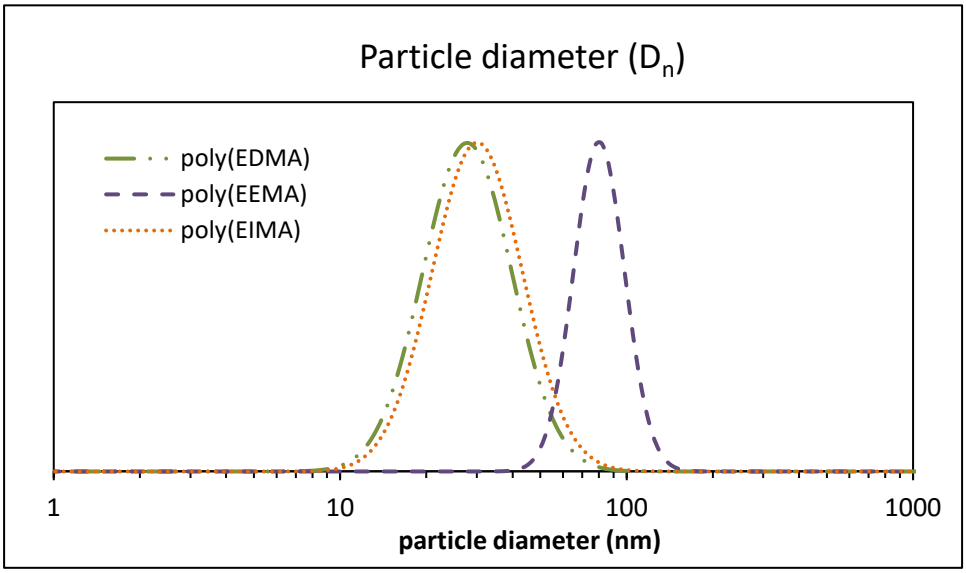

Figure A3-2. Number-average particle size distributions (Cumulants model) for poly(EDMA), poly(EIMA) and poly(EEMA) obtained from emulsion polymerization using KPS thermal initiation.

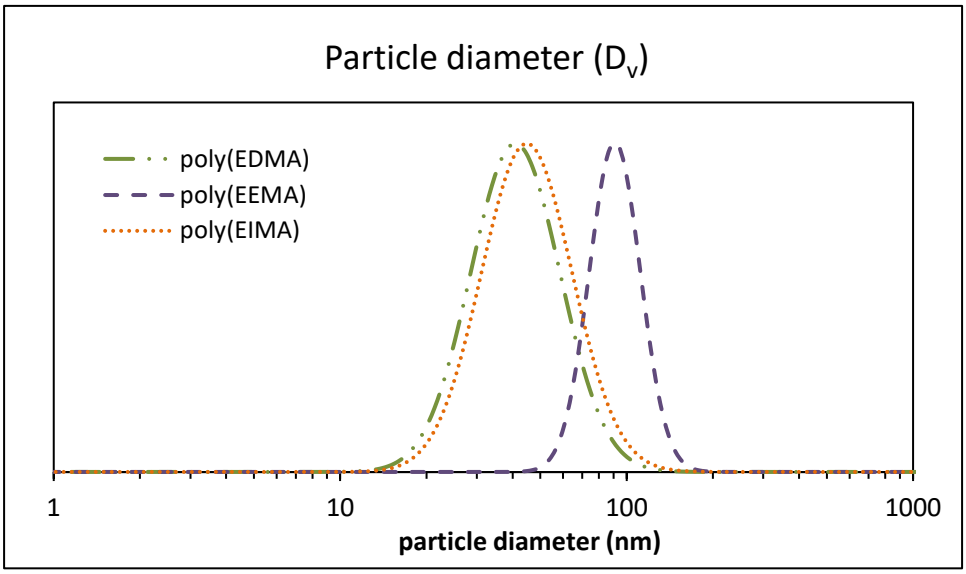

Figure A3-3. Volume-average particle size distributions (Cumulants model) for poly(EDMA), poly(EIMA) and poly(EEMA) obtained from emulsion polymerization using KPS thermal initiation.

A3.3 Emulsion polymerization using ACVA as the initiator

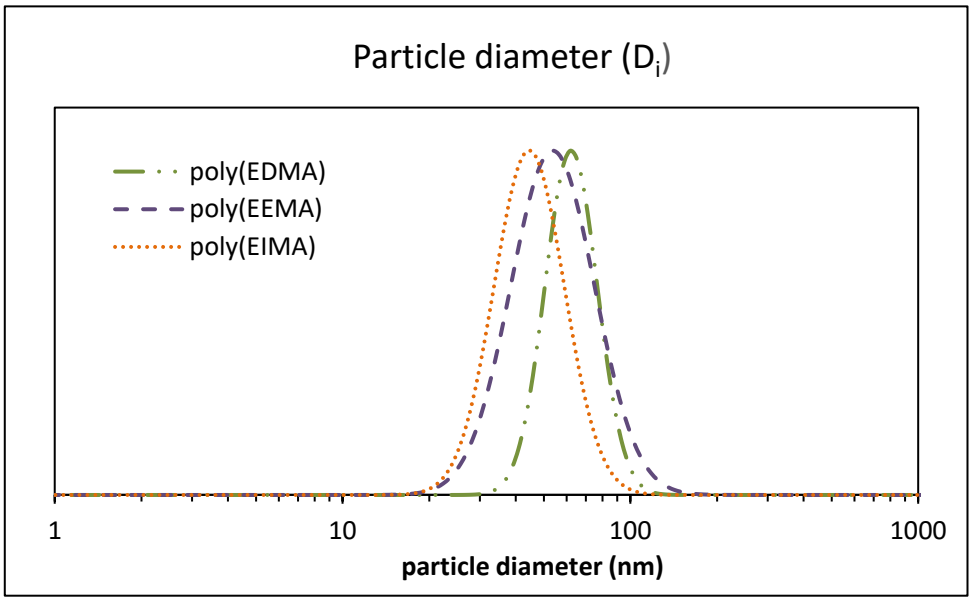

Figure A3-4. Intensity-average particle size distributions (Cumulants model) for poly(EDMA), poly(EIMA) and poly(EEMA) obtained from emulsion polymerization using ACVA thermal initiation

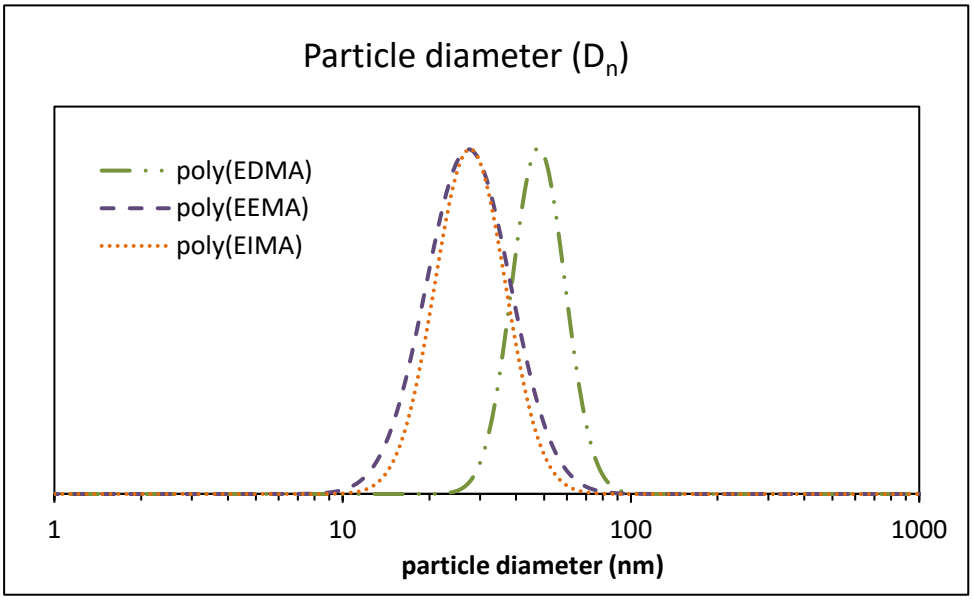

Figure A3-5. Number-average particle size distributions (Cumulants model) for poly(EDMA), poly(EIMA) and poly(EEMA) obtained from emulsion polymerization using ACVA thermal initiation

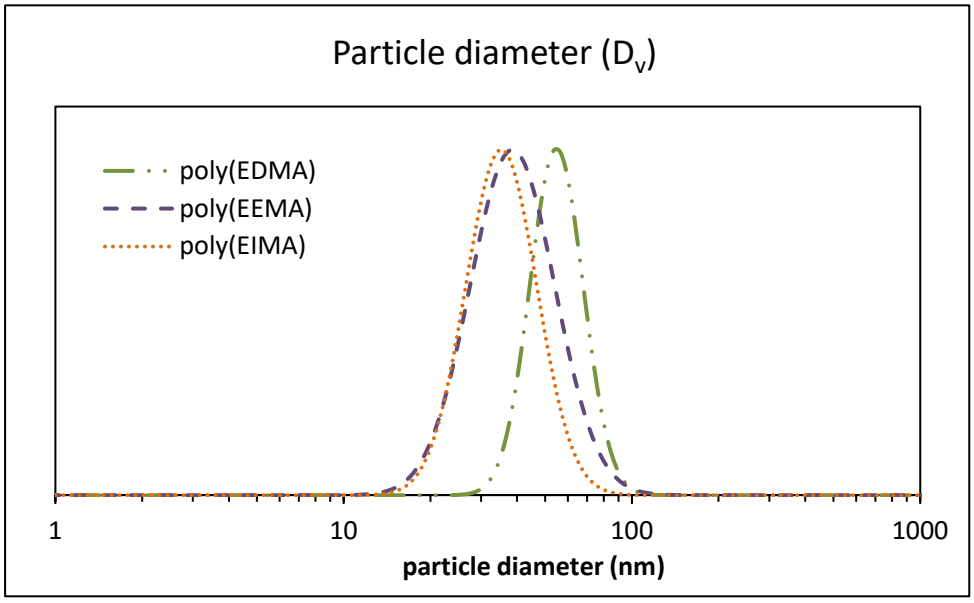

Figure A3-6. Volume-average particle size distributions (Cumulants model) for poly(EDMA), poly(EIMA) and poly(EEMA) obtained from emulsion polymerization using ACVA thermal initiation

A3.4 Emulsion polymerization using $Na_2S_2O_5$/KPS redox initiation:

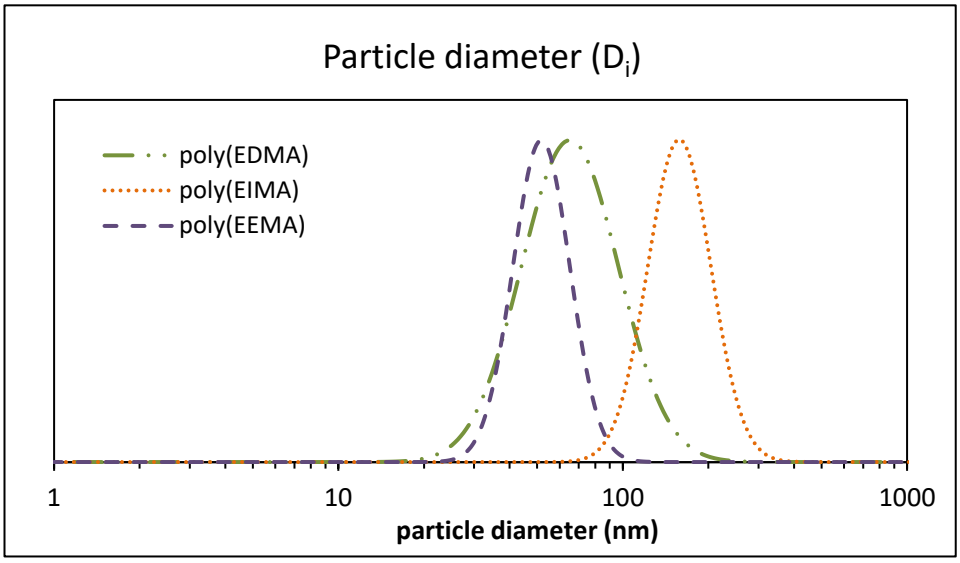

Figure A3-7. Intensity-average particle size distributions (Cumulants model) for poly(EDMA), poly(EIMA) and poly(EEMA) obtained from emulsion polymerization using $Na_2S_2O_5$/KPS Redox initiation

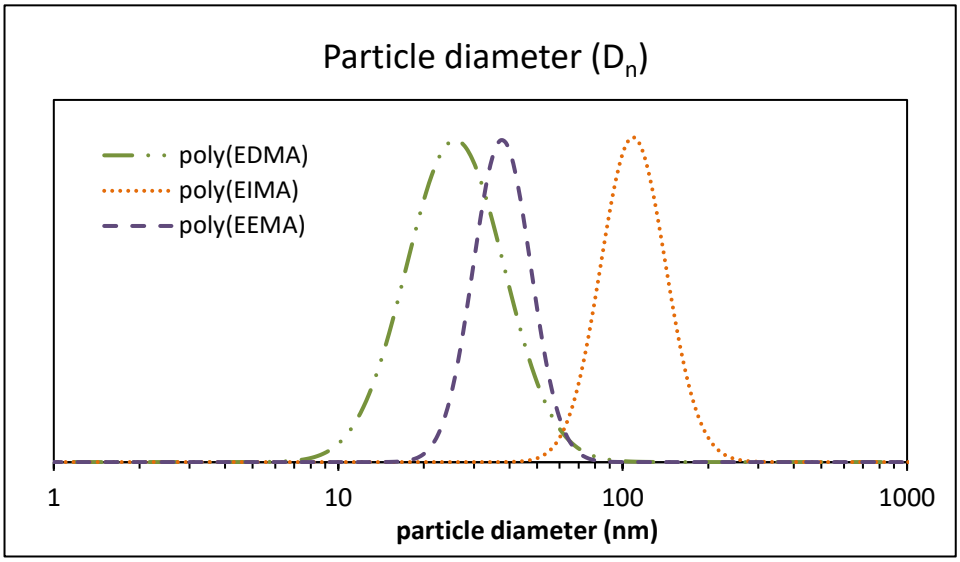

Figure A3-8. Number-average particle size distributions (Cumulants model) for poly(EDMA), poly(EIMA) and poly(EEMA) obtained from emulsion polymerization using $Na_2S_2O_5$/KPS Redox initiation

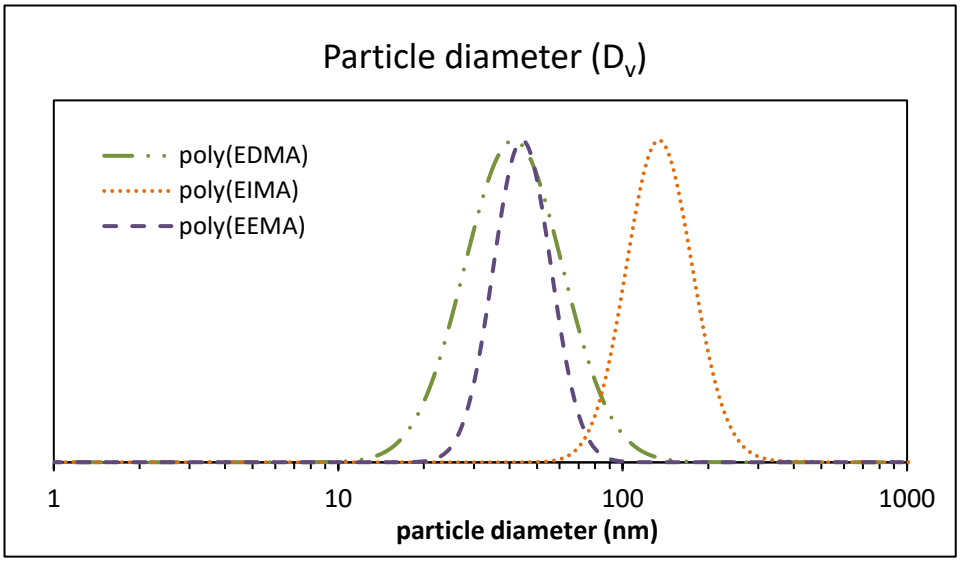

Figure A3-9. Volume-average particle size distributions (Cumulants model) for poly(EDMA), poly(EIMA) and poly(EEMA) obtained from emulsion polymerization using $Na_2S_2O_5$/KPS Redox initiation

A3.5 TEM measurements

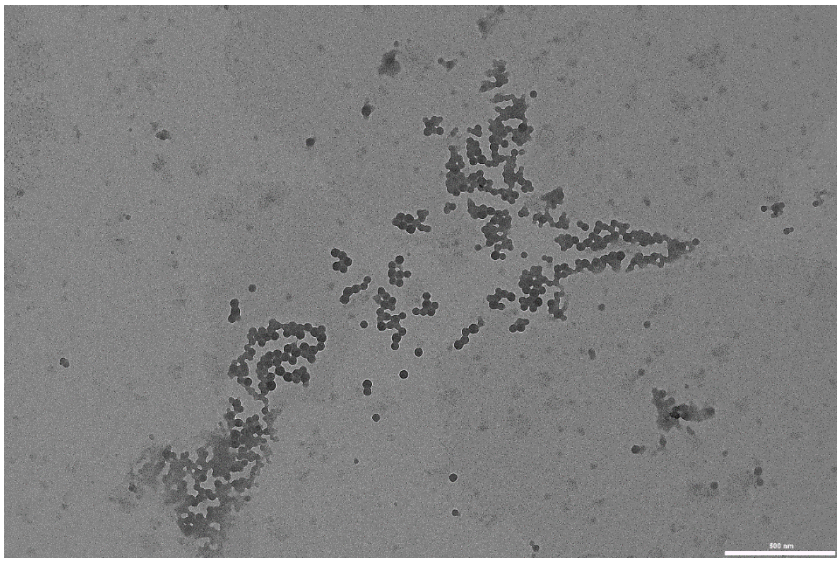

Figure A3-10. TEM image of poly(EIMA) latex obtained by emulsion polymerization using ACVA (70°C) as the initiator.

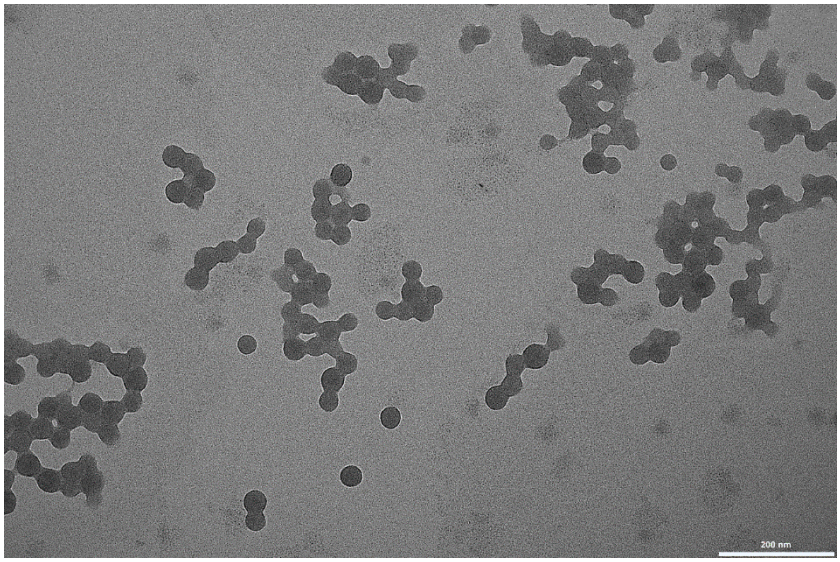

Figure A3-11. TEM image of poly(EIMA) latex obtained by emulsion polymerization using ACVA (70°C) as the initiator (Zoom). Number average particle diameter size determined from 100 particles: $D_{n,TEM}$=38 nm, Stdev 4.3 nm.

A3.6 Thermogravimetric analysis (under N_2)

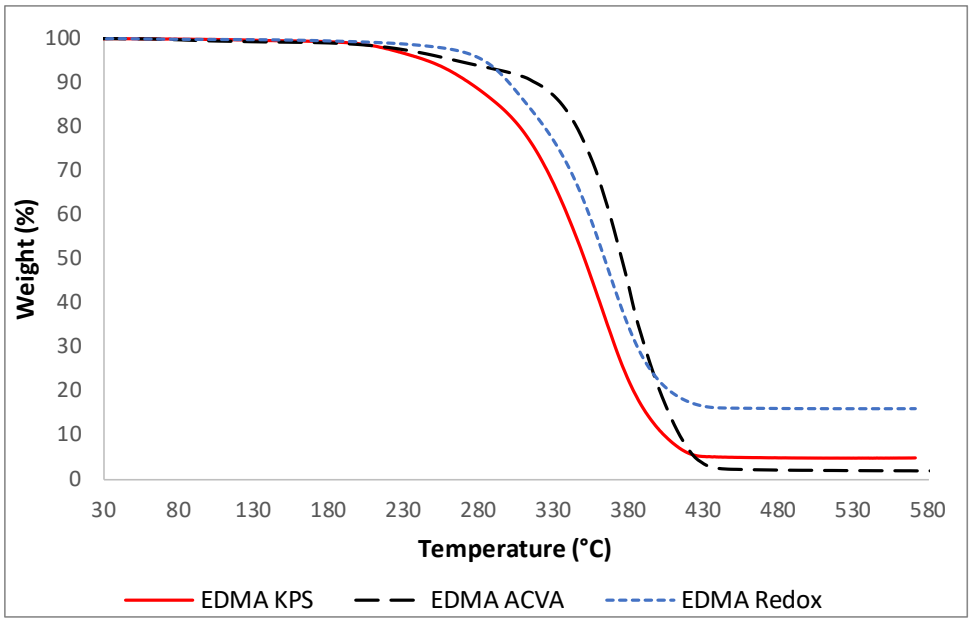

Figure A3-12. TGA curves on poly(EDMA) obtained from emulsion polymerization of EDMA using different initiators.

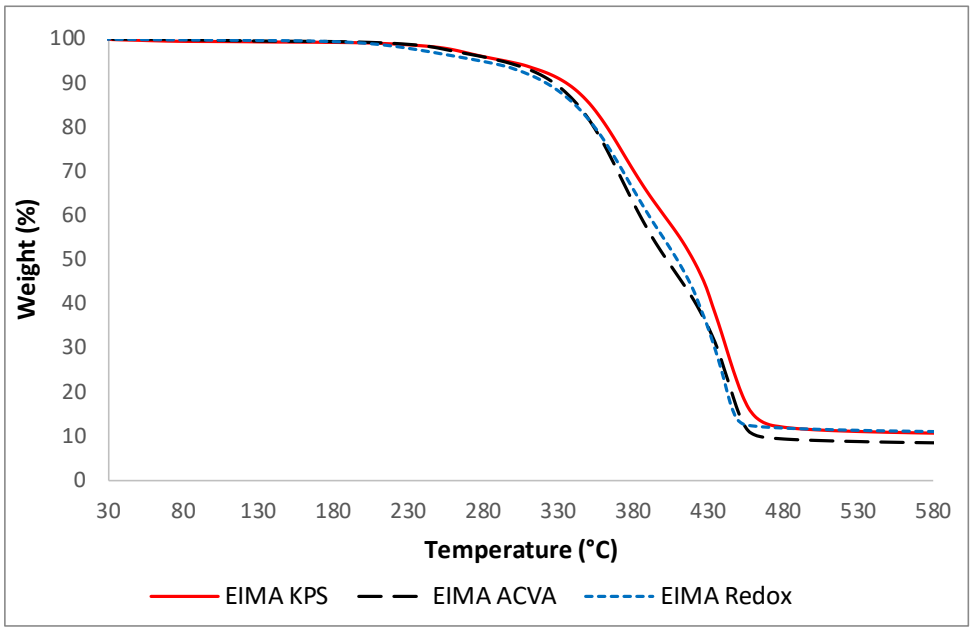

Figure A3-13. TGA curves on poly(EIMA) obtained from emulsion polymerization of EIMA using different initiators.

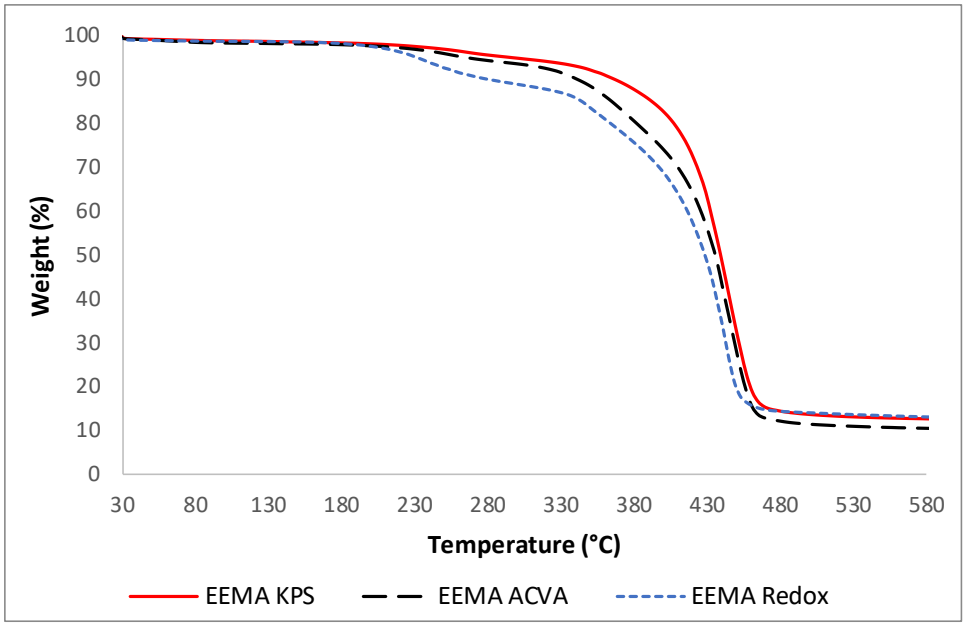

Figure A3-14. TGA curves on poly(EEMA) obtained from emulsion polymerization of EEMA using different initiators.

A3.7 DSC measurements

- Emulsion polymerization with thermal KPS initiation:

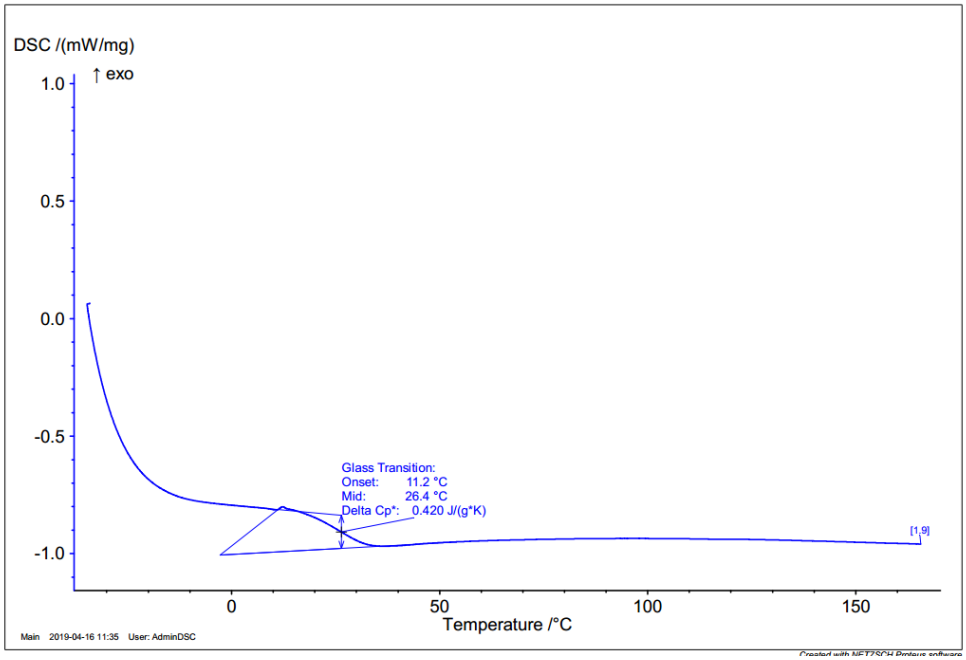

Figure A3-15. DSC measurement on poly(EDMA) from emulsion polymerization with KPS thermal initiation.

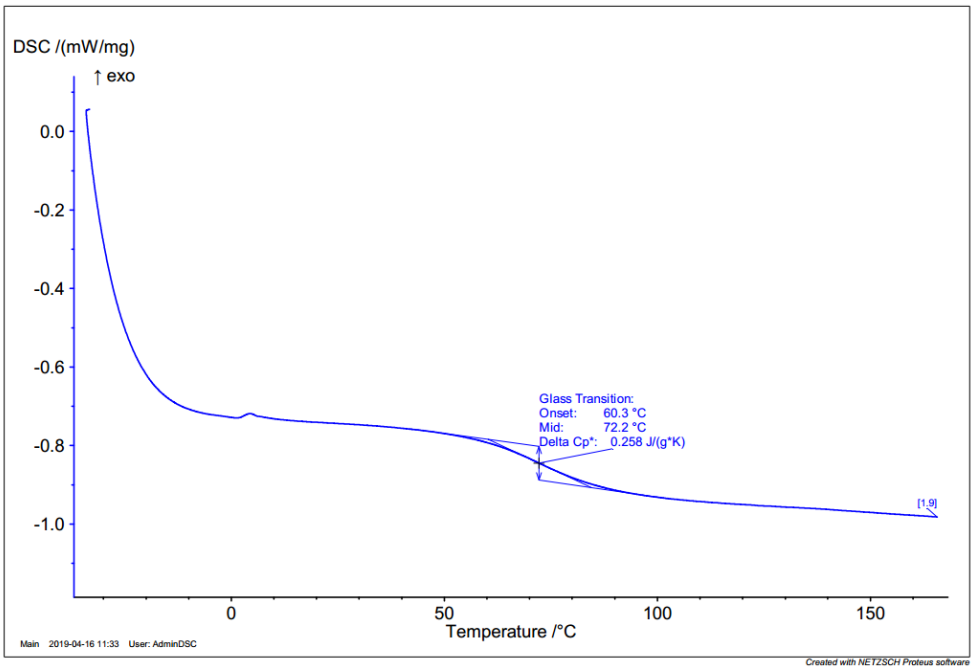

Figure A3-16. DSC measurement on poly(EIMA) from emulsion polymerization with KPS thermal initiation.

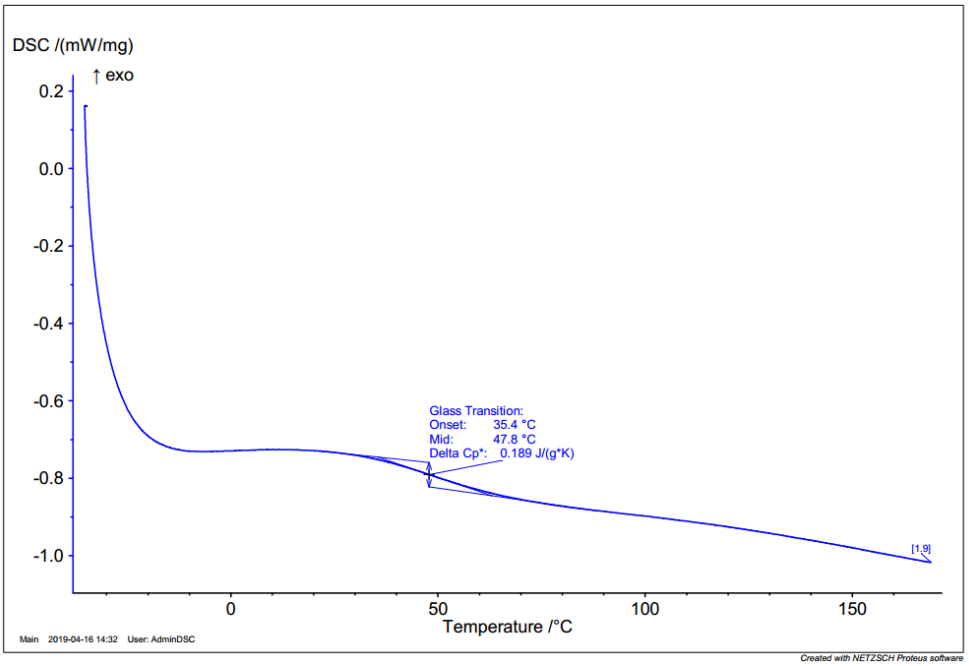

Figure A3-17. DSC measurement on poly(EEMA) from emulsion polymerization with KPS thermal initiation.

- Emulsion polymerization with thermal ACVA initiation:

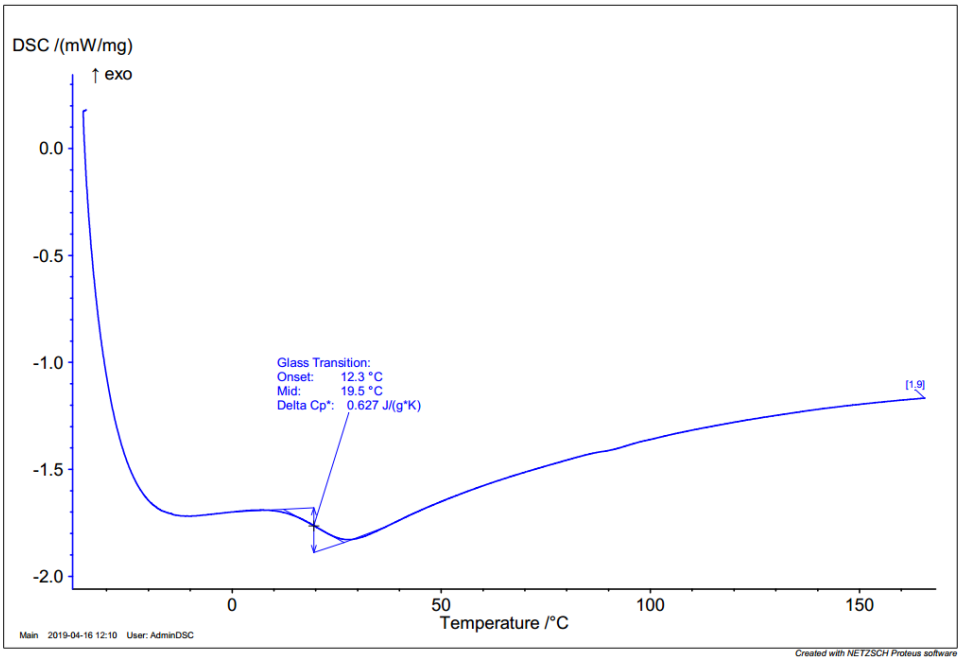

Figure A3-18. DSC measurement on poly(EDMA) from emulsion polymerization with ACVA thermal initiation.

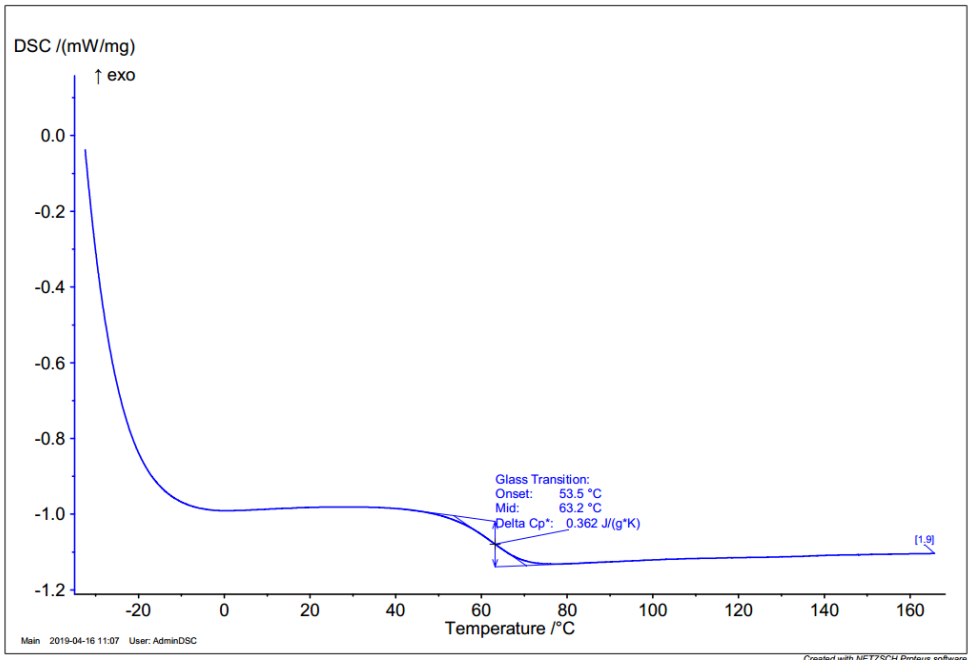

Figure A3-19. DSC measurement on poly(EIMA) from emulsion polymerization with ACVA thermal initiation.

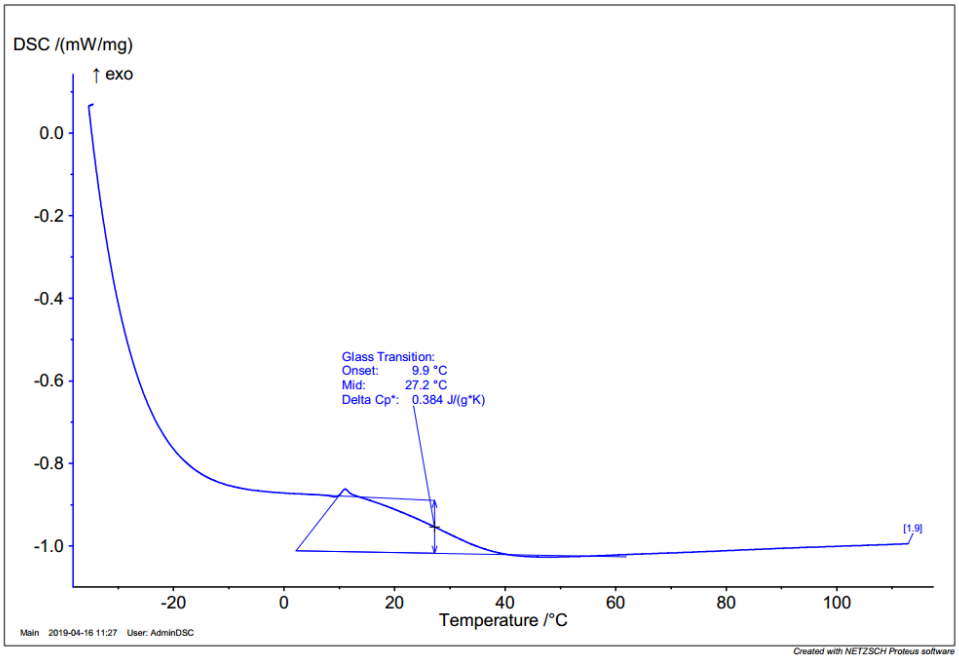

Figure A3-20. DSC measurement on poly(EEMA) from emulsion polymerization with ACVA thermal initiation.

- Emulsion polymerization with $Na_2S_2O_5$/KPS redox initiation:

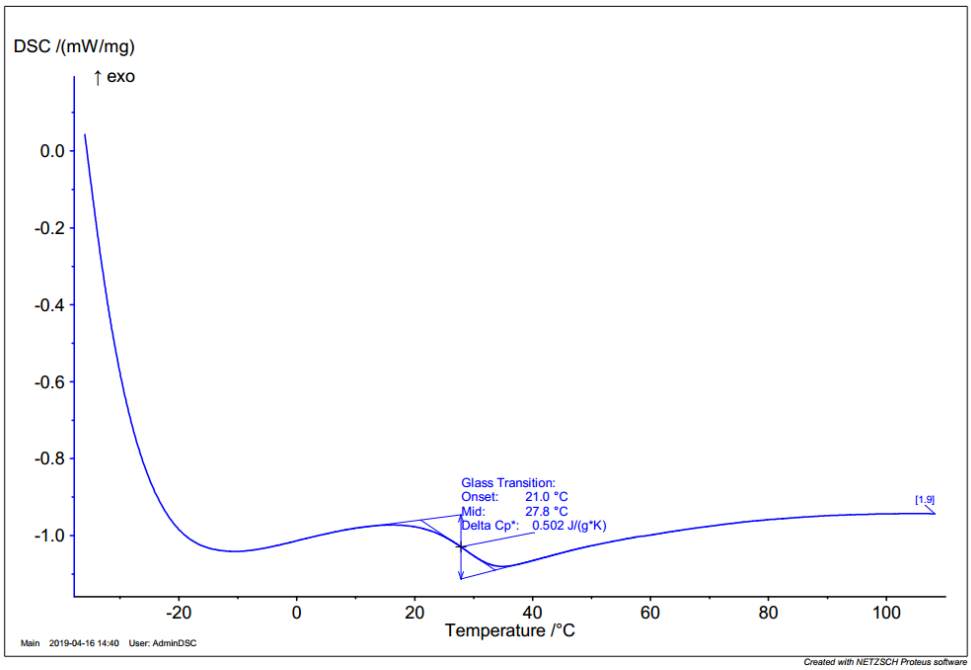

Figure A3-21. DSC measurement on poly(EDMA) from emulsion polymerization with $Na_2S_2O_5$/KPS redox initiation.

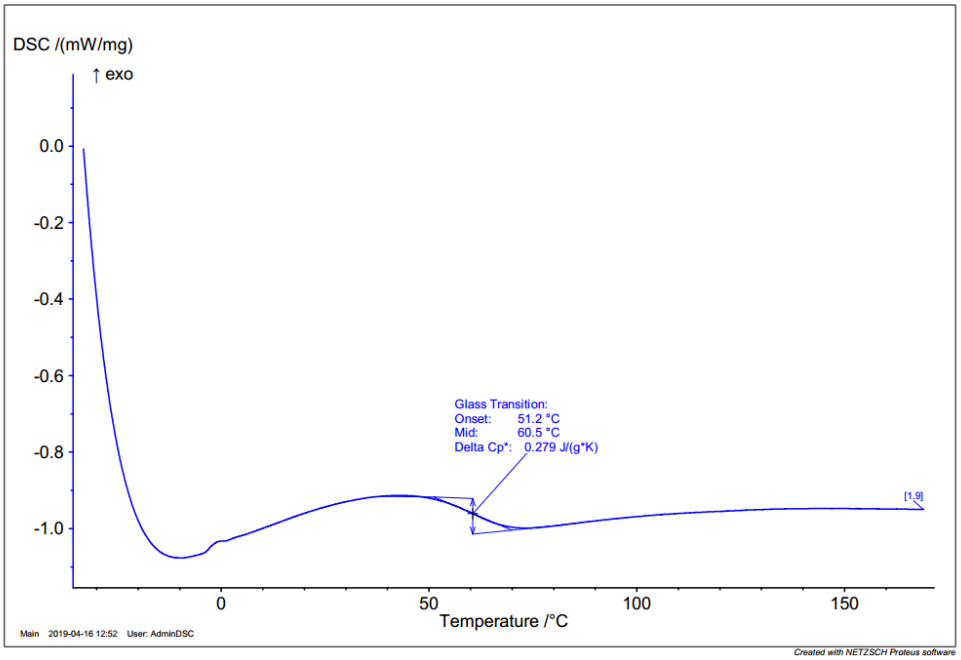

Figure A3-22. DSC measurement on poly(EIMA) from emulsion polymerization with $Na_2S_2O_5$/KPS redox initiation.

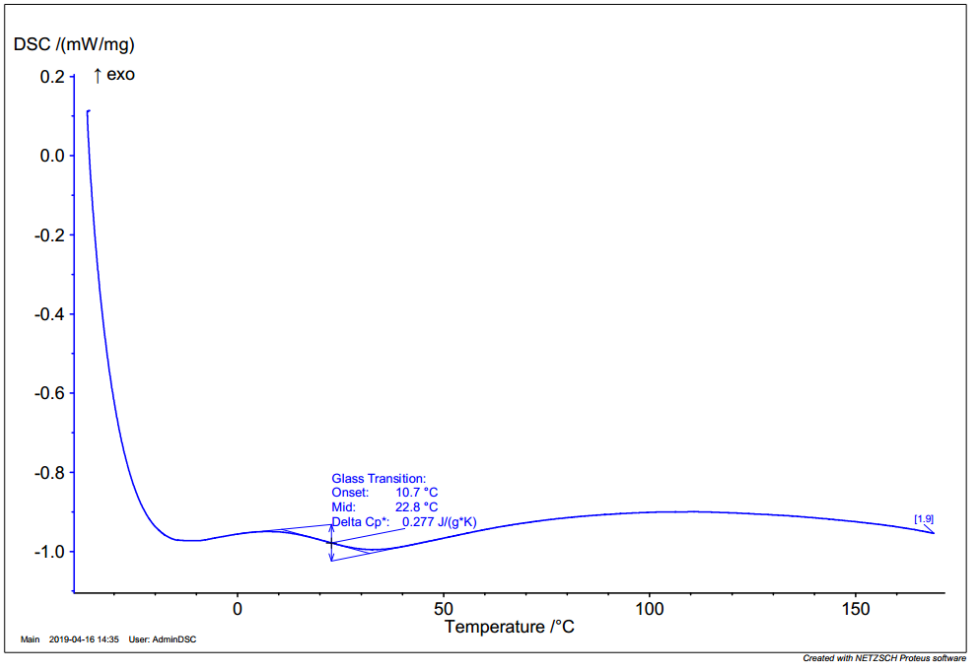

Figure A3-23. DSC measurement on poly(EEMA) from emulsion polymerization with $Na_2S_2O_5$/KPS redox initiation.

A3.8 Kinetics of polymerization:

- Calculation of Monomer conversion directly with signal of a reference peak (methoxy group of EDMA monomer) using Eq. A1-3:

$$Monomer\ conversion = 100 \times \left(1 - \left(\frac{\frac{Signal\ integration\ of\ double\ bond_{t=x}}{Number\ of\ protons\ from\ double\ bond\ signal\ _{t=x}}}{\frac{Signal\ integration\ of\ a\ reference\ signal\ (methoxy)_{t=x}}{Number\ of\ protons\ from\ reference\ signal\ (3)\ _{t=x}}}\right)\right)$$

$$Monomer\ conversion = 100 \times (1 - \left(\frac{\frac{534.84 + 535.85}{2}}{\left(\frac{3000}{3}\right)}\right)) = 46.5\%$$

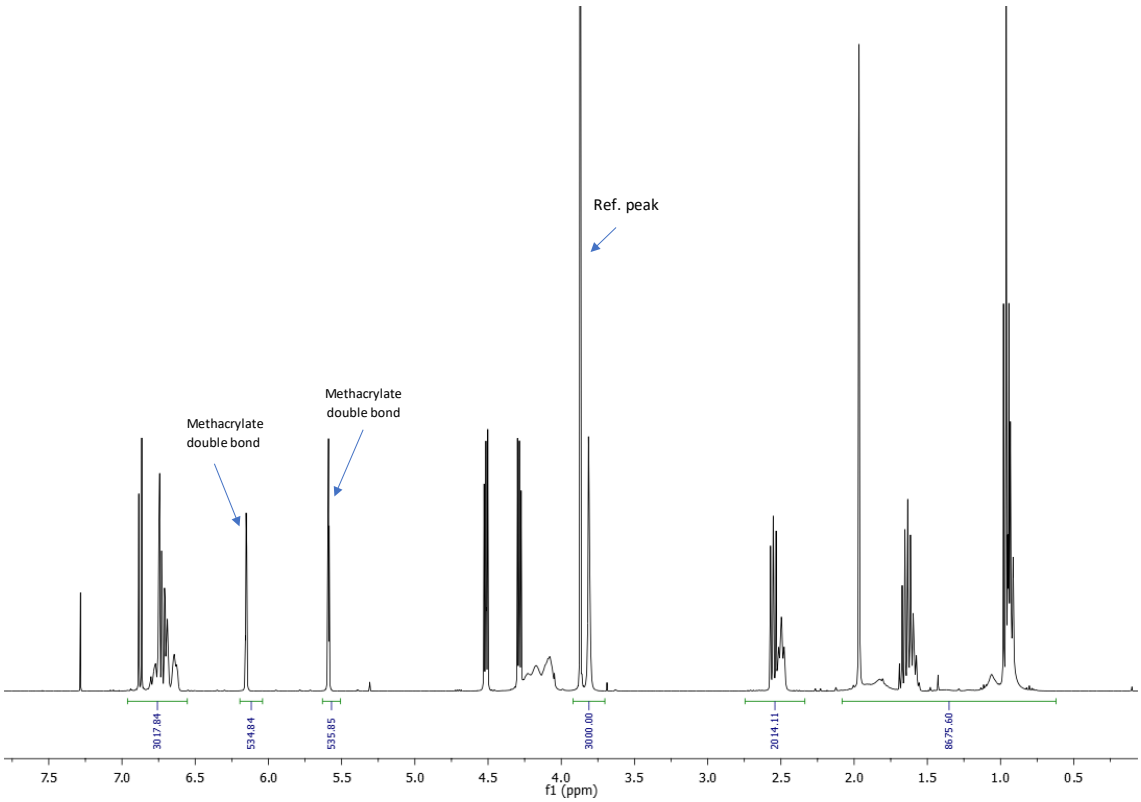

Figure A3-24. ^{1}H NMR EDMA emulsion polymerization using $Na_2S_2O_5$/KPS redox initiation system t=30 min.

Calculation example:

Monomer conversion for emulsion polymerization of EEMA at t=2 hours

- Calculation with Internal Standard (1-4-bis(trimethylsilylbenzene), BTMSB):

$$Monomer\ conversion = 100 \times \left(1 - \left(\frac{\frac{Signal\ integration_{t=x}}{IS\ integration_{t=x}}}{\frac{Signal\ integration_{t=0}}{IS\ integration_{t=0}}}\right)\right)$$ Eq. A1-2

$$Monomer\ conversion = 100 \times (1 - \left(\frac{\frac{331.46 + 333.54}{1000}}{\frac{854.23 + 826.67}{1000}}\right)) = 60.4\%$$

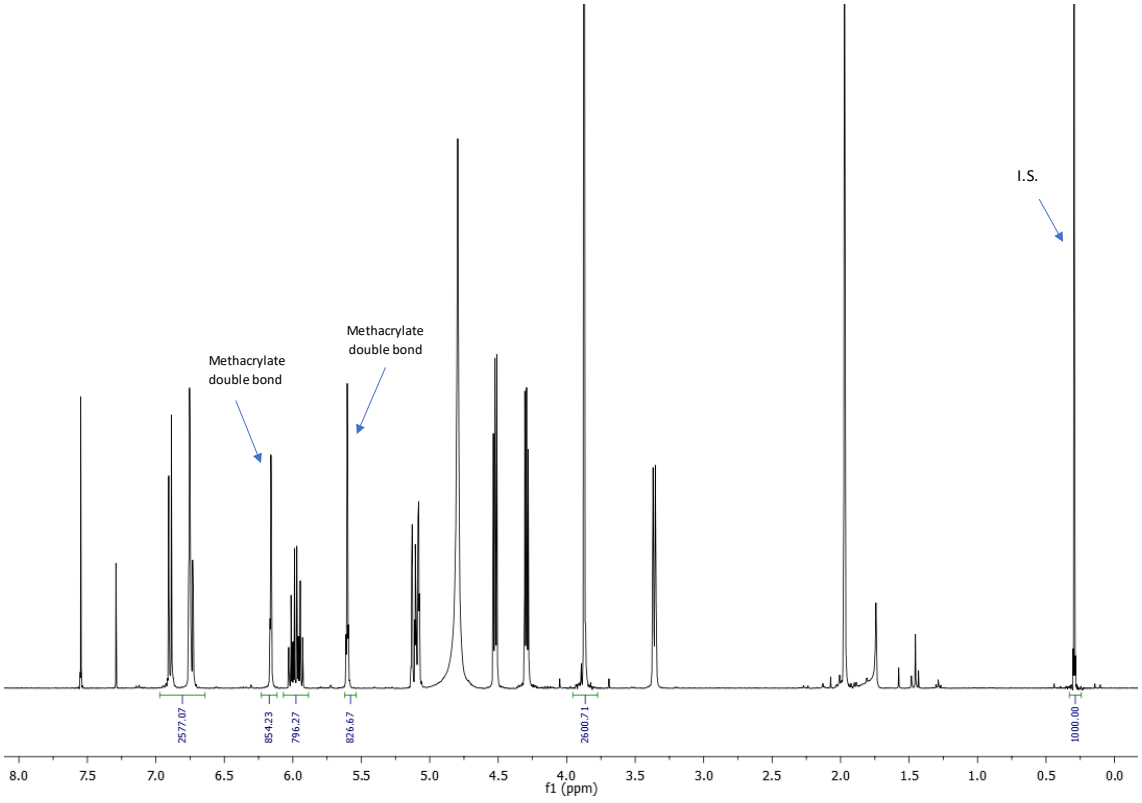

Figure A3-25. ^{1}H NMR EEMA emulsion polymerization using $Na_2S_2O_5$/KPS redox initiation system t=0 h.

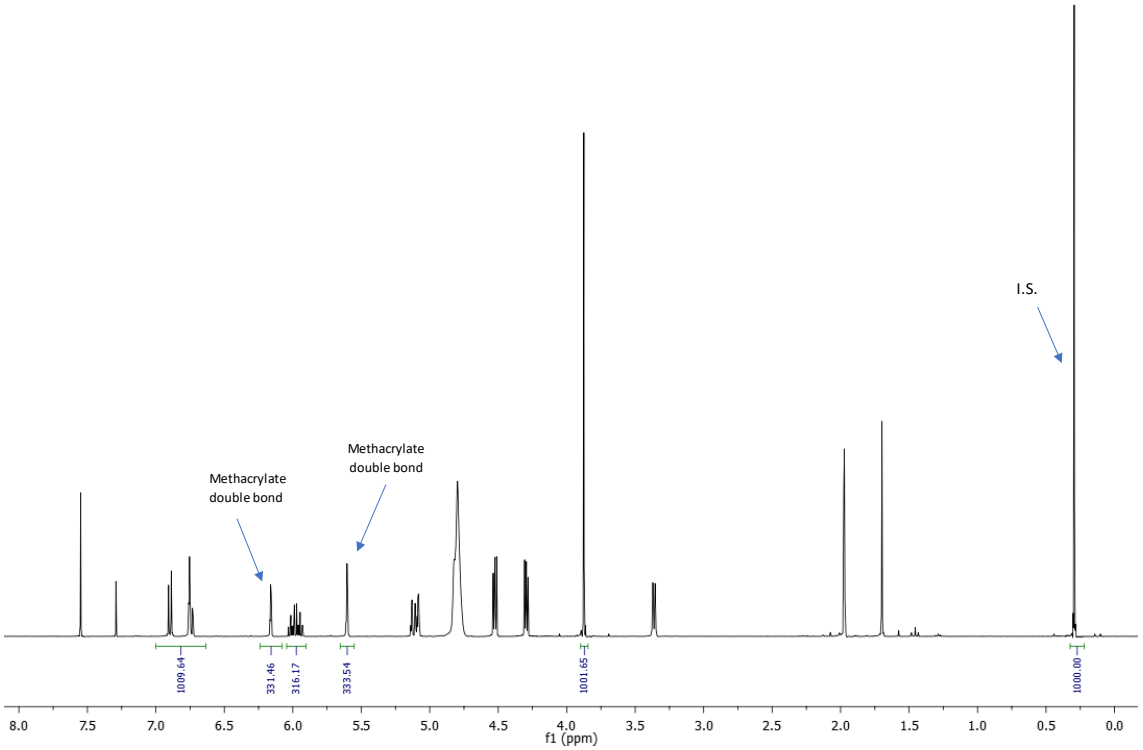

Figure A3-26. ^{1}H NMR EEMA emulsion polymerization using $Na_2S_2O_5$/KPS redox initiation system t=2 h.

A4 CHAPTER 5

A4.1 Determination of reactivity ratios

Three methods were used to determine the reactivity ratios of EDMA and MMA. All the methods used were based on the terminal model for copolymerization.

Table A4-1. Initial monomer feed molar fractions, monomer conversions, and instantaneous copolymer mole fractions for the copolymerization of EDMA with MMA in benzene-d_6 at 70°C

Expt ID	$f_{EDMA,0}$ (molar fraction)	$f_{MMA,0}$ (molar fraction)	Conversion (%)		Overall Conversion, X[a] (%)	F_{EDMA}[b] (molar fraction)	F_{MMA} (molar fraction)
			EDMA	MMA			
A	0.68	0.32	5.0	4.7	4.9	0.70	0.30
B	0.31	0.69	6.0	8.1	7.5	0.30	0.70
C	0.89	0.11	2.5	3.9	2.7	0.92	0.08
D	0.50	0.50	7.3	10.8	9.0	0.45	0.55
E	0.30	0.70	4.9	5.2	5.1	0.28	0.72
F	0.12	0.88	8.4	6.4	6.6	0.15	0.85

[a] Calculated using the formula: $Conv_{EDMA} \times f_{EDMA} + Conv_{MMA} \times f_{MMA}$

[b] Instantaneous copolymer composition calculated using Eq. A4-11

Kelen- Tüdös Linearization Method

The Kelen-Tüdös method[1] is based on the Fineman-Ross method (linearization of the copolymer equation), with the introduction of an arbitrary constant, α, which helps distribute the data more evenly as the Fineman-Ross method tends to be biased towards points at low or high monomer concentrations. Eq. A4-1 to Eq. A4-8 are used in the Kelen-Tüdös method to determine the reactivity ratios of EDMA and MMA (see Table A4-2. Parameters used in the calculation of rEDMA and rMMA using the Kelen-Tüdös methodTable A4-2 and Figure A4-1).[2]

The initial monomer concentrations, where $[M_1]_0$ and $[M_2]_0$ are the initial monomer concentrations:

$$X_0 = \frac{[M_1]_0}{[M_2]_0} \qquad \text{Eq. A4-1}$$

The rates of monomer consumption, where $R(M_1)$ and $R(M_2)$ are the rates of consumption of the two monomers:

$$n = \frac{R(M_1)}{R(M_2)} \qquad \text{Eq. A4-2}$$

The Fineman-Ross and Kelen-Tüdös constants:

$$F = \frac{{X_0}^2}{n} \qquad \text{Eq. A4-3}$$

$$G = \frac{X_0(n-1)}{n} \qquad \text{Eq. A4-4}$$

$$\alpha = \sqrt{F_{min}F_{max}} \qquad \text{Eq. A4-5}$$

$$Y = \frac{G}{\alpha + F} \qquad \text{Eq. A4-6}$$

$$X = \frac{F}{\alpha + F} \qquad \text{Eq. A4-7}$$

A plot of X vs. Y yields a straight line according to the following equation which can be solved for r_1 and r_2:

$$Y = \left(r_1 + \frac{r_2}{\alpha}\right)X - \frac{r_2}{\alpha} \qquad \text{Eq. A4-8}$$

Table A4-2. Parameters used in the calculation of r_{EDMA} and r_{MMA} using the Kelen-Tüdös method

Feed molar fractions		R(EDMA)	R(MMA)	X_o	n	F	G	α
$f_{EDMA,0}$	$f_{MMA,0}$	mmol/hr	mmol/hr					
0.16	0.84	0.0134	0.0727	0.19	0.18	0.19	0.83	0.72
0.68	0.32	0.1116	0.0483	2.15	2.31	2.00	1.22	0.72
0.31	0.69	0.0228	0.0564	0.45	0.40	0.49	0.66	0.72
0.89	0.11	0.1474	0.0127	7.72	11.61	5.13	7.05	0.72
0.12	0.88	0.0194	0.113	0.13	0.17	0.10	0.64	0.72
0.50	0.50	0.0729	0.1074	1.00	0.68	1.49	0.48	0.72

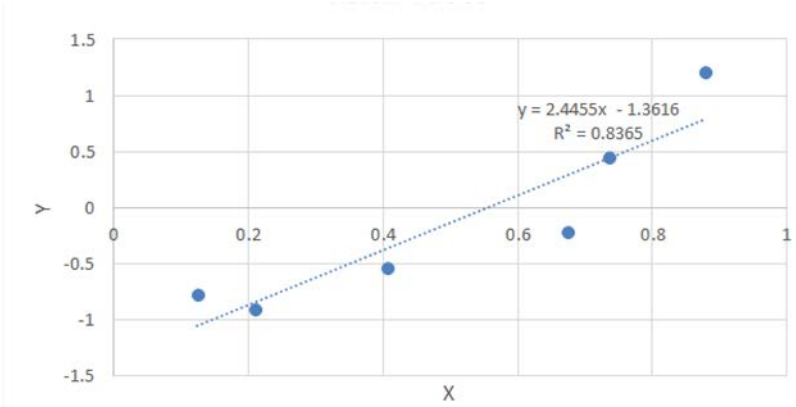

Figure A4-1. Kelen-Tüdös plot for the determination of EDMA and MMA reactivity ratios. In this case, α=0.72 giving $r_1 = r_{EDMA} = 1.08$ and $r_2 = r_{MMA} = 0.98$.

Non-linear regression

Non-linear regression was also used to evaluate the reactivity ratios of EDMA and MMA based on the method of the visualization of the sum of squared residual space proposed by van den Brink et al.[3] This method is based on the use of the integrated form of the copolymerization equation (Eq. A4-9).

$$X = 1 - \left(\frac{f}{f_0}\right)^{\alpha} \left(\frac{1-f}{1-f_0}\right)^{\beta} \left(\frac{f_0-\delta}{f-\delta}\right)^{\gamma} \qquad \text{Eq. A4-9}$$

where,

$$\alpha = \frac{r_2}{1-r_2}, \beta = \frac{r_1}{1-r_1}, \delta = \frac{1-r_1 r_2}{(1-r_1)(1-r_2)}, \gamma = \frac{1-r_2}{2-r_1-r_2}$$

and X: overall monomer conversion = $Conv_1 \times f_1 + Conv_2 \times (1-f_1)$

f: monomer 1 molar fraction = (moles monomer 1)/(moles monomer 1 + moles monomer 2)

f_0: initial monomer 1 molar fraction = (initial moles monomer 1)/(initial moles monomer 1 + initial moles monomer 2)

r_1 and r_2: reactivity ratios of monomers 1 and 2

The point estimate (best estimate of r_1 and r_2) was found by minimizing the sum of squared residuals, represented by Eq. A4-10 (where w_i are the weighting factors and L_i are the residuals). Full details of the method can be found in the article of van den Brink et al.[3] Calculations were performed using Excel 2016 software. The reported value in the article ($r_{EDMA} = 0.95$ and $r_{MMA} = 1.02$) using this method is the average obtained from 5 experiments (Table A4-3).

$$SS(r_1, r_2) = \sum_{i=1}^{n} w_i {L_i}^2 \qquad \text{Eq. A4-10}$$

A contour plot of the sum of squared residuals for arbitrary values of r_{EDMA} and r_{MMA} for experiment 1 in Table A4-3 is shown in **Figure A4-2.** Contour plot of the sum of squared residuals for arbitrary

rEMDA and rMMA values in experiment 1. In this case, it gives r1 = rEDMA = 0.99 and r2 = rMMA = 1.11. Figure A4-2.

Table A4-3. EDMA and MMA copolymerization data for reactivity ratios determination using the visualization of the sum of squared residuals method.

Expt	$f_{EDMA,0}$	$f_{MMA,0}$	EDMA conversion (%)	MMA conversion (%)	r_{EDMA}	r_{MMA}
1	0.68	0.32	0	0	0.99	1.11
			5.0	4.7		
			15.9	14.8		
			32.0	32.8		
2	0.31	0.69	0	0	0.90	1.14
			3.9	4.3		
			6.0	8.1		
			11.4	12.1		
3	0.16	0.84	0	0	0.92	0.93
			1.7	2.0		
			5.2	3.2		
			7.0	5.5		
			11.4	8.3		
			13.1	14.5		
4	0.89	0.11	0	0	0.98	0.98
			2.5	3.9		
			16.2	10.8		
			45.0	47.3		
5	0.50	0.50	0	0	0.95	0.92
			7.3	10.8		
			22.3	27.9		

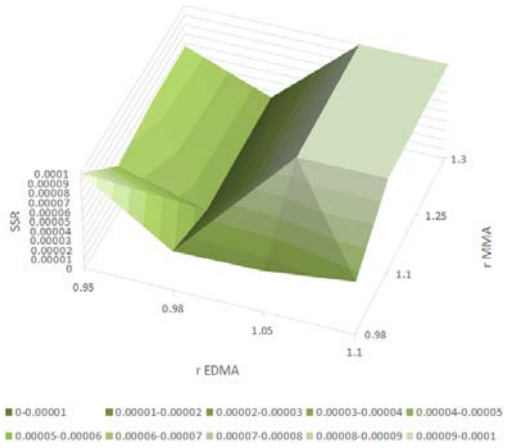

Figure A4-2. Contour plot of the sum of squared residuals for arbitrary r_{EMDA} and r_{MMA} values in experiment 1. In this case, it gives $r_1 = r_{EDMA} = 0.99$ and $r_2 = r_{MMA} = 1.11$.

The 95% joint confidence interval based on the data from Table A4-3 using the F-distribution for r_{EDMA} and r_{MMA} is shown in Figure A4-3.

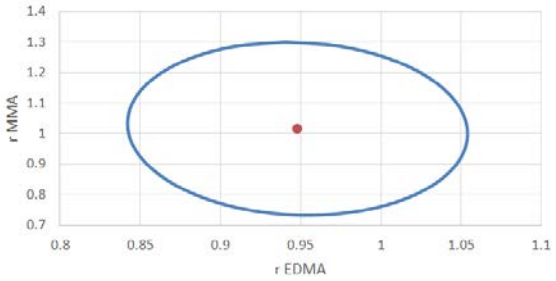

Figure A4-3. Plot of the 95% joint confidence intervals for the reactivity ratios of EDMA and MMA determined by the nonlinear least-squares method described by van den Brink et al.[3]

Non-linear curve fitting

Origin 9.0 was used to determine the EDMA and MMA reactivity ratios based on experimentally obtained data. Instantaneous copolymer compositions were calculated using the direct numerical differential method[4] (Eq. A4-11). The Levenberg-Marquardt algorithm[5] was used to fit the data to the Mayo-Lewis copolymer equation[2] (Eq. A4-12) based on the terminal model.

$$F_1 = \frac{d_{m1}}{d_{m1} + d_{m2}} \qquad \text{Eq. A4-11}$$

where, d_{m1} and d_{m2} refer to the change in moles of monomers 1 and 2 between two time intervals t_1 and t_2.

$$F_1 = \frac{r_1 f_1^{\,2} + f_1 f_2}{r_1 f_1^{\,2} + 2 f_1 f_2 + r_2 f_2^{\,2}} \qquad \text{Eq. A4-12}$$

where, F_1 is the instantaneous mole fraction of monomer 1 in the copolymer
f_1, f_2 are the mole fractions of monomers 1 and 2 in the feed
r_1 and r_2 are the monomer reactivity ratios

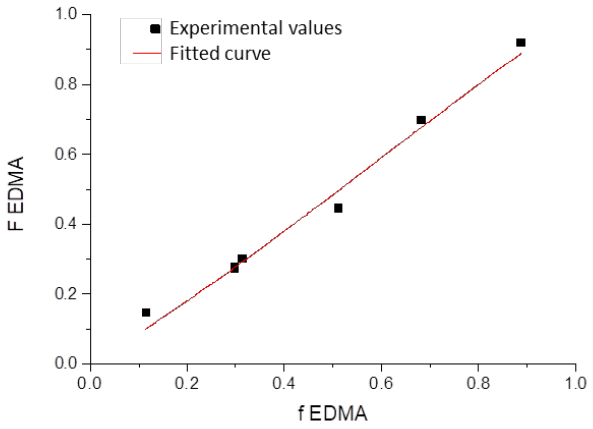

Figure A4-4. Experimental vs. fitted values of monomer feed and instantaneous copolymer composition using the Levenberg-Marquardt algorithm in Origin 9.0. The reactivity ratios of r_{EDMA} = 1.06 (standard error = 0.28) and r_{MMA} = 1.19 (standard error = 0.27) were obtained. Parameter standard errors were calculated using the error propagation formula in Origin 9.0.

A4.2 DLS

Table A4-4. Intensity-, number-, volume- and z-average particle hydrodynamic diameters of latexes prepared by emulsion polymerization in water of BA, MMA, MAA, EDMA and EEMA initiated by NaPS at 80°C at 4 h

Formulation	D_i (nm)	D_n (nm)	D_v (nm)	D_z (nm)	PDI
BA:MMA:MAA (87:12:1)	158	126	144	146	0.0411
BA:MMA:EDMA:MAA (87:6:6:1)	159	119	141	144	0.0538
BA:EDMA:MAA (87:12:1)	173	108	145	146	0.0873
BA:EDMA:EEMA:MAA (87:11:1:1)	178	153	168	168	0.0290

- Emulsion polymerization BA:MMA:MAA (87:12:1):

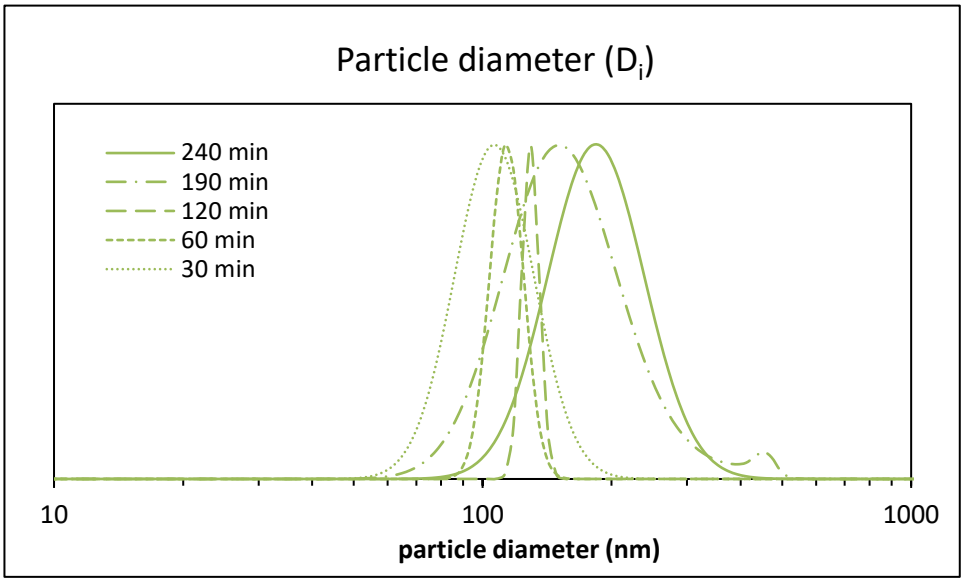

Figure A4-5. Intensity-average particle size distributions (Cumulants model) for BA:MMA:MAA (87:12:1) emulsion terpolymerization.

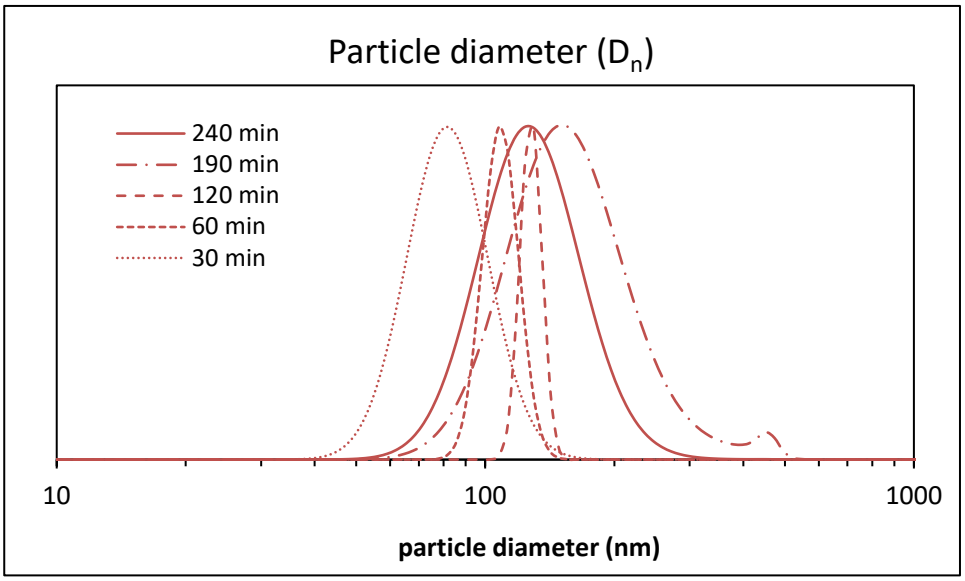

Figure A4-6. Number-average particle size distributions (Cumulants model) for BA:MMA:MAA (87:12:1) emulsion terpolymerization.

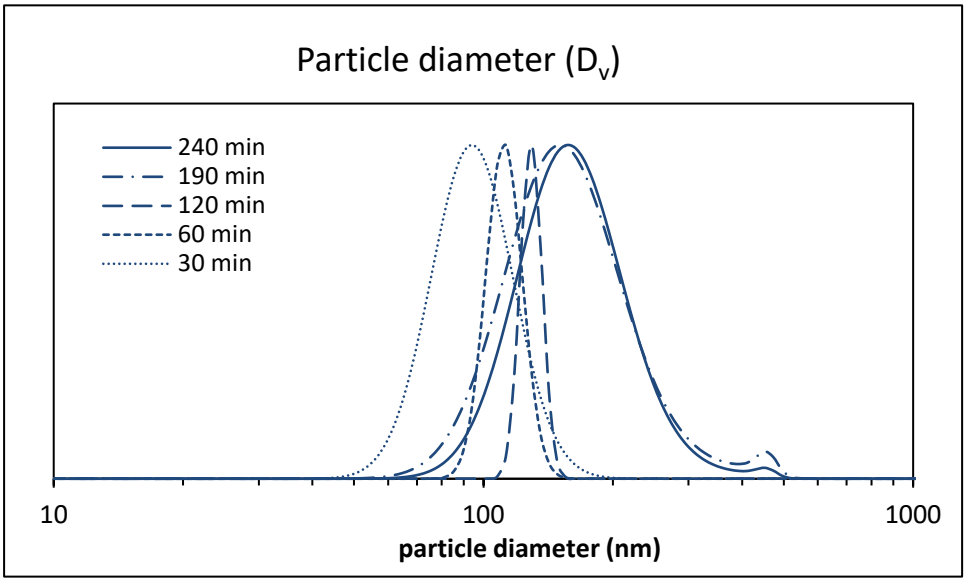

Figure A4-7. Volume-average particle size distributions (Cumulants model) for BA:MMA:MAA (87:12:1) emulsion terpolymerization.

- Emulsion polymerization BA:MMA:EDMA:MAA (87:6:6:1):

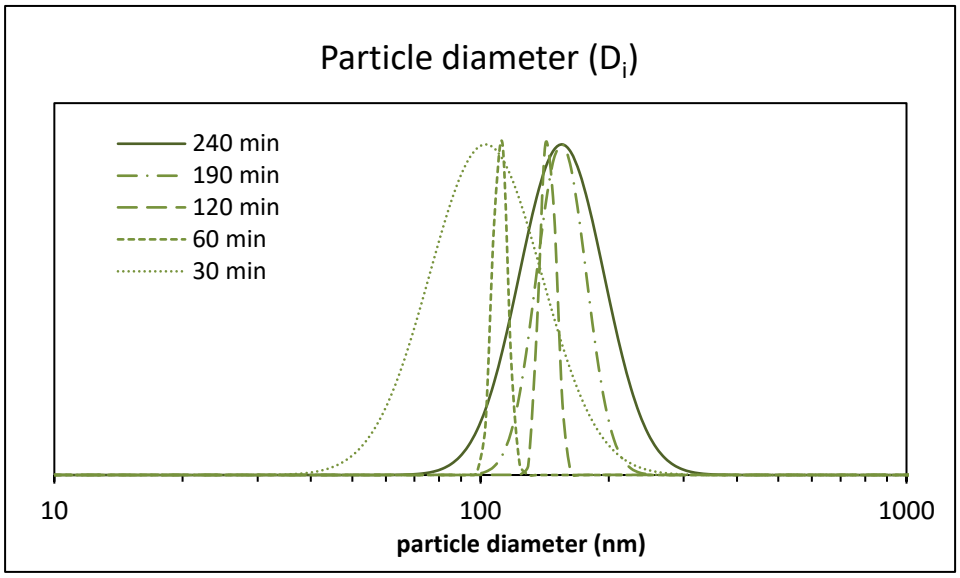

Figure A4-8. Intensity-average particle size distributions (Cumulants model) for BA:MMA:EDMA:MAA (87:6:6:1) emulsion copolymerization.

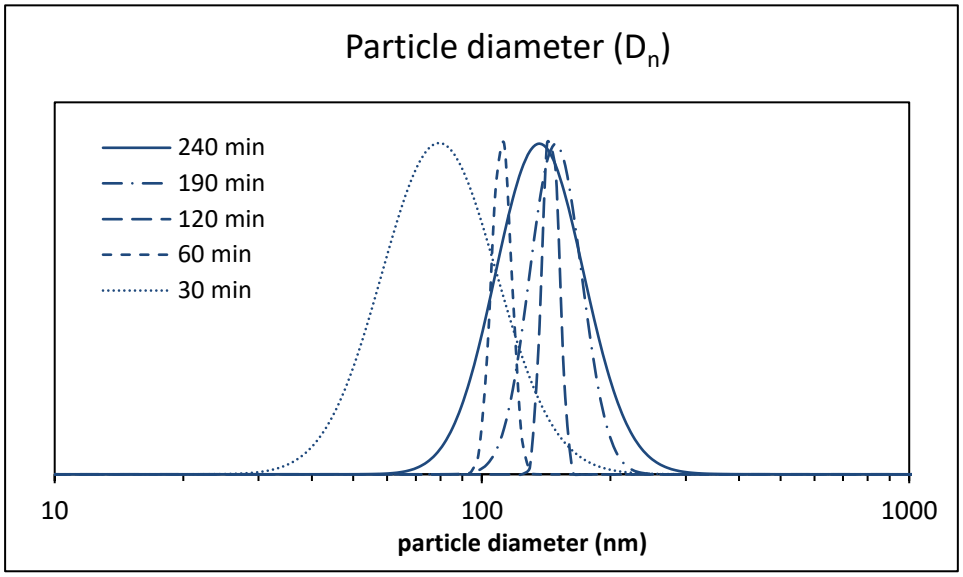

Figure A4-9. Number-average particle size distributions (Cumulants model) for BA:MMA:EDMA:MAA (87:6:6:1) emulsion copolymerization.

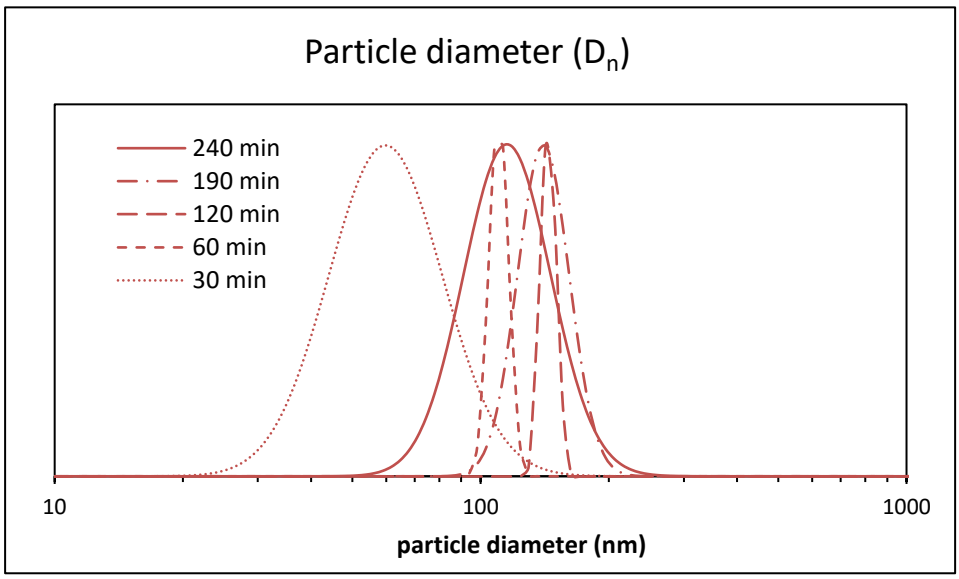

Figure A4-10. Volume-average particle size distributions (Cumulants model) for BA:MMA:EDMA:MAA (87:6:6:1) emulsion copolymerization.

- Emulsion polymerization BA:EDMA:MAA (87:12:1):

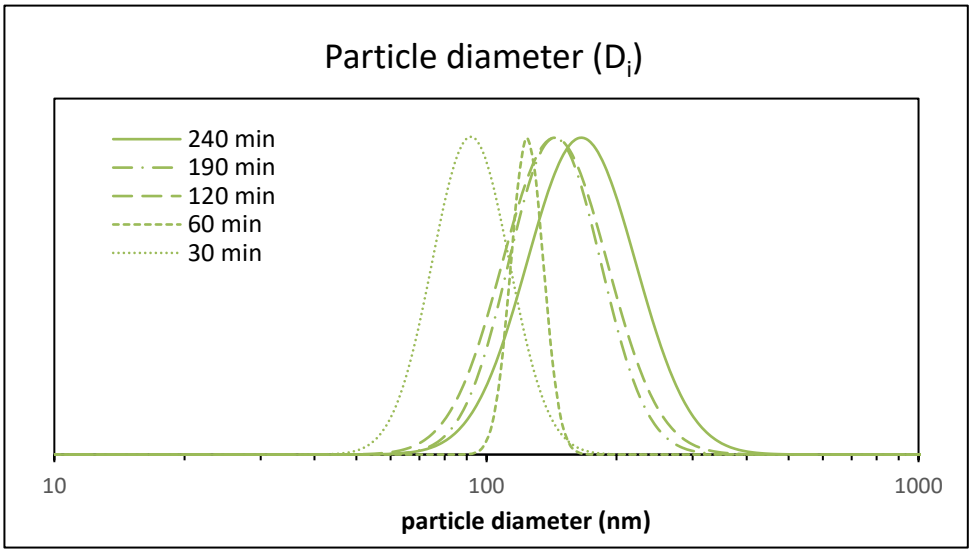

Figure A4-11. Intensity-average particle size distributions (Cumulants model) for BA:EDMA:MAA (87:12:1) emulsion terpolymerization.

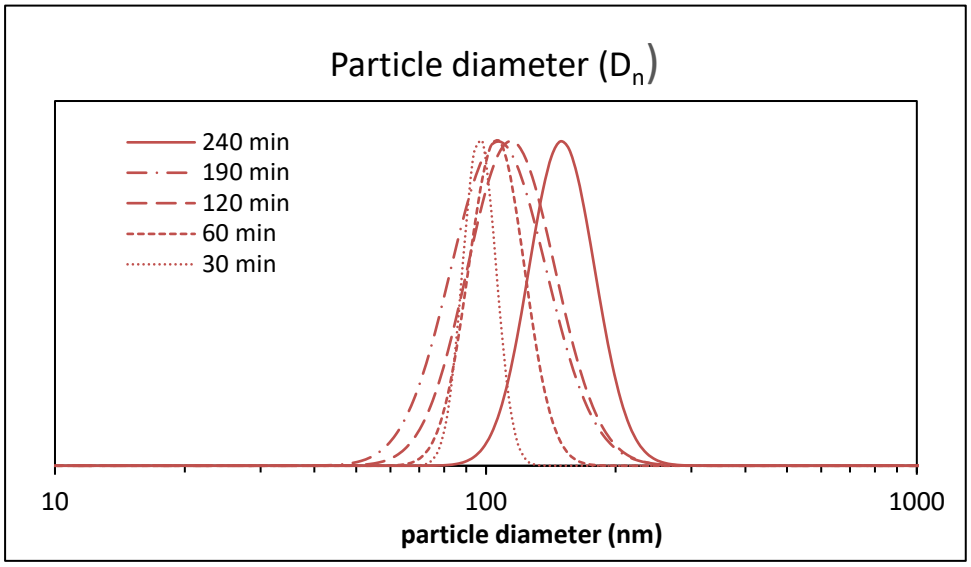

Figure A4-12. Number-average particle size distributions (Cumulants model) for BA:EDMA:MAA (87:12:1) emulsion terpolymerization.

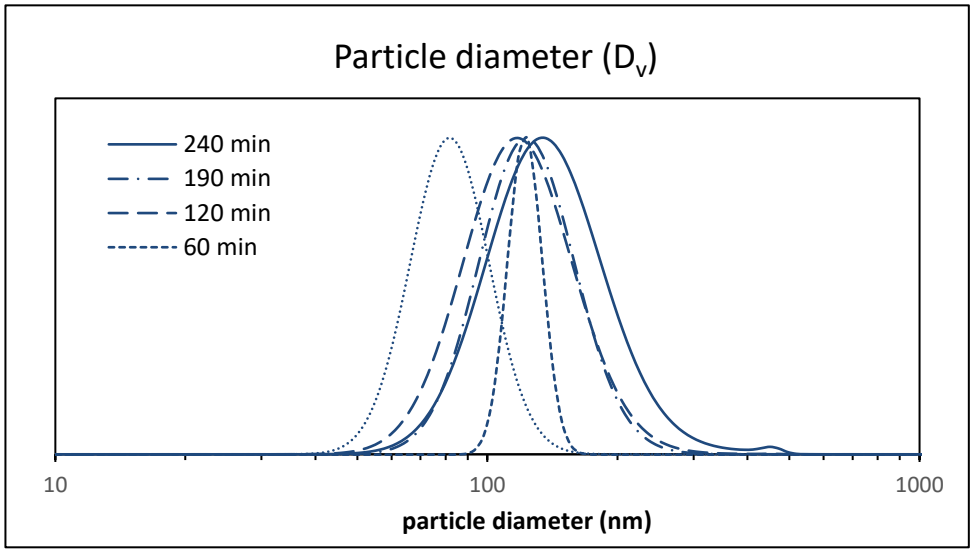

Figure A4-13. Volume-average particle size distributions (Cumulants model) for BA:EDMA:MAA (87:12:1) emulsion terpolymerization.

- Emulsion polymerization BA:EDMA:EEMA:MAA (87:11:1:1):

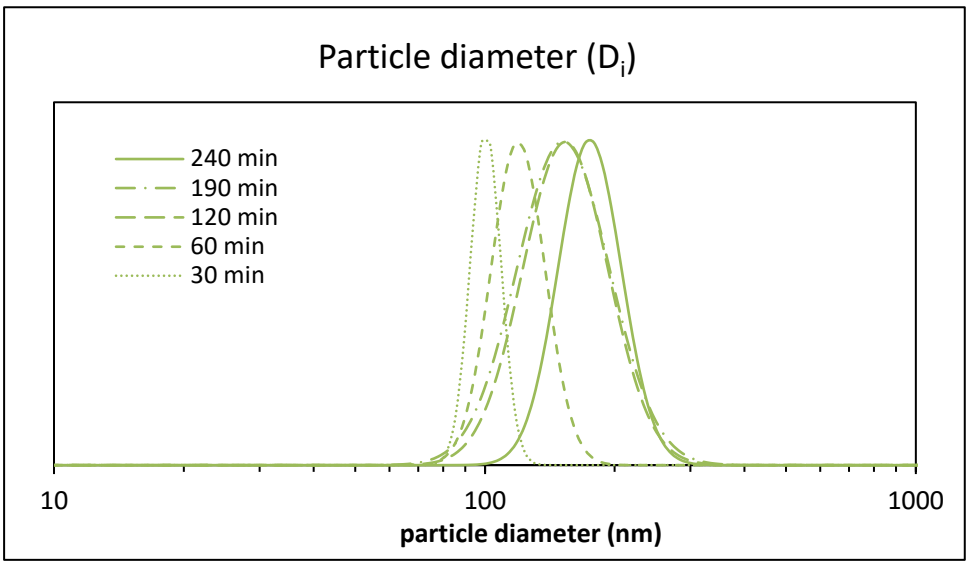

Figure A4-14. Intensity-average particle size distributions (Cumulants model) for BA:EDMA:EEMA:MAA (87:11:1:1) emulsion copolymerization.

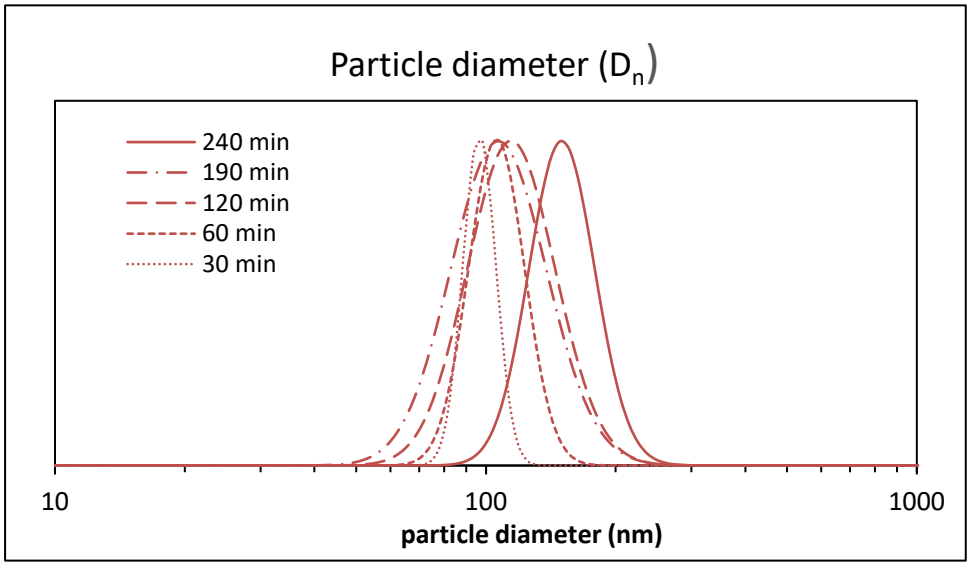

Figure A4-15. Number-average particle size distributions (Cumulants model) for BA:EDMA:EEMA:MAA (87:11:1:1) emulsion copolymerization.

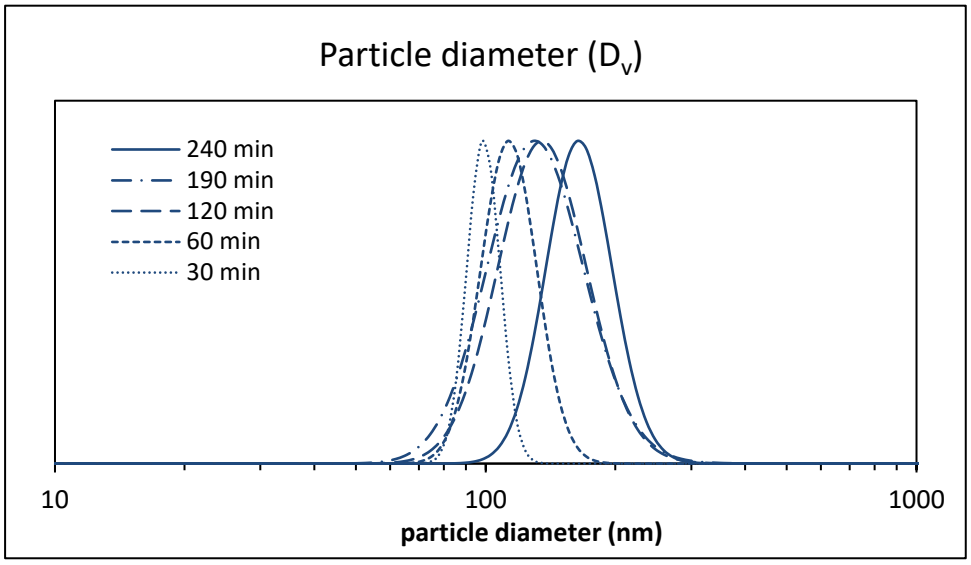

Figure A4-16. Volume-average particle size distributions (Cumulants model) for BA:EDMA:EEMA:MAA (87:11:1:1) emulsion copolymerization.

A4.3 Instantaneous and cumulative monomer conversions.

Table A4-5. Instantaneous monomer conversion of the different latex formulations

Instantaneous Conversion (%)				
Time (min)	F1	F2	F3	F4
0	0	0	0	0
30	91	85	86	87
60	89	87	83	94
120	95	94	90	92
190	93	90	95	93

Table A4-6. Cumulative monomer conversion of the different latex formulations

Cumulative Conversion (%)				
Time (min)	F1	F2	F3	F4
0	0	0	0	0
30	43	41	41	42
60	57	56	53	61
120	80	79	76	77
190	91	88	92	91
240	96	94	94	94

The monomer conversions in the reactor were measured gravimetrically. The instantaneous conversion at a given time, xi, is defined as the weight ratio of the polymer formed in the reactor to the total amount of monomer fed into the reactor by that time plus the initial charge. Overall conversion, xo, is defined as the mole or weight ratio of polymer in the reactor to the total monomer in the recipe

Instantaneous conversion was calculated using the equation:

$$Instantaneous\ Conversion(\%) = \frac{TSC_{exp,t} - TSC_{zero,t}}{TSC_{final\ (100\%conv),t} - TSC_{zero,t}} \qquad \text{Eq. A4-13}$$

where $TSC_{exp,t}$ is the total solids content at time t, $TSC_{zero,t}$ is the total solids content at zero conversion at time t, $TSC_{final\ (100\%conv),t}$ is the total solids content at 100% monomer conversion at time t.

Cumulative conversion was calculated using the equation:

$$Cumulative\ Conversion(\%) = \frac{TSC_{exp,t} - TSC_{zero,t}}{TSC_{final\ (100\%conv),final} - TSC_{zero,final}} \qquad \text{Eq. A4-14}$$

where $TSC_{final\ (100\%conv),final}$ is total solids content at 100% monomer conversion at time final, $TSC_{zero,final}$ is the total solids content at zero monomer conversion at time final.

A4.4 Thermogravimetric analysis

Table A4-7. Thermal decomposition temperatures under nitrogen for the different polymers prepared by emulsion copolymerization

TGA under N_2				
Latex	***Composition***	$T_{d,2\%}$	$T_{d,5\%}$	$T_{d,50\%}$
F1	BA:MMA:MAA (87:12:1)	310	335	395
F2	BA:MMA:EDMA:MAA (87:6:6:1)	290	320	387
F3	BA:EDMA:MAA (87:12:1)	314	340	397
F4	BA:EDMA:EEMA:MAA (87:11:1:1)	305	333	395

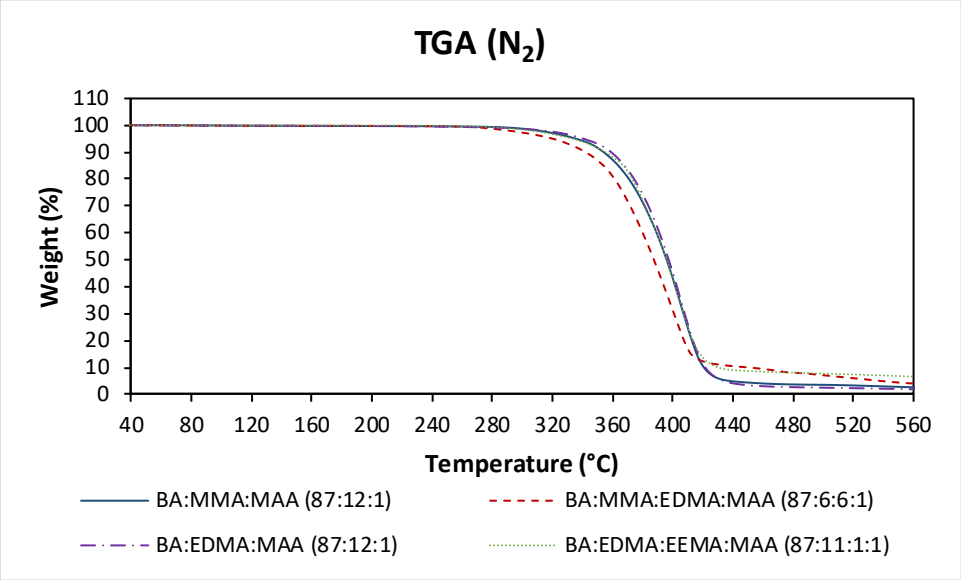

Figure A4-17. TGA curves under nitrogen of the copolymers prepared by emulsion polymerization in water.

Table A4-8. Thermal decomposition temperatures under air for the different polymers prepared by emulsion copolymerization

TGA under Air				
Latex	***Composition***	$T_{d,2\%}$	$T_{d,5\%}$	$T_{d,50\%}$
F1	BA:MMA:MAA (87:12:1)	290	320	383
F2	BA:MMA:EDMA:MAA (87:6:6:1)	295	324	388
F3	BA:EDMA:MAA (87:12:1)	293	321	385
F4	BA:EDMA:EEMA:MAA (87:11:1:1)	287	313	387

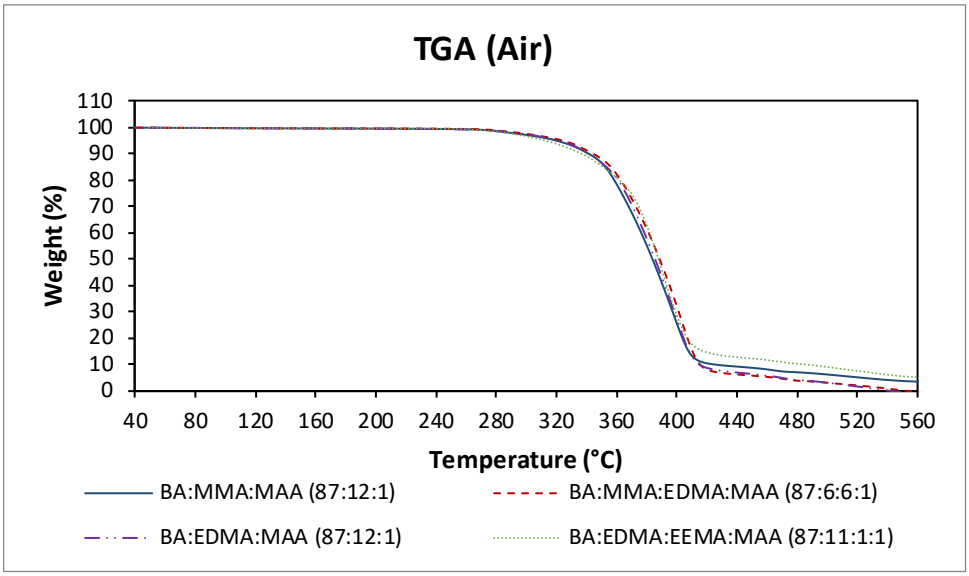

Figure A4-18. TGA curves under air of the copolymers prepared by emulsion polymerization in water.

A4.5 DSC measurements

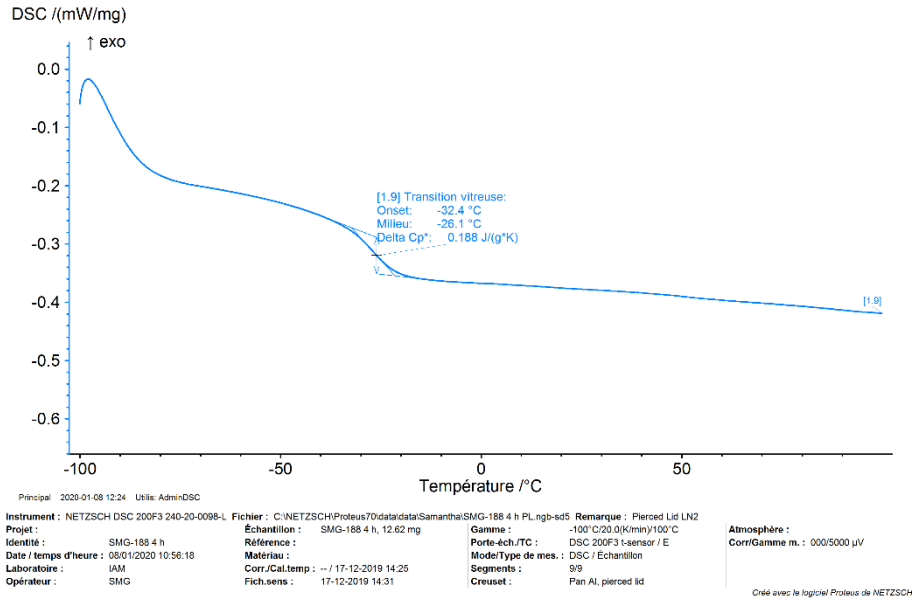

Figure A4-19. DSC measurement of the terpolymer prepared via emulsion copolymerization of BA:MMA:MAA (87:12:1) in water.

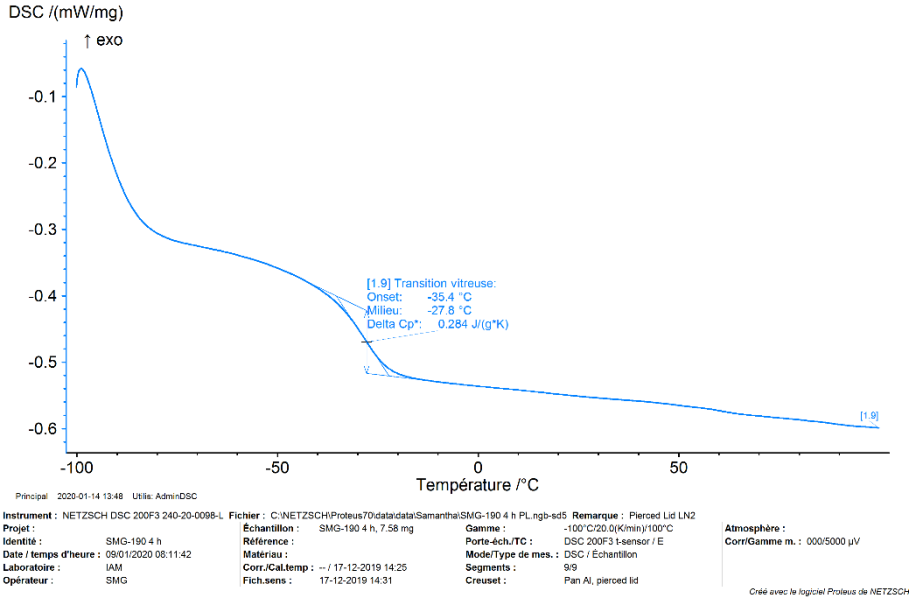

Figure A4-20. DSC measurement of the copolymer prepared via emulsion copolymerization BA:MMA:EDMA:MAA (87:6:6:1) in water.

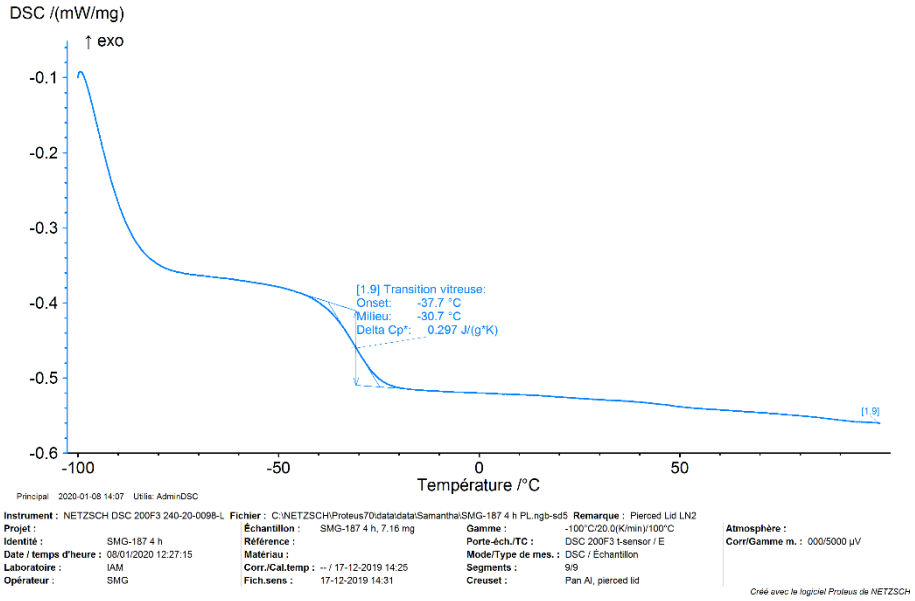

Figure A4-21. DSC measurement of the terpolymer prepared via emulsion copolymerization BA:EDMA:MAA (87:12:1) in water.

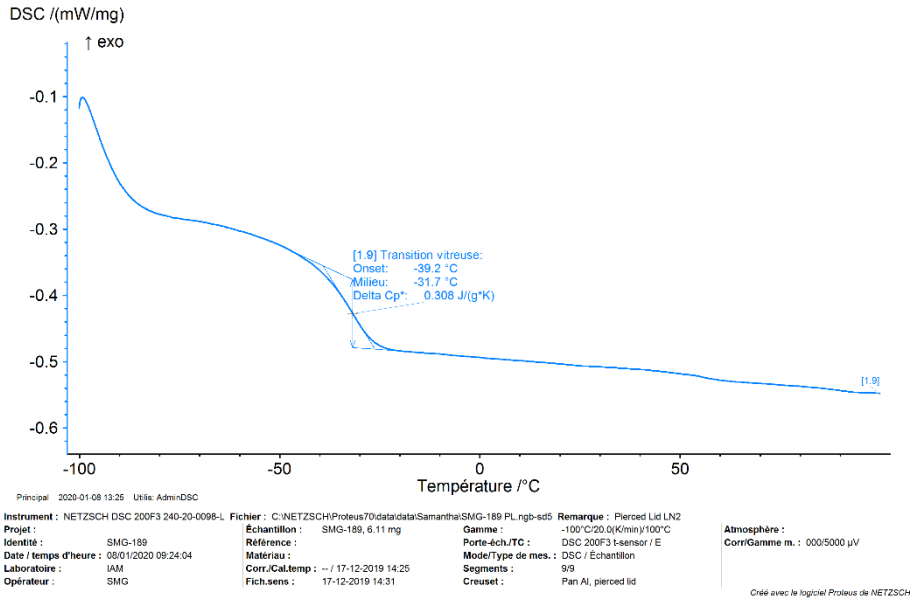

Figure A4-22. DSC measurement of the copolymers prepared via emulsion copolymerization BA:EDMA:EEMA:MAA (87:11:1:1) in water.

A4.6 SEC measurement (soluble fraction of the copolymers)

Table 4-9. Molar masses of the copolymers prepared by emulsion polymerization in water (PMMA calibration)

Formulation	M_n	M_w	Đ = M_w/M_n
BA:MMA:MAA (87:12:1)	51,700	288,300	5.58
BA:MMA:EDMA:MAA (87:6:6:1)	36,100	118,100	3.27
BA:EDMA:MAA (87:12:1)	31,200	86,600	2.78
BA:EDMA:EEMA:MAA (87:11:1:1)	20,300	51,800	2.55

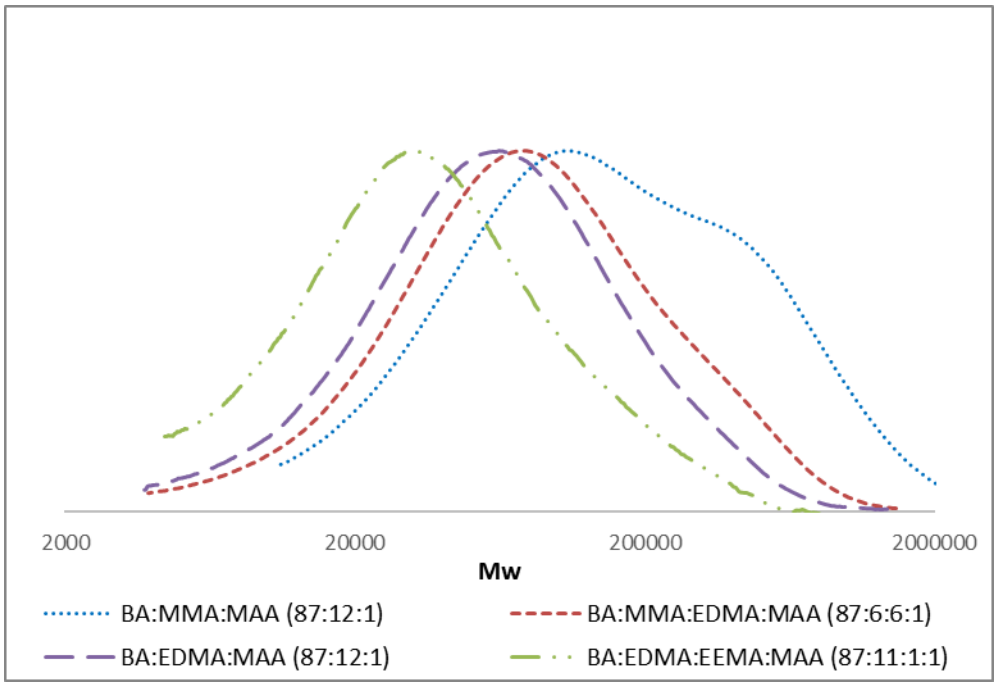

Figure A4-23. Molar mass distributions of the copolymers prepared by emulsion polymerization in water.

A4.7 Peel measurements

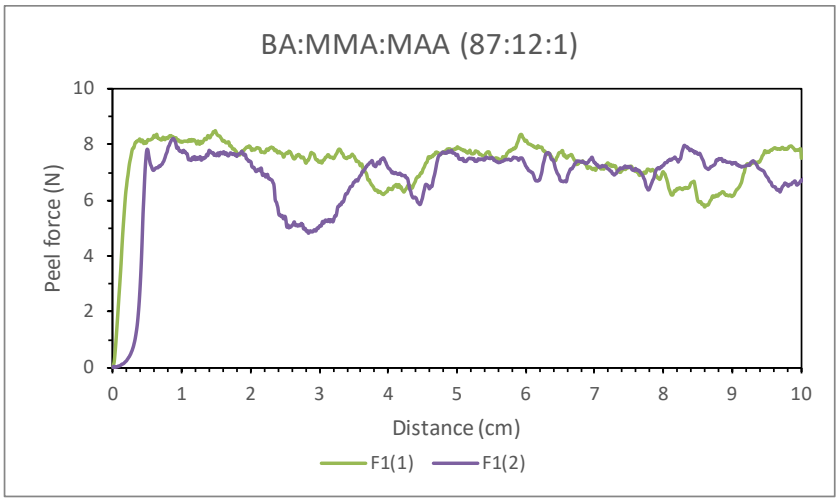

Figure A4-24. Peel measurement of F1 formulation BA:EDMA:MAA (87:12:1).

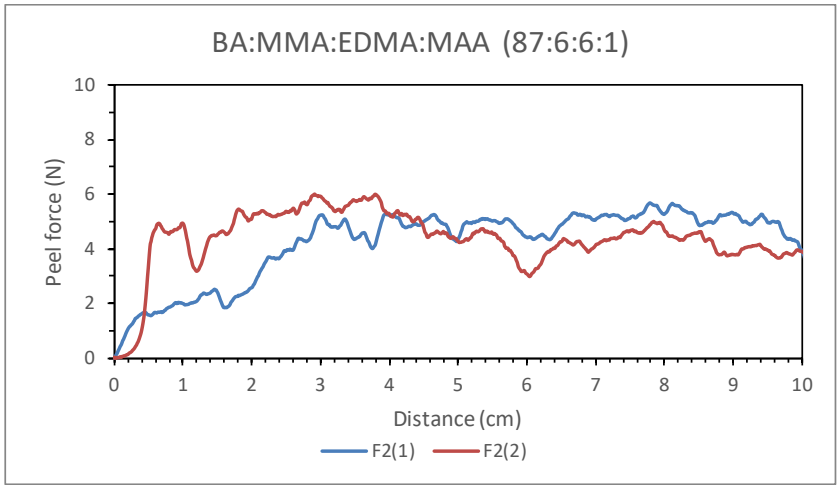

Figure A4-25. Peel measurement of F2 formulation BA:MMA:EDMA:MAA (87:6:6:1).

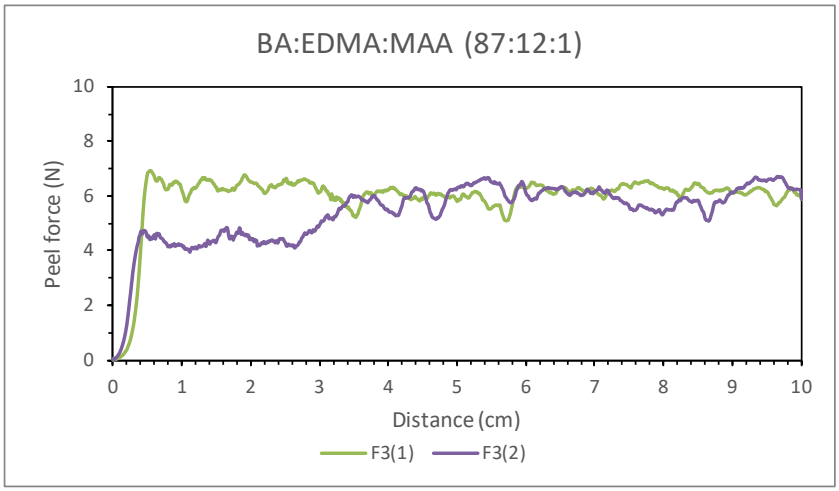

Figure A4-26. Peel measurement of F3 formulation BA:EDMA:MAA (87:12:1).

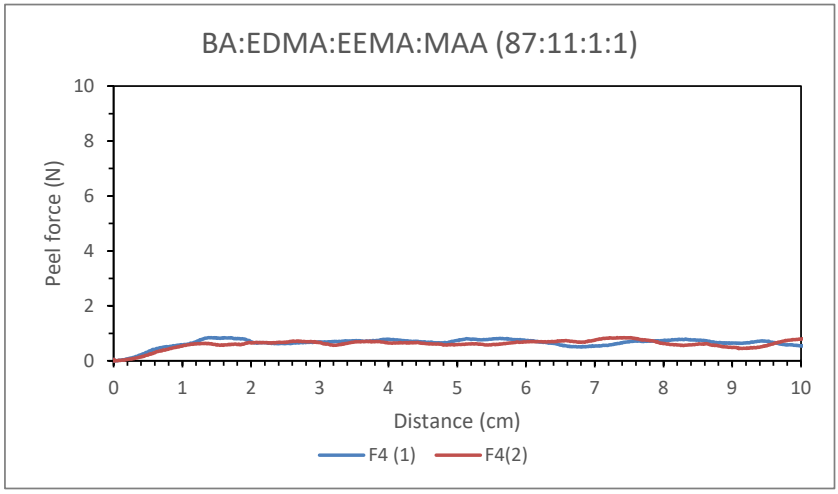

Figure A4-27. Peel measurement of F4 formulation BA:EDMA:EEMA:MAA (87:11:1:1).

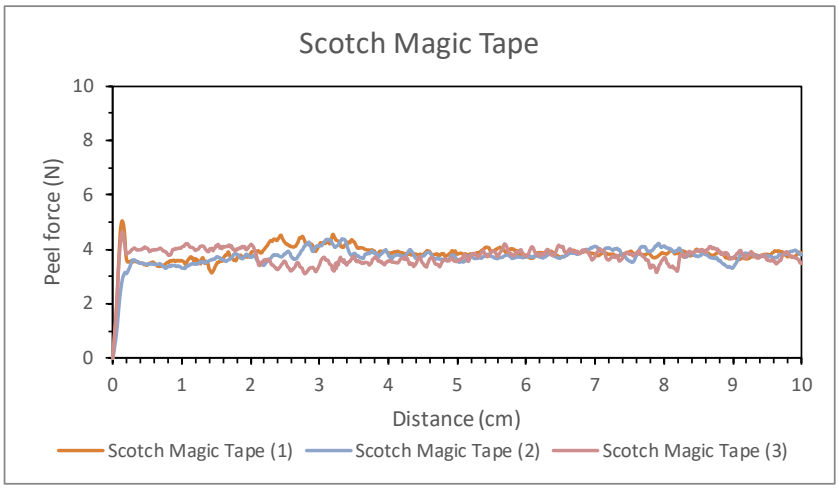

Figure A4-28. Peel measurement of Scotch Magic™ Tape.

A4.8 Tack measurement

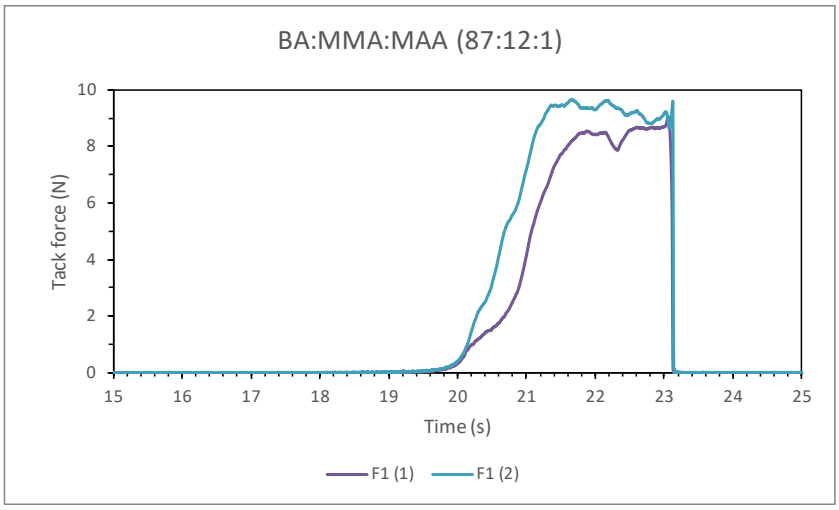

Figure A4-29. Tack measurement of F1 formulation BA:MMA:MAA (87:12:1).

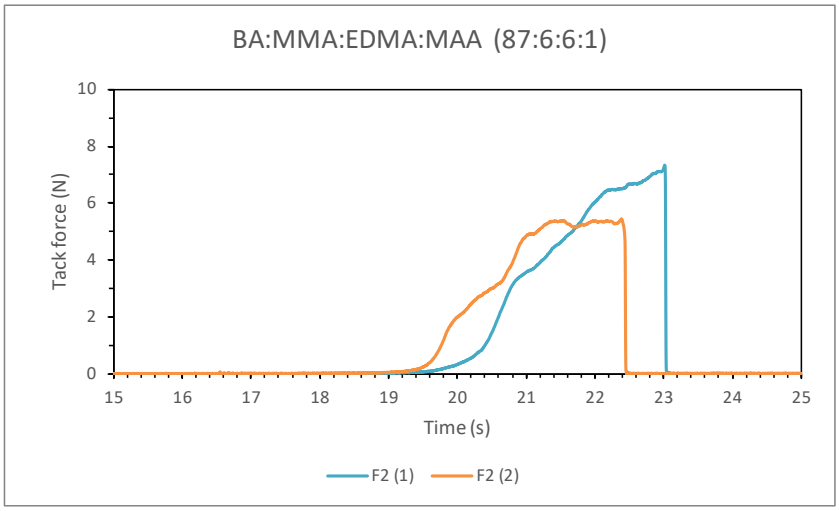

Figure A4-30. Tack measurement of F2 formulation BA:MMA:EDMA:MAA (87:6:6:1).

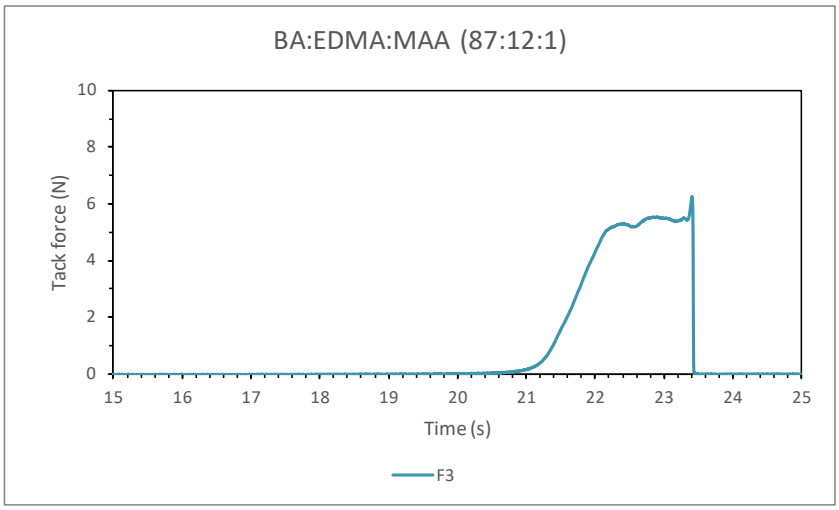

Figure A4-31. Tack measurement of F3 formulation BA:EDMA:MAA (87:12:1).

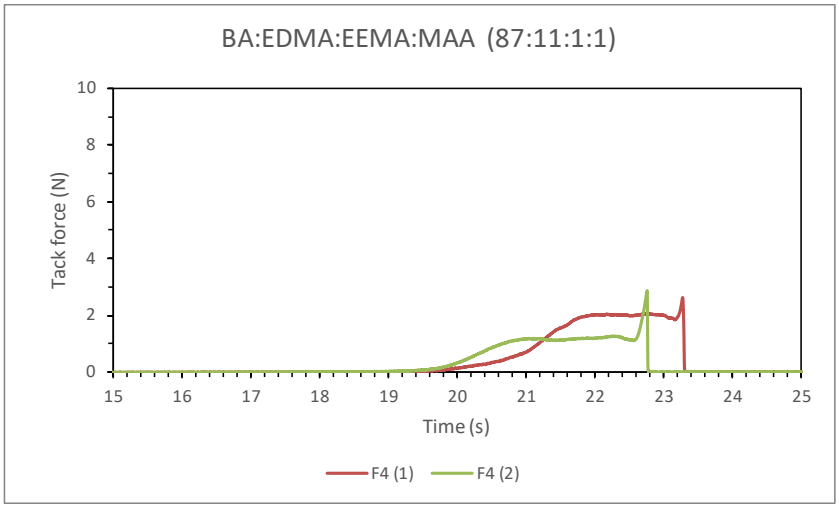

Figure A4-32. Tack measurement of F4 formulation BA:EDMA:EEMA:MAA (87:11:1:1).

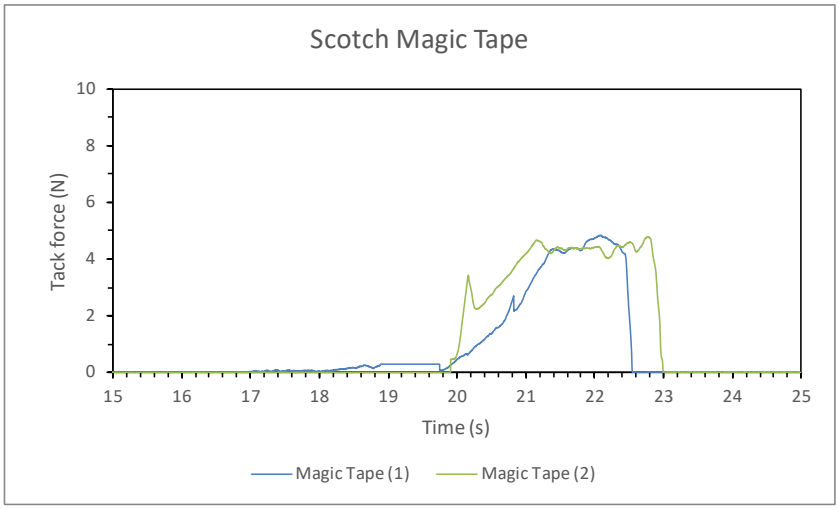

Figure A4-33. Tack measurement of Scotch Magic™ Tape.

A5 References

(1) Kelen, T.; Tüdös, F. Analysis of the Linear Methods for Determining Copolymerization Reactivity Ratios. I. A New Improved Linear Graphic Method. *J. Macromol. Sci. Part A - Chem.* **1975**, *9*, 1.

(2) Odian, G. *Principles of Polymerization*; John Wiley & Sons, Inc.: Hoboken, NJ, USA, 2004; Vol. 58.

(3) Van Den Brink, M.; Van Herk, A. M.; German, A. L. Nonlinear Regression by Visualization of the Sum of Residual Space Applied to the Integrated Copolymerization Equation with Errors in All Variables. I. Introduction of the Model, Simulations and Design of Experiments. *J. Polym. Sci. Part A Polym. Chem.* **1999**, *37*, 3793.

(4) Feng, J.; Oyeneye, O. O.; Xu, W. Z.; Charpentier, P. A. In-Situ NMR Measurement of Reactivity Ratios for Copolymerization of Methyl Methacrylate and Diallyl Dimethylammonium Chloride. *Ind. Eng. Chem. Res.* **2018**, *57*, 15654.

(5) Moré, J. J. The Levenberg-Marquardt Algorithm: Implementation and Theory; 1978; pp 105–116.

Abstract

Current environmental concerns and environmental regulations have led to the necessity to synthesize monomers and polymers from renewable resources through environmentally friendly processes. In this work, photoinduced polymerization and aqueous emulsion polymerization were selected as polymerization techniques. Natural phenols have not been widely researched and employed in the synthesis of monomers to be polymerized through the aforementioned polymerization methods. Thus, eugenol, isoeugenol and dihydroeugenol, natural phenols coming from clove oil and lignin depolymerization, were chosen as building blocks. The synthesis of eight novel monomers derived from eugenol bearing polymerizable functional groups such as (meth)acrylate, epoxy and carbonate was achieved. Successful radical polymerization in solution was achieved with the (meth)acrylated eugenol-derivatives. The polymerization rate was affected by secondary reactions involving the allylic and propenyl groups in the eugenol and isoeugenol derivatives (degradative chain transfer and cross-propagation). However, most of the allylic and propenyl groups were preserved for post-polymerization reactions. Photoinduced polymerization was executed with the methacrylate eugenol-derived monomers and monitored in the absence and presence of a photoinitiator and under air or protected from air, using Real-Time Fourier Transform Infrared Spectroscopy. The polymerization rate was again affected by the presence and reactivity of the allyl and propenyl groups in the eugenol- and isoeugenol-derived methacrylates, respectively. These groups are involved in radical addition, degradative chain transfer, and termination reactions, yielding crosslinked polymers. Without photoinitiator and in the presence of air, the formation of peroxides for eugenol and isoeugenol derivatives led to a second polymerization regime. The materials, in the form of films, were characterized by differential scanning calorimetry, thermogravimetric analysis, and contact angle. Eugenol-derived methacrylates were then homopolymerized through aqueous emulsion polymerization using three different initiation systems. Stable latexes of poly(ethoxy dihydroeugenyl methacrylate), poly(ethoxy eugenyl methacrylate) and poly(ethoxy isoeugenyl methacrylate) were successfully obtained. Glass transition temperatures of the resulting polymers ranged between 20 and 72°C. Subsequently, eugenol-derived methacrylates were copolymerized by emulsion polymerization to produce latexes for adhesive applications. Latexes containing ethoxy dihydroeugenyl methacrylate and ethoxy eugenyl methacrylate with high total solids content of 50 wt % were obtained and characterized. Latexes synthesis was carried out using a semibatch process, and latexes with particle diameters in the 159−178 nm range were successfully obtained. Glass transition temperature values of the resulting polymers ranged between −32 and −28 °C. Furthermore, tack and peel measurements confirmed the possibility to use these latexes in adhesive applications.

Keywords: Biobased monomers • photoinduced polymerization • emulsion polymerization • coatings • adhesives

Résumé

Les préoccupations et les réglementations environnementales rendent nécessaires la synthèse de monomères et de polymères à partir de ressources renouvelables en utilisant des procédés respectueux de l'environnement. Dans ce travail, la polymérisation photoinduite et la polymérisation en émulsion aqueuse ont été sélectionnées comme techniques de polymérisation. Les phénols naturels ont été peu étudiés dans la littérature pour la synthèse de monomères polymérisables par les procédés de polymérisation susmentionnés. Ainsi, l'eugénol, l'isoeugénol et le dihydroeugénol, des phénols naturels provenant de l'huile de girofle ou de la dépolymérisation de la lignine, ont donc été choisis comme matières premières. La synthèse de huit nouveaux monomères dérivés d'eugénol contenant des groupes fonctionnels polymérisables tels que les groupes (méth)acrylate, époxy et carbonate, a été réalisée. Les dérivés d'eugénol (méth)acrylés ont été polymérisés avec succès par polymérisation radicalaire en solution. La vitesse de polymérisation s'est trouvée affectée par des réactions secondaires impliquant le groupe allylique de l'eugénol et propényle de l'isoeugénol (réactions de transfert de chaîne dégradatif et de propagation croisée). Cependant, la plupart des groupes allylique et propényle ont été conservés pour des réactions de post-polymérisation. De plus, la polymérisation photoinduite a été réalisée avec les monomères méthacrylates des dérivés d'eugénol et suivi par spectroscopie infrarouge à transformée de Fourier en temps réel, en l'absence et en présence d'un photoamorceur ainsi que sous air ou à l'abri de l'air. La vitesse de polymérisation a également été affectée par la présence et la réactivité des groupes allyle et propényle dans les méthacrylates d'eugénol et d'isoeugénol, respectivement. Ces groupes sont impliqués dans des réactions d'addition de radicaux, de transfert de chaîne dégradatif, et de terminaison, donnant ainsi des polymères réticulés. Sans photoamorceur et en présence d'air, la formation de peroxydes à partir des dérivés d'eugénol et d'isoeugénol a conduit à un deuxième régime de polymérisation. Les matériaux, sous forme de films, ont été caractérisés par calorimétrie différentielle à balayage, thermogravimétrie et mesure d'angle de contact. Ensuite, les méthacrylates des dérivés d'eugénol ont été homopolymérisés par polymérisation en émulsion aqueuse en utilisant trois systèmes d'amorçage différents. Des latex stables de poly(méthacrylate d'éthoxy dihydroeugényle), poly(méthacrylate d'éthoxy eugényle) et poly(méthacrylate d'éthoxy isoeugényle) ont été obtenus avec succès. Les températures de transition vitreuse des polymères résultants se situent entre 20°C et 72°C. Par la suite, des méthacrylates des dérivés d'eugénol ont été copolymérisés par polymérisation en émulsion pour produire des latex pour des applications d'adhésifs sensibles à la pression. Des latex contenant du méthacrylate d'éthoxy dihydroeugényle (EDMA) et du méthacrylate d'éthoxy eugényle (EEMA) avec un taux de solides de 50% en poids ont été obtenus et caractérisés. La synthèse de latex a été réalisée en utilisant un procédé semi-batch, et des latex avec des diamètres de particules dans la gamme de 159-178 nm ont été obtenus avec succès. Les valeurs de température de transition vitreuse des polymères résultants se situent entre -32°C et -28°C. De plus, les mesures de pégosité (« tack ») et de pelage (« peel ») ont confirmé la possibilité d'utiliser ces latex dans des applications d'adhésifs.

Mots clés : Monomères biosourcés • polymérisation photoinduite • polymérisation en émulsion • revêtements • adhésifs